Inorganic Biochemistry of Iron Metabolism

Inorganic Biochemistry of Iron Metabolism

From Molecular Mechanisms
to Clinical Consequences
Second Edition

Robert Crichton

Université Catholique de Louvain, Belgium

With the collaboration of

Johan R. Boelaert, Volkmar Braun, Klaus Hantke, Jo J. M. Marx, Manuela Santos *and* **Roberta Ward**

Contents

6 Intracellular Iron Storage and Biomineralization   133

7 Intracellular Iron Metabolism and Cellular Iron Homeostasis   167

Preface

Two roads diverged in a yellow wood,
And sorry I could not travel both
And be one traveller, long I stood
And looked down one as far as I could

Then took the other as just as fair,

Oh, I kept the first for another day !
Yet knowing how way leads on to way,
I doubted if I should ever come back.

I shall be telling this with a sigh
Somewhere ages and ages hence:
Two roads diverged in a wood, and I –
I took the one less traveled by,
And that has made all the difference.

Robert Frost 'The road not taken' from *Mountain Interval* (1916)

When one reflects on the choice that one has made in the course of a career (and I might well have gone down the path of Kierkegardian existentialist philosophy, and ended up as a Church of Scotland minister), Frost's reflections seem particularly appropriate. I came to iron and protein chemistry simultaneously and serendipitously, via cytochrome *c* in Glasgow, insect haemoglobins in Munich, and ferritins and transferrins in Glasgow, Berlin and Louvain-la-Neuve. I have remained faithful to the proteins involved in iron metabolism for nearly forty years' and make no apology for continuing to do so.

Over this time the importance of metals in biology – described as inorganic biochemistry or bioinorganic chemistry respectively by biochemists and inorganic chemists, and more recently neutralized by the appellation 'biological inorganic chemistry – has been increasingly recognized. The growth of interest in inorganic biochemistry, as I shall call this area, has been modestly helped on its way by the author who, together with Cees Veeger from the Agricultural University in Wageningen, has organized in Louvain-la-Neuve (with the financial support, initially of the Federation of European Biochemical Societies (FEBS), and subsequently the European Union and the European Science Foundation) 15 Advanced Courses on 'Chemistry of Metals in Biological Systems'. These with the enthusiastic help of a devoted faculty, have trained more than 500 young (and not so young) biochemists, physicists, inorganic and physical chemists in the spectroscopic and biochemical techniques that enable us to investigate the role of metals in biological systems. A measure of our success was the presence 2 years ago of 35 former students among some 300 participants at the fourth European Biological Inorganic Chemistry Congress in Seville, many of who gave invited lectures. The

list of faculty reads like a roll call of Europe's best inorganic biochemists – Fraser Armstrong, Lucia Banci, Ernesto Carafoli, Bob Eady, Dave Garner, Fred Hagen, Peter Kroneck, Claudio Luchinat, Daniel Mansuy, Jan Reedijk, Helmut Sigel, Barry Smith, Alfred Trautwein, Bob Williams and Antonio Xavier, to mention but a few.

While Robert Frost might have doubted whether he would ever come back, I have done so, not by the other path but by the same, I trusts with renewed relish at the prospect of once again confronting the wonderful world of iron metabolism. At the outset of this next step, along a road already travelled, I would like first of all to address myself to you, my dear readers, and to thank you for the enormous encouragement you have given me over the last few years to continue, and develop the project that I began in 1990. This encouragement has been an important stimulus in the preparation of a second edition, if only through seeing the well-thumbed copies of the first edition on your desks and bookshelves. Another factor was hearing from so many of you about how useful you found the first edition for giving a panoramic view of iron metabolism from the point of view of a participant' who was at least prepared to come down on one side of the fence, rather than the other[†]. I continue to adopt the position that when writing a review (or even more important, as in this case, an overview), it is *important* not simply to *describe* the current literature, but to take a *reasoned position* concerning the *probability* that *one particular viewpoint is correct*.

A list of some of the inorganic elements (and a few selected non-metals) that play an important part in biology with their relative abundance in the earth's crust and in seawater, together with examples of specific functions, is presented in Table 1. The basic principles involved in the bioselection of elements conform to four fundamental rules (Frausto da Silvo and Williams, 1991; Orchiai, 1986), namely (i) the abundance of the element, (ii) its efficacy, (iii) its basic fitness for a given task, and (iv) the evolutionary pressure. A rapid examination of Table 1 shows that abundance, for example, is not an adequate requirement for biological fitness (aluminium is perhaps the best example, and owes its inclusion to the fact that it has more or less been brought into our present day biological environment by man himself). Individual elements are particularly fitted for specific functions, often as a direct consequence of their chemical properties – for instance sodium and potassium, which form complexes of very low stability and are therefore very mobile in biological media, are ideally suited for use in electrolytic circuits. Yet, if each of these elements has its own particular specificities with regard to biological function, the present text will consider one metal only (with the exception of a brief excursion into its interactions with other metals), the one that I consider to be of capital importance, namely *iron*, and that, as a glance at the table will show, has a multiplicity of functions. The reader will, I trust, forgive this selectivity, for it is with iron that I have passed the last four decades, and it is the metal with which I am most familiar. This, fortunately, does not breed contempt on my part, but rather an increasing wonder at what iron, associated with low molecular weight and protein ligands, and often with other metal and non-metal cofactors, can do in biological systems.

The importance of well-defined amounts of iron for the survival, replication and differentiation of the cells of animals, plants and almost all microorganisms (one

[†] Unlike the mythical *mugwump*, reputed to sit on fences with his *mug* on one side and his *wump* on the other.

Table 1 Relative abundance and examples of functions of inorganic elements (and a few selected non-metals) that play an important role in biology. Adapted extensively from Mason and Moore, 1982.

Metal	Crustal average (ppm)	Seawater (mg/l)	Examples of specific functions
Sodium	2.8×10^4	1.1×10^4	Osmotic control, electrolytic equilibria, currents
Magnesium	2.1×10^4	1.4×10^3	Phosphate metabolism, chlorophyll
Aluminium	8.1×10^4	1×10^{-3}	Neurotoxic, solubilized by acid rain
Silicon	2.8×10^5	3	Prevents aluminium toxicity
Potassium	2.6×10^4	3.9×10^{-2}	Osmotic control, electrolytic equilibria, currents
Calcium	3.6×10^4	4.1×10^{-2}	Second messenger, muscle activation, biominerals
Vanadium	135	2×10^{-3}	Nitrogenase, peroxidases
Chromium	100	5×10^{-4}	Glucose metabolism?
Manganese	950	2×10^{-3}	Oxygen production and metabolism, structure
Cobalt	25	4×10^{-4}	B_{12} coezymes, alkyl transfer
Nickel	75	7×10^{-3}	Hydrogenases, urease
Copper	55	3×10^{-3}	Electron transfer, oxidases, oxygen transport
Zinc	70	1×10^{-2}	Lewis acid catalysis, regulation (DNA binding)
Selenium	5×10^{-2}	9×10^{-9}	Glutathione peroxidase
Molybdenum	1.5	1×10^{-2}	Nitrogenase, oxidases, oxo-transfer
Tungsten	1.5	1×10^{-4}	Dehydrogenases
Iron	$\mathbf{5 \times 10^4}$	$\mathbf{3 \times 10^{-3}}$	**Oxygen transport, storage, activation and detoxification, electron transfer, nitrogen fixation, ribose reduction, etc.**

notable exception is the *Lactobacillus* family) is well established (Crichton, 1991). However, iron in excess is toxic, particularly in man, and iron deficiency is also a general problem in biology, such that iron homeostasis is a major preoccupation in biology. Some examples of the multiple roles of iron in biology have been selected to give the reader a panoramic view of the importance of this element. This panorama is by no means comprehensive, nor is it intended to be. It should, like the 'ameuse geule' served before the meal in many French restaurants, whet the appetite of the reader for what is to follow.

While iron is the fourth most abundant element in the earth's crust, it is only present in trace concentrations in seawater (Table 1). Indeed, it is arguably the most important transition metal ion in the oceans on account of its relatively low abundance. Throughout large regions of our oceans, low levels of iron (20–50 pM) limit primary production of phytoplankton (Martin and Fitzwater, 1989). It has been suggested that addition of substantial amounts of iron, thereby stimulating massive algal blooms which fix carbon dioxide by photosynthesis, could mitigate the greenhouse effect relatively inexpensively, (the 'iron hypothesis'). Iron enrichment in the high-nitrate, low-chlorophyll, equatorial Pacific ocean – the experiments Ironex I (Martin *et al.*, 1994) and Ironex II (Coale *et al.* – 1996), showed that iron supply controls phytoplankton photosynthesis (Behrenfeld *et al.*, 1996), resulting in enhanced algal stocks and associated macronutrient uptake (Coale *et al.*, 1996). However, modelling simulations indicate that the equatorial Pacific is unlikely to be a significant region for iron-mediated carbon sequestration, whereas the southern ocean is the largest repository of unused macronutrients in surface waters, and is thought to have a disproportionate influence on the functioning of the global

carbon cycle in both the present and the geological past. This has been recently tested by conducting the *in situ* mesoscale southern ocean iron release experiment (SOIREE) over 13 days in February 1999. The result showed that increased iron supply (up to 3 nM over an area of around 50 km^2) led to elevated phytoplankton biomass and rates of photosynthesis in surface waters, causing a large drawdown of carbon dioxide and macronutrients, mostly due to the proliferation of diatom stocks (Boyd *et al*., 2000). However, no significant iron-increased export production was observed, so it was not possible to test the second tenet of the 'iron hypothesis', namely that fixed carbon is subsequently sequestered in the deep ocean. Many oceanic bacteria have been shown to produce siderophores (see next paragraph), and although little is known about how phytoplankton sequesters iron, it seems likely that cell-surface reductases are used to obtain iron from chelated complexes (reviewed in Butler, 1999).

Ironically, the propensity of some bacteriophages and colicines to kill certain strains of *E. coli*, depends on the recognition of an outer membrane receptor, normally reserved for uptake of iron–siderophore complexes – siderophores are low molecular weight chelators secreted by microorganisms into their extracellular medium, where they complex ferric iron and transport the ferri-siderophore via a receptor-mediated mechanism into the microbial cell. The receptors for some of these siderophores were identified genetically as the receptors for T1 and other bacteriophages before their real biological role, which is to ensure the essential iron requirements of the microbial cells was identified (Neilands, 1982). Indeed the tonB protein (discussed in more detail in Chapter 3) is so named because it was the second protein component to be identified as essential for infection of *E. coli* strains by the T1 bacteriophage. The other, Ton A, originally discovered as the receptor for the phages TI, T5 and for colicin M, is now known as FhuA, the receptor for ferric hydroxamate uptake. The bacteriophages and the colicines bind to the siderophore receptors of the host bacteria, and are used to shuttle the aggressor into the inside of the bacterial cell as if it were a veritable ferri-siderophore. It is equally ironic that my first iron publication was with Volkmar Braun (Braun *et al*. 1968), who subsequently followed me to Berlin where he set up a research group to work on the bacteriophage receptors of *E. coli*, only to return to iron when it became clear that they were in fact siderophore receptors. Since his appointment to the chair of microbiology in Tübingen, he has been enormously influential in advancing our understanding of iron uptake by bacteria, *E. coli* in particular. That is why I asked him together with his long-standing collaborator Klaus Hantke, to contribute Chapter 3, although, as with all the contributed chapters, I remain responsible for their final form (or lack of it, as the case may be !).

> *And, following thee, in thy ovation splendid,*
> *Thine almoner, the wind, scatters the golden leaves*
>
> Longfellow, 'Autumn'

As I write this Preface looking out on the superbly changing colours of the 'Season of mists and mellow fruitfulness' (Keats), and trying very hard to avoid what George Bernard Shaw called the difference between inspiration and transpiration, I am reminded that not only are the golden and other colours of the leaves largely

due to iron-containing enzymes, but that as they fall, they also take with them most of the inorganic matter that constitutes the foliage of the tree. Come the springtime, all of these elements must be reassimilated from the soil by the roots and pumped, often many tens of metres, up to the branches where the leaves with their iron-intensive photosynthetic apparatus will be resynthesized. In the case of iron, this will involve the uptake of soil iron by one or more of three basic strategies: (i) protonation, i.e. acidification of the soil in order to displace the equilibrium in favour of dissociation of the $Fe(OH)_3$ complexes – Fe(III) solubility increases one-thousand fold for each unit decrease in pH;(ii) chelation, involving the release of high-affinity Fe(III) siderophores, both those synthesized and secreted by soil microorganisms and those produced by a number of plant species, and; (iii) reduction of Fe(III) by membrane-bound reductases at the plasmalemma of the plant root cells, resulting in iron being assimilated as the much more water-soluble ferrous iron.

The advent of monoclonal antibodies led to the hunt for tumour-specific antigens, particularly those expressed on the outer surface of tumour cells. Among the many candidates found was a 180-kD transmembrane disulfide-linked dimeric protein, that turned out to be the receptor for transferrin, the protein that, like Mercury, the messenger of the Gods, transports iron in the circulation and ensures the supply of iron to the mammalian cells that require it. Tumour cells (i.e. cells with an excessively high growth rate) express an extremely high level of transferrin receptors, and indeed most mammalian cells seem to regulate their iron requirements by regulating the expression of transferrin receptors. However, it has also become clear that in many mammalian cells there is reciprocal regulation of transferrin receptors and the intracellular iron storage protein, ferritin, at the level of mRNA translation, by a family of RNA-binding proteins known as iron regulatory factors. When iron is scarce TfR protein synthesis increases several fold while Ft mRNA is not translated. Inversely, in iron repletion, Ft is synthesized and Tfr mRNA is degraded.

One of the most impressive developments in our understanding of iron metabolism since publication of the first edition of this book has been the application of the revolutionary techniques of molecular biology to identify new genes, their gene products involved in iron uptake and cellular utilization, and progressively to approach an understanding of their function. The possible role of some of these new candidates implied in the uptake of iron across the gastrointestinal tract is discussed in Chapter 8. This approach, initially pioneered in the model eukaryote *Saccharomyces cerevisiae*, has not only led to our recognition of the link between iron and copper – discussed briefly later – but also to the identification of a candidate gene for genetic haemochromatosis, HFE (Feder *et al.*, 1996). Within a very short time of it's discovery, the X-ray structure of HFE has been determined, and it has been shown to form a complex with the transferrin receptor and to influence binding of diferric transferrin to its receptor. Haemochromatosis, an autosomal, recessive, HLA-linked, disease, is one of the most frequent genetic disorders in man, with an estimated carrier frequency of 1in 200 in Caucasian populations, and characterized by a defect in the regulation of iron absorption, resulting in a progressive iron accumulation in parenchymal tissues. If undiagnosed and untreated, premature death occurs as a result of liver, pancreatic and cardiac dysfunction. Some 83 % of

patients with GH have the same mutation of Tyr for Cys at position 282 of the HFE protein. Our colleague Jo Marx from the University of Utrecht, whose laboratory with Maria de Sousa of the University of Porto, developed the first animal model of the disease using β2-microglobulin knock-out mice (Santos *et al.*, 1996), has undertaken (with Manuela Santas) to contribute Chapter 9 which treats both iron overload and iron deficiency in man. While neither of these conditions is 'sexy' in terms of their treatment – the one requires iron repletion either orally or parenterally, while the other requires iron depletion by venesection – their high penetration in the human population (one in three for iron deficiency and one in two-hundred for genetic haemochromatosis) means that they merit serious clinical attention.

As we shall explain in more detail later, iron is particularly indicated for catalysis of reactions which necessitate a free radical mechanism. One such reaction, of primordial importance for DNA replication and cell division, is the transformation of ribose to deoxyribose, catalysed by ribonucleotide reductases. The best characterized enzyme, from *E. coli*, has a binuclear iron centre and a stable tyrosyl free radical as cofactor. However, as we will see in Chapter 2, iron can also catalyse reactions with molecular oxygen and its reduced forms superoxide and hydrogen peroxide, leading ultimately to production of the highly reactive hydroxyl radical. This is the so-called oxygen paradox, whereby oxygen is absolutely essential for aerobic life, yet under certain conditions, is also toxic. The capacity of iron to catalyse Fenton chemistry, with concomitant production of hydroxyl radicals, means that iron is intimately involved in a catalogue of diseases involving oxidative stress – indeed, as has been pointed out, in the former Soviet Union, cancer and atherosclerosis are now referred to as the 'rusting diseases' (Parke, 1992). This link between iron and oxidative damage is dealt with in Chapter 10 by our long-standing (and long-suffering) collaborator Roberta Ward.

Iron is necessary for the multitude of bacteria, fungi and protozoa that causes infections in vertebrate hosts, and its importance in this respect is underlined by the observations that in all such infections, iron withholding is a classic host response – plasma iron is rapidly decreased, whilst conditions of reticuloendothelial iron overload greatly increases the severity of infections. Very often the strains of microorganisms that are responsible for the most virulent infections have a specific, and often plasmid-borne, iron uptake mechanism. A good example is the ColV plasmid associated with virulence in *E.coli* strains (Williams, 1979) that codes for the aerobactin iron-transport system. Epidemiological evidence supports the role of aerobactin in bacterial virulence in meningitis, septicaemia, and epidemics of *Salmonella* poisoning. Siderophore-mediated iron uptake systems are also known as virulence factors in fish pathogens (*Vibrio anguilarum* – anguibactin), and in *Pseudomonas* species – the fluorescent pyoverdins and pyochelins (Crosa, 1989), while exogenous siderophores supplied to hosts infected with *Salmonella*, *Vibrio* and *Yersinia* can severely enhance their virulence (Weinberg, 1989). Indeed certain pathogenic bacteria do not use siderophores at all, but use iron sources that occur in their host – haem, both alone or bound to haemopexin, haemoglobin, both alone and bound to haptoglobin, while *Neisseria* and *Haemophilis influenzae* also use iron bound to transferrin and lactoferrin (see Chapter 3). Johan Boelaert, a Brugge-based clinician who has for many years charted the important relationship of iron and infection, deals with this in Chapter 11, and his emphasis on the potential

of iron depletion to combat infection is reflected in his organization of important international meetings on iron and HIV over the last few years.

Finally, we can cite the powerful fascination for human civilization of Mars, the Roman god of war and the old chemists name for iron, and Venus, the Roman goddess of love and beauty, and the alchemists, name for copper (Crichton and Pierre, 2001). During prebiotic times, water-soluble ferrous iron was present and was the form used in the first stages of life. The natural abundance and the redox properties of iron allowed the chemistry that was suited to life. At the same time, copper was in the water-insoluble Cu(I) form, as highly insoluble sulfides, and was not available for life. About 10^9 years ago, evolution of dioxygen into the earth's atmosphere began to develop. Iron was oxidized and transformed into the insoluble Fe(III)state, while at the same time the oxidation of insoluble Cu(I) led to soluble Cu(II). As iron biochemistry evolved and changed, so too a new role of copper evolved with enzymes of higher redox potentials taking advantage of the oxidizing power of dioxygen. In Roman mythology, allusions not only to interactions but even to connivances between Mars and Venus, leading even to seduction, abound (the superb representations of the love of Mars and Venus in Pompeii, for example). As we will see in our final chapter, the metabolism of iron and copper are intimately interconnected. Though little remains from the Iron Age, compared with the to Bronze Age (the alloy of copper and tin), or gold and silver, iron always has the last word:

> *'Gold is for the mistress – silver for the maid –*
> *Copper for the craftsman cunning at his trade.'*
> *'Good !' said the Baron, sitting in his hall,*
> *'But Iron – Cold Iron – is master of them all.'*
>
> Rudyard Kipling 'Cold Iron' (1902)

These few examples give only the mariner's view of the iceberg concerning the fundamental importance of iron in biological systems. There remains a great deal more that we have not seen in this titillation of the reader's palate, but we shall try to make amends in what follows. Of course, rules always must have their exceptions, and the *Lactobacillae* quoted in an earlier paragraph are no doubt that. They have evolved in ecological niches where the use of a metal other than iron for key metabolic roles was an evolutionary plus. For the vast majority of living organisms, iron is absolutely necessary for the maintenance, the defence, the differentiation and last, but by no means least, the growth and cellular division of almost all living organisms.

That is why I have devoted this book to the inorganic biochemistry of iron.

References

Behrenfeld, M.J., Bale, A.J., Kolber, Z.S., Aiken, J. and Falkowski, P.G. (1996). *Nature*, **383**, 508–10.

Boyd, P.W., Watson, A.J., Law, C.S., Abraham, E.R. *et al*. (2000). *Nature*, **407**, 695–702.

Braun, V., Crichton, R.R. and Braunitzer, G. (1968). *Hoppe Zeyler's Z. Physiol. Chem.*, **349**, 197–210.

Butler, A. (1999). *Science*, **281**, 207–10.

Coale, K.H., Johnson, K.S., Fitzwater, S.E., Gordon, R.M. *et al*. (1996). *Nature*, **383**, 495–501.

Crichton, R.R. (1991). *Inorganic Biochemistry of Iron Metabolism*, Ellis Horwood, Chichester, 263 pp.

Crichton, R.R. and Pierre, J.-L. (2001). *Biometals*, in press.

Crosa, J.H. (1989). *Microbiol. Rev.*, **53**, 517–30.

Feder, J.N., Gnirke, A., Thomas, W., Tsuchihashi, Z. *et al*. (1996). *Nat. Genet.*, **13**, 399–408.

Frausto da Silvo, J.J.R. and Williams, R.J.P. (1991). *The Biological Chemistry of the Elements*, Clarendon Press, Oxford, 561 pp.

Martin, J.H. and Fitzwater, S.E. (1989). *Nature*, **331**, 341–3.

Martin, J.H., Coale K.H., Johnson, K.S., Fitzwater, S.E. *et al*. (1994). *Nature*, **371**, 123–9.

Mason, B. and Moore, C.B. (1982). *Principles of Geochemistry*, Fourth Edition, Wiley, New York.

Neilands, J.B. (1982). *Ann. Rev. Microbiol.*, **36**, 285–309.

Orchiai, E.I. (1986). *J. Chem. Educ.*, **63**, 942–4.

Parke, D.V. (1992). *The Biochemist*, **15**, 48.

Santos, M., Schilham, M.W., Rademakers, L.H.M.P., Marx, J.J.M., de Sousa, M. and Clevers, H. (1996). *J. Exp. Med.*, **184**, 1975–85.

Weinberg, E.D. (1989). *Quart. Rev. Biol.*, **64**, 261–90.

Williams, P.H. (1979). *Infect. Immunol.*, **26**, 925–32.

The following are the list of pages where 'Plate X' appears.

Chapter 2 – 33 (2 occurances), 42(2 occurances).

Chapter 3 – 54, 58, 72.

Chapter 5 – 111 (2 occurances), 112 (2 occurances), 117, 118 (2 occurances), 120.

Chapter 6 – 146, 147, 148 (2 occurances), 149, 154.

Chapter 7 – 170, 185.

Chapter 9 – 217, 220.

Chapter 10 – 250.

Chapter 12 – 290.
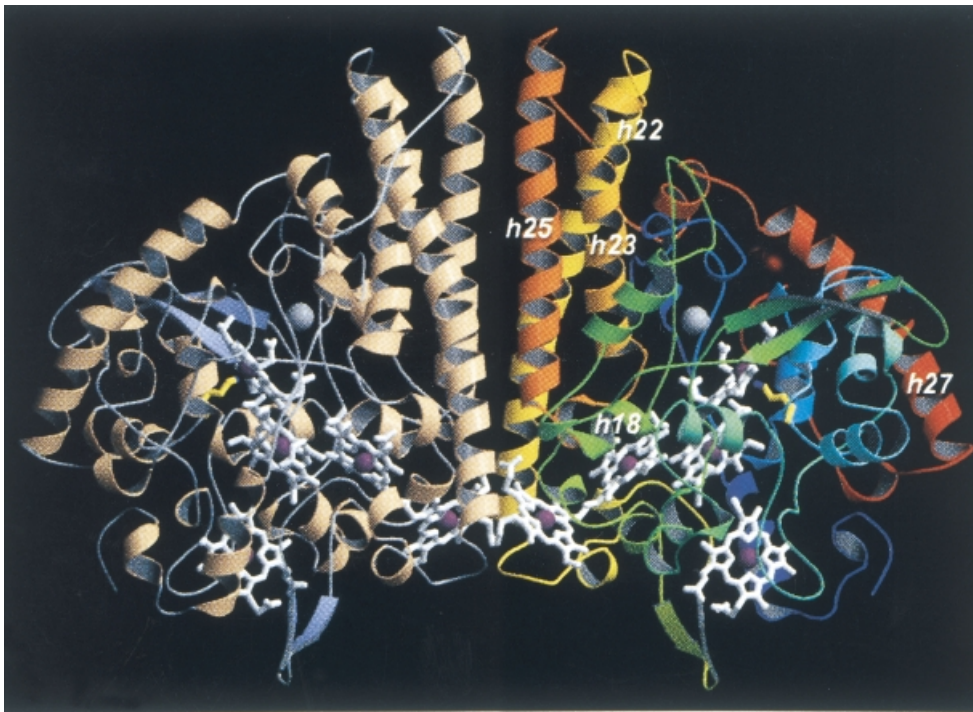
(a)
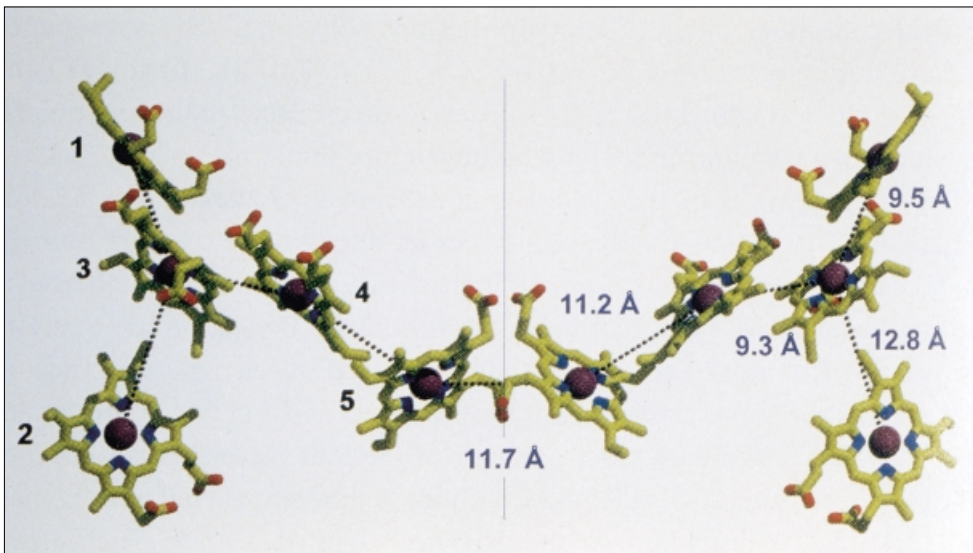
(b)

Figure 2.7 (a) A front view of the nitrite reductase dimer with the five haems in each monomer in white, a bound Ca^{2+} ion in grey and Lys-133, which coordinates the active site iron of haem 1, in yellow. (b) The haem arrangement. The overall orientation corresponds to (a), with the active site located at haem 1. Reprinted with permission from Einsle *et al.*, 1999. Copyright (1999), Macmillan Magazines Limited.

Plate 1

(a)

(b)
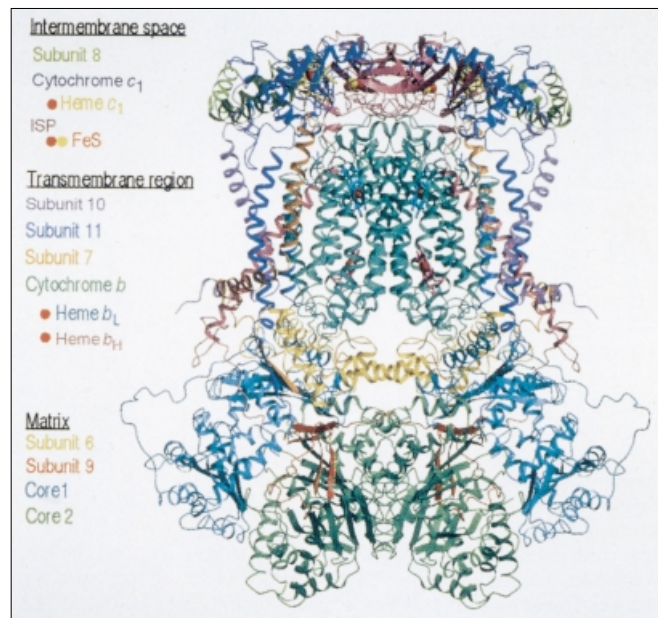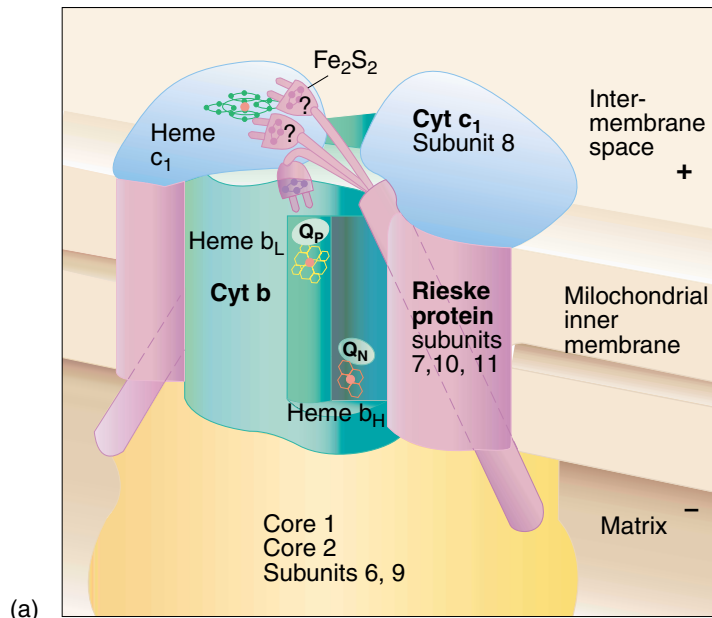
Figure 2.8 The structure of the dimeric cytochrome bc_1 complex of the respiratory chain. (a) The cave for chemistry constituted by the hollow between the two monomers (the 'essential dimer') in a cartoon representation. Reprinted with permission from Smith, 1998. Copyright (1998), American Association for the Advancement of Science. (b) The structure viewed perpendicular to the twofold axis and parallel to the membrane. All of the eleven subunits are completely traced and their sequences assigned. The top of the molecule extends 3.8 nm into the intermembrane space, the middle spans the membrane (4.2 nm), and the bottom extends some 7.5 nm into the matrix. Reprinted with permission from Iwata *et al.*, 1998. Copyright (1998) American Association for the Advancement of Science.

Plate 2
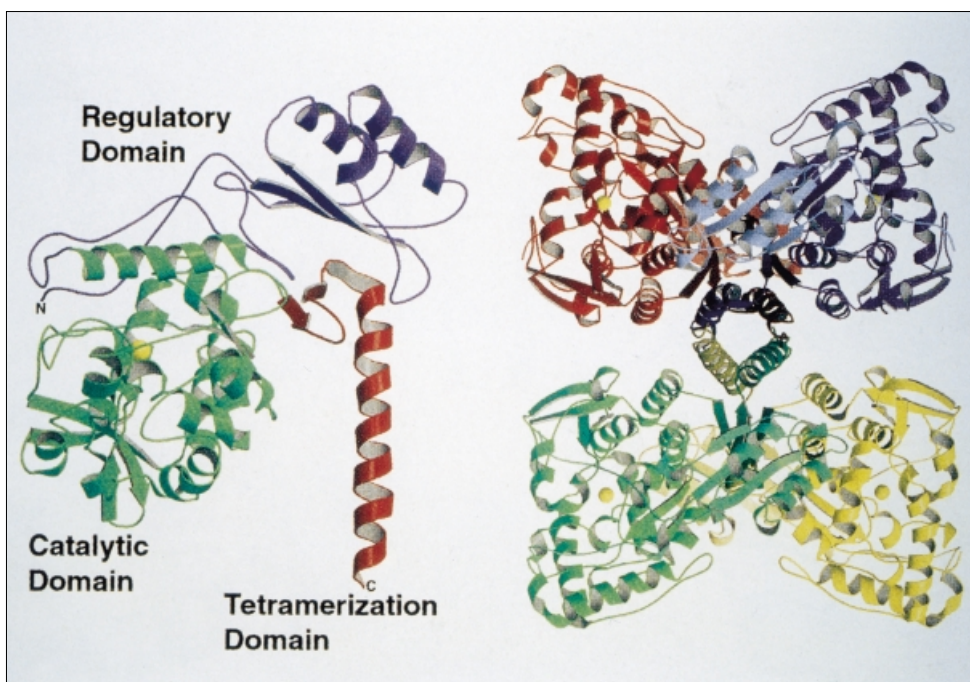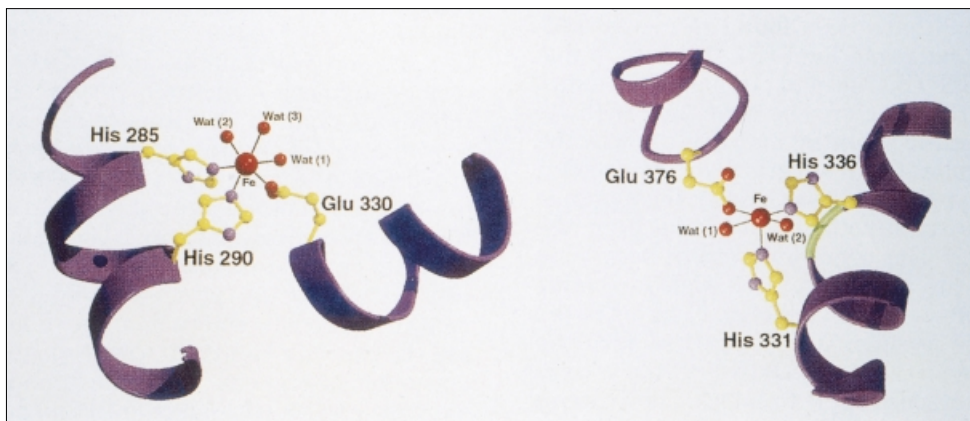
Figure 2.12 (a) Model of the human phenylalanine tetramer, created by combining the structure of the regulatory/catalytic domain crystal structure and the catalytic/tetramer domain crystal structure. The monomeric form of the enzyme is presented in the left panel, the tetramer viewed down the tetramerization domain in the right panel. (b) The metal-binding domains of phenylalanine hydroxylase and tyrosine hydroxylase are shown on the left and right respectively. (a) and (b) reprinted with permission from Flatmark and Stevens, 1999. Copyright (1999), American Chemical Society.

Plate 3
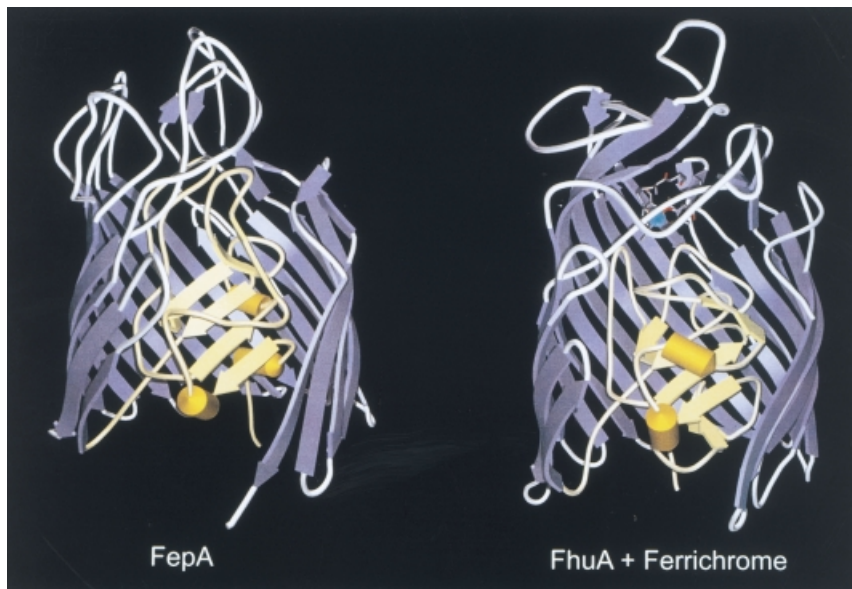
Figure 3.3 Comparison of the FepA and FhuA crystal structures. A portion of the ß-barrel (in violet is removed to show the globular cork domain (in yellow) that inserts from the periplasm into the channel of the ß-barrel. FhuA is loaded with ferrichrome (iron is shown as a green ball) (Ferguson *et al.*, 1998; Locher *et al.*, 1998). The FepA crystal structure does not reveal Fe^{3+}–enterobactin, but the FepA structure shown might be partially occupied by enterobactin (Buchanan *et al.*, 1999).
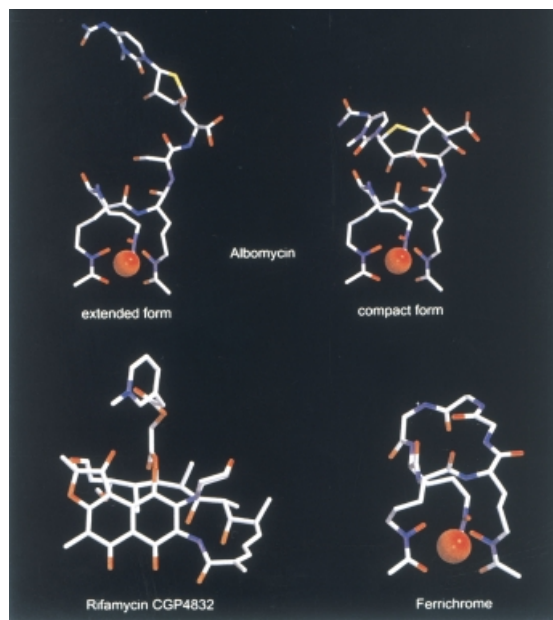
Figure 3.5 Structures of FhuA ligands as determined by X-ray analysis of co-crystals with FhuA. Albomycin adopts an extended and a compact conformation in the FhuA crystal, and rifamycin CGP 4832 binds to the same FhuA site as ferrichrome and albomycin although it assumes a different conformation.

Plate 4

Figure 3.7 The crystal structure of DtxR, a 226-residue three-domain dimeric protein, is shown. The protein, activated by cobalt (designated 1 and 2), is bound to a 21-bp DNA duplex based on the consensus operator sequence. Two DtxR dimers surround the DNA duplex, which is distorted compared to canonical B-DNA. Only domain 1, involved in DNA-binding, and domain 2, involved in dimer formation, are shown. The helices of the DNA-binding domain are indicated by H1, H2, and H3. H3 binds to the major groove of the DNA. From Pohl *et al.*, 1999, by permission of Academic Press.
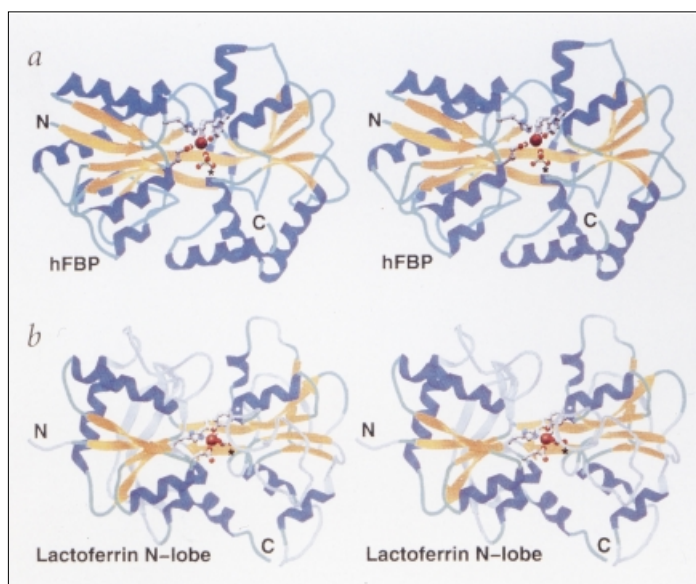
Figure 5.4 (a) Stereo ribbon representation of hFBP with Fe^{3+} ligands shown. ß-sheets are gold, α-helices are cyan, and other structures are dark blue. (b) N-lobe of lactotransferrin. Secondary structure elements are coloured as in hFBP, except for grey regions, which are those most different from hFBP. From Bruns *et al.*, 1997. Reproduced by permission of Nature Publishing Group.

Plate 5
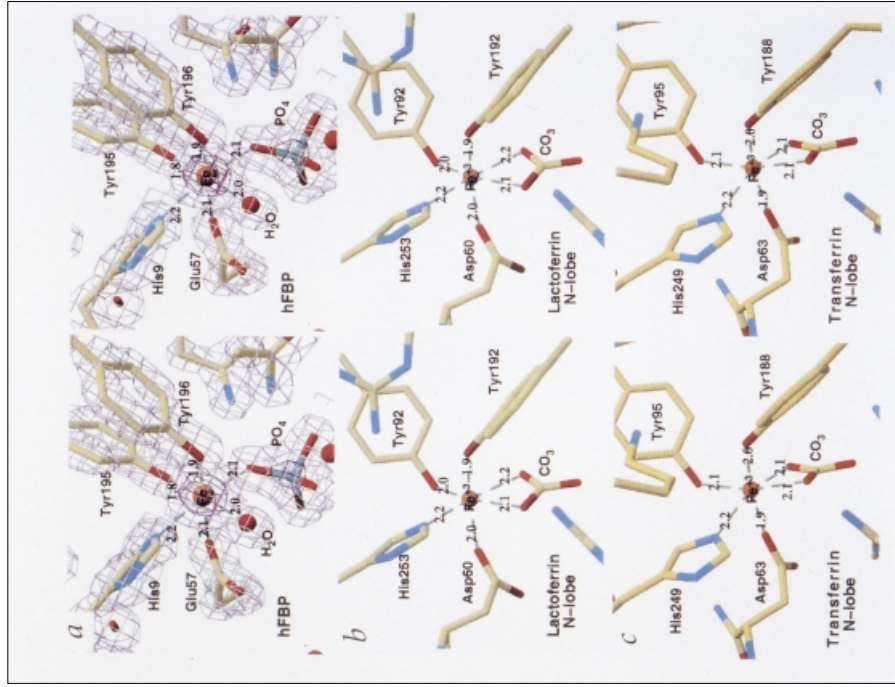
Figure 5.5 Stereo view of the Fe³⁺ binding site of (a) hFBP (b) human lactoferrin, N-lobe and (c) human transferrin (N-lobe). From Bruns, 1997. Reproduced by permission of Nature Publishing Group.
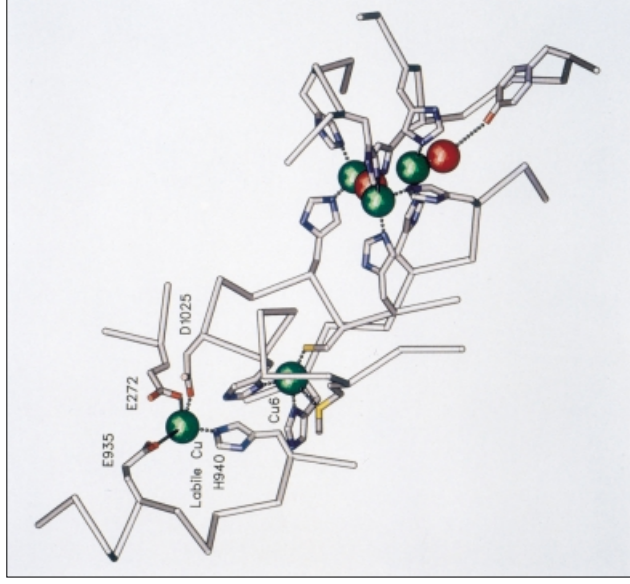
Figure 5.6 The putative metal binding site in the vicinity of the domain 6 copper atom (Cu_6) of human ceruloplasmin. The trinuclear copper cluster is located at the interface between domains 1 and 6 (bottom right of figure, copper atoms in green, water molecules in red). The green sphere at the top left of the figure represents a labile metal ion binding site (copper or iron), surrounded by His-940 and three negatively charged residues, E272 from domain 1 and E935 and D1025 from domain 6: the distance from the mononuclear copper centre is about 0.75 nm (centre of figure). The negatively charged residues Asp-1025, Glu-272 and Glu-935 could bind to a ferrous ion prior to its oxidation to the ferric state and the transfer of an electron via His-940 and the mononuclear copper towards the trinuclear centre (Adapted from Lindley (1996); figure kindly provided by Peter Lindley).

Plate 6

(a)   (b)
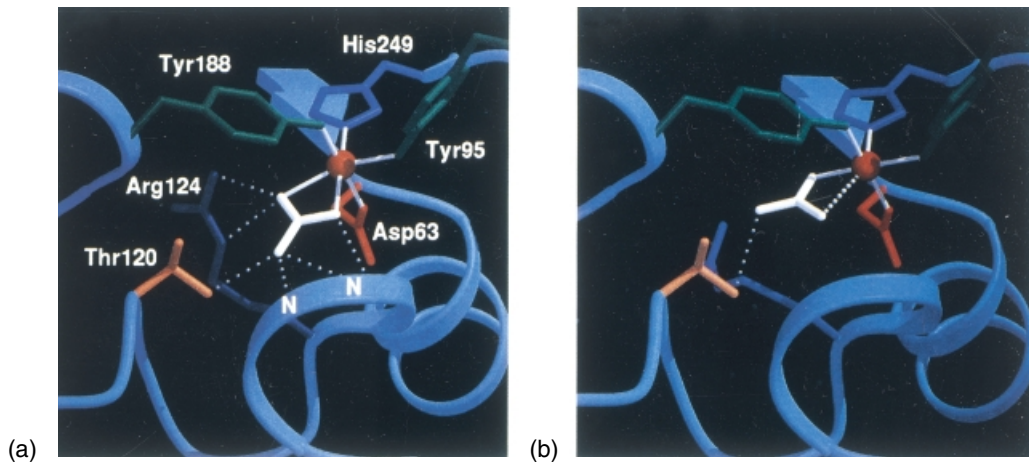
Figure 5.7 Structures of the alternative conformations of the iron-binding sites in the orthorhombic crystal form of the recombinant N-lobe of human transferrin. Reproduced with permission from MacGillivray *et al.*, 1998. Copyright (1998), American Chemical Society.
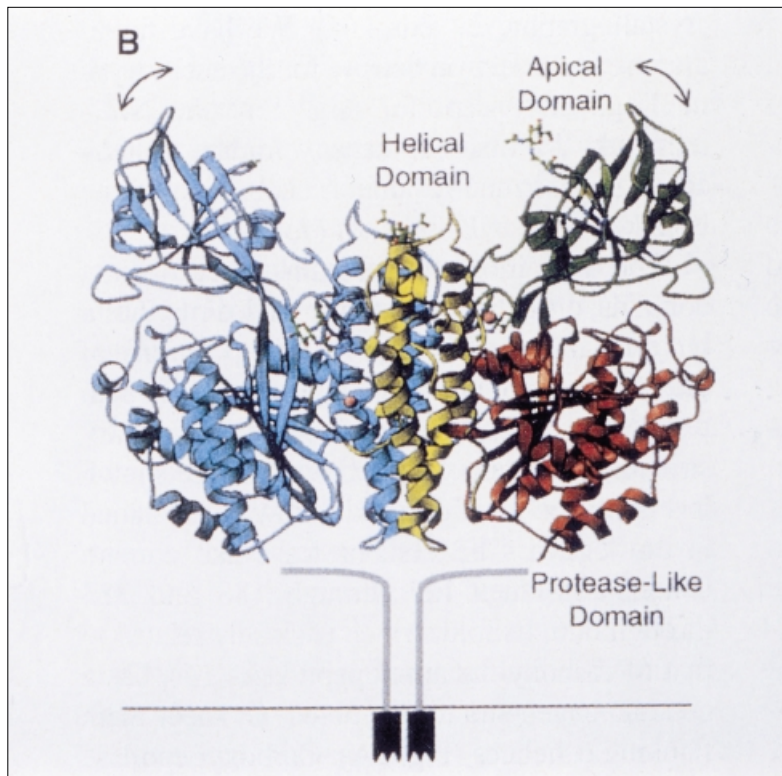
Figure 5.10 Ribbon diagram of the transferrin receptor dimer depicted in its likely orientation with regard to the plasma membrane. One monomer is blue, the other is coloured according to domain; the protease-like, apical and helical domains are red, green and yellow respectively; the stalk is shown in grey, connected to the putative membrane spanning helices in black. Pink spheres indicate the location of Sm^{3+} ions. Reprinted with permission from Lawrence *et al.*, 1999. Copyright (1999) American Association for the Advancement of Science.

Plate 7

Figure 5.12 Proposed model for binding of transferrin to the transferrin receptor. The surface of the receptor is predominantly in white, with elements of the lateral cleft that are in contact with the docked transferrin coloured according to domain as in Figure 5.10 (the opening to the vestigial protease active site is indicated by a yellow asterisk). The structure of rabbit transferrin is shown with the first and second domains of the N lobe (N_1 and N_2) being orange and red and the corresponding domains of the C lobe (C_1 and C_2) in blue and purple, respectively. The ferric ions are represented as labelled spheres and the positions of the human and rabbit transferrin glycosylation sites by white and black asterisks. White arrows indicate movements of the N_2 and C_2 domains upon iron release. The model predicts that the following regions of the transferrin receptor participate in binding of transferrin: the αII-2/βII-8 and βII-4/βII-5 loops of the apical domain, the αI-7/αI-8 loop of the protease-like domain, and the αIII-1 and αIII-5 helices of the helical domain – these regions are coloured in Figure 5.13. Together the αIII-1 and αIII-5 helices form the carboxyl-terminal face of the lateral cleft, and they may contain residues responsible for species specificity of transferrin association (Buchegger *et al.*, 1996). The αI-7/αI-8 loop might also contribute to selectivity. Reprinted with permission from Lawrence *et al.*, 1999. Copyright (1999) American Association for the Advancement of Science.

Plate 8

(a)

(b)

(c)

Figure 5.11 Individual transferrin receptor domains. Ribbon diagrams for domain I, the protease-like domain (a); domain II, the apical domain (b); and domain III, the helical domain (c). Secondary structure elements are labelled and are referred to in the text first with respect to the domain number, then with respect to the linear order of the elements within the domain. For example αI-3 refers to the third helix in the first domain. In (a), the two grey spheres indicate the positions that would be occupied by Zn^{2+} in an authentic protease. Reprinted with permission from Lawrence *et al.*, 1999. Copyright (1999) American Association for the Advancement of Science.

Figure 5.13 Ribbon diagrams of HFE, TfR and HFE-TfR structures. (a) HFE (PDB code 1A6Z). Residues substituted in HH mutations (Cys-260 and His-41) and a cluster of histidines (residues 87, 89, 94 and 123) are highlighted. (b) TfR monomer. A, apical loop (residues 312–328); PL protease-like loop (residues 469–476); C, *C*-terminal tail (residues 750–760). (c) Two views of the HFE-TfR structure related by a 90 ° rotation about the vertical axis. Chain termini nearest the predicted transmembrane region (*C*-terminus for HFE heavy chain, *N*-terminus for TfR) are labelled (left). The membrane bilayer is represented by a grey box (right). Reprinted with permission from Bennett *et al.*, 2000. Copyright (2000) Macmillan Magazines Limited.
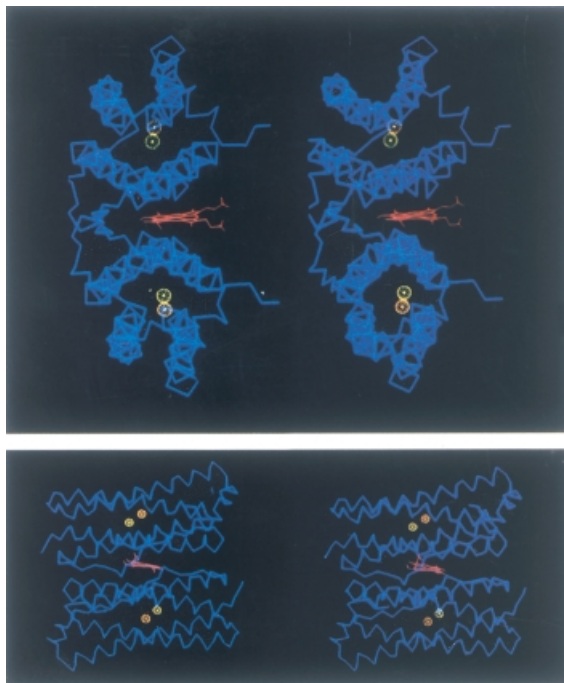
Figure 6.8 Stereoscopic view of the dimeric building block of bacterioferritin (a) twofold axis horizontal; (b) twofold axis approximately normal to the page. The protein is represented by a blue α-carbon trace, the haem by a stick model (pink) and the dinuclear metal site by dotted spheres (orange and yellow). From Frolow *et al.*, 1994. Reproduced by permission of Nature Publishing Group.

Plate 9
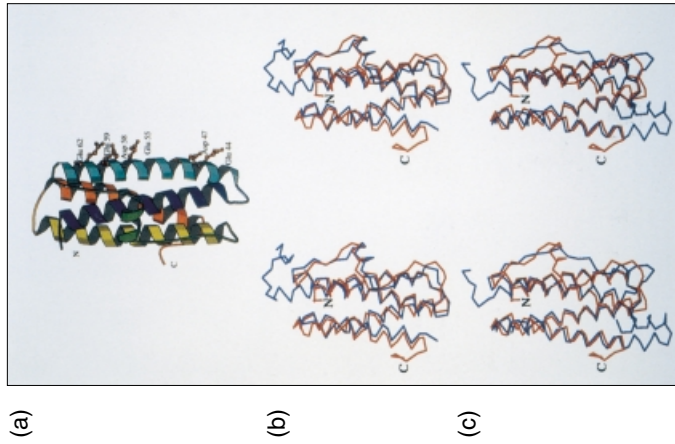
Figure 6.9 Monomer fold of *L. inocua* ferritin and comparison with related structures. (a) *L. inocua* ferritin, and comparison with (b) *E. coli* Dps, and (c) horse-spleen L-chain monomers. In (a) the A helix is coloured blue, the B helix blue–green, the C helix yellow, the D helix orange and the BC helix dark green. The *N*-terminus is on the top left of the monomer and the *C*-terminus middle left. The acidic residues of the B helix facing the inner cavity of the dodecamer are indicated. In (b) and (c) the *L. inocua* monomer is coloured red and the other monomer blue. The superpositions are based on the least squares minimization of the structurally conserved regions, i.e. the four α-helix bundle. From Ilari *et al.*, 2000. Reproduced by permission of Nature Publishing Group.
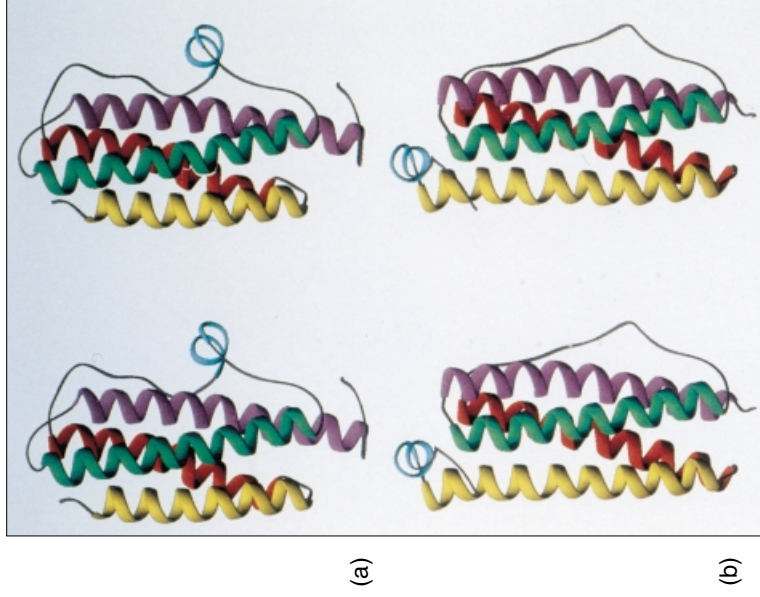
Figure 6.10 Comparison of Dps and EcFTN monomers. (a) Stereo view of Dps subunit. The *N*-terminus is located at the bottom of the four-helix bundle on the right, the *C*-terminus at the top on the left. The A helix is coloured magenta, the B helix green, the BC helix cyan, the C helix red and the D helix yellow. (b) Stereo view of EcBFR subunit in the same orientation; the colour coding is the same as in (a) except that the E helix is cyan. From Grant *et al.*, 1998. Reproduced by permission of Nature Publishing Group.

Plate 10
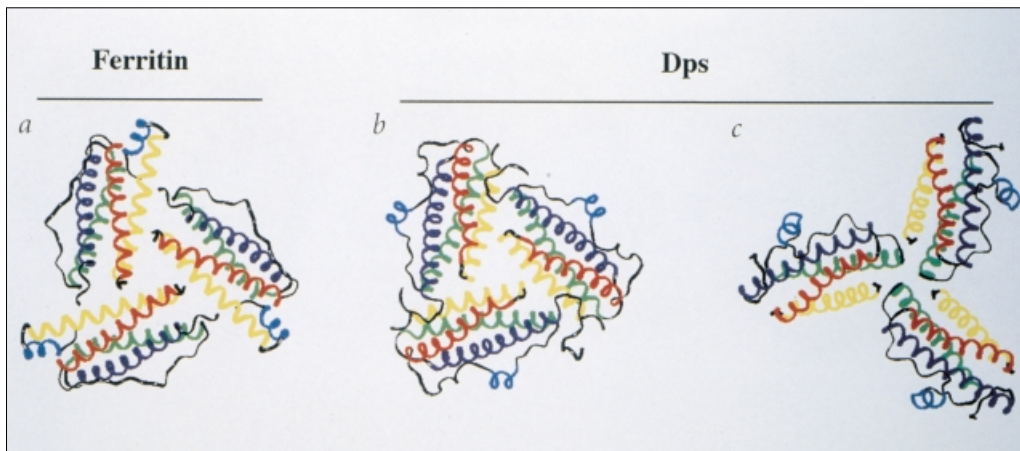
Figure 6.11 Comparison of monomer–monomer interactions in Dps and EcBFR. (a) Ribbon diagram of a trimer from the EcBFR 24-mer. (b) Ribbon diagram displaying one of the two types of trimeric interactions between monomers in the Dps dodecamer. The acidic hole in the centre of the trimer connects the exterior of the dodecamer to the hollow core. Note the similarity of this trimer to the EcBFR trimer in (a). (c) Ribbon diagram of the second type of trimeric interaction. The hole in the centre of this trimer is smaller than in the other and contains a hydrophobic constriction. Colour coding of the helices: A helices magenta, B helices green, C helices red, D helices yellow and E helix/BC helix blue. From Grant *et al.*, 1998. Reproduced by permission of Nature Publishing Group.
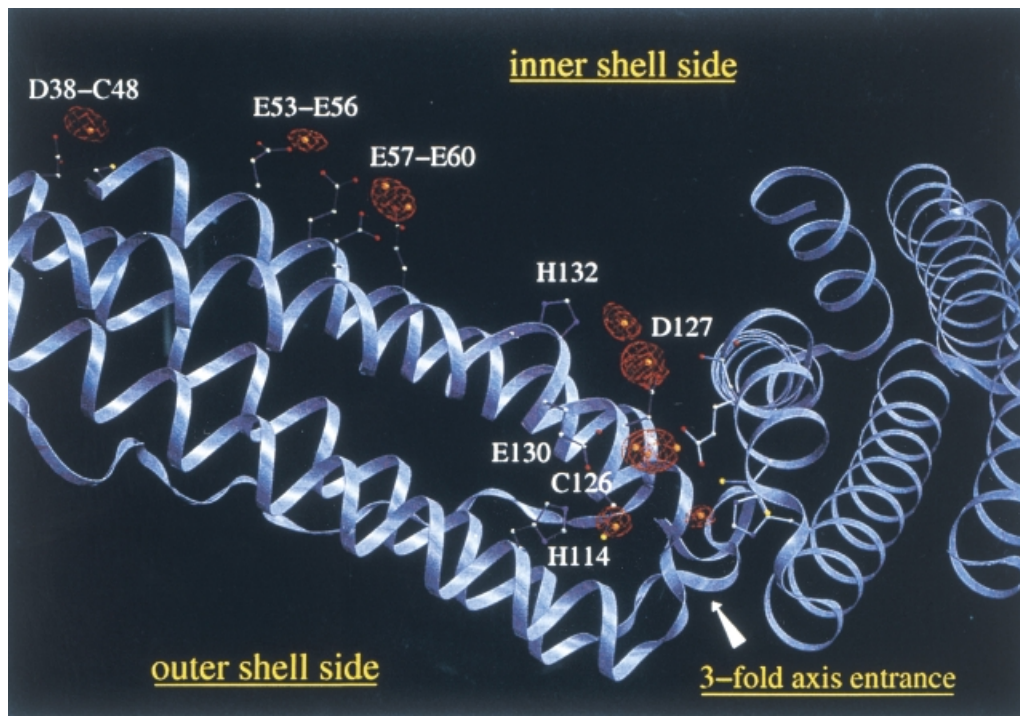
Figure 6.15 Metal binding sites on the interior face of the B helix in HoLF. From Granier *et al.*, 1998. Reproduced by permission of John Wiley & Sons, Inc.

Plate 11
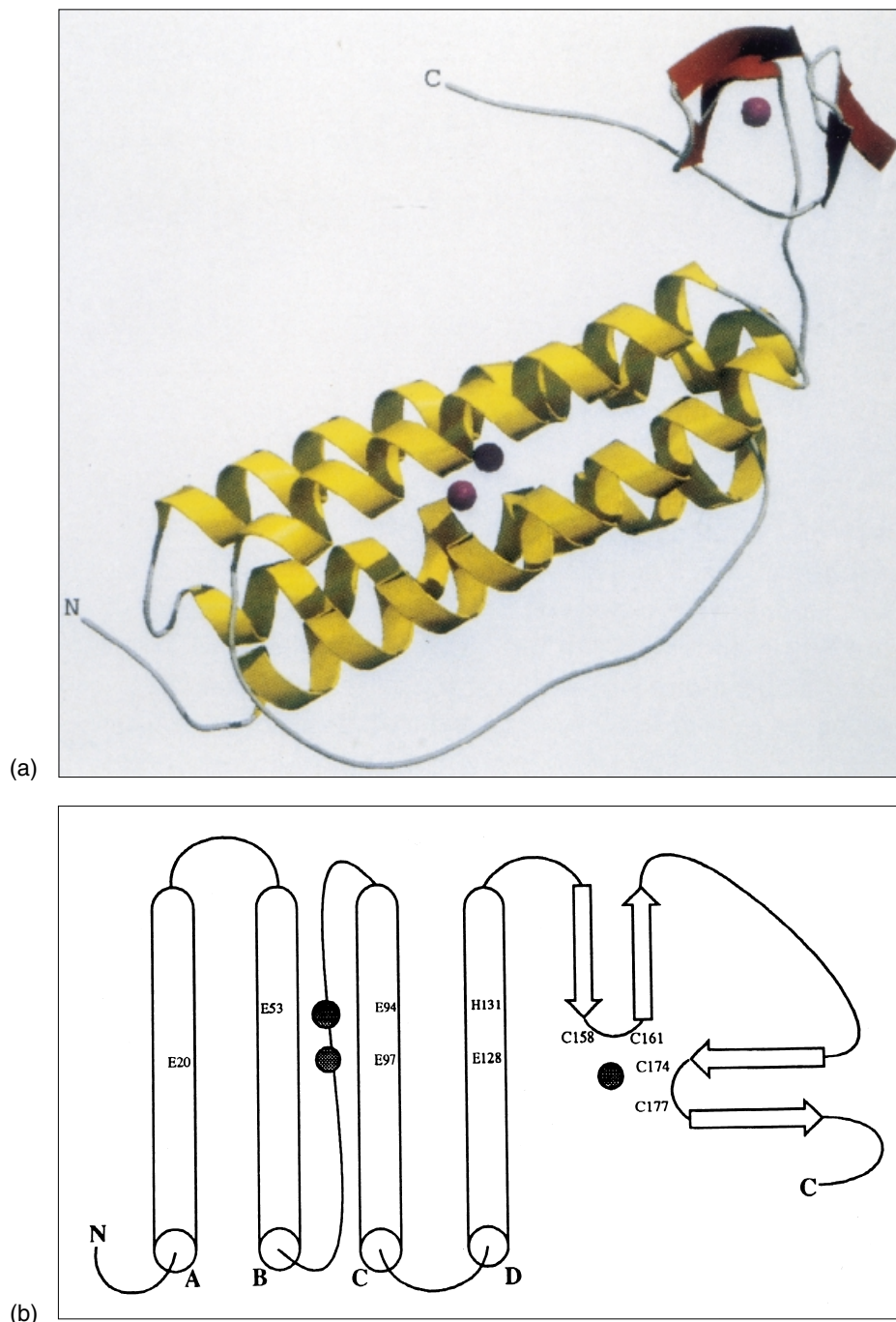
Figure 6.12 (a) The overall fold of the rubrerythrin subunit. Helical regions are in yellow, ß-sheet regions in red and iron atoms represented as magenta spheres. The *N*-terminus is to the lower left and the *C*-terminus at the top in the middle. (b) Schematic topology diagram showing the structural organization of the rubrerythrin subunit. Cylinders indicate helical regions and arrows indicate sheets. Solid circles represent iron atoms. Letters and numbers correspond to the iron ligand residues. From De Maré *et al.*, 1996. Reproduced by permission of Nature Publishing Group.

Plate 12

(a)

(b)
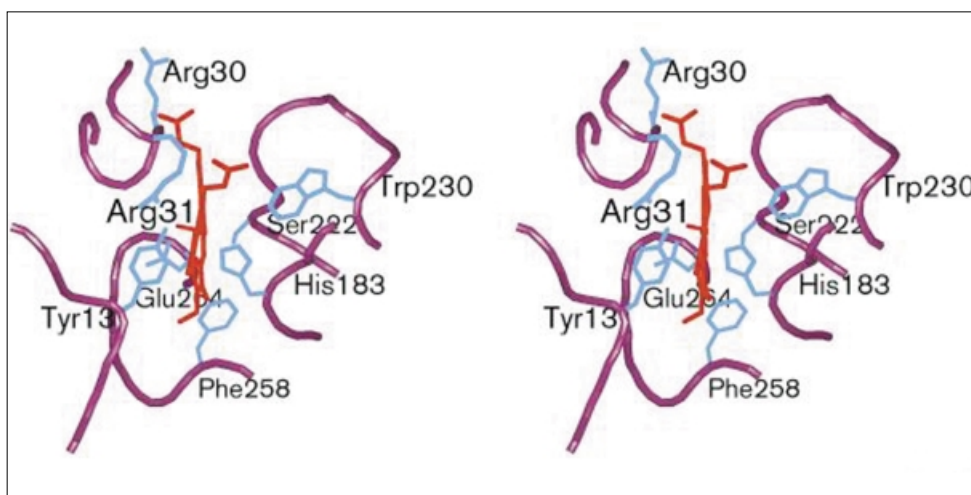
Figure 7.2 (a) Schematic representation of the structure of *B. subtilis* ferrochelatase. Domain I is coloured green and domain II blue. The parts of the chain in red build up the walls of the cleft, and the region in yellow makes the connection between the domains. The *N*- and *C*-termini are marked. (b) The proposed active site of ferrochelatase with protoporphyrin IX molecule (red) modelled into the site. The backbone atoms of the protein are in purple, the side-chains in blue. Reprinted from Al-Karadaghi *et al.*, 1997. Copyright (1997), with permission from Elsevier Science.

Plate 13

(a)

(b)
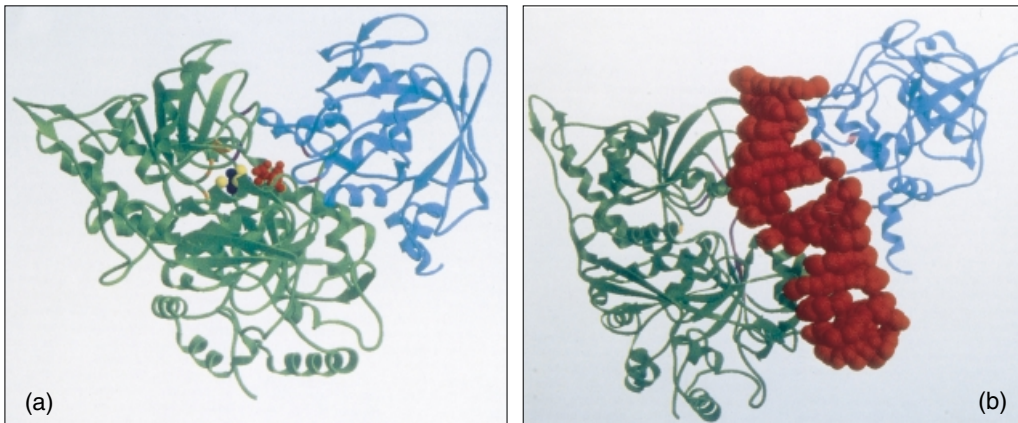
Figure 7.7 Mitochondrial aconitase as a structural model for IRP-1, in its role as a cytoplasmic aconitase (A) and IRE-binding protein (B). Based on the structure of the mitochondrial aconitase, two forms have been drawn without making allowances for differences between aconitase and IRP-1. (A) In the 4Fe–4S cluster containing enzyme, domains 1–3 (coloured in green) and 4 (coloured in blue) form a narrow cleft (closed form), where the Fe–S cluster (Fe atoms coloured in blue, S atoms coloured in yellow) is found, linked to three cysteines (orange) of the protein backbone. The substrate, citrate, (red), is situated within the cleft and interacts with both the cluster and the protein backbone (Arg-536, Arg-541, Arg-699, Arg-780, in magenta). In this conformation, the narrow cleft prevents IRE binding. (B) The apoprotein form may adopt a more open conformation via the hinge linker. Domains 1–3 and 4 may separate enough to accomodate the IRE (in red). In this form, the IRE may contact amino acids 121–130 (magenta) and the region close to C437 (orange). Reprinted from Paraskeva and Hentze, 1996. Copyright (1996), with permission from Elsevier Science.
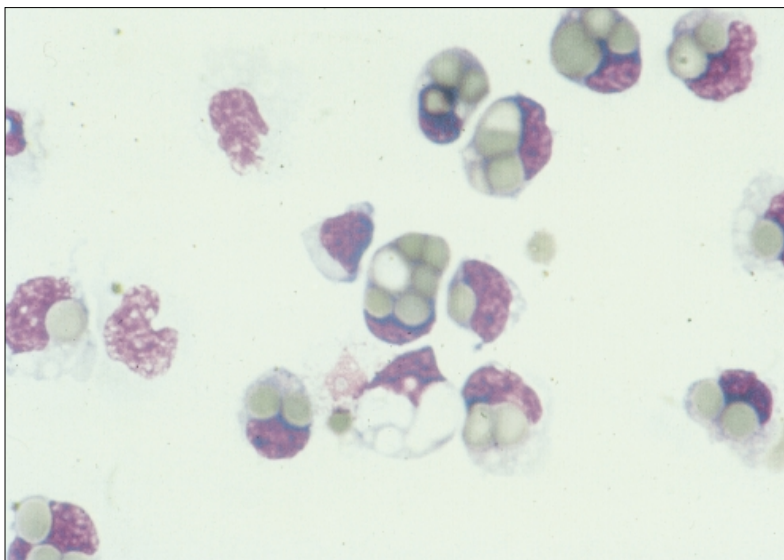
Figure 9.5 Healthy volunteer monocytes after erythrophagocytosis. Rabbit erythrocytes were incubated with heat-inactivated mouse antirabbit erythrocyte serum. Human peripheral blood monocytes (MN) were obtained after Ficoll–Paque isolation and monocyte clumping with subsequent separation from lymphocytes, yielding a 95 % pure MN population. Non-ingested erythrocytes were removed by hypotonic lysis.

Plate 14
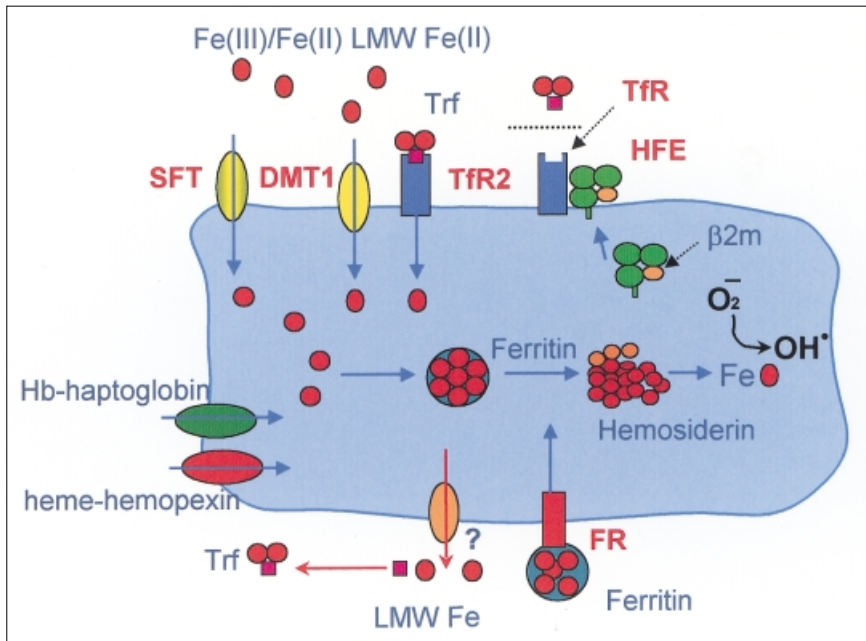
Figure 9.7 Iron transport by hepatocytes. Known proteins involved in iron transport across the plasma membrane of hapatocytes are represented. LMW = low molecular weight; Trf = transferrin; Trf-R = transferrin receptor; HFE = hamochromatosis gene product; ß2m = ß2-microglobulin; O_2^- = superoxide; OH· = hydroxyl radical; FR = ferritin receptor; SFT = stimulator of iron transport.
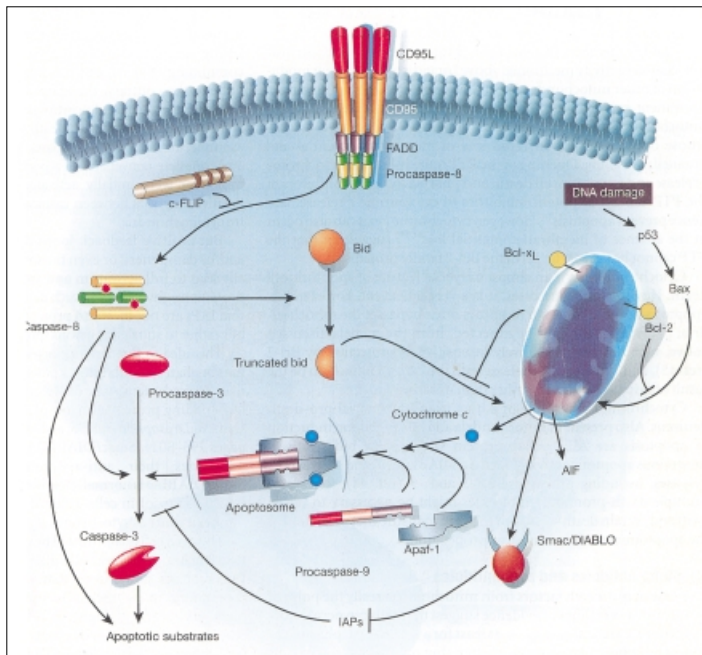
Figure 10.5 The death receptor pathway for DNA damage. Reprinted with permission from Hengartner, 2000. Copyright (2000) Macmillan Magazines Limited.

Plate 15

Figure 12.3 NMR structure of reduced CopZ. Schematic representation of the NMR-derived structure of reduced CopZ, displaying the conserved cysteine residues: α-helix (yellow), α-sheet (blue), loop or turn (red). Reprinted from Harrison *et al.*, 2000. Copyright (2000), with permission from Elsevier Science.

Figure 12.2 Copper chaperone function. (a) Copper homeostasis in *Enterococcus hirae* is affected by the proteins encoded by the *cop* operon. CopA, Cu^{1+}-import ATPase: CopB, Cu^{1+}-export ATPase: CopY, Cu^{1+}-responsive repressor: copZ, chaperone for Cu^{1+} delivery to CopY. (b) The CTR family of proteins transports copper into yeast cells. Atx1p delivers copper to the CPx-type ATPases located in the post Golgi apparatus for the maturation of Fet3p. (c) Cox17p delivers copper to the mitochondrial intermembrane space for incorporation into cytochrome c oxidase (CCO). (d) hCTR, a human homologue of CTR, mediates copper-ion uptake into human cells. CCS delivers copper to cytoplasmic Cu/Zn superoxide dismutase (SOD1). Abbreviations: IMM, inner mitochondrial membrane; OMM, outer mitochondrial membrane; PM, plasma membrane; PGV, post Golgi vessel. Reprinted from Harrison *et al.*, 2000. Copyright (2000), with permission from Elsevier Science.

Plate 16

1 Solution Chemistry of Iron in Biological Media

1.1 Aqueous Solution Chemistry of Iron

Iron, element 26 in the periodic table, is the second most abundant metal (after aluminium) and the fourth most abundant element of the earth's crust. Its position in the middle of the elements of the first transition series (so designated because their ions have incompletely filled d orbitals) implies that iron has the possibility of various oxidation states (from $-II$ to $+VI$), the principal ones being II (d^6) and III (d^5), although a number of iron-dependent monooxygenases generate high valent Fe(IV) or Fe(V) reactive intermediates during their catalytic cycle. Whereas Fe^{2+} is extremely water soluble, Fe^{3+} is quite insoluble in water ($K_{sp} = 10^{-39}$ M and at pH 7.0, $[Fe^{3+}] = 10^{-18}$ M) and significant concentrations of water-soluble Fe^{3+} species can be attained only by strong complex formation. Iron(III) is a hard acid that prefers hard oxygen ligands while iron(II) is on the borderline between hard and soft, favouring nitrogen and sulfur ligands. The interaction between Fe^{2+} and Fe^{3+} and ligand donor atoms will depend on the strength of the chemical bond formed between them. An idea of the strength of such bonds can be got from the concept of 'hard' and 'soft' acids and bases (HSAB). 'Soft' bases have donor atoms of high polarizability with empty, low-energy orbitals; they usually have low electronegativity and are easily oxidized. In contrast 'hard' bases have donor atoms of low polarizability, and only have vacant orbitals of high energy; they have high electronegativity and are hard to oxidize. Metal ions are 'soft' acids if they are of low charge density, have a large ionic radius and have easily excited outer electrons. 'Hard' acid metal ions have high charge density, a small ionic radius and no easily excited outer electrons. In general, 'hard' acids prefer 'hard' bases and 'soft' acids form more stable complexes with 'soft' bases (Pearson, 1963). Fe(III) with an ionic radius of 0.067 nm and a positive charge of 3 is a 'hard' acid and will prefer 'hard' oxygen ligands like phenolate and carboxylate to imidazole or thiolate. Fe(II) with an ionic radius of 0.083 nm and a positive charge of only 2 is on the borderline between 'hard' and 'soft' favouring nitrogen (imidazole and pyrrole) and sulfur ligands (thiolate and methionine) over oxygen ligands.

A coordination number of 6 is that most frequently found for both Fe(II) and Fe(III), giving octahedral stereochemistry although four- (tetrahedral) and,

particularly, five-coordinate complexes (trigonal bipyramidal or square pyrimidal) are also found. For octahedral complexes, two different spin states can be observed. Strong-field ligands (e.g. F^-, OH^-), where the crystal field splitting is high and hence electrons are paired, give low-spin complexes, while weak-field ligands (e.g. CO, CN^-) where crystal field splitting is low, favour a maximum number of unpaired electrons and hence give high spin complexes. Changes of spin state affect ion size of both Fe(II) and Fe(III), the high-spin being significantly larger than the low-spin ion. As we will see in Chapter 2, this is put to good use as a trigger for cooperative binding of dioxygen to haemoglobin. High-spin complexes are kinetically labile, while low-spin complexes are exchange inert. For both oxidation states, only high-spin tetrahedral complexes are formed. Both oxidation states are Lewis acids, particularly the ferric state.

The unique suitability of iron comes from the extreme variability of the Fe^{2+}/Fe^{3+} redox potential, which can be fine tuned by well-chosen ligands, so that iron sites can encompass almost the entire biologically significant range of redox potentials, from about -0.5 V to about $+0.6$ V.

1.2 Oxygen Free Radicals

Molecular oxygen was not present when life began on Earth, with its essentially reducing atmosphere, and both the natural abundance of iron and its redox properties predisposed it to play a crucial role in the first stages of life on Earth. About 1 billion (10^9) years ago, photosynthetic prokaryotes (cyanobacteria) appeared and dioxygen was evolved into the Earth's atmosphere. It probably required 200–300 million years, a relatively short period on a geological time scale, for oxygen to attain a significant concentration in the atmosphere, since at the outset the oxygen produced by photosynthesis would have been consumed by the oxidation of ferrous ions in the oceans. Once dioxygen had become a dominant chemical entity, as the Precambrian deposits of red ferric oxides bear witness, iron hydroxides precipitated. Concomitant with the loss of iron bioavailability, the oxidation of Cu(I) led to soluble Cu(II). While enzymes active in anaerobic metabolism were designed to be active in the lower portion of the redox potential spectrum, the presence of dioxygen created a need for a new redox-active metal with $E_o M^{n+1}/M^n$ from 0 to 0.8 V. Copper, now bioavailable, was ideally suited for this role, and began to be used in enzymes with higher redox potentials (as a dicopper centre in laccase and a mixed iron–copper centre in cytochrome oxidase) to take advantage of the oxidizing power of dioxygen. Some typical redox potentials for iron and copper proteins and chelates are given in Figure 1.1.

Although oxygen must ultimately completely oxidize all biological matter, its propensity for biological oxidation is considerably slowed by the fact that in its ground state (lowest energy state), it exists as a triplet spin state (Figure 1.2), whereas most biological molecules are in the singlet state as their lowest energy level. Spin inversion is relatively slow, so that oxygen reacts much more easily with other triplet-state molecules or with free radicals than it does with singlet-state molecules.

$Phen_3Fe$ **+ 1.1**		
	Ferrous or cuprous state does not give Fenton reaction	**+ 0.8 (?)** (Haemocyanin)
$(Fe(H_2O)_6$ **+ 0.77**		**+ 077** (Laccase, Type1)
	—— $(H_2O_2 \rightarrow HO^\cdot + HO^-)$ ——	
	+ 0.46	**+ 0.37** (plastocyanin)
		+ 0.33 (azurin)
(iron SOD) **+ 0.27**	***The ferrous or the cuprous state give Fenton reaction***	**+ 0.32** (Cu-ZnSOD)
(haemoglobin) **+ 0.14**		**+ 0.16** (Cu aquo)
0	***The ferric or the cupric form can be reduced by superoxide***	
	—— O_2/O_2^- **- 0.16** ——	
(horse radish peroxidase) **-0.27**	***The ferric or the cupric form is not reduced by superoxide***	
(ferredoxin) **-0.40**		
(ferritransferrin) **-0.52**		
(ferrienterobactin) **-0.75**		

Figure 1.1 Some redox potentials (in volts) of iron and copper enzymes and chelates at pH 7 relative to the standard hydrogen electrode. From Crichton and Pierre, 2001. Reproduced by permission of Kluwer academic publishers.

The arrangement of electrons in most atoms and molecules is such that they occur in pairs, each of which have opposite intrinsic spin angular momentum. Molecules having one or more unpaired electrons are termed free radicals: they are generally very reactive, and will act as chain carriers in chemical reactions. Thus, the hydrogen atom, with one unpaired electron, is a free radical, as are most transition metals and the oxygen molecule itself. The dioxygen molecule has two unpaired electrons, each located in a different π^* antibonding orbital. Since these two electrons have the same spin quantum number, if the oxygen molecule attempts to oxidize another atom or molecule by accepting a pair of electrons from it, both new electrons must have parallel spins in order to fit into the vacant spaces in the π^* orbitals. A pair of electrons in an atomic or molecular orbital would have antiparallel spins (of $+\frac{1}{2}$ and $-\frac{1}{2}$) in accordance with Pauli's principle. This imposes a restriction on oxidation by O_2, which means that dioxygen tends to accept its electrons one at a time (Figure 1.2), slowing its reaction with non-radical species (Halliwell and Gutteridge, 1984). Transition metals can overcome this spin restriction on account of their ability to accept and donate single electrons (Hill, 1981). The interaction of iron centres and oxygen is of paramount importance in biological inorganic chemistry, and we have summarized some of the main features in Figure 1.3.
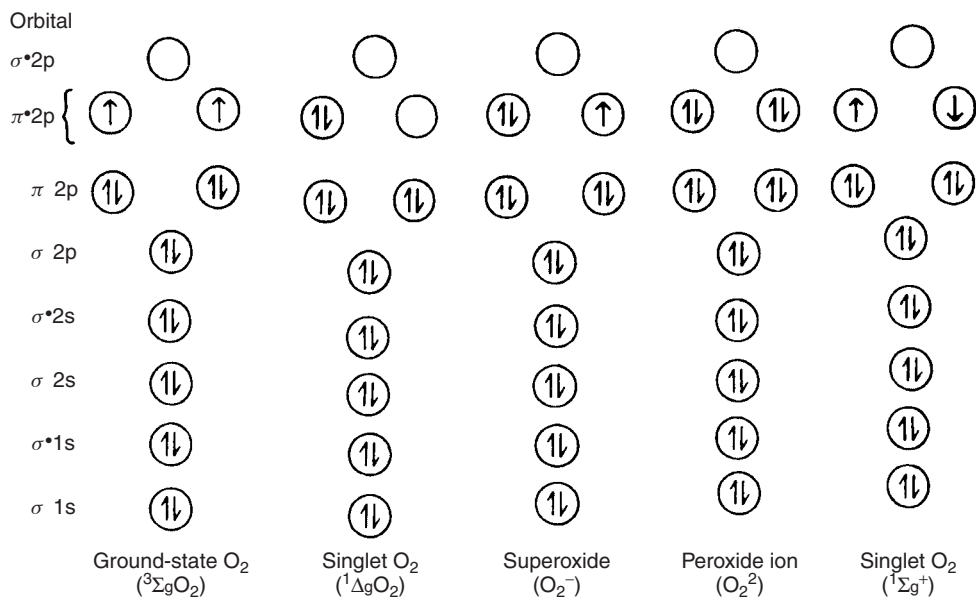
Figure 1.2 Bonding in the diatomic oxygen molecule. Reproduced with permission from Halliwell and Gutteridge, 1984. © the Biochemical Society.
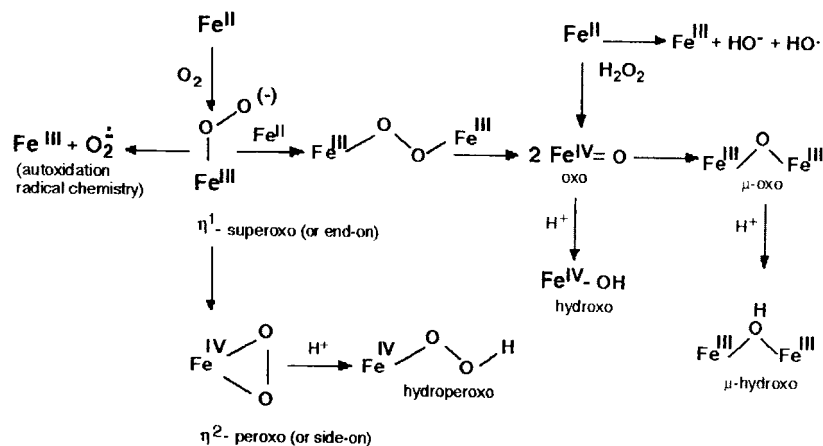
Figure 1.3 Iron–oxygen chemistry. Multi-bridged species have been omitted. From Crichton and Pierre, 2001. Reproduced by permission of Kluwer academic publishers.

The reactivity of O_2 can be increased in another way, namely by moving one of the unpaired electrons in a way that alleviates the spin restriction to give the two singlet states of O_2 (Figure 1.2). The most important of the two forms of singlet $O^1_2\delta_g$ in biological systems has no unpaired electrons, is not a radical, and can be obtained when a number of biological pigments such as chlorophylls, retinal, flavins or porphyrins, are illuminated in the presence of O_2 (Foote, 1982). When a single electron is accepted by the ground-state O_2 molecule, it must enter one of the π^* antibonding orbitals, to form the superoxide radical, O_2^-. Addition of a

second electron to O_2^- gives the peroxide ion O_2^{2-} with no unpaired electrons. At physiological pH, O_2^{2-} will immediately protonate to give hydrogen peroxide, H_2O_2. The third reactive oxygen species found in biological systems is the hydroxyl free radical. Two hydroxyl radicals, $\cdot OH$ can be formed by homolytic fission of the $O-O$ bond in H_2O_2, either by heating or by irradiation. However, as Fenton first observed in 1894 (Fenton, 1894), a simple mixture of H_2O_2 and an Fe(II) salt also produces the $\cdot OH$ radical (equation 1):

$$Fe^{2+} + H_2O_2 \longrightarrow Fe^{3+} + \cdot OH + OH^- \tag{1}$$

In the presence of trace amounts of iron, superoxide can then reduce Fe^{3+} to molecular oxygen and Fe^{2+}. The sum of this reaction (equation 2) plus the Fenton reaction (equation 1) produces molecular oxygen plus hydroxyl radical, plus hydroxyl anion from superoxide and hydrogen peroxide, in the presence of catalytic amounts of iron – the so-called Haber–Weiss reaction (equation 3) (Haber and Weiss, 1934).

$$Fe^{3+} + O_2^- \longrightarrow Fe^{2+} + O_2 \tag{2}$$

$$O_2^- + H_2O_2 \longrightarrow O_2 + \cdot OH + OH^- \tag{3}$$

Iron or copper complexes will catalyse Fenton chemistry only if two conditions are met simultaneously, namely that the ferric complex can be reduced and that the ferrous complex has an oxidation potential such that it can transfer an electron to H_2O_2. However, we must also add that this reasoning supposes that we are under standard conditions and at equilibrium, which is rarely the case for biological systems. A simple example will illustrate the problem: whereas under standard conditions reaction (2) has a redox potential of -330 mV (at an O_2 concentration of 1 atmosphere), *in vivo* with $[O_2] = 3.5 \times 10^{-5}$ M and $[O_2^-] = 10^{-11}$ M the redox potential is $+230$ mV (Pierre and Fontecave, 1999).

In aqueous solution in the absence of oxygen, iron is present as the hydrated hexa-aqua ferrous [Fe(II)] ion, $Fe(H_2O)_6^{2+}$. In the early stages of evolution the atmosphere was thought to be essentially reducing with a very low oxygen pressure, and hence a high concentration of reduced iron would have been present. It is calculated that initially, at a redox potential of -325 mV, most of the iron would have been present as Fe_3O_4 (the mixed valence mineral, magnetite), and that the concentration of Fe^{2+} could have been as high as 0.2 mM (Österberg, 1976). The appearance of molecular oxygen, which accompanied the arrival of photosynthetic organisms capable of fixation of atmospheric carbon dioxide (with concomitant water splitting to yield electrons, protons and oxygen), changed the situation dramatically, since the following reaction (equation 4, here simplified by neglecting the hydration of the ferrous ion) would result:

$$Fe(II)_{aq} + O_2 \longrightarrow Fe(III)_{aq} + O_2^- \tag{4}$$

Except at very low pH values, the hexa-aqua ferric ion, $Fe(H_2O)_6^{3+}$, would then undergo a series of hydrolysis and polymerization reactions, leading progressively to more and more insoluble ferric polynuclears which would precipitate to give the geologic evidence of atmospheric oxygenation by the presence around the

mid-Precambrian of intense red ferric oxide deposits. The inorganic chemistry involved in these processes is better understood due to the unstinting efforts of, notably, my colleague and good friend, Walter Schneider of the ETH in Zurich and his collaborators (Schneider, 1988; Schneider and Schwyn, 1987; Cornell *et al.*, 1989). The rest of this chapter concerns the pathways of ferric iron hydrolysis and polymerization, and concludes with some thoughts on biomineralization.

1.3 Iron Hydrolysis – A Ubiquitous Phenomenon

The phenomenon of hydrolysis is defined as the behaviour of metal salts when they are dissolved in water. Hydrolysis originates in the loss of protons from aqua-metal ions, and it often terminates, as in the case of iron, in the precipitation of metal hydroxides or hydrated metal oxides. Between pH 5 and pH 9, which is clearly of relevance to biological as well as aquatic systems, ferric salts hydrolyse immediately, whereas ferrous salts, in the absence of oxygen or other oxidizing agents, give solutions of ferrous aqua ions, $Fe(H_2O)_6^{2+}$. Thus, in biological media, the hydrated ferrous ion is a real species, whereas hydrated ferric ion is relatively rare, although significant concentrations of $Fe(H_2O)_6^{3+}$ will be present at very low pH values (since hydrolytic polymerization reactions involve deprotonation of the original hexa-aquo ion $Fe(H_2O)_6^{3+}$, to form hydroxo and oxo species as described below). In most lakes, estuaries, streams and rivers, iron levels are high, and Fe^{2+} is produced by photolysis of inner-sphere complexes of particulate and colloidal iron(III) hydroxides with biogenic organic ligands. Since the photic zones in which this takes place are aerobic, there is continuous reoxidation of iron to yield secondary colloidal iron(III) hydroxides. In deeper waters, settling organic matter can supply reducing equivalents to convert $FeO \cdot OH$ to Fe^{2+}. In contrast, iron levels in surface seawater are extremely low, 0.02 to 1 nM (Wu and Luther, 1996).

The hydrolysis and polymerization of iron(III) from hydrated ferrous and ferric ions can be achieved by addition of an oxidant to the former or a base to the latter. Temperature and solvent changes will also influence hydrolysis and polymerization.

1.4 Hydrolysis of Iron(III) in Acid Media – Formation of Polynuclear Species

Hydrolysis of ferric solutions is readily induced by addition of base. Initially, at rather acid pH, the purple ferric aqua-ion $Fe(H_2O)_6^{3+}$, upon addition of base undergoes the first deprotonation step (equation 5), which is followed by reversible dimerization (equation 6), giving a yellow solution of mono- and dinuclear species:

$$2Fe^{3+} + 2H_2O \longrightarrow 2FeOH^{2+} + 2H^+ \tag{5}$$

$$FeOH^{2+} + FeOH^{2+} \longrightarrow Fe_2(OH)_2^{4+} \tag{6}$$
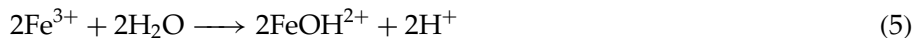
The equilibria leading to mono- and dinuclear hydrolysis products such as $FeOH^{2+}$, $Fe(OH)_2^+$ and $Fe_2(OH)_2^{4+}$ are established rapidly and are well understood

(Schneider, 1984; Schneider and Schwyn, 1987; Schneider, 1988; Cornell *et al.*, 1989). Perchlorate solutions that contain the dinuclear $Fe_2(OH)_2^{4+}$ to about 10 % of the total iron concentration can be kept unchanged for several weeks. This is by no means trivial, because it was recognized many years ago that solutions containing $Fe_2(OH)_2^{4+}$ to a significant degree are supersaturated with respect to solid phases such as FeO(OH) (Biedermann and Schindler, 1957). The low molecular species interact to produce species with a higher nuclearity (equation 7):

$$Fe_2(OH)_2^{4+} + FeOH^{2+} + H_2O \longrightarrow Fe_3(OH)_4^{5+} + H^+ \tag{7}$$
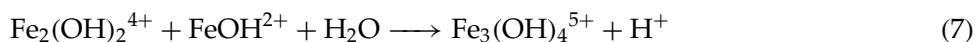
The molecular processes that occur during formation of the low nuclearity polynuclears governs the morphological properties of the end products. Various well-defined limiting stoichiometries can develop depending on the site at which a growth unit adds to the dimer, and as illustrated in Figure 1.4, even for the trimer, five different morphological arrangements are possible. The small, relatively labile, polynuclear species that develop upon further base addition polymerize further to give red–brown colloidal systems of spherical polynuclear species with limiting diameters between 3 and 5 nm. These polynuclears can be isolated as amorphous species and have been characterized by a number of techniques, including chemical analysis, ultracentrifugation, transmission electron microscopy (TEM), X-ray powder diffraction, Mössbauer, infrared and visible spectroscopy. They consist of iron cores of nuclearity, p, with OH^- and O^{2-} exclusively in bridging positions and can be represented by $Fe_pO_r(OH)_s^{3p-(2r+s)}$. Since these species are positively charged polyelectrolytes, they can be coagulated by specifically adsorbing anions. In these polynuclears the peripheral iron atoms are coordinated
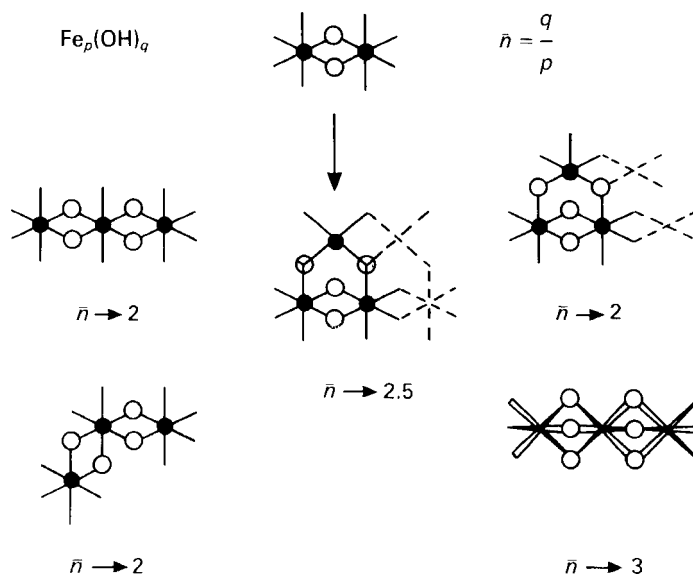
Figure 1.4 The structural variety of trinuclear ferric hydroxo complexes, $Fe_3(OH)_q^{9-q}$, that could form from $Fe_2(OH)_2^{4+}$ at low pH. Iron atoms are indicated as full circles, OH as open circles. The arrow indicates a transition from dinuclears to trinuclears ($p = 2$ to $p = 3$), which is realistic as an early step in the growth of polynuclears. (From Crichton, 1991.)

to at least one water molecule, so that deprotonation of these water molecules with increasing pH also leads to coagulation. TEM shows that the polynuclears coagulate to form chains, rafts or irregular masses.

Controlled hydrolysis of Fe(III) complexes, using for example the $[Fe_2O]^{4+}$ unit, in aqueous or non-aqueous solvents in the presence of appropriate ligands has been carried out to give a variety of products. These have been shown to contain di-, tri- and tetranuclear and even deca-, undeca-, dodeca-, heptadeca-, octadeca- and nonadecanuclear Fe(III) core structures (Gorin and Lippard, 1986; Micklitz *et al.*, 1994; Heath *et al.*, 1996; Lippard and Berg, 1994; Powell, 1998).

1.5 Formation of Precipitates

Ageing of polynuclears eventually leads either to an amorphous precipitate or to a variety of crystalline compounds. The molar ratio of excess base added per Fe(III), a, determines both the precipitation time and whether the precipitate is amorphous or crystalline. A crystalline precipitate forms in minutes or hours at a critical value of a, a_{min} which lies between 0.5 and 1.0 (Figure 1.5). At values
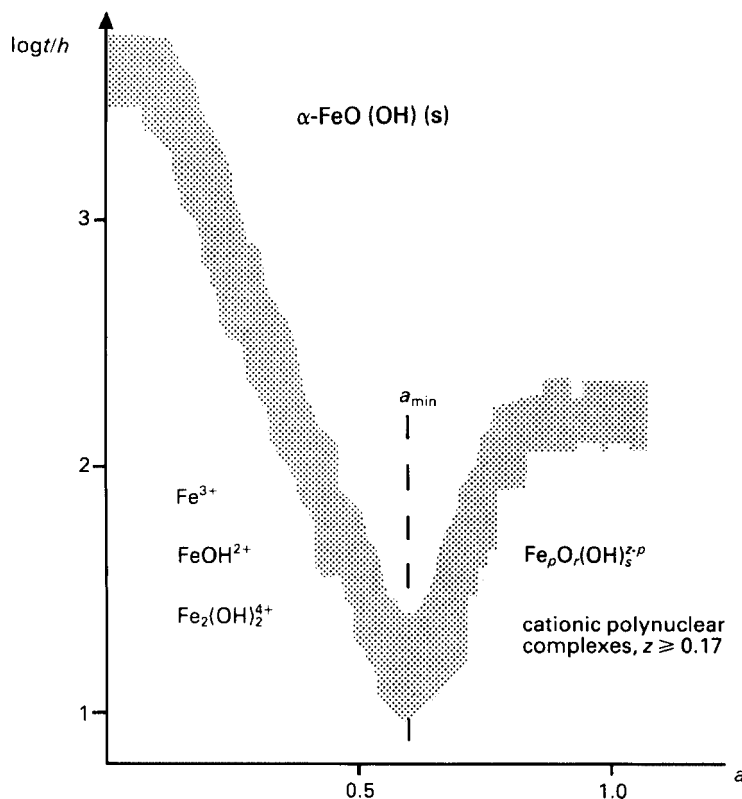
Figure 1.5   The variation of precipitation times with molar ratios of $a = HCO_3^-$ / Fe(III) for 0.6 M iron(III) perchlorate solutions. τ is the somewhat arbitrarily defined time elapsed before a Tyndall effect is observed. (From Crichton, 1991.)

of *a* less than this, a microcrystalline precipitate forms directly from a solution of low molecular weight species; polynuclears are absent. If base is added to give $a_{min} < a < 2.8$, red–brown colloidal polynuclears form, that transform slowly (weeks to months) to an amorphous precipitate or to crystalline $FeO(OH)$ or α-Fe_2O_3. Which crystalline iron hydroxide forms depends on the value of *a* and on the anion present. α-$FeO(OH)$ precipitates from ferric nitrate solutions, β-$FeO(OH)$ (mineral name akaganeite) forms when chloride is present, whereas γ-$FeO(OH)$ (lepidocrocite) forms together with α-$FeO(OH)$ from perchlorate systems. With time and a high enough temperature $FeO(OH)$ transforms in acid medium into α-Fe_2O_3.

Schneider and Schwyn (1987) showed that addition of $FeOH^{2+}$ to primary polynuclears (i.e. nuclei) leads to anisotropic growth of needle-like polynuclears, up to 70 nm in length and 30 nm in width:

$$(\text{polynuclear})_p + FeOH^{2+} \longrightarrow (\text{polynuclear})_{p+1}$$
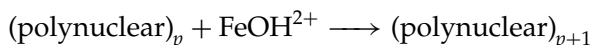
However, ageing of these virtually monodisperse systems was shown to promote an increase in width in favour of length. There was no change from hydroxo to oxo bridges, but instead there was an alteration in polynuclear shape. While the internal structure was maintained, it was found that the polynuclears became shorter and wider, as the mononuclear ferric species released from the ends of the needles by acid cleavage redeposited on the centres of the molecules.

1.5.1   Ageing of Amorphous Ferrihydrite to More-crystalline Products

Addition of sufficient base to give $a > 3$ to a ferric solution immediately leads to precipitation of a poorly ordered, amorphous, red–brown ferric hydroxide precipitate. This synthetic precipitate resembles the mineral ferrihydrite, and also shows some similarity to the iron oxyhydroxide core of ferritin (see Chapter 6). Ferrihydrite can be considered as the least stable but most reactive form of iron(III), the group name for amorphous phases with large specific surface areas (>340 m^2/g). We will discuss the transformation of ferrihydrite into other more-crystalline products such as goethite and haematite shortly, but we begin with some remarks concerning the biological distribution and structure of ferrihydrite (Jambor and Dutrizac, 1998).

Although ferrihydrite is of great importance in metallurgical processing and in the natural environment, its presence is often underestimated because of difficulties in its definitive identification, and also because of its common designation (covering a range of poorly ordered compounds) as amorphous iron hydroxide, colloidal ferric hydroxide, $Fe(OH)_3$, etc. However, it should be pointed out that ferrihydrite has been identified as a preterrestrial component of meteorites, and may be a constituent of the soils of Mars. On our planet Earth, ferrihydrite occurs widely in natural waters, in the sediments derived from these waters, and is a constituent of a wide variety of soils, particularly those formed under cool and moist conditions. It is abundantly present, though difficult to identify, in sulfide oxidation products and in the precipitates resulting from acid mine drainage, where it was identified for the first time in a biological context (Chukhrov *et al.*, 1973). Ferrihydrite is also believed to be the dominant constituent of some metallurgical processing residues. Wherever

it is found, ferrihydrite precipitation controls the level of dissolved iron in solution as well as regulating the concentration and distribution of a host of impurities.

Rapid hydrolysis of Fe(III) solutions (for example neutralization of ferric solutions with an excess of alkali) gives a red–brown precipitate of ferrihydrite. Ferrihydrite is generally classified according to the number of X-ray diffraction lines that the material gives: '2-line ferrihydrite' describes material that exhibits little crystallinity and '6-line ferrihydrite' that which has the best crystallinity. The degree of order found in ferrihydrite depends on the method of preparation and the time of its ageing. Brief heating of Fe(III) solutions to about 80°C typically produces '6-line ferrihydrite', whereas the 2-line variety is typically produced at ambient temperatures by addition of alkali to raise the pH to about 7. While there have been a number of new structural models proposed for ferrihydrite, none of them has to date received universal acceptance (Jambor and Dutrizac, 1998). However it does seem to be agreed that 'amorphous iron hydroxide' is not amorphous, has at least a low degree of crystallinity, and is synonymous with 2-line ferrihydrite. Secondly, there seems to be universal agreement that the ferrihydrite structure, although different from that of goethite, has closer similarities to the FeOOH-type minerals goethite and akaganeite, than to haematite. Despite the ease of its synthesis in the laboratory, no single formula is widely accepted. Table 1.1 shows the composition as $Fe_5HO_8 \cdot 49H_2O$ (Towe and Bradley, 1967), while the widely reported nominal formula of ferrihydrite, $5Fe_2O_3 \cdot 9H_2O$ (Towe, 1981), is thought to be excessively hydrous and, in view of the closer similarity of ferrihydrite to goethite than to haematite, it seems inappropriate to write a component of the formula as $5Fe_2O_3$. It has been demonstrated that almost all of the water can be replaced by adsorbed species in quantities that cannot be accommodated within the crystal structure. There is general agreement that the iron in ferrihydrite is octahedrally coordinated, but it is also thought that the octahedral coordination only represents the 'core' structure and that much of the surface of ferrihydrite has iron in tetrahedral coordination. These 'coordination-unsaturated' surface sites are readily accessible to the adsorption of foreign species and, together with the large surface area referred to above, may account for the high adsorptive capacity of ferrihydrite. Ferrihydrite is thermodynamically unstable and transforms with time into the more

Table 1.1 Oxides, hydroxides and oxyhydrosides of iron. Reprinted with permission from Jambor and Dutrizac, 1998. Copyright (1998) American Chemical Society.

Mineral	Nominal formula	Phase	Nominal formula
Goethite	α-FeOOH	synthetic	$Fe(OH)_2$
Akaganeite	β-FeOOH	synthetic	β-Fe_2O_3
Lepidocrocite	γ-FeOOH	synthetic	ε-Fe_2O_3
Ferroxyhite	δ-FeOOH	synthetic	FeOOH
Haematite	α-Fe_2O_3		
Maghaemite	γ-Fe_2O_3		
Magnetite	Fe_3O_4		
Wüstite	FeO		
Bernalite	$Fe(OH)_3$		
Ferrihydrite	$Fe_5HO_8 \cdot 4H_2O$		

stable crystalline oxides haematite and goethite. The dry thermal transformation of ferrihydrite to either haematite or goethite proceeds at <400°C with fine particle sizes leading directly to haematite, whereas courser material initially produces goethite. The presence of adsorbed species can drastically increase the transformation temperature – as illustrated by the observation that an Si : Fe ratio of 0.25 in ferrihydrite increases the temperature required to convert ferrihydrite to haematite to 800°C. The aqueous transformation of ferrihydrite is complex, and depends on pH, temperature, and the presence of various anions, cations and organic species in the organic slurry. The presence of foreign ions in solution can influence the kinetics of ferrihydrite transformation, altering the proportions of haematite and goethite formed or initiating the crystallization of new end products, such as lepidocrocite (Cornell, 1987). Two different reaction pathways have been identified: for the ferrihydrite-to-goethite transformation a dissolution–reprecipitation mechanism, and a dissolution–solid state transformation of ferrihydrite to haematite (Jambor and Dutrizac, 1998).

1.6 Biomineralization

Many structures formed by plants and animals are the products of biomineralization (calcium phosphate in teeth and bones, calcium in the shells of marine organisms, silicon in grasses and the shells of invertebrates). Biomineralization involves the formation of these inorganic materials under the influence of proteins, carbohydrates and lipids. The way in which biominerals grow is intimately linked to the problem of morphology, and it is difficult to think of a better introduction to this field than the pioneering work of D'Arcy Thompson, whose classic book *On Growth and Form* is essentially about biominerals (Thompson, 1968). This fascinating problem includes initiation of nucleation, growth of the inorganic crystalline phases, and definition of the volume and shape of the inorganic material, which is determined by the organic mould (lipid, protein, carbohydrate) within which the inorganic mineral structure is deposited, and is extensively reviewed by Frausto da Silva and Williams (1991) and by Mann *et al*. (1989).

The formation of the ferrihydrite core of ferritin and its transformation into haemosiderins is one example of a biomineralization process. Another is the formation of magnetite (Fe_3O_4) particles by magnetotactic bacteria. Of the 14 iron oxides, hydroxides, and oxyhydroxides that have been more or less well defined, 10 are known to occur in nature (Table 1.1). Of these, goethite, haematite and magnetite occur in sufficient abundance to be considered as rock-forming minerals. The intermediate minerals, lepidocrocite, ferrihydrite and maghaemite, are found in sediments from many localities, but they all occur much less frequently and in much lower abundance than goethite, haematite and magnetite. Nonetheless, the intermediate minerals are common, both in distribution and amounts, compared with the relative sparseness of wüstite, akaganeite, ferroxhyte and finally, bernalite, which is only known from one locality (Jambor and Dutrizac, 1998). Table 1.2 lists the diagnostic criteria for these various iron oxides.

The biological mineralizing systems for iron that have been studied the most extensively are the ferrihydrite (and, in prokaryotic ferritins, the amorphous

Table 1.2 Diagnostic criteria for iron oxide minerals.

Mineral	Colour	Most intense X-ray lines	IR bands (cm^{-1})	Magnetic hyperfine field (T)		
				295 K	77 K	4 K
Ferrihydrite	Reddish brown	2.54, 2.24, 1.97, 1.73, 1.47		–	–	47–50
Haematite	Bright red	2.70, 3.68, 2.52	345, 470, 540	51.8	54.2/53.5	54.2/53.5
Maghemite	Red to brown	2.52, 2.95	400, 450, 570, 590, 630	50	–	52.6
Magnetite	Black	2.53, 2.97	400, 590	49.1/46.0	–	–
Goethite	Yellowish brown	4.18, 2.45, 2.69	890, 797	38.2	50.3	
Lepidocrocite	Orange	6.26, 3.29, 2.47, 1.937	1026, 1161, 753	–	–	45.8
Akaganéite	Yellowish brown	3.33, 2.55, 7.47	840, 640	–	47.1, 46.7, 45.3	48.9, 47.8, 47.3
Feroxyhyte	Reddish brown	2.54, 2.22, 1.69, 1.47	1110, 920, 790, 670	42.0	53.0	53.5
Bernalite	Dark green	3.784, 1.682, 2.393, 2.676, 1.892		42.0		55.7

Adapted with permission from Schwertman and Cornell (1991) in Jambor and Dutrizac (1998). Copyright (1998) American Chemical Society.

hydrated ferric phosphate) cores of ferritins and haemosiderins, which will be considered in greater detail in Chapter 6, the magnetite laid down in the magneto-somes of magnetotactic bacteria, and the magnetite and goethite particles, which seem to be derived from ferrihydrite, in molluscan teeth (Webb *et al.*, 1989). We will consider the iron biomineralization to magnetite here.

1.6.1 Magnetite Biomineralization by Magnetotactic Bacteria

Aquatic bacteria exhibiting magnetotaxis, i.e. orienting and migrating along geomagnetic field lines, were discovered serendipitously in the early 1970s.[†] This ability is dependent on the formation of intracellular magnetic structures, the magnetosomes, which comprise nanometer-sized, membrane-bound, crystals of the magnetic iron minerals magnetite (Fe_3O_4) or greignite (Fe_3S_4). The use of magnetite for orientation purposes has also been demonstrated in bees, pigeons, and possibly in man. Magnetosome formation is achieved by a process of mineralization which involves (i) accumulation of iron within a vesicular structure; (ii) transformation of the initial iron deposit (most likely ferrihydrite) into magnetite, and (iii) crystallization of the magnetite mineral to give a particle within the vesicle with a specific size and orientation.

Magnetotactic bacteria are morphologically and metabolically diverse, including both freshwater and marine species. Their permanent magnetic dipole moments result from intracellular magnetosomes (particle dimensions invariably within the 40–120 nm size range), which are membrane-enveloped, single-crystal, particles, essentially of magnetite. The number of magnetosomes per cell is variable and depends on the environmental concentration of iron, oxygen and other chemicals. The iron content of the cells is generally high – for example in the magnetotactic spir-illum *Aquaspirillum magnetotacticum*, with an average of 20 siderosomes per cell, iron constitutes 2 % of the dry weight. In addition to Fe_3O_4, the cells contain some ferrous iron as well as hydrous ferric oxide (ferrihydrite). The process is thought (Mann and Frankel, 1989; Schuler and Frankel, 1999) to involve (i) reductive uptake of iron from the surrounding environment and its membrane transport; (ii) transport of iron, perhaps as ferritin, to and across the magnetosome membrane; (iii) precipitation of hydrated Fe(III) oxide within the magnetosome vesicles, and (iv) phase transforma-tion of the amophous Fe(III) phase – most likely ferrihydrite – to magnetite, both during the nucleation phase and during surface-controlled growth of the crystallite. The unique stage of this process appears to be transformation of the ferrihydrite to magnetite, since the initial stages are likely to involve processes similar to formation

[†] At the Marine Station at Woods Hole, Massachusetts, Richard Blakemore observed that bacteria from marine and freshwater muds accumulated at the north side of drops of water and sediment when placed upon a microscope slide, and that these bacteria swam towards and away from the south and north pole of a bar magnet respectively (Blakemore, 1975). He subsequently showed that such magnetotactic bacteria behave like self-propelled, permanent, magnetic dipole moments. Magnetotactic bacteria use magnetite, Fe_3O_4, as an internal compass with which to navigate, and in the northern hemisphere, their magnetic dipole is oriented northward, whereas magnetotactic bacteria from the southern hemisphere have their dipole oriented southward. These microorganisms, isolated in the northern hemisphere, swing northward but also downward along the earth's magnetic field lines, to avoid the higher oxygen concentrations of surface water, which are toxic to them. When transferred to the southern hemisphere they '*perd leur Nord*', and swim upward!

of the ferrihydrite cores in ferritin. Transformation of ferrihydrite to magnetite is likely to be slow, since it will require dehydration, dissolution, reprecipitation and partial reduction of the ferric iron. At neutral pH it can occur, provided that the redox potential of the reaction environment is in the range of -100 mV. However, small changes in pH can markedly influence the phase transformation processes – a slight lowering of the pH will favour more positive values of the redox potential, which would favour transformation to the less hydrated and more crystalline ferric oxides such as goethite. This mineral has been observed in the radular teeth of limpets, whereas the radular teeth of chitons contain magnetite. The subsequent crystal growth and morphology results, on the one hand, from surface reactions that are kinetically restrained, showing slow crystal growth and therefore highly ordered crystals; and on the other hand, the crystal morphology, that arises from the interaction between the growing crystal and its local environment in such a way that the ultimate form of the crystal is determined by precise biological control of crystal growth. This explains why, although the biological organization and function of the mineral phase of different magnetotactic bacteria may have a common evolutionary origin, the crystal forms found are species specific (Mann and Frankel, 1989).

1.7 References

Biedermann, G. and Schindler, P.W. (1957). *Acta Chem. Scand.*, **20**, 1376−88.

Blakemare, R.P. (1975). *Science*, **190**, 377−9.

Chukhrov, F.V., Zvyagin, B.B., Gorshkov, A.I., Yermilova, L.P. and Balashova, V.V. (1973). *Int. Geol. Rev.*, **16**, 1131−43.

Cornell, R.M. (1987). Z. *Pflanzenernähr. Dung. Bodenkd.*, **150**, 304−7.

Cornell, R.M., Giovanoli, R. and Schneider, W. (1989). *J. Chem. Tech. Biotechnol.*, **46**, 115−34.

Crichton, R.R. and Pierre, J.-L. (2001). *Biometals* (in press).

Fenton, H.J.H. (1894). *J. Chem. Soc., Trans.*, **65**, 899−910.

Foote, C.S. (1982). In *Pathology of Oxygen* (ed. Autor, A.P.), pp. 21−44, Academic Press, New York.

Frausto da Silva, J.J.R. and Williams, R.J.P. (1991). *The Biological Chemistry of the Elements*, Oxford University Press, Oxford, pp. 467−94.

Gorun, S.M. and Lippard, S.J. (1996). *Nature*, **319**, 666−8.

Haber, F. and Weiss, J. (1934). *Proc. Roy. Soc. Ser. A*, **147**, 332−51.

Halliwell, B. and Gutteridge, J.M.C. (1984). *Biochem. J.*, **219**, 1−14.

Heath, S.L., Charnock, J.M., Garner, C.D. and Powell, A.K. (1996). *Chem. Eur. J.*, **2**, 634−9.

Hill, H.A.O. (1981). *Phil. Trans. Roy. Soc. Ser. B*, **8**, 89−193.

Jambor, J.L. and Dutrizac, J.E. (1998). *Chem. Rev.*, **98**, 2549−85.

Lippard, S.J. and Berg, J.M. (1994). *Principles of Bioinorganic Chemistry*, pp. 129−130, University Science Books, Mill Valley, California, USA.

Mann, S. and Frankel, R.B. (1989). In *Biomineralization* (eds Mann, S., Webb, J. and Williams, R.J.P.), VCH, Weinheim, pp. 389−426.

Mann, S., Webb, J. and Williams, R.J.P. (1989). *Biomineralization*, VCH, Weinheim, 541 pp.

Micklitz, W., McKee, V., Rardin, R.L., Pence, L.E., Papaefthymiou, G.C., Bott, S.G. and Lippard, S.J. (1994). *J. Am. Chem. Soc.* **116**, 8061–9.

Österberg, R. (1976). In *An Introduction to Bioinorganic Chemistry* (ed. Williams, D.R) C.C. Thomas, Illinois, USA.

Pearson, R.G. (1963). *J. Am. Chem. Soc.*, **85**, 3533–9.

Pierre, J.-L. and Fontecave, M. (1999). *Biometals*, **12**, 195–9.

Powell, A.K. (1998). In *Metal Ions in Biological Systems* (eds Sigel, A. and Sigel, H.), **35**, 515–61.

Schneider, W. (1984). *Comments Inorg. Chem.*, **5**, 205–23.

Schneider, W. (1988). *Chimia*, **42**, 9–20.

Schneider, W. and Schwyn, B. (1987). In *Aquatic Surface Chemistry* (ed. Stumm, W.) pp. 167–95, Wiley, New York.

Schuler, D. and Frankel, R.B. (1999). *Appl. Microbiol. Biotechnol.*, **52**, 464–73.

Schwertmann, U. and Cornell, R.M. (1991). *Iron Oxides in the Laboratory*, VCH, New York, 137 pp.

Thompson, D.W. (1968). *On Growth and Form*, Second Edition, Cambridge University Press, Cambridge.

Towe, K.M. (1981). *J. Biol. Chem.*, **256**, 9377–8.

Towe, K.M. and Bradley, W.F. (1967). *J. Colloid Interface Sci.*, **24**, 384–92.

Webb, J., Macey, D.J. and Mann, S. (1989). In *Biomineralization* (eds Mann, S., Webb, J. and Williams, R.J.P.), VCH, Weinheim, pp. 345–87.

Wu, J. and Luther III, G.W. (1996). *Geochim. Cosmochim. Acta*, **60**, 2729–41.

2 The Importance of Iron for Biological Systems

2.1 Introduction

As we saw in Chapter 1, the aqueous solution chemistry of iron is dominated by forms of Fe^{2+} and Fe^{3+} whose complexes readily undergo electron transfer and acid–base reactions. This explains the wide range and variety of catalytic and other reactions of which the element is capable. It also underlines the importance of iron in biological systems. Another feature of iron which makes it so important is its abundance although, as was pointed out before, since the advent of oxygen into the earth's atmosphere, iron bioavailability has been seriously compromised. When we consider the extensive range of redox potentials available to the metal by varying its interaction with coordinating ligands, and add to that its capacity to participate in one-electron transfer (i.e. free radical) reactions, it is easy to see why iron is virtually indispensable for life. One such free radical reaction, rate determining in DNA synthesis, is the reduction of ribonucleotides to their corresponding deoxy ribonucleotides, catalysed by ribonucleotide reductases (RNRs), all of which are radical metalloenzymes (Stubbe and van der Donk, 1998). There are four classes of ribonucleotide reductases, I–IV. These utilize respectively for catalysis: class (I), a stable tyrosyl radical adjacent to a diferric cluster (present in a great number of organisms including *E. coli*, yeast and man); class (II), adenosyl-cobalamine (for example, in *Lactobacillus* species); class (III), found in *E. coli* grown under anaerobic conditions, a glycyl radical together with an FeS cluster; and class IV enzymes, a dimanganese cluster and a putative tyrosyl radical (in *Cornyeform* bacteria) (Figure 2.1a). It has been shown for class I and II ribonucleotide reductases, and proposed for class III and IV enzymes, that the function of all of these cofactors is to generate a thiyl radical that initiates ribonucleotide reduction. A working model for nucleotide reduction by class I enzymes is presented in Figure 2.1(b). Following hydrogen atom abstraction from the 3′-position of the ribonucleotide by the thiyl radical, subsequent elimination of the 2′-hydroxyl group as water occurs simultaneously with deprotonation of the 3′-hydroxyl. Reduction of the intermediate α-keto radical **1** via oxidation of two cysteines to the corresponding disulfide generates a 3′-deoxynucleotide radical **2**, which reabstracts the originally removed hydrogen atom from the third cysteine, yielding product and regenerating the thiyl radical. This mechanism has been supported by a great deal
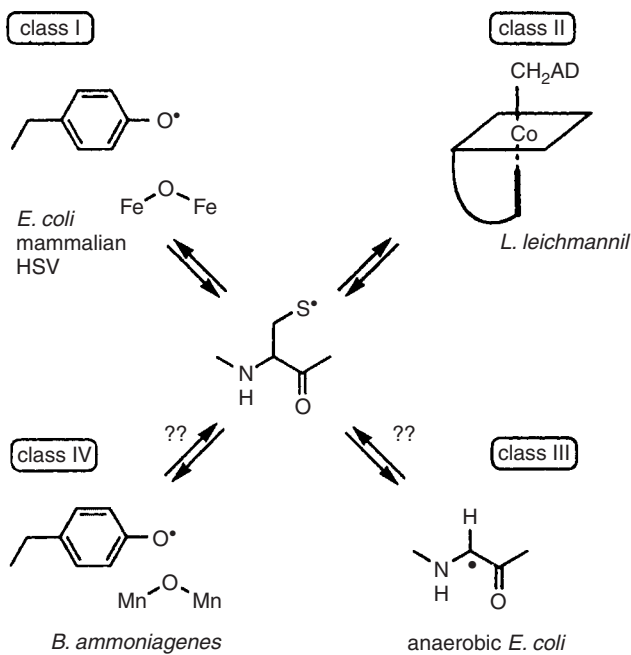
(a)
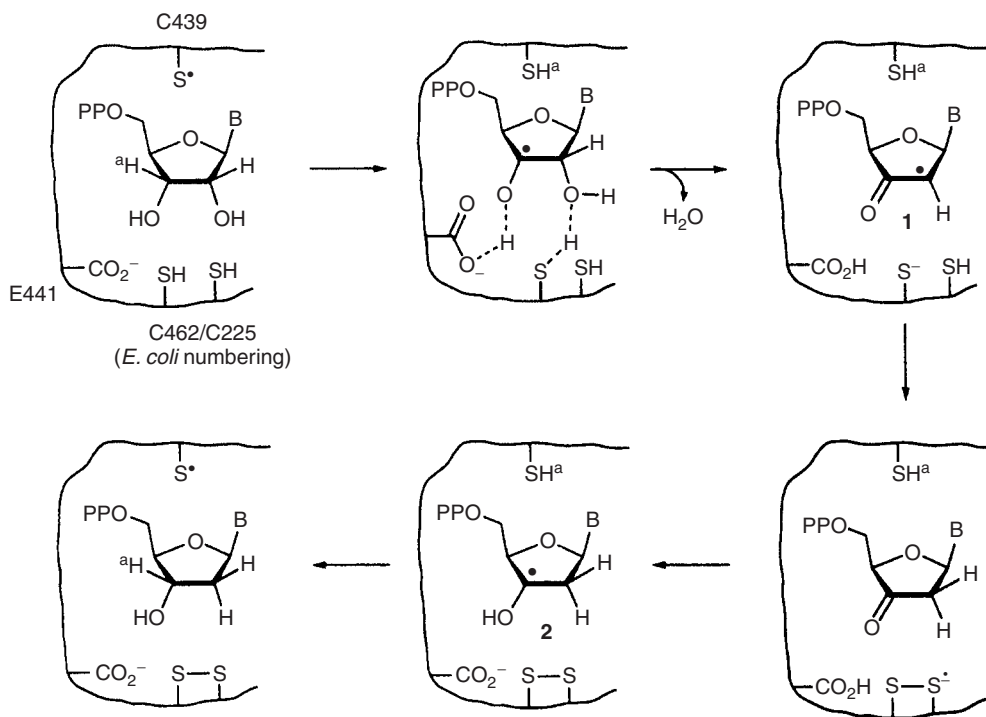
(b)

of data accumulated over the last two decades (reviewed in Stubbe and van der Donk, 1998).

In this chapter we will describe some aspects of the biological chemistry of iron, with particular reference to iron-containing enzymes. The importance of iron for biological systems can be illustrated by three simple examples. *E. coli* devotes almost 50 genes to proteins involved in iron uptake – six distinct siderophore-mediated Fe^{3+} transport systems, one for iron uptake from ferric citrate, and one Fe^{2+} transport system, yet it synthesizes only one siderophore: enterobactin. When blue–green algal blooms occur in lakes, the factor determining which algal species takes over is the efficacy of its capacity to chelate iron (Murphy *et al.*, 1976). When it is wished to determine the potential for growth of a mammalian tumour, the density of transferrin receptors, which are required for iron uptake and hence cell growth, are measured.

At the outset, before discussing the classification of iron-containing proteins, we should cover two aspects of the incorporation of iron, and indeed of most metal ions, into proteins that seem to us to be of primordial importance. Firstly, we do not know, in most cases, the mechanisms whereby metal ions are incorporated specifically into metalloproteins[†]. Secondly, metal incorporation into proteins may involve the creation of what Vallee and Williams (1968) have described as an 'entatic state', whereby binding of the metal to the protein induces functionally useful strain in the metal centre. As Williams (1995) has pointed out, the entatic state occurs in a protein when a metal is forced into an unusual, energized, geometric or electronic state, particularly by misfitting to the stable protein fold (i.e. the protein fails to provide the expected arrangement of ligating groups that is observed in model complexes with freely mobile ligands). The general idea was of catalytic perfection induced by strain, not only on the metal ion as a consequence of the geometry imposed by the ligands of the protein, but on the protein by the binding of the metal ion to it.

Metal-containing proteins present in living organisms can be classified according to a number of criteria – for example, the functional role of the metal ion, defined as (i) structural, (ii) metal-ion storage and transport, (iii) electron transport, (iv) dioxygen binding, and (v) catalytic – the latter being extremely large and diverse. We have chosen here a presentation for iron metalloproteins which is based essentially on the coordination chemistry of the metal. This has the advantage of allowing the reader more easily to appreciate the diversity of biochemical functions

Figure 2.1 (a) Classification of the four classes of ribonucleotide reductases according to the cofactors used in catalysis. It has been shown for class I and II ribonucleotide reductases, and proposed for class III and IV enzymes, that the function of all of these cofactors is to generate a thiyl radical that initiates ribonucleotide reduction. (b) A working model for the nucleotide reduction process catalysed by ribonucleotide reductases. Catalysis is initiated by hydrogen atom abstraction from the 3′ position of the substrate by the thiyl radical generated by one of the metallocofactors. After elimination of the 2′-hydroxyl group as water, the intermediate α-keto radical **1** is reduced by oxidation of two cysteines to the corresponding disulfide and the 3′-deoxyribonucleotide radical **2** re-abstracts the hydrogen atom originally removed from the third cysteine, providing the product and regenerating the original thiyl radical. (a) and (b) reprinted with permission from Stubbe and van der Donk, 1998. Copyright (1998) American Chemical Society.

[†] A notable recently identified exception is copper (see Chapter 13) for which specific chaperone proteins deliver the metal to individual copper-dependant proteins (Harrison *et al.*, 1999).

which iron can serve, as viewed through the ligands that bind it to the protein. First, we consider haemoproteins in which an iron protoporphyrin is incorporated into different apoproteins to give O_2 carriers, O_2 activators or, alternatively, electron transfer proteins. Secondly, we consider proteins containing iron–sulfur clusters, many of which are involved in electron transfer although, as we shall see, catalytic iron–sulfur clusters are also known. Finally there is a growing class of non-haem, non-iron–sulfur, iron-containing proteins which include, in addition to enzymes, proteins of iron storage and transport. It is also important to insist on the increasing contribution that bioinorganic chemistry is making in the design and synthesis of model compounds that can mimic metal–binding sites in metalloproteins – we have already alluded to this in the previous chapter.

As was pointed out in Chapter 1, in the classification of metal ions as 'hard' or 'soft' acids, Fe^{3+} can be considered as a 'hard' acid, with a preference for ligands which are 'hard' bases (Pearson, 1963), notably those which contain oxygen as a donor atom: examples are hydroxyl, carboxyl, and other oxygen containing groups. In contrast, Fe^{2+} is intermediate between a 'hard' and a 'soft' acid, and can accomodate both the 'hard' oxygen-based ligands, and the 'soft' ligands such as those containing nitrogen and sulfur. Examples are histidine, protoporphyrin, cysteine and inorganic sulfur. The distribution of the donor atoms that ligate the metal, and their geometry, will hence determine the functional properties of the metal centre. In the case where one of the coordination spheres is unoccupied, there exists the possibility of binding a 6th non-protein ligand.

2.2 Physical Techniques for the Study of Iron in Biological Systems

Before discussing the different classes of iron-containing proteins, it is perhaps appropriate to indicate briefly the physico-chemical techniques that are available for the study of iron in biological systems. While, in what follows, we will emphasize crystallographically defined metal sites, it is important to recognize that much of our information about structure–function correlations of iron sites comes from the application of spectroscopic methods in solution. Table 2.1 lists the key spectroscopic techniques that can be utilized for the study of iron-containing metalloproteins in order of increasing energy, with indications concerning the parameters accessible to the technique, and where appropriate the time scale and the information content that can be extracted from the data (Holm *et al*., 1996). The electronic properties and the high electron densities of metal ions (including iron) make them particularly amenable to physical techniques such as EXAFS, Mössbauer, resonance Raman, and electroparamagnetic resonance spectroscopies, which are rarely used by biorganic chemists. The amount of protein and the concentration required for different techniques vary widely – EPR, for example, can detect high-spin ferric ions at concentrations as low as the μM range, whereas NMR studies may require concentrations in the mM range. One drawback of the use of ^{57}Fe Mössbauer spectroscopy is the low natural abundance of this isotope (2.2 %), often necessitating enrichment of the protein, either by reconstitution from the apoprotein or, alternatively, its isolation from a growth medium containing iron salts enriched in ^{57}Fe.

Table 2.1 Spectroscopic methods in the study of iron in biological systems. Extensively modified from Holm *et al.*, 1996.

Method	Parameters	Information content
Magnetic susceptibility	Molecular g value, axial and rhombic zero field splitting, exchange interaction	Number of unpaired electrons/ground spin state; defines antiferromagnetic and ferromagnetic interactions; quantitates ground sublevel splittings
Mössbauer spectroscopy	Quadrupole coupling, isomer shift	For ^{57}Fe sites: oxidation and spin state; chemical environment
Electron paramagnetic resonance (EPR)	Quadrupole tensor, nuclear Zeeman splitting, g values, coupling constants, relaxation times	Usually for odd electron metal sites: probes groundstate wavefunction at high resolution
Electron-nuclear double resonance (ENDOR)		Combines sensitivity of EPR and high resolution of NMR to probe ligand superhyperfine interactions
Nuclear magnetic resonance (NMR)	Chemical shift, nuclear coupling constants, relaxation times	For paramagnetic proteins: enhanced chemical shift resolution, contact and dipolar shifts, spin delocalization, magnetic coupling from temperature dependence of shifts
Vibrational spectroscopy (Raman and IR)	Energies (with isotope perturbation), intensities and polarizations	Identification of ligands coordinated to a metal centre
Electronic absorption spectroscopy (ABS)	Energies, intensities, and band shapes	Direct probe of ligand field and charge transfer excited states
Magnetic circular dichroism (MCD)	Same as ABS plus circular polarization induced by applied magnetic field and magnetic susceptibility	Greater sensitivity than ABS in observing weak transitions and greater resolution due to differences in circular polarization; complimentary selection rules aiding in assignment of electronic transitions
Circular dichroism (CD)	Same as ABS plus circular polarization due to asymmetric nature of metal site	Allows detection of transitions not readily observable in absorption
Resonance Raman spectroscopy	Intensity profiles, depolarization ratios	Allows study of chromophoric active sites in biological molecules at low concentration; can provide information on metal–ligand bonding
Extended X-ray absorption fine structure (EXAFS)	Energies, intensities and polarizations	Identity of ligand atoms: distance of ligand atoms from metal: number of scattering ligands of a given type
X-ray diffraction	Atomic coordinates at a given resolution	Identity of ligands to metal centre (but distances more precise by EXAFS)

While it is often thought that X-ray crystal structures give accurate metal−ligand distances and geometries, this is not usually the case unless very high resolution can be achieved. Geometric information derived from fitting extended X-ray absorption fine structure (EXAFS) data to a model structure can be reliable to around 0.001 nm. So, when the liganding atoms to an iron site are known, EXAFS gives much more accurate distances than X-ray crystallography. More information on these techniques can be found in the references contained in the article by Holm *et al*., 1996 and in the excellent texts by Lippard and Berg (1994) and by Cowan (1997).

2.3 Haemoproteins

The first class of iron-containing proteins that we consider is that where the iron is bound to four ring nitrogen atoms of a porphyrin molecule (haem) and to one or two axial ligands from the protein. The porphyrin consists of four pyrrole rings, linked by methene bridges; in most haemoproteins it has the arrangement shown in Figure 2.2, with four methyl, two vinyl and two propionyl substituents, known as protoporphyrin IX. The enzyme ferrochelatase, located on the matrix face of the inner mitochondrial membrane, incorporates ferrous iron into protoporphyrin IX to form haem, which is subsequently incorporated into different haemoproteins. There are three types of haemoproteins: (i) oxygen carriers; (ii) activators of molecular oxygen; (iii) electron transport proteins.

2.3.1 Oxygen Carriers

In haemoglobins and myoglobins, the haem is tightly bound to the protein through a large number of hydrophobic interactions and by a single coordinate bond between the imidazole of a 'proximal histidine' and the ferrous iron (Figure 2.2b). Whether they are tetramers, dimers or monomers from mammals, insects, worms, or even the nodules of leguminous plants, and whether they bind molecular oxygen in a cooperative or a non-cooperative way, all have the common globin tertiary fold. They possess an unoccupied sixth coordination site, situated within a hydrophobic pocket, sterically hindered by the presence of distal histidine residue, and are capable of reversibly binding molecular oxygen. In contrast, simple ferrous porphyrins are irreversibly oxidized by molecular oxygen, leading ultimately to stable (μ-oxo)diiron(III) species. Reversible oxygenation at room temperature can be achieved with synthetic ferrous porphyrins by using sterically encumbered ligands to protect the O_2 binding site, thus preventing the approach of two iron−porphyrin moieties. Two examples are given in Figure 2.3, one a *picket-fence* porphyrin, in which all four pivalamido substituents project on the same side of the ring, the other a *capped* porphyrin, which binds O_2 in the presence of a large excess of axial base. The dioxygen molecule is bound end-on to the iron, both in model complexes, in haemoglobin and in myoglobin. Resonance Raman spectroscopy provides good evidence for electron transfer to dioxygen, such that we could consider oxyhaemoglobin and oxymyoglobin as ferric-superoxide complexes, in which the superoxide is stabilized by hydrogen bonding to the distal histidine proton (Figure 2.2).
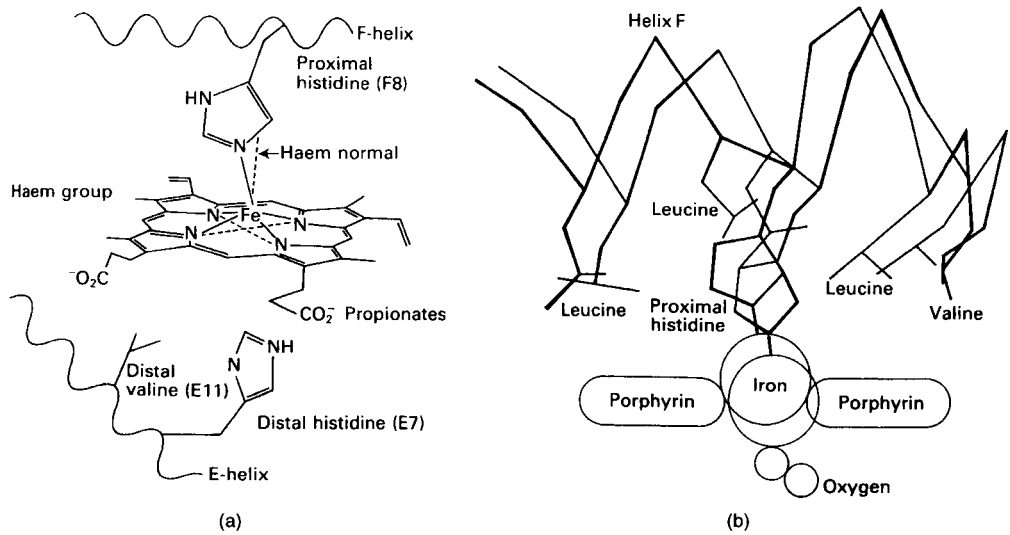
Figure 2.2 (a) A detailed picture of the haem group and its binding site within myoglobin or haemoglobin; (b) the particular changes in the globin component of haemoglobin upon O_2 binding. Reproduced from Frausto da Silva and Williams, 1991, by permission of Oxford University Press.

Picket fence porphyrin   Capped porphyrin
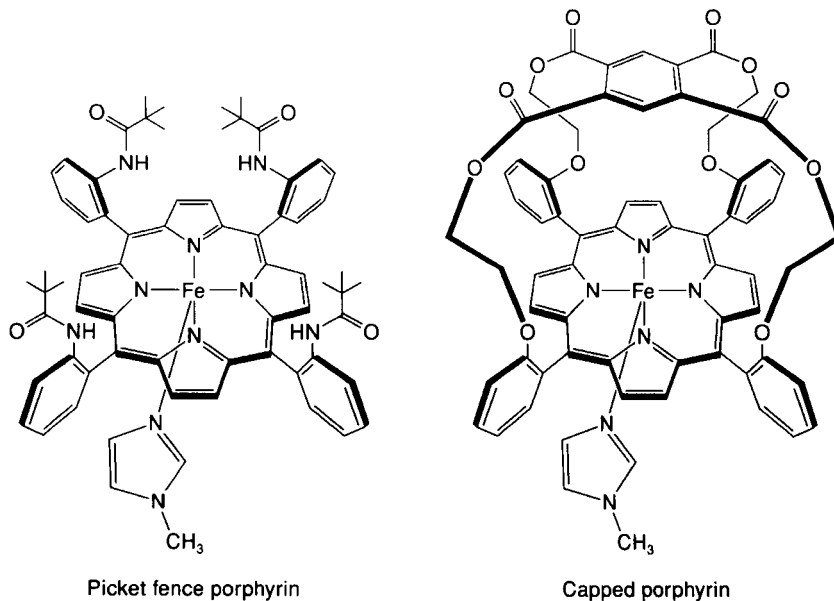
Figure 2.3 Structures of two globin compounds capable of reversible dioxygen binding. From Lippard and Berg, 1994. Reproduced by permission of University Science Books.

The most important difference between monomeric and oligomeric haemoglobins is, of course, the cooperativity of the oxygen binding by the latter – tetrameric mammalian haemoglobins fix the fourth oxygen molecule with one-hundred times greater affinity than the first. Before the high resolution structural refinements of myoglobin and haemoglobin were taken into account, it had been suggested that

the size of the iron atom might be the key factor in triggering the subunit transition from the low (deoxy, or T) to the high affinity (oxy, or R) state. The first to draw attention to this potential 'trigger' was Bob Williams (Williams, 1961). Ferrous porphyrins have six d electrons and can occupy three spin states. High-spin iron(II) porphyrins are invariably 5-coordinate with the iron atom well displaced out of the haem plane towards the single axial ligand. Six-coordinate ferrous porphyrins with two axial ligands, one on either side of the haem plane, are invariably diamagnetic and low-spin ($S = 0$). The covalent radius is such that low-spin iron(II) fits into the porphyrin core with minimum disruption and lies almost in the plane of the haem. Iron(II) porphyrins can also assume an intermediate spin state ($S = 1$) which has no biological counterpart. Model X-ray studies with porphyrin model compounds had shown that the 5-coordinate high spin Fe(II) sits a small distance out of the haem plane, whereas in the presence of a sixth coordinating ligand the low-spin Fe(II) is pulled into the haem plane (reviewed in Perutz, 1979). Perutz developed a 'stereochemical mechanism' for how haemoglobin worked, based on the observation that a number of salt bridges at the subunit interfaces present in deoxyhaemoglobin are absent from the oxy form (Perutz, 1970; Perutz *et al.*, 1998). It was proposed that upon binding of O_2 to haem in the T quaternary structure, the spin-state transition would force the iron atom into the haem plane thus pushing the haem closer to His F8, the axial fifth ligand of the haem iron, causing movement of the F-helix. This results in the breaking of a salt bridge, release of a proton, and destabilization of the structure at the subunit interface between $\alpha\beta$ dimers of the tetramer, thereby pushing the quaternary structure equilibrium towards the R-state. In this mechanism the salt bridges play three roles: (i) they stabilize the T quaternary structure relative to R; (ii) they reduce the oxygen affinity in the T state because of the energy required to break them on oxygen binding; and (iii) they release protons when they are broken, thus explaining the effect (discovered almost a century ago by the physiologist father of atomic physicist Niels Bohr, Christian), namely that the affinity of haemoglobin for oxygen is reduced when the pH decreases (Bohr *et al.*, 1904).

In myoglobin (and by homology, also haemoglobin), the N–H proton of the distal histidine E7 in the O_2 binding pocket (Figure 2.2) forms a hydrogen bond with the iron-coordinated dioxygen molecule, and imposes an angular bend on the oxygen molecule. In carbon-monoxide adducts of myoglobin and haemoglobin, the steric hindrance caused by the distal histidine results in a less favourable binding geometry (CO prefers a linear coordination). Thus, CO, a poison present both in tobacco smoke and in automobile exhausts, and also produced in the normal biological degradation of haem, binds only about 250-times more tightly than O_2 to both myoglobin and haemoglobin, whereas the affinity of free haem for carbon monoxide is much greater. This tailoring of the iron porphyrin centres to bind O_2 rather than its toxic surrogate CO, means that endogenously produced carbon monoxide did not prove lethal to man, before his discovery of means for its exogenous production. None the less, the progressive irritation of the gendarme on traffic duty on the Place de l'Etoile during the rush hour still reflects the greater affinity of his haemoglobin for CO rather than for O_2!

2.3.2 Activators of Molecular Oxygen

These haem enzymes include cytochrome oxidase, peroxidases, catalases and cyto-chrome P_{450}s. They are characterized by a penta-coordinate geometry in which the sixth site of the metal centre can bind either molecular oxygen, hydrogen peroxide or, in the case of cytochrome P_{450}s, form iron–carbon bonds with the substrate. Substrate specificity and oxygen activation is determined by the interaction between haem iron and ligands and the control of spin state (Smith and Williams, 1970). For all of them the high spin iron–porphyrin system can go to the radical cation state at a redox potential close enough to that of the couple Fe(IV)/Fe(III) to allow a ferryl type of iron to participate in chemical reactions, such as the activation of oxygen or oxidation of molecules at the expense of hydrogen peroxide.

Cytochrome oxidase, the terminal enzyme of the mitochondrial respiratory chain, spans the mitochondrial inner membrane and catalyses the reduction of molecular dioxygen to water at the rate of up to 250 molecules of O_2 per second. In addition, it couples the energy released in this process to the translocation of protons, which in turn contributes to the chemiosmotic gradient required for ATP synthesis. The primary oxygen binding site involves a haem Fe, called haem a_3 and a copper ion termed Cu_B in a binuclear site (analogous to the copper–copper centre in laccase) in which dioxygen is reduced (Figure 2.4a). Electron input to this site comes from cytochrome c by way of a second haem iron, haem a, and a second copper centre Cu_A. The crystal structure of cytochrome oxidase has been determined (Tsukihara *et al*., 1995, 1996; Iwata *et al*., 1995), and the mechanism of oxygen reduction has been studied with a variety of spectroscopic techniques (Ferguson-Miller and Babcock, 1996), so that we now have considerable insight into many aspects of the catalytic cycle. Following dioxygen binding to the fully reduced enzyme, an oxy-intermediate is formed that has the resonance Raman signature of oxyhaemoglobin or oxymyoglobin, and can be reproduced well with six-coordinate oxyhaem A model compounds. The initial reaction product with O_2 at haem a_3 binds in a relaxed, end-on configuration, with no apparent interaction with Cu_B. Two transient, but detectable, intermediates at the binuclear centre were identified and designated P and F, and while there was consensus that the F intermediate involved a ferryl-oxo intermediate at haem a_3, the structure of P (designated as P for peroxy) has been a matter of considerable controversy. However, it now seems that P also has an a_3^{4+}=O structure at the binuclear centre (reviewed in Babcock, 1999), indicating that O=O bond cleavage has already occurred at P. A simplified reaction scheme for oxygen reduction by cytochrome oxidase is presented in Figure 2.4(b) (Babcock, 1999), which highlights the analogies between the oxidase and peroxidases and catalases, in terms both of oxygen–oxygen bond cleavage chemistry, and the nature of the products of the reactions. In the oxidase, the enzyme extracts three electrons from metals in the active site – two from haem a_3 as it goes from the +2 to the +4 state and one from Cu_B as it is oxidized from cuprous to cupric – and one electron from a redox-active protein side chain. This is most likely Tyr-244, which is cross-linked to His-240, one of the Cu_B ligands. The oxy-intermediate is reduced in one step to O^- and OH^-. Both products are at the level of water, but further protonation and release only occur in later steps of the reaction.
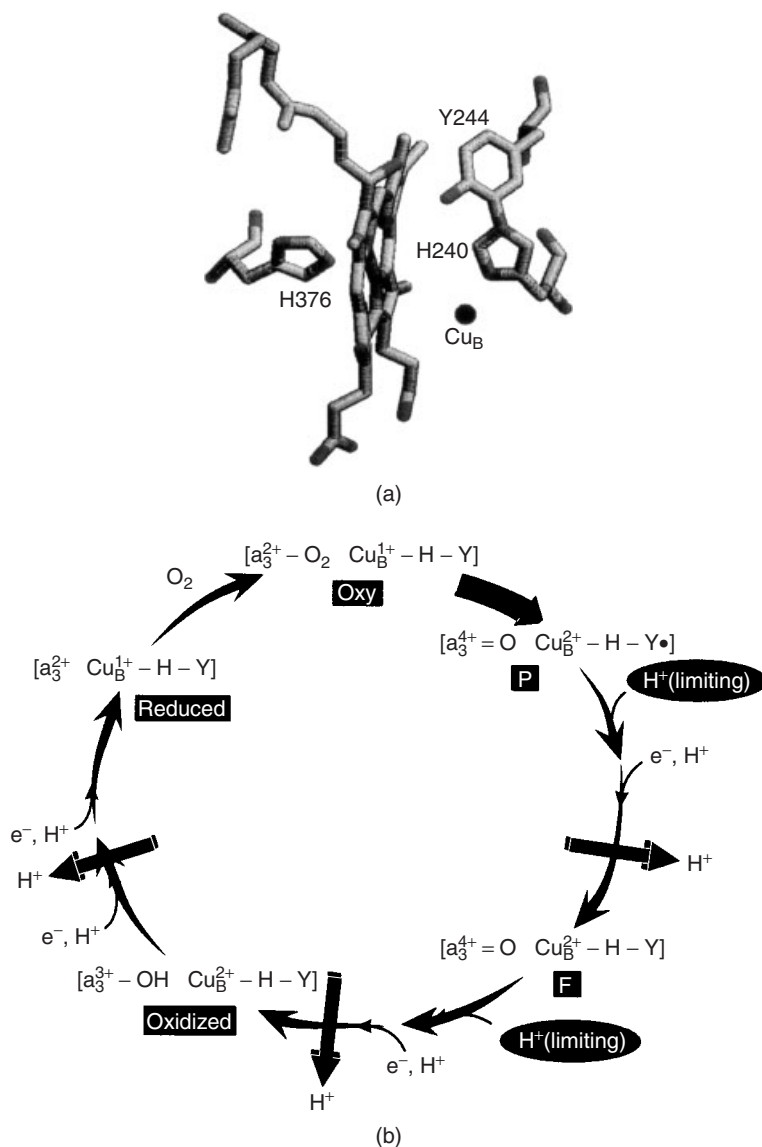
Figure 2.4 (a) The binuclear centre of cytochrome oxidase. Haem a_3, and Cu_B are shown along with the proximal ligand for the haem iron, His-376, and the Cu_B ligand His-240, which is cross-linked to Tyr. O_2 binding and reduction occurs in the region between the a_3 iron and Cu_B. (b) A simplified scheme for the reaction between cytochrome oxidase and oxygen. The binuclear site that contains haem a_3, Cu_B and the cross-linked His-240–Tyr-244 (H–Y) structure, is shown. Reduction and protonation of the oxidized form of the centre produces the reduced site, which binds oxygen to form the oxy species. This reacts further to produce *P* and *F* intermediates before regenerating the oxidized form of the enzyme. The reduction of *P* and *F* are limited by proton transfer reactions, while the steps between *P* and the reduced form of the site have been implicated in proton pumping processes (indicated by arrows). The stoichiometry of these steps is a matter of current investigation, although up to four protons can be pumped during the complete cycle. From Babcock, 1999. Copyright (1999) National Academy of Sciences, USA.

Catalases and peroxidases both promote H_2O_2 reduction by mechanisms that involve ferryl intermediates. Catalases differ from peroxidases by their ability to use H_2O_2 both as an electron acceptor and as donor, thus catalysing the disproportionation reaction (catalatic activity) (equation 1):

$$H_2O_2 + H_2O_2 \longrightarrow 2H_2O + O_2 \tag{1}$$

Both catalases and peroxidases can oxidize a variety of organic substrates (peroxidatic activity) (equation 2):

$$AH_2 + H_2O_2 \longrightarrow A + 2H_2 \tag{2}$$
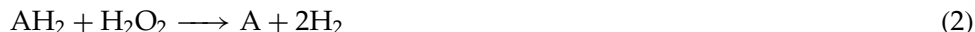
In peroxidases and catalases, the enzyme extracts one electron from haem iron in the active site and a second electron from an organic moiety to reduce H_2O_2 in one step to O^{2-} and OH^-. The immediate product of this chemistry is compound I, which contains a ferryl-oxo species, and an organic radical, analogous to the $a_3{}^{4+}{=}O$ radical found in intermediate P in cytochrome oxidase. The organic radical in compound I is reduced in a subsequent step to produce compound II, which maintains the ferryl-oxo structure, and exactly the same chemistry is found in the oxidase to produce the F intermediate (Figure 2.4b). This similarity in the chemistry catalysed by these oxygen-activating haem proteins may extend to other enzymes involved in activating and reducing oxygen and peroxides.

Prior to 1955 it was thought that the only role of oxygen in biological systems was as an electron acceptor in dioxygen-utilizing oxidase or dehydrogenase reactions. In that year Hayaishi and Mason independently demonstrated, using $^{18}O_2$, that one or both oxygen atoms of dioxygen can be directly incorporated into organic molecules (Hayaishi *et al.*, 1955; Mason *et al.*, 1955). The enzymes that incorporate oxygen atoms from molecular oxygen in such reactions were designated oxygenases by Hayaishi (1974), and can be further classified into two categories, monooxygenases (equation 3) and dioxygenases (equation 4), depending on whether one or both oxygen atoms from dioxygen are incorporated into the substrate, where XH and AH_2 represent substrate and an electron donor respectively:

$$XH + {}^*O_2 + AH_2 \longrightarrow X({}^*O)H + H_2{}^*O + A \tag{3}$$

$$XH + {}^*O_2 \longrightarrow X({}^*O_2)H \tag{4}$$

The monooxygenases require two electrons in order to reduce the second oxygen atom to water, and they are sometimes called mixed function oxidases or mixed function oxygenases, since they function both as oxygenase and oxidase. Shortly after the discovery of oxygenases, Garfinkel (1958) and Klingenberg (1958) independently described the presence of a CO-binding pigment in liver microsomes that exhibited an unusual absorption band maximum at 450 nm. Six years later Omura and Sato (1964) identified this unusual pigment as a haem protein and assigned it the name cytochrome P_{450}, without knowing what its function was. Liver microsomal P_{450} exists in multiple forms and plays important roles in the hydroxylation of endogenous physiological substrates, as well as a vast range of drugs and other compounds foreign to the organism (xenobiotics[‡]). Exposure to

---

[‡] Xenos, as Michael Flanders remarked in the Flanders and Swann recording 'At the Drop of a Hat', is the Greek word for stranger or guest; as in xenophobia – fear and hatred of guests!

such xenobiotics results in the induction of particular P_{450} proteins, and more than 450 different P_{450} enzymes are known to exist. Cytochrome P_{450}s are found in almost all mammalian tissues and organs, as well as in plants, bacteria, yeast, insects, etc., where they catalyse a panoply of different reactions, as shown in Table 2.2 (reviewed in Sono *et al.*, 1996). With the exception of microbial P_{450}s, the majority of P_{450}s are membrane bound and associated either with the inner membrane of the mitochondria or with the endoplasmic reticulum (microsomal) membrane. Most of the physiological substrates such as steroids, prostaglandins, leukotrienes and fatty acids, as well as the xenobiotics that react with P_{450}, are hydrophobic. When cytochrome P_{450} functions as a monooxygenase it requires a two-electron donor, which transfers electrons, derived from either NADH or NADPH, via electron transport protein systems (equation 5):

$$RH + O_2 + NAD(P)H + H^+ \longrightarrow ROH + H_2O + NAD(P)^+ \qquad (5)$$

There are two types of electron transport: those involving flavoproteins *and* iron–sulfur proteins, and those requiring only flavoproteins. The X-ray crystal structure of the soluble cytochrome P_{450} from *Pseudomonas putida* grown on camphor (P-45O-CAM) has been determined (Poulos *et al.*, 1985), as have several others. The haem group is deeply embedded in the hydrophobic interior of the protein, and the identity of the proximal haem iron ligand, based on earlier spectroscopic studies (Mason *et al.*, 1965) is confirmed as a specific cysteine residue.

The catalytic cycle of cytochrome P_{450} involves four well-characterized and isolable states (1–4 in Figure 2.5). The resting form of the enzyme is a hexacoordinate low-spin iron(III) state (**1**) with two axial ligands; water (or hydroxide) as the exchangeable distal ligand *trans* to the proximal cysteinate. Binding of substrate RH at a hydrophobic site on the protein close to the haem generates the pentacoordinate high-spin ferric state (**2**) with the cysteinate as the only axial ligand. The vacant coordination site will ultimately bind dioxygen. However, conversion of ferric iron from low spin to high spin results in a significant increase in redox potential (from -330 to -173 mV versus the normal hydrogen electrode), favouring electron transfer from the reductase, so that one electron coming from NAD(P)H along the electron transfer chain can form a high-spin pentacoordinate ferrous complex (**3**) which is in an open conformation for binding dioxygen (as well as a number of other ligands such as CO, isocyanides, nitrogenous bases and phosphines). Dioxygen binding to Fe(II) cytochrome P_{450} haem gives a relatively stable hexacoordinate low-spin complex, that can be described either as the ferrous-O_2 (**4a**) or the ferric-superoxo (**4b**) complex. Addition of CO to **3** gives the ferrous–CO inhibitor adduct **5** with its characteristic absorbance peak near 450 nm. States **1–5** of P_{450} have all been isolated and extensively characterized. The final intermediates of the catalytic cycle, that transfers one oxygen atom to the substrate, have not been characterized. Addition of a second electron to **4**, the rate-limiting step in the cycle, is proposed to give a ferric peroxide adduct (**6a**) which can be protonated to give the hydroperoxide complex **6b**. A second protonation of the same oxygen leads to heterolytic O–O bond cleavage, releasing water and generating the high valent porphyrin–iron-oxo complex **7**, which is assumed to have characteristics compatible with an oxo-ferryl ($Fe^{4+}=O$) porphyrin radical cation (equivalent to the peroxidase compound I described above). Whether formation of **7** occurs directly from **4**, as in cytochrome

Table 2.2 Schematic summary of the diverse reactions catalysed by cytochrome P450. Reprinted with permission from Sato *et al.*, 1996. Copyright (1996) American Chemical Society.

(a) Hydrocarbon hydroxylation

$$\text{CH} \longrightarrow \text{C–OH}$$

(b) Alkene epoxidation/Alkyne oxygenation

(i)
$$\text{C=C} \longrightarrow \text{epoxide } (\text{C–C with O})$$

(ii)
$$\text{R–C}\equiv\text{C–H} \longrightarrow \left[\begin{array}{c} \text{R} \\ \text{C=C=O} \\ \text{H} \end{array} \right] \xrightarrow{\text{H}_2\text{O}} \text{RH}_2\text{C–C(=O)–OH}$$

(c) Arene epoxidation, aromatic hydroxylation, NIH shift

$$\text{(arene with X, R)} \longrightarrow \text{(epoxide)} \longrightarrow \text{(phenol with OH, R)} + \text{(phenol with X, OH, R)}$$

(d) N-Dealkylation

$$\text{R–N(Me)–H} \longrightarrow [\text{R–N(H)–CH}_2\text{OH}] \longrightarrow \text{R–NH}_2 + \text{HCHO}$$

(e) S-Dealkylation

$$\text{R–S–Me} \longrightarrow [\text{R–S–CH}_2\text{OH}] \longrightarrow \text{R–SH} + \text{HCHO}$$

(f) O-Dealkylation

$$\text{R–O–Me} \longrightarrow [\text{R–O–CH}_2\text{OH}] \longrightarrow \text{R–OH} + \text{HCHO}$$

(g) N-Hydroxylation

$$\text{C–NH}_2 \longrightarrow \text{C–NHOH}$$

(h) N-Oxidation

$$\text{N} \longrightarrow \text{N}^+\text{–O}^-$$

(i) S-Oxidation

$$\text{R–S–Me} \longrightarrow \text{R–S}^+(\text{O}^-)\text{–Me}$$

(j) Oxidative deamination

$$\begin{array}{c} \text{NH}_2 \\ \text{R–C(Me)–H} \end{array} \longrightarrow \left[\begin{array}{c} \text{NH}_2 \\ \text{R–C(Me)–OH} \end{array} \right] \longrightarrow \text{R–C(=O)–Me} + \text{NH}_3$$

(k) Oxidative dehalogenation

$$\begin{array}{c} \text{R}_2 \\ \text{R}_1\text{–C(H)–X} \end{array} \longrightarrow \left[\begin{array}{c} \text{R}_2 \\ \text{R}_1\text{–C(X)–OH} \end{array} \right] \longrightarrow \begin{array}{c} \text{R}_2 \\ \text{R}_1\text{–C=O} \end{array} + \text{HX}$$

(l) Alcohol and Aldehyde oxidations

(i)
$$\begin{array}{c} \text{R'(H)} \\ \text{R–C(H)–OH} \end{array} \longrightarrow \left[\begin{array}{c} \text{R'(H)} \\ \text{R–C(OH)–OH} \end{array} \right] \longrightarrow \begin{array}{c} \text{R'(H)} \\ \text{R–C=O} \end{array} + \text{H}_2\text{O}$$

(ii)
$$\begin{array}{c} \text{H} \\ \text{R–C=O} \end{array} \longrightarrow \begin{array}{c} \text{OH} \\ \text{R–C=O} \end{array}$$

Table 2.2 (*continued*)

(m) Dehydrogenation

(i)
$$\underset{H_2}{C}\!-\!\underset{H_2}{C} \xrightarrow{-H} [\,\overset{H}{\underset{\bullet}{C}}\!-\!\underset{H_2}{C}\,] \xrightarrow{-e^-,\,-H^+} \overset{H}{C}\!=\!\overset{}{\underset{H}{C}}$$

(Hydroxylation) $\longrightarrow \overset{OH}{CH}\!-\!\underset{H_2}{C}$

(ii)

NHAc $\xrightarrow{-2e^-,\,-2H^+}$ NAc (quinone imine, HO → O)

(n) Dehydrations

(i) $\underset{R}{\overset{R}{C}}\!=\!N\!-\!OH \longrightarrow R\!-\!C\!\equiv\!N + H_2O$

(ii) $R\!-\!\overset{OOH}{CH}\!-\!CH\!=\!CH\!-\!R' \longrightarrow$ epoxide $R\!-\!CH(\!-\!O\!-\!)CH\!-\!R' + H_2O$

(o) Reductive dehalogenation

$R_1\!-\!\overset{R_2}{\underset{R_3}{C}}\!-\!X \xrightarrow{+e^-} R_1\!-\!\overset{R_2}{\underset{R_3}{\overset{\bullet}{C}}} + X^-$

(p) *N*-Oxide reduction

$\overset{}{N^+}\!-\!O^- \xrightarrow{+2e^-\,(+2H^+)} N\ (+H_2O)$

(q) Epoxide reduction

$$\text{(epoxide)} \xrightarrow{+2e^-,\,+2H^+} \text{(benzene)} + H_2O$$

(r) Reductive β-scission of alkyl peroxides

$$X\!-\!\overset{R}{\underset{R'}{C}}\!-\!OOH \xrightarrow{+2e^-,\,+2H^+} X\!-\!C\!=\!O + R'H + H_2O$$

(s) NO reduction

$$2NO \xrightarrow{+2e^-,\,+2H^+} N_2O + H_2O$$

(t) Isomerizations

Prostaglandin H$_2$ (PGH$_2$) $\longrightarrow$ Prostaglandin I$_2$ (PGI$_2$); Thromboxane A$_2$ (TxA$_2$)

(u) Oxidative C—C bond cleavage

(i) $HO\!-\!\overset{OH}{\underset{R,\,H}{C}}\!-\!\overset{}{\underset{H}{C}}\!-\!R' \xrightarrow[{-H_2O}]{+O_2,\,+2e^-} R\!-\!C(=O)\!-\!R' + O\!=\!CH\!-\!R'$

(ii) $\xrightarrow[{-H_2O}]{+O_2,\,+2e^-,\,+2H^+} R\!-\!C(=O)\!-\!R' + HO\!-\!C(=O)\!-\!R'$

Figure 2.5 Catalytic cycle of cytochrome P_{450} including postulated structures of putative intermediates. RH represents the substrate and R(O)H the product. The porphyrin ring is abbreviated as a parallogram with nitrogens at the corners. Adapted with permission from Sato *et al.*, 1996. Copyright (1996) American Chemical Society.

oxidase, peroxidases and catalases, remains to be established. The P_{450} cycle is completed when **7** transfers oxygen to the substrate to give the alcohol product and to regenerate **1**.

2.3.3 Electron Transport Proteins

The third class of haemoproteins is the cytochromes, in which the iron is bound in a hexacoordinate low-spin system. They were first discovered by McMunn in 1884, and called histohaematins. However, the editor and chemist Hoppe Seyler[¶] declined

[¶] These were the days of the modest 'Herausgeber' of scientific journals – Justus von Liebig's *Annalen der Chimie*, Hoppe Seyler's *Zeitschrift für Physiologische Chemie*. It is recorded that when Freidrich Meischer
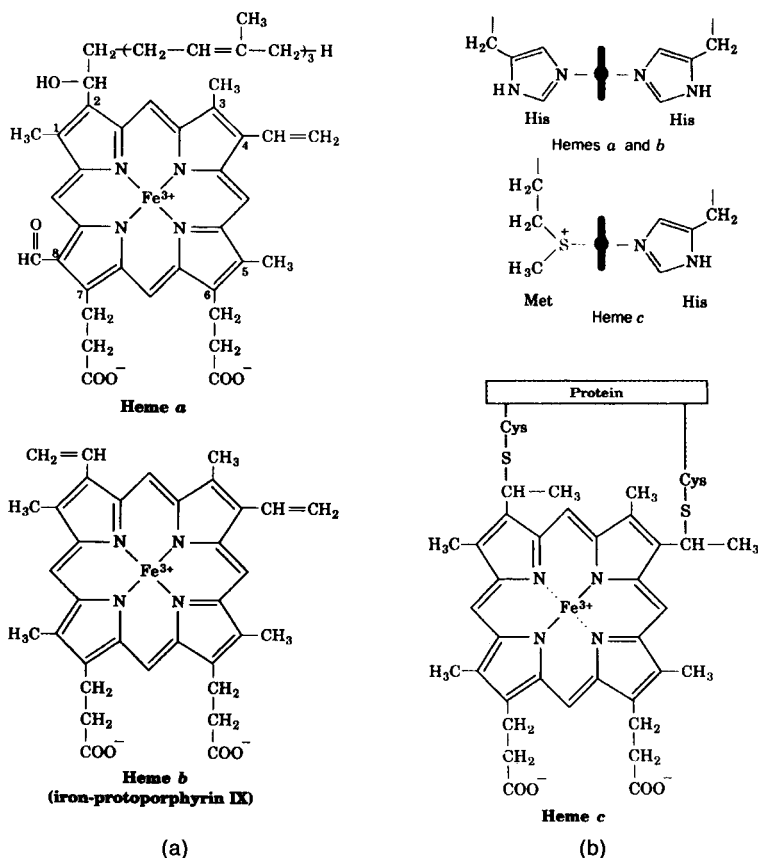
Figure 2.6   Chemical structures (a) and axial ligands (b) to the haem groups in cytochromes *a*, *b* and *c*. From Voet and Voet, 1995. Reproduced by permission of John Wiley & Sons, Inc.

to publish this discovery, so the work remained unnoticed until 1925 when David Keilin, using a hand spectroscope, rediscovered the characteristic absorption (Soret) bands of the three cytochromes *a*, *b* and *c* in respiring cells, and correctly concluded that they transferred electrons from substrate oxidation to the terminal oxidase that we know today as cytochrome *c* oxidase (Keilin, 1925). The three principal classes of cytochromes *a*, *b* and *c* have a distinctive three-banded absorption spectrum in the reduced state with an α-absorption band around 550–664 nm, a β band around 520–546 nm and a γ (Soret band) around 400–450 nm. They also differ in the nature of the side chains to their porphyrin (Figure 2.6). The *b*-type haems have protoporphyrin IX, as in haemoglobin. In the *c*-type cytochromes the vinyl groups of protoporphyrin IX form covalent thioether bonds with cysteine residues of the protein. *a*-Type haems contain a long hydrophobic tail of isoprene units attached to the porphyrin, as well as a formyl group in place of a methyl substituent. The

submitted his publication on the discovery of DNA (from pus-saturated surgical bandages), Hoppe Seyler delayed publication for a year, and accompanied Meischer's article with a confirmatory note of his own and a couple of research papers on the subject from his own laboratory. Apropos McMunn, one of my favourite textbook errors is the description of McMunn as a German biochemist!

axial ligands of haem iron vary with cytochrome type. In cytochromes *a* and *b*, both ligands are usually His residues, whereas in cytochrome *c*, one is His and the other is often Met (Figure 2.6). They are widely distributed in nature and serve as electron-carrier proteins in mitochondria, endoplasmic reticulum and photosynthetic organelles, as well as in bacterial redox chains. The iron in all cytochromes can alternate between an oxidized Fe(III) low-spin state with a single unpaired electron and a formal charge for the haem of +1, and a reduced Fe(II) low-spin form with no unpaired electrons, a net charge of zero. Since the iron remains low spin, electron transfer is greatly facilitated.

Because of its ease of isolation in a soluble form, in contrast to the rest of the proteins of the mitochondrial respiratory chain which are membrane-bound, cytochrome *c*, which serves as a mobile transporter of electrons between complex III and IV of the chain, is by far the best characterized cytochrome. It has a redox potential of +260 mV and contains one single haem group per molecule of 103–113 amino acids. The X ray structures of many eukaryotic and prokaryotic cytochromes *c* indicate the presence of the same overall molecular folding. Other members of the cytochrome *c* family can have as many as five haems with redox potentials covering the range −290 to +400 mV. The structure of a cytochrome c nitrite reductase dimer (Einsle *et al.*, 1999) is illustrated in Figure 2.7(a) (see Plate 1) with the arrangement of the five haems per monomer illustrated Figure 2.7(b). All of the haems are covalently attached to the protein, and all but haem 1 have bis-His axial ligands. The active site is haem 1, which has a single Lys residue as axial ligand, leaving the sixth coordination position free for nitrite binding. The enzyme, supplied by electrons from a further multihaem cytochrome that functions as electron donor, reduces nitrite in successive two-electron steps through the potential intermediates NO and hydroxylamine to ammonium cation: no intermediates are released.

Cytochromes, as partners of a number of respiratory chains, must interact with the other components, accepting electrons from reduced donor molecules and transferring them to appropriate acceptors. In the mitochondrial respiratory chain, electrons coming from the reduced form of coenzyme Q are transferred to complex III, which is composed of two *b* cytochromes, one [2Fe−2S] Rieske cluster and one cytochrome c_1. The crystal structure of the bovine cytochrome bc_1 complex has been determined at 0.3 nm resolution (Figure 2.8, Plate 2), including all 11 subunits (Iwata *et al.*, 1998). In Figure 2.8(a) a cartoon representation (Smith, 1998) shows that cytochrome bc_1 contains a hollow between its two monomers which allows easy shuttling of ubiquinol/ubiquinone to and from the complex and between two sites designated Q_P and Q_N. The external domain of the Rieske protein also shuttles between a site near Q_P and cytochrome c_1. For every electron transferred from Q_P through the Rieske protein and cytochrome c_1, to cytochrome *c* (not shown), two protons are deposited on the electropositive side of the membrane (the Q cycle hypothesis). The players in the Q cycle, all bound to the transmembrane domain of cytochrome *b*, are the haems b_L and b_H and their adjacent ubiquinol/ubiquinone sites, Q_P and Q_N. At Q_P, the electron transfer pathway is proposed to divide, with one electron of ubiquinol transferred to the Rieske external domain (from where it is transferred on to cytochrome c_1), while the other is recycled through the *b* haems to ubiquinone at Q_N. In Figure 2.8(b), the monomers of the bc_1 complex form a dimer (the 'essential dimer', necessary for activity, underlined by the location of the Rieske intrinsic and

extrinsic domains in opposite domains of the dimer), around a crystallographic twofold symmetry axis. The top of the molecule extends 3.8 nm into the intermembrane space (this includes major parts of cytochrome c_1 and the Rieske iron-sulfur centre). The membrane spanning region, 4.2 nm thick, includes the haem groups of both cyochrome bs, while more than half of the molecular mass of the complex, and also its widest part, extends 7.5 nm into the mitochondrial matrix (Xia *et al.*, 1997).

2.4 Iron – Sulfur Proteins

Fe–S proteins are presumed to be among the first catalysts that nature had to work with (Huber and Wächtershäuser 1998[§]). The second class of iron-containing proteins is those which contain iron atoms bound to sulfur, either forming a cluster linked to the polypeptide chain uniquely by the thiol groups of cysteine residues (rubredoxins), or else with both inorganic sulfide and cysteine thiols as ligands. Although they have a very widespread distribution in all living organisms, their recognition as a distinct class of metalloproteins took place only in the 1960 s after the discovery of their characteristic EPR spectra in the oxidized state. Iron–sulfur proteins can be classified into simple and complex iron–sulfur proteins, the latter containing, in addition to the iron–sulfur clusters, flavins, molybdenum, flavins and molybdenum, flavins and haem, etc. Their roles are numerous, ranging from electron transport (such as rubredoxins, ferredoxins) to enzymes with both redox and non-redox functions (succinate dehydrogenase, nitrogenase and aconitase for example).

Simple iron–sulfur proteins contain four basic core structures that have been characterized crystallographically both in model compounds and in iron–sulfur proteins (Holm *et al.*, 1996). They are (Figure 2.9) respectively: rubredoxins (upper panel, left), found only in bacteria, in which the [Fe–S] cluster consists of a single Fe atom in a typical mercaptide coordination, i.e. an iron centre liganded to four Cys residues; rhombic two iron–two sulfide [Fe_2–S_2] clusters which may either have all cysteine S-protein ligands (upper panel, right), or have a mixture of S- and N- (histidine) ligands (middle panel, left); cuboidal three-iron–four-sulfide [Fe_3–S_4] clusters (middle panel, right); and cubane four-iron–four-sulfide [Fe_4–S_4] clusters. Low molecular weight proteins containing the first and the last three types are generically referred to as rubredoxins (Rd) and ferredoxins (Fd), respectively. The schematic structure of these four Fe–S clusters (lower panel, centre), their electron transfer reactions and approximate ranges of potentials E_0' (pH 7) are given in Figure 2.9. In some cases, electron and proton transfer are coupled, so that the potentials are pH dependent. In addition to discrete Rd and Fd proteins as components of electron transfer pathways, the Fe–S clusters are also found within enzyme molecules themselves.

Rubredoxins do not have acid-labile sulfur as do ferredoxins, with the iron characterized by a mercaptide coordination. They are small proteins composed of some 50 amino acids. Both oxidized and reduced forms are high spin.

[§] While a passionate enthusiast for evolutionary theories, and their experimental testing, Günther Wächtershäuser is in his professional life a patents lawyer.
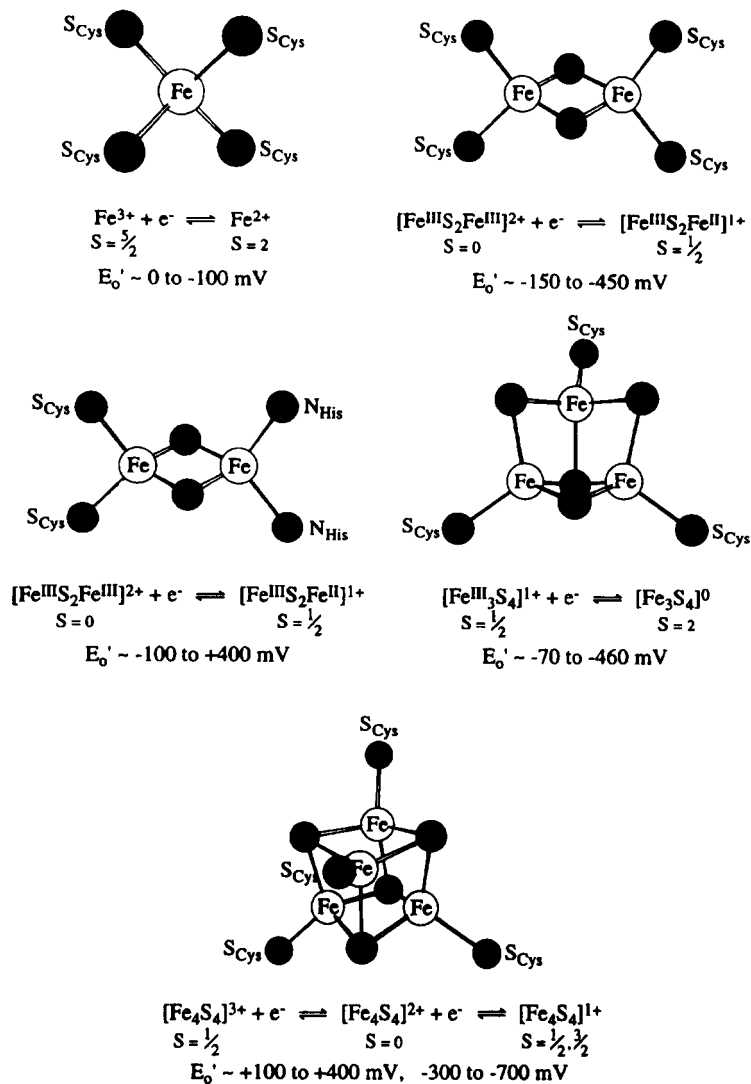
Figure 2.9 Schematic structures of Fe−S redox centres, their electron-transfer reactions and approximate range of potentials. See text for details. Individual iron atom oxidation states are not specified for delocalized cluster; spin states are indicated. Reprinted with permission from Holm *et al.*, 1996. Copyright (1996) American Chemical Society.

Fds with conventional $[Fe_2−S_2]$ clusters can undergo a one-electron transfer to a deeply valence-trapped $Fe^{III}Fe^{II}$ species. For proteins of known structure (and presumably others) one iron atom is closer to the surface (by about 0.5 nm) and it has been established that the added electron resides on that atom. No instances are known where an $[Fe_2−S_2]$ centre acts as a physiological two-electron donor or acceptor. In addition to the conventional $[Fe_2−S_2]$ ferredoxins, the electron-transfer chains of mitochondria and photosynthetic bacteria contain Rieske proteins which have a cluster with the composition $[(Cys.S)_2FeS_2Fe(N.His)_2]$, in which the two imidazole groups are bound to the same iron atom (Figure 2.9). This atom is the site

of reduction, and the presence of two neutral ligands increases the redox potential to values more positive than conventional $Fe_2-S_2]$ ferredoxins. A water-soluble fragment of a Rieske protein from bovine heart is reported to show two reductions.

The structure of the trinuclear cluster $[Fe_3S_4(S.Cys)_3]$ has been demonstrated crystallographically in two ferredoxins and in the inactive form of the citric-acid cycle enzyme, aconitase. The geometry is cuboidal, i.e. a cube with one vacancy. Under oxidizing conditions, it is probable that the reaction $[Fe_4-S_4]^{3+} \longrightarrow [Fe_3-S_4]^+ + Fe^{2+}$ occurs, the oxidized tetranuclear being insufficiently basic to retain the ferrous ion, the removal of which may be facilitated by complexation with an exogenous ligand. The cluster reconstitution reaction $[Fe_3-S_4]^0 + Fe^{2+} \longrightarrow [Fe_4-S_4]^{2+}$ occurs readily. However, the biological function of these clusters remains unclear.

Three core oxidation states are known for protein-bound $[Fe_4-S_4(S.Cys)_4]^{3+}$ clusters as illustrated in Figure 2.9. Native proteins exhibit either the $[Fe_4-S_4]^{2+,+}$ or the $[Fe_4-S_4]^{3+,2+}$ redox couple, with proteins involved in the latter couple being referred to historically as HiPIP (high-potential iron protein). The three oxidation states have not been traversed in one protein unless its tertiary structure is significantly perturbed.

There are a number of more complex Fe−S clusters whose structures are known and some of them are illustrated in Figure 2.10 (Beinert, 2000; Holm *et al.*, 1996). In the sulfite reductase of *Escherichia coli* a 4Fe−4S cluster is linked via a cysteine to the
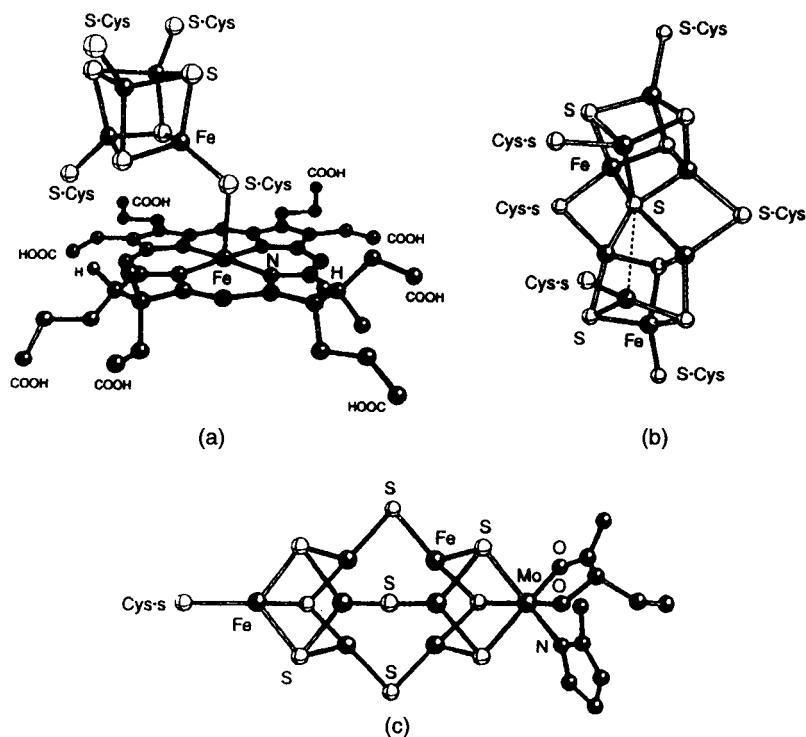
Figure 2.10 Schematic structures of (a) sulfite reductase of *Escherichia coli* in which a 4Fe−4S cluster is linked via a cysteine to the iron in a sirohaem; (b) P cluster of nitrogenase; (c) FeMoCo cluster of nitrogenase; (d) the binuclear site in *Desulforibrio gigas* hydrogenase.

(d)
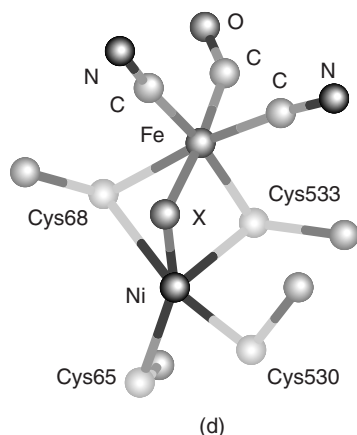
Figure 2.10 (*continued*)

iron in a sirohaem. In the nitrogenase, the X-ray structures of which are known for several nitrogen-fixing bacteria, the so-called P-cluster (P for protein versus cofactor) consists of two [Fe_4-S_3] modules linked together via two bridging cysteines and a seventh bridging sulfide, while the FeMoCo cluster (Fe–Mo cofactor) is constructed from two [Me_4-S_3] modules linked together by sulfides: the Mo, which is on the right hand side, is partially ligated by homocitrate (only two oxygen atoms shown) and a His. The 2Fe cluster found in the Ni–Fe hydrogenases has several diatomic ligands, which turn out, as predicted from spectroscopy (Pierik *et al.*, 1999) to be cyanide and carbon monoxide ligands. Similar –CO and –CN ligands are also found in all Fe hydrogenases, where the 2Fe–2S cluster is linked to a 4Fe–4S cluster. It is thought that Ni is mainly used in hydrogen uptake hydrogenases, whereas in those mostly evolving hydrogen, the 2Fe type is used. An unusual class of hybrid-cluster proteins ('prismane proteins'), of unknown physiological function, has been described in strict anaerobes but has recently been found in *E. coli* (van den Berg *et al.*, 2000).

2.5 Other Iron-containing Proteins

The third class consists of a heterogeneous collection of enzymes that contain iron in a non-haem, non iron–sulfur form. These proteins can be classified into (i) *mononuclear non-haem iron enzymes*. These include (Table 2.3) catechol and Rieske dioxygenases, involved in the degradation of aromatic molecules in the environment; lipoxygenases oxidizing fatty acids into leukotrienes and lipoxins – these are potential targets for antiinflammatory drugs; the aromatic amino-acid hydroxylases; isopenicillin *N*-synthase and deacetoxycephalosporin C synthase, important in the synthesis of β-lactam antibiotics such as penicillins and cephalosporins; enzymes involved in the post-translational modification of amino acids in collagen (prolyl and lysyl hydroxylases) and blood-clotting factors. (ii) *Dinuclear non-haem iron enzymes*. These are a number of proteins of diverse biological activity, characterized by the presence of iron–oxo-bridged di- or polyiron aggregates at their

Table 2.3 Mononuclear non-haem iron enzymes classified according both to enzyme type and reaction type. Reprinted with permission from Holm *et al.*, 1996. Copyright (1996) American Chemical Society.

Enzyme Type	Reaction Type	Representative Enzyme	Catalytic Reaction
		Mononuclear non-haem iron enzymes	
intramolecular	intradiol dioxygenation	protocatechuate 3,4-dioxygenase (PCD)	
	extradiol dioxygenation	catechol 2,3-dioxygenase (CTD)	
	hydroperoxidation	lipoxygenase (LO)	
	cis-hydroxylation	phthalate dioxygenase (PDO)	
external monooxygenase	hydroxylation	ω-hydroxylase (ωH)	

intermolecular dioxygenase

pterin-dependent hydroxylation

phenylalanine hydroxylase (PAH)

PAH (Fe^{II})

O_2, H$_4$biopterin   H$_2$O, H$_2$biopterin

α-ketoglutarate-dependent hydroxylation

clavaminate synthase (CS)

CS (Fe^{II})

O_2, α-KG CO_2, succinate

oxidase

α-ketoglutarate-dependent 4e$^-$ oxidation

clavaminate synthase

CS (Fe^{II})

O_2, α-KG   H$_2$O, CO_2, CO_2, succinate

CS (Fe^{II})

O_2, α-KG   H$_2$O, CO_2, CO_2, succinate

4e$^-$ oxidation

isopenicillin N-synthase (IPNS)

IPNS (Fe^{II})

O_2 2H$_2$O

metallic cores, and (iii) proteins involved in iron transport, either directly (transferrins) or indirectly, as receptors for the internalization of extracellular iron transport molecules (transferrin receptors and siderophore receptors).

We will deal here only with proteins of class (ii) that contain diiron centres and reserve the discussion of proteins containing polyiron oxo aggregates (ferritins) until Chapter 6. As for the proteins of class (iii), their discussion is deferred until Chapter 3 concerning siderophore receptors and Chapter 5 concerning the transferrins and their receptors respectively.

2.5.1   Mononuclear Non-haem Iron Enzymes

Dioxygen reduction (oxidase activity) and activation for incorporation into organic substrates are catalysed by a number of mononuclear non-haem iron enzymes. We will first consider the intramolecular dioxygenases, in which both atoms of oxygen are introduced into the substrate, then the monoxygenases (in which we choose to include the pterin-dependent hydroxylases), the large family of α-hetoacid-dependent enzymes, and finally isopenicillin *N*-synthase.

Dioxygenases

The catechol dioxygenases (Table 2.3) are part of nature's strategy for the degradation of aromatic compounds in the environment. They are found in soil bacteria and catalyse the final ring-opening step in the biodegradation of catechols, transforming aromatic precursors into aliphatic products. The intradiol-cleaving enzymes use Fe(III). In contrast, the extradiol-cleaving enzymes use Fe(II) (and occasionally Mn(II)), and are similar to the mammalian homogentisate 1,2-dioxygenase that operates the ring-opening of homogentisate in the oxidative degradation of phenylalanine and tyrosine. The metal sites of protocatechuate 3,4-dioxygenase, an intradiol-cleaving catechol dioxygenase, and of 2,3-dihydroxybiphenyl 1,2-dioxygenase, an extradiol-cleaving catechol dioxygenase are presented in Figure 2.11. The X-ray structure of protocatechuate 3,4-dioxygenase shows a trigonal bipyrimidal ferric iron site ion coordinated by four endogenous protein ligands (Tyr-408, Tyr-447, His-460 and His-462) with a bound solvent molecule completing the trigonal iron coordination in the equatorial plane. In contrast, the coordination geometry of 2,3-dihydroxybiphenyl 1,2-dioxygenase reveals a square pyramidal iron site with three endogenous protein ligands (His-146, His-210 and Glu-260) and two ligands derived from the solvent. The two classes of catechol diooxygenases have distinctly different regiospecificities. The intradiol-cleaving catechol dioxygenases bind substrate in a bidentate anionic mode and the mechanism proposed involves an electrophilic attack of bound substrate by O_2, whereas the extradiol-cleavage enzymes bind substrate in a bidentate monoanionic mode and their mechanism is proposed to involve nucleophilic attack of bound substrate by O_2^-. Full details on the mechanisms of these dioxygenases can be found in Que and Ho (1996).

Lipoxygenases, which catalyse the oxidation of unsaturated fatty acids containing the *cis,cis*-1,4-pentadiene moiety to the corresponding 1-hydroperoxy-*trans,cis*-2,4-diene (Table 2.3), are widely distributed in plants and animals. The mammalian
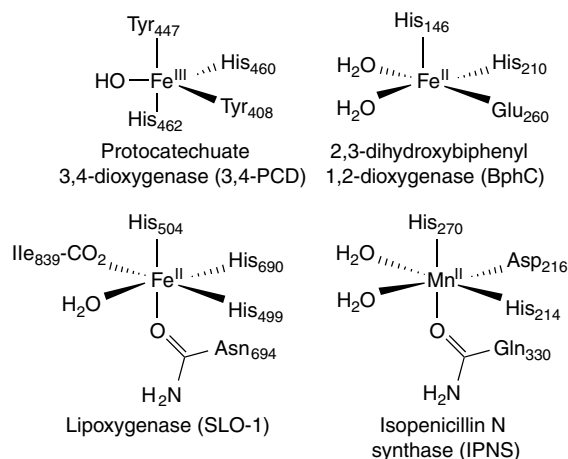
Figure 2.11 Metal coordination sites of crystallographically characterized mononuclear non-haem enzymes. Reprinted with permission from Que and Ho, 1996. Copyright (1996) American Chemical Society.

enzymes typically act on arachadonic acid to produce hydroperoxides, which are precursors of leukotrienes and lipoxins, both classes of compounds being implicated as mediators of inflammation. The crystal structures of several lipoxygenases have been determined and the iron coordination site, consisting of three histidines and one carboxylate (derived from the *C*-terminal Ile residue), is shown in Figure 2.11. In one of the lipoxygenase structures a fifth endogenous ligand, Asn-694, has also been identified. Mutagenesis of the corresponding Asn-713 in soybean lipoxygenase suggests that this Asn is not required for iron binding, but is important for catalysis. As isolated lipoxygenase is in an inactive Fe(II) high spin form, which must be oxidized to the high spin Fe(III) to elicit enzymatic activity; mechanistic proposals for lipoxygenase are summarized in Que and Ho (1996).

The Rieske oxygenases, which require a mononuclear non-haem iron centre and a Rieske-type Fe_2S_2 cluster, are involved in the oxygenation of aromatic compounds in the soil. The best studied examples are phthalate dioxygenase and 4-methoxybenzoate *O*-demethylase. The former, which catalyses the *cis*-dihydroxylation of the phthalate C4–C5 double bond (Table 2.3), is an example of a class of important *cis*-dihydroxylating enzymes (e.g. benzoate 1,2-dioxygenase, toluene 2,3-dioxygenase) which catalyse the initial step in the degradation of aromatic rings; the dihyrodiol products are precursors to catechols that are cleaved by the catechol dioxygenases described above. The mononuclear iron appears to be high spin Fe(II) and is 6-coordinated as isolated, but becomes 5-coordinate on substrate binding, presumably priming it for binding O_2.

Hydroxylases

Among the mononuclear non-haem iron enzymes catalysing hydroxylation reactions (Table 2.3) we can distinguish between intramolecular dioxygenases and external mononoxygenases. The former can be divided into those which are pterin-dependent and those which use α-ketoacids such as α-keto glutarate as obligatory

cofactor. Of the external monooxygenase family very little structural information is available for the ω-hydroxylase. In contrast, progress has been important in recent years on the phenylalanine, tyrosine and tryptophan hydroxylases of mammals, a class of functionally and structurally closely related enzymes (Flatmark and Stevens, 1999)[‖]. All of these monooxygenases (or mixed-function oxidases) share a common mechanism in which dioxygen is used by an active site containing a single weakly bound high-spin ferrous ion to incorporate one atom of the dioxygen molecule into the aromatic substrate, and the other into water with concomitant two-electron oxidation of a cofactor; this may be rubredoxin for the ω-hydroxylase, or tetrahydrobiopterin for the amino-acid hydroxylases (Table 2.3). The reactions catalysed by the latter are important in mammalian metabolism. Phenylalanine hydroxylase initiates the catabolism and detoxification of high levels of phenylalanine, while tyrosine hydroxylase and tryptophan hydroxylase catalyse the rate-limiting steps in the biosynthesis of the neurotransmitters/hormones dopamine/noradreanaline/adrenaline and serotonin, respectively.

   The amount of structural information on the aromatic amino-acid hydroxylases, particularly crystal structures of phenylalanine hydroxylase and tyrosine hydroxylase, has given us new insights into these enzymes. They are all composed of three structural and functional domains: regulatory, catalytic and tetramerization. A full enzyme structure model for phenylalanine hydroxylase is presented in Figure 2.12(a) (Plate 3). The subunit with its three domains is shown on the left and the holoenzyme tetramer on the right. The iron-binding site in phenylalanine hydroxylase and tyrosine hydroxylase are shown in Figure 2.12(b) (Plate 3). In the former the Fe(II) ion is hexacoordinate with octahedral geometry, and one of the axial water molecules (opposite His-285) is displaced upon binding of L-Phe. In tyrosine hydroxylase, the iron is thought to be pentacoordinate. A fuller discussion of these two enzymes and of the inborn errors of metabolism resulting from mutations in their amino-acid sequence can be found in Flatmark and Stevens (1999).

α-Ketoacid-dependent Enzymes

The α-ketoacid-dependent enzymes are distinguished from other non-haem iron enzymes by their absolute requirement for an α-ketoacid cofactor as well as Fe(II) and O_2 for activity. They catalyse two types of reaction (Table 2.3), hydroxylation and oxidation. In both, the α-ketoglutarate is decarboxylated and one oxygen atom introduced into the succinate formed: in the hydroxylases, the other oxygen atom is introduced into the substrate, while in the oxidases it is found in water, together with the cyclized product. In general these enzymes require one equivalent of Fe(II) an α-ketoacid, usually α-ketoglutarate and ascorbate. Examples of these enzymes include proline 4-hydroxylase, prolyl and lysyl hydroxylase, which

---

[‖] While the first of these two authors is a long-time colleague and friend, I was touched by Raymond Stevens's affiliation – Institute for Childhood and Neglected Diseases at the Scripps Institute – in a caring modern society can we still have neglected diseases of childhood? And then I return to my lecture notes on PKU and find that post-natal diagnosis is not carried out for altruistic reasons, but simply because the cost of caring for those born with the disease outweighs by a factor of ten the costs of diagnosis and perinatal care. So what happens to the Neglected and Orphan Diseases?

hydroxylate specific prolyl and lysyl residues in collagen[††] important in its maturation; thymine hydroxylase; deacetoxy/deacetylcephalosporin C synthase, which catalyses the ring expansion of isopenicillin N to deacetoxycephalosporin C and its subsequent hydrolysis to deacetylcephalosporin C; clavaminate synthase, a key enzyme in the synthesis of clavulanic acid, an important β-lactamase inhibitor; and 4-hydroxyphenylpyruvate dioxygenase, which converts 4-hydroxyphenylpyruvate to homogentisate, an important step in the catabolism of tyrosine. The latter enzyme is unusual in that it incorporates both oxygens into the same molecule, since the α-ketoacid which is decarboxylated is the side chain pyruvate of the substrate. A possible reaction mechanism for this class of enzymes involves initial ligation of the α-ketoacid to the Fe(II), followed by binding of O_2 to the Fe(II) centre forming an Fe(III)-superoxide adduct. Attack of the bound O_2 on the ligated α-ketoacid results in decarboxylation followed by substrate binding to give the oxygenated substrate, a carboxylic acid and the Fe(II) enzyme (Que and Ho, 1996). A similar class of non-haem enzyme known as ethylene-forming enzymes, do not require α-keto glutarate, using ascorbate as a stoichiometric reductant instead.

Isopenicillin N Synthase

The importance of penicillin- and cephalosporin-related antibiotics in clinical medicine cannot be underestimated, and has stimulated the study of their biosynthetic pathways. The key steps in the biosynthesis of these antibiotics in some microorganisms are the oxidative ring closure reactions of δ-(L-α-aminoadipoyl)-L-cysteinyl-D-valine (ACV) to form isopenicillin N, the precursor of penicillins and cephalosporins. The enzyme that catalyses this transformation is isopenicillin N synthase (Table 2.3), which requires Fe(II) and O_2 for activity. The overall reaction utilizes the full oxidative potential of O_2, giving two molecules of H_2O for each O_2. As we saw earlier, these enzymes are technically oxidases and the four electrons required for dioxygen reduction come from the substrate. The crystal structure of the Mn-substituted enzyme from *Aspergillus nidulans* has been reported and establishes that the six-coordinate Mn ion is bound to the enzyme through four endogenous protein ligands (two His, an Asp and a Gln) and two solvent H_2O molecules (Figure 2.11). A reaction mechanism has been proposed (Baldwin and Bradley, 1990) which is discussed in Que and Ho (1996).

Superoxide Dismutases

One last class of mononuclear non-haem iron enzyme that we have not yet considered, consists of the microbial superoxide dismutases with Fe(III) at their active site. The crystal structure of the *E. coli* enzyme shows a coordination geometry reminiscent of protocatechuate 3,4-dioxygenase, with four endogenous protein ligands, three His and one Asp residue, and one bound water molecule (Carlioz *et al.*, 1988).

[††] This of course goes a long way to explaining the association of scurvy with vitamin C deficiency, and the successful utilization by the British navy of lime juice as a means of prevention of the disease – hence the expression 'limey' for British sailors.

Table 2.4 Some properties of diiron proteins. From Kurz, 1997. Reproduced by permission of Springer-Verlag.

Protein	Source	Diiron site function	Diiron-binding sequence motif[a]	Diiron(III) solvent bridge
Hemerythrin (myohemerythrin)	Marine invertebrates	O_2 carrier	$HX_{29}HX_3EX_{16}HX_3H-X_{23/28}HX_4D$	Oxo
Ribonucleotide reductase	*E. coli*, viruses, mammals	Tyrosyl radical generator	$DX_{33}EX_2HX_{85}EX_{33}EX_2H$	Oxo
Purple acid phosphatase[b]	Plants, uterine fluid, beef spleen, bone	Phosphate ester hydrolysis	$[D_{28}DX_{31}YX_{33}NX_{33}H-X_{50}HX_{36}H]$	Hydroxo or aqua
Methane monooxygenase	Methanotrophic bacteria	Methane hydroxylation	$EX_{29}EX_2HX_{64}EX_{33}EX_2H$	Hydroxo, aqua
Ferritin, bacterioferritin	Vertebrates, bacteria	Ferroxidase (?)	$EX_{34}EX_2HX_{41}EX_{36}E$ $[EX_{32}EX_2HX_{39}EX_2H]$	?
Rubrerythrin (nigerythrin)	Anaerobic bacteria	Ferroxidase (?)	$EX_{32}EX_{40}EX_2EX_{30}EX_2H$	Oxo
Stearoyl-acyl carrier protein Δ^9-desaturase	Higher plants	HC—CH $\longrightarrow$ C=C	$EX_{37}EX_2HX_{52}EX_{32}EX_2H$	Oxo
Toluene-4-monooxygenase	*Pseudomonas* sp.	Toluene-4-hydroxylation	$[EX_{29}EX_2HX_{59}EX_{33}EX_2H]$	Hydroxo and/or aqua
Membrane stearoyl-CoA Δ^9 desaturase	Mammals, plants	HC—CH $\longrightarrow$ C=C	$[HX_{3-4}HX_{20-50}HX_{2-3}HH-X_{100-200}HX_{2-3}HH]$	Oxo (?)

[a]Sequence motifs in brackets are proposed; others are based on X-ray crystal structures of the diiron-containing proteins.
[b]May not be a diiron-oxo protein as defined here.

2.5.2   Dinuclear Non-haem Iron Enzymes

(μ-Carboxylato)diiron Proteins

A large number of proteins containing non-haem, non-sulfur, carboxylate-bridged diiron sites have been lumped together under the description 'diiron-oxo' proteins, probably due to the common misconception that all members of the family contain an oxo bridge. Although it is well established that haemerythrin, the original (and for many years the only) member of this class, contains an oxo-bridged diiron(III) site (Kurz, 1997), at least three members of the family contain diiron sites that have yet to be shown to contain a stable oxo bridge. However, they almost certainly contain hydroxy (or aqua) bridges in their diiron(III) forms. The common link in all of these 'diiron-oxo' proteins is that they react with dioxygen as part of their functional processes. A more apt structural description of metal sites of this class of proteins would be '(μ-carboxylato)diiron' (Nordlund and Eklund, 1995). They all contain a four-helix-bundle protein fold, surrounding a (μ-carboxylato)diiron core with the two iron atoms separated by 0.4 nm or less, one or more bridging
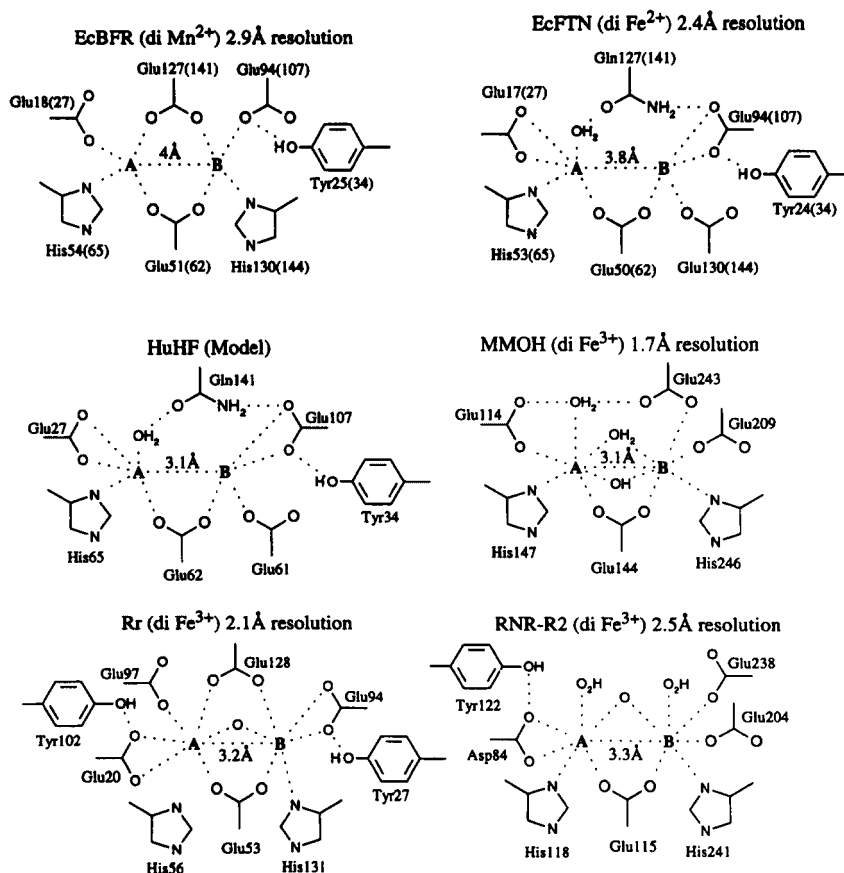
Figure 2.13   Schematic diagrams of diiron centres in rHuHF, EcFTN, EcBFR, DvRrn RNR-R2 and MMOH. Reprinted from Harrison *et al.*, 1998, by courtesy of Marcel Dekker, Inc.

carboxylate ligands, with terminal carboxylate and/or histidine ligands, and a bridging oxo, hydroxo or aqua ligand, at least at the diiron(III) oxidation level (Kurz, 1997). At least eight distinct types of protein have now been shown to have stable functional carboxylate-bridged diiron sites containing oxo, hydroxo or aqua bridges (Table 2.4). They include: haemerythrin (Hr) (and myohaemerythrin), the R2 subunit of ribonucleotide reductase (RNE-R2), purple acid phosphatase, the hydroxylase component of methane monooxygenase (MMOH), ferritins and bacterioferritins, rubrerythrin (Rr) (and nigererythrin), stearoyl–acyl carrier protein desaturase, and the hydroxylase component of toluene-4-monooxygenases. The diiron-containing purple acid phosphatases clearly belong to a separate class, since they do not have the four helix bundles found in the X-ray crystal structures of the other seven (Nordlund and Eklund, 1995), and their diiron sites do not appear to react with dioxygen, and are not discussed further. Despite the striking structural similarities, they represent an enormous functional diversity, and raise the interesting question as to how we can correlate the geometry of their diiron sites with their different reactivity towards O_2 and additional substrates. The iron ligands
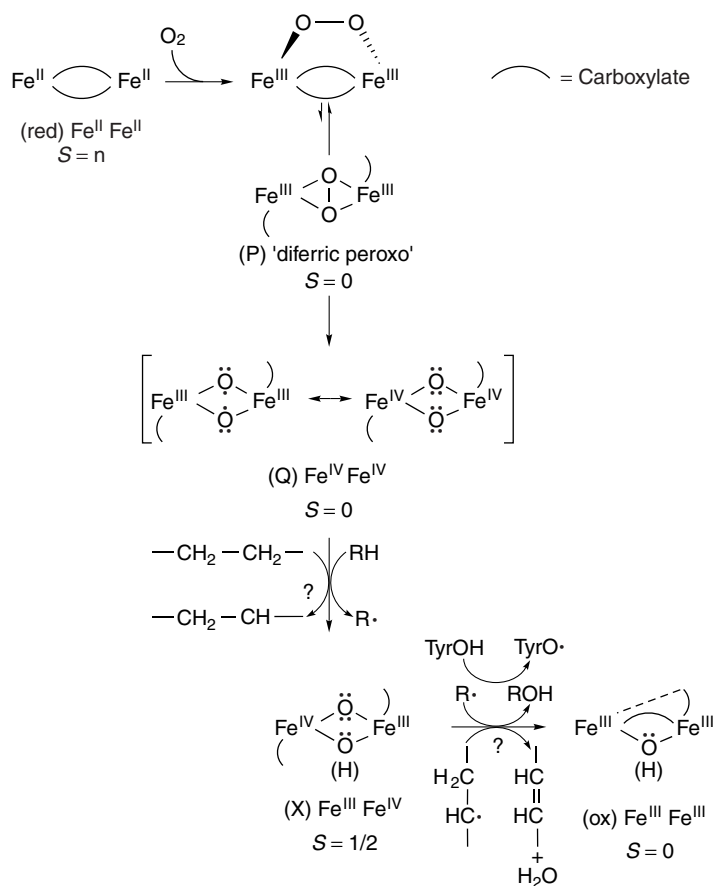
Figure 2.14   A possible scheme for the reactions of diiron centres with O_2 and substrates. Formal oxidation states, ground spin states and shorthand letter designations are listed below each diiron species. Reprinted from Kurz, 1997, by courtesy of Marcel Dekker, Inc.

in the dinuclear sites of many of these proteins are very similar, and the structures of the (μ-carboxylato)diiron cores found for MMOH, RNR-R2, DvRr and EcFTN and those deduced for EcBFR and HuHF are presented in Figure 2.13. The structure of the diiron(II) site in Hr, the sole O_2 carrier in the group, is clearly different from the others, as we can infer from the diiron sequence motifs listed in Table 2.4. The Hr diiron site is clearly more His rich, and it lacks the characteristic $(D/E)X_{30-37}EX_2H$ ligand sequence motifs, and is the only structure to have a solvent bridge in the reduced state as well. It appears that the diiron site in Hr only permits terminal O_2 coordination to a single iron atom with very little rearrangement of the diiron coordination sphere. In contrast, the oxygen-activating diiron(II) centres present open or labile coordination sites on both irons of the centre and show a much greater coordinative flexibility upon oxidation to the diiron (III) state. In both MMOH and RNR-R2, oxidation of Fe^{2+} to Fe^{2+} results in shortening of the Fe–Fe distance. Intermediates at the formal Fe(III) Fe(III) and Fe(IV) Fe(IV) oxidation levels for MMOH and formal Fe(III) Fe(IV) oxidation level for RNR-R2 have been identified during reactions of the diiron(II) sites with O_2. An $[Fe_2(\mu O_2)]^{4+,\ 3+}$ 'diamond core' structure has been proposed for the latter two oxidation levels (Figure 2.14). The intermediate at the Fe(III) Fe(IV) oxidation level in RNR-R2 is kinetically competent to generate a stable functionally essential tyrosyl radical, whilst the Fe(IV) Fe(IV) oxidation level is presumed to carry out the hydroxylation of hydrocarbons in MMOH. The mechanism of the hydroxylation remains controversial.

2.6 References

Babcock, G.T. (1999). *Proc. Natl Acad. Sci., USA*, **96**, 12971–3.

Baldwin, J.E. and Bradley, M. (1990). *Chem. Rev.*, **90**, 1079–2907.

Beinert, H. (2000). *J. Biol. Inorg. Chem.*, **5**, 2–15.

Bohr, C., Hasselbach, K.A. and Krogh, A. (1904). *Skand. Arch. Physiol.*, **15**, 401–12.

Carlioz, A., Ludwig, M.L., Stallings, W.C., Fee, J.A., Steinman, H.M. and Touati, D. (1988). *J. Biol. Chem.*, **263**, 1555–62.

Cowan, J.A. (1997). *Inorganic Biochemistry: An Introduction*, Second edition, Wiley-VCH, New York.

Einsle, O., Messerschmidt, A., Stach, P., Bourenkov, G.P. *et al*. (1999). *Nature*, **400**, 476–80.

Ferguson-Miller, S. and Babcock, G.T. (1996). *Chem. Rev.*, **99**, 2889–907.

Flatmark, T. and Stevens, R.C. (1999). *Chem. Rev.*, **99**, 2137–60.

Frausto da Silva, J.J.R. and Williams, R.J.P. (1991). *The Biological Chemistry of the Elements*, Oxford University Press, Oxford.

Garfinkel, D. (1958). *Arch. Biochem. Biophys.*, **77**, 493–509.

Harrison, M.D., Jones, C.E. and Dameron, C.T. (1999). *J. Biol. Inorg. Chem.*, **4**, 145–53.

Hayaishi, O. (1974). In *Molecular Mechanisms of Oxygen Activation* (ed. Hayaishi, O.), Academic Press, New York, pp. 1–28.

Hayaishi, O., Katagiri, M. and Rothberg, S. (1955). *J. Am. Chem. Soc.*, **77**, 5450–1.

Holm, R.H., Kennepohl, P. and Solomon, E.I. (1996). *Chem. Rev.*, **96**, 2239–314.

Huber, C. and Wächtershäuser, G. (1998). *Science*, **281**, 670–2.

Iwata, S., Lee, J.W., Okada, K., Lee, J.K. *et al*. (1998). *Science*, **281**, 64–71.

Iwata, S., Ostermeier, C., Ludwig, B. and Michel, H. (1995). *Nature*, **376**, 660–9.

Keilin, D. (1925). *Proc-R. Soc. (London)*, **98B**, 312–39.

Klingenberg, M. (1958). *Arch. Biochem. Biophys.*, **75**, 376–86.

Kurz, D.M. Jr. (1997). *J. Biol. Inorg. Chem.*, **2**, 159–67.

Lippard, S.J. and Berg, J.M. (1994). *Principles of Bioinorganic Chemistry*, University Science Books, Mill Valley, California, p. 290.

Mason, H.S., Fawlks, W. and Peterson, J. (1955). *J. Am. Chem. Soc.*, **77**, 2914–5.

Mason, H.S., North, J.C. and Vanneste, M. (1965). *Fed. Proc., Fed. Am. Soc. Exp. Biol.*, 1172–80.

Murphy, T.P., Lean, D.R.S. and Nalewajko, C. (1976). *Science*, **192**, 900–2.

Nordlund, P. and Eklund, H. (1995). *Current Opin. Struct. Biol.*, **5**, 758–66.

Omura, T. and Sato, R. (1964). *J. Biol. Chem.*, **239**, 2370–8.

Pearson, R.G. (1963). *J. Am. Chem.*, **85**, 3533–9.

Perutz, M.F. (1970). *Nature*, **228**, 726–39.

Perutz, M.F. (1979). *Ann. Rev. Biochem.*, **48**, 327–86.

Perutz, M.F., Wilkinson, A.J., Paoli, M. and Dodson, G.G. (1998). *Ann. Rev. Biophys. Biomol. Struct.*, **27**, 1–34.

Pierik, A.J., Roseboom, W., Happe, R.P., Bagley, K.A. and Albracht, S.P.J. (1999). *J. Biol. Chem.*, **274**, 3331–7.

Poulos, T.L., Finzel, B.C., Gunsalus, I.C., Wagner, G.C. and Kraut, J. (1985). *J. Biol. Chem.*, **260**, 16122–30.

Que, L. Jr. and Ho, R.Y.N. (1996). *Chem. Rev.*, **99**, 2607–24.

Smith, D. and Williams, R.J.P. (1970). *Struct. Bonding,* **7**, 1–45.

Smith, J.L. (1998). *Science*, **281**, 58–9.

Sono, M., Roach, M.P., Coulter, E.D. and Dawson, J.H. (1996). *Chem. Rev.*, **96**, 2841–2887.

Stubbe, J. and van der Donk, W.A. (1998). *Chem. Rev.*, **98**, 705–62.

Tsukihara, T., Aoyama, Y., Yamashita, E., Tomizawa, T. *et al*. (1995). *Science*, **269**, 1069–74.

Tsukihara, T., Aoyama, O., Yamashita, E., Tomizawa, T. *et al*. (1996). *Science*, **272**, 1136–44.

Vallee, B.L. and Williams, R.J.P. (1968). *Proc. Natl Acad. Sci. USA*, **59**, 198–505.

Van den Berg, W.A., Hagen, W.R. and van Dongen, W.M. (2000). *Eur. J. Biochem.*, **267**, 666–76.

Voet, D. and Voet, J.G. (1995). *Biochemistry*, Second edition, John Wiley & Sons, Chichester.

Williams, R.J.P. (1961). *Fed. Proc., Fed. Am. Soc. Exp. Biol.*, **20**, Suppl. **3**, 10–5.

Williams, R.J.P. (1985). *Eur. J. Biochem.*, **150**, 231–48.

Williams, R.J.P. (1995). *Eur. J. Biochem.*, **234**, 363–81.

Xia, D., Yu, C.A., Kim, H., Xia, J.Z., *et al*. (1997). *Science*, **277**, 60–6.

3 Microbial Iron Uptake

3.1 Introduction

Bacteria have developed a large variety of iron-uptake systems, which probably reflect the type of iron sources in their particular environment at a given time. Since the environment of the bacteria can change, for example *Escherichia coli* cells in the gut can later be found in sewage, soil, blood and the meninges, several iron-transport systems exist in parallel in one organism. In *E. coli* K-12, the standard laboratory strain used for the elucidation of *E. coli* physiology, genetics, and molecular biology, one plasmid-encoded and six chromosomally encoded iron-transport systems have been identified. This strain has maintained all of these iron-transport systems during years of cultivation in the laboratory since its isolation from the stool of a convalescent diphtheria patient in 1922.

Bacteria obtain the iron that they require by synthesizing and secreting strong and highly specific Fe^{3+}-complexing compounds, termed siderophores, which are taken up by specific transport systems. They also use ambient iron sources, such as Fe^{3+}-loaded siderophores from other bacteria and fungi, as well as haem, haemoglobin, haemopexin, transferrin, and lactoferrin from their mammalian hosts (Figure 3.1). The transport systems for the latter compounds are highly specific in that, for example, only human transferrin, and not bovine or porcine transferrins, supports growth of the human pathogens *Neisseria meningitidis* and *Haemophilus influenzae*, and only primate transferrins bind to the human pathogens (Gray-Owen and Schryvers, 1993).

Iron-transport systems are usually studied using cells in liquid cultures, which guarantees that each cell experiences the same conditions. Results obtained this way usually agree with results obtained using cells from colonies grown on nutrient agar plates. Cells in colonies are exposed to different conditions depending on their location: oxic conditions at the colony surface, microaerophilic and anoxic conditions in the centre, abundant nutrients on the agar, and limiting nutrients close to the surface of the colonies. In nature, bacteria frequently form colonies and even biofilms, and the results obtained under laboratory conditions may not strictly apply to the natural situation. However, reliable results on iron transport mechanisms, the transport proteins involved, and the regulation of transport, can only be obtained under well-defined experimental conditions. Such conditions are usually only met when using mutants in which all but the iron-transport system under study have been inactivated. Fortunately, *E. coli* K-12 synthesizes only one chromosomally
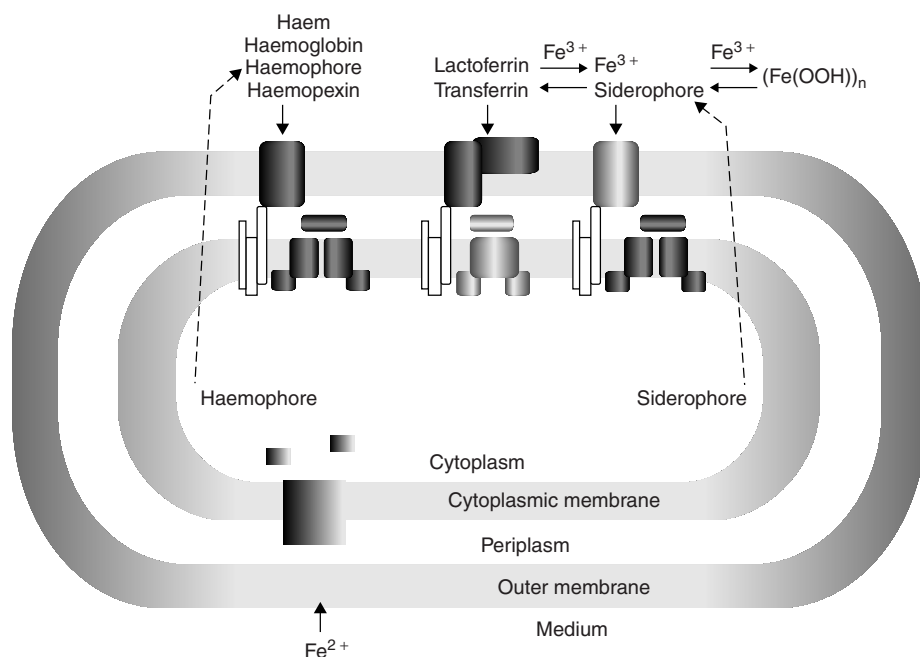
Figure 3.1 Overview of Fe^{3+}- and Fe^{2+}-uptake systems of Gram-negative bacteria. The iron donors bind to one or two outer membrane receptor proteins, which transport Fe^{3+} released from host lactoferrin and transferrin, haem and haem released from haemoglobin and haemopexin, and Fe^{3+}–siderophores synthesized by bacteria and fungi. The three proteins inserted in the cytoplasmic membrane and coupled to the receptors are TonB, ExbB, and ExbD, which provide the energy delivered by the proton-motive force of the cytoplasmic membrane for active transport across the outer membrane. Periplasmic binding proteins deliver Fe^{3+} and Fe^{3+} siderophores to one or two integral cytoplasmic membrane proteins, which translocate them into the cytoplasm at the expense of ATP provided by ATPases associated with the inside of the cytoplasmic membrane (see Figure 4 and text for further details). Transport systems in Gram-positive bacteria look the same except that an outer membrane, the receptor proteins, and the TonB, ExbB, and ExbD proteins are lacking. Under anoxic conditions, Fe^{2+} is transported by the Feo system, which differs from the Fe^{3+} transport systems.

encoded siderophore, enterobactin. Therefore, enterobactin synthesis and transport can be studied without interference from other iron-transport systems (Earhart, 1996). To identify and study other iron transport systems, an *aroB* mutant of *E. coli* K-12, that does not synthesize enterobactin, is used. Without this precaution, Fe^{3+} bound to the added siderophore may be shifted to enterobactin, and as a result, Fe^{3+}–enterobactin transport occurs. Using an *aroB* mutant, it was shown that a transport system for ferrichrome, a fungal Fe^{3+}–siderophore complex, exists in *E. coli* K-12. By supplying citrate, a Fe^{3+}–citrate transport system was discovered and characterized. By transforming *aroB* mutants with certain pColV plasmids, genes for aerobactin synthesis and Fe^{3+}–aerobactin transport were characterized. To study iron transport systems of bacteria other than *E. coli*, mutants are also used. In addition, DNA fragments encoding iron transport or siderophore biosynthesis genes of these bacteria are introduced into *E. coli* K-12 *aroB*, and the systems are subsequently characterized in this standard organism.

This chapter emphasizes common principles in bacterial iron transport without attempting to cover the many facets of the large variety of bacterial solutions to the iron supply problem. Those systems that have been most extensively studied genetically and biochemically will be discussed. A rapidly increasing body of information is being built up from comparisons of gene sequences, with the assumption that sequence similarities indicate similar functions. In most cases, this may turn out to be true, but results from purely *in silico* studies should be considered with caution. The results should be used as a guide for experiments aimed at identifying the most likely iron supply system and unravelling the way it functions. For more comprehensive reviews or reviews on specific aspects of microbial iron supply, the reader is referred to the recent publications of Braun *et al*. (1998), Hantke and Braun (2000), Crosa (1997), Wandersman and Stojiljkovic (2000), Schryvers and Stojiljkovic (1999), Mietzner *et al*. (1998), Expert *et al*. (1996) and Ratledge and Dover (2000).

3.2 Siderophores

Siderophores are iron-complexing compounds of low molecular weight that are synthesized by bacteria and fungi, and serve to deliver iron to the microbes. Because of their exclusive affinity and specificity for Fe^{3+}, natural siderophores and synthetic derivatives have been exploited in the treatment of human iron-overload diseases. The most successfully used example is Desferal®, which is the methane sulfonate derivative of iron-free ferrioxamine B, a linear trihydroxamate (Figure 3.2). Ferrioxamine was isolated in 1958 from the culture supernatant of *Streptomyces*
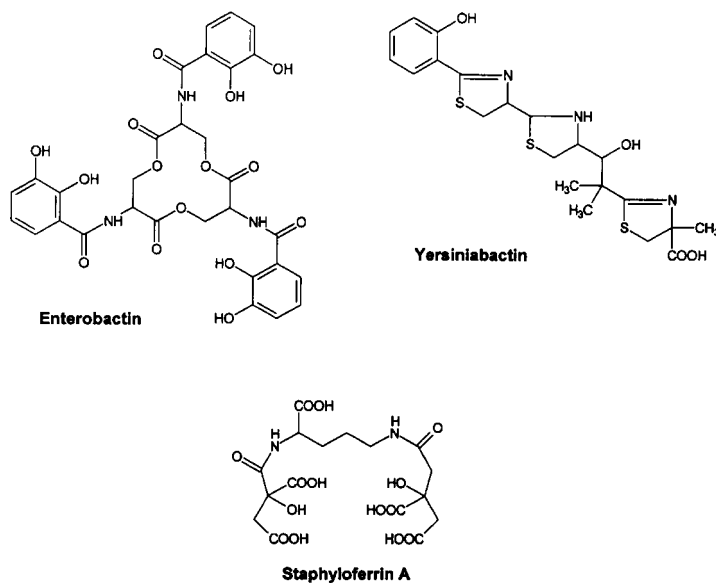
Figure 3.2 Chemical structures of selected siderophores to demonstrate the four major structural classes and the different solutions of microorganisms to scavenge iron. See for comparison the conformations of the Fe^{3+}-complexes of ferrichrome and albomycin shown in Figure 3.5.

Pseudobactin 358

Ferrichrome

Albomycin δ_2
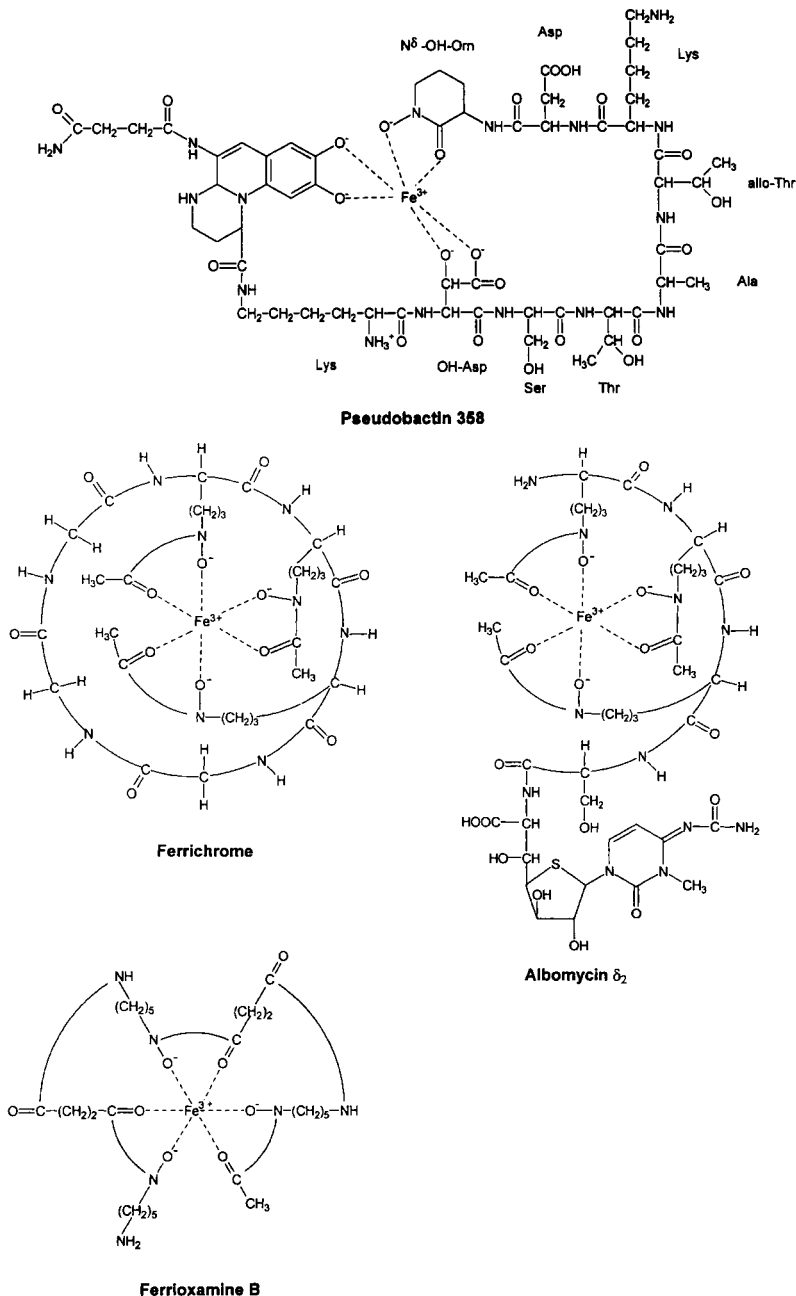
Ferrioxamine B

Figure 3.2   (*continued*)

pilosus ETH21748 after it had been recognized that ferrioxamine antagonized the killing of *Staphylococcus aureus* by ferrimycin from *Streptomyces griseoflavus* ETH 9578 (Bickel *et al.*, 1960). We now know that the antagonism is caused by competition for the same transport system. The research group at the Eidgenössische Technische Hochschule (ETH) in Zürich had actually been interested in finding new antibiotics,

and ferrimycin was the first pure siderophore antibiotic isolated. This original work and the previous isolation of ferrichrome from the culture of *Ustilago sphaerogena* (Neilands, 1952) stimulated research that resulted in the elucidation of the structures of several hundred siderophores. Siderophores are studied in order to understand the ways in which microorganisms overcome the extreme iron shortage to which they are exposed under oxic conditions; to unravel the role that iron plays in the pathogenicity of microorganisms for humans, animals, and plants; to find new siderophore antibiotics; to use them as carriers for antibiotics that otherwise would not enter microbial cells, and last but not least, to find new chelators to treat iron-overload diseases orally, in contrast to Desferal®, which has to be administered intravenously. More applications can be envisaged if siderophores can be inexpensively produced: to combat plant pathogens by iron withdrawal; to supply iron to humans, animals, and plants, and to remove rust from metal surfaces.

Siderophores can be classified into five principal groups according to their chemical structures: hydroxamates, catecholates, carboxylates, heterocyclic compounds, and mixed types (Winkelmann and Drechsel, 1997). All the natural siderophores are designed to chelate Fe(III) selectively, which under aerobic conditions is the predominant, and potentially bioaccessible form of iron in the environment (Chapter 1). This means that they usually contain hard O-donor atoms as ligands, and form thermodynamically extremely stable complexes with Fe(III)[†] Examples are given in Figure 3.2 with their corresponding pFe values in the text; ferrichrome (pFe = 25.2) is drawn such that the similarity to albomycin, a highly effective antibiotic, becomes obvious. The crystal structure of ferrichrome and the identical structure of ferrichrome bound to the FhuA outer membrane transporter show that the bound iron is not in the centre of the molecule. Rather, the hydroxamate configuration around Fe^{3+} forms a substructure separate from the peptide backbone configuration (see Figure 3.5). Ferrichrome is not only of historical interest, but represents one of the most intensively studied Fe^{3+} siderophores with regard to structure, transport, and biosynthesis (Leong and An, 1997). The same applies to enterobactin (also termed enterochelin; pFe = 35.5) (Figure 3.2), which is the prototype of the catecholate siderophores (Earhart, 1996). The X-ray structure of vanadium(IV) enterobactin shows the metal complexed by the six hydroxyl groups in the centre of the molecule (Karpishin *et al.*, 1993). Staphyloferrin A (Figure 3.2) belongs to the carboxylate siderophores and is formed by *Staphylococcus aureus* under iron-limiting growth conditions (Konetschny-Rapp *et al.*, 1990). At first glance, the simplest complex of this type is that formed by Fe^{3+} and citrate, but a closer examination reveals an iron–citrate polymer at pH 7 with a molecular weight of 2.1×10^5; the polymer dissociates predominantly into $[Fe(Cit)_2]^{5-}$ when citrate is in excess (20 mM) over Fe^{3+} (1 mM) (Pierre and Gautier-Luneau, 2000). These latter conditions are those used to study iron–citrate transport and the novel

---

[†] The stability of Fe(III)siderophore complexes can be most conveniently addressed in an empirical approach which does not require knowledge of the K_a of the ligand groups or the denticity of the complex (Raymond *et al.*, 1984). The pM value, in this case, the pFe, is defined from an equilibrium reaction (Telford and Raymond, 1996) as the negative logarithm of the free or uncomplexed Fe^{3+}_{aq} concentration (pFe = $-\log[Fe^{3+}_{aq}]$ calculated from the formation constant for a fixed set of experimental conditions: pH 7.4, a total ligand concentration of 10 μM and $[Fe^{3+}_{aq}]_{tot}$ of 1 μM. The larger the pM value for a particular ligand, the more stable is the metal complex under these standard conditions.

type of iron–citrate transport regulation in *E. coli*. Yersiniabactin (Figure 3.2), an example of a heterocyclic siderophore, was isolated from the culture supernatant of *Yersinia enterocolitica* (Drechsel *et al.*, 1995), and pseudobactin 358 (Figure 3.2) from *Pseudomonas putida* WC358 is one of the most complex heterocyclic siderophores (Abdallah, 1991).

3.2.1 FhuA-mediated Ferrichrome Transport Across the Outer Membrane of *E. coli*

Gram-negative bacteria are surrounded by an outer membrane, consisting of a typical lipid bilayer in which proteins are inserted. The best-characterized outer membrane, that of *E. coli*, forms a permeability barrier for hydrophilic substances larger than 700 Da. Smaller substances, including most nutrients, diffuse through the water-filled pores formed by the porin proteins. Many Fe^{3+}–siderophores have molecular masses larger than 700 Da, which reduces their diffusion rate through the porins to the extent that they no longer meet growth requirements. In addition, release of the siderophores into the growth medium, where they bind the scarce aqueous Fe^{3+} in equilibrium with the insoluble iron hydroxide polymers, various iron chelators, haem, transferrin, lactoferrin, or ferritin, results in a very dilute Fe^{3+} siderophore solution. This would not be sufficient to support growth by simple diffusion into the cells. The Fe^{3+}–siderophores must be extracted from the growth medium by binding to outer membrane receptor proteins, and from there they have to be actively transported across the outer membrane, through the periplasm and then across the cytoplasmic membrane to provide sufficient iron in the cytoplasm. *E. coli* needs approximately 10^5 Fe^{3+} ions per generation to synthesize haem, iron–sulfur proteins, and iron-containing redox enzymes.

Mainly the outer membrane ferrichrome receptor and transporter FhuA will be discussed because most structural and functional studies have been performed with this protein. In fact, FhuA was the first outer membrane protein identified (called TonA), with known functions as a phage and colicin receptor, that are related to iron transport (for a historical account, see Braun and Hantke 1977).

FhuA is encoded by the *fhuA* gene in the *fhuACDB* operon on the *E. coli* chromosome. The *fhuACDB* genes are cotranscribed, and transcription is regulated by a promoter upstream of *fhuA* that responds to the iron content of the cells via negative regulation by the Fur protein with one bound Fe^{2+} ion. Under iron-limiting growth conditions, Fur does not contain bound Fe^{2+}, transcription is derepressed, and the amount of FhuA protein in the outer membrane can increase from a few hundred to over 10 000 molecules per cell. Accordingly, the ferrichrome transport rate is increased. When iron is in surplus, Fe^{2+}–Fur represses transcription. Through this mechanism, the iron content of *E. coli* is regulated, which is important since a surplus of iron kills cells, mainly by damaging DNA (Touati *et al.*, 1995).

The crystal structure of FhuA, with and without bound ferrichrome, has been determined (Ferguson *et al.*, 1998; Locher *et al.*, 1998). FhuA consists of 22 antiparallel transmembrane β-strands extending from residue 161 to residue 723, which form a β-barrel (Figure 3.3, Plate 4). The β-barrel strands are interconnected by large loops at the cell surface and small turns in the periplasm. Such a β-barrel structure is the

principal arrangement of all bacterial outer membrane proteins established to date, including the porins (Koebnik *et al.*, 2000). However, in contrast to the porins, no loop from the cell surface folds inside the barrel to restrict the permeability of the channel. Rather, the FhuA barrel is closed entirely by the *N*-terminal cork domain that enters the β-barrel from the periplasmic side. More than half the FhuA is located above the bilayer membrane. It contains a cavity that is open to the external medium and separated from a periplasmic cavity by a thin short coil of amino-acid residues.

Binding of ferrichrome causes a large structural transition across the entire FhuA molecule. Ferrichrome is fixed above the cork well outside the membrane, by hydrogen bonds and van der Waals contacts, in a binding site formed by eight aromatic residues and one residue each of arginine, glutamine, and glycine. Compared with unloaded FhuA, apex B formed by residues Glu-98 to Gln-100 of the cork domain makes an α-carbon translation of 1.7 Å towards ferrichrome. This and additional movements of residues in the cork domain and the barrel domain largely maintain the FhuA secondary structure up to the periplasmic cavity. There, a short helix (residues 24 to 29) is completely unwound, and the resulting coil bends away by 180° from the previous helix axis, resulting in the transition of Glu-19 a distance 17.3 Å away from its former α-carbon position. A small structural change at the ferrichrome binding site on the cell surface is amplified to a large structural change in the periplasmic cavity. These results are in line with biochemical data that demonstrate upon binding of ferrichrome (i) conversion of isolated FhuA to trypsin resistance at Lys-67, (ii) reduction of monoclonal antibody binding to residues 21 to 59 (Moeck and Coulton, 1998), (iii) decrease in the intrinsic tryptophan fluorescence of FhuA (Locher and Rosenbusch, 1997), (iv) *in vivo* fluorescence quenching of fluorescein-maleimide bound to the genetically introduced Cys-336 residue (Bös *et al.*, 1998), and (v) increase in the formation of a chemically cross-linked complex between FhuA and TonB (Moeck *et al.*, 1997).

The activity of FhuA is dependent on energy input, which is provided by the proton-motive force of the cytoplasmic membrane since there is no energy source in the outer membrane. Energy is transmitted from the cytoplasmic membrane to the outer membrane by a complex consisting of three proteins: TonB, ExbB, and ExbD (Braun, 1995). TonB and ExbD are located in the periplasm with their *N*-termini inserted in the cytoplasmic membrane (Figure 3.4). It has been shown by genetic suppression analyses that FhuA interacts with TonB. Inactive FhuA mutants, with a mutation in the region spanning residues 7–11, which is homologous in all proteins that require TonB for transport, gain partial activity by combining with a mutant in which Glu-160 of TonB is replaced by Leu or Lys (Schöffler and Braun, 1998). This result was taken as evidence that the region covering residues 7–11 of FhuA physically interacts with the region around residue 160 of TonB. This region in FhuA was thus called the TonB box. Overexpressed TonB, which is proteolytically degraded *in vivo*, is stabilized by overexpressed FhuA, and the degree of stabilization is in agreement with the activity of the FhuA TonB box mutants (Günter and Braun, 1990). It was concluded that TonB assumes an energized conformation in response to the proton-motive force, interacts with FhuA, and allosterically opens the FhuA channel. This might occur by a small change in the conformation in the coil that separates the outer and inner cavities of FhuA. The TonB box is not seen in the crystal
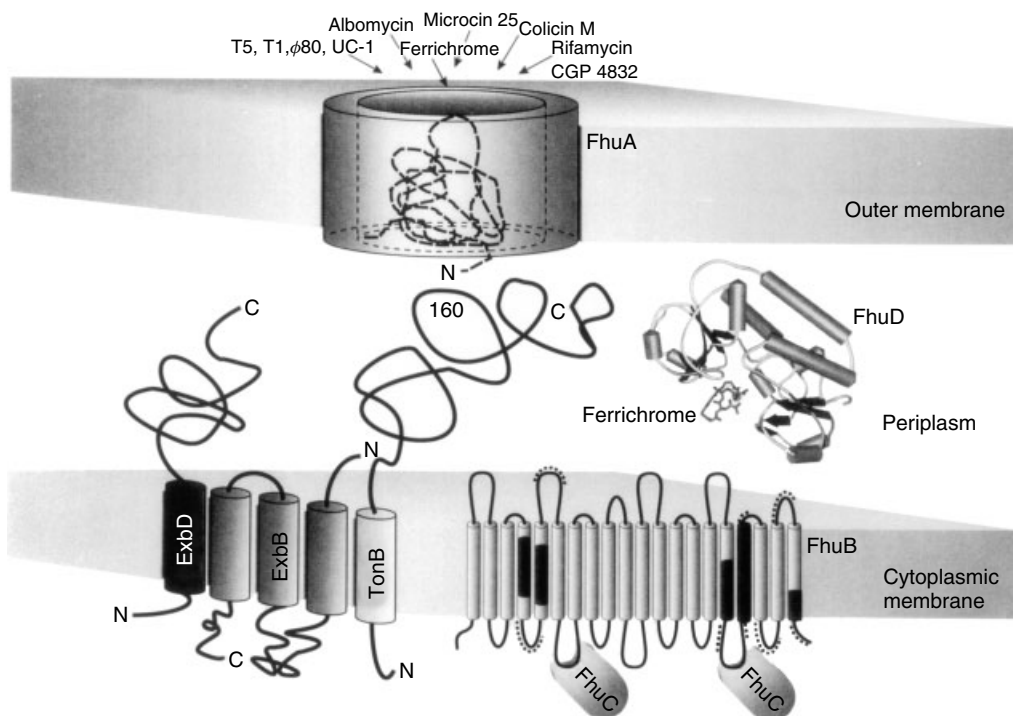
Figure 3.4 Model of the FhuA-catalysed transport of ferrichrome, albomycin, rifamycin CGP 4832, colicin M, and microcin 25 across the outer membrane of *E. coli*, of the FhuA-mediated infection by the phages T5, T1, ϕ80, and UC-1, and of ferrichrome and albomycin transport across the cytoplasmic membrane. The *N*-terminus of FhuA contains the TonB box, which is thought to interact with the Gln-160 region of TonB in the periplasm. The crystal structure of FhuD with bound ferrichrome is shown (Clarke *et al.*, 2000). The regions of FhuB that bind to FhuD, as revealed using synthetic FhuB peptides, are marked by dots in hydrophilic loops that may fold back into the predicted FhuB channel, and by shaded transmembrane segments. Two copies of FhuC, the ATPase, might bind to the indicated FhuB regions, as revealed by mutation analysis.

structure, which is only visible from residue 19, and apparently does not assume a fixed structure. Since Glu-19 is exposed to the periplasm, the TonB box is most likely located in the periplasm, where it interacts with TonB. Binding of ferrichrome enhances interaction of FhuA with TonB, so that preferentially substrate-loaded FhuA is coupled to the energy-providing Ton system (Moeck *et al.*, 1997). Under natural iron-deplete conditions, the amounts of FhuA and the other TonB-dependent transporters are much higher than the amount of TonB, which makes it necessary and economical that the channels of only substrate-loaded transporters are opened by interaction with TonB.

The crystal structure of FepA, the outer membrane transporter of Fe^{3+}–enterobactin, has also been determined (Figure 3.3), and has a structure similar to the FhuA structure (Buchanan *et al.*, 1999). In the FepA structure, the TonB box (residues 12–18) can be clearly seen located inside the barrel and extending into the periplasm, as one would expect from its interaction with the periplasmic portion of TonB.

Interaction between the region around residue 160 of TonB and the TonB box was chemically demonstrated with BtuB, the outer membrane transporter of vitamin B_{12}. This transporter functions similarly as the Fe^{3+}−siderophore receptors. Cysteines introduced into the TonB box and into the region around residue 160 of TonB cross-link spontaneously in living cells (Cadieux and Kadner, 1999). Crosslinking at several positions increases when BtuB is loaded with vitamin B_{12}, and the crosslinking pattern is changed in mutants that contain amino-acid substitutions in BtuB which impair TonB-dependent BtuB activity. Site-directed spin-labelling and electron paramagnetic resonance (EPR) studies indicated that the TonB box of BtuB, in the unliganded conformation, might be localized to a helix that forms specific interactions with side-chain residues from the periplasmic turns of the β-barrel domain of BtuB (Merianos *et al.*, 2000). Binding of vitamin B_{12} to BtuB converts this segment into an extended, disordered, and highly dynamic structure that probably extends into the periplasm to interact physically with TonB. A TonB-uncoupled TonB box mutant of BtuB shows a strongly altered EPR spectrum and no longer responds to the addition of vitamin B_{12}. These results prove beyond doubt the functional interaction of the BtuB TonB box with the region around residue 160 of TonB.

The TonB box is part of the FhuA cork domain. Deletion of the cork should abolish interaction of TonB with FhuA, and FhuA should be converted into an open channel through which ferrichrome diffuses in an energy independent manner. Removal of residues 5−160 of FhuA results in FhuAΔ5−160, which inserts into the outer membrane. Ferrichrome provided at higher concentrations supports growth of these mutant cells independent of TonB. Under these conditions, ferrichrome presumably diffuses through FhuAΔ5−160 into the periplasm. Unexpectedly, at lower ferrichrome concentrations, TonB is still required to support growth and to transport ferrichrome into the cells (Braun *et al.*, 1999). Other TonB-dependent activities of FhuA (Figure 3.4), such as transport of the antibiotics albomycin and rifamycin CGP 4832, infection by the bacterial viruses (bacteriophages) T1 and φ80, and killing of cells by the bacterial protein toxin colicin M, are also mediated by FhuAΔ5−160. All of these results point to other sites of interaction between FhuA and TonB in addition to the FhuA TonB box that contributes to the activity of FhuA. The structural transition in FhuAΔ5−160 upon binding to energized TonB presumably proceeds from the periplasm through the outer membrane to loop 4 exposed at the cell surface since loop 4 is the principal binding site for bacteriophages (Killmann *et al.*, 1995). Phages T1 and φ80 only bind to energized TonB$^+$ cells (Hancock and Braun, 1976) which probably reflects a particular loop 4 conformation. In wild-type FhuA, the predicted structural transition in the cork domain may release ferrichrome from its binding site ($K_D < 0.1$ μM). In FhuAΔ5−160, the remaining amino−acid residues in the barrel domain bind ferrichrome rather weakly (<10 % compared to wild-type FhuA). TonB interaction with the barrel domain might be sufficient to release ferrichrome from this residual site.

FhuA and FepA will prove to be the reference structures for a large group of bacterial outer-membrane transporters that take up bacterial Fe^{3+}−siderophores, Fe^{3+} released from host transferrin and lactoferrin, haem, and haem released from haemoglobin and haemopexin. It is assumed that all iron sources are transported

across the outer membrane of Gram-negative bacteria by a mechanism similar to that for ferrichrome via FhuA and Fe^{3+}–enterobactin via FepA.

3.2.2   FhuA as an Antibiotic Transporter

Albomycin is a structural analogue of ferrichrome to which an antibiotically active thioribosyl moiety has been added (Figures 3.2, 3.5 – for Figure 3.5 see Plate 4). In *E. coli*, the thioribosyl group has to be released from the Fe^{3+}–hydroxamate carrier by the intracellular peptidase N for cells to be killed. Peptidase N mutants are resistant to albomycin; and for these mutants, albomycin serves as an iron supplier (Hartmann *et al.*, 1979; Braun *et al.*, 1983). Albomycin is a highly effective antibiotic since it is actively transported and concentrated inside cells, in contrast to most antibiotics which enter cells by diffusion. Albomycin is transported across the outer membrane via FhuA. The structure of the albomycin–FhuA cocrystal reveals an identical coordination geometry around Fe^{3+}, and the same binding site as ferrichrome on FhuA (Ferguson *et al.*, 2000). The antibiotically active thioribosyl moiety extends into the surface cavity and unexpectedly assumes both an extended and a compact conformation (Figure 3.5). This allows a rather high tolerance of FhuA to ferrichrome side chains due to the space provided by the surface cavity. As the albomycin example demonstrates, active transport of synthetic siderophore-antibiotic conjugates consisting of an iron-chelating siderophore, a peptide linker, and an antibiotic group, may improve the efficacy of those antibiotics that diffuse too slowly into microorganisms to serve as therapeutic drugs (Braun, 2000).

Another unexpected observation supports the tolerance of FhuA for the transport of chemically different substrates. A synthetic rifamycin derivative, CGP 4832, is 200 times more active against *E. coli* than rifamycin because it is transported by FhuA (Pugsley *et al.*, 1987). Since CGP 4832 has structurally nothing in common with ferrichrome (Figures 3.5, 3.6) the structure of CGP-4832–FhuA cocrystals was determined (Ferguson *et al.*, 2001). CGP 4832 occupies a binding site similar to that of ferrichrome. Of the ten amino-acid residues at a distance of less than 4 Å from ferrichrome, nine also participate in binding of CGP 4832. The side chains that differ between CGP 4832 and rifamycin contribute strongly to FhuA binding, which explains the transport of CGP 4832 and lack of transport of rifamycin through FhuA.

3.2.3   Transport of Ferrichrome Across the Cytoplasmic Membrane

The Fe^{3+} taken up by bacteria at their outer membrane in the form of Fe^{3+}–siderophores, Fe^{3+}-citrate, diferric-transferrin, diferric-lactoferrin, and haem is transported by ABC transporters across the cytoplasmic membrane of Gram-positive and Gram-negative bacteria. ABC transporters consist of one or two integral membrane proteins, and one or two ATPases associated with the inner side of the cytoplasmic membrane. The bacterial ABC transporters are the most frequently occurring transporters in bacteria, and they are analogous to the family of eukaryotic multidrug resistance P-glycoproteins (MDRs). For example, in human MDR, the two intrinsic membrane proteins and the ATPases found in bacteria are combined in one polypeptide (Johnstone *et al.*, 2000). In bacteria, ATP hydrolysis
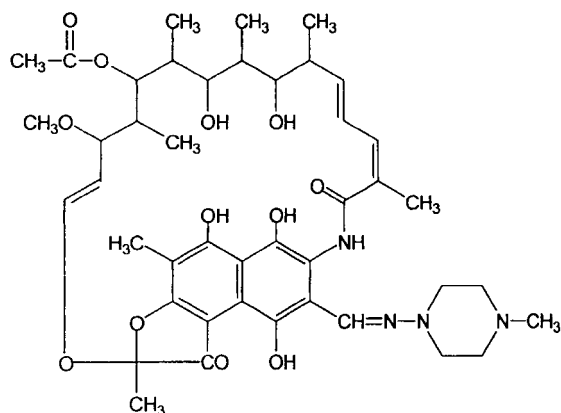
Rifamycin
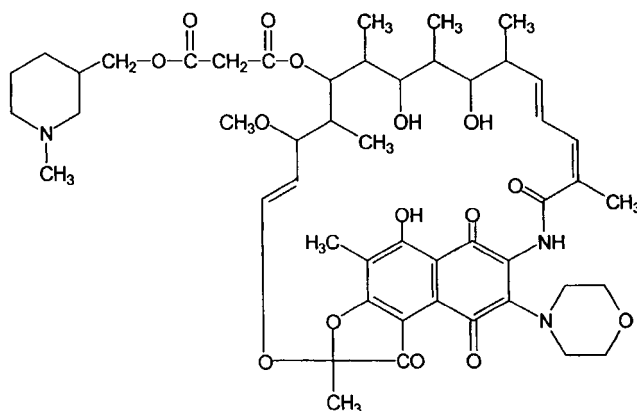
Rifamycin CGP 4832

Figure 3.6 Comparison of the chemical structures of rifamycin (Rifampicin®) and rifamycin CGP 4832; the latter is transported by FhuA. Note the entirely different chemical structures (Figure 3.2) and conformations (Figure 3.5) of the ferrichrome and albomycin FhuA transport substrates.

drives transport across the cytoplasmic membrane, in contrast to transport across the outer membrane which is energized by the proton-motive force of the cytoplasmic membrane (Bradbeer, 1993). There is no evidence that outer membrane transport and inner membrane transport are in any way mechanistically coupled. Rather, it seems that the two transport steps occur independently of each other. An additional protein, termed the binding protein, is essential for transport and is located in the periplasm of Gram-negative bacteria. In Gram-positive bacteria, which are devoid of a periplasm, corresponding binding proteins are anchored by a lipid of the murein lipoprotein type (Hantke and Braun, 1973) to the cytoplasmic membrane (Schneider and Hantke, 1993).

In the ferrichrome transport system (Figure 3.4), FhuD is the periplasmic ferrichrome binding protein, FhuB is the intrinsic cytoplasmic membrane protein, which probably evolved by fusion of two genes, and FhuC is the cytoplasmic

ATPase. Substrate-loaded FhuD protein is thought to interact with FhuB, thereby triggering ATP hydrolysis by FhuC, as has been shown for the transport systems of histidine and maltose reconstituted in lipid vesicles (Bishop *et al*., 1989; Davidson *et al*., 1992). FhuD is less specific than FhuA in that it binds and transports a variety of ferric hydroxamates, such as ferrichrome, coprogen, aerobactin, ferrioxamine B, shizokinen, rhodotorulic acid, and the antibiotic albomycin. Binding of iron(III) hydroxamates to the mature FhuD protein was shown by (i) accumulation of [^{55}Fe^{3+}]ferrichrome in the periplasm of intact cells in a FhuD-overproducing strain, which, due to a mutation in the integral membrane protein FhuB, was unable to translocate the substrate into the cytoplasm; (ii) protection of radio-labeled FhuD against proteolytic degradation by proteinase K and trypsin when loaded with those ferric hydroxamates that support growth of the bacterial cells under iron-limiting conditions (Köster and Braun, 1990), and (iii) determination of the dissociation constants of ferric hydroxamates through the concentration-dependent decrease in the intrinsic fluorescence intensity of His-tagged-FhuD (0.4 µM for ferric aerobactin, 1.0 µM for ferrichrome, 0.3 µM for ferric coprogen, and 5.4 µM for albomycin). Ferrichrome A, ferrioxamine B, and ferrioxamine E, which are poorly taken up via the Fhu system, display dissociation constants of 79, 36 and 42 µM, respectively. The dissociation constant for ferrichrome bound to FhuD is similar to the Michaelis constant determined for ferrichrome uptake into wild-type cells [K_D 0.1 µM, K_m 0.5 µM (Rohrbach *et al*., 1995)].

If FhuD delivers the ferric hydroxamates directly to the FhuB transport protein in the cytoplasmic membrane, it should physically interact with FhuB. Direct interaction was shown by (i) protection of FhuB in spheroplasts against trypsin and proteinase K degradation through FhuD (Rohrbach *et al*., 1995), (ii) cross-linking of His-tagged FhuD to FhuB, and (iii) binding of 10 and 20 amino-acid-residue peptides identical in sequence to segments of FhuB (marked in Figure 3.4) to FhuD (Mademidis *et al*., 1997; Braun and Killmann, 1999). The FhuB peptides that bind in an ELISA assay to FhuD also inhibit ferrichrome transport when they are delivered into the periplasm through a FhuA derivative that forms an open channel through the genetic excision of residues 322–355 (Killmann *et al*., 1993). In all three experiments, FhuD free of substrate was at least as effective as FhuD loaded with ferrichrome or aerobactin. This finding was unexpected since periplasmic binding proteins of ABC transporters usually assume a substrate-loaded structure that differs from the unloaded structure. The binding proteins are typically composed of two lobes connected by a hinge region. They close like a Venus fly trap when they bind the substrate. The substrate independence of the binding assays to FhuB might be explained now that the FhuD crystal structure with bound gallichrome (ferrichrome in which Fe^{3+} is replaced by Ga^{3+}) has been determined (Clarke *et al*., 2000). In contrast to other periplasmic binding proteins, including the *Haemophilus influenzae* Fe^{3+}-binding protein discussed in Chapter 5 (Bruns *et al*., 1997), the interface between the *N*-terminal and *C*-terminal domains is predominantly hydrophobic, suggesting that siderophore binding and release is not accompanied by large-scale opening and closing of the binding site. The polypeptide chain crosses only once between the *N*-terminal and *C*-terminal domains via a 23-residue kinked helix that runs the entire length of the protein and also restricts movement of the two domains. Ga^{3+}, like Fe^{3+}, in ferrichrome

is octahedrally coordinated by six oxygen donor atoms of (Gly$_3$)-(*N*-acetyl-δ-*N*-δ-hydroxy-L-ornithine)$_3$. Only three direct hydrogen bonds (two by Arg-84 and one by Tyr-106) are formed between gallichrome and FhuD in the receptor site. A similar motif is observed in FhuA, but FhuA forms more hydrogen bonds and covers the surface of ferrichrome to a much greater extent than FhuD. In fact, gallichrome is not buried in a deep cleft like ferrichrome in FhuA (Figure 3.3), but is exposed at the protein surface (Figure 3.4). This might explain the narrower substrate specificity of FhuA as compared to FhuD. Nevertheless, FhuD changes its conformation upon binding of ferrichrome, and the new conformation is recognized by FhuB, which in turn triggers ATP hydrolysis by FhuC.

Competitive peptide mapping not only revealed sites of interaction between FhuD and FhuB, but also suggested a mechanism of FhuC activation that has hitherto not been envisioned for binding-protein-dependent transport systems (Mademidis *et al.*, 1997; Braun and Killmann, 1999). As illustrated in Figure 3.4, the FhuD binding sites involve not only periplasmically exposed loops of FhuB, according to a FhuB transmembrane topology model (Groeger and Köster, 1998), but also transmembrane regions and even regions exposed to the periplasm. The latter might fold into the membrane and, together with the transmembrane regions, form a channel into which FhuD inserts when it delivers ferrichrome to FhuB. Insertion into the channel would bring FhuD into close contact with one of the FhuC binding sites at FhuB, or into direct contact with FhuC. This suggests that FhuC hydrolysis is triggered without the need of a transmembrane signal through FhuB from the periplasm to the cytoplasm, which would be required if FhuD binds only to periplasmic loops of FhuB.

The folding of FhuD has nothing in common with the folding of the *N*- or *C*-terminal lobes of transferrin and lactoferrin. There is certainly no common ancestor of FhuD-like Fe^{3+}−siderophore binding proteins and the iron-binding transferrins and lactoferrins. In contrast, as we discuss in detail in Chapter 5, the structure of the Fe^{3+} binding protein hFBP of *H. influenzae* is similar to one lobe of transferrin and lactoferrin (Bruns *et al.*, 1997). Carbonate in transferrins, which provides two oxygen molecules for Fe^{3+} binding, is replaced by phosphate in hFBP, providing only one oxygen atom, the remaining coordination site being filled by water. Similar amino-acid residues bind Fe^{3+} in hFBP and transferrin. However, they come from different parts of the molecules, which makes it unlikely that the two proteins evolved from an iron-binding common ancestor. This conclusion is supported by the fact that the structure of the transferrin lobe is most closely related to the bacterial sulfate- and phosphate-binding proteins, which are anion-binding rather than cation-binding proteins. If these proteins developed by convergent evolution instead of divergent evolution, it would be interesting to know which functional constraints resulted in similar solutions.

The ATPase activity of FhuC was originally claimed on the basis of the presence of the 'Walker A' and 'Walker B' consensus motifs[‡] and the location of FhuC

[‡] The name given to particular amino-acid sequence motifs found in ATP-binding and ATP-hydrolysing proteins, after the Cambridge biochemist John Walker who first described them. Walker received the Nobel Prize in 1999 for his determination of the crystal structure of the ATP-synthesizing F$_1$ subunit of bovine heart mitochondrial F$_1$F$_O$ ATPase.

Table 3.1 Bacterial Fe^{3+} transport systems.

Organism	Outer membrane receptor	Binding protein	Membrane component	ATP-binding component	Substrates	References
Escherichia coli	FhuA	FhuD	FhuB	FhuC	Ferrichrome	Braun *et al.*, 1998
	FhuE	FhuD	FhuB	FhuC	Coprogen	
	IutA	FhuD	FhuB	FhuC	Aerobactin	
	FecA	FecB	FecC, FecD	FecE	Ferric-dicitrate	Braun *et al.*, 1998
	FepA	FepB	FepD, FepG	FepC	Enterochelin	Earhart, 1996
	Cir, Fiu	FepB	FepD, FepG	FepC	Dihydroxybenzoylserine	
Yersinia enterocolitica	HemR	HemT	HemU	HemV	Haem	Wandersman and Stojiljkovic, 2000
Shigella dysenteriae	ShuA	ShuT	ShuU	ShuV	Haem	Wyckoff *et al.*, 1998
Serratia marcescens	HasA/HasR	Not characterized			Haem	Wandersman and Stojiljkovic, 2000
Corynebacterium diphtheriae	Not applicable	HmuT	HmuU	HmuV	Haem	Drazek *et al.*, 2000
Serratia marcescens	Unknown	SfuA	SfuB	SfuC	Iron(III)	Braun *et al.*, 1998
Yersinia pestis	Unknown	YfeA	YfeCD	YfeB	Iron	Bearden *et al.*, 1998
Vibrio anguillarum	FatA	FatB	FatC, FatD	?	Anguibactin	Crosa, 1997
Campylobacter coli	Not characterized	CeuE	CeuB, CeuC	CeuD	Enterochelin	Richardson and Park, 1995
Erwinia chrysanthemi	Not characterized	CbrA	CbrB, CbrC	CbrD	Achromobactin	Mahe *et al.*, 1995; Munzinger *et al.*, 2000
Bacillus subtilis	Not applicable	FhuD	FhuB, FhuG	FhuC	Ferrichrome	Schneider and Hantke, 1993
Staphylococcus aureus	Not applicable	?	FhuB, FhuG	FhuC	Ferrioxamine	Sebulsky *et al.*, 2000
Neisseria spp.	TbpA, TbpB	FbpA	FbpB	FbpC	Iron(III) also from transferrin	Schryvers and Stojiljkovic, 1999
	LbpA, LbpB	FbpA	FbpB	FbpC	Iron(III) also from lactoferrin	

at the inside of the cytoplasmic membrane (Schultz-Hauser *et al.*, 1992). FhuC mutants with mutations in the Walker motifs are inactive; an aspartate-to-glutamate substitution is particularly noteworthy since one CH_2 group made all the difference between active and inactive (Becker *et al.*, 1990). FhuC has now been isolated and shows ATPase activity (Dangelmayr, Engel, Killmann and Braun, unpublished).

3.2.4   Variety of Fe³⁺ Transport Systems in Bacteria

Many Fe^{3+} transport systems have been identified in various bacteria. Table 3.1 lists not only those for which sequence similarities suggest that the genes encode iron transport proteins, but also those for which biochemical studies have proved transport activities. An interesting novel mechanism for iron transport in the fresh water bacterium *Aeromonas hydrophila* has been described by means of an indiscriminant siderophore transport system composed of a single multifunctional receptor (Stintzi *et al.*, 2000). It appears that the siderophore and Fe^{3+} enter the bacterium together, and that ligand exchange occurs at the cell surface involving iron exchange between a ferric siderophore to an iron-free siderophore already bound to the receptor. This iron exchange mechanism, also found in *E. coli*, does not appear to involve a redox process, and might represent a more widely distributed microbial iron-transport system.

3.3   Ferrous Iron Transport Systems

Under anoxic conditions, ferrous iron is stable and more soluble than Fe^{3+}; this allows its transport without the need for complexation by ligands. In *E. coli*, a ferrous-iron transport system consists of three genes, *feoABC* (Kammler *et al.*, 1993). *feoB* encodes an 84-kDa protein located in the cytoplasmic membrane that shows a typical nucleotide-binding motif proximal to the *N*-terminus. This binding motif has more similarities to the GTP binding sites found in Ras proteins or elongation factors than to ATP binding sites in transporters. The function of this nucleotide binding site is unknown; it may drive transport or it may have a regulatory role. *feoA* and *feoC* encode two small proteins of less than 10 kDa with unknown functions. Mutants in *feoA* or *feoB* show a strongly reduced ferrous iron uptake. In addition, *feo* mutants are derepressed for many Fur-regulated genes, which indicates that ferrous-iron transport also contributes under aerobic conditions to the iron supply of the cells. *feo* genes have also been identified in *Salmonella typhimurium* (Tsolis *et al.*, 1996), and the genome of *Methanococcus janashii* reveals a gene similar to *feoB* (Bult *et al.*, 1996). FeoB seems to be the major high-affinity, iron-acquisition, system of *Helicobacter pylori* (Velayudhan *et al.*, 2000). Growth under iron-limiting conditions is impaired in a *feoB* mutant and cannot be restored by $FeSO_4$, but is restored by iron citrate, and by iron-loaded human transferrin and lactoferrin.

Uptake by FeoB is inhibited by the 'energy poisons'[¶] FCCP, DCCD, and vanadate. Both Fe^{3+} and Fe^{2+} serve equally well as iron sources, but Fe^{3+} provided as a citrate salt is immediately reduced to Fe^{2+}, as demonstrated by the formation of the magenta-coloured Fe^{2+}–ferrocine complex.

Fe^{2+} is also transported by the CorA protein (Hantke, 1997), a divalent cation transporter for Mg^{2+}, Co^{2+}, Mn^{2+}, and Ni^{2+} in *E. coli* and *S. typhimurium*. CorA may represent the often-mentioned 'low-affinity' iron-uptake system of *E. coli* that is suppressed in Fe^{3+} uptake studies by the addition of 0.2 mM dipyridyl and 0.1 mM nitrilotriacetate.

3.4 Iron Metabolism

While much is known about siderophore-mediated ferric-iron transport, very little is known about ferrous-iron transport and iron metabolism inside the cell. It is generally assumed that Fe^{3+} chelated to the siderophore must be reduced to allow removal from the strong claws of the chelator. Indeed, in some cases the siderophore transported iron was found 30 minutes later in the intracellular Fe^{2+} pool of the cells (Matzanke *et al.*, 1991).

The *ent–fes–fep* gene cluster is necessary for the synthesis of enterobactin and transport of the iron loaded siderophore. The *fes* gene product was shown to be necessary for utilization of the siderophore-bound iron inside the cell. The protein has an esterase activity which cleaves the ester bonds of the cyclic 2,3-dihydroxybenzoylserine ester in enterobactin. However, the esterase activity of Fes does not seem to be important for iron mobilization since Fes is also necessary for the utilization of iron from enterobactin analogues which do not have ester bonds (Heidinger *et al.*, 1983). No reductase activity has been found in Fes (Brickman and McIntosh, 1992) or in any other protein encoded in the *ent–fes–fep* gene cluster.

There is some evidence that the iron-sulfur protein, FhuF, participates in the mobilization of iron from hydroxamate siderophores in *E. coli* (Müller *et al.*, 1998; Hantke, K. unpublished observations). However, a reductase activity of FhuF has not been demonstrated. Many siderophore–iron reductases have been shown to be active *in vitro* and some have been purified. The characterization of these reductases has revealed them to be flavin reductases which obtain the electrons for flavin reduction from NAD(P)H, and whose main functions are in areas other than reduction of ferric iron (e.g. flavin reductase Fre, sulfite reductase). To date, no specialized siderophore–iron reductases have been identified. It has been suggested that the reduced flavins from flavin oxidoreductases are the electron donors for ferric iron reduction (Fontecave *et al.*, 1994). Recently it has been shown, after a fruitless search for a reducing enzyme, that reduction of Co^{3+} in cobalamin is achieved by reduced flavin. Also in this case it was suggested that cobalamins and corrinoids are reduced *in vivo* by flavins which may be generated by the flavin

---

[¶] These three substances block ATP production in quite different ways: FCCP (carbonylcyanide-*p*-trifluoromethoxyphenylhydrazone) is a proton-transporting ionophore, that uncouples oxidative phosphorylation from electron transport; DCCD (dicyclohexylcarbodiimide) inhibits proton transport through the F_O subunit of the ATPase by reacting with a Glu residue of F_O; vanadate is an analogue of phosphate.

reductase Fre and other flavin oxidoreductases (Fonseca and Escalante-Semerena, 2000). From this view point, Fes or FhuF may be enzymes that bind the siderophores and help to remove the reduced Fe^{2+} from these siderophores.

According to Mössbauer spectroscopic data, the ratio of Fe^{2+} to Fe^{3+} in a bacterial cell is roughly 1 : 1. In these spectra, iron in cytochromes, iron in [Fe–S] proteins and iron in ferritins is below 10 % of the iron content of the cell. The binding sites of the pool of iron(II) and iron(III) in the logarithmically growing cell are not known (Böhnke and Matzanke, 1995). Although the bulk of iron seems not to be stored in ferritins, two types of ferritins, the haem containing bacterioferritins and the haem-free ferritins (Andrews, 1998) are found in *E. coli* and in many other bacteria. Iron storage by these molecules is mainly observed in the stationary phase after growth in iron-rich media. In *E. coli* the function of the bacterioferritin Bfr is not clear while a mutation in the *ftnA* encoding ferritin A led to an impaired growth following a change from iron-rich to iron-poor conditions (Abdul-Tehrani *et al*., 1999). The function of the second ferritin gene *ftnB* in *E. coli* is unknown. In *Campylobacter jejuni*, ferritin seems to be important for iron storage and protection against oxidative stress by H_2O_2 and paraquat (Wai *et al*., 1996). Similarly, bacterioferritins have been shown in *Neisseria* and *Pseudomonas aeruginosa* to be important for storage and defence against oxidative stress. In the obligate anaerobe *Porphyromonas gingivalis*, a haem-free ferritin was shown to be important for iron storage (Ratnayake *et al*., 2000). However, in this case the ferritin did not protect the cells against oxidative stress.

Genes encoding bacterioferritins are often located in the vicinity of genes that encode small ferredoxins. These [2Fe–2S] ferredoxins are thought to be involved in the mobilization of iron from bacterioferritin. Interestingly the Bfd protein (bacterioferritin-associated ferredoxin) of *E. coli* shows similarity to the central region of the NifU protein. NifU is encoded in a set of genes responsible for the biosynthesis of the [Fe–S] centres of nitrogen-fixation proteins in *Azotobacter vinelandii*. Similar clusters of genes have been found in many bacteria and eukaryotes involved in the synthesis and incorporation of [Fe–S] centres (reviewed in Chapter 7). The NifU homolog IscU in *E. coli* serves as a scaffold for a labile [4Fe–4S] centre which may be used in the maturation of Fe–S proteins. The NifS homolog IscS (Agar *et al*., 2000) is a cysteine desulfurase, which liberates sulfur from cysteine and provides it for [Fe–S] cluster synthesis on IscU (Zheng *et al*., 1998; Agar *et al*., 2000). Besides IscS and IscU the chaperone Hsc66, related to the heat shock protein Hsp70, is encoded in the Fe–S synthesis gene cluster. It was demonstrated that IscU is a substrate for Hsc66, which suggests a specialized function of Hsc66 in assembly, stabilization or transfer of [Fe–S] clusters formed on IscU (Silberg *et al*., 2000). We can expect that in the course of the next few years the function of other gene products encoded in the *iscS–iscU* gene cluster will be elucidated. In *E. coli* three NifS homologues are found: IscS, Csd, and SufS. The *sufS* gene is regulated by Fur and iron in a putative operon encoding additional genes assumed to be necessary for [Fe–S]-cluster synthesis (Patzer and Hantke, 1999). A mutant in *sufS* was unable to produce the [2Fe–2S]-containing protein FhuF which is thought to be involved in iron mobilization from hydroxamate siderophores.

3.5 Iron Regulation in Bacteria – the Fur Protein

The Fur protein regulates iron uptake systems in many Gram-negative bacteria. The striking phenotype of the first *fur* mutants isolated was the overexpression of the outer membrane receptors for siderophore iron transport. In addition, excretion of siderophores under iron-rich growth conditions was observed in these mutants, indicating that the biosynthesis of siderophores is also regulated by Fur.

The Fur protein from *E. coli* was isolated in one step due to its high affinity for metal-chelate columns loaded with zinc. In DNase footprinting experiments, the Fur protein was shown to bind DNA in the promoter region of several iron-regulated genes. The consensus sequence, called the Fur box, is GATAATGATAATCATTATC. *In vitro* binding is dependent on the divalent cations $Co^{2+} \geqslant Mn^{2+} \geqslant Cd^{2+} \geqslant Cu^{2+}$ at 150 µM, while Fe^{2+} seemed to be less active at this concentration, probably due to oxidation to Fe^{3+} (De Lorenzo *et al.*, 1987). The unspecificity for divalent metals observed *in vitro* shows that the cells have to select the ions transported carefully and have to balance their active concentrations. In addition, it is a caveat for the experimenter to test a hypothesis on metal-ion specificity not only *in vitro*, but also *in vivo*.

The important regulatory metal-binding site occupied *in vivo* by Fe^{2+} is not well characterized. The metal is bound in this site by at least two histidines and one carboxylate in an axially distorted octahedral environment (Althaus *et al.*, 1999), confirming earlier work (Hamed and Neilands, 1993).

Zn^{2+} at 100 µM seems to activate the apo-Fur protein partially, possibly caused by the recently discovered tight binding of zinc to Fur. Two cysteines at positions 92 and 95 have been identified as binding sites by alkylation of cysteines in the presence and absence of zinc (Gonzalez *et al.*, 1999). In addition, from spectroscopic studies two nitrogen/oxygen binding sites were proposed for zinc. The binding of zinc is remarkable since several members of the Fur family, like the Zur (zinc uptake regulator) protein in *E. coli*, regulate genes for zinc uptake and metabolism (Patzer and Hantke, 1998). Both metal-binding sites seem to be mainly in the carboxy-terminal half of the protein, although iron might also be bound by a histidine in the *N*-terminal half of the Fur protein (Saito *et al.*, 1991).

The DNA binding site of Fur was predicted and then found to be in the *N*-terminal domain in an unusual helix-turn-helix motif (Holm *et al.*, 1994; Stojiljkovic and Hantke, 1995). The structure of Fur still remains to be determined and attempts to crystallize the protein have so far been unsuccessful.

3.5.1 The Fur Regulon

Genes regulated by Fur code for proteins that function in iron transport and iron metabolism; under aerobic conditions, iron metabolism is associated with oxidative stress. In addition, some virulence factors are regulated by Fur. Table 3.2 lists examples and functions of Fur- and iron-regulated genes in *E. coli*, including pathogenic *E. coli* strains.

Table 3.2 Proteins encoded by Fur-regulated genes in *E. coli* strains.

Promoters and genes(s)	proteins	Function (substrate)	Strain, plasmid	Reference
Siderophore biosynthesis and iron uptake				
fhuABCD	FhuA FhuBCD	Outer membrane transport (ferrichrome) Inner membrane transport (ferrichrome)	K-12	(Earhart, 1996)
FhuE	FhuE	Outer membrane transport (coprogen)	K-12	(Hantke, 1983)
fepA	FepA	Outer membrane transport (enterobactin)	K-12	(Earhart, 1996)
fepBCDG	FepBCDG	Inner membrane transport (enterobactin)		
orf43	Orf43	Function unknown, gene in the *fep* cluster		
entABCDEF	EntABCDEF	Enterobactin biosynthesis		
fepE	FepE	Function unknown, gene in the *ent* cluster		
orf 15	Orf 15	Function unknown, gene in the *ent* cluster		
fes	Fes	Iron mobilization, esterase (enterobactin)		
cir	Cir	Outer membrane transport, catechol-siderophores	K-12	(Earhart, 1996)
fiu	Fiu	Outer membrane transport catechol-siderophores	K-12	(Hantke, 1990)
fecIR	FecIR	Transmembrane regulator FecR and alternative sigma factor FecI of the Fe^{3+}–citrate uptake system, Fec	K-12	(Van hove et al., 1990)
fecABCDE	FecA FecBCDE	Outer membrane transport (ferric citrate) Inner membrane transport (ferric citrate)	K-12	(Hantke and Braun, 1998)
tonB	TonB	Energization of receptors for the uptake of siderophores, haem, and vitamin B_{12}	K-12	
exbBD	ExbBD		K-12	(Kammler et al., 1993)
feoABC	FeoABC	Ferrous iron uptake	K-12	(Muller et al., 1998)
fhuF	FhuF	Mobilization of iron from hydroxamates?	K-12	
iutA	IutA	Outer membrane transport (aerobactin)	Col V	(De Lorenzo et al., 1987)
iucABCD	IucABCD	Aerobactin biosynthesis		
fyuA	FyuA	Outer membrane transport (yersiniabactin, pesticin receptor)	EAggEC[b], UPEC[c]	(Schubert et al., 1999)

Table 3.2 (*continued*)

Promoters and genes(s)	proteins	Function (substrate)	Strain, plasmid	Reference
ybtPQ	YbtPQ	Inner membrane transport (yersiniabactin)		(Fetherston et al., 1999)
ybtX	YbtX	Inner membrane, function unknown		
ybtS	YbtS	Yersiniabactin synthesis (salicylate)		
irp1	HMWP1	Yersiniabactin synthesis		(Bach et al., 2000; Schubert et al., 1999; Bearden et al., 1997; Geoffroy et al., 2000)
irp2	HMWP2	Yersiniabactin synthesis		
irp5 (ybtE)	YbtE	Yersiniabactin synthesis		
irp4 (ybtT)	YbtT	Yersiniabactin synthesis		
irp3 (ybtU)	YbtU	Yersiniabactin synthesis and regulation		
shuA	ShuA	Outer membrane transport (haem)	EHEC[d]	(Torres and Payne, 1997)
shuTUV	ShuTUV	Inner membrane transport (haem)	EIEC[e]	
shuWXY	ShuWXY	Function unknown	UTI[f]	
shuS	ShuS	Iron mobilization?	NM[g]	
Iron metabolism and oxidative stress response				
bfd	Bfd	Mobilization of iron from bacterioferritin?	K-12	(Stojiljkovic et al., 1994)
fur	Fur	Iron regulator, cofactor Fe^{2+}	K-12	(Braun et al., 1998)
sufABCDSE	SufABCDSE	SufASE possibly iron sulfur center synthesis SufBCD unknown	K-12	(Patzer and Hantke, 1999)
mntH	MntH	Manganese transporter	K-12	(Kehres et al., 2000)
AcnA (+)[a]	AcnA	Aconitase	K-12	(Gruer and Guest, 1994)
fumA (+)	FumA	Fumarase A	K-12	

sodA	SodA	Superoxide dismutase (Mn)	K-12	(Tardat and Touati, 1993)
sodB (+)	SodB	Superoxide dismutase (Fe)	K-12	(Dubrac and Touati, 2000)
ftnA (+)	FtnA	Ferritin	K-12	(Abdul-Tehrani et al., 1999)
bfr (+)	Bfr	Bacterioferritin	K-12	
yhhX	YhhX	Unknown	K-12	(Patzer and Hantke, 2000)
gpm	PGMI	Phosphoglycerate mutase	K-12	(Tsolis et al., 1995)
mutY	MutY	8-Hydroxyguanine endonuclease	K-12	(Lee et al, 1998)
Virulence factors				
hlyCABD	HlyA	Haemolysin		(Grünig et al., 1987)
	HlyC	Acylation and activation of haemolysin		
	HlyBD	Secretion of haemolysin		
sltA	SltA	Shiga-like toxin	Lambdoid bacteriophage H19B	(De Grandis et al., 1987)
cvaAB	CvaAB	Secretion of colicin V (microcin)	Col V	(Boyer and Tai, 1998)
cvaC	CvaC	Colicin V (microcin)		
cvaI	CvaI	Immunity protein against ColV		
mcjABCD	McjA	Microcin J25 (receptor FhuA)		
	McjBC	Maturation, head–tail linkage of pro-MccJ25		
	McjD	ABC exporter		(Salomon and Farias, 1994)

[a](+)Indicates positive regulation by Fur; [b]Enteroaggregative *E. coli*; [c]Uropathogenic *E. coli*; [d]Enterohaemorrhagic *E. coli*; [e]Enteroinvasive *E. coli*; [f]Urinary tract infectious *E. coli*; [g]Neonatal meningitis *E. coli*).

3.5.2   Siderophore Biosynthesis and Uptake

The majority of Fur-regulated gene products are involved in iron uptake. Genes for transport and biosynthesis of enterobactin have been studied in *E. coli* K-12 (Earhart, 1996). It is assumed that this system is found in nearly every *E. coli* strain. Also the ferrichrome transport system seems to have a very broad distribution. The ferric citrate transport system (*fec*), however, is only present in some *E. coli* strains and may be part of a pathogenicity island.§ The aerobactin and yersiniabactin biosynthesis and transport systems are not found in all *E. coli* strains and are integrated into pathogenicity islands (Schubert *et al.*, 1999). The ability to utilize haem seems also to be a specific pathogenicity-related adaptation. Haem transport systems are used in the animal or human host, where transferrin and lactoferrin create an iron-poor environment for bacteria.

In Table 3.2, the genes of a haem uptake and yersiniabactin synthesis and uptake are listed as *E. coli* genes. However, their Fur regulation was originally defined in *Yersinia*. The function of these genes and sequence data (Fur box) provide good evidence that they are also regulated by Fur in *E. coli* strains.

3.5.3   Iron Metabolism and Oxidative Stress Response

Another group of iron-regulated genes is involved in intracellular iron metabolism, which includes iron storage and mobilization, delivery of iron to apo-enzymes, and regulation. A special problem under aerobic conditions is the Fenton chemistry of iron. Tight binding of iron within the cell is necessary in order to prohibit uncontrolled generation of oxygen radicals. However, solid knowledge of how iron is stored in growing cells is fragmentary. One condition by which the killing of *E. coli* cells by iron can be demonstrated is the addition of ferrous iron to a low-Mg^{2+} medium under aerobic conditions; otherwise, it is difficult to demonstrate the toxicity of iron for *E. coli* (Hantke, 1997). Certain combinations of mutations make the cells very sensitive to iron under aerobic conditions. For example, *fur recA* double mutants are not viable on iron-rich media under aerobic conditions (Touati *et al.*, 1995). This can be taken as evidence that in Fur mutants, a high level of free iron leads to oxidative damage of DNA, which cannot be repaired without RecA, required both for homologous recombination of DNA and for DNA repair.

From these observations, it is understandable why the Fur protein is not only autoregulated and regulated by cAMP-CAP (De Lorenzo *et al.*, 1988), but also by OxyR and SoxRS (Zheng *et al.*, 1999). After treatment of cells with H_2O_2, OxyR induces a set of genes with clear antioxidant activities. OxyR induction of Fur synthesis should diminish the formation of $HO^{\bullet}$ radicals generated by the reaction of H_2O_2 with intracellular iron. SoxRS induces oxidative stress-response genes after treatment of cells with $O_2^{\bullet-}$-generating compounds. The induction of Fur by SoxRS should decrease the generation of $HO^{\bullet}$ radicals (Zheng *et al.*, 1999).

---

§ This charming term indicates a cluster of genes, physically localized in a bacterial genome, that are associated with the virulence and hence the pathogenicity of the particular bacterial strain. The pathogenicity islands are thought to be acquired by horizontal DNA transfer from different genera since their GC content and codon usage differs from the genome.

3.5.4 Genes Regulated by Fur

An increasing number of gene products has been shown to be positively regulated by Fur. In some cases, no binding of Fur to the promoter region of the respective genes is found. The best studied case is SodB, an iron-containing superoxide dismutase that shows an iron- and Fur-dependent increase. The *sodB* mRNA half-life is reduced in a *fur* mutant, indicating that Fur regulation in this case is post-transcriptional and leads to stabilization of *sodB* mRNA (Dubrac and Touati, 2000). A palindrome followed by an AT-rich stretch of bases in the first 40 transcribed bases is important for the Fur-dependent regulation of SodB. These observations are reminiscent of the well-characterized IRE regulatory elements involved in eukaryotic iron metabolism (see Chapter 7). Also in bacteria, RNA binding activity of the aconitase AcnA has been demonstrated (see below). In the next few years we will see whether *sodB* RNA interacts with AcnA or whether Fur itself has RNA binding activity, which would explain the stabilization of *sodB* mRNA and the results on the acid-shock response described below.

Fur has a regulatory influence on the acid-shock response in *E. coli* and *Salmonella*. The acid-response reactions are important for the cells to survive when they pass the acidic gut. In *Salmonella*, a Fur-dependent, but iron-independent, regulation of acid-response genes is observed. Certain point mutations of Fur (e.g. H90R) do not respond to iron, but are able to regulate an acid-response gene (Foster, 2000). Unfortunately, the functions of the Fur-dependent gene products in acid response are not known.

3.5.5 Virulence-Associated Genes

Low-iron stress in the host is a signal for pathogenic bacteria to induce virulence factors, such as Shiga-like toxin and haemolysins (although haemolysins could also help to obtain iron from lysed cells and could be grouped under 'iron uptake').

It is interesting to note that the virulence-associated factors microcins ColV and MccJ25 are also regulated by iron and Fur. This guarantees high expression of these toxic peptides under conditions where their receptors Cir (for ColV) and FhuA (for MccJ25) are highly expressed in sensitive enterobacteria. However, production of typical colicins (proteinaceous *E. coli* toxins) like colicins I, B, and M, that also use iron-regulated receptors, is not iron dependent. The function of microcins and colicins, which is always a matter of debate, might be to stabilize the encoding genetic element (be it a plasmid or a transposon).

3.5.6 Fur-like Proteins

Fur-like proteins are found in nearly all bacteria sequenced so far, with some notable exceptions: the highly adapted and specialized pathogens, such as *Mycoplasma pneumoniae, M. genitalium, Treponema pallidum, Chlamydia*, and *Ricketsia* do not seem to contain genes encoding Fur-like proteins. Only some of the archaea, e.g. *Archaeoglobus fulgidus*, encode a Fur-like protein. In many cases, the Fur-like proteins

seem to regulate a very similar spectrum of genes such as in *E. coli*. The function of these proteins, however, has to be tested. There are subfamilies of Fur which regulate zinc utilization or oxidative stress-response genes (see below). However, in the Gram-positive bacterium *Corynebacterium diphtheriae*, it was found that the chromosomally encoded protein DtxR (<u>d</u>iphtheria <u>tox</u>in <u>r</u>egulator) mediates the well-known iron regulation of the phage-encoded toxin. Later it was shown that DtxR-like proteins regulate siderophore biosynthesis in streptomycetes. In the sequencing projects, it was found that in these Gram-positive bacteria (DNA with high $G + C$ content), *fur*-like genes are also found. Interestingly, in the two cases studied, the *fur*-like genes are cotranscribed with a catalase–peroxidase-coding gene, which indicates that in these organisms the Fur-like protein mainly regulates oxidative stress response rather than iron metabolism and uptake (Zhou *et al.*, 1999).

In the Gram-positive bacterium *Bacillus subtilis* (DNA with low $G + C$ content), three Fur-like proteins have been characterized (Bsat *et al.*, 1998). One, called Fur, regulates mainly iron uptake and siderophore biosynthesis. A second one, called PerR, regulates peroxide stress response genes and acts with manganese as corepressor. A third one, Zur, regulates genes for zinc uptake. The Zur protein found in *E. coli* shows only 25 % identity to the *B. subtilis* Zur, while the two Fur proteins have 32 % identical amino acids.

DtxR-like Regulators

As already mentioned, the first bacterial iron regulator not belonging to the Fur family was identified as being a repressor of the diphtheria toxin gene and therefore named DtxR. Similar regulators were found in mycobacteria (here called IdeR) and *Streptomyces* strains to regulate siderophore biosynthesis or siderophore uptake genes. These genes seem to regulate a spectrum of genes similar to those regulated by Fur in *E. coli*, while the Fur-like proteins in these organisms seem to regulate certain oxidative stress-response genes (see above).

The crystal structures of DtxR and IdeR provide a detailed picture of this protein family (Figure 3.7, Plate 5). The *N*-terminal domain (residues 1–73) containing a helix-turn-helix motif binds a recognition nucleotide sequence of about 21 base pairs, as is nicely shown in a cocrystal of DNA and DtxR (Pohl *et al.*, 1999). The central domain (74–140) has a function in dimerization; the role of the third carboxy-terminal domain (141–230) is uncertain. Although metal-binding sites have been defined in these crystal structures, the mechanism by which metal binding causes the structural changes between apo- and holo-repressor is not clear.

Recent studies show that not all members of the DtxR family recognize iron as a cofactor. One interesting case is TroR, which regulates a manganese transporter in *Treponema pallidum* and which accepts only Mn^{2+} as corepressor. Similarly, in *B. subtilis* with its three Fur-like proteins, the DtxR homologue MntR with Mn^{2+} as cofactor regulates two manganese transporters. It seems that this subfamily of DtxR-like proteins regulates with manganese a set of genes involved in manganese utilization.

This overview illustrates that in bacteria, the two protein families Fur and DtxR are the main regulators of iron metabolism and transport. Both repressors are also

used to regulate virulence factors of pathogenic bacteria. Low-iron stress is taken as a signal for the host environment. Another set of genes regulated by both repressors are those involved in the oxidative stress response, which is intimately connected to the peculiarities of iron reacting with oxygen. Since the oxidative burst is one of the weapons which mammalian macrophages employ to fight microbial invaders (Chapter 10), this makes these genes all the more important for the survival of pathogenic bacteria.

3.5.7 Regulation by Fe^{3+} Siderophores

Synthesis of siderophores and synthesis of the Fe^{3+}–siderophore transport systems are not only controlled by repressors such as Fur and DtxR, but might also be induced by Fe^{3+} siderophores in the growth medium, which would have the advantage that the related transport system would only be formed when the cognate Fe^{3+} siderophore is already present in the growth medium. In contrast, iron limitation derepresses gene transcription of all iron-transport systems regardless of which iron source is present. The Fe^{3+} citrate transport system of *E. coli* is an extensively studied case. Transcription of the two regulatory genes, *fecI* and *fecR*, is controlled by the Fur repressor, and they are transcribed under conditions of iron limitation. The FecI and FecR proteins are required for the response of cells to Fe^{3+} citrate in the medium (Braun, 1997). Interestingly, Fe^{3+} citrate does not need to enter cells to induce transcription of the *fecABCDE* transport genes. It binds to the outer membrane protein FecA, which functions simultaneously as a signaling protein and as a Fe^{3+} citrate transporter across the outer membrane. The information that FecA has bound Fe^{3+} citrate is transmitted to the cytoplasmic membrane protein FecR, which transmits it across the cytoplasmic membrane into the cytoplasm, where it activates the FecI protein, a sigma factor that directs the RNA polymerase to the promoter of the *fecABCDE* operon. This results, in response to the presence of Fe^{3+} citrate in the growth medium, in the transcription of the *fecABCDE* transport genes. The transport system thus formed takes up Fe^{3+} citrate across the outer membrane into the periplasm, and then transports Fe^{3+} across the cytoplasmic membrane into the cytoplasm. The information flux across three cell compartments – outer membrane, periplasm, and cytoplasmic membrane – occurs by the interaction of the FecA and FecR proteins. The *N*-terminal portion of mature FecA is localized in the periplasm (Kim *et al.*, 1997), and FecR is positioned in the cytoplasmic membrane such that residues 101–317 are within the periplasm, residues 86–100 span the cytoplasmic membrane, and residues 1–85 are in the cytoplasm (Ochs *et al.*, 1995; Welz and Braun, 1998). In an *in vitro* binding assay, FecA is retained by His-tagged FecR bound to a Ni-NTA agarose column and is co-eluted with His-FecR. In an *in vivo* assay using a bacterial two-hybrid system, $FecA_{1-79}$ interacts with $FecR_{101-317}$. Interaction of FecR with FecI has been shown *in vitro* by binding FecI to His-FecR on a Ni-NTA agarose column and by *in vivo* binding of $FecR_{1-85}$ to $FecI_{1-173}$ (Enz *et al.*, 2000).

The novel mechanism of transcriptional control of the ferric citrate transport system via transmembrane signalling is also observed in *Pseudomonas putida* and probably also occurs in *Pseudomonas aeruginosa*. Synthesis of the PupB outer

membrane transporter for the uptake of Fe^{3+} pseudobactin BN8 is induced by pseudobactin BN8, and PupB is required for induction. Two regulatory genes homologous to *fecIR* are encoded upstream of the *pupB* gene and are required for *pupB* transcription (Koster *et al.*, 1994). The genomes of *P. putida* and *P. aeruginosa* each contain approximately eight sets of genes homologous to *fecIR*, which suggests a number of FecIR-like regulatory devices in these organisms.

There are other mechanisms by which Fe^{3+} siderophores induce the formation of their cognate transport systems. The reader is referred to recent reviews (Crosa, 1997; Vasil and Ochsner, 1999; Venturi *et al.*, 1995).

3.5.8 Regulation of Outer Membrane Transporter Synthesis by Phase Variation

Phase variation is a genetic mechanism by which bacteria change the cell surface to escape the immune defence mechanisms. During DNA replication, DNA polymerase 'slips' on a string of repeated nucleotides in the template DNA, which results in the addition or deletion of one repeat unit. The repeated nucleotides can be located within the open reading frame, causing an out-of-frame mutation, or in the promoter region, causing differences in transcription levels.

Three genes of *H. influenzae, hgbA, hgbB*, and *hgbC*, which encode outer-membrane receptor proteins for haemoglobin, haemoglobin–haptoglobin, or both compounds, contain multiple repeats of tetrameric CCAA units immediately after the sequence encoding the signal peptide. The same strain grown on haem or haemoglobin synthesizes HgbA (96 % and 98 %) more frequently than HgbB (11 % and 8 %). Those cells that synthesize HbgA contain 22 or 25 CCAA repeats, which allow full-length protein synthesis; those that do not synthesize HgbA contain 23, 26, or 27 CCAA repeats, leading to premature synthesis stop. The results obtained with HgbB also related protein synthesis to the number of CCAA repeats that give rise to in-frame synthesis. HgbC is synthesized at a low level and has not been studied in detail (Ren *et al.*, 1999; Cope *et al.*, 2000).

In *Neisseria meningitidis*, haem provided by haemoglobin is transported by the two outer membrane transporters HmbR and HpuAB. Synthesis of HmbR correlates with a sequence of either 9 or 12 consecutive G nucleotides within the open reading frame; whereas, with a G track other than 9 or 12 nucleotides, there is a total lack of synthesis. Different clinical isolates display a switching between the on and off phases that differ more than 1000-fold (Richardson and Stojiljkovic, 2000). Synthesis of HpuAB also depends on phase variation of a poly(G) tract (Lewis *et al.*, 1999). HpmR synthesis in a *hpu* mutant occurs at a frequency of 10^{-3}. An even more rapid phase variation between high- and low-expression levels was found in the recently characterized ferric enterobactin receptor FetA of *Neisseria gonorrhoeae* with a frequency of phase variation of approximately 1.3 % in the on and off directions (Carson *et al.*, 2000). The number of C nucleotides in a poly(C) tract in the promoter region determines the rate of *fetA* transcription: 12 cytosines in the high transcription state and 11 cytosines in the low transcription state. Alteration of the outer membrane transporters by phase variation makes sense since they are strongly synthesized under the low-iron conditions in the human body, and antibodies to these proteins are contained in the serum of patients.

Changes in transporter proteins by high-frequency genetic mutation mechanisms, while maintaining transport activity, helps to evade the host's immune response, and in cases where the substrate specificity is changed, helps the microorganism to adapt to new iron sources.

3.5.9   Iron-related Bacterial Virulence

Solubilization of Fe^{3+} by binding to host compounds, mainly haem, haemoglobin, transferrin, and lactoferrin, clearly reduces the available iron to such low levels that bacteria without specific mechanisms for withdrawing iron from these compounds would be starved of iron, stop growing, and be non-pathogenic. Iron is the only nutrient known to be generally growth limiting and to play an important role in the virulence of bacteria. Older literature amply demonstrates the relationship between iron supply and the growth of bacteria in animal models (Weinberg 1978, 1990; Bullen and Griffith, 1987; Woodridge and Williams, 1993). However, there are relatively few data that relate virulence to specific iron-transport systems under defined *in vivo* experimental conditions. The aerobactin transport system which allows invasive *E. coli* of human and animal origin to grow in serum is such a case (Williams, 1979; Crosa, 1984). Virulence of the fish pathogen *Vibrio anguillarum* also depends on the synthesis and transport of the strain-specific siderophore anguibactin (Crosa, 1997). *Yersinia enterocolitica* only kills mice when it synthesizes yersiniabactin and a related iron-repressible outer-membrane transport protein (Heesemann *et al.*, 1993). *Y. enterocolitca* also contains a transport system for Desferal® (Bäumler and Hantke, 1992) which explains the occasional occurrence of yersiniosis in Desferal-treated patients. Iron acquisition via yersiniabactin is also important for the virulence of *Y. pestis* during the early stages of infection in mice (Bearden and Perry, 1999). In *Legionella pneumophila*, which naturally occurs in protozoa (e.g. acantamoeba), but can occasionally infect human alveolar macrophages and cause Legionnaires' disease, the *iraAB* locus is required for iron assimilation, intracellular infection, and virulence (Viswanathan *et al.*, 2000). An *ira* mutant, defective in intracellular infection, yielded 1000-times fewer bacteria from the lungs and spleen of inoculated guinea pigs compared with *ira* wild-type cells, in which a fiftyfold lower dose was used. The mutant bacteria are subsequently cleared in contrast to wild-type bacteria, which multiply. In *Salmonella typhimurium*, the *sitABCD* genes are thought to encode a complete iron-transport system. Transcription of the *sitABCD* genes is induced after invasion of the intestinal epithelium of BAB/c mice. A *sit* null mutant is attenuated in mice, which suggests that the *sit* iron transport system plays an important role in *S. typhimurium* virulence (Janakiraman and Slauch, 2000). Iron uptake is important for the virulence of *Pseudomonas aeruginosa*. A *tonB* mutant devoid of Fe^{3+} uptake via pyoverdin, pyochelin, and haem grows in the muscles and lungs of immunosuppressed mice but does not kill the animals (Takase *et al.*, 2000a). Pyoverdin and pyochelin double mutants multiply but do not kill the mice, but intranasal inoculation results in multiplication and killing (Takase *et al.*, 2000b), although growth in the lung is attenuated compared to wild-type bacteria. *H. pylori feoB* mutants do not colonize the stomach of mice after oral inoculation (Velayudhan *et al.*, 2000), showing that

the major *in vitro* high-affinity iron-transport system is also the most important one *in vivo*.

Two novel aspects of competition for iron between bacteria and their hosts has recently became apparent. Human epithelium cells infected by *N. gonorrhoeae* and *N. meningitidis* have reduced levels of transferrin receptor mRNA and cycling transferrin receptors. The ability of infected cells to internalize transferrin receptor is reduced, and the distribution between surface and cycling transferrin receptors is altered (Bonnah *et al.*, 2000). Thus, *Neisseria* interferes with transferrin–iron homeostasis not only by using transferrin iron, which is crucial for bacterial colonization in the urethra of man (Cornelissen *et al.*, 1998), but also by affecting transferrin receptor cycling. Iron withdrawal from bacterial pathogens might also involve the use of siderophore iron, in addition to binding iron to transferrin, lactoferrin, and ferritin. Human neutrophils, macrophages, and myeloid cell lines can acquire iron from pyoverdine and pyochelin of *P. aeruginosa* (Brittigan *et al.*, 2000); this may serve as a host defence mechanism to limit the availability of iron to invading *P. aeruginosa*.

3.6   Acknowledgements

3.7   References

Abdallah, M. (1991). In *Handbook of Microbial Iron Chelates* (ed. Winkelmann, G.), CRC Press, Baton Rouge, pp. 139–153.

Abdul-Tehrani, H., Hudson, A.J., Chang, Y.S., Timms, A.R. *et al.* (1999). *J. Bacteriol.*, **181**, 1415–28.

Agar, J.N., Krebs, C., Frazzon, J., Huynh B.H., Dean, D.R. and Johnson, M.K. (2000). *Biochemistry*, **39**, 7856–62.

Althaus, E.W., Outten, C.E., Olson, K.E., Cao, H. and O'Halloran, T.V. (1999). *Biochemistry*, **38**, 6559–69.

Andrews, S.C. (1998). *Adv. Microb. Physiol.*, **40**, 281–351.

Bach, S., de Almeida, A. and Carniel, E. (2000). *FEMS Microbiol. Lett.*, **183**, 289–94.

Bäumler, A.J. and Hantke, K. (1992). *Mol. Microbiol.*, **6**, 1309–21.

Bearden, S.W. and Perry, R.D. (1999). *Mol. Microbiol.*, **32**, 403–14.

Bearden, S.W., Fetherston, J.D. and Perry, R.D. (1997). *Infect. Immun.*, **65**, 1659–68.

Bearden, S.W., Staggs, T.M. and Perry, R.D. (1998). *J. Bacteriol.*, **180**, 1135–47.

Becker, K., Köster, W. and Braun, V. (1990). *Mol. Gen Genet.*, **223**, 159–62.

Bickel, H., Gäumann, E., Keller-Schierlein, W., Prelog, V. *et al.* (1960). *Experientia*, **16**, 129–33.

Bishop, L., Agbayani, H.R., Jr., Ambudkar, S.V., Maloney, P.C. and Ames, G.F.-L. (1989). *Proc. Natl Acad. Sci. USA*, **86**, 6953–7.

Böhnke, R. and Matzanke, B.J. (1995). *Biometals*, **8**, 323–30.

Bonnah, R.A., Lee, S.W., Vasquez, B.L., Enns, C.A. and So, M. (2000). *Cellular Microbiol.*, **2**, 207–18.

Bös, C., Lorenzen, D. and Braun, V. (1998). *J. Bacteriol.*, **180**, 605–13.

Boyer, A.E. and Tai, P.C. (1998). *J. Bacteriol.* **180**, 1662–72.

Bradbeer, C. (1993). *J. Bacteriol.*, **175**, 3146–50.

Braun, M., Killmann, H. and Braun, V. (1999). *Mol. Microbiol.*, **33**, 1037–49.

Braun, V. (1995). *FEMS Microbiol. Rev.*, **16**, 295–307.

Braun, V. (1997). *Arch. Microbiol.*, **167**, 325–31.

Braun, V. (2000). *Drug Resistance Updates*, **2**, 363–9.

Braun, V. and Hantke, K. (1977). In *Microbial interactions* (ed. Reisig, J.L.), Series B, Vol. 3, Chapman and Hall, London, pp. 101–37.

Braun, V. and Killmann, H. (1999). *Trends Biochem. Sci.*, **24**, 104–9.

Braun, V., Günthner, K., Hantke, K. and Zimmermann, L. (1983). *J. Bacteriol.*, **156**, 308–15.

Braun, V., Hantke, K. and Köster, W. (1998). In *Metal ions in biological systems* (eds. Sigel, A. and Sigel, H.), Marcel Dekker, New York, Vol. 35, pp. 67–145.

Brickman, T.J. and McIntosh, M.A. (1992). *J. Biol. Chem.*, **267**, 12350–5.

Brittigan, B.E., Rasmussen, G.T., Olakanmi, O. and Cox, C.D. (2000). *Infect. Immun.*, **68**, 1271–5.

Bruns, C.M., Nowalk, A.J., Arvai, A.S., McTigue, M.A. *et al.* (1997). *Nature Struct. Biol.*, **4**, 919–24.

Bsat, N., Herbig, A., Casillas-Martinez, L., Setlow, P. and Helmann, J.D. (1998). *Mol. Microbiol.*, **29**, 189–98.

Buchanan, S.K., Smith, B.S., Venkatramani, L., Xia, D. *et al.* (1999). *Nature Struct. Biol.*, **6**, 56–63.

Bullen, J.J. and Griffith, E. (eds) (1987). *Iron and Infection. Molecular, Physiological and Clinical Aspects*. John Wiley & Sons, New York.

Bult, C.J., White, O., Olsen, G.J., Zhou, L. *et al.* (1996). *Science* **273**, 1058–73.

Cadieux, N. and Kadner, R.J. (1999). *Proc. Natl Acad. Sci. USA*, **96**, 10673–8.

Carson, S.D.B., Stone, B., Beucher, M., Fu, J. and Sparling, P.F. (2000). *Mol. Microbiol.*, **36**, 585–93.

Clarke, T.E., Ku, S.-Y., Dougan, D.R., Vogel, H.J. and Tari, L.W. (2000). *Nature Struct. Biol.*, **7**, 287–91.

Cope, L.D., Hrkal, Z. and Hansen, E. (2000). *Infect. Immun.*, **68**, 4092–101.

Cornelissen, C.N., Kelley, M., Hobbs, M.M., Anderson, J.E. *et al.* (1998). *Mol. Microbiol.*, **27**, 611–6.

Crosa, J.H. (1984). *Ann. Rev. Microbiol.*, **38**, 69–89.

Crosa, J.H. (1997). *Microbiol. Molec. Biol. Rev.*, **61**, 319–36.

Davidson, A.L., Shuman, H. and Nikaido, H. (1992). *Proc. Natl Acad. Sci. USA*, **89**, 2360–4.

De Grandis, S., Ginsberg, J., Toone, M., Climie, S., Friesen, J. and Brunton, J. (1987). *J. Bacteriol.*, **169**, 4313–9.

De Lorenzo, V., Wee, S., Herrero, M. and Neilands, J.B. (1987). *J. Bacteriol.*, **169**, 2624–30.

De Lorenzo, V., Herrero, M., Giovannini, F. and Neilands, J.B. (1988). *Eur. J. Biochem.*, **173**, 537–46.

Drazek, E.S., Hammack, C.A. and Schmitt, M.P. (2000). *Mol. Microbiol.*, **36**, 68–84.

Drechsel, H., Stephan, H., Lotz, R., Haag, H. *et al.* (1995). *Liebigs Ann.*, 1727–33.

Dubrac, S. and Touati, D. (2000). *J. Bacteriol.*, **182**, 3802–8.

Earhart, C.F. (1996). In *Escherichia coli and Salmonella* (ed. Neidhard, F.C.), ASM Press, Washington DC, pp. 1075–90.

Enz, S., Mahren, S., Stroeher, U.H. and Braun, V. (2000). *J. Bacteriol.*, **182**, 637–646.

Expert, D., Enard, C. and Masclaux, C. (1996). *Trends Microbiol.*, **4**, 232–6.

Ferguson, A., Hofmann, D.E., Coulton, J.W., Diederichs, K. and Welte, W. (1998). *Science*, **282**, 2215–20.

Ferguson, A.D., Braun, V., Fiedler, H.-P., Coulton, J.W., Diederichs, K. and Welte, W. (2000). *Prot. Sci.*, **9**, 956–63.

Ferguson, A.D., Ködding, J., Walker, G., Bös, C. *et al.* (2001)., submitted for publication.

Fetherston, J.D., Bertolino, V.J. and Perry, R.D. (1999). *Mol. Microbiol.*, **32**, 289–99.

Fonseca, M.V. and Escalante-Semerena, J.C. (2000). *J. Bacteriol.*, **182**, 4304–9.

Fontecave, M., Coves, J. and Pierre, J.L. (1994). *Biometals*, **7**, 3–8.

Foster, J.W. (2000). In *Bacterial Stress Responses* (eds Storz, G., and Hengge-Aronis, R.), ASM Press Washington DC, pp. 99–115.

Geoffroy, V.A., Fetherston, J.D. and Perry, R.D. (2000). *Infect. Immun.*, **68**, 4452–61.

Gonzalez, de Peredo, A., Saint-Pierre, C., Adrait, A., Jacquamet, L., Latour, J.M. *et al.* (1999). *Biochemistry*, **38**, 8582–9.

Gray-Owen, S.D. and Schryvers, A.B. (1993). *Microb. Path.*, **14**, 389–98.

Groeger, W. and Köster, W. (1998). *Microbiol.*, **144**, 2579–769.

Gruer, M.J. and Guest, J.R. (1994). *Microbiology*, **140**, 2531–41.

Grünig, H.M., Rutschi, D., Schoch, C. and Lebek, G. (1987). *Zentralbl. Bakteriol. Mikrobiol. Hyg. [A.]*, **266**, 231–8.

Günter, K. and Braun, V. (1990). *FEBS Lett.*, **274**, 85–8.

Hamed, M.Y. and Neilands, J.B. (1993). *J. Inorg. Biochem.*, **50**, 193–210.

Hancock, R.E.W. and Braun V. (1976). *J. Bacteriol.*, **125**, 409–15.

Hantke, K. (1990). *FEMS Microbiol. Lett.*, **67**, 5–8.

Hantke, K. (1997). *J. Bacteriol.*, **178**, 6201–4.

Hantke, K. and Braun, V. (1973). *Eur. J. Biochem.*, **34**, 284–96.

Hantke, K. and Braun, V.(1998). In *Metal Ions in Gene Regulation* (eds Silver, S. and Walden, W.), Chapman and Hall, New York, pp. 11–44.

Hantke, K. and Braun, V. (2000). In *Bacterial Stress Responses* (eds Storz, G. and Hengge-Aronis, R.), ASM Press, pp. 275–88.

Hartmann, A., Fiedler, H.-P. and Braun, V. (1979). *Eur. J. Biochem.*, **99**, 517–24.

Heesemann, J., Hantke, K., Vocke, T., Saken, E. *et al.* (1993). *Mol. Microbiol.*, **8**, 397–408.

Heidinger, S., Braun, V., Pecoraro, V.L. and Raymond, K.N. (1983). *J. Bacteriol.*, **153**, 109–15.

Holm, L., Sander, C., Rüterjans, H., Schnarr, M., Fogh, R., Boelens, R. and Kaptein, R. (1994). *Protein Eng.*, **7**, 1449–53.

Janakiraman, A. and Slauch, J.M. (2000). *Mol. Microbiol.*, **35**, 1146–55.

Johnstone, R.W., Ruefli, A.A. and Smyth, M. (2000). *Trends in Biochem.*, **25**, 1–6.

Kammler, M., Schön, C. and Hantke, K. (1993). *J. Bacteriol.*, **175**, 6212–9.

Karpishin, T.B., Dewey, T.M. and Raymond, K.N. (1993). *J. Am. Chem. Soc.*, **115**, 1842–51.

Kehres, D.G., Zaharik, M.L., Finlay, B.B. and Maguire, M.E. (2000). *Mol. Microbiol.*, **36**, 1085–1100.

Killmann, H., Benz, R. and Braun V. (1993). *EMBO J.*, **12**, 3007–16.

Killmann, H., Videnov, G., Jung, G., Schwarz, H. and Braun, V. (1995). *J. Bacteriol.*, **177**, 694–8.

Kim, I., Stiefel, A. Plantör, S., Angerer, A. and Braun. V. (1997). *Mol. Microbiol.*, **23**, 333–44.

Koebnik, R., Locher, K.P. and van Gelder, P. (2000). *Mol. Microbiol.*, **37**, 239–53.

Konetschny-Rapp, S., Jung, G., Meives, J. and Zähner, H. (1990). *Eur. J. Biochem.*, **191**, 65–74.

Koster, M., van Klompenburg, W., Bitter, W., Leong, J. and Weisbeek, P. (1994). *EMBO J.*, **13**, 2805–13.

Köster, W. and Braun, V. (1990). *J. Biol. Chem.*, **265**, 21407–10.

Lee, H.S., Lee, Y.S., Kim, H.S., Choi, J.Y., Hassan, H.M. and Chung, M.H. (1998). *Free Radic. Biol. Med.*, **24**, 1193–1201.

Leong, S. and An, Z. (1997). In *Transition Metals in Microbial Metabolism* (eds Winkelmann, G. and Carrano, C.J.), Harwood Academic Publishers, Reading, pp. 51–79.

Lewis, L.A., Gipson, M., Hartmann, K., Vaughn, J. and Dyer, D.W. (1999). *Mol. Microbiol.*, **32**, 977–89.

Locher, K.B., Rees, B., Koebnik, R., Mitschler, A. *et al*. (1998). *Cell*, **95**, 771–8.

Locher, K.L. and Rosenbusch, J.P. (1997). *Eur. J. Biochem.*, **274**, 770–5.

Mademidis, A., Killmann, H., Kraas, W., Flechsner, I., Jung, G. and Braun, V. (1997). *Mol. Microbiol.*, **26**, 1109–23.

Mahe, B., Masclaux, C., Rauscher, L., Enard, C. and Expert, D. (1995). *Mol. Microbiol.*, **18**, 33–43.

Matzanke, B.F., Berner, I., Bill, E., Trautwein, A.X. and Winkelmann, G. (1991). *Biometals*, **4**, 181–5.

Merianos, H.J., Cadieux, N., Lin, C.H., Kadner, R.J. and Cafiso, D.S. (2000). *Nature Struct. Biol.*, **7**, 205–9.

Mietzner, T.A., Tenza, S.B., Adhikari, P., Vaughan, K.G. and Nowalk, A.J. (1998). *Curr. Topics Microbiol. Immunol.*, **228**, 113–35.

Moeck, G.S. and Coulton, J.C. (1998). *Mol. Microbiol.*, **28**, 675–81.

Moeck, G.S. Coulton, J.C. and Postle, K. (1997). *J. Biol. Chem.*, **272**, 28391–7.

Müller, K., Matzanke, B.F., Schünemann, V., Trautwein, A.X. and Hantke, K. (1998). *Eur. J. Biochem.*, **258**, 1001–8.

Munzinger, M., Budzikiewicz, H., Expert, D., Enard, C. and Meyer, J.M. (2000). *Z. Naturforsch. [C].*, **55**, 328–32.

Neilands, J.B. (1952). *J. Am. Chem. Soc.*, **74**, 4846.

Ochs, M., Veitinger, S., Kim, I., Welz, D., Angerer A. and Braun, V. (1995). *Mol. Microbiol.*, **15**, 119–32.

Patzer, S.I. and Hantke, K. (1998). *Mol. Microbiol.*, **28**, 1199–210.

Patzer, S.I. and Hantke, K. (1999). *J. Bacteriol.*, **181**, 3307–9.

Pierre, J.L. and Gautier-Luneau, I. (2000). *Biometals*, **13**, 91–6.

Pohl, E., Holmes, R.K. and Hol, W.G. (1999). *J. Mol. Biol.*, **292**, 653–67.

Pugsley, A.P., Zimmermann, W. and Wehrli, W. (1987). *J. Gen. Microbiol.*, **133**, 3505–11.

Ratledge, C. and Dover, L.G. (2000). *Ann. Rev. Microbiol.*, **54**, 881–941.

Ratnayake, D.B., Wai, S.N., Shi, Y., Amako, K., Nakayama, H. and Nakayama, K. (2000). *Microbiology*, **146**, 1119–27.

Raymond, K.N., Müller, G. and Matzanke, B.F. (1984). In *Topics in Current Chemistry* (ed. Boschke, F.L.), Springer-Verlag, Berlin, 49–102.

Ren, Z., Jin, H., Whitby, P.W., Morton, D.J. and Stull, T.L. (1999). *J. Bacteriol.*, **181**, 5865–70.

Richardson, A.R. and Stojiljkovic, I. (2000). *J. Bacteriol.*, **118**, 2067–74.

Richardson, D.T. and Park, S.F. (1995). *Microbiol.*, **141**, 3181–91.

Rohrbach, M.R., Braun, V. and Köster, W. (1995). *J. Bacteriol.*, **177**, 7186–93.

Saito, T., Wormald, M.R. and Williams, R.J. (1991). *Eur. J. Biochem.*, **197**, 29–38.

Salomon, R.A. and Farias, R.N. (1994). *FEMS Microbiol. Lett.*, **121**, 275–9.

Schneider, R. and Hantke K. (1993). *Mol. Microbiol.*, **8**, 111–21.

Schöffler, H. and Braun V. (1998). *Mol. Gen. Genet.*, **217**, 378–83.

Schryvers, A.B. and Stojiljkovic, I. (1999). *Mol. Microbiol.*, **32**, 1117–23.

Schubert, S., Rakin, A., Fischer, D., Sorsa, J. and Heesemann, J. (1999). *FEMS Microbiol. Lett.*, **179**, 409–14.

Schultz-Hauser, G., Köster, W., Schwarz, H. and Braun, V. (1992). *J. Bacteriol.*, **174**, 2305–11.

Sebulsky, M.T., Hohnstein, D., Hunter, M.D. and Heinrichs, D.E. (2000). *J. Bacteriol.*, **182**, 4394–4400.

Silberg, J.J., Hoff, K.G., Tapley, T.L. and Vickery, L.E. (2000). *J. Biol. Chem.*, in press.

Stintzi, A., Barnes, C., Xu, J. and Raymond, K.N. (2000). *Proc. Natl Acad. Sci., USA*, **97**, 10691–96.

Stojiljkovic, I. and Hantke, K. (1995). *Mol. Gen. Genet.*, **247**, 199–205.

Stojiljkovic, I., Bäumler, A.J. and Hantke, K. (1994). *J.Mol.Biol.*, **236**, 531–45.

Takase, H., Nitanai, H., Hoshino, K. and Otani, T. (2000a). *Infect. Immun.*, **68**, 4498–504.

Takase, H., Nitanai, H., Hoshino, K. and Otani, T. (2000b). *Infect. Immun.*, **68**, 1834–9.

Tardat, B. and Touati, D. (1993). *Mol. Microbiol.*, **9**, 53–63.

Telford, J.R. and Raymond, K.N. (1996). In *Comprehensive Supramolecular Chemistry*, Vol. 1 (eds Lehn, J.M. and Gokel, G.W.), Pergamon Press, London, 245–66.

Torres, A.G. and Payne, S.M. (1997). *Mol. Microbiol.*, **23**, 825–33.

Touati, D., Jacques, M., Tardat, B., Bouchard, L. and Despied, S. (1995). *J. Bacteriol.*, **177**, 2305–14.

Tsolis, R.M., Bäumler, A.J., Stojiljkovic, I. and Heffron, F. (1995). *J. Bacteriol.*, **177**, 4628–37.

Tsolis, R.M., Bäumler, A.J., Heffron, F. and Stojiljkovic, I. (1996). *Infect. Immun.*, **64**, 4549–56.

Van Hove, B., Staudenmaier, H. and Braun, V. (1990). *J. Bacteriol.*, **172**, 6749–58.

Vasil, M.L. and Ochsner, U.A. (1999). *Mol. Microbiol.*, **34**, 399–413.

Velayudhan, J., Hughes, N.J., McColm, A.A., Bagshaw, J., Clayton, C.L., Andrews, S.C. and Kelly, D.J. (2000). *Mol. Microbiol.*, **37**, 274–86.

Venturi, V., Weisbeek, P. and Koster, M. (1995). *Mol. Microbiol.*, **17**, 603–10.

Viswanathan, V.K., Edelstein, P.H., Pope, C.D. and Cianciotto, N.P. (2000). *Infect. Immun.*, **68**, 1069–79.

Wai, S.-N., Nakayama, K., Umene, K., Moriya, T., Amako, K. (1996). *Mol. Microbiol.*, **20**, 1127–34.

Wandersman, C. and Stojiljkovic, I. (2000). *Curr. Opinions Microbiol.*, **3**, 215–20.

Weinberg, E.D. (1978). *Microbiol. Rev.*, **42**, 45–66.

Weinberg, E.D. (1990). *Drug Metabolism Reviews*, **22**, 531–79.

Welz, D. and Braun, V. (1998). *J. Bacteriol.*, **180**, 2387–94.

Williams, P.H. (1979). *Infect. Immun.*, **26**, 925–32.

Winkelmann, G. and Drechsel, H. (1997). *Microbial Siderophores*. VCH Weinheim, Germany.

Woodridge, K.G. and Williams, P. (1993). *FEMS Microbiol. Rev.*, **12**, 325–48.

Wyckoff, E.E., Duncan, D., Torres, A.G., Mills, M., Maase, K. and Payne, S. (1998). *Mol. Microbiol.*, **28**, 1139–52.

Zheng, L., Cash, V.L., Flint, D.H. and Dean, D.R. (1998). *J. Biol. Chem.*, **273**, 13264–72.

Zheng, M., Doan, B., Schneider, T.D. and Storz, G. (1999). *J. Bacteriol.*, **181**, 4639–43.

Zhou, P., Borovok, I., Lucana, D.O., Müller, D. and Schrempf, H. (1999). *Microbiol.*, **145**, 549–59.

4 Iron Uptake by Plants and Yeast

4.1 Iron Acquisition by Plants

4.1.1 Introduction

> *Thy steps are by the farmer's prayers attended;*
> *Like flames upon the altar shine the sheaves;*
> *And, following thee, in thy ovation splendid,*
> *Thine almoner, the wind, scatters the golden leaves!*

'Autumn' Henry Wadsworth Longfellow (1807–1882)

Those leaves bear with them most of the inorganic, as well as much of the organic, matter that constitutes the tree, and come the springtime these minerals must be reassimilated from the soil by the roots of the tree and, in many cases, pumped up to the branches where their iron-intensive photosynthetic apparatus will be resynthesized. Mineral nutrition in plants is an important factor in both growth and development and, as a consequence, in crop productivity. However, at the molecular level, our knowledge concerning the acquisition, assimilation and storage of most essential metal ions is rather limited. Iron is one of the three nutrients that most commonly limit plant growth but, unlike the other two limiting nutrients – nitrogen and phosphorus – iron deficiency is not easily remedied by fertilizers because the added iron becomes unavailable in the form of insoluble iron hydroxides. Iron is important not only because of its role in fundamental processes such as photosynthesis, respiration, nitrogen fixation and DNA synthesis, but also because of its involvement in key enzymes of plant hormone synthesis, such as lipoxygenases (Siedow, 1991) and ethylene-forming enzymes (Bouzayen *et al.*, 1991). Despite the fact that iron represents 4–5 % of the total solid mineral composition of soils, it is generally present as poorly soluble ferrihydrite, and its bioavailability is further decreased at the neutral and alkaline pH values found in semiarid, calcareous soils.[†] Discrepancies between the solubility of iron in the soil and the demand for iron are the primary cause of iron-deficiency chlorosis in plants. The concentration

---

[†] Which are estimated to represent over one-third of the world's surface area, and account for 44 million acres of cropland in the United States.

of soluble Fe^{3+} decreases by one-thousandfold for every unit of increase in the pH, such that it is virtually unavailable above pH 4. Plants require approximately 10–20 nM for growth, but in calcareous soils total soluble iron reaches no more than 100 μM. Without active mechanisms for extracting iron from the soil, most plants would therefore exhibit symptoms of iron deficiency, such as leaf intraveinal chlorosis (Guerinot and Yi, 1994; Briat *et al*., 1995). However, since the solubility of iron in soils will also be affected by the redox potential and pH, it is clear that in flooded or waterlogged acidic soils, where O_2 availability is low, Fe^{2+} can attain high concentrations and become toxic to the plants by producing reactive oxygen free radicals such as $OH^{\bullet}$. These can of course damage cellular components leading to loss of cellular integrity and eventually cell death (Guerinot and Yi, 1994; Briat *et al*., 1995). The immobility of plants also results in large differences of iron availability in their immediate environment. It is on account of these problems of limited solubility on the one hand and potential Fe^{2+} toxicity on the other that plants have evolved mechanisms to control iron fluxes. These responses are mediated by signals, most of which are still not well characterized, but which result in the control of iron uptake by the roots, long-distance iron transport between roots and shoots, in sensing the iron status of the leaves and signalling it to the roots, in subcellular iron distribution, and in detoxifying and buffering iron when it is in excess (Briat *et al*., 1995).

4.1.2 Iron Acquisition by the Roots of Plants

Dicotyledons and Non-grass Monocotyledons (Strategy I) – Ferrous Iron Transport

In the absence of iron stress, i.e. in iron-sufficient conditions, all plant roots reduce Fe(III) chelates, and transport Fe(II) through the plasma membrane by a constitutive plasma membrane-bound ferric reductase (Briat *et al*., 1995; Bienfait, 1985). However, physiological responses to iron-deficiency stress, which result in increased iron acquisition, can be classified into two different strategies (Römheld and Marschner, 1986). Dicotyledons[‡] and non-graminaceous monocotyledons utilize what is commonly referred to as Strategy I, in which they respond to iron stress by an increased root-reducing capacity. In contrast, graminaceous species (grasses), which are much less susceptible to iron chlorosis, especially when grown in alkaline soils, use Strategy II, and under iron deficiency they produce non-protein amino acids called phytosiderophores, which are released from their roots.

In iron-deficient conditions Strategy I plants (Figure 4.1) acidify the soil, through the activation of a specific H^+-ATPase (Guerinot and Yi, 1994), increase their reducing capacity at the root plasma membrane, and possibly also release reductants into the rhizosphere.[¶] They also release iron chelators, such as caffeic acid

---

[‡] The distinction between mono-and dicotyledonous plants is quite simple: monocotyledons are flowering plants which have only one seed leaf, and usually have parallel-veined leaves, flower parts in multiples of three, and no secondary growth in stems and roots, whereas dicotyledons are flowering plants with two seed leaves (cotyledons), net-veined leaves, flower parts in fours and fives, and in woody plants have cambium, a layer of formative cells between the wood and the bark; the cells increase by division and differentiate to form new wood and bark.

[¶] The rhizosphere is the part of the soil enclosing and influenced by the roots of a plant.

from soybeans and tomato, pistidic acid from pigeon pea, or alfafuran from alfalfa (Mori, 1998). The low pH increases iron solubility which, together with the phenolic chelators, releases iron from soil ferrihydrite. The Fe(III)chelate is reduced by an inducible plasma-membrane-bound reductase and transported into the cells by an Fe(II) transporter (Guerinot and Yi, 1994; Briat *et al.*, 1995; Bienfait, 1985). This enhanced reductase activity coincides with the spatial and temporal alteration of root morphology. In the roots of Fe-starved non-gramminaceous plants, formation of root hairs is increased and the root cortex shows increased cell wall ingrowth into cytoplasm (so-called transfer cells) with dense cytoplasm and cell wall protuberances, that are supposed to increase the surface area of the epidermal cell membranes for proton extrusion (Kramer *et al.*, 1980; Schmidt and Bartels, 1996). The transfer cells, which have numerous mitochondria and an extensive rough endoplasmic reticulum, are not found in grasses (Strategy II plants). The enhanced plasma membrane reductase activity coincides spatially and temporally with the morphological responses, although the two are controlled separately (Moog *et al.*, 1995).

As we will see later in this chapter, there are striking similarities between the uptake of iron in Strategy I plants and in the yeast, *Saccharomyces cerevisiae* (Eide, 1998). Yeast ferric reductases and both high- and low-affinity ferrous transporters have been cloned, and mutants deficient in these genes have been used to try to clone the corresponding plant genes by functional complementation using *Arabidopsis thaliana* (for which the complete genome sequence is now available). The FRO2 gene, which is expressed in iron-deficient roots of *Arabidopsis*, has been cloned recently by PCR, using oligonucleotides derived from the yeast ferric reductase FRE1 and FRE2 sequences (Robinson *et al.*, 1999), and appears to represent the ferric chelate reductase. The reducing equivalents are supplied by transmembrane

(a)
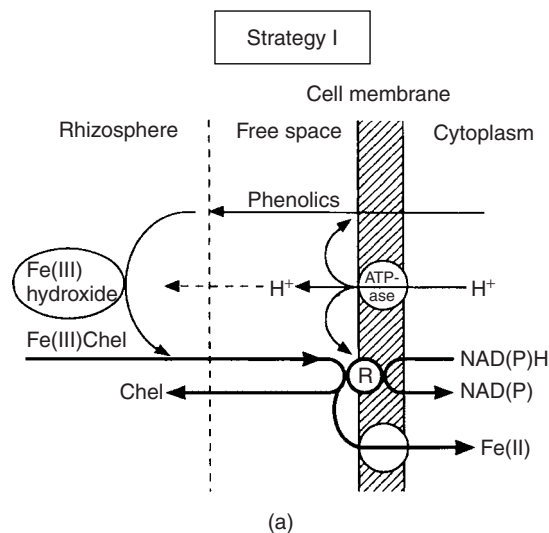
Figure 4.1 (a) Mechanism of iron absorption of Strategy I in the roots of dicots and non-graminaceous monocots. (b) Mechanism of iron absorption of Strategy II in the roots of graminaceous plants. Reprinted from Mori, 1998, by courtesy of Marcel Dekker, Inc.
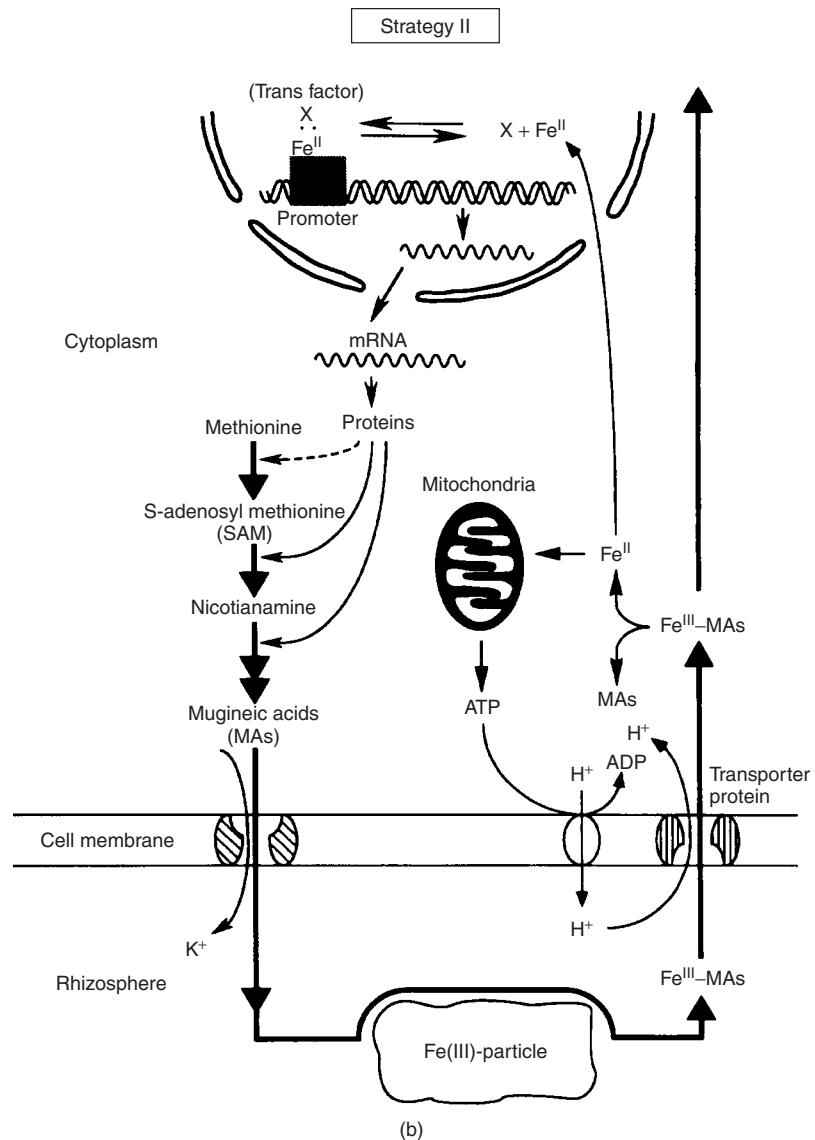
Figure 4.1 (*continued*)

electron transfer from cyosolic NADPH to extracellular iron compounds which serve as electron acceptors, and this is an obligatory step required for iron uptake. FRO2 belongs to a superfamily of flavocytochromes (Figure 4.2) that transport electrons across membranes. It has intramembrane binding sites for haem (four His residues which are predicted to bind two haems) and cytoplasmic binding sites for nucleotide cofactors (FAD and NADPH) that donate and transfer electrons. By analogy with the human phagocytic NADPH oxidase gp91phox (Chanock *et al.*, 1994) and yeast ferric-chelate reductases such as FRE1 (Dancis *et al.*, 1990) and FRP1 (Roman *et al.*, 1993), it is proposed that FRO2 transfers electrons from cytosolic donors to FAD, and then through two consecutive haem groups to single
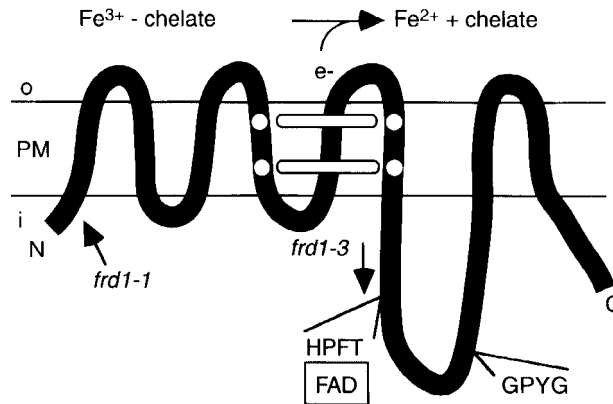
Figure 4.2 Hypothetical plasma membrane (PM)-associated structure of FRO2. Four histidine residues (white spots) predicted to coordinate two intramembraneous haem groups (white bars) are indicated, as are the tetrapeptide binding sites for FAD and NAD(P)H. The sites of mutations in the FRO gene are indicated (*frd1-1*, *frd1-3*); i, inside cell; o, outside cell. Reprinted with permission from Nature (Robinson *et al.*, 1999). Copyright (1999) Macmillan Magazines Limited.

electron acceptors (Fe^{3+}-chelate) on the opposite face of the membrane (Figure 4.2). The reduced iron is then transported across the root plasma membrane by Fe(II) transporters.

A putative *Arabidopsis* ferrous transporter, IRT1, has been cloned (Eide *et al.*, 1996) using the yeast double mutant *fet3 fet4* (ferrous transporter) impaired in both high- and low-affinity ferrous transporters. IRT1 is not equivalent to either FET3 or FET4, but rather seems to be a new class of eukaryotic metal-ion transporter, with related sequences in rice, yeast, nematodes and humans. The gene codes for a predicted protein of 339 amino acids, with eight transmembrane domains and four HisGly repeats, constituting potential metal-binding domains between transmembrane domains 3 and 4. IRT1 transcripts were detected in *Arabidopsis* in roots where they accumulated in response to iron deficiency. Under these conditions there were increased levels of root-associated Mn, Zn and Co (Korshunova *et al.*, 1999), and IRT1 cDNA was found to complement mutant strains of yeast defective in either Mn or Zn uptake, but not a Cu uptake-defective mutant. Iron uptake in IRT1-expressing yeast was inhibited by several transition metals, Cd, Co, Mn and Zn. Taken together these data indicate that IRT1 is a broad-range metal-ion transporter in plants.

Although the IRT1/ FRO2 system is likely to be a major component in iron-uptake systems in *Arabidopsis*, and in other Strategy I plants, other proteins might also be involved. In rice, *Oriza sativa* (Os) three genes coding for proteins similar to the mammalian *Nramp* genes (Chapters 5 and 8) have been cloned (Belouchi *et al.*, 1995,1997), and in *Arabidopsis thaliana* (At) the sequence of five NRAMP proteins has been determined (Curie *et al.*, 2000). It has been shown that *AtNramp 1* and *OsNramp 1* can complement the *fet3 fet4* yeast mutant defective in both high- and low-affinity ferrous transport. The *AtNramp 1* transcript accumulates in response to iron deficiency in roots but not in leaves, and its overexpression in transgenic *A. thaliana* plants leads to an increased resistance to toxic iron concentrations (Curie *et al.*, 2000). These results indicate that *AtNramp1* participates in the control of iron

homeostasis in plants. cDNAs corresponding to three of the five *AtNramp* genes have been cloned and characterized (Tomine *et al.*, 2000) and shown to be involved in transport of both iron and cadmium in *Arabidopsis*.

Since Strategy I is accompanied by altered root morphology, the possible involvement of plant hormones in the regulation of iron stress has been proposed (Kramer *et al.*, 1980). The reciprocal involvement of auxin and abscisic acid in stimulation of ATP-driven proton extrusion in iron-deficient plants seems likely (Landsberg, 1986). Ethylene synthesis is regulated by iron (Bouzayen *et al.*, 1991), and ethylene has also been shown to be involved in Fe-deficiency-induced Fe(III) reduction (Romero and Alcantara, 1994). However, recent analysis of 45 *Arabidopsis* mutants defective in hormone metabolism and/or root hair formation indicated that hormones are not required for ferric chelate reductase activity, and once again underlined that the morphological and physiological components of the iron-stress syndrome are regulated separately (Schmidt *et al.*, 2000).

Graminaceous Plants (Strategy II) – Ferric Iron Transport

Strategy II plants (grasses) respond to iron deficiency by releasing phytosiderophores (Figure 4.1), which can chelate poorly soluble iron from soils, in the form of phosphates or hydroxides, by the formation of Fe(III)–phytosiderophore complexes. The Fe–phytosiderophore complex is then taken up at the root plasma membrane via an as yet uncharacterized specific transporter (Mihashi and Mori, 1989; Römheld and Marschner, 1986). Phytosiderophores chelate and solubilize soil iron efficiently at high pH values and high concentrations of bicarbonate (Inoue *et al.*, 1993; Takagi *et al.*, 1988) whereas bicarbonate inhibits the solubilization of Fe(III) by proton release accompanied by an increase in the reducing capacity at the roots (Strategy I) (Coulombe *et al.*, 1984; Touleau *et al.*, 1992). This ecological advantage of Strategy II plants favours grasses over non-graminaceous species in bicarbonate buffered soils (Chen and Barak, 1982). Phytosiderophores, non-proteinogenic secondary amino acids of molecular weight around 320, are synthesized from nicotianamine to give the so-called mugineic acids (Shojima *et al.*, 1990), which can effectively chelate ferric iron via their amino and carboxyl groups (Mino *et al.*, 1983). Nicotianamine (Figure 4.3) is synthesized by the condensation of three molecules of *S*-adenosyl methionine in a reaction catalyzed by nicotianamine synthase (Shojima *et al.*, 1990), an enzyme that has an increased activity in response to iron deficiency which is one-hundredfold higher in roots than in leaves. Nicotianamine synthase has been purified to homogeneity from iron-deficient barley roots (Higuchi *et al.*, 1994) as a homodimer of subunit molecular weight of 30 kD, which appears to be absent in iron-sufficient barley roots. The nicotianamine synthase genes have been recently cloned, and form a multigene family in the barley and rice genomes (Higuchi *et al.*, 1999). Nicotianamine is found in every plant so far investigated, although its eventual role in iron metabolism remains unknown, whereas the mugineic acid family of phytosiderophores is only found in graminaceous plants.

Nicotianamine is converted to a first phytosiderophore, 2′-deoxymugeneic acid, by amino transfer and subsequent reduction (Figure 4.3). Nicotianamine amino-transferase, which catalyzes the initial amino transfer reaction, the first step
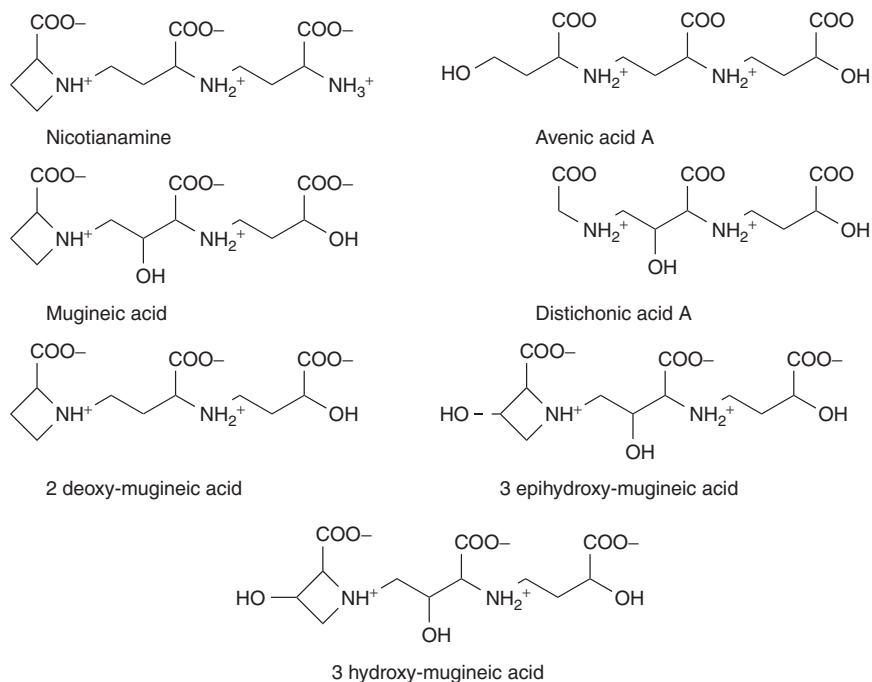
Figure 4.3   Structures of nicotianamine and mugineic acids.

in the unique biosynthetic pathway to mugineic acids, has been purified from iron-deficient barley roots. Two distinct cDNA clones have been identified, and their deduced amino-acid sequences found to be homologous to several aminotransferases, and they shared consensus sequences for the pyridoxal phosphate binding-site lysine residue and its surrounding residues (Takahashi *et al.*, 1999). The 2′-deoxymugeneic acid is subsequently converted to the other phytosiderophores, mugineic acid and 3-epihydroxy mugineic acid (Figure 4.3) by consecutive hydroxylation steps. Transcripts of two candidate cDNAs cloned by differential screening (*ids2* and *ids3*) ('iron-deficiency specific') specifically accumulate in roots of barley grown under iron-deficient conditions, and code for two putative polypeptides of 338 and 169 amino acids respectively. Ids2 and Ids3 share a region similar to the functional domain of α-ketoglutarate dioxygenases (Chapter 2), and are therefore good candidates for these two hydroxylation steps in phytosiderophore biosynthesis (Nakanishi *et al.*, 1993; Okumura *et al.*, 1994). Recently it has been shown that the activity of adenine phosphoribosyltransferase is induced by iron deficiency in barley roots, and in the roots of other graminaceous plants such as rye, maize and rice, but not in the roots of a non-graminaceous plant, tobacco (Itai *et al.*, 2000). The role of adenine phosphoribosyltransferase, which mediates AMP synthesis through the transfer of adenine to phosphoribosylpyrophosphate with release of pyrophosphate, in the biosynthesis of mugineic acids may be related to adenine salvage in the methionine cycle.

The mugineic acid family of phytosiderophores comprises six compounds: mugineic acid, avenic acid, 3-hydroxymugeneic acid, 3-epihydroxymugeneic acid,

2′-deoxymugeneic acid, and disticonic acid. We have described above how three of them are formed. Of the others, avenic acid and disticonic acid are probably derived from 2′-deoxymugeneic acid and 3-epihydroxymugeneic acid respectively by ring opening, and 3-hydroxymugeneic acid by hydroxylation of mugineic acid (summarized in Ma and Nomoto, 1996). Following their synthesis in response to iron stress, the phytosiderophores are secreted into the rhizosphere (Figure 4.1), where they complex and solubilize Fe(III). The Fe(III)-phytosiderophore is presumed to be transported across the root plasma membrane by a specific transporter(Mihashi and Mori, 1989), although it has not yet been characterized at the molecular level. Once inside the cell, the iron is released by a ferric reductase. Preliminary characterization of an NADH-dependent ferric chelate reductase from maize (Bagnaresi and Pupillo, 1995) suggests that it has similar properties to the ferric chelate reductase of tomato, a Strategy I plant (Bagnaresi *et al.*, 1997), and that both belong to the cytochrome b_5 reductase flavoprotein family.

Mutants Affected in Iron Transport

Mutants which affect iron acquisition in plants can be classified into two major groups – those deficient in iron uptake and those in which iron uptake is deregulated (Briat and Lobréaux, 1997). Among the former, mutants defective in acidification and chelate reduction have been identified in both tomato (Ling *et al.*, 1996) and muskmelon (Jolley *et al.*, 1991), but the precise nature of the defect is not yet known. As described above, in Arabidopsis, 'ferric chelate reductase defective' mutants have been characterized (Yi and Guerinot, 1996) and mutations in the FRO2 gene shown to account for the impaired activity of ferric chelate reductase in two mutants (Robinson *et al.*, 1999); one is a nonsense mutation in the first exon of FRO2, the other is substitution of a Thr codon for a Met codon in the deduced tetrapeptide FAD-binding site (Figure 4.2). Two maize mutants have been described (Basso *et al.*, 1994) which develop intraveinal chlorosis – ys1 and ys3 ('yellow' stripes). The former is responsible for a defect in the transport of the Fe(III)-deoxymugineic acid through the root plasma membrane. Since in the ys1 mutant, siderophore synthesis and secretion is normal, it is likely that the YS1 protein is the phytosiderophore transporter (or one of its subunits), or a factor regulating its synthesis. While the ys2 mutant has the same characteristics as ys1, it seems likely that here the secretion of the phytosiderophores into the rhizosphere may be the step which is affected.

   In the second class of mutants, the plant behaves as if it were iron deficient even when grown in iron-sufficient conditions. This results in excessive iron accumulation in shoots, leading to retarded growth and the development of necrotic spots on the leaves. Two such mutants have been described in pea, brz ('bronze') and dgl ('degenerative') which both seem to have increased rates of Fe(III) reduction and uptake, as well as increased capacity to acidify the rhizosphere (Kneen *et al.*, 1990; Grusak *et al.*, 1990; Grusak and Pezeshgi, 1996). A tomato mutant cln ('chloronerva') has been described with constitutive expression of iron uptake responses, a phenotype similar to the pea mutants. Even in the presence of iron it has high ferric reductase activity, extrudes high levels of protons, and accumulates high levels of iron in the shoots (Ling *et al.*, 1996). Biochemically, chloronerva is an auxotroph for

nicotianamine, and map-based cloning has shown that, based on enzyme activity and sequence similarity to the coding DNA sequence of the purified barley enzyme, the chloronerva gene encodes the enzyme nicotianamine synthase (Ling *et al.*, 1996). This raises the interesting question of just what the role of nicotianamine in iron metabolism might be. It has been suggested that the deficiency in nicotianamine synthesis might cause a defect in long-distance signalling of the iron status of the shoots to the roots in both the pea and tomato mutants (Grusak and Pezeshgi, 1996; Stephan and Sholz, 1993).

4.2 Plant Ferritins

Free iron in biological systems is both poorly soluble and potentially toxic, and it must therefore be maintained in a safe and soluble form. Plant ferritins have been detected in the stroma of plastids,[§] and are observed to accumulate in non-green plastids, such as proplastids, etioplasts and amyloplasts, and are found in specific tissues such as shoots, root apex, seeds and nodules. Exogenous treatment with ozone or ethylene, as well as impaired photosynthesis or iron overload, induce ferritin accumulation in chloroplasts, suggesting that both developmental and environmental signals are involved in plant ferritin gene regulation. Plant ferritin subunits are synthesized as a precursor with a transit peptide required for plastid import. Plant ferritins have an additional sequence in their *N*-terminus compared with animal ferritins in the form of an *α*-helical extension peptide, localized on the outer face of the protein shell. The extension peptide is the site of free-radical cleavage during iron exchange *in vitro* (Laulhère *et al.*, 1989), and possibly *in vivo* (Lobréaux and Briat, 1991), leading to ferritin degradation.

4.2.1 Developmental Regulation of Ferritin Synthesis

Whereas immunoblotting of protein extracts from pea vegetative organs does not detect ferritin throughout the plant life cycle (Lobréaux and Briat, 1991), ultrastructural analysis shows that in some tissues ferritins accumulate in non-green plastids (Seckbach, 1982). Ferritin subunit levels increase in seeds during their maturation, and are detected in dry seeds. During germination, ferritins are degraded, apparently by a free-radical mechanism, consistent with the hypothesis that the pool of iron stored in seed ferritin is mobilized during germination, and that the protein shell is degraded. In maize leaves, ferritin is found in young leaf sections and in the tip section containing senescent cells, but not in the central part of the leaf, where mature chloroplasts abound (Theil and Hase, 1993), implying that ferritin is both a source of iron for iron-containing proteins involved in photosynthesis (cytochromes and iron–sulfur proteins) and a means of sequestering potentially toxic iron when chloroplasts degenerate. Both ferritin mRNA and ferritin subunits

---

[§] Plastids are any of a number of interrelated organelles occurring in the cytoplasm of plant cells in which starch, oil, protein, pigments, etc., are stored. The chlorophyll-containing chloroplasts, the site of photosynthesis, are referred to as green plastids.

are detected in soybean nodules before the accumulation of the key iron proteins required for nitrogen fixation, nitrogenase and leghaemoglobin (Ragland and Theil, 1993). In mature nodules, lower levels of ferritin are found, although mRNA levels remain unchanged. Thus ferritin seems to function as reserve of iron for both photosynthesis and nitrogen fixation. The targeting of plant ferritin to plastids is assured at the molecular level by a transit peptide at the *N*-terminal extremity of the protein (Heijne *et al.*, 1989). In addition to this peptide, it appears from model-building studies with pea ferritin (Lobréaux *et al.*, 1992a) that there is a 24-residue extension peptide compared with mammalian ferritins, which is the site for free-radical cleavages during iron exchanges *in vitro* (Laulhère *et al.*, 1989) and possibly *in vivo* (Lobréaux and Briat, 1991), leading to ferritin degradation.

4.2.2   Iron-regulated Expression of Ferritin Genes

Accumulation of plant ferritin is induced by stress conditions such as iron overload or treatment with ozone, and during recovery from iron deficiency, when it buffers iron availability in plastids (Van der Mark *et al.*, 1983; Proudhon *et al.*, 1989). Unlike the situation in animal cells, where ferritin synthesis is regulated at the level of ribosomal mRNA translation by the binding activity of iron regulatory proteins (Chapter 7), no such regulatory sequences have been found in plant ferritin cDNAs or genes, and no iron regulatory protein binding activities have been found in plant cell extracts. When plant cells are overloaded with iron, levels of ferritin mRNA increase (Lescure *et al.*, 1991; Lobréaux *et al.*, 1992b), and are regulated in soybean cell suspension cultures at the level of DNA transcription (Lescure *et al.*, 1991). Two pathways seem to be involved in the accumulation of ferritin mRNA in response to iron. One involves the plant stress hormone abscisic acid: iron overload in maize plantlets leads to a fivefold increase in abscisic acid levels in roots and leaves, and ferritin mRNA levels are increased by exogenous abscisic acid treatment (Lobréaux *et al.*, 1993). The other pathway seems to be mediated by iron-mediated oxidative stress. In conditions of iron overload, using derooted maize plantlets from abscisic-acid-deficient mutants, treatment with glutathione or *N*-acetyl cysteine (a precursor for glutathione synthesis) abolished the increase in ferritin mRNA. Hydrogen peroxide treatment performed in low iron concentrations led to an increased ferritin mRNA transcript level (Lobréaux *et al.*, 1995), and similar results were obtained using *Arabadopsis thaliana* plantlets (Gaymard *et al.*, 1995). In maize, two subclasses of ferritin cDNAs have been cloned (Fobis-Loisy *et al.*, 1995); the mRNA transcripts of one of these accumulates in response to both iron and abscisic acid treatments, whereas the transcript of the other only increases with iron treatment.

4.3   Iron Acquisition by Yeast

The budding yeast *Saccharomyces cerevisiae* is an extremely attractive eukaryotic model system for the study of genes involved in iron metabolism. This is because of its short generation time, the ease with which relatively large amounts of

biomass can be grown relatively inexpensively on defined media, and the fact that its complete genome has been recently sequenced (Goffeau *et al.*, 1996). The yeast genome is small (6043 genes), most yeast genes do not, unlike most other eukaryotes, have introns, so that a genomic library is essentially equivalent to a cDNA library. Yeast favours homologous recombination, unlike mammals, and it is comparatively easy to inactivate specific genes. Finally, it turns out that not only do many of the mechanisms involved in iron uptake and metabolism in mammalian systems have homologous systems in yeast, but many of the genes involved in iron acquisition in yeast have homology with human genes that cause disease states in man when they are functionally inactive (Askwith and Kaplan, 1998).

4.3.1 Introduction – Pathways for Iron Uptake

Just as was seen with bacterial systems, as represented by *E. coli*, so yeast has multiple transport systems for iron (for a recent review see Ardon *et al.*, 2000). At present we know of five systems, described in detail below, and which are:

  (i)   A low-affinity Fe(II) iron-transport system coded by the *FET4* gene.

 (ii)   A high-affinity iron-transport system consisting of the proteins coded by the *FET3* gene (a ferroxidase) and the *FTR1* gene (an Fe(III) permease).

(iii)   Divalent cation/ proton symports of the *SMF* gene family, which are homologous to the mammalian transporter DMTI (Chapters 5 and 8).

(iv)   Two different transport systems able to mediate uptake of iron from iron−siderophore complexes secreted by other organisms. One system uses the high affinity system [(ii) above] while the second requires the products of the *ARN* gene family.

 (v)   A transport system for recovery of iron from the vacuole which comprises the *FET5* and *FTH1* gene products.

These different systems come into operation under different conditions both environmental and in terms of growth requirements. As we will see later in this chapter, yeasts do not appear to have a mechanism for iron excretion, so that their cellular iron homeostasis, as in *E. coli*, relies on tight control of uptake and eventually storage. As we will see when we examine these iron uptake systems in detail, most of them require ferrous iron, rather than ferric. This implies that the first step required for iron transport is the reduction of Fe^{3+} to Fe^{2+} by membrane-bound reductases.

4.3.2 Cell Surface Reductases

As we saw in the previous section, Strategy 1 plants utilize ferric reductases, with NADPH as electron donor, coupled to proton extrusion and a specific Fe(II) transport system localized in the root plasma membrane. *Saccharomyces cerevisiae* also uses cell surface reductases to reduce ferric iron, and in early studies (Lesuisse *et al.*, 1987;

Raguzzi *et al*., 1988), it was shown that iron uptake in yeast requires (a) reduction of Fe(III) by an NADPH-dependent enzyme and (b) subsequent transfer of Fe(II) into the cell. This transfer could be inhibited by other divalent cations. In further studies, the yeast plasma membrane reductase was extensively purified (Lesuisse *et al*., 1990). Subsequently, two ferric reductase genes were identified in yeast, designated *FRE1* and *FRE2*, that have 25 % amino-acid sequence identity (Dancis *et al*., 1990; Georgatsou *et al*., 1997): deletion of both *FRE1* and *FRE2* results in complete loss of reductase activity. FRE1 has a molecular weight of 78.8 kDa (Shatwell *et al*., 1996) and has sequence homology to the large subunit, gpP1phox of the NADPH oxidase localized in the plasma membrane of human phagocytic cells (Chanock *et al*., 1994). As was discussed for the *FRO2* gene of *Arabidopsis thaliana* (Figure 4.2), FRE1 is thought to be a transmembrane flavocytochrome b_{558} electron-transfer protein, with NADPH and FAD binding domains at its cytosolic face, and a pair of intramembrane haems which transfer electrons one at a time to Fe(III) at the external surface of the cell. If this comparison holds good, we might expect that FRE1 is part of a larger electron-transfer chain, which would supply electrons to NADPH through an NADPH dehydrogenase. A gene of as yet unclear function, *UTR1* was found to affect ferrireductase activity (Lesuisse *et al*., 1996). Five more genes with significant homology to *FRE1* to *FRE2* have been found within the yeast genome (Martins *et al*., 1998), but their possible role in iron uptake is not established. The regulation of the *FRE* genes is thought to involve the transcription factor Aft1p, which binds to most of the *FRE* genes under conditions of low iron and activates their transcription. The analogous transcription factor for copper uptake in yeast is Mac1p, and *FRE1* contains two Mac1p binding sites in its promotor region (Martins *et al*., 1998), underlining the close linkage between the physiology of iron and copper. The ferrireductases FRE1 and FRE2 not only reduce Fe(III) but also reduce Cu(II), which supplies Cu(I), the substrate for the cell surface copper transporters *CTR1* and *CTR3* described in Chapter 13.

4.3.3   Iron Uptake Across the Plasma Membrane

Low Affinity Iron-Transport System

The need for the *FRE1/FRE2* ferrireductase system for cell survival can be circumvented by supplying yeast with iron as Fe^{2+}, and as was shown earlier, other divalent cations can compete for Fe^{2+} uptake (Lesuisse *et al*., 1987). The low-affinity iron-uptake pathway was identified by screening for genes capable of restoring normal growth in strains in which the *FET3* gene had been deleted ($\Delta fet3$). These strains were still able to grow on an iron-rich medium, indicating that there was an alternative iron-uptake system. The *FET4* gene, when overexpressed, allowed growth of the $\Delta fet3$ strain on low iron media (Dix *et al*., 1994). Fet4p is a 63 kD integral membrane with six transmembrane domains, and has all the characteristics of a classic plasma membrane permease (Dix *et al*., 1997), unlike Fet3p. Deletion of both *FET3* and *FET4* abolishes measurable iron accumulation. The K_m for Fet4p mediated iron transport is 30 μM, and it can transport other transition metals such as Cu^{2+}, Mn^{2+} and Cd^{2+} (Dix *et al*., 1994, 1997). Transcription of *FET4* is regulated

by iron requirements, but neither by Aft1 p (Dix *et al.*, 1997), nor by other transition metals. In the absence of *FET3* and low iron conditions, *FET4* mRNA levels are increased, resulting in increased transport not only of iron, but of other transition metal ions, such that high levels of Fet4p can lead to cell death due to toxic metal accumulation (Li and Kaplan, 1998). Under anaerobic conditions *FET4* is the most important iron-transport system, in yeast, probably because transcription of *FET3* and other Aft1 p regulated genes, such as the *FRE* genes, is decreased in anaerobic conditions (Hassett *et al.*, 1998).

High Affinity Iron-Transport System

As pointed out above, the ferrireductase system is not essential for cell survival, and it can be separated from iron-transport activity by modulation of experimental conditions (Eide *et al.*, 1992). From studies of the concentration dependence of iron uptake, it became clear that there were at least two transport pathways (Eide *et al.*, 1992); one high affinity, selective for iron and tightly regulated, and a low affinity pathway, which as we saw above, is shared by other divalent metal ions and is less tightly regulated. Genetic screens were devised to identify the *FET3* gene (Askwith *et al.*, 1994), which is able to restore the growth capacity of mutants with normal ferrireductase activity and which were unable to grow on low iron medium, or for that matter to accumulate iron presented as Fe^{2+}. Fet3p shows extensive homology with the family of multicopper oxidases, which includes ascorbate oxidaze, laccase and ceruloplasmin, which couple the oxidation of substrates with the four-electron reduction of molecular oxygen to water. This represents a kind of cumulative, even vaguely cooperative process, where the enzymes oxidize their substrates sequentially, storing the abstracted electrons until, when the fourth electron has been removed from the substrate, they attack the dioxygen molecule in a concerted fashion, without release of reactive oxygen species, and transform it into two molecules of water. Like all multicopper oxidases, Fet3p has three spectroscopically different forms of copper, one Type 1 copper, one Type 2 copper and two Type 3 coppers; the Type 2 and Type 3 coppers are assembled in a trinuclear copper centre. The mammalian serum multicopper oxidase, ceruloplasmin, as we will see later (Chapter 5) has long been suggested to function as a ferroxidase to facilitate iron binding to the mammalian iron-transport protein transferrin. It turns out that Fet3p also has ferroxidase activity (De Silva *et al.*, 1995), and this turned out to be the key to unravelling the role of this protein in the high-affinity iron-uptake pathway. However, there was one very big problem – Fet3p contains only a single transmembrane domain, in its carboxyl terminus (De Silva *et al.*, 1995), and so it cannot be an ion channel. How does the iron get transported across the yeast cell plasma membrane? The breakthrough came with the identification of the *FTR1* gene, which encodes a protein predicted to have six transmembrane domains and a potential iron-binding site (Stearman *et al.*, 1996). Site-directed mutagenesis of the iron-binding motif REGLE in *FTR1* showed that these amino acids are required for iron transport. Transcription of both *FTR1* and *FET3* are increased in low iron conditions by the action of the transcription factor *AFT1*, and both have a single Aft1p binding site in their promoter region. Figure 4.4 presents a
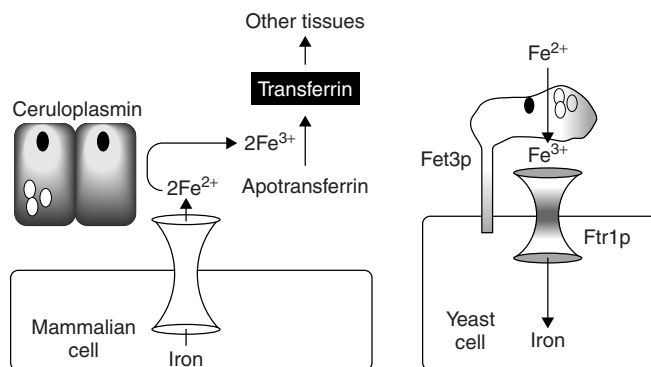
Figure 4.4 Comparison of oxidase-dependent iron transport in mammals and yeast. In mammals, the plasma glycoprotein cerulpolasmin mediates iron oxidation, facilitating iron export from the cells and delivery to other tissues throughout the body. In yeast, Fet3p, an integral membrane protein mediates iron oxidation, resulting in plasma membrane iron transport through the permease Ftr1p. Reprinted from Askwith and Kaplan, 1998. Copyright (1998), with permission from Elsevier Science.

comparison between the oxidase-dependent iron transport out of mammalian cells with the oxidase/permease transport of iron into yeast cells. All the present evidence suggests that Fet3p and Ftr1p are the only plasma membrane proteins required for high-affinity iron transport, and that they need to form a complex (Stearman *et al*., 1996; Askwith and Kaplan,1997) in order to be translocated to the surface of the plasma membrane. However, a number of other genes are required for the assembly of these proteins, many of them for the insertion of copper into the multicopper oxidase Fet3p. Defects in copper transport or in intracellular copper metabolism result in decreased iron uptake by the high affinity system and in the appearance of apo-Fet3p at the cell surface. Six genes have been identified that are involved in the mechanism of Fep3p assembly. Subsequent to reduction of copper by the membrane ferrireductases, high-affinity copper transport across the yeast plasma membrane is mediated by Ctr1p and Ctr2p. Cytosolic Atx1p, a specific cytosolic copper chaperone, delivers copper to the vesicular copper transporter Ccc2p, a P-type ATPase which transports copper across the vesicle membrane. Ccc2p is the yeast protein which corresponds to the proteins mutated in Menkes and Wilson's disease in man (which is discussed in more detail in Chapter 12). The major function of Ccc2p is to load Fet3p with copper. Disruption of any of the genes involved in the cellular copper transport system composed of Ctr1p, Atx1p and Ccc2p results in deficiency of Fet3p activity and of high affinity iron transport (Askwith and Kaplan, 1998). The way in which Fet3p is affected by copper homeostasis is illustrated in Figure 4.5.

Two more genes required for Fet3p assembly are *GEF2* and *GEF1*. *GEF2* is a subunit of the H^+-ATPase that is required for the acidification of both vacuoles and endosomes. This indicates that copper loading of Fet3p requires an acidic pH. And, finally, *GEF1* encodes a voltage-regulated chloride channel (Greene *et al*., 1993). The requirement for a chloride channel appears to be twofold; (i) to dissipate the unfavourable electrochemical potential within the vesicle, resulting in a lower pH and a higher Cu^+ concentration (Gaxiola *et al*., 1998), and (ii) because chloride is directly required for copper insertion into apoFet3p (Davis-Kaplan *et al*., 1998).
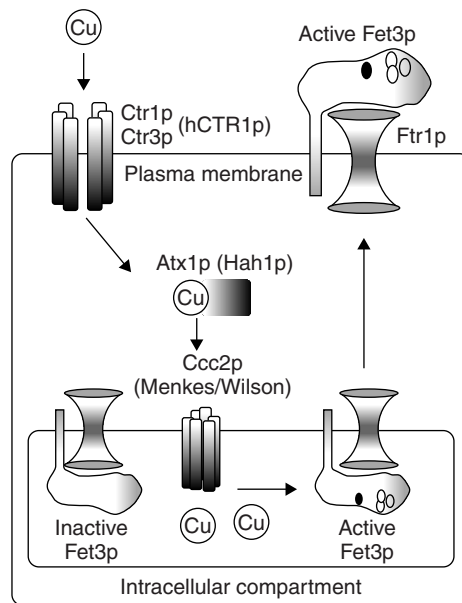
Figure 4.5 Fet3p and copper homeostasis. Defects in the plasma membrane transporters Ctr1 and Ctr3, the cytosolic copper chaperone Atx1p, or the vesicular copper transporter Ccc2p affect Fet3p activity. Reprinted from Askwith and Kaplan, 1998. Copyright (1998), with permission from Elsevier Science.

SMF Family of Transporters

The *SMF* family consists of three genes *SMF1*, *SMF2* and *SMF3*; the proteins encoded are 45 % identical with as many as ten transmembrane domains (Supek *et al*., 1997). They were first identified as Mn^{2+} transporters, but a possible role in iron transport was indicated in view of their homology with the mammalian iron transporter DMT1 (also known as NRAMP2 or DCT1), which has been implicated in iron transport across the intestinal tract and across the endosomal membrane within cells. DMT1 has a broad range of specificity and is thought to act as a divalent cation/ H^+ symport (Gunshin *et al*., 1997). Deletion of both *SMF1* and *SMF2* results in hypersensitivity to oxidative stress; this phenotype can be complemented by transformation of the deletion strains with a high copy plasmid containing DMT1 (Pinner *et al*., 1997). *SMF1* and *SMF2* can mediate H^+-coupled iron transport using an oocyte expression system (Chen *et al*., 1999), but *SMF3* cannot. The role of the *SMF* gene family in iron transport in yeast is unclear. They may be responsible for some part of iron uptake, since a Δ*fet3*Δ*fet4* strain can still grow on a rich medium containing moderate amounts of iron. *SMF1* and *SMF2* are not transcriptionally regulated by iron.

Siderophore-mediated Iron Uptake

Saccharomyces cerevisiae does not itself synthesize or secrete siderophores. However, somewhat like *E. coli* (Chapter 3), it can take up iron–siderophore

complexes secreted into its environment by other microorganisms. This was elegantly demonstrated using the Δ*fet3*Δ*fet4* deletion strain, which cannot grow on minimal media. (Lesuisse *et al*., 1998). Both hyroxamate siderophores (ferricoprogen, ferriferricrocin and ferrioxamine B) and the catecholate siderophore ferrienterobactin allowed growth on minimal media. Using a mutant that was unable to utilize ferrioxamine B iron for growth and complementation of the phenotype with a genomic library, the *SITI* gene was identified as encoding a ferrioxamine B permease (Lesuisse *et al*., 1998). A further five genes have been identified in *S. cerevisiae* which are homologous to *SITI* (Heymann *et al*., 2000; Yun *et al*., 2000a), three of which, like *SITI*, are iron regulated by Aft1p. These four iron-regulated genes were termed *ARN* genes (**AFT1 r**egulo**n**), with *SITI* now *ARN3*. Other siderophores, such as ferrichrome and fusarinines can be taken up by the *ARN* genes (Yun *et al*., 2000b). Two different mechanisms have been demonstrated for ferrioxamine B uptake (Yun *et al*., 2000a). One involves the reduction and release of the iron from the ferrisiderophore by the membrane ferrireductases, followed by uptake via the Fet3p/Ftr1p system. The second, seen only in the absence of Fet3p, requires members of the *ARN* family.

Recovery of Iron from the Vacuole

When the complete yeast genome was examined a homologue of *FET3* was found, designated *FET5*, with all of the sequence features expected of a multicopper oxidase (Spizzo *et al*., 1997). The corresponding Fet5p protein is not located at the plasma membrane, but is localized to the vacuole, where it is found complexed to an *FTR1* homologue Fth1p (Urbanowski and Piper, 1999). In the absence of Fet5p, Fth1p is not found in the vacuole, but is retained in the reticuloendoplasmic reticulum. It was further shown that Fth1p and Fet5p are physically associated, suggesting that like Fet3p and Ftr1p they form an oxidase/permease pair whose role may be to mobilize iron from the vacuole to the cytoplasm. This still leaves the unresolved question as to how the oxidase/permease are positioned in the vacuole membrane such that they regard the inside of the vacuole as 'outside' and the cytoplasm as 'inside' the cell, by analogy with the Fet3p/Ftr1p system. It also raises the question of how iron accumulates in the vacuole, which is where we found iron accumulation when yeast was iron loaded (Raguzzi *et al*., 1988). We also noted that vacuolar iron could subsequently be mobilized for haem synthesis in the mitochondria – perhaps this is the role of the *FET5/FTP1* system, namely to liberate iron from the storage vacuole, where it has been deposited when it is in excess, for future utilization.

4.4   Intracellular Iron Metabolism

In the absence of a demonstrable yeast iron-storage protein (ferritin), we have to recognize that, despite our substantial advances in understanding iron uptake in yeast, we know practically nothing about intracellular iron metabolism – except that is for iron transport into, and out of, mitochondria.

4.4.1 Mitochondrial Iron Transport

As we will see in Chapter 7, the mitochondria are not only the energy powerhouse of the cell, they is also the site of both haem (Lange *et al.*, 1999) and iron–sulfur cluster (Lill *et al.*, 1999) biosynthesis. The proteins that contain haem and iron–sulfur clusters are not all located in the mitochondria, which makes the mitochondria a focal point of intracellular iron metabolism. We recognize that mitochondrial iron transport must occur, although we do not quite know how it functions, but from recent work it seems that there must be a mitochondrial iron cycle (Radisky *et al.*, 1999), such that mitochondria not only import iron but also export it. Analysis of the function of the gene *YFH1* (Babcock *et al.*, 1997), which is a homologue of the mammalian gene Frataxin (mutated in Friedrich's ataxia), shows that is involved in mitochondrial iron efflux. Yfh1p is a protein of 125 amino acids localized in the matrix of the mitochondria. The phenotypes of strains in which *YFH1* has been deleted reflect respiratory incompetence and decreased cytosolic iron, which are the result of mitochondrial iron accumulation. The excedent of mitochondrial iron produces increased amounts of hydroxyl radical which in turn damages mitochondrial proteins, lipids and DNA.∥ The damage to mitochondrial DNA generates respiratory incompetent yeast, termed *petites*, which can survive because they regenerate cytosolic NADH by fermentation. Although the ATP yield is much less than by respiration (about twentyfold), their survival strategy lies in what Louis Pasteur described as '*la vie sans air*' (life without air). The *petite* mutants should in fact have a selective advantage because they no longer produce toxic reactive oxygen species at the mitochondrial inner membrane. It has been established that Yfh1p mediates iron efflux from mitochondria (Radisky *et al.*, 1999), yet it is located in the matrix and has no transmembrane domain. It may function either by regulating iron transport, or by keeping iron in a form that is recognized by an as yet to be discovered transport protein. Transcription of *YFH1* is not iron regulated.

Although iron–sulfur proteins are found in various cellular localizations in eukaryotic cells, mitochondria are the major site of Fe–S cluster biosynthesis (Lill *et al.*, 1999). Deletions in nuclear genes involved in mitochondrial iron–sulfur cluster formation lead to massive accumulation of iron in mitochondria (Chapter 7). For example, deletion of *ATM1*, a mitochondrial ATPase, which seems to be responsible for the export of Fe–S clusters, leads to respiratory incompetence, excessive iron accumulation and leucine auxotrophy (Kispal *et al.*, 1999). In Δ*yfh1* cells there is only partial loss of mitochondrial Fe–S enzymes and the cells are not leucine auxotrophs.

∥ This constitutes what is often termed the oxygen paradox. The symbiotic cohabitation of a prokaryotic cell within a eukaryotic host enabled the mitochondrial respiratory chain to produce much more ATP than could be achieved by fermentation: two ATP molecules are produced by homolactic fermentation (e.g. in muscle) or by alcoholic fermentation (e.g. in yeast) per molecule of glucose, whereas the combined operation of shuttles for transferring electrons from cytoplasmic NADH to mitochondria, transfer of pyruvate into the mitochondrial matrix and its conversion to acetyl CoA, the citric-acid cycle together with the mitochondrial electron transport chain and its associated ATP synthase raises this figure to 36–38 ATP molecules per molecule of glucose. However there is a price to be paid. The transfer of electrons along the respiratory chain generates reactive oxygen species, notably the hydroxyl radical which can provoke oxidative damage. This is the essence of the paradox – dioxygen is both beneficial yet at the same time potentially toxic. More on this subject in Chapter 10.

It thus seems unlikely thatYfh1p plays a role in either Fe–S cluster formation or their export.

4.4.2 Iron Storage in *S. cerevisiae*

Despite extensive efforts, it has proved extremely difficult to find evidence for iron storage proteins like the ferritins found in bacteria, plants, animals and almost every other living organism (see Chapter 6). Scrutiny of the *S. cerevisiae* genome fails to reveal any gene with convincing homology to consensus sequences for ferritins. We did obtain small amounts of a protein of molecular weight around 270–280 kD, with a subunit molecular weight of 12–13 kD from substantial quantities of bakers' yeast (1–2 kg) using classical protein chemical techniques (Raguzzi *et al.*, 1988; Raguzzi, 1989). Subsequent efforts to obtain further information by microsequencing techniques were unsuccessful (Crichton, unpublished data). We did find that growth of *S. cerevisiae* on iron-rich medium led to iron accumulation in the vacuole (Raguzzi *et al.*, 1988), and that this iron could subsequently be utilized for mitochondrial haem synthesis. It has been pointed out that the concentrations of iron used were non-physiological, and would lead to repression of both high- and low-affinity iron uptake systems (Ardon *et al.*, 2000), and it has been suggested that iron might be stored in the cytoplasm (Radisky *et al.*, 1999). Other studies have implied that the vacuole is indeed the site of iron, and possibly other metal ion, sequestration (Bode *et al.*, 1995). As is always the case in science, time alone will tell.

4.5 Iron Transport in Other Fungi

As we have seen in the previous chapter, it is almost unavoidable for one particular organism to become the focus of all kinds of research, simply because of the advantages which it presents. As in bacteria with *E. coli*, *S. cerevisiae* has been the yeast of choice over the last few decades. This is certainly not unrelated to the ease of genetic manipulation of this fungal species which passes much of its life cycle in the haploid state, unlike many other fungi of pathological or economic importance, which are diploid.[††] Several pathogenic yeasts that cause infections in man are known (see Chapter 11). *Candida albicans* is responsible for a great number of oral and vaginal mucosal infections, as well as systemic infection, particularly when cellular immunity is compromised, and is genetically related to *S. cerevisiae*. It has a number of components in common with *S. cerevisiae* (Eck *et al.*, 1999; Morrissey *et al.*, 1996; Yamada–Okabe *et al.*, 1996) including a ferrireductase and an oxidase/permease high-affinity iron-transport system. *Cryptococcus neoformans* causes meningitis, particularly in patients with cellular immunological deficiency, and is often found in patients with AIDS. Although *C. neoformans* and

---

[††] Haploid cells have only a single copy of each chromosome. This occurs normally in the mature germ cell. Diploid cells, in contrast have two copies of each chromosome: most normal somatic cells are diploid. The fact that yeast cells are haploid renders genetic analysis much easier because one has taken sex out of the equation – the question remains whether it is as much fun?

S. cerevisiae are evolutionary distinct members of the fungal family (Basidiomycetes and Ascomycetes respectively), *C. neoformans* under conditions of iron stress also expresses a plasma-membrane ferric reductase which provides Fe^{2+} for both a low and high affinity transmembrane transport system (Nyhus *et al.*, 1997). This fungus can also take up iron from ferric-siderophores such as ferrioxamine B. *Histoplasma capsulata* not only secretes five different hydroxamate siderophores and appears to have a high affinity ferric reductase system, it seems also to take up iron from the hosts's diferrictransferrin (Howard, 1999). *Ustilago maydis* is a fungal pathogen of maize, which produces ferrichrome siderophores (Budde and Leong, 1989). Using fluorescent biomimetic analogues of ferrichrome and ferrioxamine B (another hydroxamate siderophore not produced by *Ustilago maydis*), two different uptake pathways were established (Ardon *et al.*, 1997, 1998). The ferrichrome–iron complex enters the cell, the iron is removed and the ferrichrome is secreted back into the medium, whereas iron uptake from ferrioxamine B appeared to involve extracellular reduction without entry of the siderophore into the cell.

The accumulation of iron by pathogenic fungi is often associated with virulence, and it had been hoped that drugs based on components of their iron uptake systems might prove a valuable site of attack. In the case of *Candida albicans*, a mutant defective in *FET3* was found to be just as infectious as wild type strains in a mouse model of systemic candidiasis (Eck *et al.*, 1999), suggesting that other iron-uptake pathways must exist. As the genome sequences of pathogenic fungi become available, it should be possible to identify the genes for iron–transport systems. However, if the experience with *S. cerevisiae* is anything to go by, we may find that there are multiple iron-uptake mechanisms which may prevent an easy solution to fungal pathogenicity through such an approach.

4.6 References

Ardon, O., Weizmann, H., Libman, J., Shanzer, A., Chen, Y. and Hadar, Y. (1997). *Microbiology*, **143**, 2625–31.

Ardon, O., Nudelman, R., Caris, C., Libman, J., Shanzer, A., Chen, Y. and Hadar, Y. (1998). *J. Bacteriol.*, **180**, 2021–6.

Ardon, O., Kaplan, J. and Martin, B.D. (2001). In *Molecular and Cellular Iron Transport*, Marcel Dekker Inc, New York.

Askwith, C. and Kaplan, J. (1997). *J. Biol. Chem.*, **272**, 401–5.

Askwith, C. and Kaplan, J. (1998). *TIBS*, **23**, 135–8.

Askwith, C., Eide, D., Van Ho, A., Bernard, P.S. *et al.* (1994). *Cell*, **76**, 403–10.

Babcock, M., de Silva, D., Oaks, R., Davis-Kaplan, S. *et al.* (1997). *Science*, **276**, 1709–12.

Bagnaresi, P. and Pupillo, P. (1995). *J. Exp. Bot.*, **46**, 1497–1503.

Bagnaresi, P., Basso, B. and Pupillo, P. (1997). *Planta*, **202**, 427–34.

Basso, B., Bagnaresi, P., Bracale, M. and Soave, C. (1994). *Maydica*, **39**, 97–105.

Belouchi, A., Cellier, M., Kwan, T., Saini, H.S., Leroux, G. and Gros, P. (1995). *Plant Mol. Biol.*, **29**, 1181–96.

Belouchi, A., Kwan, T. and Gros, P. (1997). *Plant Mol. Biol.*, **33**, 1085–92.

Bienfait, H.F. (1985). *J. Bioenerg. Biomembr.*, **17**, 73–83.

Bode, H.P., Dumschat, M., Garotti, S. and Fuhrmann, G.F. (1995). *Eur. J. Biochem.*, **228**, 337–42.

Briat, J.-F. and Lobréaux, S. (1997). *Trends Plant Sci.*, **2**, 187–93.

Briat, J.-F., Fobis-Loisy, I., Grignon, N., Lobréaux, S. *et al.* (1995). *Biol. Cell*, **84**, 69–81.

Bouzayan, M., Felix, G., Latché, A., Pech, J.C. and Boller, T. (1991). *Planta*, **184**, 244–7.

Budde, A.D. and Leong, S.A. (1989). *Mycopathologia*, **108**, 125–33.

Chanock, S.J., Elbenna, J., Smith, R.M. and Babior, B.M. (1994). *J. Biol. Chem.*, **269**, 24519–22.

Chen, X.Z., Peng, J.B., Cohen, A., Nelson, H., Nelson, N. and Hediger, M.A. (1999). *J. Biol. Chem.*, **274**, 35089–94.

Chen, Y. and Barak, P. (1982). *Adv. Agron.*, **35**, 217–40.

Coulombe, B.A., Chaney, R.L. and Wiebold, W.J. (1984). *Soil Sci. Soc. Am. J.*, **48**, 1297–1301.

Curie, C., Alonso, J.M., Le Jean, M., Ecker, J.R. and Briat, J.-F. (2000). *Biochem. J.*, **347**, 749–55.

Dancis, A., Klausner, R.D., Hinnebusch, A.G. and Barriocanal, J.G. (1990). *Mol. Cell. Biol.*, **10**, 2294–301.

Davis-Kaplan, S.R., Askwith, C.C., Bengtzen, A.C., Radisky, D. and Kaplan, J. (1998). *Proc. Natl Acad. Sci., USA*, **95**, 13641–5.

De Silva, D.M., Askwith, C.C., Eide, J. and Kaplan, J. (1995). *J. Biol. Chem.*, **270**, 1098–1101.

Dix, D.R., Bridgham, J.T., Broderius, M.A., Byersdorfes, C.A. and Eide, D.J. (1994). *J. Biol. Chem.*, **269**, 26092–9.

Dix, D.R., Bridgham, J.T., Broderius, M.A. and Eide, D.J. (1997). *J. Biol. Chem.*, **272**, 11770–7.

Eck, R., Hundt, S., Hartl, A., Roemer, E. and Kunkel, W. (1999). *Microbiology*, **145**, 2415–22.

Eide, D.J. (1998). *Ann. Rev. Nutr.*, **18**, 441–69.

Eide, D., Broderius, M., Fett, J. and Guerinot, M.L. (1996). *Proc. Natl Acad. Sci.*, USA, **93**, 5624–8.

Eide, D., Davis-Kaplan, S., Jordan, I., Sipe, D. and Kaplan, J. (1992). *J. Biol. Chem.*, **267**, 20774–81.

Fobis-Loisy, I., Loridon, K., Lobréaux, S., Lebrun, M. and Briat, J.F. (1995). *Eur. J. Biochem.*, **231**, 609–19.

Gaxiola, R.A., Yuan, D.S., Klausner, R.D. and Fink, G.R. (1998). *Proc. Natl Acad. Sci.*, USA, **95**, 4046–50.

Gaymard, F., Boucherez, J. and Briat, J.F. (1995). *Biochem. J.*, **318**, 67–73.

Georgatsou, E., Mavrogiannis, L.A., Fragiadakis, G.S. and Alexandraki, D. (1997). *J. Biol. Chem.*, **272**, 13786–92.

Goffeau, A., Barrell, B.G., Bussey, H., Davis, R.W. *et al.* (1996). *Science*, **274**, 546, 563–7.

Greene, J.R., Brown, N.H., Di Domenico, B.J., Laplan, J. and Eide, D.J. (1993). *Mol. Gen. Genet.*, **241**, 542–53.

Grusak, M.A. and Pezeshgi, S. (1996). *Plant Physiol.*, **110**, 329–34.

Grusak, M.A., Welch, R.M. and Kochian, L. (1990). *Plant Physiol.*, **94**, 1353–7.

Guerinot, M.L. and Yi, Y. (1994). *Plant Physiol.*, **104**, 815–20.

Gunshin, H., Mackenzie, B., Berger, U.V., Gunshin, Y. *et al.* (1997). *Nature*, **388**, 482–8.

Hassett, R.F., Romeo, A.M. and Kosman, D.J. (1998). *J. Biol. Chem.*, **273**, 7628–36.

Heijne, G.V., Steppuhn, J. and Herrmann, R.G. (1989). *Eur. J. Biochem.*, **180**, 535–45.

Heymann, P., Ernst, J.F. and Winkelmann, G. (2000). *FEMS Microbiol. Lett.*, **186**, 221–7.

Higuchi, K., Kanazawa, K., Nishizawa, N.K., Chino, M. and Mori, S. (1994). *Plant Soil*, **165**, 173–9.

Higuchi, K., Suzuki, K., Nakanishi, H., Yamaguchi, H., Nishizawa, N.K. and Mori, S. (1999). *Plant Physiol.*, **119**, 471–80.

Howard, D.H. (1999). *Clin. Microbiol. Rev.*, **12**, 394–404.

Inoue, K., Hiradate, S. and Takagi, S. (1993). *Soil Sci. Soc. Am. J.*, **57**, 1254–60.

Itai, R., Suzuki, K., Yamaguchi, H. *et al*. (2000). *J. Exp. Bot.*, **51**, 1179–88.

Jolley, V.D., Brown, J.G. and Nugent, P.E. (1991). *Plant Soil*, **130**, 87–92.

Kispal, G., Csere, P., Prohl, C. and Lill, R. (1999). *EMBO J.*, **18**, 3981–89.

Kneen, B.E., La Rue, T.A., Walch, R.M. and Weeden, N.F. (1990). *Plant Physiol.*, **93**, 717–22.

Korshunova,Y.O., Eide, D., Clark, W.G., Guerinot, M.L. and Pakrasi, H.B. (1999). *Plant Mol. Biol.*, **40**, 37–44.

Kramer, D., Römheld, V., Landsberg, E.C. and Marschner, H. (1980). *Planta*, **147**, 335–9.

Landsberg, E.C. (1986). *Plant Physiol.*, **82**, 511–7.

Lange, H., Kispal, G. and Lill, R. (1999). *J. Biol. Chem.*, **274**, 18989–96.

Laulhère, J.-P., Labouré, A.M. and Briat, J.F.(1989). *J. Biol. Chem.*, **264**, 3629–35.

Lescure, A.M., Proudhon, D., Pesey, H., Ragland, M., Theil, E.C. and Briat, J.F. (1991). *Proc. Natl. Acad. Sci.,* USA, **88**, 8222–6.

Lesuisse, E., Raguzzi, F. and Crichton, R.R. (1987). *J. Gen. Microbiol.*, **133**, 3229–36.

Lesuisse, E., Crichton, R.R. and Labbe, P. (1990). *Biochim. Biophys. Acta*, **1038**, 253–9.

Lesuisse, E., Casteras-Simon, M. and Labbe, P. (1996). *J. Biol. Chem.*, **271**, 13578–83.

Lesuisse, E., Simon-Casteras, M. and Labbe, P. (1998). *Microbiology*, **271**, 3455–62.

Li, L. and Kaplan, J. (1998). *J. Biol. Chem.*, **273**, 22181–87.

Lill, R., Diekert, K., Kaut, A., Lange, *et al*. (1999). *Biol. Chem.*, **380**, 1157–66.

Ling, H.Q., Pich, A., Scholz, G. and Ganal, M.W. (1996). *Mol. Gen. Genet.*, **252**, 87–92.

Lobréaux, S. and Briat, J.-F. (1991). *Biochem. J.*, **274**, 601–6.

Lobréaux, S., Yewdall, S., Briat, J.-F. and Harrison, P.M. (1992a). *Biochem. J.*, **288**, 931–9.

Lobréaux, S., Massenet, O. and Briat, J.-F. (1992b). *Plant Mol. Biol.*, **19**, 563–75.

Lobréaux, S., Hardy, T. and Briat, J.-F. (1993). *EMBO J.*, **12**, 651–7.

Lobréaux, S., Thoiron, S. and Briat, J.-F. (1995). *Plant J.*, **8**, 443–9.

Ma, J.F. and Nomoto, K. (1996). *Physiol. Plant.*, **97**, 609–17.

Martins, L.J., Jensen, L.T., Simons, J.R., Keller, G.L. and Winge, D.R. (1998). *J. Biol. Chem.*, **273**, 23716–21.

Mihashi, S. and Mori, S. (1989). *Biol. Metals*, **2**, 146–54.

Mino, Y., Ishida, T., Ota, N., Inoue, M. *et al*. (1983). *J. Am. Chem. Soc.*, **105**, 4671–6.

Moog, P.R., van der Kooij, T.A.W., Briggeman, W., Schiefelbein, J.W. and Kniper, P.J.C. (1995). *Planta*, **195**, 505–13.

Mori, S. (1998). In *Metal Ions in Biological Systems* (eds Sigel, A. and Sigel, H.), **35**, 215–38.

Morrissey, J.A., Williams, P.H. and Cashmore, A.M. (1996). *Microbiology*, **142**, 485–92.

Nakanishi, H., Okumura, N., Umehara, Y., Nishizawa, N.K., Chino, M. and Mori, S. (1993). *Plant Cell Physiol.*, **34**, 401–10.

Nyhus, K.J., Wilborn, A.T. and Jacobsen, E.S. (1997). *Infec. Immun.*, **65**, 434–8.

Okumura, N., Nishizawa, N.K., Umehara, Y., Ohata, T. *et al.* (1994). *Plant Mol. Biol.*, **254**, 705–19.

Pinner, E., Gruenheid, S., Raymond, M. and Gros, P. (1997). *J. Biol. Chem.*, **272**, 28933–8.

Proudhon, D., Briat, J.F. and Lescure, A.M. (1989). *Plant Physiol.*, **90**, 586–90.

Radisky, D.C., Babcock, M.C. and Kaplan, J. (1999). *J. Biol. Chem.*, **274**, 4497–9.

Ragland, M. and Theil, E.C. (1993). *Plant Mol. Biol.*, **21**, 555–60.

Raguzzi, F. (1989). Doctoral thesis, Université de Louvain.

Raguzzi, F., Lesuisse, E. and Crichton, R.R. (1988). *FEBS Lett.*, **231**, 253–8.

Robinson, N.J., Procter, C.M., Connolly, E.L. and Guerinot, M.L. (1999). *Nature*, **397**, 694–7.

Romero, F.J. and Alcantara, E. (1994). *Plant Physiol.*, **105**, 1133–8.

Roman, D.G., Dancis, A., Anderson, G.J. and Klausner, R.D. (1993). *Mol. Cell. Biol.*, **13**, 4342–50.

Römheld, V. and Marschner, H. (1986). *Plant Physiol.*, **80**, 175–80.

Schmidt, W. and Bartels, M. (1996). *Plant Physiol.*, **110**, 217–25.

Schmidt, W., Tittel, J. and Schikora, A. (2000). *Plant Physiol.*, **122**, 1109–18.

Seckbach, J.J. (1982). *J. Plant Nutr.*, **5**, 369–94.

Shatwell, K.P., Dancis, A., Cross, A.R., Klausner, R.D. and Segal, A.W. (1996). *J. Biol. Chem.*, **271**, 14240–4.

Shojima, S., Nishizawa, N.K., Fushiya, S., Nozoe, S., Irifune, T. and Mori, S. (1990). *Plant Physiol.*, **93**, 1497–1503.

Siedow, J.N. (1991). *Ann. Rev. Plant Physiol. Plant Mol. Biol.*, **42**, 145–188.

Spizzo, T., Byersdorfer, C., Duesterhoeft, S., Eide, D. (1997). *Mol. Gen. Genet.*, **256**, 547–56.

Stearman, R., Yuan, D.S., Yamaguchi-Iwai, Y., Klausner, R.D. and Dancis, A. (1996). *Science*, **271**, 1552–7.

Stephan, U.W. and Scholz, G. (1993). *Physiol. Plant*, **88**, 522–29.

Supek, F., Supekova, L., Nelson, H. and Nelson, N. (1997). *J. Exp. Biol.*, **200**, 321–30.

Takagi, S., Nomoto, K. and Takemoto, T. (1984). *J. Plant Nutr.*, **7**, 469–77.

Takahashi, M., Yamaguchi, H., Nakanishi, H., Shioiri, T., Nishizawa, N.K. and Mori, S. (1999). *Plant Physiol.*, **82**, 511–17.

Theil, E.C. and Hase, T. (1993). In *Iron Chelation in Plants and Soil Microorganisms* (eds Barton, L.L. and Hemings, B.,) Academic Press, New York, pp. 133–156.

Tomine, S., Wang, R., Ward, J.M., Crawford, N.M. and Schroeder, J.I. (2000). *Proc. Natl Acad. Sci., USA*, **121**, 947–56.

Touleau, V., Sentenac, H., Thibaud, J.B., Davidian, J.C. *et al.* (1992). *Planta*, **186**, 212–18.

Urbanowski, J.L. and Piper, R.C. (1999). *J. Biol. Chem.*, **274**, 38061–70.

Van der Mark, F., van der Briel, W. and Huisman, H.G. (1983). *Biochem. J.*, **214**, 943–50.

Yamada-Okabe, T., Shimmi, O., Doi, R., Mizumoto, K, Arisawa, M. and Yamada-Okabe, H. (1996). *Microbiology*, **142**, 2515–23.

Yi, Y. and Guerinot, M.L. (1996). *Plant J.*, **10**, 835–44.

Yun, C.W., Ferea, T., Rashford, J., Ardon, *et al*. (2000a). *J. Biol. Chem.*, **275**, 10709–15.

Yun, C.W., Tiedeman, J.S., Moore, R.E. and Philpott, C.C. (2000b). *J. Biol. Chem.*, **275**, 16354–9.

5 Cellular Iron Uptake in Mammals

5.1 The Transferrins

The transferrins are a family of iron-binding proteins found in the physiological fluids of many vertebrates. Their discovery in egg white and serum is an excellent example of serendipity.[†] Ovotransferrin, originally called conalbumin, was first purified from raw egg white by Osborne and Cambell (1900), although its identification as the antimicrobial agent of egg white (Alderton *et al.*, 1946), the properties of which are abolished by the addition of iron (Schade and Caroline, 1944) followed almost half a century later. Likewise, siderophilin, the iron-binding protein of human serum, the antibacterial properties of which are also abolished by iron, was purified by Schade and Caroline (1946). The 'red protein' of pig plasma was purified by Laurell and Ingelman (1947) and in the same year the name 'transferrin' was proposed (Holmberg and Laurell, 1947), and has since been used as the generic name for proteins of this family. The initial discovery of the transferrins was made possible by their potent antibacterial activities – by depriving bacteria of iron they contribute to the defence of mammalian cells against infection. The iron-binding protein of human milk, which plays a similar antibacterial role, was discovered almost simultaneously by Montreuil *et al.* (1960) and Johansson (1960), and is usually referred to as lactoferrin. In vertebrates, transferrins are found in many body fluids including serum, milk, tears, and saliva as well as being secreted by leukocytes(lactoferrin). Ovotransferrin is present in avian egg white while melanotransferrin, a cell surface glycoprotein, identified by sequence homology as a member of the family (Rose *et al.*, 1986), is anchored to the membranes of melanocytes and other cells by a glycosyl–phosphatidylinositol linkage. Although only the *N*-lobe of melanotransferrin has a functional iron-binding site (Baker *et al.*,

---

[†] Horace Walpole in a letter to his friend Horace Mann, wrote on January 28, 1754:
 'I once read a silly fairy tale, called ''The Three Princes of Serendip'': as their highnesses travelled, they were always making discoveries by accidents and sagacity, of things they were not in quest of: for instance, one of them discovered that a mule blind of the right eye had travelled the same road lately, because the grass was eaten only on the left side, where it was worse than on the right – now do you understand ''serendipity''?'
 For Walter Gratzer (a regular contributor to *Nature*), serendipity is not that when you drop your buttered toast on the floor that it falls, as it invariably does, buttered side down, but that when you pick it up you discover the contact lens that you lost a few days earlier.

1992) it none the less appears to provide a receptor-independent but saturable route for transferrin iron uptake by melanoma cells (Richardson and Baker, 1994). Originally thought to be restricted to vertebrates, transferrin-like proteins have been isolated, characterized and cloned from two insects, the tobacco hornworm and the cockroach (Bartfeld and Law, 1990; Jamroz *et al.*, 1993). Whereas the principal role of transferrins is to control iron levels in body fluids with a resultant bacteriostatic effect, serum transferrin has the specific role of transporting iron in vertebrates from sites of absorption and haem degradation to sites of utilization (for erythropoeisis) and storage (in ferritin).

   Most transferrins are glycoproteins of molecular weight around 80 kD, composed of a single polypeptide chain of 680 amino-acid residues able to bind tightly, but reversibly, two Fe^{3+} ions with concomitant binding of two carbonate anions, as was first established for human serotransferrin (Schade *et al.*, 1949). A number of other synergistic anions can serve as bridging ligands between the protein and the metal ion *in vitro*. The role of the bridging anion may be to prevent water from binding in the coordination sphere of the metal, locking the metal firmly to the protein and avoiding hydrolysis. *In vitro*, iron can be released from serum transferrin by acidification (Surgenor, 1949). A number of other metals can bind to transferrins in addition to Fe(III), including Al(III), Ga(III), Cr(III), Cu(II), Mn(III), Co(III), Cd(II), Zn(II) VO(II), Sc(II), Ni(II) as well as many lanthanides and actinides, but there is no clear evidence that this has any physiological significance with the possible exceptions of the vanadyl ion VO(II) and Al(III). While recognizing that neither of these latter two metal ions can properly be considered as representing 'normal' physiology, when they are introduced into the biosphere, for example as vanado-porphyrins in the emissions from fossil-fuel-fired electric power generating plants, or by leaching and solubilization of aluminium in the soil by acid rains, transferrin serves to transport them in vivo. It has recently been suggested that chromium, known to be a micronutrient for mammals for four decades, is transported from mobile pools to insulin-sensitive cells by transferrin (Vincent, 2000).

5.1.1   Structure of Transferrins

Determination of the amino-acid sequence of human serum transferrin (MacGillivray *et al.*, 1983) and of human lactoferrin (Metz-Boutique *et al.*, 1984) revealed an internal two-fold sequence repeat. The amino-terminal half has approximately 40 % sequence identity with the carboxyl-terminal half. Similar results have subsequently been found for a number of other transferrins (Baldwin, 1993), suggesting that the modern transferrins have evolved by a gene duplication event from an ancestral gene coding for a protein of molecular weight around 40 kD and with a single metal-binding site. Subsequent duplications of this gene would have given rise to the transferrins, lactoferrins, ovotransferrins and melanotransferrins that we find today. Crystallographic studies, on human lactoferrin (Anderson *et al.*, 1987, 1989), human serotransferrin (Bailey *et al.*, 1988) and ovotransferrin (Kurokawa *et al.*, 1995) have shown that the polypeptide chain is folded into two structurally homologous lobes referred to as the N- and C-lobes. The same folding pattern, found in a number of other transferrins as well as
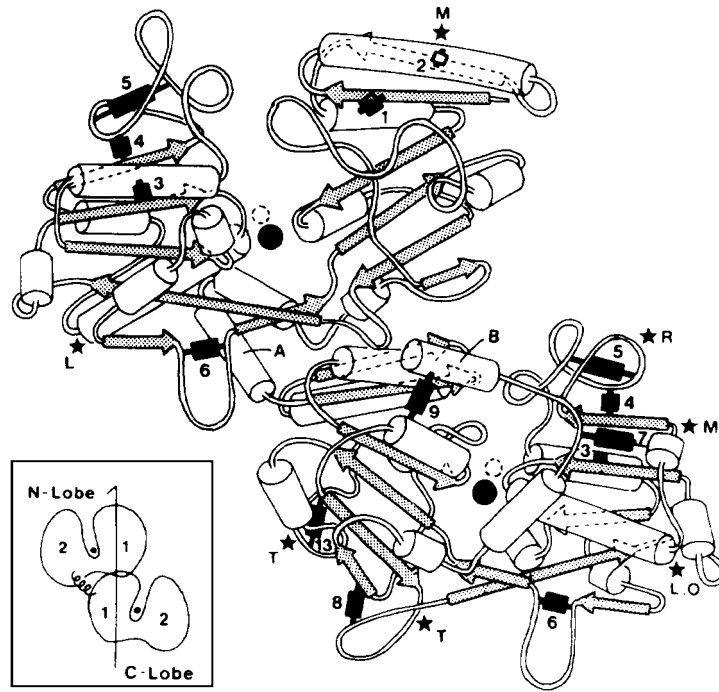
Figure 5.1 Schematic diagram of the lactoferrin molecule. The positions of carbohydrate attachment are marked with a star. O, ovotransferrin; T, human serotransferrin; L, human lactoferrin; R, rabbit serotransferrin; M, melanotransferrin; A, the connecting helix; B, the *C*-terminal helix. The disulfide bridges are indicated by heavy bars, and the iron and carbonate binding sites by filled or open circles, respectively. Reprinted from Baker *et al.*, 1987. Copyright (1987), with permission from Elsevier Science.

various fragments, mutants, and metal- and anion-substituted proteins, is shown in schematic form for human lactoferrin in Figure 5.1. The organization of the human serotransferrin and hen ovotransferrin genes are consistent with this evolutionary history (Park *et al.*, 1985; Schaeffer *et al.*, 1987). Each gene contains 17 exons separated by 16 introns. Exon 1 codes for a signal peptide, while the remaining 16 exons code for the mature transferrin molecule. Fourteen of these exons constitute seven homologous pairs, coding for corresponding regions in each of the lobes, while the remaining two are unique to the *C*-terminal lobe. The *N*-terminal lobe in Figure 5.1 is at the top and the *C*-terminal lobe at the bottom. They are both made up of some 330 amino acids, joined by a short connecting peptide which, in lactoferrin, forms a three-turn α-helix. Each lobe contains an iron binding site located deep in the cleft between two dissimilar α/β-globular domains, 1 and 2, each of about 160 residues, that follow the folding pattern shown in Figure 5.2. All four domains have a similar super-secondary structure consisting of a central core of five or six irregularly twisted β-sheets of similar topology, with α-helices packed on either side of them. The first 90 or so residues form part of domain 1. The polypeptide chain then crosses to domain 2 via a long β-strand, e. The next 160 residues form the whole of domain 2, and the chain then returns via a long β-strand, j, to complete the folding of domain 1, and finally an α- helix runs back across the domain interface
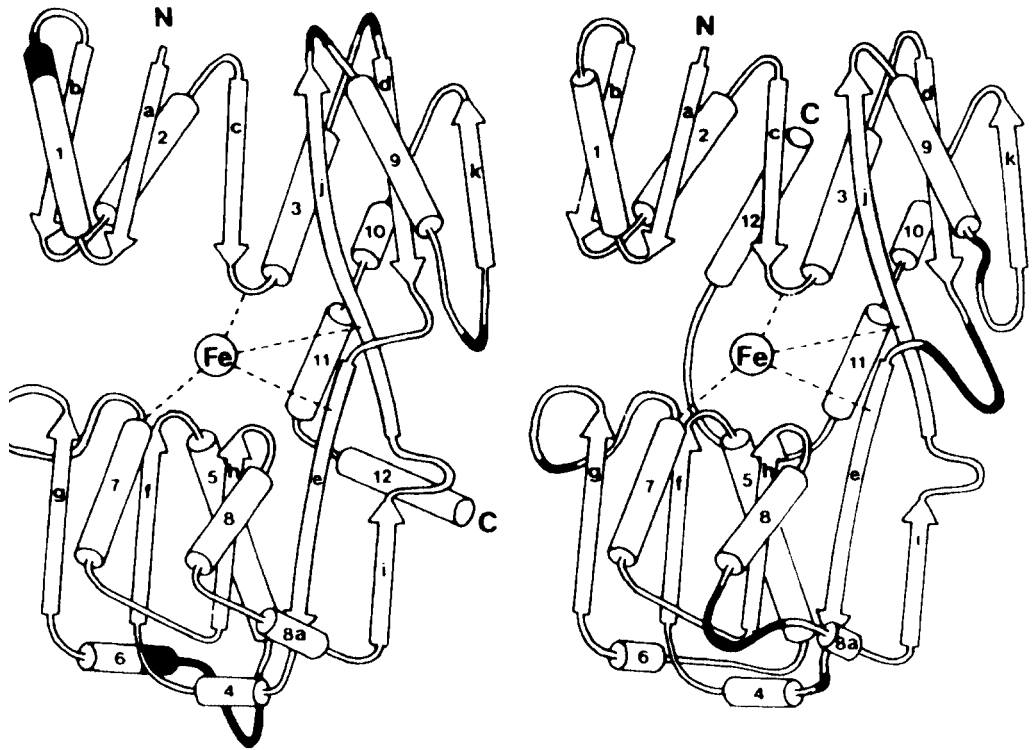
Figure 5.2 Schematic representation of the folding pattern for the N-lobe (left) and C-lobe (right) of human lactoferrin. From Anderson *et al.*, 1989. Reproduced by permission of Academic Press.

to domain 2. The pair of antiparallel β-strands e and j, which run behind the iron binding site, forms a flexible hinge between the two domains. Disulfide bridges, six in the *N*-lobe and ten in the *C*-lobe are represented as heavy bars. Many of these disulfide bridges are conserved in other transferrins, but none of them crosses from one lobe to the other, which explains how single half-molecules can be isolated from many species of transferrin by proteolytic cleavage in the helix A which joins the *N*- and *C*-lobes.

The determination of the structure of the iron transporter, ferric-binding, protein (hFBP)[‡] from *Haemophilus influenzae* (Bruns *et al.*, 1997) at 0.16 nm resolution shows that it is a member of the transferrin superfamily, which includes both the transferrins and a number of periplasmic binding proteins (PBP). The PBPs transport a wide variety of nutrients, including sugars, amino acids and ions, across the periplasm from the outer to the inner (plasma) membrane in bacteria (see Chapter 3). Iron binding by transferrins (see below) requires concomitant binding of a carbonate anion, which is located at the *N*-terminus of a helix. This corresponds to the site at which the anions are specifically bound in the bacterial periplasmic sulfate- and

---

[‡] Gram-negative pathogenic bacteria such as *Haemophilus*, *Neisseria, Serratia* and *Yersinia* acquire free iron directly from the transferrin (Tf) or lactoferrin (Lf) of their host. Fe^{3+} is extracted from Tf or Lf at the outer membrane by receptor proteins which are specific for Tf (Tbp1 and Tbp2) or Lf (Lbp1 and Lbp2), and transported to an inner membrane permease by a periplasmic ferric binding protein (Fbp).
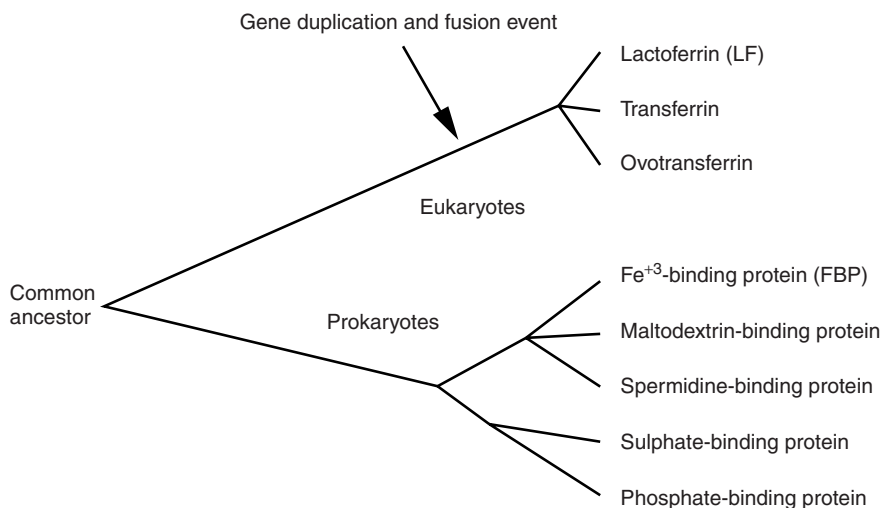
Figure 5.3   The deduced evolutionary tree for selected members of the transferrin superfamily, based on comparisons of structures and sequences. The tree combines the transferrins with a number of prokaryotic periplasmic transport proteins. From Bruns *et al.*, 1997. Reproduced by permission of Nature Publishing Group.

phosphate-binding proteins (Pflugrath and Quiocho, 1985; Luecke and Quiocho, 1990). This led to the suggestion that the transferrins could have arisen by divergent evolution and subsequent duplication from an anion-binding precursor common to the transferrins and the periplasmic binding proteins (Baker *et al.*, 1987).

HFBP is a member of the class II periplasmic binding proteins, which include those specific for phosphate (Pbp), sulfate and maltodextrin, and Figure 5.3 presents the deduced evolutionary tree for selected members of the transferrin superfamily, based on comparison of structures and sequences. The polypeptide topology of hFBP and the *N*-lobe of human lactoferrin are compared in Figure 5.4 (Plate 5). The apparent homology between the transferrins and the periplasmic binding proteins implies evolution from a common ancestor that existed prior to the divergence of prokaryotes and eukaryotes, about 1500 million years ago. Despite their structural similarities the periplasmic binding proteins have less than 20 % sequence identity with one another and less than 10 % identity with the transferrins.

5.1.2   Transferrin Iron Binding and Release

The iron binding sites of both the *N*- and *C*-lobes of transferrins are highly conserved (Figure 5.5, Plate 6) consisting of four protein ligands together with a carbonate ion as a bidentate ligand to the metal. The iron binding sites in transferrins and hFBP have nearly ideal octahedral metal coordination, with tight yet reversible Fe^{3+} binding (affinity constant $= 10^{19}$–10^{20} M^{-1}). Whereas the iron binding site in transferrins is buried, the Fe^{3+} binding site in hFBP is substantially more exposed to solvent. This is explained by the different relative orientation of the two domains, and the existence of an additional loop in the transferrins which covers the binding site (Figure 5.4). In hFBP the Fe^{3+} is bound by five oxygen ligands and a single

nitrogen. The protein ligands are two tyrosines, one histidine and one glutamate: the phosphate provides only one oxygen with a water molecule filling the remaining coordination site to the iron (Figure 5.4). The phosphate in hFBP is bound in a similar way to the phosphate in Pbp and in an analogous position to both the sulfate ion in Sbp and the carbonate ion in the transferrins. However, the tyrosine and histidine ligands in Fbp come from completely different parts of the protein fold as compared with their counterparts in lactoferrin and transferrin: only the carboxylate ligands (Glu-57 in hFBP, Asp-63 in Tf and Asp-60 in Lf come from a spatially equivalent position in the two proteins, after the third β-strand in domain 1 (Figure 5.4). The common anion-binding fold of Fbp and transferrins suggests divergent evolution from a common PBP-like anion-binding protein, whereas the selection of similar iron-binding ligands coming from different structural origins suggests convergent evolution to an optimized ligand geometry for binding of Fe^{3+}.

Apotransferrin binds iron rapidly *in vitro* and seems quite able to oxidize Fe^{2+} and incorporate it in the Fe^{3+} form (Gabor and Aisen, 1970). However, ceruloplasmin,[¶] a copper-containing plasma glycoprotein, while likely to be multifunctional (Frieden and Hsieh, 1976), was reported to have ferroxidase activity, and it has been suggested that this is its principal physiological role. In view of the danger that 'free' Fe^{2+} will lead to the production of the highly toxic hydroxyl radical ($OH^\bullet$) (see Chapter 10), it is suggested that *in vivo* ceruloplasmin has a custodial role, mediating the release of Fe^{2+} from cells and ensuring that it is subsequently incorporated into apotransferrin in the Fe^{3+} form (Lindley, 1996). The structure of human ceruloplasmin has been solved at a resolution of 0.3 nm (Zaitseva *et al.*, 1996). It contains six copper atoms, three mononuclear sites and one trinuclear cluster. The organization of the trinuclear cluster and the closest mononuclear site (Figure 5.6, Plate 6) is essentially that found in ascorbate oxidase (Messerschmidt *et al.*, 1992), suggestive of an oxidase activity for ceruloplasmin in blood. In addition, ceruloplasmin has at the outside of the molecule, approximately 0.7–0.8 nm from this mononuclear site, a flexible putative metal-binding site consisting of a His and three carboxylates, an Asp and two Glu's (Figure 5.6), which could constitute an oxidation site for Fe^{2+}, by analogy with the ferroxidase sites in H chain ferritins (see Chapter 6). Whether or not the putative iron-binding sites play a role in the known ferroxidase of ceruloplasmin remains to be established, but it has become clear that ceruloplasmin plays a key role in cellular iron metabolism and is intricately linked with serum transferrin. At present we do not understand where and how iron is bound to apotransferrin *in vivo*.

The iron-binding sites have been characterized by crystallographic studies on several transferrins, and in Figure 5.7 (Plate 7) that of the *N*-lobe of human lactoferrin is presented. The 3+ charge on the ferric ion is matched by the three anionic ligands Asp-63, Tyr-95 and Tyr-188 (the fourth, His-249, is neutral), while the charge on the carbonate anion is almost matched by the positive charge on Arg-124 and the

[¶] Ceruloplasmin is a protein for which many functions have been proposed – somewhat akin to Pirandello's *Six Characters in Search of an Author*, ceruloplasmin has long been a protein in search of a function. However, its importance in iron metabolism has been underlined by the observation of systemic iron loading in the tissues of patients with aceruloplasminaemia and other mutations in the ceruloplasmin gene. For further information on copper and iron interactions, see Chapter 12.

N-terminus of helix 5. This explains why the synergistic anion is necessary for iron binding, since it effectively neutralizes the positive charge in the putative binding pocket and supplies two oxygen ligands to bind the metal. The carbonate anion binds to the *N*-terminus of helix 5 (involving residues 124–136) through hydrogen bonds to the main chain amide nitrogens of Ala-126 and Gly-127, and is also hydrogen bonded to the side chain oxygen of Thr-120 and to two of the nitrogens of Arg-124. In addition, Ser-125 forms a hydrogen bond to the second carbonyl oxygen of Asp-63, bridging domains 1 and 2. The protein ligands (Figure 5.2) come from the two β-strands that connect domains 1 and 2 (Tyr-95 in strand e and His-249 in strand j), from a loop between β-strand c and α-helix 3 (Asp-63), and from the *N*-terminus of helix 7 in domain 2 (Tyr-188). The binding site is extremely well designed to accommodate the ferric cation and the synergistic carbonate anion.

Substantial conformation changes accompany iron binding and release as shown by crystallographic studies on human apolactoferrin (Anderson *et al.*, 1990) and, at lower resolution, duck apoovotransferrin (Rawas *et al.*, 1996). X-Ray and light scattering together with EXAFS studies in solution (Grossmann *et al.*, 1992, 1998) show that all transferrins undergo similar structural changes. Iron binding or release is accompanied by a 'Venus' fly trap'[§] mechanism, similar to that observed in the periplasmic binding proteins (Quiocho, 1990), where large scale domain movements mediated by a hinge in the two antiparallel β-strands that run behind the iron-binding site in each lobe, results in opening or closing of the binding cleft of each lobe. A schematic representation of the N-lobe polypeptide chain fold, showing the conformational change between 'open' and 'closed' forms of human lactoferrin, where the N-lobe is opened by some 54°, is shown in Figure 5.8 (Anderson *et al.*, 1990). The opening of the cleft exposes a cluster of basic residues (Arg-121, Arg-219 and Lys-301), which were previously buried within it. It is proposed that the sequence of events upon binding starts with the carbonate anion being attracted into
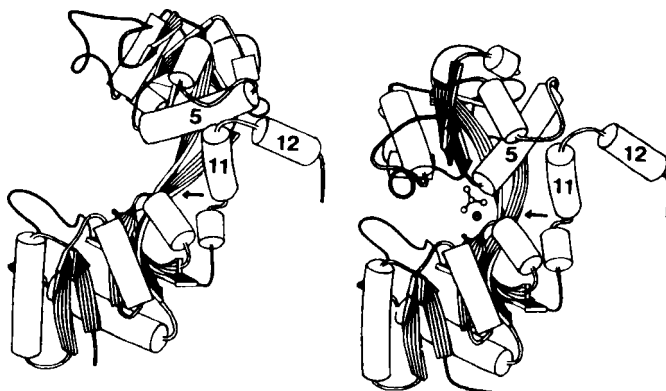
Figure 5.8 A schematic representation of the N-lobe polypeptide chain fold, showing the conformational change between 'open' and 'closed' forms of human lactoferrin. Reprinted with permission from Nature (Anderson *et al.*, 1990). Copyright (1990) Macmillan Magazines Limited.

[§] Venus' fly trap: a white-flowered swamp flower of the sundew family, native to the Carolinas, having leaves with two hinged blades that snap shut to trap insects.

the interdomain cleft, where it binds to the *N*-terminus of helix 5 (involving residues 124–136) through hydrogen bonds to the main-chain amide nitrogens of Ala-126 and Gly-127, and is also hydrogen bonded to the side-chain oxygen of Thr-120 and to two of the nitrogens of Arg-124 (Figure 5.7). Four of the six metal-binding ligands (Tyr-92 and Tyr-192, both from domain N2 and two of the carbonate oxygens) are now in a position to bind the Fe^{3+} to the N2 domain. Binding is completed as the N2 domain rotates and the cleft is closed bringing the last two ligands, Asp-63 and His-29 into coordination with the metal, with the second carbonyl oxygen of Asp-63 further linking the two domains by hydrogen bonding to Ser-125 (Anderson *et al.*, 1989). However, while this is a not implausible model for iron uptake by apotransferrin *in vitro*, we must await further information concerning it's *in vivo* applicability.

With regard to iron release from transferrin, there is a well established cellular cycle involving the endocyosis of diferric transferrin bound to its receptor (see below), which leads to iron release within the confines of the endosome at pH values below 6, followed by recycling of apotransferrin and the transferrin receptor to the plasma membrane where apotransferrin is released and both it and the receptor are reutilized. Studies with non-physiological anions such as oxalate and malonate in place of carbonate have shown that these anions allow binding of diferric transferrin to its receptor, but inhibit iron acquisition by cells, implying involvement of carbonate in iron release. This has led to the proposition that protonation of the carbonate and a change in anion coordination from bidentate to monodentate could be the first step in dissociation of the metal–transferrin complex. The transferrin receptor is also involved in the iron release mechanism, as will be discussed below (Bali and Aisen, 1991; Sipe and Murphy, 1991; Egan *et al.*, 1993). Residues involved in the hydrogen bonding network around the iron-binding site, the so-called 'second coordination shell' must also play a role in iron release, since the primary iron-coordination spheres in the *N*-and *C*-lobes in different transferrins are structurally identical, yet their iron release properties differ. For example, the *N*-lobe of human transferrin releases iron below pH 6, about one pH unit higher than the *C*-lobe and two pH units higher than lactoferrin. A possible explanation for the pH dependence of iron release was proposed by Dewan and colleagues based on the 0.23 nm resolution crystal structure of ferric ovotransferrin *N*-lobe (Dewan *et al.*, 1993). Two lysine residues (Lys-206 and Lys-296 in the human transferrin numbering) appeared to be so close to one another (side chain NZ atoms only 0.23 nm apart) that they could not both be protonated. It was suggested that the pK_a of one of the lysine residues was abnormally low (less than 5.9, the pH at which the crystals were grown), and that it would not be positively charged. At lower pH values, the NZ amino group of this lysine would be protonated, the two charged lysine residues would repel one another, acting as a dilysine trigger and providing the electrostatic force required to open the cleft containing the iron-binding ligands. These two Lys residues, which belong to different domains and lie immediately behind the iron-binding site, are present in the *N*-lobes of human transferrin and ovotransferrin, but not in their *C*-lobes, or in lactoferrin.

A recently obtained high resolution structure of two crystal forms of the *N*-lobe of human serum transferrin (at 0.16 and 0.18 nm resolution) shows disorder at the iron-binding sites (MacGillivray *et al.*, 1998). Model building and refinement show

that there are two alternative conformations of the carbonate anion, the side chain of Arg-124 and several solvent molecules, with the A conformation (occupancy 0.63–0.65) corresponding to the structure of the iron-binding site found in other transferrins, whereas in the alternative B conformation (occupancy 0.35–0.37) the carbonate has rotated 30° relative to the iron atom, and the side chain of Arg-124 has moved to accomodate the new position of the carbonate (Figure 5.7). In the A conformation the Arg-124 side chain is folded around the carbonate ion with both the NE and NH2 atoms of Arg-124 hydrogen bonded to the carbonate O2 atom: the carbonate oxygen atoms also receive hydrogen bonds from Thr-120 and the main-chain amide nitrogen atoms of Ala-126 and Gly-127 at the terminus of helix 5 (residues 124–136**).** The hydrogen bonding of the carbonate ion is considerably disrupted in the B conformation: the hydrogen bonds with the N-terminus of helix 5 have been lost, and, in the orthorhombic crystal form shown in Figure 5.7(b), so have both of the hydrogen bonds with Arg-124. A number of solvent molecules is also displaced. The same type of movement of the anion is found in two mutants of human lactoferrin *N*-lobe, in which the anion-binding arginine has been mutated, and in which iron binding is destabilized (Faber *et al*., 1996). Concomitant with this anion movement, a number of conformational changes occur that result in partial removal of the anion from the metal, a substantial weakening of hydrogen bonding between anion and protein, and greatly decreased binding affinity between the metal, the anion and the protein. Thus protonation of the carbonate ion could be the first step in iron release: the decreased charge on the resulting bicarbonate would lead to its detachment from the helix 5 *N*-terminus, as well as from Arg-124, and a change from bidentate to monodentate anion coordination. In the dilysine trigger model, the next step would be protonation of either Lys-206 or Lys-296, followed by opening of the cleft and release of the anion. Thereafter the other metal-binding ligands would be removed, perhaps first His-249 and Asp-63 from domain 1, before Tyr-95 and Tyr-188. Interestingly, in the mutant His249Glu, the crystal structure shows that Glu-249 is directly bound to iron and that a local movement of Lys-296 has broken the dilysine interaction: despite the loss of this potentially pH–sensitive interaction, the mutant is only slightly more acid stable than wild type, and releases iron only slightly faster (MacGillivray *et al*., 2000). Likewise, protonation of His-249 as the pH decreases might also be an important factor in iron release (Jeffrey *et al*., 1997; El Hage Chagine and Pakdaman, 1995). Interactions with 'second shell' amino-acid residues in the binding cleft (i.e. amino acids involved in the hydrogen bonding network around the primary iron coordination sphere), can also profoundly affect metal binding (He *et al*., 1998).

5.2 Iron Uptake by Mammalian Cells – Uptake of Transferrin-bound Iron

5.2.1 The Transferrin Receptor

From early studies with doubly labelled transferrin it became clear that whereas iron is rapidly cleared from the circulation, the protein recycles many times – in

man the half-life of transferrin is about 7.6 days, whereas that of transferrin-bound iron is around 1.7 hours (Katz, 1961). It can be estimated that the transferrin molecule undergoes more than one hundred cycles of iron binding, transport and release, before it is finally removed from the circulation. Further, it was shown that treatment of reticulocytes with trypsin abolished iron uptake, suggesting that there was a membrane receptor for transferrin (Jandl *et al.*, 1959). This led to the proposal of a plasma-to-cell cycle for transferrin (Jandl and Katz, 1963) in which the iron-loaded transferrin released its iron within the cell, where it remained, whilst the apotransferrin was released back to the circulation in search of more iron. Before discussing the transferrin-to-cell cycle we will discuss our present knowledge concerning the transferrin receptor (TfR), which has been the object of a considerable amount of scientific activity in the last twenty years.[‖]

In essentially all proliferating, differentiating and haemoglobin synthesizing mammalian cells, iron uptake is mediated by transferrin receptors, which all have very similar structures. They are disulfide-linked homodimers consisting of two identical glycosylated subunits of apparent molecular weight 90 000. In humans, the gene for the transferrin receptor is located on the long arm of the same chromosome 3 as are the genes for transferrin, melanotransferrin and ceruloplasmin (Rabin *et al.*, 1985). The transferrin receptor, in common with the other so-called type II transmembrane proteins, does not have a cleavable signal sequence and during its synthesis is inserted into the rough endoplasmic reticulum with the *N*-terminus facing the cytoplasm (Zerial *et al.*, 1986). Such transmembrane proteins lacking the *N*-terminal signal peptide are thought to have made an early appearance in the course of biochemical evolution (Sabatini *et al.*, 1982). The subunit, a transmembrane polypeptide of 760 amino acids, consists of a short amino-terminal cytoplasmic domain (residues 1–67), that contains the internalization motif YTRF, a single hydrophobic transmembrane region (residues 68–88), that is presumed to contain the signal for translocation across the plasma membrane of the cell (Zerial *et al.*, 1986), and a large extracellular portion (ectodomain, residues 89–760), that contains a binding site for the transferrin molecule (Figure 5.9). The two subunits are linked by two intermolecular disulfide bonds, one formed by Cys-89 and one by Cys-98 of each subunit, located in the extracellular domain of the protein close to the cell membrane (Jing and Trowbridge, 1987). There is a third cysteine residue at position 62 just at the internal face of the cytoplasmic membrane, which is the site of acylation by a palmitate residue, although abolition of the acylation site by site-directed mutagenesis has little effect on receptor function (Jing and Trowbridge, 1990). The cytoplasmic domain of the receptor can also be phosphorylated by protein kinase C at Ser-24 (Davis *et al.*, 1986); phosphorylation does not appear greatly to affect receptor function (Rothenberger *et al.*, 1987). The receptor is *N*-glycosylated at Asn residues 251, 317 and 727 (Omary and Trowbridge, 1981) and *O*-glycosylated at residue Thr-104 (Hayes *et al.*, 1992). Mutated receptor lacking *N*-glycosylation sites shows impaired transferrin-binding activity, reduced intersubunit disulfide

---

[‖] With the advent of monoclonal antibodies, the search for *tumour-specific antigens* became the biggest cottage industry since unemployment. It rapidly became apparent that a 90 kD disulfide-bridged transmembrane protein was present in many tumour cells – it was the transferrin receptor, and as they say, the rest is history. It has become a standard procedure to determine the *in vivo* growth potential of tumours by measuring transferrin receptor expression.
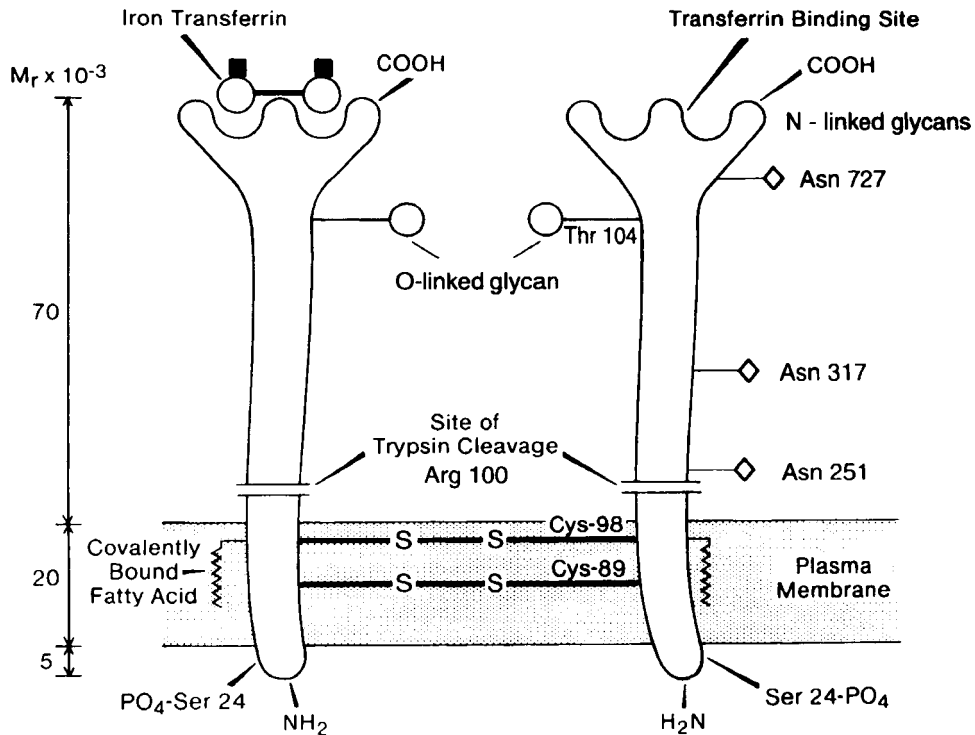
Figure 5.9 Diagrammatic representation of the transferrin receptor. Adapted from Aisen, 1998, by courtesy of Marcel Dekker, Inc.

bonding and decreased surface expression (Williams and Enns, 1991). Electron cryomicroscopy shows that the transferrin receptor has a globular extracellular structure separated from the membrane by a stalk of about 3.0 nm in length (Fuchs *et al.*, 1998). The stalk presumably includes the residues immediately following the transmembrane region, including the *O*-linked glycan and the two intermolecular disulfide bonds. The extracellular domain can be isolated by trypsin digestion as a soluble fragment containing residues 121–760; it is not disulfide linked, yet it is a dimer which binds two molecules of transferrin with normal affinity as well as antibodies directed against the receptor, and corresponds to the large globular structure seen by electron microscopy. A similar fragment is found as a normal component of human serum, where its level is inversely correlated with body iron stores, as will be discussed in more detail in Chapter 9.

The equivalent of the tryptic fragment of human transferrin receptor has been expressed in Chinese hamster ovary cells and its structure determined at a resolution of 0.32 nm (Lawrence *et al.*, 1999). The asymmetric unit of the crystals contains four transferrin receptor dimers. Interpretable electron density is found for the entire tryptic fragment except for Arg-121 at the amino terminus, and density is also seen for the first *N*-acetylglucosamine residue at each of the *N*-glycosylation sites. The transferrin receptor monomer is made up of three distinct domains, organized such that the dimer is butterfly shaped (Figure 5.10, Plate 7). The likely orientation of the dimer with respect to the plasma membrane has been assigned on the basis of the

amino terminal positions. The first, protease-like, domain contains residues 122 to 188 and 384 to 606. It has a fold similar to carboxy- or aminopeptidase (Chevrier *et al.*, 1996), consisting of a central, seven-stranded mixed B-sheet with flanking helices (Figure 5.11(a), Plate 8). An unusual feature is an intramolecular disulfide bridge involving Cys-556 and Cys-558. The second, apical domain, contains residues 189 to 383, and can best be described as a β-sandwich in which the two sheets are splayed apart, with an α-helix (α II-2) running along the open edge (Figure 5.11(b)). A similar structure has been seen in domain 4 of aconitase (Robbins and Stout, 1989). The apical domain is inserted between the first and second strands of the central β sheet in the protease-like domain. The third, helical domain (Figure 5.11(c)) contains residues 607 to 760, and is essentially a four-helix bundle (like ferritin, see Chapter 6), formed by the two parallel helices αIII-3 and αIII-6 as the second and fourth helices of the bundle with the first and third helices of the bundle each broken in two (αIII-1 and αIII-2 constituting the first helix and αIII-4 and αIII-5 the third). The large loop-like insert between αIII-4 and αIII-5 has contacts with both the apical and the protease-like domains, as well as with its counterpart across the molecular twofold axis. The helical domain seems to be particularly important for receptor dimerization, since it contacts each of the three domains in the dimer partner.

5.2.2 Transferrin Binding to Its Receptor

In the light of the (albeit low resolution) structure of the transferrin receptor there has been much speculation as to how, and where, transferrin is bound to the receptor protein. We know that the transferrin receptor binds two transferrin molecules, probably non-cooperatively. We also know that the two lobes of diferritransferrin are quite similar, particularly in the first coordination sphere of the iron, and that iron release probably involves substantial opening of the interdomain cleft. We also assume, as outlined below, that during the physiologically relevant release of iron from the transferrin–receptor complex within the endosome (see below) during the transferrin to cell cycle, the complex does not dissociate, the implication being that the complex must withstand a hinge-like opening of both lobes. We also know from studies with the *N*- or *C*-lobes of transferrin that the interactions between the *C*-lobe and the transferrin receptor are much stronger – the binding constant for the *C*-lobe is one-tenth that of intact transferrin (Zak *et al.*, 1994; Mason *et al.*, 1997), which might imply that the contacts between the *C*-lobe and the receptor are more extensive than those with the *N*-lobe. An additional consideration is that on the convoluted surface of the transferrin receptor dimer, there are lateral facing clefts and a bowl-like depression at the top of the molecule (Figure 5.12, Plate 8). This central bowl is not sufficiently large to accomodate two transferrin molecules without extensive interference, leaving the lateral clefts as more likely sites of interaction. All three domains of a single monomer contribute to the surface of each cleft, which opens inward toward what would be the catalytic site of a structurally related protease. Apparent surface complementarity was found between transferrin and the lateral clefts of the transferrin receptor, which allowed docking of the two molecules by inspection, followed by rigid body refinement (Lawrence *et al.*,

1999). The resulting model (Figure 5.12)[††] takes many of these considerations into account: (i) most contacts with transferrin involve the C_1 domain, with additional contributions from the N_1 domain, particularly near to its carboxyl terminus; (ii) the N_2 and C_2 domains of transferrin have only minor interactions with the receptor; (iii) the motions required within each lobe for iron release are easily tolerated; (iv) the largest continuous patch of conserved surface residues in human and rabbit transferrin is found at the interface in the model between the apical domain of the transferrin receptor and the N_1 and C_1 domains of transferrin; (v) the glycosylation sites in human and rabbit transferrins, which are not required for interacton with the receptor point away from the receptor. This model predicts that the following regions of the transferrin receptor participate in binding of transferrin: the αII-2/βII-8 and βII-4/βII-5 loops of the apical domain, the αI-7/αI-8 loop of the protease-like domain, and the αIII-1 and αIII-5 helices of the helical domain – these regions are coloured in Figure 5.13 (see Plate 9). Together the αIII-1 and αIII-5 helices form the carboxyl-terminal face of the lateral cleft, and they may contain residues responsible for species specificity of transferrin association (Buchegger *et al.*, 1996). The αI-7/αI-8 loop might also contribute to selectivity. It is also speculated that hinge motions of the apical domain, as shown by the arrows in Figure 5.10, could stimulate iron release by favouring the apo conformation of transferrin, resulting in the movements of the N_2 and C_2 domains upon ferric iron release (Figure 5.12). The helical domain has been implicated in transferrin binding from studies with human/chicken chimaeric transferrin receptor (Buchegger *et al.*, 1996), while the presence of a conserved Arg–Gly–Asp sequence at positions 646–648 in human, mouse, rat, chicken and Chinese hamster transferrin receptor, together with site-directed mutagenesis studies, localizes the binding site at least to include these residues within helix 3 of the helical domain (Dubljevic *et al.*, 1999).

A human cDNA highly homologous to the transferrin receptor, has been identified and reported to encode a protein, designated TfR2, which binds diferrictransferrin and mediates iron uptake of transferrin-bound iron (Kawabata *et al.*, 1999). A mouse orthologue of human TfR2 has been found independently (Fleming *et al.*, 2000); its transcript does not contain the iron-responsive elements (IREs) found in the 3′-untranslated sequences of TfR mRNA (see a discussion of this in Chapter 7), consistent with the observation that TfR2 allows continued uptake of Tf-bound iron by hepatocytes even after TfR has been down-regulated by iron overload. Comparison of the human TfR2 and TfR genes shows that none of the IREs in the TfR gene are conserved in the TfR2 gene. It therefore seems likely that human TfR2 mRNA is also insensitive to regulation by cellular iron status, and that TfR2 contributes to the susceptibility of the liver to iron loading in hereditary haemochromatosis. The observation that the TfR knockout mutation in the mouse leads to an embryonic lethal phenotype (Levy *et al.*, 1999) shows that TfR2 cannot compensate for TfR, perhaps reflecting its absence of expression in placenta as well as a number of other tissues (Fleming *et al.*, 2000).

[††] While wishing to show no disrespect, as a professor in a Catholic University, it has often seemed to me that the modern art of molecular modelling for proteins, and perhaps particularly for protein–protein interactions might best be accomodated in the curriculum as an interfaculty course with the title 'Molecular Theology'.

5.2.3   **Transferrin Receptor Binding to Hereditary Haemochromatosis Protein HFE**

As we will see in Chapter 9, the gene mutated in the iron-overload disease, hereditary haemochromatosis (HH), encodes for a 384-residue type I transmembrane glycoprotein, HFE, which is homologous to Class I MHC molecules and associates with the Class I light chain β2-microglobulin (Feder *et al*., 1996). The HFE molecule, unlike other Class I MHC molecules, that function in the immune system by presenting peptide antigens to T cells, does not bind peptides or perform any known immune function. Most HH patients are homozygous for a mutation which converts Cys-260 to Tyr, eliminating a disulfide bond in HFE and preventing its association with β2-microglobulin and its expression at the cell surface in cell cultures (Feder *et al*., 1997; Waheed *et al*., 1997). A second mutation (His41Asp) is found on the other chromosome of about 70 % of patients heterozygous for the Cys260Tyr mutation (Feder *et al*., 1996): this mutation does not prevent association with β2-microglobulin or cell-surface expression (Feder *et al*., 1997; Waheed *et al*., 1997). The crystal structure of the soluble ectodomain of human HFE has been determined at a resolution of 0.26 nm (Lebron *et al*., 1998), and is presented in Figure 5.13(a), see Plate 9. There is a connection between HFE and its anticipated role in iron overload: it was found that HFE binds to the transferrin receptor (Parkkila *et al*., 1997; Feder *et al*., 1998) and decreases its affinity for diferric transferrin five-to ten-fold (Feder *et al*., 1998). HFE binds tightly to transferrin receptor at the pH of the cell surface, but not at pH 6.0, which suggests that HFE would dissociate from the transferrin receptor within acidified endosomes (Lebron *et al*., 1998; Lebron and Bjorkmann, 1999). *In vitro* studies show that HFE and diferritransferrin can bind simultaneously to the transferrin receptor forming a ternary complex (Lebron *et al*., 1998) consisting of one diferritransferrin and one HFE bound per transferrin receptor complex (Lebron *et al*., 1999). HFE is thought to inhibit transferrin-binding to the receptor (Feder *et al*., 1998; Gross *et al*., 1998) by binding at or near to the transferrin binding site on the receptor (Lebron *et al*., 1999).

The crystal structure at 0.28 nm resolution of the complex between the ectodomains of human HFE and the transferrin receptor has been determined (Bennett *et al*., 2000) and is presented in Figure 5.13(c) (the TfR structure using the same colour coding is given in Figure 5.13(b)). The structure consists of two HFE molecules bound to one transferrin receptor homodimer, with their overall orientations indicating that the molecules interact while anchored in the plane of a common membrane. It is assumed that around nine residues in the extracellular domain of HFE in an extended configuration could hold the HFE molecules, oriented with their long axes roughly parallel to the plane of the membrane in a 'lying-down' orientation, some 3.0 nm from the plane of the common membrane (Figure 15.13(c)). It comes as no surprise that the principal contacts essentially involve helices αIII-1 and αIII-3 from the helical domain of the receptor which, as we have seen above, have also been proposed from modelling studies as being involved in the interaction between the receptor and transferrin. The αIII-3 helix of the receptor (residues 640–662) and the α1 helix of HFE are antiparallel to each other and interact over nearly the entire lengths of both helices (around five turns). The short αIII-1 helix from TfR (residues 614–626) interacts in a parallel arrangement with the *C*-terminal region of HFE α1 helix: the hydrophobic core of this pair

consists of Leu-619 and Val-622 from TfR packed against Val-78 and Trp-81 of HFE. Mutagenesis of these two residues in HFE either shows no detectable binding (Val78Ala) or greatly reduced affinity – around 5000-fold (Trp81Ala) (Lebron and Bjorkman, 1999). Residues of TfR that interact at the interface with HFE are Leu-619, Val-622 and Arg-623 of helix αIII-1, Gln-640, Arg-646 and Asp-648 of helix αIII-3, and Arg-629 in helix αIII-2, which makes several polar interactions with residues in the α1 and α2 helices of HFE. With the exception of Arg-629, all of these residues have been implicated in the TfR–transferrin interface (see above).

In solution, HFE binds to TfR with nanomolar affinity at pH 7.5, but weakly, or not at all at pH 6.0 (Lebron *et al.*, 1998; Lebron and Bjorkman, 1999), suggesting perhaps that HFE dissociates from TfR in acidified endosomes, although in cell lines overexpressing HFE, HFE associates with TfR throughout the biosynthetic pathway and colocalizes with transferrin in intracellular acidic vesicles (Gross *et al.*, 1998). Biochemical studies have shown that HFE and diferrictransferrin can bind simultaneously to TfR to form a ternary complex (Lebron *et al.*, 1998), consisting of one HFE and one diferrictransferrin bound per TfR homodimer (Lebron *et al.*, 1999), and that HFE inhibits the interaction of TfR with transferrin (Feder *et al.*, 1998; Gross *et al.*, 1998) by binding at or near the transferrin binding site on TfR (Lebron *et al.*, 1999). It has been shown that TfR is required for, and controls the assembly, intracellular transport and surface expression of HFE, and because surface-expressed HFE and TfR remain firmly associated physically, only the fraction of TfR that is associated with HFE during biosynthesis is affected functionally (Salter-Cid *et al.*, 1999). These authors present, in their view, convincing evidence that HFE not only blocks transferrin binding to TfR on the extracellular side of the cell, but also inhibits internalization of the TfR in the cytoplasm: thus, HFE inhibition of TfR function is responsible for the diminished uptake of transferrin-bound iron. HFE indirectly regulates iron homeostasis by functioning as a negative modulator of TfR.

5.2.4 The Transferrin-to-cell Cycle

Haemoglobin-synthesizing immature erythroid cells, placental tissues and rapidly dividing cells, both normal and malignant[‡‡], obtain the iron that they require via receptor-mediated uptake from transferrin. The plasma iron pool (essentially transferrin-bound iron) in man amounts to some 4 mg, although the daily turnover is over 30 mg: the transferrin is normally only 30 % saturated, so that the bulk of the transferrin lacks iron at one or both sites. It is therefore of great importance that the transferrin receptor can distinguish between apotransferrin and iron-loaded transferrin at the plasma membrane, with its slightly alkaline pH of 7.4. In the rabbit, apotransferrin is bound with only one twenty-fifth of the affinity of diferritransferrin, whilst the two monomeric forms bind six- to seven-times less tightly (Young *et al.*, 1984). It is not clear if the same holds for human transferrin and its receptor. Studies with recombinant N and C lobes of transferrin have shown that

---

[‡‡] The use of specific antireceptor antibodies to measure transferrin receptor expression has become routine practice to determine the *in vivo* growth potential of tumours.

while both lobes interact with the receptor, the interactions between the *C*-lobe and the receptor are much stronger than with the *N*-lobe (Zak *et al.*, 1994; Mason *et al.*, 1997), perhaps suggesting that human monoferritransferrin loaded in the *N*-lobe, with its *C*-lobe in the open state, might not be an effective iron donor.

After binding to its receptor at the plasma membrane, in a step which does not require energy, the diferric transferrin–receptor complex invaginates into a clathrin-coated pit (Figure 5.14). Clathrin molecules assemble into a basket-like network on the cytoplasmic side of the membrane, and this assembly process starts to shape the membrane into a vesicle. A small GTP-binding protein, called dynamin, assembles around the neck of each deeply invaginated coated pit. The dynamin then hydrolyses its bound GTP, causing the ring to constrict and pinch off the vesicle from the membrane. This is a coated vesicle, a membranous sac encased in a polyhedral framework of clathrin and its associated coat proteins. One of these, adaptin 2, not only binds the coat to the vesicle membrane but also helps to select ligand molecules for transport. Ligand molecules for onward transport, like transferrin, are recognized by their plasma membrane receptor – the adaptins help to capture specific ligand molecules by trapping the ligand's receptors that bind them. In this way a selected set of ligand molecules, in our case diferritransferrin, bound to its specific receptor, is incorporated into the lumen of each newly formed clathrin-coated vesicle. After budding is complete, the coat proteins are removed,
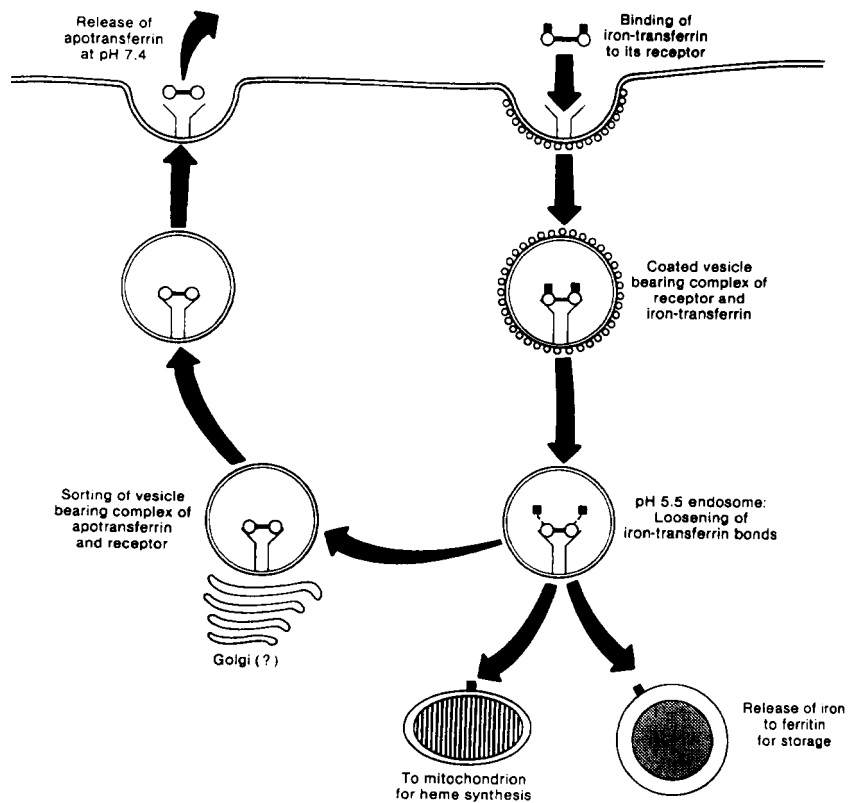
Figure 5.14   The transferrin to cell cycle. (From Crichton, 1991.)

resulting in the formation of smooth-surfaced vesicles. These naked transport vesicles can then fuse with the target membranes of endosomes. Fusion of the two membranes delivers the vesicle contents into the interior of the endosome, and adds the vesicle membrane to the target (endosomal) membrane. The interior of the endosome compartment is maintained at a pH of around 5–6 by the action of an ATP-dependent proton pump in the endosomal membrane that pumps protons into the endosome lumen from the cytosol. The endosomal compartment acts as the main sorting station in the inward endocytic pathway. The acidic environment of the endosome plays a crucial role in the sorting process by causing many receptors to release their bound ligand. These early endosomes containing transferrin bound to its receptor, are rapidly sorted to deflect them from lysosomal degradation. However, as was pointed out above, iron release from transferrin at mildly acidic pH values when it is bound to its receptor is facilitated compared to iron release from free diferrictransferrin (Bali and Aisen, 1991; Bali *et al.*, 1991; Sipe and Murphy, 1991). Thus, within the endosome the transferrin receptor facilitates iron release from transferrin, presumably by protonation of the carbonate and opening of the jaws of the iron-binding pocket(s), yet the apotransferrin, which retains a high affinity for its receptor at acidic pH values, unlike most other protein ligands, remains bound to its receptor and is recycled with it back to the plasma membrane. There, at the slightly alkaline extracellular pH, apotransferrin dissociates from the receptor and is released to go off into the circulation in search of iron. This constitutes the transferrin-to-cell cycle, which, given the high affinity of apotransferrin for the receptor at acidic pH values and its low affinity at pH 7.4, is expected to function in one direction only, namely to take iron into cells that have transferrin receptors.

The natural resistance associated macrophage protein (Nramp) gene family is composed of two members in mammals. Nramp1 is expressed primarily in primary macrophages and macrophage cell lines, where it is localized to late endosomes/lysosomes (Gruenheid *et al.*, 1999; Blackwell *et al.*, 2000). Mutations in this locus cause susceptibility to infectious diseases (more of this in Chapter 11). Nramp2 (Gruenheid *et al.*, 1995), now designated DCT1 (divalent cation transporter protein), present in many cell types, including haematopoietic precursors and macrophages, is expressed as a 90–100 kD integral membrane protein extensively modified by glycosylation (>40 % of molecular mass), which is localized primarily to recycling endosomes, and also to a lesser extent at the plasma membrane, where it colocalizes with transferrin (Su *et al.*, 1998; Gruenheid *et al.*, 1999). There are many compelling arguments that this 12-transmembrane domain protein functions as the apical iron transporter in the small intestine. DMT1 is not specific for Fe(II) and transports other divalent metal ions (Gunshin *et al.*, 1997). The same missense mutation (Gly185Arg) is found in the *DCT1* gene in two different inherited anaemias in rodents, microcytic anaemia (*mk*) in the mouse (Fleming *et al.*, 1997) and the Belgrade (*b*) rat (Fleming *et al.*, 1998), both of which are characterized by defective duodenal iron absorption and by inefficient iron uptake by erythroid precursors. The Belgrade rat has been particularly well studied and it appears that while the erythroid precursor cells are able to take up iron into an endosomal compartment by receptor-mediated endocytosis from transferrin, they are subsequently unable to export iron from the endosome into the cytoplasm for haemoglobin synthesis. The endosomal iron is mostly returned to the cell surface and released. The mutation

found in DCT1 of *mk* and *b* animals lies within the predicted transmembrane domain 4, which is highly conserved among Nramp proteins, including Nramp family members that have been described in bacteria, flies, worms and plants (Cellier *et al.*, 1995). Site-directed mutagenesis of DCT1 in this region (Su *et al.*, 1998) showed that only the Gly185Arg mutation seemed to affect iron transport directly, whereas other mutations only compromised protein stability. The Gly185Arg mutant DCT1 was expressed at the cell surface and in endosomes, indicative that the residue at position 185 has a key role in the transmembrane passage of iron. While Nramp2 appears to be important for iron transport out of the early endosome, there has not as yet been convincing evidence concerning the reductase that is assumed to reduce the iron, which as we have seen above is released from transferrin as Fe^{3+}.

5.2.5 Receptor-independent Uptake of Transferrin Iron

Another potential source of iron, at least for hepatocytes, is receptor-independent uptake of iron from transferrin. This appears to involve an iron uptake pathway from transferrin which is neither suppressed in hepatocytes by antibodies to TfR (Trinder *et al.*, 1988), nor by transfection of HuH-7 hepatoma cells with transferrin receptor anti-sense cDNA (Trinder *et al.*, 1996). The same pathway may also be utilized for iron uptake from isolated transferrin *N*-lobe, which is not recognized by the receptor (Thorstensen *et al.*, 1995). The possible role of TfR2 in this process remains to be established, as does the physiological importance of this pathway in intact liver. Human melanoma cells (Richardson and Baker, 1994) and Chinese hamster cells lacking transferrin receptors but transfected with melanotransferrin (Kennard *et al.*, 1995) use another pathway for transferrin iron uptake, independent of the transferrin receptor, but utilizing iron transfer from transferrin or simple iron chelates to membrane-anchored melanotransferrin, and from there onwards into the cellular interior.

5.3 Iron Uptake by Mammalian Cells – Uptake of Non-transferrin Bound Iron

Transferrin iron uptake via receptor-mediated endocytosis has clearly appeared fairly late in evolution, when we consider that the bilobal iron-binding protein is found only as far back as insects[¶¶]. As we have seen in the preceding chapters, iron-uptake mechanisms involving the synthesis of more or less specific siderophores have evolved together with strategies implying the solubilization of insoluble ferric iron by the combined effects of pH and reduction, and even the development of receptor proteins capable of taking up transferrin-, lactoferrin- or haem-bound iron from specific hosts.

[¶¶] Although, on an evolutionary time scale, this was recent: the last common ancestor of vertebrates and arthropods existed some 600 million years ago (Jamroz *et al.*, 1993)

5.3.1 Non-protein-Bound Iron

Two inherited disorders provide evidence for transferrin-independent iron transport of iron (De Silva *et al.*, 1996). In congenital hypotransferrinaemia, a rare disease of humans and rodents, affected individuals have undetectable levels of transferrin, together with anaemia due to iron-limited erythropoiesis, yet they develop tissue iron overload. When hypotransferrinaemic mice are given radio iron, it is absorbed by the digestive tract and accumulated in a variety of parenchymal tissues, principally the liver. By contrast, iron administered to such mice that have been made transferrin replete distributes to haematopoietic tissues, underlining both the existence of a transferrin-independent cellular iron-uptake system, and a tissue-distribution pattern that depends on the presence or absence of transferrin (Bernstein, 1987; Craven *et al.*, 1987). In humans with hereditary haemochromatosis, a defect in the regulation of intestinal iron absorption, homozygotes have extensive hepatic iron overload, as well as iron accumulation in many other organs. Transferrin saturation may approach 100 %, yet despite this, increased intestinal iron absorption continues. As we have seen above, it may be that some of this transferrin-bound iron is taken up in liver by TfR2. However, in hereditary haemochromatosis and in other iron loading disorders such as transfusion-dependent thalassaemia, important amounts of non-transferrin bound iron (NTBI) are found in serum, to a large extent complexed to citrate (Grootfeld *et al.*, 1989). This iron is thought to be much more reactive and available than transferrin-bound iron, and to pose a much greater problem in terms of potential toxicity (Herschko *et al.*, 1978). NTBI transport has been studied using ferric citrate, ferric nitrilotriacetate and other chelators (Graham *et al.*, 1998; Scheiber-Mojdehkar *et al.*, 1999; Gutierrez *et al.*, 1998). Iron administered as ferric citrate in intact animals mostly goes to the liver, where some of it is eliminated by biliary excretion (Brissot *et al.*, 1994). Studies in rat hepatocyte cell cultures (Rakba *et al.*, 1998) have shown that ferric citrate is extremely cytotoxic, in contrast to iron administered as ferritin or as iron dextran (Rakba *et al.*, 1998; Aouad *et al.*, 2000), and that citrate-mediated iron uptake is inhibited in a dose dependent fashion by diferric transferrin, and even more effectively by apotransferrin (Graham *et al.*, 1998; Scheiber-Mojdehkar *et al.*, 1999). NTBI uptake by hepatocytes is regulated by the iron status of the liver, is not regulated by iron regulatory proteins (see Chapter 7), and may involve more than one transport system (Scheiber-Mojdehkar *et al.*, 1999).

It has been suggested that membrane ferric iron reductases[§§] are involved in, and perhaps even essential for, NTBI uptake and acquisition by cells (Inman and Wessling-Resnick, 1993; Randell *et al.*, 1994). A novel factor involved in cellular iron

---

[§§] We should underline the cautionary remarks of our old friend and colleague Phil Aisen: 'Assay of true ferric iron reductase is not as simple as many reports suggest. The use of so-called ferrous iron chelators to report on iron reduction can be misleading. Although these chelators display intense colours only when binding Fe^{2+}, due to charge to ligand transfer, they also form colourless complexes with Fe^{3+} (Smith and Martell, 1975). More importantly, the high reduction potentials of the Fe^{2+}/Fe^{3+} couple in these complexes, which may exceed $+1100$ mV (Buettner, 1993), and the extremely strong binding of Fe^{2+}, make their complexes with Fe^{3+} potent oxidants which can drive, and not simply report on, ferric iron reduction (Thorstensen and Aisen, 1990). A far more rigorous approach would be to use non-perturbing techniques such as EPR and Mössbauer spectroscopy. Difficulties in their use would be more than compensated in the reliability of the results: **uncritically accepting a poor experiment is not justified by difficulty in doing a good one**' (Aisen, 1998).

assimilation called SFT (Stimulator of Fe Transport) has been identified (Gutierrez *et al.*, 1997) which stimulates iron uptake by cultured cell lines from both transferrin- and non-transferrin-bound iron. Expression of SFT mRNA is enhanced by iron chelation and down-regulated by high levels of iron in HeLa cells and SFT transcript levels are also up-regulated in haemochromatosis patients (Yu *et al.*, 1998). A low affinity system for uptake of Fe(II) has been found (Savigni and Morgan, 1998) in reticulocytes of the Belgrade rat (which has a missense mutation in DCT1 – see Chapter 8).

Yet another potential pathway for NTBI uptake by intestinal and erythroid cells has been proposed involving integrins and mobilferrin (Conrad and Umbreit, 1993; Conrad *et al.*, 1994), although its physiological relevence remains uncertain.

5.3.2 Ferritin-bound Iron

A number of different cell types has been found to have ferritin receptors, which could have important consequences as a source of iron in view of the high average iron content of ferritin molecules (typically 2500–3000 iron atoms/molecule compared with a maximum of two for iron-saturated transferrin). However, apart from the unusual case of guinea pig erythroid precursor cells and rat hepatocytes, an iron-donating function for ferritin has not been conclusively demonstrated. The former take up ferritin iron in a saturable, time- and temperature-dependent fashion, characteristic of receptor-mediated endocytosis, with up to 70 % of the iron appearing subsequently in haem (Pollack and Campana, 1981; Blight and Morgan, 1983). *In vivo* studies show that almost all of radio-iron labelled ferritin injected into rats is taken up by the liver (Unger and Hershko, 1974). *In vitro*, primary cultures of hepatocytes take up ferritin in a manner consistent with receptor-mediated endocytosis (Osterloh and Aisen, 1989), and the ferritin protein is degraded in lysosomes and its iron reutilized for hepatocyte ferritin synthesis (Sibille *et al.*, 1988, 1989). The possible role of ferritin in the reflux of iron from reticuloendothelial cells to parenchymal cells in secondary iron overload will be discussed in greater detail in Chapter 7.

5.3.3 Haemopexin as an Iron Transporter

Turnover of haem proteins, particularly haemoglobin, potentially leads to release of free haem into extracellular fluids, where it can be a source of free radical formation and a major source of iron for invading bacterial pathogens (Lee, 1995). Protection is afforded by haemopexin, a 60-kD serum protein whose structure has been recently determined (Paoli *et al.*, 1999), which binds haem with high affinity ($K_d < 1$ pM), and delivers the haem to target cells such as liver via specific receptors. Internalization of the haem–haemopexin complex releases haem for intracellular degradation by haem oxygenase, stimulates intracellular protective mechanisms including induction of haem oxygenase 1 and the anti-apoptotic transcription factor NFκB. In this way, haem binding and transport by haemopexin provides protection against both extracellular and intracellular damage by free haem, limits access by pathogenic organisms to haem, and conserves iron by recycling the haem iron. The importance of haem–haemopexin as a cellular iron source is probably rather limited under normal physiological conditions.

5.4 **References**

Aisen, P. (1998). In *Metal Ions in Biological Systems* (eds Sigel, A. and Sigel, H.), **35**, 585–631.

Alderton, G., Ward, W.H. and Ferold, H.L. (1946). *Arch. Biochem. Biophys.*, **11**, 9–12.

Anderson, B.F., Baker, H.M., Dodson, E.J., Norris, G.E., Rumball, S.V., Waters, J.M. and Baker, E.N. (1987). *Proc. Natl Acad. Sci., USA*, **84**, 1769–73.

Anderson, B.F., Baker, H.M., Norris, G.E., Rice, D.W. and Baker, E.N. (1989). *J. Mol. Biol.*, **209**, 711–34.

Anderson, B.F., Baker, H.M., Norris, G.E., Rumball, S.V. and Baker, E.N. (1990). *Nature*, **344**, 784–7.

Aouad, F., Florence, A., Zhang, Y., Collins, F. *et al.* (2001). *Hepatology*, submitted for publication.

Bailey, S., Evans, R.W., Garratt, R.C., Gorinsky, B. *et al.* (1988). *Biochem.*, **27**, 5804–12.

Baker, E.N., Rumball, S.V. and Anderson, B.F. (1987). *TIBS.*, **12**, 350–3.

Baker, E.N., Baker, H.M., Smith, C.A., Stebbins, M.R. *et al.* (1992). *FEBS Lett.*, **298**, 215–8.

Baldwin, G.S. (1993). *Comp. Biochem. Physiol. B*, **106**, 203–8.

Bali, P.K. and Aisen, P. (1991). *Biochem.*, **30**, 9947–52.

Bali, P.K., Zak, O. and Aisen, P. (1991). *Biochem.*, **30**, 324–8.

Bartfeld, N.S. and Law, J.H. (1990). *J. Biol. Chem.*, **265**, 21684–91.

Bennett, M.J., Lebron, J.A. and Bjorkman, P.J. (2000). *Nature*, **403**, 46–53.

Bernstein, S.E. (1987). *J. Lab. Clin. Med.*, **110**, 690–705.

Blackwell, J.M., Searle, S., Goswami, T. and Miller, E.N. (2000). *Microbes Infect.*, **2**, 317–21.

Blight, G.D. and Morgan, E.H. (1983). *Br. J. Haematol.*, **55**, 59–71.

Brissot, P., Zanninelli, G., Guyader, D., Zeind, J. and Gollan, J. (1994). *Am. J. Physiol. Gastrointest. Liver Physiol.*, **267**, G135–G142.

Bruns, C.M., Nowalk, A.J., Arvai, A.S., McTigue, M.A. *et al.* (1997). *Nature Struct. Biol.*, **4**, 919–23.

Buchegger, F., Trowbridge, I.S., Liu, L.F., White, S. and Collawn, J.F. (1996). *Eur. J. Biochem.*, **235**, 9–17.

Buettner, G.R. (1993). *Arch. Biochem. Biophys.*, **300**, 535–43.

Cellier, M., Prive, G., Belouchi, A., Kwan, T. *et al.* (1995). *Proc. Natl Acad. Sci., USA*, **92**, 5105–10.

Chevrier, B., d'Orchymont, H., Schalk, C., Tarnus, C. and Moras, D. (1996). *Eur. J. Biochem.*, **237**, 393–8.

Conrad, M.E. and Umbreit, J.N. (1993). *Am. J. Hematol.*, **42**, 67–73.

Conrad, M.E., Umbreit, J.N., Moore, E.G., Uzel, C. and Berry, M.R. (1994). *J. Biol. Chem.*, **269**, 7169–73.

Craven, C.M., Alexander, J., Eldridge, M., Kushner, J.P., Bernstein, S. and Kaplan, J. (1987). *Proc. Natl Acad. Sci., USA*, **84**, 3457–61.

Davis, R.J., Johnson, G.L., Kelleher, D.J., Anderson, J.K., Mole, J.E. and Czech, M.P. (1986). *J. Biol. Chem.*, **261**, 9034–41.

De Silva, D.M., Askwith, C.C. and Kaplan, J. (1996). *Physiol. Rev.*, **76**, 31–47.

Dewan, J.C., Mikami, B., Hirose, M. and Sacchettini, J.C. (1993). *Biochem.*, **32**, 11963–8.

Dubljevic, V., Sali, A. and Goding, J.W. (1999). *Biochem. J.*, **341**, 11–14.

Egan, T.J., Zak, O. and Aisen, P. (1993). *Biochem.*, **32**, 8162–7.

El Hage Chahine, J.-M. and Pakdaman, R. (1995). *Eur. J. Biochem.*, **230**, 1102–10.

Faber, H.R., Baker, C.J., Day, C.L., Tweedie, J.W. *et al.* (1996). *Biochem.*, **35**, 14473–9.

Feder, J.N., Gnirke, A., Thomas, W., Tsuchihashi, Z. *et al.* (1996). *Nature Genet.*, **13**, 399–408.

Feder, J.N., Tsuchihashi, Z., Irrinki, A., Lee, V.K. *et al.* (1997). *J. Biol. Chem.*, **272**, 14025–8.

Feder, J.N., Penny, D.M., Irrinki, A., Lee, V.K. *et al.* (1998). *Proc. Natl Acad. Sci. USA*, **95**, 1472–7.

Fleming, M.D., Romano, M.A., Su, M.A., Garrick, L.M. *et al.* (1998). *Proc. Natl Acad. Sci. USA*, **95**, 1148–53.

Fleming, R.F., Migas, M.C., Holden, C.C., Waheed, A. *et al.* (2000). *Proc. Natl Acad. Sci., USA*, **97**, 2214–9.

Frieden, E. and Hsieh (1976). *Adv. Enzymol.*, **44**, 187–236.

Fuchs, H., Lücken, U., Tauber, R., Engel, A. and Reinhard, G. (1998). *Structure*, **6**, 1235–43.

Gabor, B.P. and Aisen, P. (1970). *Biochim. Biophys. Acta*, **221**, 228–33.

Graham, R.M., Morgan, E.H. and Baker, E. (1998). *Eur. J. Biochem.*, **253**, 139–45.

Grootveld, M., Bell, J.D., Halliwell, B., Aruoma, O.I., Bomford, A. and Sadler, P.J. (1989). *J. Biol. Chem.*, **264**, 4417–22.

Gross, C.N., Irrinki, A., Feder, J.N. and Enns, C.A. (1998). *J. Biol. Chem.*, **273**, 22068–74.

Grossmann, J.G., Neu, M., Pantos, E., Schwab, F.J. *et al.* (1992). *J. Mol. Biol.*, **225**, 811–9.

Grossmann, J.G., Crawley, J.B., Strange, R.W., Patel, K.J. *et al.* (1998). *J. Mol. Biol.*, **279**, 461–72.

Gruenheid, S., Cellier, M., Vidal, S. and Gros, P. (1995). *Genomics*, **25**, 514–25.

Gruenheid, S., Canonne-Hergaux, F., Gauthier, S., Hackam, D.J., Grinstein, S. and Gros, P. (1999). *J. Exp. Med.*, **189**, 831–41.

Gunshin, H., McKenzie, B., Berger, U.V., Gunshin, Y. *et al.* (1997). *Nature*, **388**, 482–8.

Gutierrez, J.A., Yu, J., Rivera, S. and Wessling-Resnick, M. (1997). *J. Cell Biol.*, **149**, 895–905.

Gutierrez, J.A., Inman, R.S., Akompong, T., Yu, J. and Wessling-Resnick, M. (1998). *J. Cell Physiol.*, **177**, 585–92.

Hayes, G.R., Enns, C.A. and Lucas, J.J. (1992). *Glycobiology*, **2**, 355–9.

He, Q.Y., Mason, A.B., Woodworth, R.B., Tam, B.M. *et al.* (1998). *J. Biol. Chem.*, **273**, 17018–24.

Herschko, C., Graham, G., Bates, G.W. and Rachmilewitz, E.A. (1978). *Brit. J. Haematol.*, **40**, 255–63.

Holmberg, C.G. and Laurell, C.B. (1947). *Acta Chem. Scand.*, **1**, 944–50.

Inman, R.S. and Wessling-Resnick, M. (1993). *J. Biol. Chem.*, **268**, 8521–8.

Jamroz, R.C., Gasdaska, J.R., Bradfield, J.Y. and Law, J.H. (1993). *Proc. Natl Acad. Sci., USA*, **90**, 1320–4.

Jandl, J.M., Inman, J.K., Simmons, R.L. and Allen, D.W. (1959). *J. Clin. Invest.*, **38**, 161–85.

Jandl, J.M. and Katz, J.H. (1963). *J. Clin. Invest.*, **42**, 314–26.

Jeffrey, P.D., Bewley, M.C., MacGillivray, R.T.A., Mason, A.B., Woodworth, R.B., and Baker, E.N. (1997). *Biochem.*, **37**, 13978–86.

Jing, S. and Trowbridge, I.S. (1987). *EMBO J.*, **6**, 327–31.

Jing, S. and Trowbridge, I.S. (1990). *J.Biol. Chem.*, **265**, 11555–9.

Johansson, B. (1960). *Acta Chem. Scand.*, **14**, 510–2.

Katz, J.H. (1961). *J. Clin. Invest.*, **40**, 2143–52.

Kawabata, H., Yang, R., Hirama, T., Vuong, P.T. *et al*. (1999). *J. Biol. Chem.*, **274**, 20826–32.

Kennard, M.L., Richardson, D.R., Gabathuler, R., Ponka, P. and Jefferies, W.A. (1995). *EMBO J.*, **14**, 4178–86.

Kurokawa, H., Mikami, B. and Hirose, M. (1995). *J. Mol. Biol.*, **254**, 196–207.

Laurell, C.B. and Ingelman, B. (1947). *Acta Chem. Scand.*, **1**, 770–6.

Lawrence, C.M., Ray, S., Babyonyshev, M., Galluser, R., Borhani, D.W. and Harrison, S.C. (1999). *Science*, **286**, 779–82.

Levy, J.E., Jin, O., Fujiwara, Y., Kuo, F. and Andrews, N.C. (1999). *Nat. Genet.*, **21**, 396–9.

Lebron, J.A. and Bjorkman, P.J. (1999). *J. Mol. Biol.*, **289**, 1109–18.

Lebron, J.A., West, A.P. and Bjorkman, P.J. (1999). *J. Mol. Biol.*, **294**, 239–45.

Lee, B.C. (1995). *Mol. Microbiol.*, **18**, 383–90.

Lindley, P.F. (1996). *Rep. Prog. Phys.*, **59**, 867–933.

Luecke, H. and Quiocho, F.A. (1990). *Nature*, **347**, 402–6.

MacGillivray, R.T., Mendez, E., Shewale, J.G., Sinha, S.K., Lineback-Zins, J. and Brew, K. (1983). *J. Biol. Chem.*, **258**, 3543–53.

MacGillivray, R.T.A., Moore, S.A., Chen, J., Anderson, B.F. *et al*. (1998). *Biochem.*, **37**, 7919–28.

MacGillivray, R.T.A., Bewley, M.C., Smith, C.A., Quing-Yu, H. *et al*. (2000). *Biochem.*, **39**, 1211–6.

Mason, A.B., Tam, B.M., Woodworth, R.C., Oliver, R.W.A. *et al*. (1997). *Biochem. J.*, **326**, 77–85.

Messerschmidt, A., Steigemann, W., Huber, R., Lang, G. *et al*. (1992). *Eur. J. Biochem.* **209**, 597–602.

Metz-Boutique, H.H., Jollès, J., Mazurier, J., Schoentgen, F. *et al*. (1984). *Eur. J. Biochem.*, **145**, 659–76.

Montreuil, J., Tornelat, J. and Mullet, S. (1960).) *Biochim. Biophys. Acta*, **45**, 413–21.

Omary, M.B. and Trowbridge, I.S. (1981). *J. Biol. Chem.*, **256**, 12888–92.

Osborne, T.C. and Cambell (1900). *J. Am. Chem. Soc.*, **22**, 422–6.

Osterloh, K. and Aisen, P. (1989). *Biochim. Biophys. Acta*, **1011**, 40–45.

Paoli, M., Anderson, B.F., Baker, H.M. and Morgan, W.T. (1999). *Nature Struct. Biol.*, **6**, 926–31.

Park, I., Schaeffer, E., Sidoli, A., Baralle, F.E., Cohen, G.N. and Zakin, M.M. (1985). *Proc. Natl. Acad. Sci., USA*, **82**, 3149–53.

Parkkila, S., Waheed, A., Britton, R.S., Feder, J.N. *et al*. (1997). *Proc. Natl Acad. Sci. USA*, **94**, 2534–9.

Pflugrath, J. and Quiocho, F. (1985). *Nature*, **314**, 257–60.

Pollack, S. and Campana, T. (1981). *Biochem. Biophys. Res. Commun.*, **100**, 1667–72.

Quiocho, F.A. (1990). *Phil. Trans. R. Soc. B*, **326**, 341–52.

Rabin, M., McLelland, A., Kühn, L.C. and Ruddle, F.H. (1985). *Am. J. Hum. Genet.*, **37**, 1112–6.

Randell, E.W., Parkes, J.G., Olivieri, N.F. and Templeton, D.M. (1994). *J.Biol. Chem.*, **269**, 16046–53.

Rakba, N., Aouad, F., Henry, C., Caris, C. *et al.* (1998). *Biochem. Pharmacol.*, **55**, 1797–1806.

Rawas, A., Muirhead, H. and Williams, J. (1996). *Acta Crys.*, **D52**, 464–8.

Richardson, D.R. and Baker, E. (1990). *Biochim. Biophys. Acta*, **1053**, 1–12.

Richardson, D.R. and Baker, E. (1994). *J. Cell. Physiol.*, **161**, 160–8.

Robbins, A.H. and Stout, C.D. (1989). *Proteins*, **5**, 289–312.

Rose, T.M., Plowman, G.D., Teplow, D.B., Dreyer, W.J., Hellstrom, K.E. and Brown, J.P. (1986). *Proc. Natl Acad. Sci., USA*, **83**, 1261–5.

Rothenberger, S., Iacopetta, B.J. and Kühn, L.C. (1987). *Cell*, **49**, 423–431.

Sabatini, D.D., Kreibich, G., Morinoto, T. and Adensick, M. (1982). *J. Cell Biol.*, **92**, 1–22.

Salter-Cid, L., Brunmark, A., Li, Y., Leturcq, D. *et al.* (1999). *Proc. Natl Acad. Sci., USA*, **96**, 5434–9.

Savigni, D.L. and Morgan, E.H. (1998). *J. Physiol.*, **508**, 837–50.

Schade, A.L. and Caroline, L. (1944). *Science*, **100**, 14–15.

Schade, A.L. and Caroline, L. (1946). *Science*, **104**, 340–1.

Schade, A.L., Reinhart, R.W. and Levy, H. (1949). *Arch. Biochem. Biophys.*, **20**, 170–2.

Schaeffer, E., Lucero, M.A., Jeltsch, J.-M., Py, M.-C. *et al.* (1987). *Gene*, **56**, 109–16.

Scheiber-Mojdehkar, B., Zimmermann, I., Dresow, B. and Goldenberg, H. (1999). *J. Hepatol.*, **31**, 61–70.

Sibille, J.-C., Kondo, H., and Aisen, P. (1988). *Hepatology*, **8**, 296–301.

Sibille, J.-C., Ciriolo, M., Kondo, H., Crichton, R.R. and Aisen, P. (1989). *Biochem. J.*, **262**, 685–8.

Sipe, D.M. and Murphy, R.F. (1991). *J. Biol. Chem.*, **266**, 8002–7.

Smith, R.M. and Martell, A.E. (1975) *Critical Stability Constants*, Vol. **2**, New York, Plenum Press.

Su, M.A., Trenor, C.C., Fleming, J.C., Fleming, M.D. and Andrews, N.C. (1998). *Blood*, **92**, 2157–63.

Surgenor, D.M., Koechlin, B.A. and Strong, L.E. (1949). *J. Clin. Invest.*, **28**, 73–96.

Thorstensen, K. and Aisen, P. (1990). *Biochim. Biophys. Acta*, **1052**, 29–35.

Thorstensen, K., Trinder, D., Zak, O. and Aisen, P. (1995). *Eur. J. Biochem.*, **232**, 129–33.

Trinder, D., Morgan, E.H. and Baker, E. (1988). *Biochim. Biophys. Acta*, **943**, 440–6.

Trinder, D., Zak, O. and Aisen, P. (1996). *Hepatology*, **23**, 1512–20.

Unger, A. and Hershko, C. (1974). *Br. J. Haematol.*, **28**, 169–79.

Vincent, J.B. (2000). *J. Nutr.*, **130**, 715–8.

Waheed, A., Parkkila, S., Zhou, X.Y., Tomatsu, S. *et al.* (1997). *Proc. Natl Acad. Sci. USA*, **94**, 12384–9.

Williams, A.M. and Enns, C.A. (1991). *J.Biol. Chem.*, **266**, 17648–54.

Young, S.P., Bomford, A. and Williams, R. (1984). *J. Biol. Chem.*, **219**, 505–10.

Yu, J., Yu, Z.K. and Wessling-Resnick, M. (1998). *J. Biol. Chem.*, **273**, 34675–8.

Zaitseva, I., Zaitsev, V., Card, G., Moshkov, K. *et al*. (1996). *J. Biol. Inorg. Chem.*, **1**, 15–23.

Zak, O., Trinder, D. and Aisen, P. (1994). *J. Biol. Chem.*, **269**, 7110–4.

Zerial, M., Lelancon, P., Schneider, C. and Garoff, H. (1986). *EMBO J.*, **5**, 1543–50.

6 Intracellular Iron Storage and Biomineralization

6.1 Intracellular Iron Storage

We have pointed out in an earlier chapter that while nearly all forms of life require iron, the element has unfavourable chemical properties that lead to the formation of insoluble ferric-hydroxide polymers and toxic free radicals. After dealing with the transport components involved in moving iron between cells and into cells, we now come to the storage forms of iron within cells, that sequester the metal in a non-toxic and bioavailable form. Historically, the first of these to be observed within mammalian cells was haemosiderin, which was identified histologically as iron-rich granules in tissues, that gave an intense Prussian blue reaction with potassium ferrocyanide (Perls, 1867). It was first isolated by Cook (1929) and described as consisting of 'organic granules impregnated with some form of ferric oxide'. It is insoluble, visible by light microscopy as golden-yellow intracellular granules and is localized in membranous structures termed siderosomes (Richter, 1978), which appear to be derived from lysosomes. It has a variable but higher iron content than ferritin, and represents the vast majority of the excess iron stored in clinical iron overloading disorders. Ferritin was first crystallized from horse spleen by the Czech physiologist Vilem Laufberger[†] as an 'iron-rich protein', which he speculated correctly, served as a depot of iron in the body (Laufberger, 1937). The name was adapted from the iron-rich protein that Naunyn Schmiedeberg had isolated from pig liver in 1894 and had called 'ferratin'. Both ferritin and haemosiderin consist of a central inorganic ferric oxyhydroxide core, which in ferritin is surrounded by a well organized apoferritin protein shell. The protein component of haemosiderin is poorly characterized, but seems to contain some apoferritin, or degradation products of apoferritin. Haemosiderin is

---

[†] Laufberger had tried to obtain the protein from horse liver, but it did not crystallize, and as he described to me when I met him in Prague some years ago, in those days everyone wanted to have protein crystals as a criteria of purity. Although James Sumner had crystallized jack bean urease in 1926, his preparations were somewhat impure, and it was only in the mid-1930s, when John Northrop and Moses Kubnitz showed that there is a direct correlation between the enzymatic activities of crystalline pepsin, trypsin and chymotrypsin that the protein nature of enzymes was generally accepted.

thought to be derived from the intralysosomal aggregation and degradation of ferritin.

In normal human subjects, some 25 % of total body iron (800–1000 mg) is present in the storage forms, mostly as ferritin. Whereas it is likely that all mammalian cell types contain some ferritin, haemosiderin in normal subjects is essentially restricted to cells of the reticuloendothelial system. Ferritin turns out to be almost universal in its distribution: ferritin and ferritin-like proteins have been found in all organisms except for one or two archaebacteria. In contrast, haemosiderin has not been found to any extent outside of iron-loaded animals, except for a brief report of a phytosiderin in pea seeds (Laulhere *et al.*, 1989).

6.1.1   Ferritin: Distribution and Primary Structure

We begin with a definition of what constitutes ferritin – typically it is an oligomeric protein of 24 identical or similar subunits, each of molecular weight around 20 kD, forming a hollow protein shell with an external diameter of 12–13 nm, inside diameter of 7–8 nm, molecular weight about 500 kD, capable of storing up to 4500 iron atoms in a water-soluble, non-toxic, bioavailable form as ferric hydroxyphosphate micelles. There is one exception to this definition, namely the ferritin from the Gram-positive bacterium *Listeria inocua* (Bozzi *et al.*, 1997) which, unlike classical ferritins, contains twelve subunits. If however, we consider the characteristic four-helical bundle with a dimetallic-binding site as a signature of ferritins (at least H-chain ferritins), we rapidly find ourselves in the presence not of a superfamily, but of a veritable evolutionary dynasty, as was pointed out in Chapter 2[‡].

Ferritins have been found in a wide range of species, and sequence data – some, as in the first ever sequence of horse spleen apoferritin (Heusterspreute and Crichton, 1981) determined by direct methods, but many now by DNa sequencing[¶], have been deposited for more than 70 ferritins. They vary in length from 154-185 residues per subunit. Some ferritins have *N*-terminal extensions which lie on the outside of the assembled shell and target the ferritin to a specific destination such as plastids in plants and yolk sac in snails (Andrews *et al.*, 1992; Lobréaux *et al.*, 1992). For example, pea ferritin is synthesized with an *N*-terminal extension of 75 residues, which is missing from the mature protein. The first part of this extension is a chloroplast-targetting sequence of 47 residues, which is lost on entry into the plastid. The second part, an extension peptide, is lost prior to assembly of the

---

[‡] As Brian Hartley once memorably remarked 'the trouble with discussing evolution is that we weren't there when it happened!'

[¶] A year after the publication of the horse-spleen sequence (essentially L-chain), we had determined the sequence of human spleen apoferritin (Wustefeld and Crichton, 1982). By careful analysis, Chantal Wustefeld had found peptide sequences corresponding to about 70 residues, that did not fit in to the principal sequence (which we now know to be L). We published this data together with the main sequence, pointing out that it was probably that of the H subunit – and the rest as they say is history. The teams of cloners and DNA sequencers published the complete H sequence a few years later – today it would take only a few weeks! We also got one amino-acid residue wrong out of 174 in the horse-spleen sequence, namely residue 193, which we identified as Leu, the cloners identified as Pro, and, in our 0.2 nm resolution structure, we confirmed as Pro (Gallois *et al.*, 1997): *sic transit gloria* proteomics vs genomics – but at least we knew what the protein did!

24-subunit oligomer, and its loss is a prerequisite for assembly (Proudhon *et al.*, 1989) Yet another ferritin-like protein, artemin, has *C*-terminal extensions that fill the cavity and prevent iron storage (De Graaf *et al.*, 1990). Mammals contain two ferritin subunits of distinct amino-acid sequences, known as H and L. In Table 6.1 we have compared the amino-acid sequences of four mammalian ferritins, two L chains (horse and human) and two H chains (human and rat). The H-chain is typically longer than L-chain, by four amino-acid residues at the *N*-terminus and three or four residues at the *C* terminus (in the rest of this chapter, numbering is

Table 6.1 Amino-acid sequence alignment of four mammalian ferritins (Horse L chain, HoL; Human L chain, HuL; Human H chain, HuH; Rat H, RaH) and of one of the ferritins, FTN, and the bacterioferritin, BFR of *Eschericia coli*

```
        1    5      10         20          30         40
HoL     SSQIRQNYSTEVEAAVNRLVNLYLRASYTYLSLGFYFDRD
HuL     ----------D------S------Q----Y----------
HuH     TTAST--V----HQDS---I--QI--E-Y---VY--MSY-----
RaH     TTASP--V----HQDS---I--QI--E-Y---VY--MSC-----
FTN         MLKP-MIEKL-EQMNLE-YS-LLYQQMSAWCYSH
BFR         MKGD-K-INYL-KLLGNE-V-INQYFLHARM-K..

             50         60         70         80
HoL     DVALEGVCHFFRELAEEKREGAERLLKMQNQRGGRALFQD
Hul     -------S---------E----Y-----------------
HuH     ----KNFAKY-LHQSHEE--H--K-M-L-------IFL--
RaH     ----KNFAKY-LHQSHEE--H--K-M-L-------IFL--
FTN     ..TF—-AAA-LRRH-QEEMTHMQ—-FDYLTDT-NLPRINT
BFR     NWG-KRNLDVEYHESIDEMKHAD-YIERILFLE-LPNL--

             90        100        110        120
HoL     LQKPSQDEWGTTLDAMKAAIVLEKSLNQALLDLHALGSAQ
HuL     IK--AE----K-P------MA-E-K-------------R
HuH     IK--DC-D-ESG-N--EC-LH-E-NV--S--E--K-ATDK
RaH     IK--DR-D-ESG-N--RC-LH-E--V--S--E--K-ATDK
FTN     VES-.FA-YSSLDELFQETYKHEQLIT-KINE-AHAAMTN
BFR     -G-L..NIGEDVEEMLRSDLA-ELDGAKN-REAIGYADSV

            130        140        150        160
HoL     ADPHLCDFLESHFLDEEVKLIKKMGDHLTNIQRLVGSQAG
HuL     T---------T-------------------LH--G-PE--
HuH     N-------I-T-Y-N-Q--A--EL---V--LRKMGAPES-
RaH     N-------I-T-Y-N-Q--S--EL---V--LRKMGAPES-
FTN     Q-YPTFN—-QW.YVS-QHEEE-LFKSIIDKLSLAG..KS-
BFR     H-YVSR-MMIE.I-RDEEGH-DWLETE-DL--KMG.....

            170
HoL     LGEYLFERLTLKHD
HuL     --------------
HuH     -A----DKH--GDSDNES
RaH     MA----DKH--G-GDES
FTN     E-LYFIDKELSTLDTQN
BFR     -QNYLQAQIREEG
```

$H_{24} L_0$

Hela cells

Muscle
Thymus
Red blood cells

Brain
Heart

Lymphocytes

Liver
Spleen

Serum
$H_0 L_{24}$
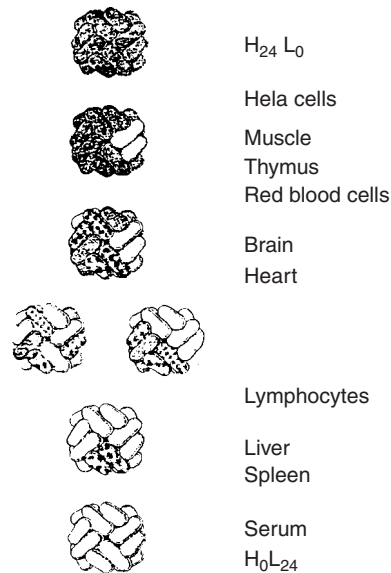
Figure 6.1 Schematic representation of human 'isoferritins' of different subunit composition. Each ferritin subunit is represented as a 'sausage' and subunits are packed in a symmetrical shell. Twelve of the 24 subunits are visible, with H-chain subunits stippled and L-chain subunits plain. Homopolymers of H-chain and L-chain subunits are at the top and bottom of the figure respectively. The sources of various ferritins are listed in the right hand column. Reprinted from Harrison and Arosio, 1996. Copyright (1996), with permission from Elsevier Science.

based on the H-subunit[§]). Whereas the H and L sequences, show only about 54 % identity, about 90 % of H-chain residues and 85 % of L-chain residues are identical. With two kinds of subunits for a 24-subunit molecule, one can build 25 'isoferritins' (Figure 6.1). Although no one would pretend to be able to isolate and characterize all of them, variations in the amount of the two subunits produced in different tissues would mean that for example, in human muscle heteropolymers rich in H subunits are predominant, whereas in liver and spleen the population of ferritin molecules has a much greater content of the L subunit. As we will see later, the effective storage of iron in mammalian ferritins requires contributions from both types of subunit. This seems to explain why we find heteropolymers rather than homopolymers, and that homopolymers are only found in pathological situations such as the Hereditary Hyperferritinaemia–Cataract Syndrome (HHCS) described in the next chapter, where L-chain homopolymers, devoid of iron, are found (Levi *et al.*, 1998). As we progress along the phylogenic tree, from mammals to other vertebrates (Figure 6.2), we encounter ferritins (sometimes with as many as three chains, as for example in the tadpole) which all have amino-acid sequences much closer to mammalian H-chain than to L-chain ferritins. This is also true of the ferritins of invertebrates and of plants (roughly 50 % identical to H-chains of mammals and 40 % to L-chains). Once we reach the prokaryotes a new class of ferritins appears,

[§] This is done 'à contre coeur', since the L-chain sequence was the first to be established. However, it makes little sense to refer to the amino terminus of H-chain ferritins as −1, −2, etc.
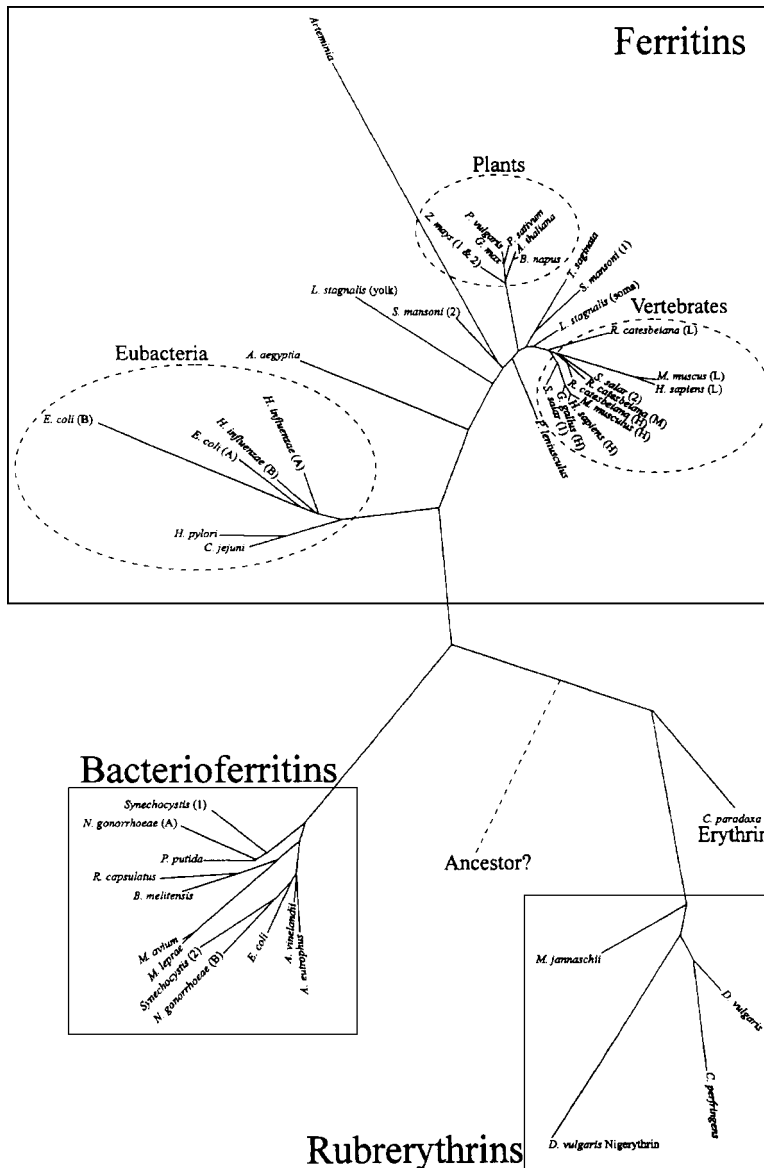
Figure 6.2 Phylogenetic tree showing the evolutionary relationship between members of the ferritin-bacterioferritin–rubreyrthrin superfamily. Reprinted from Harrison *et al.*, 1998, by courtesy of Marcel Dekker, Inc.

namely the bacterioferritins, which are haem containing; prokaryotes also contain haem-free ferritins. The samples of two representative bacterial ferritins from *E. coli*, one FTN, without haem and one, BFR with haem are also included in Table 6.1. The bacterial ferritins diverge even further from animal ferritins with only around 20 % identical residues. However, the two *E. coli* ferritins, BFR and FTN, show only 14 % identity with each other., The characteristic residues exclusive to H subunits but not to L, involved, as we will discuss later, in the primary site of

iron oxidation (the ferroxidase site), Glu-27, Glu-62, His-65 and Gln-141, are almost entirely conserved in the four H-type chains in Table 6.1 (the exception is residue 141 of BFR, which is Glu as in L ferritins). These four residues are also conserved in plant ferritins, and three of the four are also conserved in rubrerythrins, another family of bacterial proteins that are related in their structure and evolution to ferritins and bacterioferritins. The rubrerythrins contain an *N*-terminal four-helix bundle similar to bacterioferritins with a similar diiron cluster, as well as a *C*-terminal rubredoxin-like domain containing an Fe–Cys$_4$ cluster[||].

Finally, before passing to a discussion of the three-dimensional structure of the ferritin family, what of organisms which do not contain ferritins? With the increasing number of genome sequences now available and in the course of determination, we can only make what is at best a progress report. Recently it has become apparent that a number of archaebacteria, particularly hyperthermophiles, such as *Pyrococcus furiosus*, *T. maritima*, *M. thermoautotrophicum*, *A. fulgidus* do have ferritin-like proteins. However, the yeast *Saccharomyces cerevisiae* does not appear to have a ferritin, bacterioferritin or rubrerythrin sequence, nor does *Mycoplasma genitalium*, *Streptococcus pyrogenes* nor two *Pyrococcus* genomes (*P. horikoshii* and *P. abyssi*). Why these organisms do not appear to have members of the ferritin family may be attributable to their very low sequence similarity to other family members (we recall the case of BFR and FTN of *E. coli* mentioned above), or else they simply do not have ferritins. A good control for a genuine non-ferritin containing organism would be *Lactobacillus* sp. – which apparently has evolved in the total absence of iron.

6.1.2 Ferritin: Three-dimensional Structure

Horse-spleen apoferritin crystallizes in a face-centred, close-packed, cubic arrangement, in the space group F432, with molecules at the 432 symmetry points of the crystal lattice (Harrison, 1959). This publication was the logical extension of the DPhil thesis of the Oxford chemist Pauline M. Cowan (as she was before her marriage to Roy Harrison), and represented the first publication in what was to be a long and distinguished series of contributions on ferritin from the undisputed Iron Lady of iron metabolism[††].

The crystallization of horse spleen apoferritin was in fact a fortuitous coincidence, because, as we mentioned earlier, attempts to crystallize horse-liver ferritin were not successful, whereas the iron-rich ferritin from horse spleen could be crystallized (Laufberger, 1937). This was certainly related to the relatively high content of H subunits (average composition $L_{12}H_{12}$) in horse liver (something that was only discovered 50 years later). It has generally proved very difficult if not impossible to crystallize heteropolymers, and the best results in crystallographic terms have been obtained with recombinant homopolymers. As will be discussed later in this chapter,

---

[||] Interestingly an 'erythrin', without the *C*-terminal rubredoxin domain is found, perhaps appropriately in *Cyanophora paradoxa*, where, like the rubrerythrins, its function is unknown.

[††] It is interesting that another Iron Lady, also an Oxford chemist and an exact contemporary at Sommerville College of Pauline Harrison, was Britain's longest serving prime minister of this century, and its first woman prime minister, Mrs Margaret Thatcher. The political views of the two Iron Ladies could not, however, have been more different (but that is a different story).

at least as far as mammalian ferritins are concerned, the study of homopolymers represents a convenient, but none the less non-physiological simplification. Yet the first three-dimensional structure of a ferritin to be described at a final resolution of 0.26 nm (Rice *et al.*, 1983; Ford *et al.*, 1984) was that of horse spleen, with an average composition of about $L_{21}H_3$ (although the crystallization step may have selected a population with an even higher content of L subunits). Since, in the cubic space group F432 all subunits are statistically equivalent, the electron-density contours can be interpreted solely in terms of the predominant L subunit. Since this pioneering step, an important number of ferritin crystal structures have been determined. First, we describe the three-dimensional structure of the L-chain apoferritin molecule, which was the first high resolution (0.19–0.2 nm) structure of a mammalian ferritin to be determined (Gallois *et al.*, 1997; Hempstead *et al.*, 1997). We continue this structural cornucopia with H-chain apoferritins, bacterioferritins and finish with a consideration of rubrerythrins, Dps proteins and *Listeria* ferritin.

L-Chain Ferritins

The arrangement of the 24 subunits of the apoferritin molecule in their 432 symmetry viewed down a fourfold axis is presented in Figure 6.3. Also included in Figure 6.3 is a labelling scheme of symmetry related subunits and a representation of the subunit as a ribbon diagram of the α-carbon backbone. Of the 174 amino-acid residues of the L-chain 140 (80 %) are found in five α-helices. Each of the 24 subunits consists
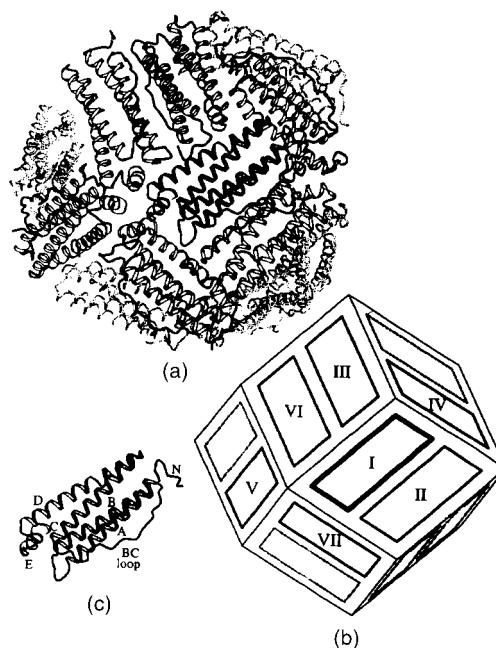
Figure 6.3 Structure of recombinant HoLF: (a) a half shell showing the relative positions and interfaces between symmetry-related subunits; (b) schematic diagram indicating labelling used for symmetry-related subunits; (c) detail of a single subunit. From Hempstead *et al.*, 1997. Reproduced by permission of Academic Press.

of a long central bundle of four parallel and antiparallel helices, A (residues 13–42), B (48–77), C (95–125) and D (126–161) with a left-handed twist, with a fifth short helix E (163–174) butting on to one end of the α-helical bundle, and a long extended loop, BC. The subunit is roughly cylindrical, a little more than 5 nm long and 2.5 nm wide. The *N*-terminus of the subunit (residues 5–12 in *H*-chain numbering) lies on the outside surface of the assembled molecule, and makes a number of intra- and intersubunit interactions. The long helices have intramolecular contacts which extend over a length of 3.5 nm with the fourth helix, D, protruding beyond this contact region. At the end of this helix the chain folds sharply back on itself such that the helix E lies roughly at 60° to the principal helix bundle. Helices A, B and C are about 4.3 nm long, D 5.2 nm and E 1.6 nm. There are short non-helical regions at the *N*- and *C*-termini and at the AB and DE turns. Helices B and C are connected at opposite ends by the long loop BC (residues 78–94) which stretches along the length of the helical bundle. The loop BC and the sides of helices A and C form the outside of the molecule, while helices B and D face the inside surface. A break in hydrogen bonding at His-136 causes a kink in the long D helix, that allows it to extend to the external surface. Within the subunit there are extensive side-chain interactions. At the two ends of the helical bundle many side chains in the L subunit interact to form tightly packed hydrophobic cores whereas in the centre there are a number of buried polar and hydrophilic residues that form a network of hydrogen bonds with a buried salt bridge between Lys-62 and Glu-107 and 141; Glu107 also interacts with Y34 (Figure 6.4). The contacts between helix E and the subunit are mediated through hydrophobic interactions with Phe-170 and Leu-175 and hydrogen bonds involving Glu-167. In both H and L subunits helical residues in the central bundle must be disposed in such a way that one side of the
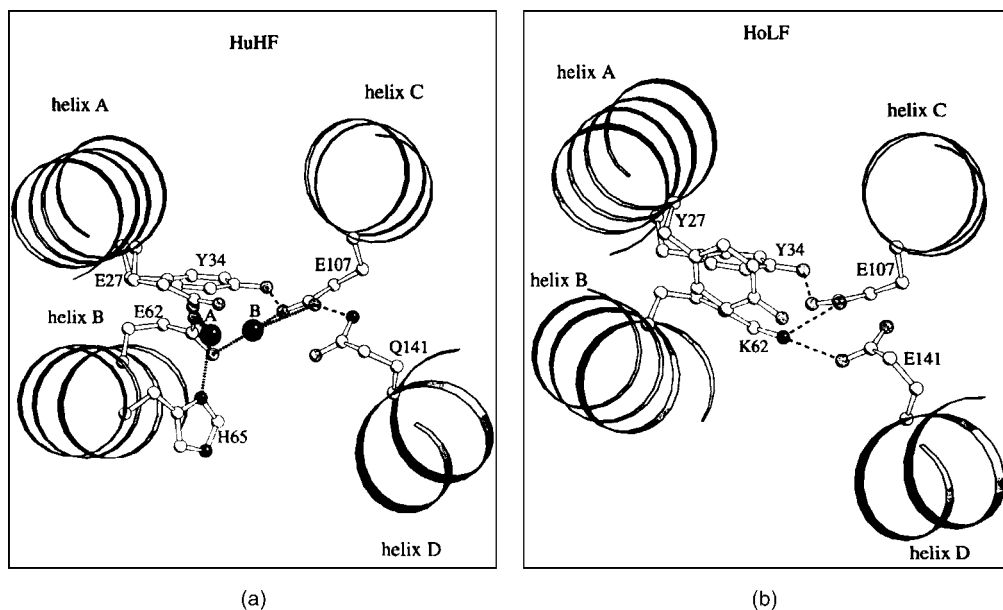
Figure 6.4 Central hydrophilic region within a subunit of (a) HuHF, and (b) HoLF. From Chasteen and Harrison, 1999. Reproduced by permission of Academic Press.

helix is predominantly hydrophobic and the other hydrophilic. The hydrophobic helical sides face each other in the largely apolar interior of the subunit while the hydrophilic groups lie mainly on the outside of the bundle.

The L subunits assemble into a compact, symmetrical and extremely stable apoferritin shell, by association with six other subunits, reducing their solvent-accessible surface area by 46 % (Hempstead *et al.*, 1997). Horse spleen apoferritin resists temperatures in excess of 80°C, is not dissociated into subunits between pH 3 and 11, nor by 10 M urea or 7 M guanidine at pH values above 6, and recombinant horse L-chain apoferritin is even more stable (Gallois *et al.*, 1997). Each subunit forms one long contact (I : II) (Figure 6.3) along a 2.2 nm long interface with an antiparallel neighbour involving many hydrophobic residues both from helix A (Val-24, Leu-28, Tyr-32 and Leu-35) and from the loop BC (Phe-82, Leu-85 and Pro-88). Their interaction with the corresponding region of a second subunit buries these hydrophobic residues from solvent and, in the process generates a twofold symmetry axis. Together with its related counterpart in a neighbouring subunit, two BC loops form a section of antiparallel β-sheet within the dimer. Interdigitation of hydrophobic side chains from BC and BC′ between those from A and A′ prevent contact between helix A and its dyad related A′ in the dimer. This also causes helices B and B′ on the inside surface of the molecule to be held apart, resulting in the formation of a partial groove on the inside surface. At the extreme ends of the dimer interface there is a salt bridge between Asp-45 on the AB turn and Arg-79 at the start of the BC loop. Towards the centre of the dimer interface (Figure 6.5(a)), a cluster of glutamate side chains from the B-helix, Glu-57, Glu-60, Glu-61 and Glu-64, extend into the cavity in a diamond shaped array. Glu-67 forms an salt bridge with Arg-63 of the same subunit while the two guanidino groups of the Arg-63 side chains face each other across the twofold axis and point into the cavity. It is in this relatively uncrowded central pocket in the dimer interface that protoporphyrin IX (Figure 6.5(b)) is found to bind (Précigoux *et al.*, 1994; Michaux *et al.*, 1996). Interestingly, when metalloporphyrins are diffused into crystals of horse spleen apoferritin, the porphyrin is found to be demetallated (Michaux *et al.*, 1996). A mechanism[‡‡] has been proposed to explain demetallation of haem. involving attack on the tetrapyrrole nitrogens of the protoporphyrin IX by protons derived from protein carboxylic acid groups and subsequent complexation of the iron by the corresponding carboxylates, together with binding of the protoporphyrin IX in the preformed pocket in the inner surface of the apoferritin molecule (Crichton *et al.*, 1997). We will return to the question of porphyrin binding later, when we discuss bacterioferritins.

There is a second long interface stretching between the threefold and fourfold axes, involving both hydrophobic and hydrophilic interactions. Close to the threefold axis is an intersubunit salt bridge between Asp-139 of subunit I and His-128 in III, which links the *N*-terminal end of helix D (III) to a position near the kink in helix D (I). Further along the interface, *N*-terminal residues 6–12 of subunit III make several interactions with the *C*-helix of subunit I, including several which are mediated

[‡‡] The mechanism has been described as involving a combination of a nesting and a molecular vacuum cleaner effect. To succeed in placing such expressions in the august pages of the scientific literature is, I suppose a sort of scientific hedonism.
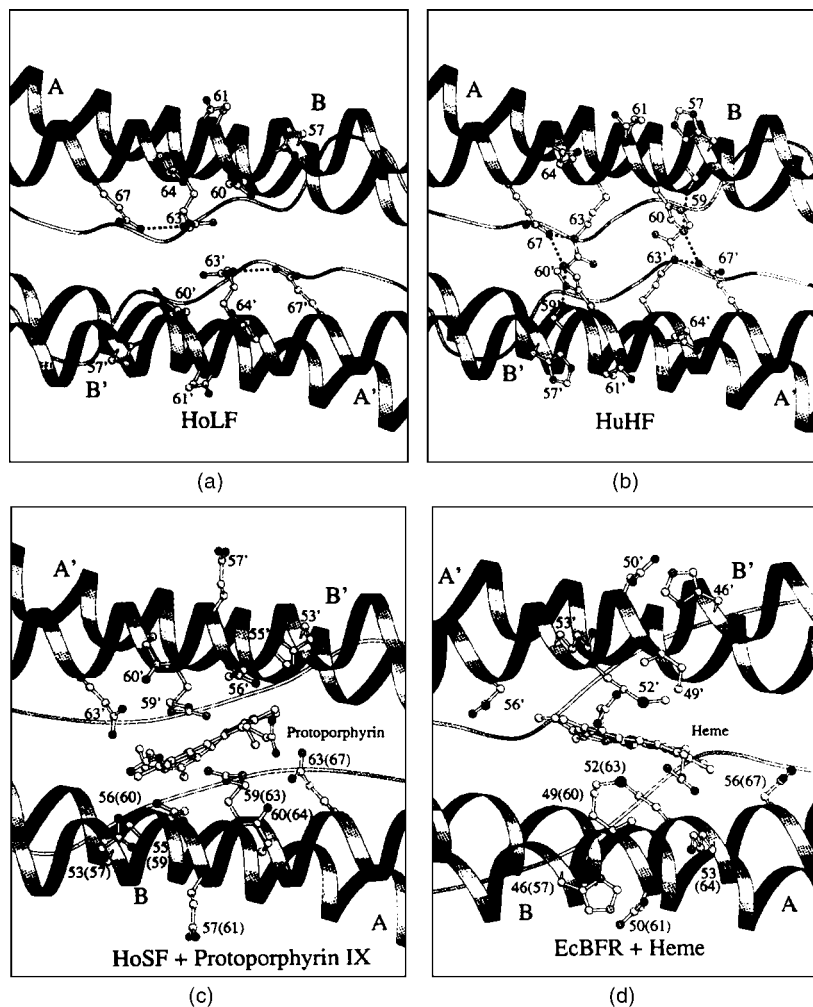
Figure 6.5 Central part of I : II intersubunit interfaces of (a) recombinant HoLF; (b) recombinant HuHF; (c) protoporphyrin IX nesting in the interface of HoLF; (d) haem binding in EcBFR. Reprinted from Harrison *et al.*, 1998, by courtesy of Marcel Dekker, Inc.

through water molecules. Further along this interface the *C*-terminus of helix A and the AB turn of subunit VI are linked to helix D of subunit I, and again there is a chain of water molecules between subunits.

Yet another hydrophobic region is found on the surface of one face of the E helix, comprising Leu-165, Tyr-168, Leu-169, Leu-173, together with Leu-158 near the *C*-terminus of helix D. In the oligomeric L-chain protein structure this second hydrophobic patch is buried in the six channels along the fourfold axes (Figure 6. 6). This is a left-handed bundle of four parallel E helices, which are lined by 12 leucine residues, Leu-165, Leu-169 and Leu-173 that lie along one edge of each of the E helices of four neighbouring subunits; this gives a long apolar channel, 1.25 nm in length, and relatively narrow – it is accessible to a 0.2 nm diameter probe (Hempstead *et al.*, 1997). The E helices protrude a short distance into the cavity, and
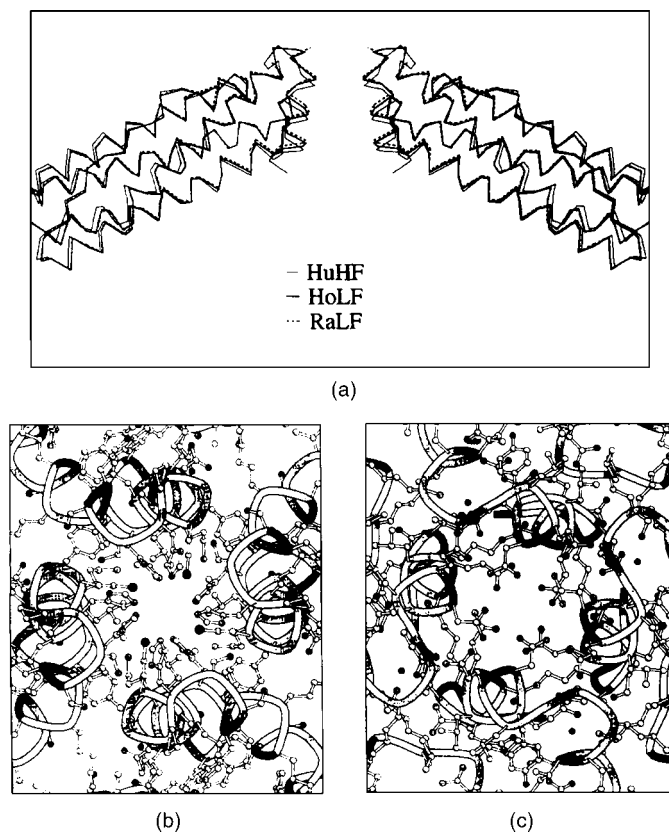
Figure 6.6 E helices around the fourfold axes in four ferritins and EcoBFR. (a) Superposition of α-carbon traces for three mammalian ferritins, HuHF, HoLF and RaLF; (b) BfLF; (c) EcBFR. (a) is viewed perpendicular to and (b) and (c) along the fourfold axis. Reprinted from Harrison *et al.*, 1998, by courtesy of Marcel Dekker, Inc.

the last three amino acids at the *C*-terminus of the chain and the inner part of the channel are polar – Lys-176, His-177 and Asp-178; the latter two are disordered.

The eight threefold axes (Figure 6.7) are funnel shaped with a wider entrance at the outside of the molecule and a narrow passage (0.34 nm wide and about 0.6 nm long). The amino-acid residues that neighbour and line these channels include residues from the *C*-terminus of helix C and those of the *N*-terminus of helix D. These residues (117 to 137) are highly conserved in L subunits with only three positions out of twenty-one being substituted. These same residues are also highly conserved in H chains (Table 6.1) although there are nine positions where H-chains differ from L-chains. Many of the H for L changes are found in or close to the wider end of the channel, whereas the narrow region is highly conserved in all ferritins. It is extremely hydrophilic in the narrow inner region, with three Glu-134 residues, towards the outer surface of the protein shell, and three Asp-131 residues, towards the inner surface (one from each of the three D helices), which are conserved in both H and L subunits and predominantly hydrophilic in its wider entrance region. The funnel shaped design of the channels could allow ions or molecules approaching the shell to find these channels more easily than if they were narrow throughout
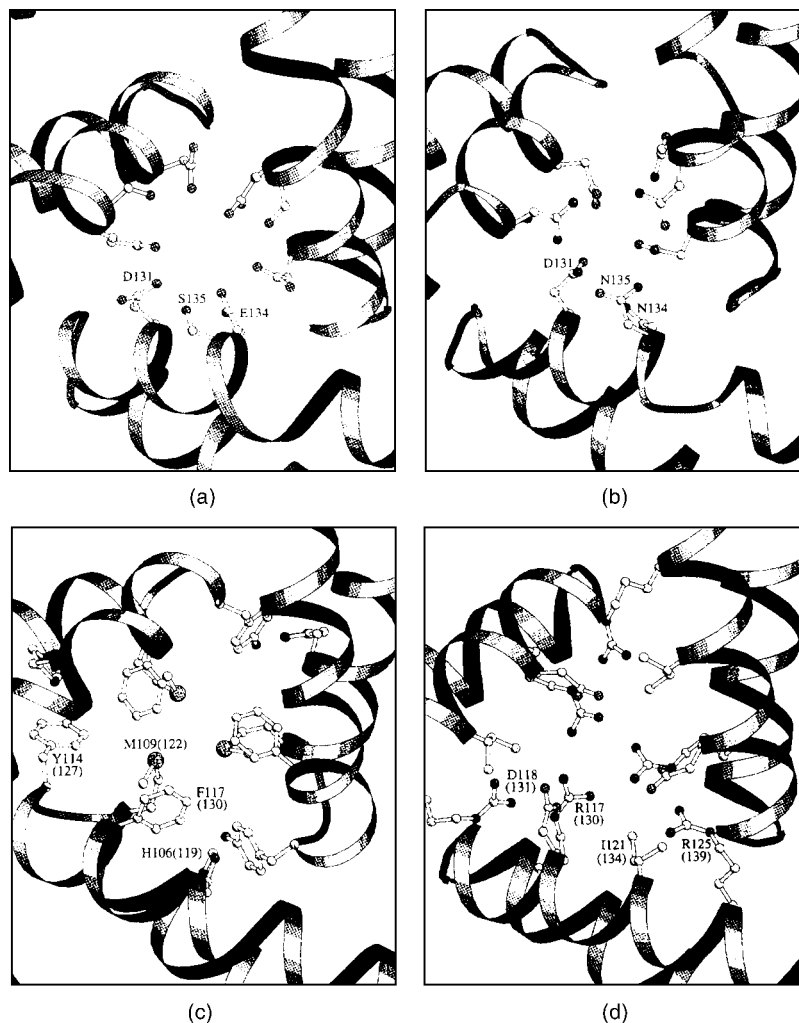
Figure 6.7 Residues close to the threefold axes in (a) BfLF; (b) Sma-1; (c) EcFTN; (d) EcBFR. Viewed along the threefold axis from the inside surface. Reprinted from Harrison *et al.*, 1998, by courtesy of Marcel Dekker, Inc.

their length of about 1.2 nm. In the crystals the clusters of Glu and Asp residues each bind a Cd^{2+} ion. The threefold and fourfold channels may provide routes for entry and exit of iron, water and other small molecules and ions into the aqueous cavity of the protein shell.

The structure of bullfrog L-chain ferritin has been determined at a resolution of 0.22 nm (Trikha *et al.*, 1994, 1995), and is extremely similar to HoLF. Recombinant bullfrog L ferritin has 52 % sequence identity with HoLF (and 61 % with HuHF). The D-helix is kinked, as in HoLF, but hydrogen bonding is interrupted by *cis*-Pro in place of His at position 136, which distorts helix D. The central hydrophilic region of the subunit is very different from HoLF (Figure 6.4), with only Tyr-34 and Glu-61 in common. In the dimer interface (between subunit I and II) Arg-63 is replaced by Lys-63, which no longer makes a salt bridge with Glu-67. The diamond

cluster of four Glu residues is conserved on the cavity side of the B helices at the I–II dimer interface. Despite changes in the two of the residues lining the fourfold channel (Met-165 for Leu and His-173 for Leu), the channel retains its predominantly hydrophobic character (Figure 6.6).

H-chain Ferritins

It was impossible to obtain X-ray quality crystals from recombinant human H-chain ferritin and so metal bridge crystal contacts, to mimic the situation in HoLF, were engineered by the mutation of Lys-86 to Gln (Lawson *et al.*, 1991). The mutated protein crystallized not, as expected, from $CdSO_4$, but from $CaCl_2$. The structure of vertebrate H-chain ferritins must resemble that of L-chain ferritins, since they form copolymers, and indeed, the structure of recombinant human H-chain ferritin was determined at a resolution of 0.19 nm using HoSF as a starting model (Hempstead *et al.*, 1997). That H- and L-chain structures are very similar is borne out by the observation that the root-mean-square deviations between α-carbons of HoLF and HuHF following superposition of four-helix bundles, is 0.04 nm. Helices A, B and C are of the same length as in HoLF, but D and E are both shorter in HuHF (D126–159 and E163–174 instead of D126–161 and E162–174), and there is a DE turn of three residues (160–162) in place of a sharp bend. There is also a *cis* -Pro at residue 161 in HuHF in place of a *trans* -Ser in HoLF and BfLF. However, the most important changes between H and L subunits are situated within the subunit bundle and at the I–II dimer interface. Of the seven residues found in the central hydrophilic region within the subunit bundle in HoLF, only three are conserved in HuHF (Tyr-34, Glu-61 and Glu-107). Although the central intrasubunit salt bridge between Lys-62 and Glu-107 is gone, Tyr-34 and Glu-107 are virtually in identical positions in both proteins, as are Gln-141 and Glu-141 in HuHF and HoLF respectively. However, the site is now capable of the binding and rapid oxidation of two ferrous ions (the ferroxidase activity discussed below). The constellation of residues constituting the 'ferroxidase' centre, Glu-27, Tyr-34, Glu-61, Glu-62, His-65, Glu-107 and Gln-141, are found in all animal H-chains, most plant ferritins and non-haem containing bacterial ferritins. All but two of these residues (Glu-27 and Glu-61) are found in haem-containing bacterioferritins as well. Four of them are present in BfLF (Tyr-34, Glu-61, Glu-62 and His-65), but they do not confer ferroxidase activity (Trikha *et al.*, 1994, 1995). At the I-II dimer interface there are significant changes. Arg-63 (I) faces across the interface between subunits and forms hydrogen bonds to Ser-59 (II) (Ala in HoLF), as does Glu-67 (I) to His-60(II), blocking the groove between BI and BII (Figure 6.5), and potentially preventing the binding of protoporphyrin IX to HuHF. The diamond cluster of glutamates found in HoLF and BfLF is disrupted, with both Glu-57 and Glu-60 replaced by His. The residues lining the fourfold channel with one change (His-173 for Leu), are still hydrophobic in character (Figure 6.6). In HuHF crystals Ca^{2+} is bound to all six carboxyl of the conserved Asp-131 and Glu-134 in the threefold channel (Figure 6.7).

 The detailed high-resolution structure of the non-haem-containing ferritin of *E. coli* EcFTNA has been recently published (Stillman *et al.*, 2000) and shows considerable structural similarity to human H-chain ferritin (r.m.s. deviation of main chain

atoms 0.066 nm), despite the low sequence identity of only 22 %. While little conservation of residues involved in inter subunit interactions was found, many of the conserved residues were seen to be clustered in the centre of the four-helix bundle. All seven residues of the ferroxidase centre of HuHF are found in EcFTN: the centre lies at the inner end of a hydrophobic channel. There are considerable changes in the intersubunit interactions around the twofold axis, including Met-51 of EcFTN replacing Arg-63 of HuHF, which means that the hydrophilic interactions made by the latter are absent in EcFTN. All four glutamates found in the diamond cluster of HoLF are replaced by Arg-45, Gln-48, Thr-52 and Gln-55 in EcFTNA. The threefold channel (Figure 6.7). is also very different with the Asp-131 and Glu-134 residues of vertebrate ferritins replaced in the sequence by Asn-118 and Gln-121 respectively in EcFTNA. However, neither of these residues points towards the threefold axis in EcTFN, and instead the channel is lined by the hydrophobic residues Met-109 and Phe-117. In contrast the fourfold axis contains Glu-149 and Phe-153, which changes the character of the channel substantially (Figure 6.6).

Bacterioferritins

That there was a ferritin in bacteria came as a great surprise, but to find that it contained a haem component, and had previously been classified as a cytochrome 75 years ago, was more than a novelty. As Frolow *et al.* (1994) pointed out, bacterioferritin was identified by its optical spectrum in whole cells of *E. coli* and named cytochrome b_1 by David Keilin in 1934 (Keilin, 1934), and isolated 30 years later (Deeb and Hager, 1964) without the authors realizing that it was a ferritin. Likewise when it was first isolated from *Azotobacter vineladii* (Bulen *et al.*, 1973), it was called 'non-haem iron cytochrome *b*', no doubt because at that time the prevailing opinion was that ferritin, though widely distributed in the animal and plant kingdom, was absent in prokaryotes. Bacterioferritins, as isolated from many bacteria, and identified in the gene sequences of quite a few others, contain iron–protoporphyrin IX as an integral part of the protein. Spectroscopic studies using EPR and MCD suggested that the axial ligands of iron in bacterioferritins were both Met sulfurs (Cheesman *et al.*, 1990), as did EXAFS studies (George *et al.*, 1993). The X-ray structure of *E. coli* bacterioferritin (EcBFR) clearly established that this was the case (Frolow *et al.* 1994), and also that EcBFR has a typically ferritin-like structure, both in terms of its subunit conformation and shell packing (Figure 6.8, Plate 9). The EcBFR subunit, like most ferritins, has a hydrophilic region at the centre of its four-helical bundle with hydrophobic regions at each extremity, that contains, in common with HuHF and EcFTN, five of the residues of the ferroxidase site (Glu-27, Tyr-34, Glu-62, His-65 and Glu-107), which together with Glu-141 and His-144, form the ligands of the ferroxidase site that is described below. The long, mostly hydrophobic I : II intersubunit contact supplies a nesting site, not this time for protoporphyrin IX, but for haem (Figure 6.5(d)) with two symmetry-related Met-63 residues as axial ligands to the metal centre. An examination of bacterioferritin sequences suggests that many have replacements which would cause loss of ferroxidase activity and/or of haem binding. Bacterioferritins have a variety of polar or non-polar residues at the equivalent positions of Asp-131

and Glu-134 in the threefold channel, although one of the two residues is always either Asp or Glu – in EcBFR we have Asp-131 and Ile-134 (Figure 6.7). The fourfold channels of EcBFR are very different from what we have seen before. The DE turn and the E helix are much shorter (only six residues compared to 9–13 residues in ferritins), the four E helices are twisted in a right handed sense, and the channels are lined by only two residues from each helix, Asn-167 and Gln-170 (Figure 6.6), which are conserved in most BFRs.

Ferritin-like Proteins

An oligomeric spherical protein complex, containing up to 50–100 iron atoms per oligomer, was isolated from the Gram-positive bacterium *Listeria innocua*, which had all of the functional properties of an authentic ferritin (Bozzi *et al.*, 1997). At neutral pH values, *Listeria* ferritin accelerates Fe^{2+} oxidation about fourfold with respect to autooxidation (Stefanini *et al.*, 1999), and as in classical ferritins, the iron is sequestered inside the protein cavity which can accomodate a maximum of 500 iron atoms (Bozzi *et al.*, 1997). However, *Listeria* ferritin has structural features similar to a class of DNA-binding proteins designated Dps (DNA-binding proteins from starved cells), which are expressed in bacteria under conditions of oxidative or nutritional stress (Grant *et al.*, 1998). A search of the SwissProt Data Base with the *Listeria* ferritin as a probe only retrieves protein sequences belonging to the Dps family. The quaternary structure of the apoferritin cage in *L. inocua*, unlike classical ferritins, contains 12 subunits (molecular weight 240 kD, diameter 9 nm) and resembles that of *E. coli* Dps (Ilari *et al.*, 2000). The X-ray crystal structure of *L. inocua* ferritin has been solved at 0.235 nm resolution by molecular replacement using the coordinates of Dps from *E. coli* (Grant *et al.*, 1998) as a search model (Ilari *et al.*, 2000). The *L. inocua* ferritin monomer consists of a four-helix bundle that closely resembles that of *E. coli* Dps and other ferritins (Figure 6.9, Plate 10), yet, like DPS, it assembles into a dodecamer with 23 symmetry. The four helices (A–D) are packed by hydrophobic interactions: helices B and C are connected by a long loop that divides the *N*- and *C*-terminal portions of the molecule. A short helix in the middle of the loop in one subunit interacts with that of another subunit related by a twofold symmetry axis. The ferritin monomer lacks the *N*-terminal tail present in Dps that is thought to mediate its interaction with DNA and the short *C*-terminal E-helix, which in all other ferritins makes the interactions along the fourfold symmetry axes. The dodecameric quaternary structure is formed by four trimers placed at the vertices of a tetrahedron and has an internal diameter of about 4 nm, half the size of vertebrate ferritins. This corresponds to an internal cavity about one-eighth that of typical ferritin shells, in excellent agreement with the respective capacity to store iron (500 versus 4500 atoms per oligomer). The relatively large negatively charged channels along the threefold axes may provide the pathway for iron entry into the negatively charged internal cavity. The *L. inocua* ferritin sequence does not contain any of the canonical ferroxidase centre residues, but does have a cluster of carboxylate residues in the B-helix (Figure 6.9) similar to the iron core nucleation site in ferritin L-chains. Examination of the electron density map reveals 12 iron atoms on the inner surface of the hollow protein core, which shows strong similarities with known ferroxidase sites, and is discussed below. The

L. inocua ferritin site however, is the first described so far that has ligands belonging to two different subunits, and is not contained within a four-helix bundle. Recently it has been suggested that the neutrophil-activating protein of *Helicobacter pylori*, the major antigen of the immune response in infected individuals, is also a dodecameric ferritin, capable of binding up to 500 iron atoms per oligomer (Tonello *et al.*, 1999).

Under conditions of nutritional or oxidative stress, *E. coli* produces high levels of a 19-kD protein, Dps, which binds DNA with no apparent sequence specificity (Almiron *et al.*, 1992). A diverse family of proteins with sequence homology to Dps has been identified in other prokaryotes, including two other functionally similar DNA-binding proteins in *Synechococcus* sp. (Pena and Bullerjahn, 1995) and *Bacillus subtilis* (Chen and Helmann, 1995), and the functional ferritin from *L. inocua* described above (Bozzi *et al.*, 1997). The crystal structure of Dps from *E. coli* has been determined at a resolution of 0.16 nm (Grant *et al.*, 1998). The monomer clearly has the same four helix bundle core as bacterioferritin (Figure 6.10, Plate 10). The r.m.s. deviation between C_α positions in the cores of the aligned bundles is 0.11 nm (Grant *et al.*, 1998). The Dps dodecamer has no fourfold interactions. However, its 23 symmetry leads to two non-equivalent environments around the threefold axes (Figure 6.11, Plate 11), one corresponding to the interactions between monomers on the 'front of the dodecamer', and the other to interactions around the same threefold on the 'back side of the dodecamer'. At the *N*-terminal end of the Dps four-helix bundle, the packing around the threefold axes is similar to the packing in ferritin. The other threefold interaction takes place at the *C*-terminal end of the Dps bundle, where the ferritin monomer makes fourfold interactions with its neighbours. The ferritin-like threefold channels (Figure 6.11) in both Dps and *L. inocua* ferritin are lined with acidic residues, as in other ferritins. Despite its structural homology with bacterioferritins, Dps does not appear to have a ferroxidase centre, since the corresponding residues in the centre of the four-helix bundle include one histidine, two phenylalanines, two leucines and one tyrosine. However, in *E. coli* Dps, a lead ion binds in essentially the same place as iron in *L. inocua* ferritin (Grant *et al.*, 1998), with striking similarity in metal-coordinating ligands. This strongly suggests that *E. coli* Dps may also have ferroxidase activity (Ilari *et al.*, 2000), a property that may help in protecting DNA from oxidative stress by sequestering iron as proposed by Grant *et al.* (1998). The ligands corresponding to the observed (His-31, Asp-51, Glu-62) and putative (His-43, Asp-47) iron ligands in *L. inocua* ferritin belong to the group of 15 highly conserved amino acids found in all members of the Dps family

It has been suggested (Bozzi *et al.*, 1997; Grant *et al.*, 1998) that Dps and *L. inocua* ferritin represent examples of a family of ancestral dodecameric protein which had as function to trap, but not to mineralize, metal ions, and that the ability to oxidize and mineralize iron efficiently and to form fourfold interactions came later. The hollow-cored dodecameric motif exemplified by Dps and *L. inocua* ferritin has clearly been adapted to a number of functions, since in addition to DNA binding and iron storage, other family members include a novel pilin, a bromoperoxidase and several other proteins of unknown function (Grant *et al.*, 1998).

Rubrerythrin is the trivial name given to a family of non-haem iron proteins that have been isolated from a number of bacteria (Figure 6.2). The structure of the best characterized rubrerythrin, that from *Desulfovibrio vulgaris*, has been determined by

X-ray crystallography (De Maré *et al.*, 1996). It is a tetramer of two-domain subunits (Figure 6.12, Plate 12), each subunit containing a four-helix bundle surrounding a diiron−oxo site and a *C*-terminal rubredoxin-like FeS$_4$ domain. The diiron−oxo site contains a larger number of carboxylate ligands and a higher degree of solvent exposure than do those in other diiron−oxo proteins. The four-helix bundle of rubrerythrin closely resembles those of ferritin and bacterioferritin subunits, suggesting a relationship between these proteins. Recombinant rubrerythrin oxidized by O$_2$ has been found to catalyse the oxidation of Fe^{2+} to Fe^{3+} *in vitro* (Bonomi *et al.*, 1996). This O$_2$-driven ferroxidase activity of rubrerythrin is of the same order of magnitude as H-chain ferritins, and both the diiron-oxo and rubredoxin-like iron centres are apparently required for this activity. The physiological role of rubrerythrin remains to be determined. Both types of iron site have unusually high reduction potentials (>200 mV). These relatively high potentials and the putative cytoplasmic localization of the protein (due to the lack of a signal sequence) have made placing rubrerythrin in any known electron transport chain difficult.

6.1.3 The Mineral Core

The cores of individual mammalian ferritin molecules are clearly visible by transmission electron microscopy as well defined nanoparticle crystallites encapsulated within the protein shell which can attain a size close to that of the 8 nm interior diameter of the protein shell (Massover, 1993). This is illustrated in Figure 6.13 for a sample of human ferritin. The amount of iron in the core is variable, and can range from zero to a maximum of approximately 4500 atoms (Fischbach and Anderegg, 1965); this corresponds to the capacity of the internal cavity for Fe(III) as
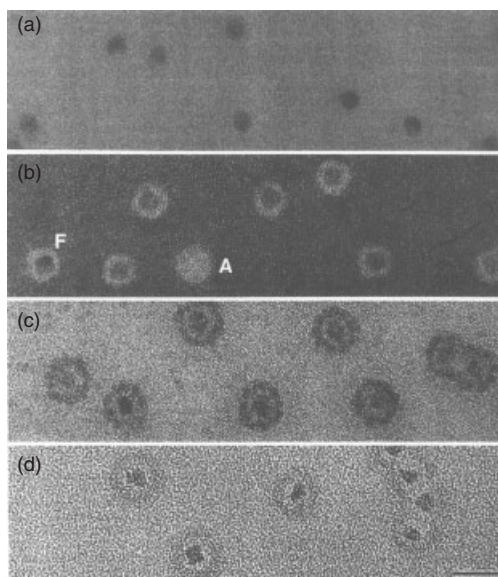
Figure 6.13 Electron micrograph of human spleen ferritin viewed at a magnification of × 170 000 after negative staining with uranyl acetate. Both the darkly coloured iron-rich cores and the clear-coloured protein shells are clearly visible. (From Crichton, 1991.)

ferrihydrite, namely about 259 nm^3. However, unlike the highly conserved protein shell described above, the structure of the iron core is very variable from species to species. This is due to an important extent to differences in composition, mostly in the content of inorganic phosphate, which varies from 44 Fe/P$_i$ in ferritin isolated from the haemolymph of the limpet *Patella laticostata* (St. Pierre *et al.*, 1990), to 1.7 Fe/P$_i$ in ferritin from the bacterium *Pseudomonos aeruginosa* (Mann *et al.*, 1986).

The mineral cores in mammalian ferritins typically consist of single or multiple crystallites of ferrihydrite (see Chapter 1 for a more detailed review), with varying degrees of crystallinity as judged by X-ray or electron diffraction, electron microscopy, Mössbauer spectroscopy and EXAFS (reviewed in Chasteen and Harrison, 1999; Ward *et al.* 2000), and with a variable, but rather low content of phosphate (about one P per ten Fe atoms in horse-spleen ferritin). In general, the iron centres appear (from iron-edge EXAFS) to be in predominantly octahedral environments, with each iron atom surrounded by an average of close to six oxygen atoms at a distance of about 0.2 nm; beyond this first shell, around a further 1.5 iron centres are seen at 0.3 nm and about 1.1 at 0.34 nm (Mackle *et al.*, 1991). Although it is difficult to assign numbers of scatterers from EXAFS data, the fact that there are relatively few iron centres in the second shell is further evidence for the disorder prevalent within the mineral cores of ferritin (Powell, 1998).

In contrast, most bacterioferritin cores have P : Fe ratios of 1 : 1 to 1 : 2, poor crystallinity, very low magnetic blocking temperatures and consist essentially of hydrated ferric phosphate. These differences appear to reflect the levels of phosphate found in bacterial and animal cells (Mann *et al.*, 1987). Plant ferritins (see Chapter 4) are eukaryotic ferritins that are found in the more prokaryotic type of environment of the plastids, with a high phosphate concentration. This is reflected in the observation that plant ferritin mineral cores also have a high phosphate content and are amorphous (Wade *et al.*, 1993; Waldo *et al.*, 1995). Whereas the small amounts of phosphate in mammalian ferritins appear to be largely surface absorbed, the large amounts of phosphate in bacterioferritins and plant ferritins penetrates throughout the core, and the mineral can be more appropriately thought of as an amorphous hydrated iron(III) phosphate (Mann *et al.*, 1986; Wade *et al.*, 1993). Indeed it has been suggested that the role of bacterioferritins might be as phosphate-storage rather than iron-storage molecules (Powell, 1998). In high phosphate cores, an Fe−P distance of 0.325 nm is observed, and the absence of an Fe−Fe distance of 0.35 nm, typical of mammalian ferritins indicates considerable loss of long-range order (Waldo *et al.*, 1995; Rohrer *et al.*, 1990).

When pea seed apoferritin is reconstituted *in vitro* in the absence of phosphate, the reconstituted mineral core consists of crystalline ferrihydrite (Rohrer *et al.*,1990; Wade *et al.*, 1993; Waldo *et al.*, 1995). Conversely, horse spleen ferritin reconstituted in the presence of phosphate produces an amorphous core (Rohrer *et al.*,1990; St. Pierre *et al.*, 1996)

However, ferritins isolated from the bacterium *Pseudomonos aeruginosa* (Mann *et al.*, 1986) and from the chiton *Acanthopleura hirtosa* (St. Pierre *et al.*, 1990) have iron cores of limited crystallinity, despite having P : Fe ratios of around 1 : 40, perhaps suggesting that core crystallinity is influenced by the rate of iron deposition as well as by the composition of the medium. The way in which phosphate may influence core development is discussed below.

The magnetic properties of the ferritin core have been extensively investigated, and it is generally agreed that the electron-spin magnetic moments of the individual Fe^{3+} ions within the ferritin core are antiferromagnetically coupled. However, because cancellation of individual magnetic moments is incomplete, the core crystallite itself has a residual net magnetic moment, giving rise to the phenomenon known as superparamagnetism, which can be studied by Mössbauer spectroscopy. Relaxometry and magnetometry of ferritin are techniques which appear to have great potential for the study of ferritin iron uptake (for recent reviews see Brooks *et al.*, 1998; Herynek *et al.*, 2000).

6.1.4 Iron Deposition in Ferritin

Early studies indicated that the oxidation of ferrous iron by dioxygen is accelerated in the presence of apoferritin (Bielig and Bayer, 1955; Niederer, 1970; Macara *et al.*, 1972; Bryce and Crichton, 1973; Bakker and Boyer, 1986). The ferric iron then undergoes hydrolysis and is deposited as ferrihydrite within the protein shell in mammalian ferritins. The iron uptake process is now thought to involve the following steps which are described in greater detail below: (i) uptake of Fe(II) into the protein shell through the hydrophilic threefold channels; (ii) oxidation of ferrous iron by the dinuclear ferroxidase sites situated within the four-helix bundle of H-chain subunits by molecular O_2, producing H_2O_2; (iii) migration of Fe(III) from the ferroxidase sites to sites of nucleation on the interior surface of the L-chain subunits of the protein shell, which facilitates mineralization; (iv) growth of the ferrihydrite mineral core via iron oxidation and mineralization on the surface of the growing crystallite. The subject has been recently reviewed (Chasteen, 1998; Chasteen and Harrison, 1999).

Iron Pathways into Ferritin

We assume that all substances involved in ferritin iron deposition or mobilization – Fe^{2+}, Fe^{3+}, O_2, reductants and chelators – gain access to the interior of the apoferritin protein shell. The possible pathways by which they might penetrate into the protein include the six channels along the fourfold axes and the eight channels along the threefold axes. The X-ray crystallographic observation of metal binding (Cd^{2+}, Zn^{2+}, Ca^{2+} and Tb^{3+}) to the six conserved carboxylates suggests that the threefold channels (Figure 6.7) are the most likely route for iron entry into animal ferritins (Lawson *et al.*, 1991; Hempstead *et al.*, 1997). [113]Cd NMR studies show that Fe^{2+} competes with Cd^{2+} binding to HoSF in the channels (Stefanini *et al.*, 1989). Other evidence that the threefold channels are involved in Fe^{2+} transport to the central cavity comes from chemical modification and site-directed mutagenesis studies (Stefanini *et al.*, 1989; Desideri *et al.*, 1991; Treffry *et al.*, 1993; Levi *et al.*, 1996). Studies of metal binding and of metal-binding stoichiometry also support the notion of the threefold channels as pathways for iron entry into ferritin (Lee *et al.*, 1994; Jacobs *et al.*, 1989; Hilty *et al.*, 1994).

Although channel mutations and chemical modifications reduce rates of iron oxidation and uptake, they do not completely abolish the ferroxidase activity of
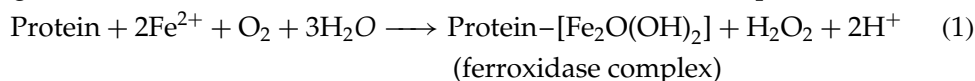
the protein, suggesting perhaps that other, less efficient, pathways may exist. Fe^{2+} entering via the threefold channels would not only need to pass through the channels (1.2 nm in length) but also traverse a distance of about 2 nm along a hydrophilic pathway from the inside of the channel to the oxidation site (Treffry *et al.*, 1993). Calculations of electrostatic potentials in HuHF (Douglas and Ripoli, 1998), which show that the negative outer entrance is surrounded by patches of positive potential and that this arrangement leads to electrostatic fields directing cations towards the channel entrance, support the threefold route. The region of negative potential extends through the threefold channel to the interior of the molecule. Iron incorporation into the dodecameric *L. innocua* ferritin also conforms to this general picture of an electrostatic gradient through the negatively charged hydrophilic pores at the threefold axes guiding iron to the ferroxidase centre (Ilari *et al.*, 2000). EcFTN has hydrophobic residues (Met-122 and Phe-130) protruding into the threefold channels, whilst its fourfold channels are lined by Glu-165, Phe-169 and Glu-173. In BFRs one of the two residues in the channel is always either Asp or Glu.

Iron Oxidation at Dinuclear Centres

We have seen in Chapter 2 that HuHF, EcFTN and EcBFR are members of a large class of (μ-carboxylato)diiron proteins that includes methane and toluene monooxygenases, stearoyl–acyl carrier protein desaturase, ribonucleotide reductase and rubreythrins. The diiron centre, located in the central region of the four-helix subunit bundle (Figure 6.4) was identified by a large number of kinetic experiments with recombinant HuHF as well as with HuLF and HoLF as the catalytic ferroxidase centre (Levi *et al.*, 1988, 1989, 1992; Treffry *et al.*, 1993, 1995). Substitution of residues at the ferroxidase centre of HuHF, such as E27A, E62 K + H65 G, H107A and Y34F, results in greatly decreased ferroxidase activity (Lawson *et al.*, 1989; Bauminger *et al.*, 1991a, 1993; Treffry *et al.*, 1992, 1995, 1997; Sun *et al.*, 1993). Rapid oxidation, which is complete in less than 10 s for HuHF at 48 Fe(II)/protein, pH 6.5, requires binding of iron(II) at both sites A and B (Figure 6.4) (Treffry, 1995, 1997).

The stoichiometries of both oxygen consumption and of proton release subsequent to Fe(III) hydrolysis have been determined by using a combined oximeter and pH stat (Yang *et al.*, 1998). The overall reaction at the ferroxidase centre is postulated to be:

$$\text{Protein} + 2Fe^{2+} + O_2 + 3H_2O \longrightarrow \text{Protein} - [Fe_2O(OH)_2] + H_2O_2 + 2H^+ \quad (1)$$
$$\text{(ferroxidase complex)}$$

Taken together, the stoichiometry of 2Fe(II)/O_2, and the structure of the ferroxidase iron site suggest that the first step after iron(II) binding, as was proposed some years ago (Crichton and Roman, 1978), would be transfer of two electrons, one from each Fe(II), to a dioxygen molecule bound at the same site, to give a formal peroxodiferric intermediate: formally dioxygen binding, followed by Fe(II) oxidation (equations 2 and 3):

$$\text{Protein} - [Fe_2]^{4+} + O_2 \longrightarrow \text{Protein} - [Fe_2^{4+}O_2]^{4+} \quad (2)$$
$$\text{(dioxygen complex)}$$

$$\text{Protein} - [Fe_2^{4+}O_2]^{4+} \longrightarrow \text{Protein} - [Fe_2^{6+}O_2^{2-}]^{4+} \quad (3)$$
$$\text{(peroxo intermediate)}$$
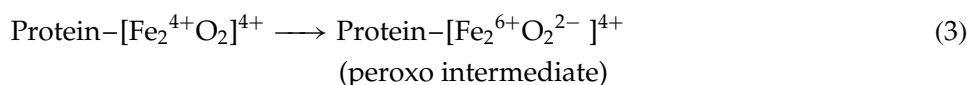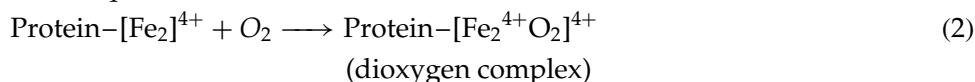
An initial blue/purple coloured species (A_{max} 550–650 nm) which forms and decays rapidly after addition of 48 or fewer Fe(II) atoms/ apoferritin molecule is now thought to be a diferric peroxo intermediate (Zhao *et al.*, 1997; Pereira *et al.*, 1998; Moënne-Loccoz *et al.*, 1999) on the basis of its spectroscopic similarities with known diferric–peroxo complexes. A second intermediate, with spectral properties typical of μ-oxobridged Fe(III) dimers, which appears after formation of the blue complex, has been identified (Bauminger *et al.*, 1991a,b, 1993; Treffry *et al.*, 1992; Yang *et al.*, 1998) This leads to the proposal that the peroxo intermediate would then undergo iron(III) hydrolysis (equations 4 and 5) to give first the μ-oxobridged Fe(III) dimer and then upon addition of another two molecules of H_2O, a protein–[$Fe_2O(OH)_2$] species at the ferroxidase centre:

$$\text{Protein–[Fe}_2^{6+}\text{O}_2^{2-}\text{]}^{4+} + \text{H}_2\text{O} \longrightarrow \text{Protein–[Fe}_2\text{O]}^{4+} + \text{H}_2\text{O}_2 \tag{4}$$

$$(\mu\text{-oxobridged complex})$$

$$\text{Protein–[Fe}_2\text{O]}^{4+} + 2\text{H}_2\text{O} \longrightarrow \text{Protein–[Fe}_2\text{O(OH)}_2\text{]} + 2\text{H}^+ \tag{5}$$
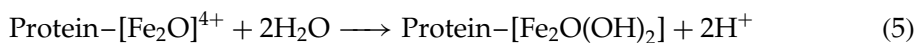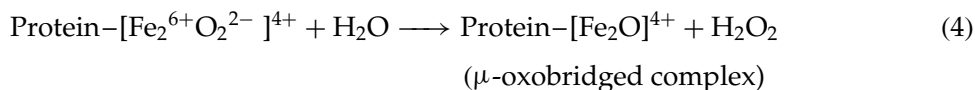
The recent detection of a peroxodiferric intermediate in the ferritin ferroxidase reaction establishes the ferritin ferroxidase site as being very similar to the sites in the O_2-activating (μ-carboxylato)diiron enzymes described in Chapter 2. However, how can we explain that the peroxodiferric intermediate decays in totally different ways? In ferritins it forms diferric oxo or hydroxo precursors which are transferred to biomineralization sites with release of hydrogen peroxide. In methane monooxygenase its decay produces a potent oxidant (Q), which oxidizes organic substrates such as methane (Figure 6.14) and forms a diferric product that is reduced back to the initial diferrous state by a reductase. It has been suggested that the explanation lies in the unusually short Fe–Fe distance found in the diiron (μ-1,2-peroxodiferric) intermediate (Hwang *et al.*, 2000) that forms in the early steps of ferritin biomineralization (0.253 nm compared with distances of 0.31 to 0.4 nm in
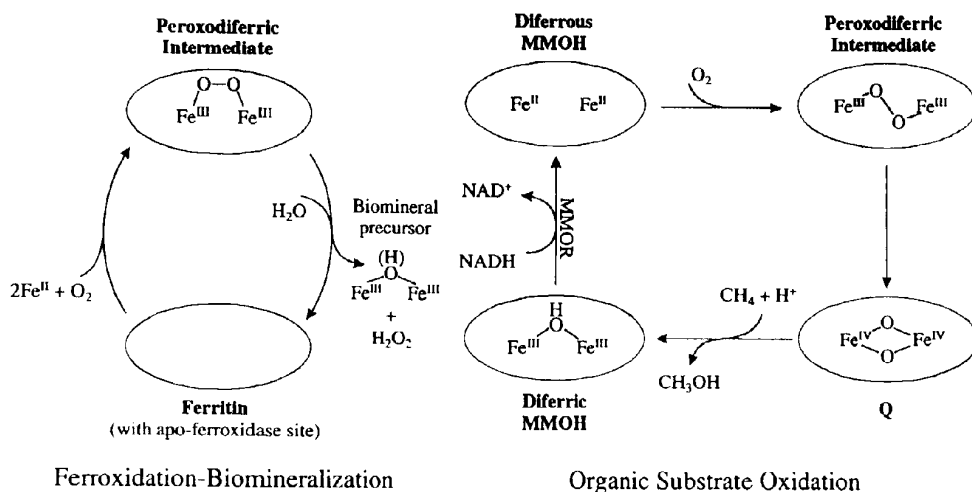
Figure 6.14 Comparison of the role of peroxodiferric–protein complexes. Reprinted with permission from Hwang *et al.*, 2000. Copyright (2000) American Association for the Advancement of Science.

previously characterized diiron sites). The short Fe–Fe distance requires a small Fe–O–O angle (106–107°), which might impose a geometry favourable to decay of the peroxodiferric complex by release of H_2O_2 and μ-oxo or μ-hydroxo diferric precursors of biomineralization rather than by oxidation of an organic substrate.

Ferrihydrite Nucleation Sites

The initial stages of iron incorporation requires the ferroxidase sites of the protein. Thereafter the inner surface of the protein shell provides a surface which supplies ligands that can partially coordinate iron but which leave some coordination spheres available for mineral phase anions, thereby enabling the biomineralization process to proceed, with formation of one or more polynuclear ferrihydrite crystallites. Iron is transferred from the ferroxidase sites to the core nucleation sites by the net reaction (Yang *et al.*, 1998):

$$\text{Protein}-[\text{Fe}_2\text{O}(\text{OH})_2] + \text{H}_2\text{O} \longrightarrow \text{Protein} + 2\,\text{FeOOH}_{\text{core}} + 2\,\text{H}^+ \qquad (6)$$

Several binding sites for Tb^{3+} or Cd^{2+} ions have been identified in the interior of the apoferritin protein shell, some of which may be iron-binding sites (Harrison *et al.*, 1989; Granier *et al.*, 1998). In HoSF and HoLF, two sites were identified on the inner surface of the B helix at the subunit dimer interface (Figure 6.15, Plate 11) which bind two Cd^{2+} ions. One involves Glu-57 and Glu-60 as ligands and the other Glu-61 and Glu-64 (Granier *et al.*, 1998). In H-chain ferritins the first pair of Glu-57 and Glu-60 are both replaced by His and only a single Tb^{3+} is found bound to Glu-61 and Glu-64 (Lawson *et al.*, 1991).

The diamond cluster of Glu residues in the central part of I : II intersubunit interface in L-chain ferritins extends across the twofold axes because of symmetry (Figure 6.5a), and represents a potential ferrihydrite nucleation site. L-chains are more efficient in promoting nucleation than are H-chains, and amino-acid substitutions or chemical modification at these residues lead to diminished core formation (Levi *et al.*, 1989, 1992, 1994; Lawson *et al.*, 1991; Wade *et al.*, 1991; Bauminger *et al.*, 1991a; Crichton *et al.*,1996; Santambrogio *et al.*, 1996). Core formation could be initiated by proximal binding of two Fe^{3+} at the putative ferrihydrite 'heteronucleation' centre (Gallois *et al.*, 1997; Granier *et al.*, 1998; Hempstead *et al.*, 1997).

It has been proposed that Glu-61 could alternately act as a ligand to the ferroxidase site and to the nucleation site, and hence serve as a go-between to move iron (eventually in both directions) from one site to another (Lawson *et al.*, 1991). What is clear is that modification of both the ferroxidase centre and the nucleation centre leads to ferritins which do not oxidize or incorporate iron (Wade *et al.*, 1991; Sun *et al.*, 1993).

Studies using UV and Mössbauer spectroscopy indicated that the μ-oxobridged dimers on the ferroxidase sites split prior to their transfer to the cavity, in the sequence dimer → monomer → cluster (Bauminger *et al.*, 1991a). The ratio of iron in clusters/monomers increases as the number of Fe atoms/molecule was increased from 4 to 40 (Bauminger *et al.*, 1991a), probably reflecting the stabilization of the ferrihydrite core as it increases in size, a consequence of the decrease in surface free energy of the nanoparticle. Splitting of the oxobridge may occur through the

addition of a water molecule to give two monomeric $[Fe(OH)_2]^+$ ions followed by migration into the cavity to form the core as in equation (6).

Hence, the overall reaction for iron oxidation and hydrolysis at the ferroxidase centre, followed by further hydrolysis and migration to the core nucleation sites (equation 7) is:

$$2\,Fe^{2+} + O_2 + 4\,H_2O \longrightarrow 2\,FeOOH_{core} + H_2O_2 + 4H^+ \tag{7}$$
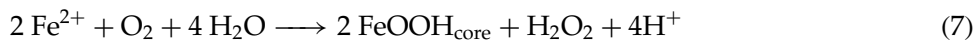
Crystal Growth

Once nucleation has taken place, the role of the protein is to maintain the growing ferrihydrite core within the confines of the protein shell, thus maintaining the insoluble ferric oxyhydroxide in a water-soluble form. We have seen how the inner surface of the protein is involved in initiating ferrihydrite formation with concomitant production of H_2O_2. As we saw in Chapter 1, if this encounters free Fe(II), this could lead production of hydroxyl radicals with potentially damaging effects on lipids, nucleic acids and proteins. Such radical reactions are seen with HoSF *in vitro* (Chen-Barrett *et al.*, 1995), but when Fe(II) is added at 200 or more atoms/molecule, H_2O_2 is not produced, since the oxidation stoichiometry approaches 4Fe(II)/ O_2 with production of water instead of H_2O_2 (Sun *et al.*, 1993; Yang *et al.*, 1998). What the situation is *in vivo*, since we can only with difficulty begin to envisage what iron levels might be attained, is virtually impossible to guess.

We now consider how the biomineralization chamber which is constituted by the interior of the apoferritin protein shell influences the growth of the core. Once sufficient core has been developed (>100 Fe atoms), Fe(II) oxidation and hydrolysis can proceed (Yang *et al.*, 1998) on the mineral surface of the growing core (equation 8):

$$4\,Fe^{2+} + O_2 + 6\,H_2O \longrightarrow 4\,FeOOH_{core} + 8H^+ \tag{8}$$
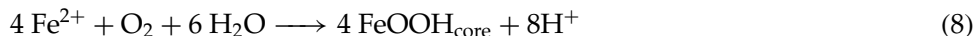
While core formation during hydrolysis of Fe(III) produces electrically neutral ferrihydrite, it also produces protons: two per Fe(II) oxidized and hydrolysed, whether due to iron oxidation and hydrolysis at the ferroxidase centre, followed by further hydrolysis and migration to the core nucleation sites (equation 7) or by direct Fe(II) oxidation and hydrolysis on the mineral surface of the growing core (equation 8). These protons must either be evacuated from the cavity or their charges must be neutralized by incoming anions, and it seems likely that both mechanisms are employed. In most ferritin molecules, some hydroxyl ions of the core (mostly on the core surface) are replaced by phosphate ions (Huang *et al.*, 1993), while electrostatic calculations indicate that expulsion of protons (as well as Fe^{3+} or Fe^{2+} ions) or uptake of orthophosphate (or other anions such as chloride) would be facilitated by the electrostatic field gradient through the threefold channels in human H-chain ferritin (Douglas and Ripoli, 1998).

Iron oxidized by ferritin must be at or near the outer surface of the apoferritin molecule, since iron appears to be exchanged between ferritin molecules, as shown by Mössbauer spectroscopy (Bauminger *et al.*, 1991a,b) and by the observation that iron oxidized by ferritin can be taken up directly by apotransferrin (Bakker and Boyer, 1986; Jin and Crichton, 1987).

6.1.5 Iron Mobilization from Ferritin

Storage iron, whether it be haemosiderin or ferritin, can be mobilized to meet body iron requirements. The molecular mechanisms that allow iron release *in vivo* are not understood. Most of the studies on iron mobilization have used *in vitro* systems involving the incubation of ferritin or haemosiderin, either with chelators alone or with low-molecular-weight reducing agents in the presence of non-physiological Fe(II) chelators, such as 2,2′-bipyridine (Sirivech *et al*., 1974), bathophenanthroline sulfonate (Biemond *et al*., 1986) or ferrozine (Boyer *et al*., 1988). The concerns emitted by Phil Aisen (Aisen, 1998) concerning their use in the demonstration of 'true' ferric iron reductase activity (Chapter 5) need to be reechoed here. It should also be underlined that placing a large excess of a powerful Fe(II) chelator in the presence of a reducing agent and Fe(III) is tantamount to placing a bar magnet in the presence of a large number of iron filings – what we referred to earlier as a molecular vacuum cleaner effect. Whatever equilibrium existed between different iron species before addition of the chelator/reductor, we are certainly far from it after their addition. Mobilization of ferritin iron by direct chelation is rather slow. Among the reducing agents employed we can discount dithionite (Granick and Michaelis, 1943) and thioglycollate (Crichton, 1973) as being non-physiological (although they are used for routine laboratory preparation of apoferritin from ferritin). Among the 'physiological' reducing agents that have been used, together with a non-physiological Fe(II) chelator, are dihydroflavins (Sirivech *et al*., 1974; Funk *et al*., 1986), superoxide (Bolann and Ulvik, 1987; Thomas *et al*., 1985; Monteiro and Winterbourn, 1988), dihydrolipoate and related thiols (Bonomi and Pagani, 1986) and ascorbate or the mono-dehydroascorbate radical (Bienfait and Van den Briel, 1980). None of these is clearly involved in mobilization of ferritin iron *in vivo*, nor is it clear what the biological chelator of Fe(II) would be. An interesting exception may be that encountered in the chloroplast, where the balance between overall iron release (ascorbate >2.5 mM) or uptake (ascorbate <2.5 mM) by plant ferritin from ferric citrate (Laulhère and Briat, 1993) occurs at physiological ascorbate concentrations (Law *et al*., 1983). When iron is electrochemically reduced in the absence of a chelator, the Fe(II) remains within the protein shell and for each Fe(III) reduced to Fe(II), $2H^+$ are taken up (Watt *et al*., 1985).

In the static crystal structure the threefold and fourfold channels of the ferritin molecule have a diameter of not more than a few tenths of a nanometre, yet solution studies by X-ray and neutron scattering and by NMR show that sugars and other small molecules of diameter larger than this (0.7–1.0 nm) can penetrate into the interior of the protein shell (Fischbach and Anderegg, 1965; Stuhrmann *et al*., 1976; Yang and Nagayama, 1995). That the channels between subunits can admit molecules of larger diameter than that observed in the crystals is also underlined by the X-ray crystallographic localization in the interior surface of a number of heavy-metal binding sites (Banyard *et al*., 1978; Hoare *et al*., 1975), and of protoporphyrin IX bound at the inner surface of horse apoferritins (Précigoux *et al*., 1994; Gallois *et al*., 1997). The kinetics of mobilization of ferritin iron by a number of reducing agents are fast enough to imply that access to the interior of the protein shell is not rate-limiting (Funk *et al*., 1986). Rates of iron release by a series of organic reductants correlate better with redox potential than with molecular size, again suggesting that

rate of penetration of the protein shell is not a determining factor (Jacobs *et al.*, 1989). Dihydroflavodoxin, a protein of molecular weight 30 kD, can reduce ferritin iron under anaerobic conditions (Watt *et al.*, 1988), which might result from electron tunnelling through the protein shell. An alternative might be that electron transfer to the ferritin core occurs by mediation of channel-bound Fe^{2+} or Fe^{3+}.

6.1.6 Haemosiderin

As mentioned earlier, haemosiderin was the first storage form of iron to be identified (Perls, 1867) and isolated (Cook, 1929). The name is perhaps misleading – while the source of haemosiderin iron is haem, the iron cores of haemosiderin contain non-haem iron. It is found in conditions of iron overload, usually associated with toxic pathological states in man, but frequently found as a normal physiological response without any toxicity in many birds, and animals (e.g. marmosets, lemurs, horses and reindeer – reviewed in Ward *et al.*, 2000). Haemosiderin appears upon EM examination as massive clusters of irregular, electron-dense particles, most of which are enclosed within membranous structures, thought to be iron-laden secondary lysosomes which have been described as siderosomes (Iancu, 1989; Richter, 1984). Electron micrographs of iron-loaded tissue and of siderosomes from human and avian (Order Passeriformes[¶¶]) spleen are presented in Figure 6.16. In man, haemosiderin is present in relatively small amounts in normal tissue, but accumulates during iron overload (Seldon *et al.*, 1980). Haemosiderin as isolated is typically a water-insoluble protein of ill-defined nature with a high iron-to-protein ratio, which can be solubilized by the use of alkali and detergents (Weir *et al.*, 1984). Ultrastructural immuno-gold staining showed that siderosome granules are recognized by anti-ferritin antibodies, although their immunoreactivity is significantly lower than that of cytosolic ferritin (Cooper *et al.*, 1988), thus supporting the view that haemosiderin is a lysosomal degradation product of ferritin (Richter, 1978). However, incubation of ferritin with purified lysosomes does not yield haemosiderin (Iancu and Neustein, 1977), suggesting that other reactions are involved in its formation. This seems to be confirmed for phytosiderin, an insoluble iron-containing product isolated from pea seed, which contains a peptide derived by radical mediated cleavage of 20 *N*-terminal residues from the ferritin subunit (Laulhère *et al.*, 1989). Evidence for proteolytic cleavage in haemosiderins of both human and animal origin have been reported (Ward *et al.*, 1989, 1994; Andrews *et al.*, 1987a,b).

On the basis of a number of physico-chemical methods (Mössbauer spectroscopy, electron diffraction, EXAFS) the iron cores of naturally occurring haemosiderins isolated from various iron-loaded animals and man (horse, reindeer, birds and human old age) were consistently shown to have ferrihydrite-like iron cores similar to those of ferritin (Ward *et al.*, 1992, 2000). In marked contrast, in the tissues of patients with two pathogenic iron-loading syndromes, genetic haemochromatosis and thalassaemia, the haemosiderins isolated had predominantly amorphous ferric oxide and goethite cores, respectively (Dickson *et al.*, 1988; Mann *et al.*, 1988;

[¶¶] Better known as the common starling.
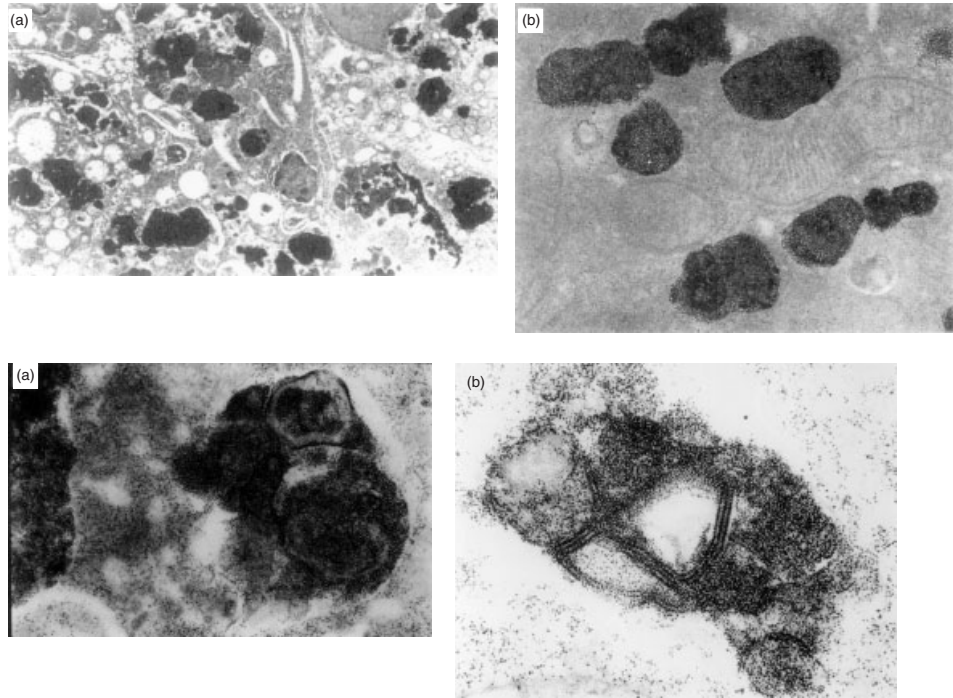
Figure 6.16 Top: Electron micrographs of iron-overloaded human spleen (a) and of an avian species (Order passeriformes) (b), showing clumps of densely stained material throughout the tissue, haemosiderin. Bottom: Electron micrographs of siderosomes from (a) human spleen and (b) an avian species (Order passeriformes). Iron-rich particles can be seen within the membrane-bound structure. Hexagonal arrangements and clusters of unbound ferritin are also seen. Unstained, magnification $\times$ 120 000. Reprinted from Ward *et al.*, 2000. Copyright (2000), with permission from Elsevier Science.

Mackle *et al.*, 1991; Ward *et al.*, 1994, 2000). The transformation of ferrihydrite to goethite (see Chapter 1) would require solubilization and reprecipitation. That desferrioxamine chelation therapy might have contributed to this transformation, as originally hypothesized (Ward *et al.*, 1992), seems unlikely in the light of studies on haemosiderin isolated from thalassaemic patients untreated with chelators (Ward *et al.*,1994), and from a marine mammal, *Dugong dugong* (Chua-anusorn *et al.*, 1994). Both have goethite as the predominant mineral phase. Prolonged centrifugation in potassium iodide enables a non-ferritin, non-haemosiderin fraction termed prehaemosiderin to be isolated; the structure of its iron cores resembled that of the corresponding haemosiderins, i.e. goethite-like in thalassaemia and ferrihydrite-like in the other conditions (Ward *et al.*, 1994). This implies that there may be multiple mechanisms of haemosiderin formation, and that the intrinsic toxicity of haemosiderin iron may vary with its origin.

6.2 Biomineralization

The underlying chemistry of iron biomineralization has been discussed in Chapter 1, and in this present section we discuss the way in which the apoferritin protein

shell functions as a reaction vessel for the formation of mineralized nanoparticles (reviewed in Powell, 1998). We have already seen that by varying the experimental conditions, iron oxyhydroxide cores similar to those observed in mammalian ferritins can be loaded into apobacterioferritins (Wade *et al.*, 1993; Mann *et al.*, 1987; Ringeling *et al.*, 1994). In the same way, mammalian ferritins can load cores of varying composition *in vitro*. For example, under conditions of high pH and limited oxygen, one can produce (Meldrum *et al.*, 1992) ferritin cores corresponding to the magnetic, mixed-valence minerals, magnetite (Fe_3O_4) and maghaemite (γ-Fe_2O_3, a defect structure of magnetite). Other nanoparticle mineral cores have been produced, including greigite (Fe_3S_4), and $MnOOH$ and Mn_3O_4 cores within the ferritin protein shell (Meldrum *et al.*, 1991; Douglas *et al.*, 1995). Such experiments, while of great interest, do not give us much insight into the process of ferritin mineralization itself. Perhaps more interesting are more recent studies (St. Pierre *et al.*, 1996) which indicate that cores displaying different crystallites and compositions can be formed in a tailored fashion by varying the temperature of loading and the amount of phosphate present, although many problems resulting from the polydispersity[§§] of the core particles were apparent (at the extremes going from fully loaded molecules with 4500 iron atoms to others that were almost empty). These studies however underline the central difficulty in obtaining samples of a sufficient degree of homogeneity to give interpretable results at the (potential) atomic resolution of the physical techniques used.

When we consider the different types of iron environment which are found in loaded ferritin cores we can distinguish three types of sites: (i) iron atoms at nucleation sites, which have coordination spheres containing both organic ligands from the protein, and inorganic ligands from the mineral surface; (ii) purely inorganic iron atoms which are in environments corresponding to the bulk mineral phase; and (iii) iron atoms at the surface of the mineral which like those at the nucleation sites may have ligands both from the mineral phase and also from outside the mineral core (water, phosphate or ligands from the protein itself). A number of cluster aggregates have been synthesized and proposed as models of the ferritin core, and the molecular structure of one such Fe_{19} cluster system, which shares quite similar EXAFS characteristics with horse spleen ferritin (Heath *et al.*, 1996) is shown in Figure 6.17, and it is hoped that their structural characterization at atomic resolution will help in our understanding of the mineral core of ferritin.

We can briefly conclude that the mineralization process of iron in ferritin cores is a difficult process to follow experimentally. While we believe that iron is delivered for storage within the protein cavity as Fe(II), and that an oxidation step occurs in the formation of the ferritin iron core, it is not clear what percentage of iron oxidation occurs on the growing surface of the mineral and what at the catalytic ferroxidase

---

[§§] It is unfortunately the case that when we incubate apoferritin with a certain number of iron atoms (for example as ferrous ammonium sulfate), the product, after elimination of non-protein-bound iron, does not have a homogeneous distribution of iron: molecules which were able to (i) take up iron rapidly through the three fold channels, (ii) quickly transfer it and form a diiron centre on a ferroxidase site, and (iii) to transfer the iron inward to a nucleation site, where (iv) it will begin to catalyse iron oxidation on the surface of the growing crystallite, will accumulate iron much more rapidly, and in much greater amounts than molecules in which steps (i), (ii) and (iii) are slower, for whatever reasons (perhaps most importantly *subunit composition*, and the *disposition of subunits* of the two types H and L, one with regard to the other). This polydispersity makes the analysis of the process of iron uptake extremely difficult.
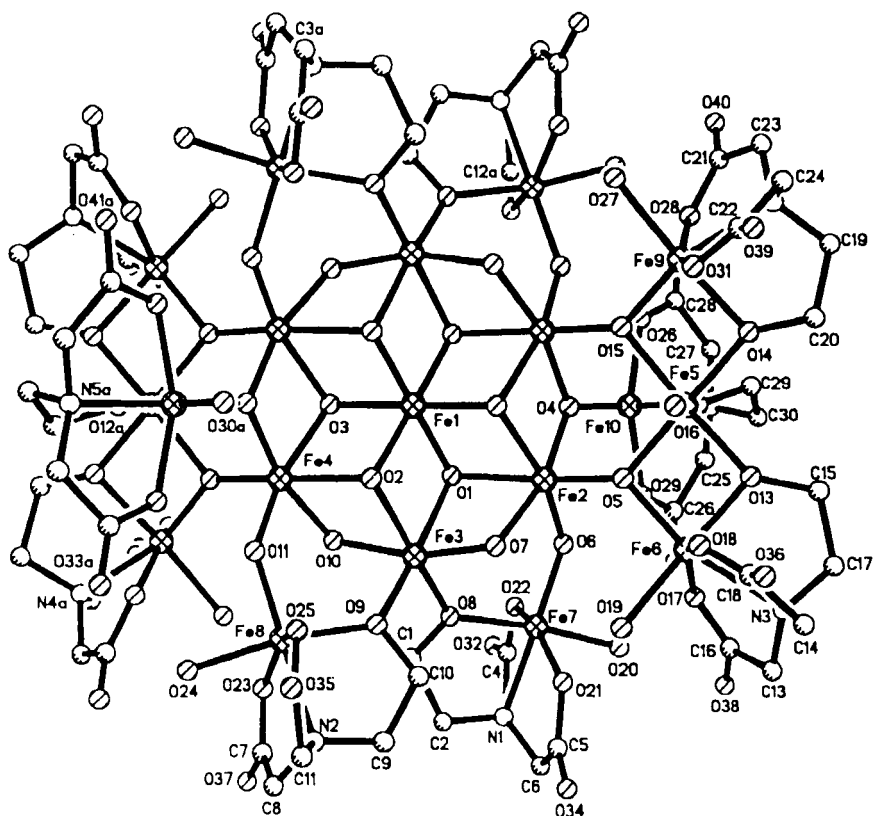
Figure 6.17 The molecular structure of the Fe_{19} crust cluster system. Reprinted from Powell, 1988, by courtesy of Marcel Dekker, Inc.

sites. It may be that the major function of the channels leading to and from the cavity is to provide a pathway for protons and electrons, controlling the redox potential and the pH, and influencing the nature of the mineral formed (Powell, 1998). While mammalian ferritins have cores composed largely of a ferrihydrite-like iron(III) oxyhydroxide mineral whereas bacterioferritins have an essentially amorphous hydrated iron phosphate, it is clear that by varying the *in vitro* loading conditions, each of these apoferritins can be used as reaction vessels to lay down iron cores analogous to the other.

6.3 References

Aisen, P. (1998). In *Metal Ions in Biological Systems* (eds Sigel, A. and Sigel, H.), Marcel Dekker, New York, **35**, 617.

Almiron, M., Link, A.J., Furlong, D. and Kolter, R.A. (1992). *Genes Dev.*, **6**, 2646–54.

Andrews, S.C., Treffry, A. and Harrison, P.M. (1987a). *Biochem. J.*, **245**, 439–46.

Andrews, S.C., Treffry, A. and Harrison, P.M. (1987b). *Biochem. J.*, **245**, 447–53.

Andrews, S.C., Brady, M.C., Treffry, A., Williams, J.M. *et al.* (1988). *Biol. Metals*, **1**, 33–42.

Andrews, S.C., Arosio, P., Bottke, W., Briat, J.-F. *et al*. (1992). *J. Inorg. Biochem.*, **47**, 161–74.

Bakker, G.R. and Bayer, R.F. (1986) *J. Biol. Chem.* **261**, 13182–5.

Banyard, S.H., Stammers, D.K and Harrison, P.M. (1978). *Nature*, **271**, 282–4.

Bauminger, E.R., Harrison, P.M., Hechel, D., Nowik, I. and Treffry, A. (1991a). *Biochim. Biophys. Acta*, **1118**, 48–58.

Bauminger, E.R., Harrison, P.M., Hechel, D., Nowik, I. and Treffry, A. (1991b). *Proc. R. Soc. London Ser. B*, **244**, 211–17.

Bauminger, E.R., Harrison, P.M., Hechel, D., Hodson, N.W. *et al*. (1993). *Biochem. J.*, **296**, 709–19.

Bielig, H.G. and Bayer, E. (1985). *Naturwissenschalt*, **42**, 125–6.

Biemond, P., Swaak, A.J.G., Beindorff, C.M. and Koster, J.K. (1986). *Biochem. J.*, **239**, 169–73.

Bienfait, H.F. and Van den Briel, M.L. (1980). *Biochim. Biophys. Acta*, **631**, 507–10.

Bolann, B.J. and Ulvik, R.J. (1987). *Biochem. J.*, **243**, 55–9.

Bonomi, F. and Pagani, S. (1986). *Eur. J. Biochem.*, **155**, 295–300.

Bonomi, F., Kurtz, D.M. and Cui, X. (1996). *J. Inorg. Biochem.*, **1**, 69–72.

Bozzi, M., Mignogna, G., Stetarini, S., Barra, D. *et al*. (1997). *J. Biol. Chem.*, **272**, 3295–65.

Boyer, R.F., Grabill, T.W. and Petrovich, R.M. (1988). *Anal. Biochem.*, **174**, 17–22.

Brooks, R.A., Vymaza, J., Goldfarb, R.B., Bulte, J.W.M. and Aisen, P. (1998). *Magn. Reson. Med.*, **15**, 227–35.

Bryce, C.F.A and Crichton, R.R. (1973) *Biochem. J.* **133**, 301–9.

Bulen, W.A., Le Comte, J.R. and Lough, S. (1973). *Biochem. Biophys. Res. Commun.*, **54**, 1274–81.

Chasteen, N.D. (1998). In *Metal Ions in Biological Systems* (eds. Sigel, A. and Sigel, H.), Marcel Dekker, New York, **35**, 479–514.

Chasteen, N.D. and Harrison, P.M. (1999). *J. Struct. Biol.*, **126**, 182–94.

Cheesman, M.R., Thomson, A.J., Greenwood, C., Moore, G.R. and Kadir, F. (1990). *Nature*, **346**, 771–3.

Chen, L. and Helmann, J.D. (1995). *Mol. Microbiol.*, **18**, 295–300.

Chen-Barrett, Y., Harrison, P.M., Treffry, A., Quail, M.A. *et al*. (1995). *Biochem.*, **34**, 7847–53.

Chua-anusorn, W., St.-Pierre, T.G., Black, G., Webb, J., Macey, D.J. and Parry, D. (1994). *Hyperfine Interact.*, **91**, 899-

Cook, S.F. (1929). *J. Biol. Chem.*, **82**, 595–609.

Cooper, J.P., Iancu, T.C., Ward, R.J., Guttridge, K.M. and Peters, T.J. (1988). *Histochem. J.*, **20**, 499–509.

Crichton, R.R. (1973). *Struct. Bonding*, **17**, 67–134.

Crichton, R.R. (1991). *Inorganic. Biochemistry of Iron Metabolism*, Ellis Horwood, Chichester.

Crichton, R.R. and Roman, F. (1978). *J. Mol. Catal.*, **4**, 75–82.

Crichton, R.R., Herbas, A., Chavez Alba, O. and Roland, F. (1996). *J. Biol. Inorg. Chem.*, **1**, 567–74.

Crichton, R.R., Soruco, J.-A., Roland, F., Michaux, M.-A. *et al*. (1997). *Biochem.*, **36**, 15049–54.

Deeb, S.S. and Hager, L.P. (1964). *J. Biol. Chem.*, **239**, 1024–31.

De Graaf, J., Amons, R. and Moeller, W. (1990). *Eur. J. Biochem.*, **193**, 737–50.

De Maré, F., Kurtz, D.M. and Nordlund, P. (1996). *Nature Struct. Biol.*, **3**, 539–46.

Desideri, A., Stefanini, S., Polizio, F., Petruzella, R. and Chiancone, E. (1991). *FEBS Lett.*, **287**, 10–14.

Dickson, D.P.E., Reid, N.M.K., Mann, S., Wade, V.J., Ward, R.J. and Peters, T.J. (1988). *Biochim. Biophys. Acta*, **957**, 81–90.

Douglas, T. and Ripoli, D.R. (1998). *Protein Sci.*, **1**, 1083–91.

Fischbach, F.A. and Anderegg, J.W. (1965). *J. Mol. Biol.*, **14**, 458–73.

Ford, G.C., Harrison, P.M., Rice, D.W., Smith, J.M.A. (1984). *Phil. Trans. R.Soc. Lond. B*, **304** 551–65.

Frolow, F., Kalb (Gilboa), A.J. and Yariv, J. (1994). *Nature Struct. Biol.*, **1**, 453–60.

Funk, F., Lenders, J.-P., Crichton, R.R. and Schneider, W. (1986). *Eur. J. Biochem.*, **152**, 167–72.

Gallois, B., Langlois d'Estaintot, B., Michaux, M.-A., Dautant, A. *et al.* (1997). *J. Biol. Inorg. Chem.*, **2**, 360–7.

George, G.N., Richards, T., Bare, R.E., Gea, Y. *et al.* (1993). *J. Am. Chem. Soc.*, **115**, 7716–8.

Granier, T., Comberton, G., Gallois, B., Langlois d'Estaintot, B. *et al.* (1998). *Proteins, Struct. Funct. Genet.*, 31 477–85.

Granick, S. and Michaelis, L. (1943). *J. Biol. Chem.*, **147**, 91–7.

Grant, R.A., Filman, D.J., Finkel, S.E., Kolter, R. and Hogle, J.M. (1998). *Nature Struct. Biol.*, **5**, 294–303.

Harrison, P.M. (1959). *J. Mol. Biol.*, **1**, 69–80.

Harrison, P.M. and Arosio, P. (1996). *Biochim. Biophys. Acta*, **1275**, 161–203.

Harrison, P.M., Artymuik, D.W., Ford, G.C., Lawson, D.M. *et al.* (1989). In *Biomineralization* (eds. Mann, S., Webb, J. and Williams, R.J.P.), pp. 257–94, VCH Weinheim'.

Harrison, P.M., Hempstead, P.D.,Artymuik, P.J. and Andrews, S.C. (1998). In *Metal Ions in Biological Systems* (eds Sigel, A. and Sigel, H.), Marcel Dekker, New York, **35**, 436–77.

Heath, S.L., Charnock, J.M., Garner, C.D. and Powell, A.K. (1996). *Chem. Eur. J.*, **2**, 634–9.

Hempstead, P.D., Yewdall, S.J., Fernie, A.R., Lawson, D.M. *et al.* (1997). *J. Mol. Biol.*, **268**, 424–48.

Herynek, V., Bulte, J.W.M., Douglas, T. and Brooks, R.A. (2000). *J. Biol. Inorg. Chem.*,**5**, 51–6.

Heusterspreute, M. and Crichton, R.R. (1981). *FEBS Lett.*, **129**, 322–7.

Hilty, S., Webb, B., Frankel, R.B. and Watt, G.D. (1994). *J. Inorg. Biochem.*, **56**, 173–185.

Hoare, R.J., Harrison, P.M. and Hoy, T.G. (1975). *Nature*, **255**, 653–4.

Huang, H., Watt, R.F., Frankel, R.B. and Watt, G.D. (1993). *Biochem.*, **32**, 1681–7.

Hwang, J., Krebs, C., Huynh, B.H., Edmondson, D.E., Theil, E.C. and Penner-Hahn, J.E. (2000). *Science*, **287**, 122–5.

Iancu, T.C. (1989). *Ultrastruc. Pathol.*, **13**, 573–84.

Iancu, T.C. and Neustein,H.B. (1977). *Br. J. Haematol.*, **37**, 527–35.

Ilari, A., Stefanini, S., Chiancone, E. and Tsernoglou, D. (2000). *Nature Struct. Biol.*, **7**, 38–43.

Jacobs, D., Watts, G.D., Frankel, R.B. and Papaefthymiou, G.C. (1989). *Biochem.*, **28**, 9216–21.

Jin, Y. and Crichton, R.R. (1987). *FEBS Letts.*, **215**, 41–6.

Keilin, D. (1934). *Nature*, **133**, 290–1.

Laufberger, V. (1937). *Bull. Soc. Chim. Biol.*, **19**, 1575–82.

Laulhère, J.P., Laboure, A.M. and Briat, J.F. (1989). *J. Biol. Chem.*, **264**, 3629–35.

Laulhère, J.P. and Briat, J.F. (1993). *Biochem. J.*, **290**, 693–9.

Law, M.Y., Charles, S.A. and Halliwell, B. (1983). *Biochem. J.*, **210**, 899–903.

Lawson, D.M., Treffry, A., Artymiuk, P.J., Harrison, P.M. *et al*. (1989). *FEBS Lett.*, **254**, 207–10.

Lawson, D.M., Artymiuk, P.J., Yewdall, S.J., Smith, J.M.A. *et al*. (1991). *Nature*, **349**, 541–4.

Lee, M., Arosio, P., Cozzi, A. and Chasteen, N.D. (1994). *Biochem.*, **33**, 3679–89.

Levi, S., Luzzago, A., Cesareni, G., Cozzi, A. *et al*. (1988). *J. Biol. Chem.*, **263**, 18086–92.

Levi, S., Salfeld, J., Franceschinelli, F., Cozzi, A., Dorner, M.H. and Arosio, P. *et al*. (1989). *Biochem.*, **28**, 5179–84.

Levi, S., Yewdall, S.J., Harrison, P.M., Santambrogio, P. *et al*. (1992). *Biochem. J.*, **288**, 591–6.

Levi, S., Santambrogio, P., Cozzi, A., Rovida, E. *et al*. (1994). *J. Mol. Biol.*, **238**, 649–54.

Levi, S., Santambrogio, P., Corsi, B., Cozzi, A. and Arosio, P. (1996). *Biochem. J.*, **317**, 467–73.

Levi, S., Girelli, D., Perrane, F., Past, M. *et al*. (1998). *Blood*, **91** 4180–7.

Lobréaux, S., Yewdall, S.J., Briat, J.-F. and Harrison, P.M. (1992). *Biochem. J.*, **288**, 931–9.

Macara, I.G., Hoy, T.G. and Harrison, P.M. (1972). *Biochem. J.*, **126**, 151–62.

Mackle, P., Garner, C.D., Ward, R.J. and Peters, T.J. (1991).*Biochim. Biophys. Acta*, **1115**, 145–50.

Mann, S., Bannister, J.V. and Williams, R.J.P. (1986). *J. Mol. Biol.*, **138**, 225–32.

Mann, S., Williams, J.M., Treffry, A. and Harrison, P.M. (1987). *J. Mol. Biol.*, **198**, 405–16.

Mann, S., Wade, V.J., Dickson, D.P.E., Reid, N.M. *et al*. (1988). *FEBS Lett.*, **234**, 69–72.

Massover, W.H. (1993). *Micron*, **24**, 389–437.

Meldrum, F.C., Wade, V.J., Nimmo, D.L., Heywood, B.R. and Mann, S. (1991). *Nature*, **349**, 684–7.

Meldrum, F.C., Heywood, B.R. and Mann, S. (1992). *Science*, **257**, 522–3.

Michaux, M.-A., Dautant, A., Gallois, B., Granier, T., d' Estaintot, B.L. and Précigoux, G. (1996). *Proteins*, **24**, 314–21.

Moënne-Loccoz, P., Krebs, C., Herlihy, K., Edmondson, D.E. *et al*. (1999). *Biochem.*, **38**, 5290.

Monteiro, H.P. and Winterbourn, C.C. (1988). *Biochem. J.*, **256**, 923–8.

Niederer, W. (1970). *Experientia*, **26**, 218–20.

Pena, M.O. and Bullerjahn, G.S. (1995). *J. Biol. Chem.*, **270**, 22478–82.

Pereira, A.S., Small, W., Krebs, C., Tavanes, P. *et al*. (1998). Biochem., **37**, 9871–6.

Perls, M. (1867). *Virchows Arch.A*, **39**, 44–8.

Powell, A.K. (1998). In *Metal Ions in Biological Systems* (eds. Sigel, A. and Sigel, H.), Marcel Dekker, New York, **35**, 515–61.

Précigoux, G., Yariv, J., Gallois, B., Dautant, A., Courseille, C. and d'Estaintot, B.L. (1994). *Acta Cryst.*, **D50**, 739–43.

Proudhon, D., Briat, J.-F. and Lescure, A.-M. (1989). *Plant Physiol.*, **90**, 586–90.

Rice, D.W., Ford, G.C., White, J.L., Smith, J.M.A. *et al*. (1983). *Adv. Inorg. Biochem.*, **5**, 39–50.

Richter, G.W. (1978). *Am. J. Pathol.*, **91**, 363–97.

Richter, G.W. (1984). *Lab. Invest.*, **50**, 26–35.

Ringeling, P.L., Davy, S.L., Monkara, F.A., Hunt, C., Dickson, D.P.E., McEwan, A.G. and Moore, G.R. (1994). *Eur. J. Biochem.*, **223**, 847–55.

Rohrer, J.S., Islam, Q.T., Watt, G.D., Sayers, D.E. and Theil, E.C. (1990). *Biochem.*, **29**, 259–64.

Santambrogio, P., Levi, S., Cozzi, A., Corsi, B. and Arosio, P. (1996). *Biochem. J.*, **314**, 139–44.

Seldon, C., Owen, M., Hopkins, J.M.P. and Peters, T.J. (1980). *Br. J. Haematol.*, **44**, 593–603.

Sirivech, S., Freiden, E. and Osaki, S. (1974). *Biochem. J.*, **143**, 311–15.

Stefanini, S., Desideri, A., Vecchini, P., Drakenberg, T. and Chiancone, E. (1989). *Biochem.*, **28**, 378–82.

Stillman, T.J., Hempstead, P.D., Artymiuk, P.J., Andrews, S.C. *et al.* (2000). *J. Mol. Biol.*, in press.

Stefaini, S., Cavallo, S., Montagnini, B. and Chiancone, E. (1999). *Biochem. J.*, **338**, 71–5.

St. Pierre, T.G., Harris, L., Webb, J. and Macey, D.J. (1990). *Inorg. Chem.*, **29**, 1870–4.

St. Pierre, T.G., Chan, P., Bauchspiess, K.R., Webb, J. *et al.* (1996). *Coord. Chem. Rev.*, **151**, 125–43.

Stuhrmann,, H.B., Haas, J., Ibel, K., Koch, M.H.J. and Crichton, R.R. (1976). *J. Mol. Biol.*, **100**, 399–413.

Sun, S., Arosio, P., Levi, S. and Chasteen, N.D. (1993). *Biochem.*, **36**, 9362–9.

Thomas, C.D., Morehouse, L.A. and Aust, S.D. (1985). *J. Biol. Chem.*, **260**, 3275–80.

Tonello, F., Dundon, W.G., Satin, B., Molinari, M. *et al.* (1999). *Mol. Microbiol.*, **34**, 238–46.

Treffry, A., Hirzmann, J., Yewdall, S.J. and Harrison, P.M. (1992). *FEBS Lett.*, **302**, 108–12.

Treffry, A., Bauminger, E.R., Hechel, D., Hodson, N.W., Nowick, I., Yewdall, S.J. and Harrison, P.M. (1993). *Biochem. J.*, **296**, 721–8.

Treffry, A., Zhao, Z.W., Quail, M.A., Guest, J.R. and Harrison, P.M. (1995). *Biochem.*, **34**, 15204–13.

Treffry, A., Zhao, Z.W., Quail, M.A., Guest, J.R. and Harrison, P.M. (1997). *Biochem.*, **36**, 432–41.

Trikha, J., Waldo, J.S., Lewandowski, F.A., Ha, Y. *et al.* (1994). Protein, **18**, 107–18.

Trikha, J. Theil, E.C. and Allewell, N.M. (1995). *J. Mol. Biol.*, **228**, 949–67.

Wade, V.J., Levi, S., Arosio, P., Treffry, A., Harrison, P.M. and Mann, S. (1991). *J. Mol. Biol.*, **221**, 1443–52.

Wade, V.J., Treffry, A., Laulhère, J.-P., Bauminger, E.M. *et al.* (1993). *Biochim. Biophys. Acta*, **1161**, 91–6.

Waldo, G.S., Wright, E., Wang, Z.H., Briat, J.-F., Theil, E.C. and Sayers, D.E. (1995). *Plant Physiol.*, **109**, 797–802.

Ward, R.J., O'Connell, M.J., Dickson, D.P.E., Reid, N.M. *et al.* (1989). *Biochim. Biophys. Acta*, **993**, 131–3.

Ward, R.J, Ramsey, M.H., Dickson, D.P.E., Florence, A. *et al.* (1992). *Eur. J. Biochem.*, **209**, 847–50.

Ward, R.J, Ramsey, M.H., Dickson, D.P.E., Hunt, C. *et al.* (1994). *Eur. J. Biochem.*, **225**, 187–94.

Ward, R.J., Legssyer, R., Henry, C. and Crichton, R.R. (2000). *J. Inorg. Biochem.*, **79**, 311–7.

Watt,, G.D., Frankel, R.B. and Papefthymiou, G.C. (1985). *Proc. Natl Acad. Sci., USA*, **82**, 3640–3.

Watt,, G.D., Jacobs, D. and Frankel, R.B. (1988). *Proc. Natl Acad. Sci., USA*, **85**, 7457–61.

Weir, M.P., Gibson, J.F. and Peters, T.J. (1984). *Biochem. J.*, **223**, 31–8.

Wustefeld, C. and Crichton, R.R. (1982). *FEBS Lett.*, **150**, 43–8.

Yang, D. and Nagayama, K. (1995). *Biochem. J.*, **307**, 253–6.

Yang, X., Chen-Barrett, T., Arosio, P. and Chasteen, N.D. (1998). *Biochem.*, **26**, 9763–97.

Zhao, Z.W., Treffry, A., Quail, M.A., Guest, J.R. and Harrison, P.M. (1997). *J. Chem. Soc., Dalton Trans.*, 3977–8.

7 Intracellular Iron Metabolism and Cellular Iron Homeostasis

7.1 Intracellular Iron Metabolism

7.1.1 The Labile Iron Pool

We have seen in Chapter 5 that extracellular iron can be taken up by various routes: (i) from transferrin, via its receptor mediated pathway; (ii) from transferrin, by the receptor independent pathway; (iii) from ferritin; (iv) from non-transferrin bound iron; (v) from other sources (like haem, in one of its many forms). Once it has been taken up by cells it enters a pool of labile, cytosolic iron. This iron is available for haem synthesis and for iron incorporation into iron-dependent enzymes and ferritin. Enlargement of this pool stimulates ferritin synthesis. Iron also enters this transit pool not only from outside the cell, but also as a result of endogenous haem breakdown and the mobilization of ferritin iron. As we will see in Chapter 10, this is the pool of intracellular iron that we suspect is responsible for oxygen-mediated iron toxicity. It is generally thought that this pool is of low molecular weight, and that it is probably the major site of iron chelation by chelators such as desferrioxamine. Hence the different names proposed for it – chelatable iron pool, transit pool, LMWIP (low molecular weight iron pool), and most recently LIP (labile iron pool). Despite many efforts to uncover this Holy Grail of intracellular iron metabolism, its nature still remains undefined. It has been described, by the author, as 'somewhat like the Loch Ness monster, only to disappear from view before its presence, or indeed its nature, can be confirmed' (Crichton, 1984).

There are essentially two problems concerning the LIP, which we will consider in turn. Firstly, what is the concentration of iron in the LIP? And secondly, what is its nature? Perhaps, we should add a codicil, namely how can we measure either of these without provoking a redistribution of iron which totally distorts the subsequent picture. In order to circumvent this problem, *in vivo* approaches have been developed, which we will now discuss – however, the ideal solution to resolving the problem raised in our codicil would be to use truly 'non-invasive' analytical methods, which do not perturb subtle intracellular equilibria.

A method has been proposed for evaluation of LIP concentration in living cells based on the fluorescent probe calcein (Breuer *et al.*, 1995; Epsztejn *et al.*, 1997). The authors assumed that calcein bound Fe^{2+}. However, a more recent thermodynamic and kinetic study indicates that the preferred form bound is Fe^{3+}, and that calcein is a good chemosensor of Fe^{3+} (Thomas, *et al.*, 1999). The iron

is bound rapidly, stoichiometrically and reversibly to form fluorescent quenched CA–Fe complexes. Cells are loaded with CA using its acetomethoxy precursor; intracellular concentrations of the probe of 1–10 μM are attained without affecting cellular viability. The estimated values of LIP, defined operationally as the sum of 'free' and CA-bound iron of the cell for resting erythroid and myeloid cells was in the range 0.2–1.5 μM.

It has been calculated from considerations of solubility in the absence of chelate effects, that upper limits of Fe^{2+} in the range of 10^{-7}–10^{-9} M and of Fe^{3+} of the order of 10^{-17}–10^{-19} M could be expected. Why the values observed by the calcein method should be higher than those predicted may reflect on the one hand the effect of potential chelators in increasing the amount of iron in solution, but perhaps also the effect of the calcein in drawing iron out of compartments which would not normally be part of the LIP (something that we have referred to in another context as a 'molecular vacuum cleaner effect', Crichton *et al.*, 1997). Whatever the absolute value of the iron concentration in the LIP, there can be no doubt that the calcein method has allowed a number of interesting studies to be carried out, that have established that the LIP can undergo dynamic changes in response to various treatments (Breuer *et al.*, 1996; Konijn *et al.*, 1999), that it is downregulated by the induction of ferritin synthesis (Epsztejn *et al.*, 1999) and that it is a key component of the oxidative stress response (Breuer *et al.*, 1997; Staubli and Boelsterli, 1998; Lipinski *et al.*, 2000).

The nature of the LIP remains as uncertain today as it did 10 years ago, when it was suggested that the dominant ligand was either AMP or ATP (Weaver and Pollack, 1989). The candidates are just as numerous, including nucleoside phosphates, citrate, pyrophosphate and amino acids, but we are still confronted with the dilemma that as soon as we break open a cell, we no longer have a cell, and there will inevitably be some unavoidable reequilibration between ligands during subsequent fractionation. One approach which has the virtue of being non-invasive and should not perturb the system is Mössbauer spectroscopy. The drawbacks, as we have pointed out in Chapter 2, are the requirements for considerable enrichment in ^{57}Fe, lack of sensitivity and limitations on the amount of information concerning the chemical environment of the metal. However, it could give valuable information concerning the valence state of the iron, which is still uncertain.

7.1.2 Haem Biosynthesis

Mitochondria are not only the powerhouse of the cell, supplying abundant ATP through the coupling of active proton pumping across their inner membrane with the transfer of electrons along the respiratory chain, they are also the alpha and omega of haem biosynthesis. Before the reader starts searching for the Four Horsemen of the Apocalypse, a quick look at Figure 7.1 should prove reassuring. The overall pathway of haem biosynthesis begins in the mitochondria, with the condensation of succinyl CoA coming from the citric-acid cycle with glycine to form δ-aminolaevulinate, which is expedited forthwith into the cytoplasm. There, the synthesis of the tetrapyrroleporphyrin nucleus continues apace, until the oxidative decarboxylation of coproporphyrinogen III to protoporphyrinogen
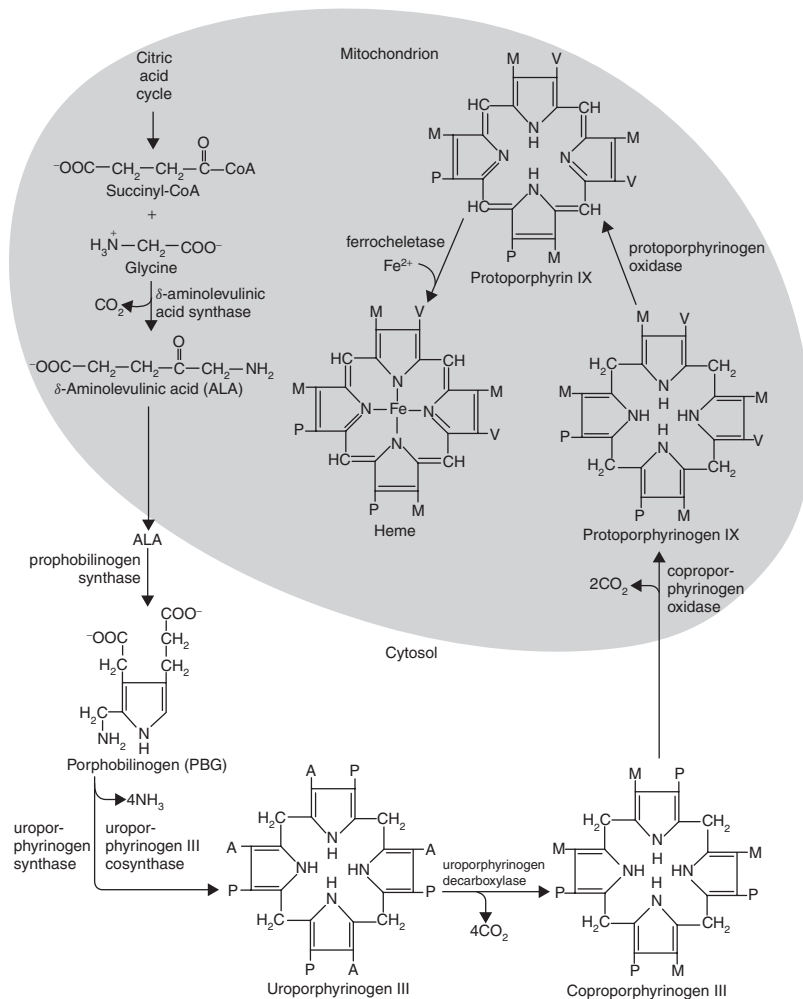
Figure 7.1 The overall pathway of haem biosynthesis. δ-Aminolaevulinate (ALA) is synthesized in the mitochondrion, and is transferred to the cytosol where it is converted to porphobilinogen, four molecules of which condense to form a porphyrin ring. The next three steps involve oxidation of the pyrrole ring substituents to give protoporphyrinogen IX, whose formation is accompanied by its transport back into the mitochondrion. After oxidation to protoporphyrin IX, ferrochelatase inserts Fe^{2+} to yield haem. A, P, M and V represent, respectively acetyl, propionyl, methyl and vinyl ($-CH_2=CH_2$) groups. From Voet and Voet, 1995. Reproduced by permission of John Wiley & Sons, Inc.

IX is accompanied by its transport back into the mitochondria whence it came, to undergo oxidation of its methylene groups to protoporphyrin IX and insertion of iron to yield the end product, haem. The two major sites of haem biosynthesis are erythroid cells, which synthesize around 85 % of the body's haem groups, and the liver, which synthesizes most of the remainder. A major function of haem in liver is as the prosthetic group of cytochrome P_{450}, the importance of which in detoxification has been discussed in Chapter 2. The liver cell must synthesize cytochrome P_{450} throughout its lifetime in quantities that vary with conditions. In contrast, the

developing erythroid cell only engages in haem synthesis when it differentiates, and then it is a one-time synthesis in vast quantities to accompany globin production and ensure the haemoglobin content that will last for the erythrocyte's lifetime. Haem and globin synthesis cease upon red cell maturation. This means that haem synthesis in liver and erythroid cells is regulated in a quite different way. In liver, the main control site is δ-aminolaevulinate synthase, which is regulated by haemin, the Fe(III) oxidation product of haem, by three mechanisms: (i) feedback inhibition, (ii) inhibition of transport of the enzyme from its site of synthesis in the cytosol to the mitochondria, and (iii) repression of the enzyme's synthesis. In differentiated erythroid cells (reticulocytes), haem stimulates protein synthesis, inducing synthesis of globin to ensure that haem and globin are synthesized in the correct ratio for assembly into haemoglobin, but also induces the synthesis of the haem biosynthetic pathway enzymes. The control of haem synthesis in erythroid cells seems to be at the level of ferrochelatase, and porphobilinogen deaminase, rather than δ-aminolaevulinate synthase. However, as we will see below, the translation of δ-aminolaevulinate synthase mRNA is regulated by iron availability, increasing when iron is abundant.

Ferrochelatase (protohaem ferrolyase), is the terminal enzyme in haem biosynthesis, catalysing the insertion of ferrous iron into protoporphyrin IX (Figure 7.1). They are monomeric proteins of molecular weight between 36–40 kD, that are found in all cells, but at different cellular locations depending upon the organism. In bacteria, ferrochelatase is found in the cytoplasm or associated with the cytoplasmic membrane; in higher plants it is found in both chloroplasts and mitochondria, while in yeast and mammalian cells, it is a mitochondrial inner-membrane associated protein, with its active site facing the mitochondrial matrix. Sequence data is available for more than 30 prokaryotic and eukaryotic ferrochelatases, but so far not Archaebacteria including bacteria, plants and animals. In the case of the latter, their overall sequence homology is rather low, with only about 20 amino-acid residues being invariant, some of which have been shown to be directly involved in catalysis (Kohno *et al.*, 1994; Gora *et al.*, 1996). Mutations in the ferrochelatase gene in humans can cause erythropoietic protoporphyria (Lamoril *et al.*, 1991). The three-dimensional structure of *Bacillus subtilis* ferrochelatase, a water-soluble protein of 310 amino-acid residues, has been determined at a resolution of 0.19 nm (Al-Karadaghi *et al.*, 1997). The structure has been compared to known protein structures, and it was found that the overall fold of ferrochelatase was most similar to that of bacterial periplasmic binding proteins. The polypeptide is folded into two similar domains each with a four-stranded parallel β-sheet flanked by α-helices (Figure 7.2, Plate 13). Structural elements from both domains build up a cleft that contains several of the invariant amino-acid residues, including His-183, which is found to bind the metal ion in crystals soaked with gold and cadmium solutions. It has previously been suggested that this histidine is involved in binding of ferrous ions. It is proposed that porphyrin binds in the structurally conserved cleft, which also includes the metal-binding site, and that the cleft region is likely to have different conformations upon substrate binding and release. The ferrochelatase sequences of some species (as compared to the *B. subtilis* protein) have *N*- and *C*-terminal extensions that may form additional structural elements not present in the *B. subtilis* enzyme. Mammalian ferrochelatases, contain an essential nitric-oxide

sensitive [2Fe−2S] cluster coordinated by four cysteine residues whose spacing in the primary sequence is unique to animal ferrochelatase, and is also found in the enzyme from *Drosophila melanogaster* (Sellers *et al.*, 1998). Three of them are located in the *C*-terminal extension (Cys-403, Cys-406 and Cys-411) while the fourth is Cys-196 (Sellers *et al.*, 1998; Crouse *et al.*, 1996). Human ferrochelatase has been crystallized (Burden *et al.*, 1999): the crystals diffract to resolution higher than 0.2 nm. The enzyme is a homodimer with one [2Fe−2S] cluster/subunit with a midpoint potential of −453 mV. As in the *B. subtilis* enzyme, each subunit is made up of two superposable domains and two extensions, one associated with the iron−sulfur cluster and one which lines the surface of the active site cleft (Dailey, 1994). The redox state of the enzyme is not important for function, suggesting that, while the iron−sulfur cluster may be required for structural reasons, it is not involved in the reaction. A chimeric mutant has been constructed, which is predominantly human, but with the last 40 amino acids from *S. cerevisiae*; it does not have a [2Fe−2S] cluster, but is still active (Medlock and Dailey, 2000).

   Many invariant residues which have been shown to be important for enzyme activity are distributed in and around the cleft, strongly supporting the suggestion that protoporphyrin IX binds there, including metal-binding residue His-183. Figure 7.2(b) presents a proposal for the active site of ferrochelatase with the protoporphyrin molecule modelled into the site. The porphyrin is oriented with its propionyl groups directed towards the surface of the molecule, where Arg-30 and Arg-31 are located. The presence of bound metal in the crystal structure suggests that porphyrin binding is not a prerequisite for metal-ion binding. The general mechanism for porphyrin metallation, deduced from non-enzymic systems, involves the following steps: deformation of the tetrapyrrole macrocycle; outer-sphere complex formation; breaking of bonds between the metal and the protein ligands; first metal−nitrogen bond formation, followed by second metal−nitrogen bond formation; and finally release of two protons and the completion of metallo-porphyrin formation (Hambright and Chock, 1974; Lavallee, 1988). The function of ferrochelatase would be to accelerate the rate-limiting steps, namely tetrapyrrole distortion, outer sphere coordination, protein ligand dissociation from the metal and proton extraction from the porphyrin. How this is achieved remains to be established, but the investigation will be greatly helped by determination of the structures of the enzyme with substrate and substrate analogues, and help our understanding of the molecular mechanisms behind erythrpoietic porphyria.

7.1.3 Friedrich's Ataxia and Mitochondrial Iron Metabolism

Friedrich's ataxia, the most common of early-onset inherited ataxias,[†] accounts for about one half of all cases of hereditary ataxia reported in Europe and the USA. The gene, which has only five exons, codes for a small protein called frataxin, of 210 amino acids. The most common mutation is the expansion of a

---

[†] Ataxia – total or partial inability to coordinate voluntary bodily movements, particularly muscular movements. Friedrich's ataxia, an autosomal recessive trait with a prevalence of about 2 per 100 000, is a lethal disease, defined as neurological (affecting the nervous system), but most patients die from cardiomyopathy.

GAA trinucleotide repeat: normal individuals may have up to 27 repeats, whereas affected individuals have in excess of 100 repeats. While the normal frataxin protein continues to be synthesized, the expanded repeat decreases the amount of protein which is produced (reviewed in Kaplan, 1999). As we saw in Chapter 4, although the frataxin sequence gave little indication concerning its function, studies with the yeast orthologous protein YFH1 showed that reduced levels of the protein led to an increase in mitochondrial iron concentration, accompanied by decreased mitochondrial respiration (Kaplan, 1999). Indeed it was clear that there is a dynamic mitochondrial iron cycle (Radisky *et al.*, 1999), involving both mitochondrial iron import and export, but also showing that mitochondria can export iron not only in the form of haem, but also in the form of iron–sulfur clusters (Kispal *et al.*, 1997). Frataxin is localized to mitochondria and is highly expressed in neuronal and cardiac tissue (Kaplan, 1999). Iron deposits have been found in the myocardium of Friedrich's ataxia patients, and myocardial respiration has been found to be defective: cardiac biopsies revealed deficits in iron–sulfur enzymes, without any apparent effect on activities of tricarboxylic acid cycle enzymes (Rötig *et al.*, 1997). It now seems well established that Friedrich's ataxia is a mitochondrial disease (Kaplan 1999), but the mechanisms responsible for the mitochondrial defect remain to be established, although all of the indications are that, as in yeast, they are associated with excessive mitochondrial iron accumulation, particularly in brain and cardiac tissue.

The uptake of iron by mitochondria from potential components of the LIP, has been studied. Saturable and reversible binding to mitochondria of iron complexed to ATP, pyrophosphate, nitrilotriacetate, citrate, ADP and GTP has been observed, but we are still no wiser as to the nature of the transporter. Genes homologous to the CCC1 gene, which suppresses mitochondrial damage in the yeast model of Friedrich's ataxia by limiting mitochondrial iron accumulation, have been found in plants, bacteria and the archae, but not in either invertebrates (*C. elegans*) or vertebrates (Chen and Kaplan, 2000). At the moment in time when we begin to realize the potential toxicity of excess iron in mitochondria, we desperately need to understand how mitochondrial iron homeostasis is regulated, and in particular how mitochondria take up iron.

7.1.4 Synthesis of Non-haem Iron Centres

As we saw in Chapter 2, iron-sulfur clusters are found ubiquitously as functional units in many redox, catalytic or regulatory processes. However, it is only recently that the biosynthesis of Fe/S proteins has been subjected to analysis by the combination of genetic and biochemical approaches. Clearly, the first requirement for the biosynthesis of Fe/S clusters is for enzymes that can produce elemental sulfur from cysteine and, furthermore, that can carry this sulfur in the form of protein-bound persulfide to the sites of synthesis. Studies on the biosynthesis of the metalloclusters of nitrogenase in *Azotobacter vinelandii* led to the identification of NifS and NifU as essential components for full activation and cluster assembly in both nitrogenase component proteins. On the basis of sequence homology with the *nif* genes that specifically target nitrogenase Fe–S cluster biosynthesis, an *isc*

(iron−sulfur cluster) gene cluster was identified in a wide range of prokaryotes (both nitrogen-fixing and not), and proposed to be responsible for general Fe−S cluster biosynthesis. Two of the nine *isc* genes, *iscS* and *iscU*, are homologous to NifS and NifU. The Isc proteins in general, and IscS and IscU in particular, have been widely conserved throughout evolution, underlining the idea that Fe−S clusters are among the most ancient types of prosthetic groups. IscU is considered to be one of the most conserved amino-acid sequences in nature (Hwang *et al.*, 1996). In the past 2 years, proteins homologous to the prokaryotic *iscS* and *iscU* gene products have been shown to be involved in Fe−S cluster assembly in eukaryotes (Kispal *et al.*, 1999; Schilke *et al.*, 1999; Strain *et al.*, 1998; Land and Rouault, 1998). IscS is a homodimeric pyridoxal phosphate-dependent L-cysteine desulfurase which initiates Fe/S cluster formation by producing elemental sulfur and alanine (Zheng *et al.*,1993). It was predicted that the putative active intermediate for the delivery of zero valency sulfur would be an enzyme-bound persulfide (Zheng *et al.*, 1994), formed by nucleophilic attack of an active-site Cys residue on the pyridoxal−phosphate-bound substrate, L-cysteine. Recent X-ray crystal analysis of two members of this general class of enzymes have confirmed this mechanistic proposal (Kaiser *et al.*, 1999; Fujii *et al.*, 2000). IscU corresponds to the *N*-terminal domain of NifU, and recent studies have indicated that IscU functions as a scaffold for the IscS-mediated assembly of both [2Fe−2S] and [4Fe−4S] clusters that are subsequently used for the maturation of apo Fe−S proteins (Agar *et al.*, 2000).

Although in eukaryotic cells Fe−S proteins are localized in mitochondria, the cytosol and the nucleus, mitochondria are the main sites of Fe−S cluster biosynthesis in the cell. Mitochondria contain an Fe−S cluster biosynthesis apparatus resembling that of prokaryotic cells, that consists of some ten proteins, including a cysteine desulfurase, a ferredoxin involved in reduction, and two chaperones (Lill *et al.*, 1999). The functional orthologue of IscS, the essential mitochondrial protein Nfs1p, is not only involved in generating mitochondrial Fe−S clusters, but is also necessary for the biosynthesis of extramitochondrial proteins (Kispal *et al.*, 1999). The mitochondrial ferredoxin Yah1 is also required both for generation of Fe−S proteins inside the mitochondria, and in the cytosol (Lange *et al.*, 2000). Export of components required for assembly of cytosolic Fe−S proteins is mediated by the ATP-binding cassette transporter Atm1p of the mitochondrial inner membrane (Kispal *et al.*, 1999; Leighton and Schatz, 1995). A possible substrate for Atm1p might be an Fe−S cluster that has been stabilized for transport. Constituents of the cytosol involved in the incorporation of Fe−S clusters into apoproteins, including the IRPs described later in this chapter, have not yet been described. Many of the mitochondrial proteins involved in Fe−S cluster formation are known to be essential. A conspicuous phenotypic consequence of defects in the biogenesis of Fe−S proteins is the drastic accumulation of iron within the mitochondria. To date, increases in mitochondrial iron concentration have been reported for Atm1p, Ssq1p, Nfs1p, Yah1p and a combined inactivation of Isu1p and Nfu1p (Kispal *et al.*, 1997; Knight *et al.*, 1998; Kispal *et al.*, 1999; Schilke *et al.*, 1999; Lange *et al.*, 2000). We discussed earlier the elevated iron levels found in mutants of the mitochondrial matrix protein, frataxin; a regulatory role for frataxin in Fe−S cluster assembly has been suggested, based on observed defects in the mitochondrial aconitase activity (Rötig *et al.*, 1997; Foury, 1999). In none of these cases do we understand the mechanism by which

unregulated iron uptake occurs. However, based on the specific function of Atm1p in the biosynthesis of extramitochondrial but not intramitochondrial Fe−S proteins (Kispal *et al.*, 1999), it has been proposed that an extramitochondrial Fe−S protein might play a decisive role in the regulation of iron uptake by the organelles (Lange *et al.*, 2000).

As discussed in Chapter 2, there are a number of important iron-containing enzymes which have neither haem nor Fe−S clusters. While we assume that they get their iron from the LIP, it is not yet established whether or not there are specific enzyme systems involved in the metal-ion insertion.

7.1.5 Intracellular Haem Degradation – Haem Oxygenase

Yet another source of iron within the cell is provided by the degradation of haem, which is catalysed by haem oxygenase. The enzyme haem oxygenase catalyses the NADPH, O_2 and cytochrome P_{450} reductase-dependent oxygenation of haem to iron, CO and biliverdin (Figure 7.3). Humans and other mammals have two isoenzymes, HO-1 and HO-2, which are products of separate genes. Human HO-1 is a 288-residue protein which is found at highest levels in the spleen, where recycling of erythrocytes takes place, but is also found in liver, where haem derived from cytochrome p_{450} is degraded, and in other tissues. It is regulated at the transcriptional level by porphyrins, metals, progesterone, and a variety of other molecules, and is involved in response to oxidative stress, ischaemia, hypoxia and other disease states. Human HO-2, a 316-residue protein, is constitutively expressed at high levels in the testis and some regions of the brain. This has led to the proposal that the principal role of HO-2 is the production of CO as a neural messenger. Some bacterial forms of HO have physiological importance for humans – the HO of *Corynebacterium diphtheriae* is important for pathogen acquisition of iron from host haem. All of the known HOs are homologous and their sequences align well throughout the length of the soluble 215 residue *C. diphtheriae* enzyme. Many, however, including HO-1 and HO-2, have *C*-terminal extensions with membrane anchors that are both localized in the microsomal membrane. Human haem oxygenase 1, which has had its crystal structure determined at 0.2 nm resolution (Schuller *et al.*, 1999), is not the full length HO-1 protein, but is a *C*-terminally truncated protein lacking the 55-residue membrane anchoring domain and which, like the bacterial and algal proteins, is soluble. It is, however, enzymatically active and interacts with its normal partner, cytochrome P_{450} reductase in a similar manner to the full length protein (Wilks *et al.*, 1995).

The reaction sequence of haem oxygenase is presented in Figure 7.3. In the first step, a ferrous haem−O_2 complex is thought to undergo an internal electron shift to form a ferric peroxyhaem intermediate, which then reacts regiospecifically with the α-bridge carbon to form α-hydroxyhaem. A second O_2 then reacts with α-hydroxyhaem, forming verdohaem and liberating CO. A third O_2 next reacts with verdohaem to form an enzyme-bound Fe(III)−biliverdin complex. On reduction of the iron atom, Fe^{2+} and biliverdin IXα are released from the enzyme. At various steps, reducing equivalents (indicated by [H]) are required. The microsomal haem oxygenases of animals derive these reducing equivalents from NADPH via the
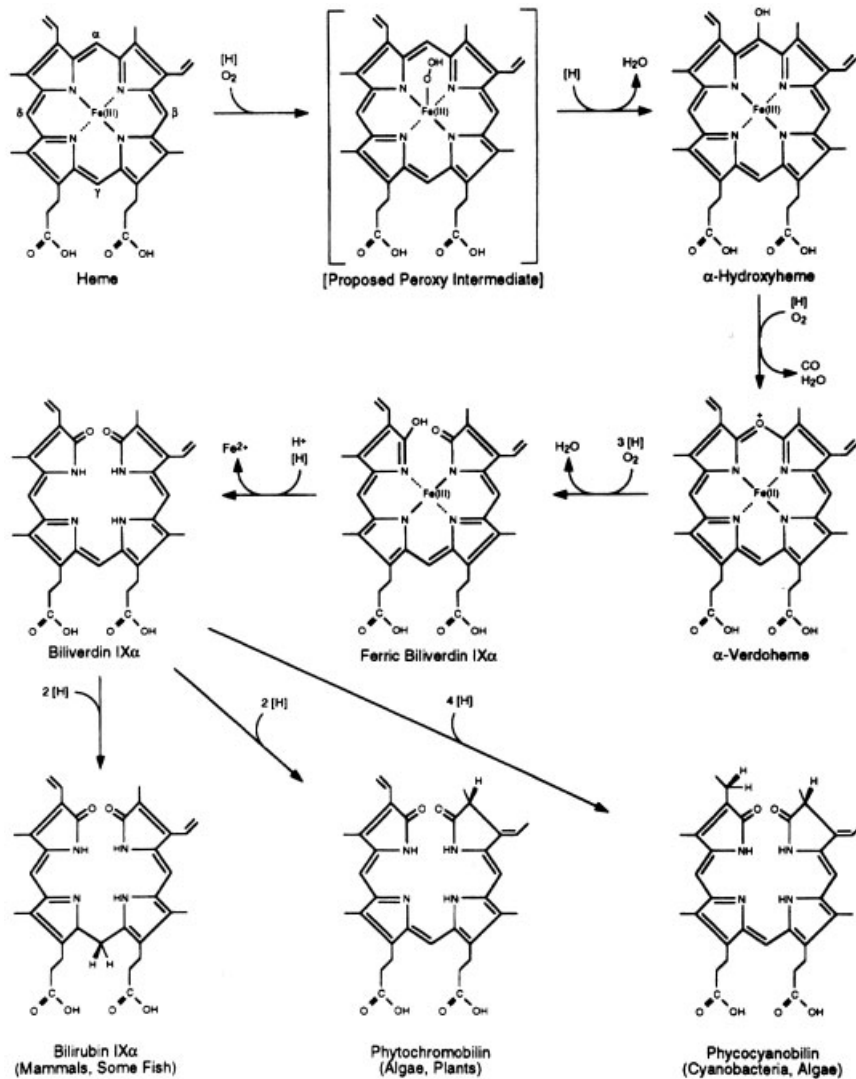
Figure 7.3 Reaction sequence for haem oxygenase. In the first step, a ferrous haem–O_2 complex is thought to undergo an internal electron shift to form a ferric peroxyhaem intermediate, which then reacts regiospecifically with the α-bridge carbon to form α-hydroxyhaem. Then a second O_2 reacts with α-hydroxyhaem, forming verdohaem and liberating CO. A third O_2 next reacts with verdohaem to form an enzyme-bound Fe(III)–biliverdin complex. On reduction of the iron atom, Fe^{2+} and biliverdin IXα are released from the enzyme. At various steps, reducing equivalents (indicated by [H]) are required. The microsomal haem oxygenases of animals derive these reducing equivalents from NADPH via the microsomal NADPH–cytochrome P_{450} reductase, whereas the soluble bacterial and algal enzymes get their reducing equivalents from ferredoxin. In mammals and some fish, biliverdin is reduced enzymatically to the potent antioxidant bilirubin, while in plants, algae and cyanobacteria, biliverdin is the precursor of photosensory pigments and light-harvesting pigments. From Beale and Jeh, 1999. Reproduced by permission of Nature Publishing Group.

microsomal NADPH-cytochrome P_{450} reductase, whereas the soluble bacterial and algal enzymes get their reducing equivalents from ferredoxin. In mammals and some fish, biliverdin is reduced enzymatically to the potent antioxidant bilirubin, while in plants, algae and cyanobacteria, biliverdin is the precursor of photosensory pigments and light-harvesting pigments. The degradation of haem still poses enigmas. How does haem oxygenase achieve its extraordinary regioselectivity, such that only the α-meso haem position is oxygenated? Why is the relatively inocuous haem molecule enzymatically transformed into a toxic product that is difficult to excrete (not only must biliverdin be reduced to bilirubin, but the latter must be glycosylated before it can be excreted in the bile)? And haem oxygenase also produces CO, which can potentially displace O_2 from haemoglobin and myoglobin. Yet another 'affaire à suivre'.

7.2   Metal Ion Homeostasis

Sometimes old ideas not only have a 'cachet', but a certain prescience, which years later becomes all too obvious. When the great French physiologist Claude Bernard[‡] talked of living organisms having two different 'environments' – that of their 'habitat' (their external environment which could change enormously, and indeed abruptly) and their 'mileu intérieur'(which needs to be kept more or less constant, otherwise the mechanisms of adaptation cannot function and the species will die) – he could have been speaking precisely about the major subject of this chapter, namely homeostasis. This is illustrated by a diagram attributed to Bertrand, in which the efficacy of a chemical substance (for example a metal ion) for the well-being of a biological system is represented as a function of its concentration. As the concentration increases, biological function gets better, until a plateau is reached, where a little bit more or less, doesn't matter. However, beyond this plateau, increasing concentrations of the substance have toxic effects – don't forget that even sodium chloride or water for that matter are toxic in excess. So the basic definition of homeostasis, whether for a metal ion, like iron, or anything else, is to maintain the 'milieu intérieur' at an appropriate level, but not to allow it to fall below minimum requirements, nor to exceed toxic levels.

   Iron homeostasis in mammalian cells is regulated by balancing iron uptake with intracellular storage and utilization. As we will see, this is largely achieved at the level of protein synthesis (translation of mRNA into protein) rather than at the level of transcription (mRNA synthesis), as was the case in microorganisms. This is certainly not unrelated to the fact that not only do microbial cells have a much shorter division time than mammalian cells, but that one consequence of this is that the half-life of microbial mRNAs is very much shorter (typically minutes rather than the hours or often days that we find with mammals). This makes it much easier to control levels of protein expression by changing the rate of specific mRNA synthesis by the use of inducers and repressors. So how do mammalian cells

[‡] His affirmation 'La methode, c'est toute' could also be taken today as the anthem of the genomics movement, except that they have not realized the irony of the obvious; namely that gene sequences neither tell us what the protein in question looks like, nor even more importantly, what it does.

arrange to regulate the translation of stable mRNAs? A relatively simple but effective solution to this problem was suggested some 30 years ago by the Russian biochemist Alex Spirin[¶], namely, that the translational control of specific mRNAs might be mediated by specific proteins (Spirin, 1969). Regulatory sequences in mRNAs are generally located in the non-coding or untranslated regions (UTRs) of the mRNA, situated at the 5′- and 3′-extremities of the coding part of the mRNA sequence: those in the former are usually associated with the initiation of translation, in other words ribosome binding, whereas those at the 3′-UTR are associated with mRNA stability and degradation, i.e. mRNA turnover. We now recognize that, if such RNA-binding proteins could bind to some mRNAs in their 5′-UTRs to prevent their translation, and to other mRNAs in their 3′-UTRs to prevent their degradation by intracellular ribonucleases, this would constitute the kind of reciprocal regulatory system that we are looking for – and this is precisely the system that was found for the iron storage and uptake proteins, ferritin and the transferrin receptor.

Fifty-five years ago, the expression of ferritin in animal cells was found to be directly regulated by changes in dietary iron (Granick, 1946). Twenty years later, it was proposed that this regulation involved translational control (Drysdale and Munro, 1966). Hamish Munro and his colleagues then showed[§] that the activation of ferritin synthesis in iron-loaded rats is insensitive to transcription inhibitors, and is associated with a shift of ferritin mRNA from translationally inactive ribonucleoprotein particles to polyribosomes, which are active in protein biosynthesis. This established beyond any doubt that this regulation cannot be at the level of transcription but must operate at the level of translation (Zähringer *et al.*, 1976). Direct measurement of ferritin mRNA levels confirmed the translational control of ferritin synthesis. In the absence of any change in ferritin mRNA levels, differences of up to two orders of magnitude in rates of ferritin protein biosynthesis were observed (Cairo *et al.*, 1985; Aziz and Munro, 1986; Rouault *et al.*, 1987).

The 5′-UTRs of both H- and L-chain ferritin mRNAs from a number of species contain putative stem-loops (Aziz and Munro, 1987) in which there is a highly conserved sequence of 28 nucleotides showing almost perfect homology (97 % phylogenetic sequence conservation) for both H and L mRNAs isolated from many animal species (human, rat, mouse, rabbit, chicken and frog). These sequences are known as iron regulatory elements (IREs) and they also have extensive homology with the single IRE found in both the 5′-UTR of erythroid-cell δ-aminolaevulinate synthase and mitochondrial aconitase, as well as with those found in the 3′-UTR of transferrin receptor mRNA. The IREs form hairpin structures in the respective

---

[¶] It is an unfortunate consequence of the use of Christian name abbreviation (A. Spirin), that Alex always evokes for me a well known analgesic, antipyretic and antiinflammatory agent, which John Vane showed in 1971 to be an inhibitor of the synthesis of prostaglandins from arachadonic acid.

[§] It would be impossible not to mention here Hamish Munro, one of my teachers at Glasgow University, whose enormous contribution to the elucidation of the regulation of ferritin synthesis was of fundamental importance. Apart from being an outstanding scientist, Hamish had a vein of humour which was typically Scottish. Two examples will suffice: a question posed to 2nd year medical students asked them to reflect on the reasons for a high incidence of scurvy in bachelors and widowers in the West of Scotland (simple explanation: they don't cook potatoes, which are the principal source of vitamin C in the population). Solution proposed by a promising future high flying medic – this presumably indicates that vitamin C is synthesized in the human body during sexual intercourse: or, of course, there were statistics based on a population of the British medical profession 'broken down by age and sex'.

mRNAs, that are recognized by *trans*-acting proteins, known as iron-regulatory proteins (IRPs), which control the rate of mRNA translation or stability.

7.2.1 Structural Features of IREs

The presence of IREs in vertebrates (mammals, birds and amphibia), and also in invertebrates (arthropods and molluscs) confirms their early evolutionary origin. It also corroborates evidence of the conservation of IRE-binding activity in annelid worms and insects, and the lack of such activity in yeast, bacteria or plants (reviewed in Hentze and Kühn, 1996). Their primary structure is highly conserved in evolution, suggesting precise structural constraints in their secondary and tertiary structure necessary for binding to IRPs. The sequences of the IREs found in vertebrate mRNAs for ferritin H and L subunits, erythroid cell δ-aminolaevulinate synthase and mitochondrial aconitase show 96–99 % identity, and even when invertebrates are included, sequence conservation is still very high. In contrast the IREs found in the 3′-UTR of TfR mRNAs (stability IREs), while highly conserved among themselves, share only 35–52 % sequence identity with the group of IREs found in the 5′-UTR (translation IREs). The canonical IRE is predicted to be capable of forming a stable stem-loop with an upper part consisting of double-stranded, five-base-pair long helix of variable sequence, topped by a six-nucleotide loop with the concensus sequence 5′-CAGUGN-3′. A small asymmetrical bulge is found invariably below the paired stem which contains a conserved unpaired C as the first nucleotide 5′ of the stem (Hentze *et al.*, 1988), followed by a second base-paired region, again of variable sequence which stabilizes the IRE hairpin (Figure 7.4a). The bulge with a single unpaired C is characteristic of some IREs, while in others (notably ferritin IREs) the bulge consists of the C and two additional 5′ nucleotides across from an single free 3′ nucleotide. When compared with the translation IREs, the TfR IREs have many more AU base pairs in their lower stems: three of the five (a, b, e) have 100 % AU base pairs in the lower stems, the other two (c, d) have 80 %. This contrasts with 40 % AU base pairs in the lower stems of translation IREs. Multiple AU-rich sequences are a feature of other rapid-turnover elements of several mRNAs, such as *c-myc*, *c-fos*, interleukin-2 and interleukin-6 (reviewed in Theil, 1998). Extensive studies have been carried out on sequence and structure constraints for recognition. Wild-type IRE's bind to IRP-1 with high affinity (K_d of the order of 10–30 pM) (Haile *et al.*, 1989; Barton *et al.*, 1990). However, deletions, particularly in the loop or the bulge region, drastically reduce binding to IRP-1 (Hentze *et al.*, 1987; Henderson *et al.*, 1994; Jaffray *et al.*, 1993). Point mutations which disrupt the upper helix were found to be non-functional, whereas complementary mutations restoring the double strandedness are tolerated (Barton *et al.*, 1990; Leibold *et al.*, 1990; Bettany *et al.*, 1992). Exchanges in the first five loop nucleotides and the bulge nucleotides usually cause a marked decrease in binding to IRP-1 (Barton *et al.*, 1990; Leibold *et al.*, 1990; Jaffray *et al.*, 1993; Henderson *et al.*, 1994).

An extensive analysis of the best IRP-1 binding sequences (from a pool of 16 384 different IRE variants) showed that the selected consensus corresponded exactly to the phylogenetically conserved IRE motif (Henderson *et al.*, 1994). A certain number of single or double mutations was tolerated at virtually every permuted position.
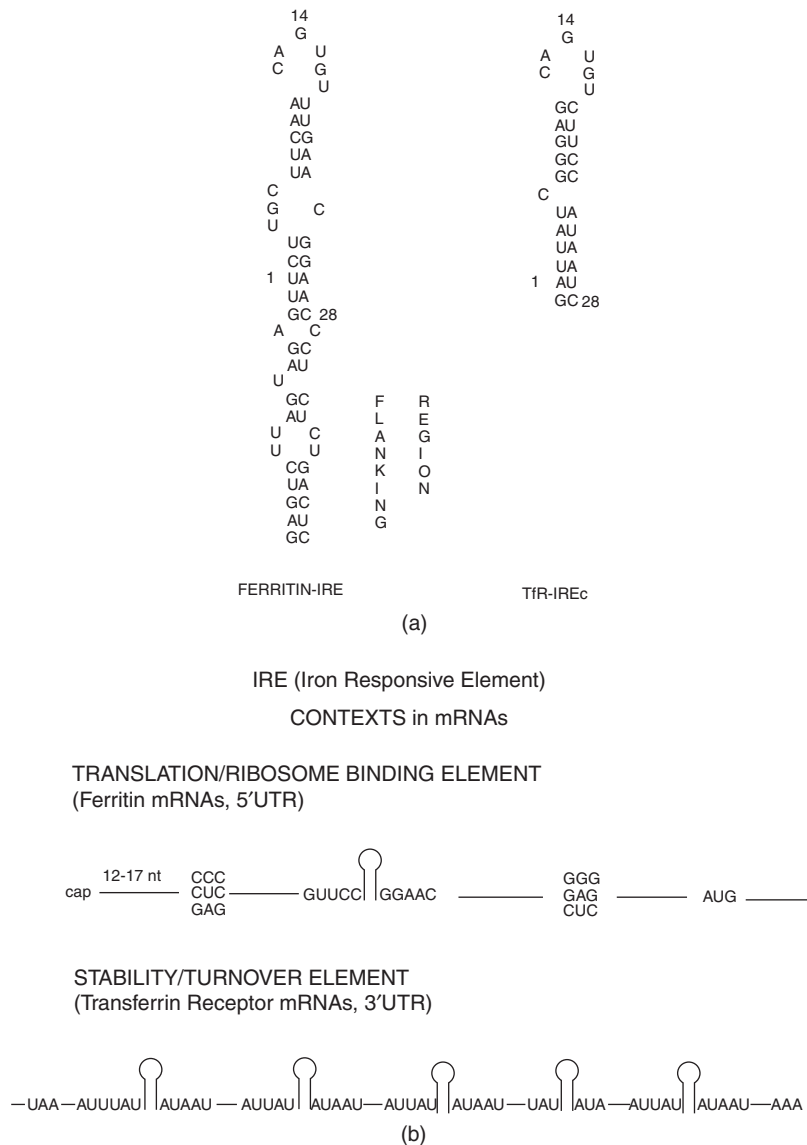
Figure 7.4 (a) IREs in eukaryotic mRNAs: the secondary structures of ferritin and transferrin receptor IREs. (b) The IRE localization in mRNAs: the translation/ribosome binding element in the 5′-UTR of ferritin mRNA is above, that of the stability/turnover element in the 3′-UTR of transferrin receptor mRNA is below. Adapted from Theil, 1998, by courtesy of Marcel Dekker, Inc.

Evidence was also found for an interaction between nucleotides one and five of the loop (Figure 7.4a). Double mutations at loop residues C^1 and G^5 altered to U^1 and A^5 were frequently selected, and they bound IRP-1 with affinities similar to wild-type IRE (Henderson *et al.*, 1994), as did a G^1C^5 (but not a A^1U^5) pair (Henderson *et al.*, 1996). Base interactions within the loop have also been observed in NMR studies of the IRE structure (Sierzputowsa-Gracz *et al.*, 1995). IRE mutants were found which selectively bind to IRP-1, but not to IRP-2 (Henderson *et al.*, 1994); a set of double

mutants specific for IRP-2 have also been described (Henderson *et al.*, 1996). The relevence of selective binding of one or other of the IRPs by IREs in a physiological context remains unclear.

7.2.2 Hereditary Hyperferritinaemia – Cataract Syndrome

However, mutations in the IRE of the ferritin L subunit mRNA and its gene have been found to be associated with an unusual autosomal dominant disorder, first described in 1995 in two families, one French and one Italian, as the Hereditary Hyperferritinaemia–Cataract Syndrome (HHCS) (Girelli *et al.*, 1995a,b; Bonneau *et al.*, 1995). The condition is characterized by the combination of congenital bilateral cataract and marked elevation of serum ferritin levels (>1000 µg/l). The hyperferritinaemia was found not to be related to iron overload and entirely due to the increase of the L-subunit, as determined by subunit-specific immunoassay. It was clearly distinguishable from genetic haemochromatosis because of (i) dominant transmission; (ii) lack of any relation with HLA, and (iii) normal to low serum iron and transferrin saturation without evidence of parenchymal iron overload. When patients with the syndrome are subjected to unnecessary phlebotomies, they rapidly develop iron-deficient anaemia (reversed by iron therapy), despite persistently elevated levels of serum ferritin. The initial description of HHCS was rapidly followed by molecular characterization; they were shown to have a single base substitution, the **Paris** mutation at position 13 (A to G) and the **Verona 1** mutation at position 14 (G to C) (Beaumont *et al.*, 1995; Girelli *et al.*, 1995a,b), both in the IRE loop (Figure 7.4). Several other mutations have subsequently been described: in **Pavia 1**, a single base change in the bulge (G5 to A) and in **Pavia 2** two single base changes in the lower stem (Cazzola *et al.*, 1997) are characterized by moderately elevated serum ferritin levels associated with mild cataract and asymptomatic cataract respectively. In **Verona 2**, a 29 base-pair deletion removes the whole 5′ sequence involved in base pairing to form the IRE stem (Girelli *et al.*, 1997) resulting in severe cataract. All of the mutations are assumed, to varying degrees, to affect IRP-binding, and to result in the worst cases in quasiconstitutive synthesis of L-subunit ferritin. In a recent study (Allerson *et al.*, 1999) *in vitro* binding affinity of IRP for HHCS mutant IREs was measured and it was found that decreases in binding affinity correlated with clinical severity. Analysis of ferritins in lympho-blastoid cell lines and in the lenses of subjects with HHCS (Levi *et al.*, 1998) showed that in HHCS cells, L-ferritin levels were up to twenty-times higher than in control cells, with about half of the L-chain assembled in homopolymers which did not incorporate iron. L-Chain accumulation also takes place in the lens, where it may induce cataract formation by altering the equilibrium between other water-soluble proteins, particularly crystallins and/or antioxidant properties. It had been reported that lens epithelial cells actively synthesize ferritin, especially in response to oxidants (McGahan *et al.*, 1994). However, in more recent studies, although high levels of L-ferritin mRNA were found in lenses from guinea pigs and humans (similar to those of major lens crystallins), lens ferritin was undetectable by Western blots (Cheng *et al.*, 2000). The mechanism of cataract formation in HHCS remains obscure, although it seems likely that cataract formation is a direct consequence of

cellular L-ferritin overproduction. At the very least, HHCS should be considered as a serious possibility by haematologists in the differential diagnosis of unexplained hyperferritinaemia.

7.2.3   mRNA Translation – IRE Translation Regulators

The location of the IRE in the 5′-UTR of ferritin mRNA suggested that it functioned to control initiation of translation and ribosomal binding. Deletion of the 5′-UTR of human H chain mRNA led to a constitutively high level of mRNA translation and all short term iron regulation was lost (Hentz *et al.*, 1987; Aziz and Munro, 1987). Further deletion analysis and cloning of the sequence into the 5′-UTR of two different reporter genes identified a region approximately 35 bases long, that is both necessary and sufficient for translational regulation by iron (Hentze *et al.*, 1987; Caughman *et al.*, 1988). The position of the single-copy 5′-UTR IREs in ferritin, erythroid cell δ-aminolaevulinate synthase and mitochondrial aconitase mRNAs is absolutely crucial for their activity as translational regulators. They are all located within 40 nucleotides or fewer from the 5′- m^7G cap of the mRNA (Figure 7.4), and when IRP binds, the complex prevents the stable association of the small ribosomal complex (the 43S preinitiation complex) with mRNA (Gray and Hentze, 1994). The functional importance of this is evident: placement of an IRE of more than 60 nucleotides downstream from the cap permits 43S preinitiation complex binding, and profoundly decreases translational control by IRE/IRP complexes in transfected cells (Goosen *et al.*, 1990; Goosen and Hentze, 1992). In more recent studies it has been shown that although the cap-binding complex eIF4F assembles even when IRP-1 is bound to the cap-proximal IRE, this assembly is futile, because bridging interactions between eIF4F and the small ribosomal subunit cannot be established in the presence of IRP-1 (Muckenthaler *et al.*, 1998).

The way in which ferritin and erythroid δ-aminolaevulinate synthase are regulated by IRP is illustrated in Figure 7.5. In (A), with IRP not bound to the IRE (1) binding of the 43S pre-initiation complex (consisting of the small ribosomal 40S subunit, plus the ternary complex containing the initiator Met-tRNA$_i$^{Met}, eukaryotic initiation factor eIF-2 and GTP) to the mRNA is assisted by initiation factors associated with this complex, as well as additional eukaryotic initiation factors (eIFs) which interact with the mRNA to facilitate 43S association. Subsequently (2), the 43S preinitiation complex moves along the 5′-UTR towards the AUG initiator codon, (3) GTP is hydrolysed, initiation factors are released and assembly of the 80S ribosome occurs. Protein synthesis from the Open Reading Frame (ORF) can now proceed. In (B) with IRP bound to the IRE, access by the 43S pre-initiation complex to the mRNA is sterically blocked, and no protein synthesis can occur. Despite the presence of high and relatively invariable concentrations of the corresponding mRNA, in the presence of active IRP-1/2, competition for binding to their respective binding sites means that IRP-1/2 bound to the IRE prevents the stable association of the 43S complex and translation of this mRNA.

The regulatory network of IRPs appears also to connect the synthesis of protoporphyrin IX in erythroid cells, and of certain mitochondrial iron−sulfur proteins to iron bioavailability (reviewed in Hentze and Kühn, 1996). mRNAs encoding erythroid
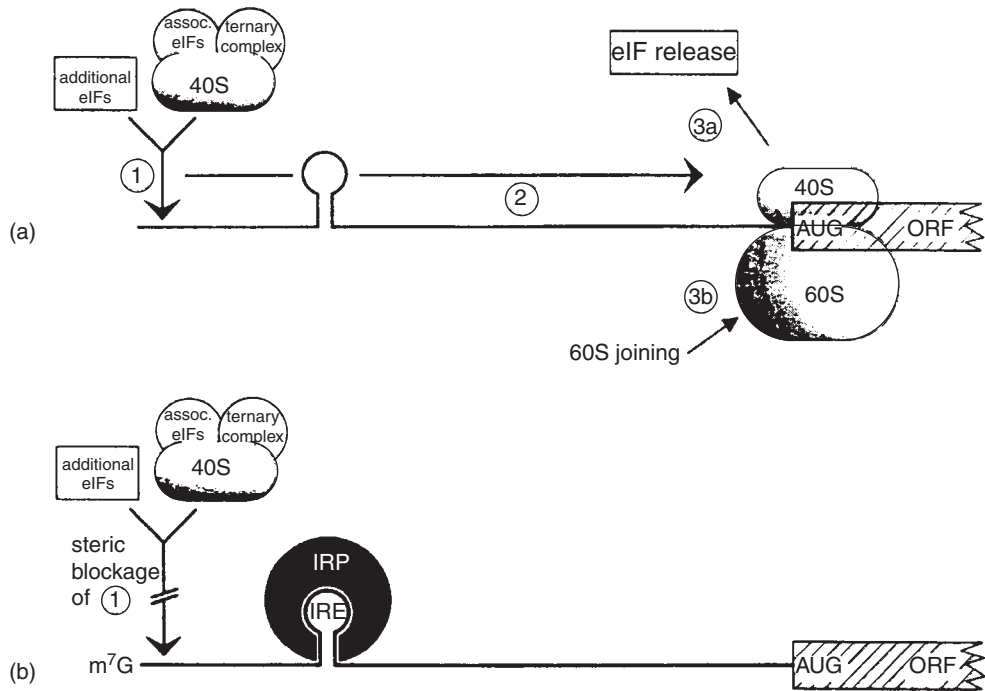
Figure 7.5   Model of ferritin (and erythroid α-aminolaevulinate synthase) translation/ribosome binding regulation by IRP. In (a), with IRP not bound to the IRE (1) binding of the 43S preinitiation complex (consisting of the small ribosomal 40S subunit, GTP and Met–tRNA^{Met}) to the mRNA is assisted by initiation factors associated with this complex, as well as additional eukaryotic initiation factors (eIFs) that interact with the mRNA to facilitate 43S association. Subsequently (2), the 43S preinitiation complex moves along the 5′-UTR towards the AUG initiator codon, (3) GTP is hydrolysed, initiation factors are released and assembly of the 80S ribosome occurs. Protein synthesis from the open reading frame (ORF) can now proceed. In (b) With IRP bound to the IRE, access of the 43S preinitiation complex to the mRNA is sterically blocked. From Gray and Hentze, 1994, by permission of Oxford University Press.

δ-aminolaevulinate synthase, mammalian mitochondrial aconitase and mitochondrial succinate dehydrogenase subunit b of *Drosophila melanogaster*, each has an IRE in their 5′-UTR, that seems to function in a similar way to ferritin mRNA, namely acting as translational control elements. The inhibitory effect of activated IRPs on erythroid δ-aminolaevulinate synthase, the first enzyme of the haem biosynthesis pathway, could serve to reduce excessive protoporphyrin IX production under conditions of iron insufficiency, although this remains to be established (we refer the reader to the previous section on haem biosynthesis, particularly the different regulation of this pathway in liver as compared to erythroid cells). Likewise, the link between iron and mitochondrial energy metabolism, while still unclear, could be related to the prevention of oxidative stress. As will be discussed in Chapter 8, the mRNA of the putative basolateral iron transport protein of the small intestine, IREG1 contains a functional IRE in its 5′-UTR (McKie *et al.*, 2000). Whether this functions in response to levels of enterocyte IRP activity remains to be established.

7.2.4 mRNA Stability – IRE Turnover Regulators

An IRE mRNA stability element has, until recently, only been found in the transferrin receptor mRNA. There are five IREs in the 3′-UTR of TfR mRNA, which are highly conserved (Figure 7.4). They all share the same structural features with other IRE's (folded hairpin loop sequence, stem with 9–10 base pairs and a C-residue in a bulge), sufficient for IRP recognition. Deletion mapping of the regulatory sequences has shown that they consist of two necessary areas of about 200 nucleotides each, separated by some 250 nucleotides (Müllner and Kühn, 1988; Casey *et al.*, 1988a). *In vitro* binding studies indicate that at least four IREs are accessible for IRP-binding (Müllner *et al.*, 1989). However, only some 250 nucleotides, including IREs B, C and D (Figure 7.6), are required for regulation (Müllner and Kühn, 1988; Casey *et al.*, 1989). Mutational studies confirmed this – when the minimally required IREs are mutated such that IRP cannot bind, the mRNA becomes constitutively unstable (Casey *et al.*, 1989), whereas mutations or deletions of the destabilizing regions, give rise to a constitutively stable mRNA (Casey *et al.*, 1988b; Müllner and Kühn, 1988; Casey *et al.*, 1989). Specific cleavage of TfR mRNA in the 3′-UTR close to the previously mapped instability elements has been identified, and, unlike several other unstable mRNAs, does not appear to require prior poly(A) tail shortening (Binder *et al.*, 1994). A model for the regulation of the transferrin receptor mRNA stability by IRE/IRP interactions in the 3′-UTR is presented in Figure 7.6. IRP binding protects the mRNA from an initial endonucleolytic clip, which occurs (presumably in a region between IRE_C and IRE_D) when the transcript is not protected.

One other case has been reported of an IRE in a 3′-UTR. The divalent cation transporter protein (DCT1, sometimes referred to as Nramp2) mRNA exists in two alternative splice forms, one of which has a stem loop structure in its 3′-UTR that closely resembles IREs. The structure, some 30 base pairs downstream from the translational stop codon, contains a consensus loop CAGUGN sequence after a single C-nucleotide bulge and a five-base-pair stem. There is an additional pyrimidine residue bulge on the opposite side of the stem, which is unique to DMT1 (Gunshin *et al.*, 1997). It is not known if the IRE in DCT1 mRNA regulates its stability via IRP binding as is the case for TfR.

7.2.5 Iron Regulatory Proteins 1 and 2

The first direct evidence that there are specific IRE-binding proteins came from the use of electrophoretic mobility shift assays and UVcross-linking using IRE-containing mRNAs (Leibold and Munro, 1988; Rouault *et al.*, 1988). Two closely related cytosolic IRE-binding proteins (now known as iron regulatory proteins – IRPs), designated IRP-1 and IRP-2 have now been identified in many mammalian cell types. They act as iron sensors, essentially by existing in two different conformations. When iron is in short supply, the IRPs can bind with high affinity to the IREs. When iron supply to cells is increased, IRP-1 is postranslationally inactivated, whereas IRP-2 is rapidly degraded. Both IRP-1 and IRP-2 have high affinities for wild-type IREs (Henderson *et al.*, 1993; Guo *et al.*, 1994; Samaniego *et al.*,
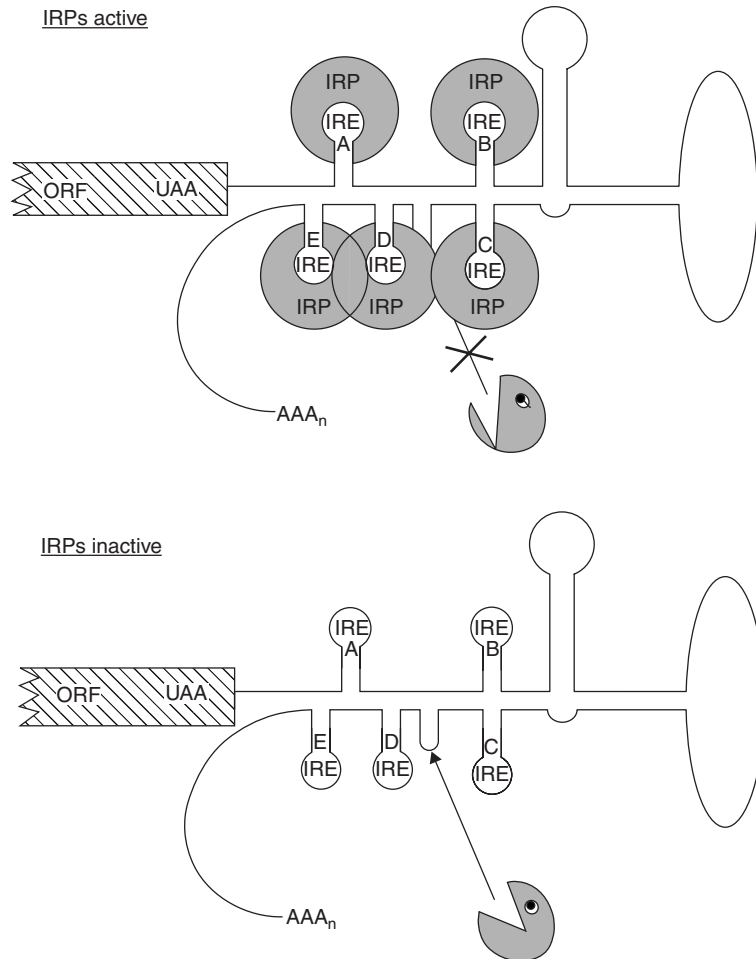
Figure 7.6 Model of regulation of transferrin receptor mRNA stability/turnover by IRE/IRP interactions in the 3′-UTR. The 3′-UTR of TfR mRNA including five IREs (A–E) and other structural features are indicated, including the stop codon UAA at the end of the open reading frame (ORF), and the poly-A tail. The bipartite regulatory region consists of the two areas that are separated by the large loop on the right, and that may be brought into closer proximity by long range RNA/RNA interactions. IRP binding (*top*) protects the mRNA from an initial endonucleolytic clip, which occurs (presumably in a region between IRE$_C$ and IRE$_D$) when the transcript is not protected (*bottom*). From Hentze and Kühn, 1996. Copyright (1996) National Academy of Sciences, USA.

1994), are strongly induced in iron-deficient cells, and rapidly lose their IRE-binding capacity after iron administration.

IRP-1 is expressed in all vertebrate tissues (Müllner *et al.*, 1992; Henderson *et al.*, 1993; Patino and Walden, 1992) with measured levels of between 50 000 to 100 000 molecules per cell (Müllner *et al.*, 1989; Haile *et al.*, 1989). In cultured cells, only about 10 % are active in IRE binding in normal medium, whereas the active IRP-1 pool reaches virtually 100 % after treatment with an iron chelator for 15 h. Alterations in IRP-1 activity occur without significant changes in the total amount

of IRP-1 (total IRP activity can be measured by addition of 2 % mercaptoethanol, which converts IRP-1 into an active IRE-binding form). Purification and cloning of IRP-1 showed that it is a monomeric cytoplasmic protein comprising 889 amino acids with a predicted molecular weight of 98 kD. The amino-acid sequence shows extensive homology to mitochondrial and bacterial aconitases, enzymes with a 4Fe−4S cluster involved in the conversion of citrate to isocitrate, including three cysteine residues (Cys-437, 503 and 506) which anchor the iron−sulfur cluster into the mitochondrial and bacterial enzymes (Hirling *et al.*, 1994). On the basis of the crystal structure of the mitochondrial aconitase, it is proposed that the apo-IRP-1 (without its iron−sulfur cluster) is able to bind to RNA (Figure 7.7, Plate 14) with high affinity, whereas the holo-IRP-1 (with the 4F−4S cluster) is unable to bind RNA, but has aconitase activity[||]. IRP-1 is presumed to form a four-domain protein with a deep cleft between domains 1−3 (coloured in green) and domain 4 (in blue), connected by a flexible hinge linker. Solution studies imply that amino-acid residues 121−130 and the region close to Cys-437 are directly in contact with IRE, and these are also coloured respectively in magenta and orange in Figure 7.7 (Paraskeva and Hentze, 1996). In the presence of ferrous iron and sulfide *in vitro*, and in iron−replete cultured cells, IRP-1 is converted into an aconitase. Mutagenesis of the three Cys residues thought to anchor the iron-sulfur cluster to Ser abolishes aconitase activity and leads to constitutive RNA binding (Hirling *et al.*, 1994). Cells that express such a protein are deregulated in both TfR and ferritin expression (De Russo *et al.*, 1995). The 4Fe−4S cluster-containing IRP-1 is inactive in IRE binding, whereas in iron deficient cells, the apoprotein form accumulates and is active in binding to IREs (Figure 7.8). The interconversion of these two forms constitutes the iron sensor referred to above, which in iron-replete cells allows ferritin synthesis to take place while in iron-deficient cells it increases transferrin receptor synthesis.

IRP-2 is less abundant than IRP-1 in most cells, and its tissue distribution indicates greatest expression in intestine and brain (Henderson *et al.*, 1993; Samaniego *et al.*, 1994). Human IRP-2 is 57 % identical and 79 % similar to human IRP-1, but is slightly larger with a molecular weight of 105 kD due to the presence of a 73 residue inclusion as compared to IRP-1. No aconitase activity has been found for IRP-2, although similar cysteine residues that coordinate the iron−sulfur cluster in IRP-1 are conserved in IRP-2 (Cys-512, -578 and -581). Whereas the apoprotein binds to IREs like IRP-1, in contrast to IRP-1, IRP-2 is degraded in iron-replete cells (Figure 7.8). This degradation is mediated through the 73 residue inclusion domain (Iwai *et al.*, 1995): its deletion stabilizes IRP-2, whereas when it is grafted onto IRP-1 it confers iron-dependent degradation of the hybrid protein. Pulse-chase experiments demonstrate that iron administration results in a threefold increase in the degradation rate of IRP-2, which is prevented by inhibitors which block proteosome[††] formation, but not by inhibitors of lysosomal proteases or calpain

---

[||] This figure is yet another example (see Chapter 5) of what might be considered Molecular Theology. On a more serious note we do not know what, if any, the physiological significance of a cytoplasmic aconitase might be, particularly since we do not know of any mammalian cytoplasmic pathways for isocitrate metabolism.

[††] Proteins which are destined for degradation by the proteosome are first modified by the enzyme-catalysed attachment of numerous molecules of the protein ubiquitin, through amino groups to the protein targeted for degradation. This marks out the protein for ATP-dependent hydrolysis by the 26S proteosome, releasing peptides and ubiquitin
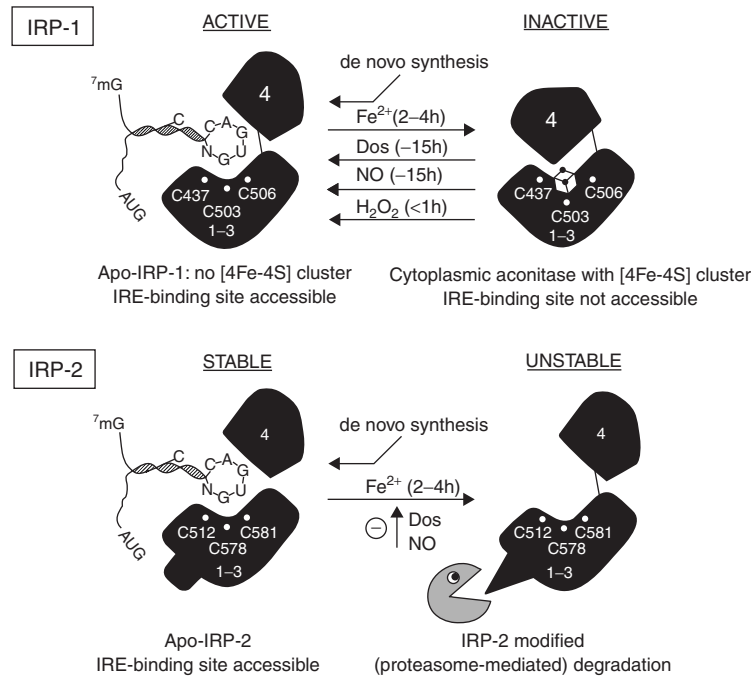
Figure 7.8 Regulation of IRP-1 and IRP-2. The two IRPs are shown as homologous four domain proteins that bind to IREs (left) In iron-replete cells, IRP-1 assembles a cubane Fe−S cluster that is liganded via cys-437, -503 and -506. Similar cysteines are conserved in IRP-2 (Cys-512, -578 and -581), but it is unresolved as to whether they also coordinate an Fe−S cluster. (right) In iron-replete cells, IRP-2 is targeted for destruction via a specific region (shaded in black), whereas IRP-1, with a 4Fe−4S cluster, is stable and active as a cytoplasmic aconitase. Multiple signals induce IRE-binding by IRP-1 with distinct kinetics. Whether or not NO and H_2O_2 induce IRP-1 by apoprotein formation remains to be addressed directly. From Hentze and Kühn, 1996. Copyright (1996) National Academy of Sciences, USA.

(Iwai *et al.*, 1995; Guo *et al.*, 1995). It seems therefore highly probable that the proteosome (and also ubiquitinylation) is involved in IRP-2 degradation.

A more detailed discussion of the role of IRPs in pathobiology, particularly the effects of oxygen and nitrogen-based free radicals on their activities is presented in Chapter 10. For a recent review see Cairo and Pietrangelo, (2000).

7.3 References

Agar, J.N., Krebs, K., Frazzon, J., Huynh, B.H., Dean, D.R. and Johnson, M.K. (2000). *Biochem.*, **39**, 7856−62.

Al-Karadahgi, S., Hansson, M., Nikonov, S., Jönsson, B. and Hederstedt, L. (1997). *Structure*, **5**, 1501−10.

Allerson, C.R., Cazzola, M. and Rouault, T.A. (1999). *J. Biol. Chem.*, **274**, 26439−47.

Aziz, N. and Munro, H.N. (1986). *Nucleic Acids Res.*, **14**, 915−27.

Aziz, N. and Munro, H.N. (1987). *Proc. Natl Acad. Sci., USA*, **84**, 8478−82.

Barton, H.A., Eisenstein, R.S., Bomford, A. and Munro, H.N. (1990). *J. Biol. Chem.*, **265**, 7000–8.

Beale, S.I. and Yeh, J.I. (1999). *Nature Struct. Biol.*, **6**, 903–5.

Beaumont, C., Leneuve, P., Devaux, I., Scoazec, J.-Y. *et al.* (1995). *Nature Genet.*, **11**, 444–6.

Bettany, A-J., Einsenstein, R.S and Munro, H.N. (1992). *J. Biol. Chem.*, **267**, 16531–1.

Binder, R., Horowitz, J.A., Basilion, J.P., Koeller, D.M., Klausner, R.D. and Harford, J.B. (1994). *EMBO J.*, **13**, 1969–80.

Bonneau, D., Winter-Fuseau, I., Loiseau, M.-N., Amati, P. *et al.* (1995). *J. Med. Genet.*, **32**, 778–9.

Breuer, W., Epsztejn, S. and Cabantchik, Z.I. (1995). *J. Biol. Chem.*, **270**, 24209–15.

Breuer, W., Epsztejn, S. and Cabantchik, Z.I. (1996). *FEBS Lett.*, **382**, 304–8.

Breuer, W., Greenberg, E. and Cabantchik, Z.I. (1997). *FEBS Lett.*, **403**, 213–9.

Burden, A.E., Wu, C., Dailey, T.A., Busch, J.L. *et al.* (1999). *Biochem. Biophys. Acta*, **1435**, 191–7.

Cairo, G. and Pietrangelo, A. (2000). *Biochem. J.*, **352**, 241–50.

Cairo, G., Bardella, L., Schiaffonati, L., Arosio, P., Levi, S. and Berneli-Zazzera, A. (1985). *Biochem. Biophys. Res. Commun.*, **133**, 314–21.

Casey, J.L., Di Jeso, B., Rao, K., Klausner, R.D. and Harford, J.B. (1988a). *Proc. Natl Acad. Sci., USA*, **85**, 1787–91.

Casey, J.L., Hentze, M.W., Koeller., D.M., Caughman, S.W. *et al.* (1988b). *Science*, **240**, 924–8.

Casey, J.L., Koeller, D.M., Ramin, V.C., Klausner, R.D. and Harford, J.B. (1989). *EMBO J.*, **8**, 3693–9.

Caughman, S.W., Hentze, M.W., Rouault, T.A., Harford, J.B. and Klausner, R.D. (1988). *J. Biol. Chem.*, **264**, 19048–52.

Cazzola, M., Bergamaschi, G., Tono, L., Arbustini, E. *et al.* (1997). *Blood*, **90**, 814–21.

Chen, O.S. and Kaplan, J. (2000). *J. Biol. Chem.*, **275**, 7626–32.

Cheng, Q., Gonzalez, P. and Zigler, J.S., Jr. (2000). *Biochem. Biophys. Res. Commun.*, **270**, 349–55.

Crichton, R.R. (1984). *Trends Biochem. Soc.*, **9**, 283–6.

Crichton, R.R., Soruca, J.A., Roland, F., Michaux, M.-A. *et al.* (1997). *Biochem.*, **36**, 15049–54.

Crouse, B.R., Sellers, V.M., Finnegan, M.G., Dailey, H.A. and Johnson, M.K. (1996). *Biochem.*, **35**, 16222–9.

Dailey, H.A., Finnegan, M.G. and Johnson, M.K. (1994). *Biochem.*, **33**, 403–7.

De Russo, P.A., Philpott, C.C., Iwai, K., Mostowski, H.S., Klausner, R.D. and Rouault, T.A. (1995). *J. Biol. Chem.*, **270**, 15451–4.

Drysdale, J.W. and Munro, H.N. (1966). *J. Biol. Chem.*, **241**, 3630–7.

Epsztejn, S., Kakhlon, O., Glickstein, H., Breuer, W. and Cabantchik, Z.I. (1997). *Anal. Biochem.*, **248**, 31–40.

Epsztejn, S., Glickstein, H., Picard, V., Slotki, I.N. *et al.* (1999). *Blood*, **94**, 3593–603.

Ferreira, G.C., and Huyn, B.H. (1994). *J. Biol. Chem.*, **269**, 7062–5.

Foury, F. (1999). *FEBS Lett.*, **456**, 281–4.

Fujii, T., Maeda, M., Mihara, H., Kurihara, T., Esaki, N. and Hata, Y. (2000). *Biochem.*, **39**, 1263–73.

Girelli, D., Olivieri, O., De Franceschi, L., Corrocher, R., Bergamaschi, G. and Cazolla, M. (1995a). *Br. J. Haematol.*, **90**, 931-.

Girelli, D., Corrocher, R., Bisceglia, L., Olivieri, O. *et al.* (1995b). *Blood*, **86**, 4050-3.

Girelli, D., Corrocher, R., Bisceglia, L., Olivieri, O. *et al.* (1997). *Blood*, **90**, 2084–8.

Goosen, B. and Hentze, M.W. (1992). *Mol. Cell. Biol.*, **12**, 1959–66.

Goosen, B., Caughman, S.W., Harford, J.B., Klausner, R.D. and Hentze, M.W. (1990). *EMBO J.*, **9**, 4127–33.

Gora, M., Grzybowska, E., Rytka, J. and Labbe-Bois, R. (1996). *J. Biol. Chem.*, **271**, 11810–6.

Granick, S. (1946). *J. Biol. Chem.*, **164**, 737–46.

Gray, N.K. and Hentze, M.W. (1994). *EMBO J.*, **13**, 3882–91.

Gunshin, H., McKenzie, B., Berger, U.V., Gunshin, Y. *et al.* (1997). *Nature*, **388**, 482-8.

Guo, B., Yu, Y. and Leibold, E.A. (1994). *J. Biol. Chem.*, **269**, 24252–60.

Guo, B., Phillips, J.D., Yu, Y. and Leibold, E.A. (1995). *J. Biol. Chem.*, **270**, 21645–51.

Haile, D.J., Hentze, M.W., Rouault, T.A., Harford, J.B. and Klausner, R.D. (1989). *Mol. Cell. Biol.*, **9**, 5055–61.

Hambright, P. and Chock, P.B. (1974). *J.Am. Chem. Soc.*, **96**, 3123-31.

Henderson, B.R., Seiser, C. and Kühn, L.C. (1993). *J. Biol. Chem.*, **268**, 27327–34.

Henderson, B.R., Menotti, E., Bonnard, C. and Kühn, L.C. (1994). *J. Biol. Chem.*, **269**, 17481–9.

Henderson, B.R., Menotti, E. and Kühn, L.C. (1996). *J. Biol. Chem.*, **271**, 4900–8.

Hentze, M.W. and Kühn, L.C. (1996). *Proc. Natl Acad. Sci., USA*, **93**, 8175–82.

Hentze, M.W., Rouault, T.A., Caughman, S.W., Dancis, A., Harford, J.B. and Klausner, R.D. (1987). *Proc. Natl Acad. Sci., USA*, **84**, 6730–4.

Hentze, M.W., Caughman, S.W., Casey, J.L., Koeller, D.M. *et al.* (1988). *Gene*, **72**, 201–8.

Hirling, H., Henderson, B.R. and Kühn, L.C. (1994). *EMBO J.*, **13**, 453–61.

Hwang, D.M., Dempsey, A., Tan, K.T. and Liew, C.C. (1996). *J. Mol. Evol.*, **43**, 536–40.

Iwai, K., Klausner, R.D. and Rouault, T.A. (1995). *EMBO J.*, **14**, 5350–7.

Jaffray, S.L., Haile, D.J., Klausner, R.D. and Harford, J.B. (1993). *Nucleic Acids Ras.*, **21**, 4627–31.

Kaiser, J.T., Clausen, T., Bourenkow, G.P., Bartunik, H.D., Steinbacher, S. and Huber, R. (2000). *J. Mol. Biol.*, **297**, 451–64.

Kaplan, J. (1999). *Proc. Natl Acad. Sci., USA*, **96**, 10948–9.

Kispal, G., Csere, P., Guiard, B. and Lill, R. (1997). *FEBS Lett.*, **418**, 346–50.

Kispal, G., Csere, P., Prohl, C. and Lill, R. (1999). *EMBO J.*, **18**, 3981–9.

Knight, S.A., Sepuri, N.B., Pain, D. and Dancis, A. (1998). *J. Biol. Chem.*, **273**, 18389–93.

Kohno, H., Okuda, M., Furukawa, T., Tokunaga, R. and Taketani, S. (1994). *Biochim. Biophys. Acta*, **1209**, 95–100.

Konijn, A.M., Glickstein, H., Vaisman, B., Meyron-Hotz, E.G., Slotki, I.N. and Cabantchik, Z.I. (1999). *Blood*, **94**, 2128–34.

Lamoril, J., Boulechfar, S., de Verneuil, J., Grandchamp, B., Nordamn, Y. and Deybach, J.-C. (1991). *Biochem. Biophys. Res. Commun.*, **181**, 594–9.

Land, T. and Rouault, T.A. (1998). *Mol. Cell*, **2**, 807–15.

Lange, H., Kaut, A., Kispal, G. and Lill, R. (2000). *Proc. Natl Acad. Sci., USA*, **97**, 1050–5.

Lavallee, D.K. (1988). *Mol. Struct. Energ.*, **9.**, 279–314.

Leibold, E.A. and Munro, H.N. (1988). *Proc. Natl Acad. Sci., USA*, **85**, 2171–5.

Leibold, E.A. and Laudano, A. and Yu, Y. (1990). *Nucleic Acids RES.*, **18**, 1819–24.

Leighton, J. and Schatz, G. (1995). *EMBO J.*, **14**, 188–95.

Levi, S., Girelli, D., Perrone, F., Past, M. *et al.* (1998). *Blood*, **91**, 4180–7.

Lill, R., Diekert, K., Kaut, A., Lange, H. *et al.* (1999). *Biol. Chem.*, **380**, 1157–66.

Lipinski, P., Drapier, J.-C., Oliviera, L., Retmanska, H., Sochanowicz, B. and Kruszewski, M. (1999). *Blood*, **95**, 2960–6.

McGahan, M.C., Harned, J., Grimes, A.M. and Fleisher, L.N. (1994). *Exp. Eye Res.*, **59**, 551–5.

McKie, A.T., Marciano, P. Raefs, A., Breman, K. *et al.* (2000). *Molecular Cell*, **5**, 299–309.

Medlock, A.E. and Dailey, H.A. (2000). *Biochem.*, **39**, 7461–7.

Muckenthaler, M., Gray, N.K. and Hentze, M.W. (1998). *Mol. Cell*, **2**, 383–8.

Müllner, E.W. and Kühn, L.C. (1988). *Cell*, **53**, 815–25.

Müllner, E.W., Neupert, B. and Kühn, L.C. (1989). *Cell*, **58**, 373–82.

Müllner, E.W., Rothenberger, S., Müllner, A.M. and Kühn, L.C. (1992). *Eur. J. Biochem.*, **208**, 597–605.

Paraskeva, E. and Hentze, M.W. (1996). *FEBS Letts.*, **389**, 40–3.

Patino, M.M. and Walden, W.E. (1992). *J. Biol. Chem.*, **267**, 19011–6.

Radisky, D.C., Babcock, M.C. and Kaplan, J. (1999). *J. Biol. Chem.*, **274**, 4497–9.

Rötig, A., de Lonlay, P., Chretien, D.,Foury, F. *et al.* (1997). *Nature Genet.*, **17**, 215–7.

Rouault, T.A., Hentze, M.W., Dancis, A., Caughman, S.W., Harford, J.B. and Klausner, R.D. (1987). *Proc. Natl Acad. Sci., USA*, **84**, 6335–9.

Rouault, T.A., Hentze, M.W., Dancis, A., Caughman, S.W., Harford, J.B. and Klausner, R.D. (1988). *Science*, **241**, 1207–10.

Samaniego, F., Chin, J., Iwai, K., Rouault, T.A. and Klausner, R.D. (1994). *J. Biol. Chem.*, **269**, 30904–10.

Schilke, B., Voisine, C., Beinert, H. and Craig, E. (1999). *Proc. Natl Acad. Sci., USA*, **96**, 10206–11.

Schuller, D.J., Wilks, A., Ortiz-de-Montellano, P.R and Poulos, T.L., (1999). *Nature Struct. Biol.*, **6**, 860–7.

Sellers, V.M., Wang, K.F., Johnson, M.K. and Dailey, H.A. (1998). *J. Biol. Chem.*, **273**, 22311–6.

Sierzputowsa-Gracz, H., McKenzie, R.A. and Theil, E.C. (1995). *Nucleic Acids Res.*, **23**, 146–53.

Spirin, A.S. (1969). *Eur. J. Biochem.*, **10**, 20–35.

Staubli, A. and Boelsterli, U.A. (1998). *Am. J. Physiol.*, **274**, G1031–7.

Strain, J., Lorenz, C.R., Bode, J., Garland, S. *et al.* (1998). *J. Biol. Chem.*, **273**, 31138–44.

Thomas, F., Serratrice, G., Beguin, C., Aman, E.S. *et al.* (1999). *J. Biol. Chem.*, **274**, 13375–83.

Theil, E.C. 1998). In *Metal Ions in Biological Systems* (eds Sigel, A. and Sigel, H.). **35**, 403–34.

Voet, D. and Voet, J.G. (1995). *Biochemistry*, Second edition, John Wiley & Sons, Chichester.

Weaver, J. and Pollack, S. (1989). *Biochem. J.*, **261**, 787–92.

Wilks, A., Black, S.M., Miller, W.L. and Ortiz de Montellano, P.R. (1995). *Biochem.*, **34**, 4421–7.

Zähringer, J., Baliga, B.S. and Munro, H.N. (1976). *Proc. Natl Acad. Sci., USA*, **73**, 857–61.

Zheng, L., White, R.H., Cash, V.L., Jack, R.F. and Dean, D.R. (1993). *Proc. Natl Acad. Sci., USA*, **90**, 2754–8.

Zheng, L., White, R.H., Cash, V.L. and Dean, D.R. (1994). *Biochem.*, **33**, 4714–20.

# 8 Iron Absorption in Mammals with Particular Reference to Man

8.1 Iron Metabolism in Man: An Overview

In humans the body iron content is normally 40–50 mg Fe/kg body weight with typically higher values in men than in women. Circulating red cells contain most of this iron bound in the haem prosthetic group of the oxygen transport protein, haemoglobin (about 30 mg Fe/kg). A further 4 mg Fe/kg is found in muscle in the form of the oxygen storage protein myoglobin, and about 2 mg Fe/kg in various tissues as other haemoproteins, iron–sulfur proteins and non-haem, non iron–sulfur proteins, the complexity of which has been reviewed in Chapter 2. Most of the remaining iron (10–12 mg Fe/kg in men and around 5 mg Fe/kg in women) is stored essentially in the liver, spleen, bone marrow and muscle, as ferritin and haemosiderin (see Chapter 6), while only a tiny fraction of total body iron, around 3 mg, circulates in the plasma and other extracellular fluids bound to the iron-transport protein, transferrin (Bothwell *et al.*, 1979). This transport compartment (see Chapter 5), despite its size, is by far the most dynamic iron compartment in the body because, as we have seen, its iron normally turns over at least ten times every day.

   The major pathways of internal iron exchange between different body compartments are well established in man (Figure 8.1). As we outline below, iron absorption and excretion are mutually adjusted and in the normal subject represent about 1 mg/day in each direction, such that iron is tightly conserved. Transferrin in plasma and extracellular fluids transports iron between the different cellular compartments. About four-fifths of this exchange, under normal conditions, cycles through the erythron and the macrophages which phagocytose senescent erythrocytes. Plasma and extracellular fluid iron cycles to the bone marrow where it is incorporated into haem to supply the haemoglobin in newly formed red-cell precursors. The erythrocytes circulate in the peripheral blood stream for about 120 days, and thereafter the senescent erythrocytes are taken up by phagocytosis in the spleen and to a lesser extent in the liver by macrophages that digest the haemoglobin and release the iron to plasma transferrin. In the course of each cycle a small amount
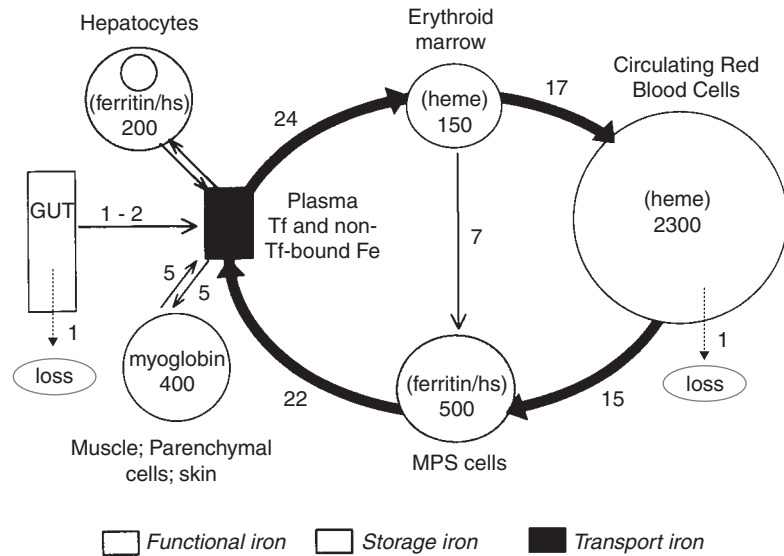
Figure 8.1   Body iron stores and daily iron exchange. The figure shows a schematic representation of the routes of iron movement in normal adult male subjects. The plasma iron pool is about 4 mg (transferrin-bound iron and non-transferrin-bound iron), although the daily turnover is over 30 mg. The iron in parenchymal tissues is largely haem (in muscle) and ferritin/haemosiderin (in hepatic parenchymal cells). Dotted arrows represent iron loss through loss of epithelial cells in the gut or through blood loss. Numbers are in mg/day. Transferrin – Tf; haemosiderin – hs; MPS – mononuclear phagocytic system, including macrophages in spleen and Kupffer cells in liver.

of iron is transferred to storage sites where it is incorporated into ferritin and subsequently into haemosiderin. Some of the storage iron is released to the plasma, and a small proportion of the newly formed erythrocytes (some 10 %) is destroyed within the bone marrow and their iron is released, thus escaping from the major circulatory part of the cycle: this is referred to as ineffective erythropoiesis. The numbers alongside the arrows in Figure 8.1 indicate the amount of iron (mg) that enters and leaves each of these compartments in normal healthy adults every day. Storage iron is usually present in roughly equal amounts in the macrophages of the reticuloendothelial system, in hepatic parenchymal cells, and in skeletal muscle. The overall extent of iron exchange by hepatocytes is much less (about one-fifth) than that by reticuloendothelial cells.

8.2   Sources of Dietary Iron in Man and the Importance of Luminal Factors

The capacity of the human body to excrete iron is severely limited as compared with most other mammals (Finch *et al*., 1978). Iron loss in human beings (per kg body weight) is only one-tenth that of other mammals (Dubach *et al*., 1955; Green *et al*., 1968; Finch *et al*., 1978) and human dietary intake only one-fiftieth to one-hundredth that of other mammals. It follows, as was originally suggested by McCance and

Widdowson (1937), that iron balance in man is primarily determined by iron absorption. There is a reciprocal relationship between iron stores and iron absorption: as stores decline, absorption increases. Similarly the rate of erythropoiesis (red cell development) is a major determinant of iron absorption: enhanced erythropoietic activity is linked to increased iron absorption. The principal site of iron absorption is the upper part of the gastrointestinal tract (the duodenum). Both the amount and bioavailability of dietary iron, together with the pH and motility of the gut lumen and other factors, influence iron absorption. These different factors do not, however, regulate iron absorption: this is thought to be carried out by the intestinal mucosa, which under normal circumstances adjusts the amount of dietary iron absorbed so that it just compensates for the iron that is lost by excretion. Since the human body lacks effective means of iron excretion, this means that only very small amounts of dietary iron are absorbed – in males about 1 mg/day to compensate for daily iron losses of about the same amount (14 μg/kg). Two-thirds of this comes from the gastrointestinal tract by exfoliation of mucosal cells and loss of red cells, and one-third by exfoliation of cells from the skin and the urinary tract. In premenopausal women the average daily absorption is about double that in men, largely because of blood losses during menstruation (typically around 20 mg/period), resulting in a net daily iron loss of around 2 mg (30 μg/kg). Iron absorption increases significantly during pregnancy (2.7 mg/day on average, but up to 5–6 mg/day in the last trimester) and during lactation (less than 0.3 mg/day).

Iron absorption from the diet depends not only on the iron content, but on its composition. Typical Western diets contain about 5–6 mg iron per 1000 kcal, with very little variation from meal to meal: this corresponds to a total daily intake of 12–18 mg for most subjects. There are two major pools of food iron: haem iron and non-haem iron. Haem iron is highly bioavailable and well absorbed – 20–30 %, regardless of other dietary or physiological variables (FAO/WHO, 1988). The haem iron in meat is absorbed as intact metalloporphyrin via specific, high-affinity mucosal brush-border haem-binding sites; this may be a receptor-mediated process. Haem itself is poorly absorbed, probably due to the formation of macromolecular haem polymers. In contrast, haem given as haemoglobin is well absorbed since it is maintained in its monomeric state by the primary amines released during the proteolysis of globin. Haem bioavailability can be substantially reduced by baking or prolonged frying.

Non-haem iron in food enters an exchangeable pool where it is subject to the interplay of luminal factors which both promote and inhibit its absorption. The major enhancers of non-haem iron absorption are meat and organic acids. Ascorbic acid is the most powerful promoter of these. It can, of course, reduce poorly soluble ferric iron to the more soluble ferrous state, but it could also chelate ferric chloride in the acidic pH of the stomach; this complex would remain not only stable, but soluble, at the alkaline pH prevailing in the gastrointestinal tract. Prolonged heating leads to the destruction of ascorbic acid and has a deleterious effect on the bioavailability of iron – so please don't cook the life out of green vegetables! A number of organic acids, notably citrate, malate, lactate and tartrate, also enhance non-haem iron bioavailability.

Inhibitors of non-haem iron absorption include polyphenols and phytates. The former, secondary plant metabolites rich in phenolic hydroxyl groups, are found

in a high molecular form in tea (tannins) but polyphenols are also present in vegetables, legumes and condiments. Phytates, which constitute 1–2 % by weight of many cereals, nuts and legumes, also inhibit dietary iron bioavailability, probably due to the complexation of iron to form di-and tetraferric phytates, which are poor sources of iron. Other inhibitors of non-haem iron absorption are thought to be wheat bran and other components of dietary fibre complexes, calcium and phosphorus acting together, perhaps due to the formation of poorly available calcium–phosphate–iron complexes, and dietary protein particularly from soy beans, nuts and lupines.

Diets rich in enhancers such as meat and/or ascorbate have high iron bioavailability (about 3 mg absorbed/day) whereas diets with inhibitors such as polyphenols and phytates are poor sources of iron (less than 1 mg/day) (Bothwell *et al.*, 1989). The human body is genetically adapted to haem iron absorption, a throwback to the days when man was a hunter. The progressive change in dietary habits that began with the introduction of the cultivation of grain about 10 000 years ago, has led to the replacement of well absorbed haem iron by less well absorbed non-haem iron from a cereal diet. The poor availability of dietary iron, particularly amongst the economically underprivileged, explains in large part the estimated more than 500 million persons throughout the world suffering from anaemia due to dietary iron deficiency (Chapter 9). With the current tendency in Western society to adopt a vegetarian regime, particularly among young women, we can expect a significant increase in anaemia, exacerbated by the progressive decrease in caloric intake (which of course correlates with dietary iron). Also, at the opposite extreme, an only slightly enhanced excessive mucosal iron absorption can lead to parenchymal iron overload sufficient to cause tissue damage, a condition unique to man – genetic haemochromatosis is probably the most frequent inherited disease in humans (Chapter 9).

8.3 Molecular Mechanisms of Mucosal Iron Absorption

Since the first edition of this book was published, our knowledge of candidate proteins that may be involved in mucosal iron absorption has greatly increased, although we cannot yet say the same of our understanding of their precise role in this process. In what follows we will first try to characterize these proteins, frequently identified from the analysis of genetic abnormalities in both animals and humans, and then endeavour to present a coherent picture of their potential role in iron handling by the mucosa. They intervene in three distinct steps: the uptake of iron from the lumen of the gut across the brush border at the apical pole of the intestinal mucosal cell; the transport of iron across the mucosal cell, associated with its eventual sequestration into an intramucosal pool that can potentially be lost when the mucosal cell reaches the end of its short life cycle; and release of iron at the basolateral pole of the mucosal cell to the plasma transport protein, transferrin. However, first, we should paint a brief picture of the life cycle of the intestinal mucosal cell (Figure 8.2). Iron absorption is most active in the proximal small intestine, mostly in the duodenum, and to a lesser extent in the upper ileum. Rat duodenal cells (enterocytes) divide within the crypts of Lieberkühn: at this stage
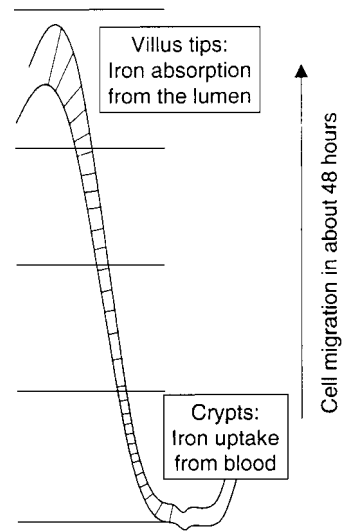
Figure 8.2 Rat duodenal cells divide in the crypts of Lieberkühn and differentiate while migrating to the villus tips within approximately 48 h. The crypt cells take up iron from the blood, and are thereby able to sense the body's state of iron repletion. They migrate to the villus tips where this information determines their iron absorption capacity from the intestinal lumen. Adapted from Schumann *et al.*, 1999, by permission of Blackwell Science.

the crypt cell, which requires iron both for cell division and for development, but lacks absorptive capacity, must obtain its iron from the plasma. In contrast, as it differentiates while migrating to the villus tips, within the space of approximately 48 h the enterocyte will progressively absorb iron from the lumen of the intestinal tract. These absorptive enterocytes are often called brush-border cells, because of the brushlike mass of microvilli on their apical surface. This serves to increase the area of apical membrane which is actively involved in the transport of nutrients, including iron, from the intestinal tract into the cells. Already in 1963, William Crosby advanced the hypothesis of regulation of iron balance by the intestinal mucosa (Crosby, 1963), based on the observation that subsequent to alterations in body iron levels, a delay of 2 to 3 days is required before any change in iron absorption occurs – a delay corresponding approximately to the life span of the enterocyte. The idea was that within the crypts of Leiberkühn, as the future enterocytes are formed, they are programmed with 'messenger iron' which is a direct reflection of body iron stores (Conrad *et al.*, 1963). As they differentiate into enterocytes and migrate into the absorptive zone of the villus, this messenger iron regulates iron absorption, possibly by interaction with iron carriers, potentially at both the apical and the basolateral membrane.

At the villus tips, the enterocytes are sloughed off (together with their intracellular content) to be phagocytosed in the intestinal tract, and those nutritive elements such as iron that have been taken up during the villal phase of their cycle, but not transferred across the cells to the bloodstream at the basolateral surface, are lost. More-recent evidence suggests that exfoliation of enterocytes is not the principal route of cell loss from the villi, but that loss of apical epithelial cells occurs by apoptosis (Hall *et al.*, 1994). The cellular fragments so formed are phagocytosed by apically located macrophages. This could explain the iron deposits found in intestinal macrophages together with their increased ferritin content in iron-loaded animals (Astaldi *et al.*, 1966; Refsum and Schreiner, 1980; Oates and Morgan, 1997). Such iron-loaded macrophages could penetrate the apical villus epithelium and be lost with their iron content into the intestinal lumen (Astaldi *et al.*, 1966). We

shall return to the life cycle of the enterocyte at the end of this description of iron uptake, transfer and release, when we discuss the regulation of iron absorption under normal physiological conditions.

8.3.1   Iron Uptake at the Apical Pole

Mucosal cells can take up iron from the lumen across their brush border membranes by at least two separate pathways, both of which are thought to be receptor mediated. Non-haem dietary iron seems most likely to be taken across the brush border membrane after reduction by an apical, membrane-bound, ferrireductase and subsequent transport of the Fe^{2+} by a divalent metal-ion transporter protein, known both as DCT1 and Nramp2.

Evidence for a duodenal ferric reductase that displays adaptive responses to iron status, increasing in hypoxia, in atransferrinaemic animals and in iron deficiency, has been found (Raja *et al.*, 1992), its partial purification and characterization from human duodenal microvillous membranes has been described (Riedel *et al.*, 1995), and it has also been reported to be present in a number of intestinal-like cell lines, such as CaCo2 cells (Ekmekcioglu *et al.*, 1996). Duodenal biopsies from patients with genetic haemochromatosis show increased ferric reductase activity and iron absorption as compared with controls (Raja *et al.*, 1996), and its activity has also been demonstrated in human leucocytes, monocytes and macrophages (Partridge *et al.*, 1998). Earlier investigations suggested that the reductase was associated with a haem-containing *b*-type cytochrome (Pountney *et al.*, 1999). Very recently a cDNA, Dcytb (for duodenal cytochrome *b*) has been isolated which encodes a plasma membrane dihaem protein in mouse duodenal mucosa (McKie *et al.*, 2001). Dcytb has a 45–50 % similarity to the cytochrome b_{561} family of plasma membrane reductases, is highly expressed in the brush border membrane of duodenal enterocytes and induces ferric reductase activity when expressed in *Xenopus* oocytes and cultured cells. Duodenal expression levels of Dcytb mRNA and protein are regulated by changes in physiological modulators of iron absorption, indicating that Dcytb provides an important element in the iron absorption pathway.

We have previously encountered the proton-coupled divalent cation transporter protein, DCT1 in the transport of free Fe(II) derived from transferrin across the endosomal membrane and into the cytoplasm (Chapter 5). DCT1, also designated as Nramp2 and DMT1 (Gruenheid *et al.*, 1995; Gunshin *et al.*, 1997; Fleming *et al.*, 1997), has also been implicated in the rapid uptake of dietary Fe(II) from the intestinal mucosa. It is not specific for Fe(II) and also transports other divalent metal ions, including cobalt, manganese and lead (Gunshin *et al.*, 1997). The same missense mutation (G185R) in the *DCT1* gene is found in two different inherited anaemias in rodents, both of which are characterized by defective duodenal iron absorption. These are microcytic anaemia (*mk*) in the mouse (Fleming *et al.*, 1997) and the so-called Belgrade (*b*) rat, which has an autosomal, recessively inherited, microcytic, hypochromic anaemia, associated with defects in both gastrointestinal iron absorption and reticulocyte iron uptake (Fleming *et al.*, 1998). DCT1 generates two alternatively spliced mRNAs, one of which has an IRE in its 3′-UTR (Canonne-Hergaux *et al.*, 1999), and only this form of DCT1 is dramatically upregulated in

the proximal part of the duodenum upon dietary iron starvation. Immunostaining shows that it is abundant under iron deplete conditions in the villi of the proximal duodenum but absent in the crypts (Canonne-Hergaux *et al*., 1999). DCT1 is expressed in the apical membrane of the human intestinal epithelial cell line CaCo2, where it mediates a proton-dependent iron-transport mechanism with a substrate preference for iron over other divalent cations (Tandy *et al*., 2000). It has been reported that duodenal levels of DCT1 mRNA are increased in haemochromatosis patients (Zoller *et al*., 1999) as well as in a mouse model of haemochromatosis (Fleming *et al*., 1999).

A number of other candidates for apical iron transfer have been described. Iron is more efficiently absorbed from human milk by suckling infants than from cow milk or infant formulas, and a role for lactoferrin in iron uptake in infants has been proposed (Davidson *et al*., 1994). A transferrin-like GPI (GlycoPhospho-Inositol)-linked iron-binding protein was reported at the apical surface of porcine fetal intestine (Danielsen and van Deurs, 1995). Uptake of iron from an intra-luminal mucin chelate (Conrad *et al*., 1991) via a surface integrin (Conrad *et al*., 1993) and subsequent transfer to a small (56 kD) cytosolic protein designated as mobilferrin (Conrad *et al*., 1990) has been described, and it is proposed that the integrin–mobilferrin system facilitates the absorption of dietary inorganic ferric iron (Conrad *et al*., 1999).

Iron is also taken up by mucosal cells in the form of haem, although as mentioned above, in the presence of primary amines derived from proteolysis, haem uptake is greatly enhanced, probably due to prevention of haem polymer formation. Since it is much more efficiently absorbed than non-haem iron, it is of major importance in haem-rich diets. Although specific mucosal receptors for haem have been described (Grasbeck *et al*., 1979), it is still uncertain as to whether or not haem has a receptor-mediated uptake pathway. After its entry into the mucosal cell, haem is degraded by the microsomal haem oxygenase in a complex series of reactions requiring NADPH and molecular oxygen to form carbon monoxide, bilirubin and ferrous iron, as in other tissues. As was mentioned earlier (Chapter 5), the X-ray crystal structure of human haem oxygenase 1 (HO-1) has been determined (Schuller *et al*., 1999). The importance of the enzyme for mammalian iron homeostasis has been shown in mice lacking functional HO-1. These animals are anaemic and have abnormally low levels of serum iron, despite having high levels of liver and kidney iron, which leads to oxidative damage (Poss and Tonegawa, 1997a,b). Haem oxygenase is present in higher concentrations in the duodenum than in the rest of the small intestine, and its activity increases in iron deficiency such that the rate of haem catabolism is more rapid. The free haem-derived Fe^{2+} thereafter enters the common intracellular iron pool and its fate follows that of inorganic iron.

8.3.2   Iron Transfer Across the Mucosal Cell

The *transfer* step involves the passage of iron that has been taken up at the apical, brush border membrane across the mucosal epithelial cell to the basolateral membrane, where it is transferred to the circulation. However, not all the iron taken up from the lumen into the cell is transferred. As a function of the body's

requirements for iron (essentially determined by the rate of erythropoiesis) a variable proportion could be sequestered within the mucosal cell, eventually to be discarded into the gastrointestinal tract when the cell exfoliates. It was suggested by Hahn *et al*. (1943) that iron absorbed from the gut in excess of body requirements might be incorporated into mucosal cell ferritin, where it would somehow function as a 'mucosal block' against unnecessary assimilation of dietary iron. The mucosal cell would thus function as a gatekeeper, preventing the onward transfer of unwanted dietary iron. We will return to this notion later when we consider the regulation of iron absorption, which clearly implies some kind of signal coupling the amount of iron entering the mucosa from the lumen as well as the proportion that is subsequently transferred into the plasma, for the body's iron requirements. What then, are the different forms of iron that we can observe within the mucosal cell?

Current opinion is that both haem and non-haem iron arrive within the enterocyte as Fe^{2+}, and it is concluded that this constitutes the 'labile' cytosolic iron pool. While in the graphical representation at the end of this section, we will refer to this 'transit' pool, its nature is not as well established as the other LIPs referred to in Chapter 6.

There is no doubt that ferritin represents the best characterized pool of iron within the mucosal cell. However, as we pointed out above, it is important to distinguish between enterocytes at various stages of their development. Immunohistochemical localization of ferritin protein in rats showed that in iron-deficient animals no ferritin was seen in any epithelial cells of the crypts or villi. In iron-loaded animals and in control animals, ferritin protein was also absent from the crypt epithelial cells, but it was seen in the cytoplasm of enterocytes in increasing amounts, commencing in the midvillus region and reaching its highest levels at the villus tips (Oates and Morgan, 1997). Using *in situ* hybridization techniques it was shown that in all iron status groups, ferritin mRNA was seen at highest levels in epithelial cells of the crypt and in macrophages within the lamina propria and at lowest levels in villus epithelial cells. These authors concluded that in undifferentiated crypt cells, ferritin genes are transcribed but not translated, whereas after differentiation, ferritin mRNA translation is controlled by cellular iron stores. Another protein which has made regular appearances in mucosal cell literature is transferrin, together with its receptor. As pointed out in Chapter 6, neither of these proteins ever gets into the cytosol, being restricted within endosomal and recycling vesicles. We will, however, return to ferritin and the basolateral membrane transferrin receptor later in our consideration of how iron absorption might be regulated.

There are other candidates for a role in cytosolic iron transport within the enterocyte, notably the previously mentioned small protein called mobilferrin (Conrad *et al*., 1990). Another cytosolic complex labelled during iron transport was called paraferritin on account of its high molecular weight – it appears to consist of at least four polypeptides, closely associated with one another. Antibody studies have identified the presence of integrin, mobilferrin, and flavin monooxygenase, while biochemical studies indicate that it has an NADPH-dependent monoxygenase ferrireductase activity (Umbreit *et al*., 1996). It is suggested that its role is to make ferrous iron available for production of iron-containing proteins (Uzel and Conrad, 1998). Precisely what the requirement for this large ferrireductase within the mucosal cell might be, particularly when iron appears to be delivered as Fe^{2+}, is not yet clear.

8.3.3 Release of Iron at the Basolateral Membrane and Uptake by Apotransferrin

While we may have savoured the final characterization of a long awaited ferrireductase to accompany DCT1 at the enterocyte's apical pole, and long appreciated the patient wait of mucosal ferritin to be crowned star of mucosal cellular iron homeostasis, it is at the basolateral membrane that there has been the greatest flurry of activity in the last few years. It was no surprise to find transferrin receptors at the basolateral membrane, which, as we inferred above, would supply the preenterocyte with the iron from the plasma that would be necessary for its division and differentiation during its 48-hour Odyssey from the crypts of Lieberkühn up to the tips of the villi. However, we did not expect to find that the gene product of genetic haemochromatosis, HFE, discovered in 1996 (Feder *et al.*, 1996) associates with the transferrin receptor (Feder *et al.*, 1998; Parkkila *et al.*, 1997) and decreases five to ten fold its affinity for its natural ligand, diferrictransferrin, (Feder *et al.*, 1998). Not only was the X-ray crystal structure of HFE determined (Lebron *et al.*, 1998), but a mere two years later, the crystal structure of the HFE-transferrin receptor complex was also established (Bennett *et al.*, 2000). We have also discovered a new member of the pantheon of classical Greek mythology, in the form of a GPI-anchored multicopper ferroxidase, called hephaestin (Vulpe *et al.*, 1999) that appears to be involved in iron egress from intestinal enterocytes into the circulation. Finally, the long-sought duodenal iron-export protein, was identified independently by three groups, and called respectively IREG1 (McKie *et al.*, 2000), ferroportin (Donovan *et al.*, 2000) or MTP (Abboud and Haile, 2000).

We begin with the transferrin receptor (TfR). Developing enterocytes in the crypts of Lieberkühn express transferrin receptors at their basolateral membranes (Anderson *et al.*, 1991, 1994; McKie *et al.*, 1996). Radioiron administered from the blood side is restricted to enterocytes in the crypt compartment in rats (Conrad and Crosby, 1963; Schumann *et al.*, 1999), where it enables the cells to acquire the quantities of iron from the blood that will be necessary for their differentiation and division during their progress along the pathway from crypt to apical villus. Likewise, in human duodenal biopsies, the crypt cell fraction showed dramatically higher transferrin-bound iron uptake than villus cells (Waheed *et al.*, 1999). The possible role of TfRs during the absorptive phase of the enterocyte's progress towards the tip of the villus and its ultimate demise remain unclear, although it seems unlikely that they play a major role in active iron uptake by the villus enterocytes. In rats and guinea pigs, duodenal iron uptake from the gut lumen, on the other hand, is restricted to enterocytes in the upper part of the villi (O'Riordan *et al*, 1997; Chowrimootoo *et al.*, 1992), while in human duodenum, the villus cells showed an uptake of ionic iron (from the apical side) two or three times higher than crypt cells (Waheed *et al.*, 1999).

Genetic haemochromatosis (GH) is an autosomal recessive disease in which patients chronically absorb a slightly greater amount of dietary iron than normal from the gastrointestinal tract, resulting in deposition of excess iron particularly in the parenchymal cells of the liver, pancreas and heart (reviewed in the next chapter). The gene mutated in GH codes for a transmembrane glycoprotein, HFE, homologous to Class I Major Histocompatibility Complex (MHC), which associates with a Class I light chain β2-microglobulin. Most GH patients are homozygous for a mutation

that converts Cys-260 to Tyr (Feder *et al.*, 1996), eliminating a disulfide bond in HFE and preventing its association with β2-microglobulin and its expression at the cell surface in cell-culture models (Feder *et al.*, 1997; Waheed *et al.*, 1997). Both HFE and TfR are expressed in crypt enterocytes of human duodenum, and Western blots show that HFE is physically associated with both TfR and β2-microglobulin in crypt enterocytes (Waheed *et al.*, 1999). *In vitro* it was observed that the HFE associates with TfR (Parkkila *et al.*, 1997; Feder *et al.*, 1998) and decreases its affinity for diferric transferrin by a factor of 5 to 10 (Feder *et al.*, 1998). Further details of the interaction of HFE and Tfr (Lebron *et al.*, 1998) together with the crystal structure of the HFE-TfR (Bennett *et al.*, 2000) are presented in Chapter 5. It has been postulated that HFE protein modulates the uptake of transferrin-bound iron by crypt enterocytes, and is involved in the mechanism by which crypt enterocytes sense the level of body iron stores. The classical GH mutation, Cys292Tyr, could in some way provide a paradoxical signal in crypt enterocytes that programmes them to absorb more dietary iron when they mature to villus enterocytes (Waheed *et al.*, 1999).

While both TfR and HFE are important in regulating iron influx into the enterocyte across the basolateral membrane during its crypt phase, other proteins have recently been identified which are implicated in iron egress from the villus enterocyte into the circulation where the natural receptor is assumed to be apotransferrin. The first of these was discovered by a genetic approach to identify the gene mutant in *sla* mice. These mice which have a genetically inherited sex-linked anaemia (hence *sla*), have a block in intestinal iron transport and develop a severe microcytic hypochromic anaemia. Their mature epithelial cells take up iron normally from the intestinal lumen, but fail to transfer it to the circulation. The iron accumulated in the enterocytes is lost during subsequent turnover of the epithelial epithelium. The mutant gene in *sla* mice was identified and designated *Heph* – it encodes a transmembrane-bound ceruloplasmin homologue, which is highly expressed in intestine (Vulpe *et al.*, 1999). The hephaestin[†] protein is a multicopper ferroxidase which appears to be necessary for iron egress from intestinal enterocytes into the circulation, and represents a major link between iron and copper metabolism in mammals (see Chapter 13). Hephaestin appears to be inserted into the basolateral membrane by a GPI (Glyco-Phospho-Inositol)-anchor, where it may intervene together with the basolateral iron transporter to load iron onto apotransferrin (see below).

It had long been expected that an iron transporter would be found at the basolateral membrane of the enterocyte responsible for the exportation of iron from the enterocytes into the portal vein circulation, and it turns out that three groups appear to have made this discovery almost simultaneously (McKie *et al.*, 2000; Donovan *et al.*, 2000; Abboud and Haile, 2000). The first of these, IREG1, was originally identified by subtractive cloning techniques (McKie *et al.*, 1998), and isolated and

---

[†] Hephaestus was the Greek god of fire, son of Zeus and Hera, and husband of Aphrodite. Homer called him *chalkeas*, the metalworker, the most skilful of all of the gods in a domain which could not be done without the use of fire. The myths tell us that Aphrodite (the Roman goddess Venus) was once unfaithful to her husband with Ares, the powerful god of war (the Roman god Mars). Skilled craftsman that he was, Hephaestus made nets of metal hammered so thin they were as invisible as spider's webs, and he spread them on the bed he shared with Aphrodite, and pretended to be called away to his forge. Returning to find Ares and Aphrodite entangled in his net, he thus made fools of the illicit couple in front of all of the gods. See Chapter 13 for more on Venus (copper) and Mars (iron).

characterized as a novel cDNA from duodenal mucosa of homozygous atrans-ferrinaemic mice which exhibit abnormally high rates of iron absorption (McKie *et al.*, 1998, 2000). IREG1 is a transmembrane protein, with ten potential membrane-spanning regions, that localizes to the basolateral membrane of polarized epithelial cells; both its mRNA and protein expression are increased under conditions of increased iron absorption, and the 5'-UTR of the Ireg1 mRNA contains a functional IRE. IREG1 stimulates iron efflux following expression in *Xenopus* oocytes. Alignment of human, rat and mouse IREF2 protein sequences shows a high degree of conservation, and IREG1-related proteins have been identified (McKie *et al.*, 2000) both in plants (*Arabidopsis thaliana*) and nematode worms (*Caenorhabditis elegans*). Increased levels of *Ireg1* mRNA levels were also found in duodenal biopsies from three GH patients. Ferrroportin (Donovan *et al.*, 2000) was cloned as the gene responsible for the hypochromic anaemia of the zebrafish mutant *weissherbst*. It is also a multiple transmembrane domain protein which is required for transport of iron from maternally derived yolk stores to the circulation and it also functions as an iron exporter when expressed in *Xenopus* oocytes. A similar protein is found expressed both at the basolateral surface of duodenal enterocytes and of placental syncytiotrophoblasts suggesting that it not only functions in iron export from the intestine, but also in iron transfer from mother to embryo. It may also function in iron release from macrophages, since high levels of expression are found in Kupffer cells (Donovan *et al.*, 2000). Comparison of the cDNA sequences of IREG1 and ferroportin confirms that they are the same. Yet a third group (Abboud and Haile, 2000) has reported an apparently identical gene and called it MTP1 (Metal Transporter Protein), expressed in tissues involved in body iron homeostasis, including the reticuloendothelial system, the duodenum and the pregnant uterus. MTPI is homologous to the DCT1 family of metal transporters, and is localized to the
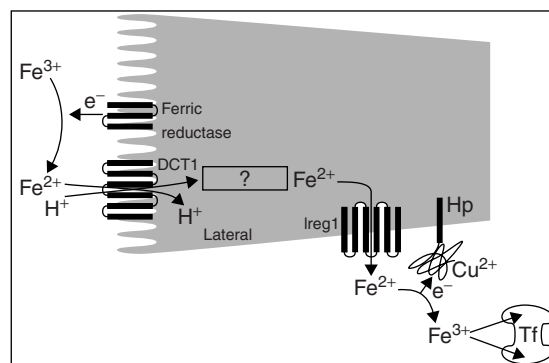
Figure 8.3 A model of iron transport across the intestine. Reduction of ferric complexes to the ferrous form is achieved by the action of the brush border ferric reductase. The ferrous form is transported across the brush border membrane by the proton-coupled divalent cation transporter (DCT1) where it enters an unknown compartment in the cytosol. Ferrous iron is then transported across the basolateral membrane by IREG1, where the membrane-bound copper oxidase hephaestin (Hp) promotes release and binding of Fe^{3+} to circulating apotransferrin. Except for hephaestin the number of transmembrane domains for each protein is not shown in full. Reprinted from McKie *et al.*, 2000. Copyright (2000), with permission from Elsevier Science.

basolateral membrane of duodenum epithelial cells and the cytoplasm of reticuloen-dothelial system cells. Iron deficiency induces MTP1 expression but downregulates it in the liver. Like IREG1 and ferroportin, MTP1 has a 5′-UTR IRE sequence.

The way in which these different partners may be involved in iron uptake across the intestine is presented in Figure 8.3. Reduction of ferric complexes to the Fe^{2+} form is achieved by the action of the brush border ferric reductase. The Fe^{2+} is transported across the brush border membrane by the proton-coupled divalent cation transporter (DCT1) where it enters an unknown compartment in the cytosol. Fe^{2+} is then transported across the basolateral membrane by IREG1, where the membrane-bound copper oxidase hephaestin (Hp) promotes release and binding of Fe^{3+} to circulating apotransferrin.

8.4 A Model of Iron Uptake and Regulation of Iron Homeostasis by the Enterocyte

We have attempted to synthesize much of the data presented above in two diagrammatical representations. In the first (Figure 9.4a), we consider the situation of the crypt cell at the beginning of its differentiation into an enterocyte, and before it has begun its climb towards the tip of the villus. We assume that at this stage in its development, the crypt cell has no absorptive capacity and that it takes up the iron necessary for its future differentiation and growth from circulating diferritransferrin (Fe_2Tf) via its basolateral TfR. This is in agreement with the observation that when radio iron is administered parenterally[‡] it is almost exclusively taken up by crypt entrocytes (Oates and Morgan, 1996; Schumann *et al.*, 1999; Waheed *et al.*, 1999). There is little evidence for TfR expression in differentiated villus cells, and both TfR and HFE are immunolocalized mainly to the crypt cells (Parkkila *et al.*, 1997; Bannerjee *et al.*, 1986; Anderson *et al.*, 1990), where it has been demonstrated that both proteins are physically associated (Waheed *et al.*, 1999). Transfection studies carried out in normal cells show that HFE and TfR associate soon after synthesis and colocalize in the perinuclear region, on the cell surface and in endosomes (Gross *et al.*, 1998). At the cell surface, HFE complexed to TfR increases the dissociation constant of transferrin for its receptor tenfold (Gross *et al.*, 1998; Feder *et al.*, 1998), whereas the Cys282Tyr mutant of HFE has no effect (Feder *et al.*, 1998). This is not surprising, since mutant HFE neither binds to TfR nor reaches the cell surface (Feder *et al.*, 1998). HFE does not remain at the cell surface, but traffics with TfR to transferrin-positive internal compartments (Gross *et al.*, 1998). Using a HeLa cell line in which HFE expression is controlled by tetracycline, it has been shown that HFE expression reduces iron uptake from transferrin by one-third without affecting endocytic or exocytic rates of TfR cycling (Roy *et al.*, 1999). In normal individuals, the interaction of the wild-type HFE protein, expressed basolaterally in the crypt cells (Parkkila *et al.*, 1997), with β2-microglobulin and TfR enables a coherent message to be transmitted to the enterocyte concerning the state of body

---

[‡] Parenteral – brought into the body by some other way than the digestive tract, such as by subcutaneous or intravenous injection.

iron stores and/or erythropoeisis. This could set the 'messenger iron' level via the IRP1 and 2 proteins (Figure 9.4a). It has been demonstrated that IRP1 activity decreased in crypt enterocytes 12 hours after administration of parenteral iron, but remained high at the villus tips (Schumann *et al.*, 1999), whereas after 48 hours, when the iron-containing enterocytes had migrated to the vileus tips, IRP1 activity in villus-tip enterocytes had decreased. IRP2 activity was not significantly changed. Intestinal iron absorption decreased with the same delay as IRP1 activity after intravenous iron administration. This implies that IRP activity (and particularly IRP1) serves as the molecular imprint which determines how much iron will be taken up by the villus enterocyte and delivered to the blood circulation in the portal vein. The way in which this message is erroneously transmitted to the developing enterocyte in GH will be considered in Chapter 9, but it is of interest to note here that studies on duodenal biopsies of GH patients indicate that IRP binding activities are either similar (Flanagan *et al.* 1995) or consistently higher (Pietrangelo *et al.*, 1995) than controls. Ferritin expression is also decreased in the enterocytes from duodenal biopsy specimens of GH patients (Francanzani *et al.*, 1989; Basclain *et al.*, 1998).

Iron is taken up from the intestinal tract by the enterocyte (Figure 9.4b) at the apical (brushborder) membrane by one of two pathways. The first involves either the combined action of the newly characterized ferric reductase and the proton-coupled divalent metal-ion transporter Nramp2, or alternatively, direct transport of Fe^{2+} produced in the upper part of the intestine by biological reducing agents like ascorbate, via Nramp2. The second pathway involves an as yet uncharacterized brushborder membrane system which transports haem into the enterocyte. Once inside the cell, haem oxygenase using both O_2 and a source of reducing equivalents converts the haem to CO, water, biliverdin and Fe^{2+}. By analogy with other mammalian haem oxygenases, we assume that the enterocyte enzyme is localized in the microsomal membrane, together with another microsomal protein, known as cytochrome P_{450} reductase, or cytochrome c reductase, which supplies electrons from NADPH. Fe^{2+} from both pathways then enters an unknown cytosolic compartment, and we might reasonably assume that this iron is in equilibrium with, and provides iron to, the enterocyte ferritin pool. The Fe^{2+} is subsequently transported across the basolateral membrane by IREG1 (ferroportin). It is postulated that IREG1 and hephaestin could work together to promote release and binding of Fe^{3+} to circulating apotransferrin.

Ferritin protein is not seen in crypt cells, but is detected with increasing staining in the apical two-thirds of the villus cells of both control and iron-loaded rats: ferritin staining increases with iron loading (Oates and Morgan, 1997). This is consistent with cellular iron levels regulating ferritin mRNA translation and with ferritin functioning to store iron that has been taken up in excess of requirements, and is the basis of the mucosal block theory (Hahn *et al.*, 1943), which proposed that the iron trapped in ferritin in the enterocyte prevented iron from being transferred to the bloodstream, and that it would subsequently be lost when the enterocyte was exfoliated at the villus tip. If we were to extend this concept of a mucosal block, we would assume that the input from the transferrin receptor/HFE system at the basolateral membrane in crypt cells would set the levels of IRP activity to reflect the iron status of the whole organism. This would mean that, under normal

circumstances (i.e. in the absence of large fluxes in iron content in the intestinal tract), the amount of dietary iron traversing the enterocyte and actually being transferred to the circulation would depend on IRP activity (which had been preset at the level of the crypts). This implies that the 'messenger iron' of Crosby would be manifested in the RNA-binding activity of the IRPs, indeed that the IRPs would function as the endogenous sensor of iron in the intestinal mucosa, as was suggested in a recent study (Schumann *et al.*, 1999).

We can speculate that in the absorptive zone of the villus, the enterocyte regulates its iron absorption as a function of the 'message' that has been programmed into the IRP proteins (Figure 9.4b). In this context, we should note that both the putative apical transport (DCT1) and basolateral (IREG1) transport proteins have IREs, respectively in their 3'- and 5'-UTRs (as discussed in Chapter 9), but that to date their direct involvement with IRPs remains to be established.

8.5 References

Abboud, S. and Haile, D.J. (2000). *J. Biol. Chem.*, **275**, 19906–12.

Anderson, G.J., Powell, L.W. and Halliday, J.W. (1990). *Gastroenterology*, **98**, 576–85.

Anderson, G.J., Walsh, M.D., Powell, L.W. and Halliday, J.W. (1991). *Br. J. Haematol.*, **77**, 229–36.

Anderson, G.J., Powell, L.W. and Halliday, J.W. (1994). *Gastroenterology*, **106**, 414–22.

Astaldi, G., Meardi, G. and Lisino, T. (1966). *Blood*, **28**, 70–82.

Basclain, K.A., Shilkin, K.B., Withers, G., Reed, W.D. and Jeffrey, G.P. (1998). *J. Gastroenterol. Hepatol.*, **13**, 624–34.

Bannerjee, D., Flanagan, P.R., Cluett, J. and Valberg, L.S. (1986). *Gastroenterology*, **91**, 861–9.

Bennett, M.J., Lebron, J.A. and Bjorkman, P.J. (2000). *Nature*, **403**, 46–53.

Bothwell, T.H., Charlton, R.W., Cook, J.D. and Finch, C.A. (1979). *Iron Metabolism in Man*. Blackwell, Oxford.

Bothwell, T.H., Baynes, R.D., MacFarlane, B.J. and MacPhail, A.P. (1989). *J. Int. Med.*, **226**, 357–65.

Brune, R.E., Magnusson, B., Persson, H. and Hallberg, L. (1986). *Am. J. Clin. Nutr.*, **43**, 438–43.

Canonne-Hergaux, F., Gruenheid, S., Ponka, P. and Gros, P. (1999). *Blood*, **93**, 4406–17.

Chowrimootoo, G., Debnam, E.S., Srai, S.K. and Epstein, O. (1992). *Exp. Physiol.*, **77**, 177–83.

Conrad, M.E. and Crosby, W.H. (1963). *Blood*, **22**, 406–15.

Conrad, M.E., Umbreit, J.N., Moore, E.G., Peterson, R.D.A. and Jones, M.B. (1990). *Blood*, **81**, 517–21.

Conrad, M.E., Umbreit, J.N. and Moore, E.G. (1991). *Gastroenterology*, **100**, 129–36.

Conrad, M.E., Weintraub, L.R. and Crosby, W.H. (1963). *J. Clin. Invest.*, **43**, 963–74.

Conrad, M.E., Umbreit, J.N., Peterson, R.D.A., Moore, E.G. and Harper, K.P. (1993). *J. Biol. Chem.*, **265**, 5273–9.

Conrad, M.E., Umbreit, J.N. and Moore, E.G. (1999). *Am. J. Med. Sci.*, **318**, 213–29.

Cook, J.D., Marsaglia, G., Eschbach, J.W., Funk, D.D. and Finch, C.F. (1970). *J. Clin. Invest.*, **49**, 197–205.

Crosby, W.H. (1963). *Blood*, **22**, 441–9.

Danielsen, E.M. and van Deurs, B. (1995). *J. Cell Biol.*, **131**, 939–50.

Davidson, L., Kastenmayer, P., Yuen'o *et al*. (1994). *Pediatr. Res.*, **35**, 117–24.

Donovan, A., Brownlie, A., Zhou, Y., Shepard, J. *et al*. (2000). *Nature*, **403**, 776–81.

Dubach, R., Moore, C.V. and Callander, S.T. (1955). *J. Lab. Clin. Med.*, **45**, 599–15.

Ekmekcioglu, C., Feyertag, J. and Marktl, W. (1996). *J. Nutr.*, **126**, 2209–17.

FAO/WHO (Food and Agriculture Organization/World Health Organization) (1988) Requirements of Vitamin A, Iron, Folate and Vitamin B_{12}. Joint Expert Consultation Report. FAO Food and Nutrition Series 23, FAO, Rome.

Feder, J.N., Gnirke, A., Thomas, W., Tsuchihashi, Z. *et al*. (1996). *Nature Genet.*, **13**, 399–408.

Feder, J.N., Tsuchihashi, Z., Irrinki, A., Lee, V.K. (1997). *J. Biol. Chem.*, **272**, 14025–8.

Feder, J.N., Penny, D.M., Irrinki, A., Lee, V.K. *et al*. (1998). *Proc. Natl. Acad. Aci. USA*, **95**, 1472–7.

Finch, C.A., Ragan, H.A., Dyer, I.A. and Cook, J.D. (1978). *Proc. Soc. Exp. Biol. Med.*, **159**, 335–8.

Flanagan, P.R., Hajdu, A. and Adams, P.C. (1995). *Hepatology*, **22**, 828–32.

Fleming, M.D., Trenor, C.C., Su, M.A., Foernzler, D. *et al*. (1997). *Nature Genet.*, **16**, 383–6.

Fleming, M.D., Romano, M.A., Su, M.A., Garrick, L.M., Garrick, M.D. and Andrews, N.C. (1998). *Proc. Natl Acad. Aci. USA*, **95**, 1148–53.

Fleming, R.E., Migas, M.C., Zhou, X., Jiang, J. *et al*. (1999) *Proc. Natl Acad. Aci. USA*, **96**, 3143–8.

Francanzani, A.L., Fargion, S., Romano, R., Piperno, A. *et al*. (1989). *Gastroenterology*, **96**, 1071–8.

Granick, S. (1946). *J. Biol. Chem.*, **164**, 737–46.

Grasbeck, R., Kouvonen, I., Lundberg, M. and Tenhunen, R. (1979). *Haematologica*, **23**, 5–9.

Green, R., Charlton, R.W., Seftel, H., Bothwell, T.H. *et al*. (1968). *Am. J. Med.*, **45**, 336–53.

Gross, C.N., Irinki, A., Feder, J.N and Enns, C.A. (1998). *J. Biol. Chem.*, **273**, 220687–74

Gruenheid, S., Cellier, M., Vidal, S. and Gros, P. (1995). *Genomics*, **25**, 514–25.

Gunshin, H., McKenzie, B., Berger, U.V., Gunshin, Y. *et al*. (1997). *Nature*, **388**, 482–8.

Hahn, P.F., Bale, W.F., Ross, J.F., Balfour, W.F. and Whipple, G.F. (1943). *J. Exp. Med.*, **78**, 169–88.

Hall, P.A., Coates, P.J., Ansari, B. and Hopwood, D. (1994). *J. Cell Sci.*, **104**, 3569–77.

Lebron, J.A., Bennett, M.J., Vaughn, D.E., Chirino, A.J. (1998). *Cell*, **93**, 111–23.

McCance, R.A. and Widdowson, E.M. (1937). *Lancet ii*, 680–4.

McKie, A.T., Raja, K.B., Peters, T.J., Farzaneh, F., and Simpson, R.J. (1996). *Am. J. Physiol*, **271**, G772-G779.

McKie, A.T., Wehr, K., Simpson, R.J., Peters, T.J., Hentze, M.W. and Farzaneh, F. (1998). *Biochem. Soc. Trans.*, **26**, S264.

McKie, A.T., Marciano, P., Rolfs, A., Brennan, K. *et al*. (2000). *Molecular Cell*, **5**, 299–309.

McKie, A.T., Barrow, D., Latunde-Dada, G.O., Rolfs, A. *et al*. (2001). *Science*, **291**, 1755–9.

Oates, P.S. and Morgan, E.H. (1996). *Anat. Rec.*, **246**, 364–71.

Oates, P.S. and Morgan, E.H. (1997). *Am. J. Physiol.*, **273**, G636–46.

O'Riordan, D.K., Debnam, E.S., Sharp, P.A., Simpson, R.J., Taylor, E.M. and Srai, S.K. (1997). *J. Physiol.*, **500**, 379–84.

Parkkila, S., Waheed, A., Britton, R.S., Feder, J.N. *et al*. (1997). *Proc. Natl Acad. Aci. USA*, **94**, 2534–9.

Partridge, J., Wallace, D.F., Raja, K.B., Dooley, J.S. and Walker, A.P. (1998). *Biochem. J.*, **336**, 541–3.

Pietrangelo, A., Casalgrandi, G., Quaglino, D., Gualdi, R. *et al*. (1995). *Gastroenterology*, **108**, 208–17.

Poss, K.D. and Tonegawa, S. (1997a). *Proc. Natl Acad. Aci. USA*, **94**, 10919–24.

Poss, K.D. and Tonegawa, S. (1997b). *Proc. Natl Acad. Aci. USA*, **94**, 10924–30.

Pountney, D.J., Raja, K.B., Simpson, R.J. and Wrigglesworth, J.M. (1999). *Biometals*, **12**, 53–62.

Raja, K.B., Simpson, R.J. and Peters, T.J. (1992). *Biochim. Biophys. Acta*, **1135**, 141–6.

Raja, K.B., Pountney; D.J., Bomford, A.B., Przemioslo, R. *et al*. (1996). *Gut*, **38**, 765–9.

Refsum, S.B. and Schreiner, B. (1980). *Scand. J. Gastroenterol.*, **15**, 1013–20.

Riedel, H.-D., Remus, A.J., Fitscher, B.A. and Stremmel, W. (1995). *Biochem. J.*, **309**, 745–8.

Roy, C.N., Penny, D.M., Feder, J.N. and Enns, C.A. (1999). *J. Biol. Chem.*, **274**, 9022–8.

Schuller, D.J., Wilks, A., Ortiz de Montellano, P.R. and Poulos, T.L. (1999). *Nature Struct. Biol.*, **6**, 860–7.

Schumann, K., Moret, R., Kunzle, H. and Kühn, L.C. (1999). *Eur. J. Biochem.*, **260**, 362–72.

Tandy, S., Williams, M., Leggett, A., Lopez-Jimenez, M. *et al*. (2000). *J. Biol. Chem.*, **275**, 1023–9.

Umbreit, J.N., Conrad, M.E., Moore, E.G., Desai, M.P. and Turrens, J. (1996). *Biochem.*, **35**, 6460–9.

Uzel, C. and Conrad, M.E. (1998). *Semin. Hematol.*, **35**, 27–34.

Vulpe, C.D., Kuo, Y.M., Murphy, T.L., Cowley, L. *et al*. (1999). *Nature Genet.*, **21**, 195–9.

Waheed, A., Parkkila, S., Zhou, X.Y., Tomatsu, S. *et al*. (1997). *Proc. Natl Acad. Aci. USA*, **94**, 12384–9.

Waheed, A., Parkkila, S., Saarnio, J., Fleming, R.E. *et al*. (1999). *Proc. Natl Acad. Aci. USA*, **96**, 1579–84.

Zoller, H., Pietrangelo, A., Vogel, W. and Weiss, G. (1999). *Lancet*, **353**, 2120–3.

9 Pathophysiology of Iron Deficiency and Iron Overload in Man

9.1 Introduction: Acquired and Genetic Disorders of Iron Metabolism

Iron related disorders leading either to exhausted or to overloaded iron stores, are extremely common in all parts of the world. Iron deficiency as a cause for anaemia has been recognized for centuries. Probably the first report on the beneficial effects of iron in anaemia comes from Greece in 1500 BC. It was told that prince Iphyclus of Thesaly suffered from sexual impotence (Fairbanks *et al.*, 1971). He was treated by the physician Melampus who scraped the rust from the blade of an old knife into some wine, which was given to Iphyclus to drink. The result was spectacular: the impotence of Iphyclus was cured and the dynasty of Thesaly was saved. The cause of the discomfort of the prince may have been blood loss from playing with another, hopefully not rusty, knife. Interestingly, impotence may also be caused by severe iron overload. Although the pathophysiology is rather different, many symptoms of iron deficiency are identical with those observed in haemochromatosis. In both conditions the cause can be acquired or inherited, or even a combination of both. The most common acquired causes of iron deficiency are blood loss and dietary defects. However, inherited defects in iron transport, anywhere between the lumen of the gut and the mitochondria of erythroblasts, can also cause iron deficiency. Iron overload can be caused by repeated blood transfusions, if the anaemia is not caused by iron deficiency, poorly indicated iron injections, and increased absorption of iron in hereditary or secondary iron overload, the latter often resulting from inherited haemolytic anaemias.

In this chapter we will focus on pathophysiological aspects of iron deficiency and iron overload, describing functional relations between cells and organs as a link between biochemistry and medicine. Clinical, diagnostic and therapeutic aspects will only be mentioned if particularly relevant for pathophysiology.

9.2 Body Iron Regulation

9.2.1 Communication Between Iron Donor and Iron Acceptor Cells

The biochemistry and physiology of iron absorption, iron transport in plasma, iron incorporation into cells and iron storage are described in detail in Chapters 5, 6 and 8 of this book. In healthy subjects all these processes are meticulously maintained in balance, procuring sufficient iron for production of haemoglobin and other iron proteins but avoiding iron-related tissue damage, the latter mainly caused by iron-catalysed generation of toxic oxygen metabolites (Gutteridge, 1994; Marx and van Asbeck, 1996). There must be communication between different cells and organs, and also within a single cell, in order to maintain an appropriate balance (Aisen *et al.*, 1999). About 1 mg iron, from a total body content of 3000–4000 mg in normal men, is lost per day. This is nicely compensated for by absorption of an equal amount from the diet which must contain between 10 and 15 mg of iron per day to allow this level of iron absorption. Fertile women need to absorb about 30 mg more iron per month to compensate for menstrual blood loss and to prevent iron deficiency anaemia. Signals to inform the gut that not enough iron is delivered to the bone marrow, inducing an increase in iron transport by intestinal mucosal cells, should reach these cells through the plasma. In the opposite situation, if the body is loaded with iron, intestinal absorption should be blocked.

   Organs and cells communicate through the plasma, which may be considered the central compartment in iron metabolism. Essentially the body contains three types of cells: (a) those that need to obtain iron from plasma for growth or for the production of iron-proteins (iron acceptor cells), (b) those that are involved in red-cell catabolism, iron storage or iron absorption, and need to export iron towards the plasma (iron donor cells), and (c) cells, such as hepatocytes, that are able to take up (and release) iron for the protection of other more vulnerable cells in the body (Santos *et al.*, 2000a). Iron transport and storage in these cells is modified in situations of iron deficiency and iron overload. Figure 9.1 provides a simple representation of communication between iron donor and acceptor cells. The plasma is the central pool, donating transferrin-bound iron (Tf-Fe) to cells that need iron for cell division or production of iron-containing proteins. The majority of plasma iron goes to erythroblasts in the bone marrow (BM) for haemoglobin (Hb) synthesis. Iron enters the plasma from iron donor cells, mainly from the macrophage system (MPS) and intestinal mucosal cells, most probably as Fe(II). The majority of this iron is rapidly oxidized and bound to transferrin (Tf-Fe). In particular, in iron overload considerable amounts of iron remain as non-transferrin bound iron (NTBI), attached to a variety of ligands (de Valk *et al.*, 2000a; Loreal *et al.*, 2000). Most NTBI is taken up by hepatocytes via the portal venous system. In haemochromatosis, NTBI may enter many other cells, resulting in tissue damage. Red blood cells (RBC) are destroyed in spleen and liver macrophages. Iron leaves these cells not only from the cytosolic labile pool, but also as ferritin and haemoglobin (Moura *et al.*, 1998a), most of which is rapidly cleared by specific receptors on hepatocytes (Hershko *et al.*, 1972; Hershko, 1975). Erythroblasts are also able to utilize iron offered as ferritin (Meyron-Holtz *et al.*, 1999). All molecular species of iron remain increased in plasma in cases of haemolysis. In dyserythropoietic anaemias, intramedullar destruction
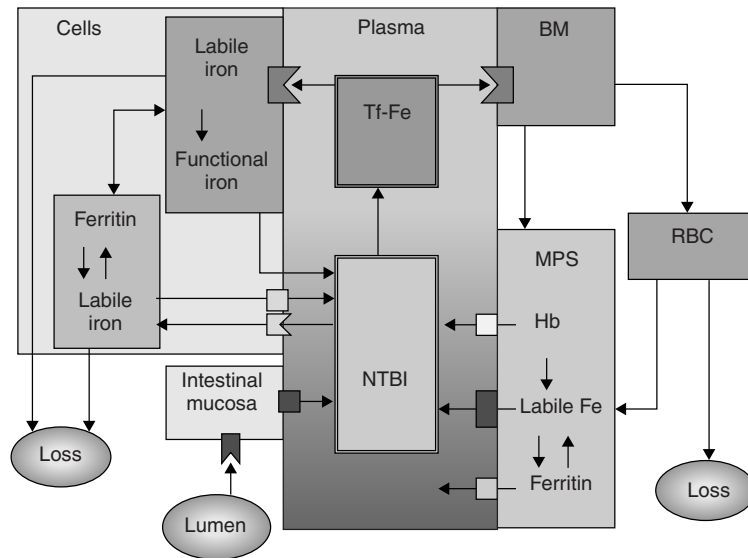
Figure 9.1 Interaction of iron-donor and iron-acceptor cells. The plasma donates trans-ferrin-bound iron (Tf-Fe) to cells that need iron for cell-division or production of iron proteins, mainly erythroblasts in the bone marrow (BM). The majority of iron is used for haemoglobin (Hb) synthesis. Iron enters the plasma from iron donor cells, mainly the macrophage system (MPS) and intestinal mucosal cells. Normally this iron is rapidly bound to transferrin (Tf-Fe). In situations of transferrin saturation, an intermediate form, non-transferrin bound iron (NTBI), exists attached to a variety of ligands. Most NTBI is taken up by hepatocytes. Red blood cells (RBC) are destroyed in macrophages. Iron leaves these cells as low-molecular-weight complexes, as ferritin and as haemoglobin, most of which is rapidly cleared by hepatocytes. In dyserythropoietic anaemias, intramedullar destruction of erythroblasts and red cells causes a direct flux of iron to bone marrow MPS. In all cells iron first enters a labile iron pool which is used as a source of iron for production of essential iron-containing proteins, or else is sequestered into ferritin. Iron is lost from the body together with exfoliating cells or during blood loss.

of erythroblasts and red cells causes a direct flux of iron to bone marrow MPS. In all cells iron first enters a cytosolic labile pool of Fe(II) from which it is used for production of essential iron-containing proteins, or else is sequestered into ferritin (Breuer *et al.*, 1995). Iron is lost from the body together with exfoliating cells, mainly from the gut, or during blood loss.

Fluxes of iron from the plasma towards BM and other tissues can be quantified by ferrokinetic studies, using ^{59}Fe and sophisticated computer models (Ricketts *et al.*, 1975; Ricketts and Cavill, 1978; Barosi *et al.*, 1978; Stefanelli *et al.*, 1980). Plasma iron turnover (PIT), erythroid iron turnover (EIT), non-erythroid iron turnover (NEIT), marrow iron turnover (MIT), and tissue iron turnover (TIT) could be calculated in many disorders of iron metabolism and in all kinds of anaemias. Iron is rapidly cleared from the plasma in iron deficiency and in haemolytic anaemias. If more iron is needed for erythropoiesis, more transferrin receptors (TfR) are expressed on erythroblasts, resulting in an increased flux of iron from intestinal mucosal cells towards the plasma. In haemolytic anaemias MPS, and subsequently hepatocytes, are overloaded. In hereditary haemochromatosis too much iron is absorbed by an intrinsic defect of gut mucosal cells. As this iron is not needed for erythropoiesis,

TfR is low in these patients, PIT is normal and most iron is stored in hepatocytes. In patients with hypoplastic anaemias and with transfusion iron overload, the BM cannot utilize iron, resulting in low TfR expression and decreased iron absorption. Quantitative analysis of all iron fluxes, which can be deduced from Figure 9.1, can assist in understanding the clinical expression of mutations of proteins involved in iron transport.

An impressive number of proteins that are involved in iron transport have been identified in recent years (Andrews, 1999; Griffiths *et al.*, 1999). Most of them can either be up-regulated or down-regulated in situations of iron deficiency and different forms of iron overload, in order to maintain a safe iron balance. However, variations in the absolute levels or genetic defects of these proteins may cause iron overload or iron deficiency. In many forms of iron-related pathology detailed information can be obtained using appropriate animal models.

9.2.2 Maintenance of Iron Balance in Cells

In 1976, Hamish Munro proposed a model for the translational control of ferritin synthesis (Zähringer *et al.*, 1976), which not only represents a crucial and remarkably far-sighted contribution to our understanding of cellular iron metabolism, but also in the more general context of the posttranscriptional control of gene expression.
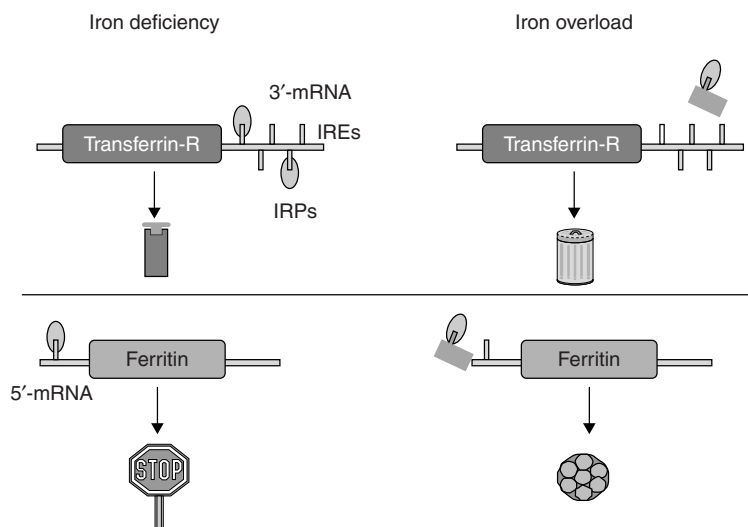
Figure 9.2 Production of transferrin receptor and ferritin is regulated on the level of mRNA by iron responsive proteins. Iron responsive elements (IREs) in mRNA of the transferrin receptor (TfR) are localized in the 3′-mRNA region, and in mRNA of ferritin in the 5′-mRNA promotor region. The system is designed to allow the cells to procure iron from the plasma, by expressing more transferrin receptors, if they need iron for production of proteins, and to protect cells against potentially toxic iron by expressing ferritin molecules, able to hide Fe(III) within its core. The system is regulated by iron responsive protein 1 (IRP). In iron deficiency IRP inhibits RNase attack of TfR mRNA, and inhibits production of ferritin while sitting on an IRE in the 5′-mRNA region. If the LIP contains abundant amounts of iron, modified IRP has no affinity for IRE, resulting in destruction of TfR mRNA. At the same time free IRE on ferritin mRNA allows sufficient expression of ferritin.

Cellular iron homeostasis is regulated by the interaction of iron responsive elements (IREs) and iron responsive proteins (IRP), as described in Chapter 7. IREs are folded RNA-hairpin structures with a number of conserved unpaired nucleotides which are found in the 3′-untranslated region of transferrin receptor mRNA, and in the 5′-untranslated region of ferritin subunits (and some other iron-related proteins). The translation of these mRNAs is regulated by the binding of the IRPs to their cognate IREs in conditions of iron paucity, resulting in synthesis of transferrin receptor, whereas ferritin synthesis is blocked. In contrast, in conditions of iron surfeit, the IRPs do not bind to the mRNAs, ferritin is synthesized and transferrin receptor mRNA is degraded (reviewed in Chapter 7 and in Cairo and Pietrangelo, 2000). A simple scheme, representing translational regulation of TfR and ferritin in situations of high and low intracellular concentrations of labile iron, is depicted in Figure 9.2. The system is designed to allow the cells to procure iron from the plasma by expressing more transferrin receptors when they need iron for the production of iron-containing proteins, and to protect the cells against potentially toxic levels of iron within the low molecular iron pool (LIP) by expressing ferritin molecules, able to store potentially toxic iron within its core. The behaviour of IRPs in intestinal mucosal cells is expected to be of pivotal interest for iron homeostasis in the whole body, in particular in the crypts of Lieberkühn where it is thought that the levels of expression of iron-transporting proteins and iron-storage proteins is set, thus determining how much dietary iron is allowed to cross the enterocyte once it reaches the phase of active absorption in the intestinal villi (Chapter 8).

9.3 Iron Absorption in Disorders of Iron Metabolism

The mechanism of iron absorption, and the involvement of recently detected proteins in iron transport, is described in detail in Chapter 8. Our understanding of iron absorption at the molecular level is growing rapidly. This knowledge is essentially based on detailed quantitative information on iron absorption in normal subjects, in patients with iron deficiency, hereditary and secondary iron overload, and inflammation (Heinrich *et al.*, 1966; Marx, 1979a; Werner and Kaltwasser, 1987; Wienk *et al.*, 1999). By using a whole body counter, with ^{59}Fe as a tracer, and [^{51}Cr]CrCl$_3$ as a non-absorbable indicator, it was possible to analyse different steps of iron absorption: the uptake of iron by the mucosal microvillus membrane, the proportional transport of iron by the basolateral membrane, and the final retention of iron in the body at about two weeks after ingestion of an oral test dose (Marx, 1979b; Marx *et al.*, 1980; Marx and van den Bent 1981). The method was adapted for use in animals like rats (Wienk *et al.*, 1997), mice (Santos *et al.*, 1997a), calves (Miltenberg *et al.*, 1993) and birds (Mete *et al.*, 2001). The double-isotope approach allows identification of iron transport modifications at the microvillus membrane, in intracellular pathways and at the basolateral membrane, and can also be applied to knock-out mice. Site-specific effects of molecular defects of transport proteins on iron absorption can be evaluated *in vivo* in man and in animals. If an animal model were to be claimed to exhibit similar defects to those observed in man, it would be proof that it had an identical pattern of iron absorption to the corresponding human disorder. This was clearly demonstrated in β2-microglobulin knock-out mice, which showed identical defects of iron transport, in particular of iron absorption, to

Figure 9.3 The whole-body counter of University Medical Centre, Utrecht, The Netherlands. The counter has a mobile shadow shield with two NaI(Tl) scintillation detectors (4 × 6 in) placed at opposite sites of the subject. The lead shielding is 100 cm long with a diameter of 90 cm. The scanner moves on rails over a distance of 240 cm with an adjustable speed. Extreme variations in geometry yield practically the same value for ^{59}Fe activity. The equipment can be used for measurements in man and small animals.

those observed in patients with hereditary haemochromatosis (Santos *et al.*, 1998). The changes could easily be distinguished from adaptive responses to anaemia, increased erythropoiesis, iron deficiency and artificial iron loading. The whole-body scanner of the University Medical Centre, Utrecht (The Netherlands), which has now been used for almost 30 years in clinical and experimental iron absorption studies, is shown in Figure 9.3 (Marx, 1979a,b).

Figure 9.4 (a) Schematic representation of iron absorption in normal subjects. The upper panel represents a mature intestinal mucosa cell at the tip of a villus. The lower panel represents an early cell in a crypt of Lieberkühn. NRAMP2 = natural-resistance-associated macrophage protein2; DMT1 = divalent metal transporter 1; IREG1 = iron-regulated transporter 1; HaemTr = haem transporter; HaemOx = haem oxygenase I; IRE = iron responsive element; IRP = iron responsive protein; HFE = the 'haemochromatosis gene' product; β2m = β2-microglobulin; DcytB = duodenal cytochrome B; TfR = transferrin receptor.

The situation prevailing in the crypt cell at the beginning of its differentiation into an enterocyte and before it has begun to climb towards the villus is shown in the lower panel. The cell's iron requirements are supplied by receptor-mediated diferric transferrin uptake from the basolateral membrane. The TfR in turn is involved in an interaction with the HFE protein, which decreases the affinity of TfR for diferric transferrin. The level of transferrin saturation, or some other factor, determines the amount of iron taken up, and presets the IRP system at a level that corresponds to the iron requirements of the organism.

In the enterocyte as it enters the absorptive zone near to the villus tips, dietary iron is absorbed either directly as Fe(II) after reduction in the gastrointestinal tract by reductants like ascorbate, or after reduction of Fe(III) by the apical membrane ferrireductase Dcytb, via the divalent transporter Nramp2 (DCT1). Alternatively, haem is taken up at the apical surface, perhaps via a receptor, and is degraded by haem oxygenase to release Fe(II) into the same intracellular pool. The setting of IRPs (which are assumed to act as iron biosensors) determines the amount of iron that is retained within the enterocyte as ferritin, and that which is transferred to the circulation. This latter process is presumed to involve IREG 1 (ferroportin) and the GPI-linked hephaestin at the basolateral membrane with incorporation of iron into apotransferrin. (b) A representation of iron absorption in HFE-related haemochromatosis.

(a)

(b)
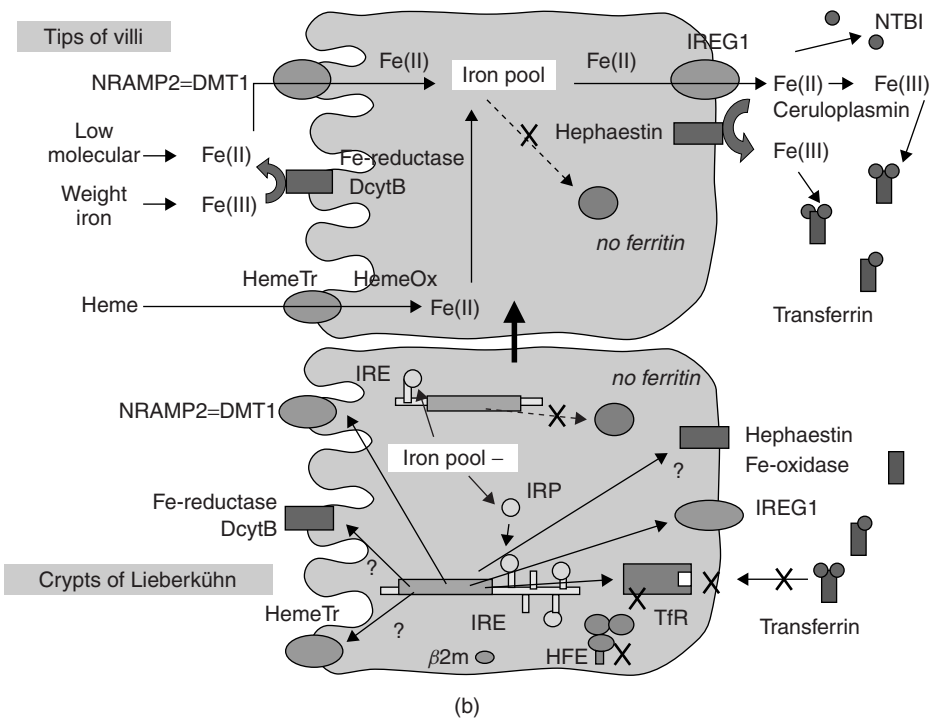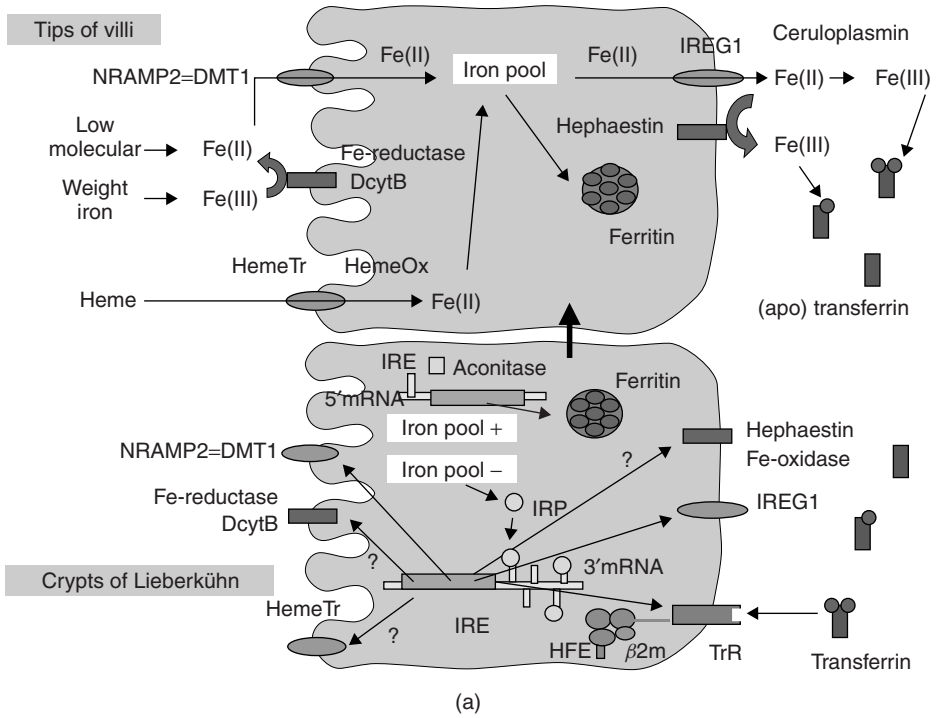
In Figure 9.4(a) we have summarized iron transport by intestinal mucosa cells. Known iron transport proteins, described in more detail in Chapter 8, are included. It is essential to make the difference between mature mucosa cells at the tips of the villi, and developing cells in the crypts of Lieberkühn. The total lifetime of duodenal mucosa cells is not more than two days. Considering the time needed for moving from the crypts towards the tips of the villi, each mucosa cell sees some iron passing by before the cell is released to the intestinal lumen only once or twice in its lifetime, eventually after phagocytosis by local macrophages. The events depicted in Figure 9.4 correspond to the situation where mucosal cells have been exposed to physiological amounts of iron from the diet. If the mucosa is flooded with iron, as may happen during oral treatment of iron deficiency or in iron intoxication, other events may prevail. Fe(II) may then not only use the physiological pathway involving NRAMP2 and IREG1, but may damage cell membranes by formation of toxic oxygen metabolites and by lipid peroxidation, allowing rapid diffusion of Fe(II) towards the plasma (Marx and Aisen, 1981; Fodor and Marx, 1988). However let us first briefly summarize the physiological pathway taken by dietary iron that reaches the microvillus surface in a water-soluble form. As transport of iron across the microvillus membrane by NRAMP2 (also described as DCT1 or DMT1), a divalent metal transporter (Gunshin *et al.*, 1997), will only transport iron as Fe(II), transport across the apical membrane must be preceded by a Fe-reductase step in the close vicinity of the transporter (Riedel *et al.*, 1995). This activity may be provided by a duodenal cytochrome *B* (DcytB). In the reducing environment of the cytosol, iron will remain long enough in the Fe(II) state to reach the basolateral membrane or to encounter a ferritin molecule, which incorporates it as Fe(II) (Chapter 6). If there are many ferritin molecules available (this is the normal situation), then much of the iron will be trapped in ferritin and retained in the mucosal cell; this will be reflected *in vivo* as a low mucosal transfer of iron (Marx, 1979a,b).

In iron deficiency, mucosal cells, like other cells in the body, hardly produce any ferritin and most of the iron crossing the apical membrane is available for transport to the plasma, which is effected by the newly discovered basolateral iron transporter IREG1 (McKie *et al.*, 2000), also known as ferroportin (Donovan *et al.*, 2000) or MTP1 (Abboud and Haile, 2000). It seems that there are hardly any quantitative restrictions for basolateral Fe(II) transport. Once Fe(II) has entered the mucosal cell it has only two choices: either to be trapped by ferritin or to be transported to the plasma. It is thought that IREG1 facilitates diffusion of Fe(II) across the basolateral membrane of the enterocyte. It has been known for many years that iron entering the portal circulation is in the ferrous state (Wollenberg *et al.*, 1990), and the flux of iron across the basolateral membrane may be significantly driven by oxidation of the highly soluble Fe(II) to much less soluble Fe(III). This could be catalysed either by the recently discovered multicopper oxidase hephaestin, localized in the basolateral membrane, or by ceruloplasmin in the plasma. The Fe(III) so formed would be rapidly bound to plasma ligands, essentially apotransferrin, except in situations of saturation of the binding capacity of the plasma transporter when it would also bind to other ligands such as citrate, constituting the so-called non-transferrin bound iron (NTBI). Iron export from the enterocyte would also be influenced by the velocity of the blood flow in the portal system. It is obvious

from numerous studies that iron deficiency results in a high mucosal uptake (with up-regulation of NRAMP2) and a high mucosal transfer of iron (with low mucosal ferritin and a considerable increase of free iron-binding sites on plasma transferrin). Iron absorption is, however, also increased in secondary iron overload due to increased erythropoiesis in severe haemolysis and dyserythropoiesis. In such conditions ferrokinetic studies have demonstrated an enormously increased plasma iron turnover, apparently induced by increased expression of transferrin receptors on erythropoietic cells (Barosi *et al.*, 1978; Stefanelli *et al.*, 1980). Although plasma iron saturation is rather high, this is more than compensated for by the very high plasma-iron turnover, offering a number of free iron sites on transferrin which may even exceed that found in iron deficiency (Marx, 1982). In normal subjects, and certainly in iron deficiency, all iron from mucosal cells entering plasma will bind to transferrin. Though Fe(II) can also be autoxidized to bind to transferrin, this takes time. After absorption iron can be detected in plasma as potentially toxic Fe(II) (Wollenberg *et al.*, 1990). It is an important task of hephaestin (and possibly ceruloplasmin) to facilitate oxidation of Fe(II), which will allow rapid binding of iron to transferrin and its delivery to cells expressing IRP-regulated transferrin receptors, thus preventing endothelial damage and uptake of iron instead by hepatocytes.

Expression of proteins involved in mucosal iron transport is regulated in dividing cells in the crypts of Lieberkühn, as hypothesized in Figure 9.4. There can be little doubt that IRPs play a decisive role here. In the crypts, abundant concentrations of transferrin receptor (TfR) can be identified on the basolateral membrane of enterocytes; once the cells have reached the tips of the villi, the transferrin receptors have disappeared. With normal plasma iron saturation, the labile iron pool in young mucosal cells will be high, IRP binding to IREs will be low, and ferritin can be synthesized. In the adult absorbing cell, this will restrict mucosal iron transfer to the plasma. As mRNAs of NRAMP2 and IREG1 carry IREs, similar to the transferrin receptor but not always in the same region, sufficient amounts of those proteins will be expressed to allow adequate mucosal uptake and basolateral transport of iron. In iron-deficient young mucosal cells, IRP binding to IREs must be increased. Despite more copies of TfR little iron is entering the cells, as transferrin has just delivered all its iron to the bone marrow. As a result also NRAMP2 and probably IREG1 will be up-regulated, allowing a much higher mucosal uptake (Canonne-Hergaux *et al.*, 1999) and a complete transfer of all Fe(II) entering the cell to and across the basolateral membrane, the latter because no iron trap in the form of ferritin is available.

The peculiar thing in hereditary haemochromatosis (HH) is that the intestinal mucosal cell behaves essentially like an iron deficient cell. Iron absorption is always high if related to the body's iron needs. In HH subjects with normal plasma ferritin values, both mucosal uptake and mucosal transfer of iron often exceed values found in patients with uncomplicated iron deficiency (Marx, 1979b). In fact the situation with respect to iron absorption in mature intestinal mucosal cells, as depicted in Figure 9.4(b), is identical to that in iron deficiency, except for the difference in plasma iron saturation. It was already known that mucosal cells in HH contain no ferritin, explaining the high mucosal transfer of iron (Francanzani

et al., 1989). Recent work has made it clear that in HH, NRAMP2 is greatly over-expressed, explaining the high mucosal uptake of iron observed in this condition (Zoller *et al*., 1999; Fleming *et al*., 1999). There are indications that IREG1, which carries an IRE in its 5′-UTR, is also regulated by IRP in a similar way in iron deficiency and HH (McKie *et al*., 2000)[†]. Although there is only circumstantial evidence, observations in HH point to a situation where there is a low concentration of iron in the labile iron pool in the preenterocyte as it leaves the crypts and begins to migrate towards the villi. Yet, iron in plasma is abundantly available, with transferrin saturated with iron, so we might conclude that binding of transferrin to its receptors on the basolateral membrane must be defective in HH. Since the TfR itself is normal in HH (Tsuchihashi *et al*., 1998), this might suggest insufficient expression of TfR on the basolateral membrane. In iron-poor cells, however, more then enough TfR is produced. It must be concluded, therefore, that the transport of the transferrin-TfR complex from the cell membrane is impaired. The Cys-282Tyr mutation of the HFE gene must be responsible for this functional defect. The biochemical basis of this mutation is disruption of a disulphide bridge, which prohibits locking in of a β2-microglobulin molecule, required for membrane expression of classical and non-classical MHC class I molecules like HFE (Waheed *et al*., 1997). This also explains why β2-microglobulin knockout mice are virtually perfect models for human HH (Santos *et al*., 1996, 1997a,b). Apparently HFE functions as a chaperone protein for TfR, perhaps facilitating its migration to the cell membrane (Feder *et al*., 1998). There is much confusion about the affinity of transferrin for TfR compared to that of the TfR-HFE complex. Experiments have been performed in a variety of cell types, the majority of which are not relevant for studies on iron absorption (Gross *et al*., 1998; Roy *et al*., 1999). In experiments using gut crypt and villus cells from human duodenum coexpression in crypt enterocytes of HFE, β2-microglobulin and TfR was clearly observed (Waheed *et al*., 1999). In the design of further studies one should take into account that the interactions of normal and mutated HFE with TfR, and its role in the cellular procurement of transferrin-bound iron, may be completely different in enterocytes and macrophages as compared with, say, hepatocytes, pancreas, heart and, in particular, bone marrow. One of the classical features of HH is that iron overload, with altered iron absorption, coexists with a state of completely normal erythropoiesis. Although defective coexpression of HFE–TfR on the enterocyte basolateral membrane could explain the pathophysiology of iron absorption in HH, TfR-mediated endocytosis should be fully intact in erythroblasts. Because many patients with the clinical picture of HH are not carrying the homozygote Cys-282Tyr mutation of HFE, other molecular defects may lead to misinterpretation of the body iron status by crypt enterocytes, leading to increased intestinal iron transport. The outline of the puzzle of iron absorption becomes clearer, but there remain many missing pieces which must still be fitted into the puzzle.

[†] This constitutes one of the many anomalies found in trying to explain how the IRP system regulates iron uptake in normal and disease conditions. An IRE located in the 5′-UTR would be expected to prevent formation of the initiation complex required for translation of the mRNA (see Chapter 7 for details), yet the results reported by McKie *et al*., show the opposite, i.e. when IRP binding activity is high, both IREG1 mRNA and protein levels are increased.

9.3.1 Genotype and Phenotype of Animal and Human Iron Disorders

Before the recent identification of many new genes involved in iron transport and homeostasis, a lot was already known about the phenotype of many iron disorders. Clinicians provided detailed descriptions of diseases related to iron deficiency and iron overload, and animal models allowed us to gain even more insight into the biochemistry and pathophysiology of the human disorders (Santos *et al.*, 2000b; Ramm, 2000; Smith, 2000). An overview of genes that may affect iron metabolism in man, together with the relevant animal model, is provided in Table 9.1. If the gene products are projected into Figures 9.1 and 9.4, a clear picture of the variety of phenotypes in patients with mutations of those genes emerges. It is possible to predict phenotypes of not-yet-identified disorders of iron transport and storage. Patients with all those disorders will exist, sometimes with a diagnosis of iron deficiency or iron overload of unknown origin! Close cooperation of clinical scientists and biochemists is needed to fill in all gaps of our knowledge of iron disorders in the near future.

9.3.2 Macrophages and Hepatocytes in Disorders of Iron Metabolism

After a lifetime of 100–120 days, effete red blood cells are recognized, phagocytosed and destroyed by macrophages, mainly in the spleen and the liver. A macrophage is capable of processing one erythrocyte, or over 200 million iron atoms, per hour. In man about 360×10^9 erythrocytes are processed per day (Aisen, 1982). As an normal adult human requires an average of 21 mg iron each day for haemoglobin synthesis, with only about 1 mg coming from absorption, it is easy to calculate that macrophages contribute much more to iron influx into the plasma than do intestinal enterocytes. Macrophages are well protected against the potential hazards of iron exposure. In the longer term, however, this does not hold true for patients with severe haemolytic anaemias (who develop secondary iron overload), as they develop a functional asplenia as a result of destruction by iron. It is known from *in vitro* studies with monocytes and macrophages that not all of the iron derived from red cell destruction leaves the cell as single iron atoms able to bind rapidly to transferrin. Release of iron from macrophages in the form of ferritin has been identified (Kondo *et al.*, 1988). The release of haemoglobin after erythrophagocytosis has also been described, but some authors have considered this to be an artefact of loading the macrophage with too many erythrocytes (Kondo *et al.*, 1988; Custer *et al.*, 1982).

In a recent series of experiments, in which human monocytes (MN) and monocyte-derived macrophages (MDM) were loaded *in vivo* with ^{59}Fe-labelled, opsonized rabbit red blood cells, it was established that red-cell-derived iron leaves MN and MDM in at least three molecular forms: low molecular weight (chelatable) iron complexes, ferritin and haemoglobin. By carefully manipulating the amount of phagocytosed red blood cells per MN or MDM, it was ensured that no cell damage occurred (Moura *et al.*, 1998b). Figure 9.5 (Plate 14) shows harmful over-loading of MN with erythrocytes, which will occasionally occur *in vivo* during haemolysis. Intracellular kinetics of [59Fe]iron release from red blood cells, the

Table 9.1 Genes that may affect iron metabolism in man.

Gene	Function	Animal model	(Anticipated) phenotype of human disease
DCT1/ Nramp2 (Gunshin *et al.*, 1997)	Transports iron across microvillus membrane; endosomal Fe(II) iron transport	*mk mice* (Fleming *et al.*, 1997) *Belgrade (b) rat* (Fleming *et al.*, 1998)	Iron-deficiency anemia, unresponsive to oral iron therapy; failure of iron transport out of endosomes
SFT (Gutierrez *et al.*, 1998)	Stimulator of iron transport in endosomes (Fe(II) and Fe(III))	?	Mild iron-deficiency anaemia?
HFE/MS2 (Feder *et al.*, 1996; Hashimoto *et al.*, 1997).	Associates with transferrin receptor (Feder *et al.*, 1998; Bennett *et al.*, 2000); ? regulates intracellular iron levels	$\beta 2m^{-/-}$ *mice* (Santos *et al.*, 1996; de Sousa *et al.*, 1994; Rothenberg and Voland, 1996; *HFE*$^{-/-}$ *mice* (Zhou *et al.*, 1998)	Hereditary haemochromatosis; increased iron absorption; parenchymal iron overload
Sla (Anderson *et al.*, 1998), Haephaestin (Vulpe *et al.*, 1999)	Transport of iron across intestinal basolateral membrane; ferroxidase activity	*sla mice* (Manis, 1971; Huebers *et al.*, 1973; Vulpe *et al.*, 1999); *sex-linked anemia*	Iron-deficiency anaemia; decreased intestinal iron transfer
IREG1 (McKie *et al.*, 2000)	Transport of iron across intestinal basolateral membrane	?	Iron-deficiency anaemia
Ceruloplasmin	Ferroxidase activity	*Cp*$^{-/-}$ *mice* (Harris *et al.*, 1999)	Aceruloplasminaemia (Logan *et al.*, 1994; Takahashi *et al.*, 1996); deficient iron mobilization; low serum iron; tissue iron overload
Hemox1	Haem oxygenase: Catabolism of cellular haem to bilirubin, carbon monoxide and free iron	*hemox1*$^{-/-}$ *mice* (Poss and Tonegawa, 1997)	Impaired haem catabolism; impaired absorption of iron from meat; anaemia; inflammation
Hemox2	Iron recycling	*hemox2*$^{-/-}$ *mice* (Dennery *et al.*, 1998)	Lung iron accumulation; idiopathic pulmonary siderosis (Dearborn, 1997)
Transferrin	Iron transport in plasma and into cells	*hpx mice* (Huggenvik *et al.*, 1989; Bernstein, 1987; Craven *et al.*, 1987; Goya *et al.*, 1972)	Hypotransferinemia (Goya *et al.*, 1972); microcytic anaemia; increased iron absorption; parenchymal iron overload
Transferrin receptor	Iron transport into cells	*Trfr*$^{-/-}$ *mice* (Levy *et al.*, 1999)	Impaired erythroid and neurologic development, and abnormal iron homeostasis

Table 9.1 *(continued)*

Gene	Function	Animal model	(Anticipated) phenotype of human disease
Transferrin receptor-2	Iron transport into hepatocytes		Hereditary haemochromatosis (Camaschella *et al.*, 2000); increased iron absorption; parenchymal iron overload
Frataxin (Campuzano *et al.*, 1996)	Mitochondrial iron transport	*frataxin$^{-/-}$ mice* (Cossee *et al.*, 2000)	Friedreich's ataxia (Harding, 1981; Lamarche *et al.*, 1984; Rotig *et al.*, 1997); neurodegeneration and cardiac myopathy; embryonic lethality
L-ferritin	Iron storage	?	Hereditary hyperferritinaemia-cataract syndrome (Girelli *et al.*, 1995; Aguilar-Martinez *et al.*, 1996; Mumford *et al.*, 1998; Martin *et al.*, 1998)
H-ferritin	Iron storage	*H-ferritin$^{-/-}$ mice* (Ferreira *et al.*, 2000)	Early embryonic lethality
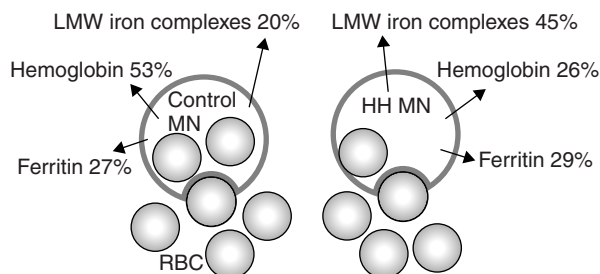
Figure 9.6 Iron release from monocytes after erythrophagocytosis. Relative release (%) of [^{59}Fe]iron molecular species from monocytes (MN) during the first 24 hours following erythrophagocytosis. MN from patients with hereditary haemochromatosis (right) take up fewer red blood cells (RBC) and released more ^{59}Fe as low-molecular-weight (LMW) complexes as compared with MN from normal controls (left).

molecular forms in which ^{59}Fe accumulated in MN or MDM, and the release of these iron species to the medium, could be followed (Moura *et al.*, 1998a). Experiments were performed with MN and MDM derived from normal donors and from Cys 282Tyr homozygote HH patients. One unexpected observation was that erythrophagocytosis by MN and MDM from HH patients was decreased, compared with donors, in 100 % of the experiments (Moura *et al.*, 1998b). Further experiments did not reveal a different level of expression of receptors or FcγRIIa polymorphism as a cause of altered phagocytosis in HH (Moura *et al.*, 1997). Results for iron release by MN after erythrophagocytosis in normal controls and HH patients are summarized in Figure 9.6. After 24 hours control MN released 20 % ^{59}Fe as

low-molecular-weight Fe-complexes, 27 % as ferritin and 53 % as haemoglobin. MN from HH patients released 45 % ^{59}Fe as low-molecular-weight Fe-complexes, 29 % as ferritin and 26 % as haemoglobin (Moura *et al.*, 1998a). Similar results were obtained in monocytes–macrophages from subjects carrying the C282Y mutation of the HFE protein which were transfected with wild-type HFE (Montosi *et al.*, 2000), raising the accumulation of radio iron delivered by ^{55}Fe-Tf in these cells by 50 %. Compared with normal controls and patients with secondary iron overload, an inappropriately increased activity of IRP was found in monocytes of untreated HH patients (Cairo *et al.*, 1997). In contrast to normal subjects, this high IRP binding activity in HH monocytes could not be down-regulated by inflammation (Recalcati *et al.*, 1998). All these results are (patho)physiologically highly relevant. As these iron species are released to the portal system (from the spleen) or come into direct contact with hepatocytes (from Kupffer cells) most iron, if not bound to transferrin, will be rapidly cleared by the hepatocytes. It has been known for some time that hepatocytes express receptors for non-transferrin bound iron (NTBI) (Scheiber-Mojdehkar *et al.*, 1999), ferritin (Sibille *et al.*, 1988), haemoglobin and Hb–haptoglobin complexes (Hershko *et al.*, 1972). It was calculated that in humans about 26 mg of Hb–haptoglobin complex is cleared per litre per minute ($T^{1/2}$ in the rat is 7 minutes) (Hershko *et al.*, 1972; Kino *et al.*, 1980). Especially in haemolytic anaemias with secondary haemosiderosis, rapid release of iron in the form of Hb may protect macrophages against oxidative damage. The finding that there is a considerably increased rapid release of low-molecular-weight iron by macrophages of HH patients finally explains the consistently high plasma iron saturation in HH and the presence of NTBI in their plasma (Loreal *et al.*, 2001); (de Valk *et al.*, 2000a). This could not only be a result of increased iron absorption but could also be caused by greater iron release from macrophages, which already accounts for more than 90 % of daily iron influx into the plasma. It also explains why in HH, in contrast with secondary iron overload, macrophages (including Kupffer cells) contain only normal or low amounts of iron. This is consistent with the finding that less HFE is expressed in Cys282Tyr homozygote HH macrophages as compared with control cells (Parkkila *et al.*, 2000).

The liver is the first organ to be severely damaged in HH and other forms of secondary iron overload that are associated with increased absorption of iron. As was just mentioned, hepatocytes express a variety of receptors to remove potentially toxic forms of iron from plasma. A simplified picture of the role of the hepatocyte in iron uptake and release is given in Figure 9.7 (Plate 15). Known mechanisms of iron uptake by parenchymal cells have already been described in Chapter 5. An interesting new iron transporter in hepatocytes is TfR2, a protein that is not regulated by IRP and that seems only to be expressed on hepatocytes (Fleming *et al.*, 2000). From all these different molecular sources, iron will finally be released, entering the cytosolic labile iron pool (LIP). The hepatocyte itself however, does not need much iron. Consequently iron from the LIP will either be stored in ferritin or be rapidly exported to the plasma in a form that can easily bind to transferrin. Our description of a macrophage *to* hepatocyte *to* plasma pathway, of a variety of molecular iron species, seems at first sight to be complicated. However, each step makes sense. Also, the pathway allows adequate availability for erythropoiesis of all the iron derived from erythrophagocytosis.

9.4   Iron Deficiency

9.4.1   Prevalence and Global Distribution of Iron Deficiency

Worldwide, iron deficiency causes anaemia in more than 500 million people (DeMaeyer and Adiels-Tegman, 1985). The most important causes in less developed countries are infection with parasites and severe malnutrition. These causes are rare in the developed part of the world (Marx, 1997). The prevalence of anaemia in Europe and North America is 1 % in adult males and 14 % in adult females; this is compared with 27 % and 48 % in males and females respectively in Africa, and 40 % and 57 % in South Asia (DeMaeyer and Adiels-Tegman, 1985). Iron deficiency is responsible for more than half of these cases. Consequently, completely different strategies of prevention and diagnosis are needed in those populations. In developed countries iron deficiency is often symptomatic of blood loss, and the physician must identify its causes. Preventive donation of iron is only justified in well defined subpopulations, especially neonates, and may be considered as an appropriate therapy in rapidly growing children and adolescents, in pregnant women, blood donors, and in under-privileged socioeconomic groups (Marx, 1997).

9.4.2   Acquired Iron Deficiency

Iron-deficiency anaemia results from a discrepancy between iron availability and the amount required for production of red blood cells. The causes of acquired iron deficiency in so-called underdeveloped and developed countries must be differentiated. In underdeveloped countries, the main causes of iron deficiency are (a) the poor availability of iron in the diet due to low haem and high fibre and phytate content (D'Souza *et al.*, 1987), and (b) chronic blood loss due to hookworm, schistosomiasis and malaria (Stoltzfus *et al.*, 1997; Olsen *et al.*, 1998; Dreyfuss *et al.*, 2000). Inflammation and vitamin A deficiency often interfere with the above causes of iron deficiency, causing a mixed type of anaemia. In underdeveloped countries diet improvement, iron fortification of natural foods and eradication of parasites will have a much higher impact than will refinement of diagnostic procedures and therapy of iron-deficiency anaemia.

   Organs responsible for development of iron-deficiency anaemia are: the uterus (increased menstrual blood loss, pregnancy), the oesophagus (varicose veins in patients with liver cirrhosis), the stomach and bulbus duodeni (hiatus hernia, aspirin and detrimental effects of other non-steroidal antiinflammatory drugs, peptic ulcer, carcinoma, partial gastrectomy), the small intestine (hookworm, coeliac disease, diverticulosis, morbus Crohn, angiodysplasia), the colon and rectum (carcinoma, diverticulosis, angiodysplasia, varices, colitis) and, rarely, the kidney and lung. Increased demands for iron, not met by adequate iron intake, occur in premature infants, during any period associated with increased growth, and during pregnancy. Poor diet is also a cause of iron deficiency in some socioeconomic groups in developed countries. Female blood donors in particular may develop iron deficiency. Self-inflicted blood loss is a diagnosis that should be considered if no cause can be found for severe iron-deficiency anaemia.

9.4.3 Genetic Forms of Iron Deficiency

Genetic forms of iron deficiency are uncommon but are none the less very interesting from a pathophysiological point of view. Mutations in any protein that is involved in the transport of iron from the gut to the site of haem synthesis in the mitochondrion may cause iron deficiency. Such causes may be suspected if a patient with iron deficiency and without any sign of abnormal blood loss, does not restore haemoglobin concentration upon adequate therapy with oral iron. These patients usually react favourably if treated with parenteral iron, except those with a defect of erythroblast iron transporters. Highly suspicious are those patients with iron deficiency from early childhood, in particular if the condition runs in the family. The diagnosis can be confirmed with radionuclide iron absorption studies, measuring mucosal uptake and mucosal transfer of iron, combined with ^{59}Fe-ferrokinetic studies. In Table 9.1 candidate genetic defects of iron transport with a possible phenotype of iron deficiency are indicated.

9.4.4 Clinical Stages of Iron Deficiency

Iron deficiency can be caused by severe acute blood loss. The result will be anaemia without the typical characteristics of iron deficiency. The pattern is different, and well defined, in chronic iron deficiency. The essential characteristic is that iron released from macrophage and hepatocyte stores, together with dietary iron supply, are insufficient to deliver enough iron for erythropoiesis. During the first stage, called *pre-latent iron deficiency*, all storage iron will be mobilized (Verloop, 1970). This may be 'diagnostically silent' as laboratory parameters still remain within normal limits, although serum ferritin concentration and, for example, bone marrow iron stores (ferritin and haemosiderin) gradually decrease. Due to a higher need for haemoglobin production, iron absorption may already be increased, and signs of 'functional iron deficiency' may be observed, such as increased zinc protoporphyrin levels (Hershko *et al.*, 1985). During the second stage, *latent iron deficiency*, haemoglobin concentration is still normal. Diagnostic criteria for iron deficiency, however, are now easily recognizable: decreased serum ferritin, low serum iron, high serum transferrin (and consequent low iron saturation of transferrin), increased plasma levels of soluble transferrin receptor (Mast *et al.*, 1998; Skikne *et al.*, 1990). In the third stage, *iron deficiency anaemia*, haemoglobin concentration (Hb) decreases. Initially, mean corpuscular volume (MCV) and mean corpuscular haemoglobin (MCH) are still normal. In the chronic phase, with a further decrease of Hb, MCV and MCH can become very low, together with the appearance of pathological erythroblasts in the bone marrow and a pathological morphology of red cells in the peripheral blood. Continuous shortage of iron may profoundly affect production of Hb while the impact on muscular myoglobin is less pronounced (Celsing *et al.*, 1988). However, iron-containing enzymes such as cytochromes may be affected by iron shortage (Dhur *et al.*, 1989).

9.4.5 Symptoms and Signs of Iron Deficiency

Most symptoms and signs of iron-deficiency anaemia are non-specific. Laboratory tests for anaemia and iron deficiency are therefore included in almost every evaluation of any patient with vague symptoms. As a result, iron deficiency is often found by chance. Symptoms and signs of iron deficiency include: fatigue, headache, dizziness, impaired physical capacity, increased susceptibility to infections, retardation of growth and cognitive performance (in infants and children) (Oski, 1993), pale skin and mucous membranes, glossitis, fissuring of the corner of the mouth, brittle nails, koilonychias (spoon nails), unusual dietary craving (called *pica*, well known in pregnancy, e.g. for ice), atrophic gastritis with decreased acid secretion in severe cases (which is unfavourable for iron absorption) (Baynes, 1994). Iron plays an important role in infection, immunity and inflammation (Brock, 1994). Clinical evidence that iron deficiency impairs resistance to infection, however, is conflicting as most studies were poorly controlled and performed in Third World countries.

9.4.6 Treatment of Iron Deficiency

In developed countries the physician is only allowed to even consider treatment of iron deficiency if its cause is diagnosed, or proper further evaluation is initiated. Treatment of iron deficiency anaemia is rather simple and inexpensive in most subjects and entails oral treatment with ferrous salts. Despite lower absorption of iron, there is renewed interest in therapeutic use of ferric maltose, suggesting that a large influx of Fe(II) from therapeutic doses may cause oxidative damage (Fodor and Marx, 1988; Geisser, 1998). Although treatment failure mostly results from an inadequate dose, persistent blood loss which exceeds iron absorption and poor compliance, failure may also be the result of malabsorption. The cause may be bowel inflammation in the duodenal region, coeliac disease or a genetic defect of one of the proteins involved in intestinal iron absorption. In these patients, parenteral treatment is needed with iron–sucrose or iron–dextran complexes (the latter is not available now in many countries because of severe side effects). If the iron transport defect is (also) localized in the erythron, any form of iron therapy will remain ineffective.

9.5 Iron Overload

9.5.1 The $\beta2m^{-/-}$ Mouse as a Model for Human Hereditary Haemochromatosis

Although many animal models for iron overload exist, some mimicking certain aspects of HH, the β2-microglobulin knockout mouse is of special interest as it revealed for the first time crucial aspects of the pathogenesis of human HH in an animal model, and also because it underlines the important links between iron metabolism and the immune system. Hepatic iron overload in β2-microglobulin (β2m)-deficient mice appeared to be similar to that found in HH, with pathological iron depositions occurring predominantly in liver parenchymal cells (de Sousa *et al.*,

1994). In such mice, cell surface expression of MHC class I molecules is severely decreased, and as a consequence they lack $CD8^+$ lymphocytes. Progressive iron deposition in the liver of β2m-deficient mice was reported, increasing with supplemental dietary iron, and associated with an increased incidence of hepatocellular carcinoma (Rothenberg and Voland, 1996). More recently, it was demonstrated that β2m-deficient mice have a fourfold increase in plasma iron concentrations, increased transferrin saturation (>80 %) and increased hepatic iron as compared with normal control mice (Santos *et al.*, 1996). Furthermore, mucosal uptake of ferric, but not ferrous, iron and the subsequent mucosal transfer into the plasma was inappropriately increased in β2 m knockout mice (Santos *et al.*, 1998). Importantly, mice in which the CD8 molecule has been disrupted, ($CD8^{-/-}$) and mice that lacked the endoplasmic reticulum transporter for Class I associating peptides ($TAP1^{-/-}$) had a normal iron metabolism (Santos *et al.*, 1996). These observations strongly suggest the involvement of a major histocompatibility complex (MHC) Class I-like, β2m-dependent gene product in iron absorption. The finding of a novel gene of the MHC-Class I family, *HFE*, that is mutated in the majority of HH patients provided further independent support for the proposed causative role of a β2m-dependent gene in HH and its involvement in iron absorption (Feder *et al.*, 1996). Using the recently characterized $HFE^{-/-}$ mouse it was decisively demonstrated that mutations which disrupt the function of the *HFE* gene product result in HH (Zhou *et al.*, 1998).

One of the distinguishing features of the pathology in HH is initial deposition of iron in the parenchymal cells of affected tissue, with insignificant early involvement of macrophages. Reconstitution of lethally irradiated β2m-deficient mice with normal haematopoietic donor cells redistributes the iron from parenchymal cells to Kupffer cells in the liver but does not correct the inappropriate iron absorption (Santos *et al.*, 1996). In addition, both $\beta2m^{-/-}$ and $HFE^{-/-}$ mice have a significantly lower capacity to store iron in the spleen as compared with B6 control mice on the same diet (Zhou *et al.*, 1998; Santos *et al.*, 1996). It seems that the lack of appropriately formed HFE–β2m complexes leads to lower iron deposits in these cells. Ultimately, the lower iron loading capacity of the spleen may be related to a lower capacity of MPS cells to store iron, which may be caused by decreased erythrophagocytosis (Moura *et al.*, 1998a) and increased release of low-molecular-weight iron (Moura *et al.*, 1998b). Iron handling and storage in macrophages and epithelial intestinal cells may thus be similar, in that they may be regarded as iron-donor cells, and also because in HH they both behave as iron-deficient cells.

9.5.2 Adaptive Response of Iron Absorption in Iron-overload Diseases

Body iron content is the principal factor in the regulation of iron absorption (Marx,1979a,b). However, other physiological variables, such as erythropoietic rate (Bothwell, 1968), hypoxia (Raja *et al.*, 1988) and inflammation (Weber *et al.*, 1988) also influence iron absorption. In normal individuals, if the rate of erythropoiesis is stimulated by blood loss, dyserythropoiesis or acute haemolysis, iron absorption is increased. Conversely, if erythropoiesis is inhibited by hypertransfusion, starvation or descent from high altitude to sea level, then iron absorption decreases. The adaptive response of iron absorption to increased erythropoiesis, stimulated

by blood loss or acute haemolysis, remains intact in $\beta 2m^{-/-}$ mice and is indistinguishable from control wild type mice (Santos *et al.*, 1998). This suggests that the regulatory mechanism(s) of iron absorption operating in these situations are independent of the expression of *HFE*. In contrast, when iron stores are altered through dietary manipulations or parenteral iron injections, both steps of mucosal uptake and mucosal transfer are quantitatively affected in $\beta 2m^{-/-}$ mice (Santos *et al.*, 1998). Therefore, the expression of the defect in iron absorption in the $\beta 2m^{-/-}$ mice is clearly quantitative, suggesting an involvement of HFE $\beta 2m$ complexes in delivering information to intestinal epithelial cells about the iron status of the body. Delivery of the signal for adaptive regulation of intestinal absorption is dependent on plasma transferrin, since in human transferrin deficiency, as in iron-loaded hypotransferrinaemic (*hpx*) mice, increased iron absorption occurs despite the presence of systemic iron overload (Craven *et al.*, 1987). The recent finding that HFE associates with the transferrin receptor, forming a ternary HFE/transferrin receptor/iron-saturated transferrin complex, further supports this notion (Bennett *et al.*, 2000).

9.5.3 Causes of Iron Overload

Many external and internal causes of iron overload can be identified in man (Brissot *et al.*, 2000). A physician who finds laboratory evidence of iron overload cannot simply diagnose haemochromatosis. Sometimes sophisticated methods, including genetic investigations, liver biopsy and analysis of iron absorption and ferrokinetics, are needed to obtain a proper diagnosis (Brissot *et al.*, 2000). An overview of causes of iron overload is given in Table 9.2. From this list, and the variety of molecular defects of iron-related proteins (Figure 9.4 and Table 9.1), one can conclude that many subjects must have complicated and compound forms of iron overload. Polymorphisms of proteins that are not yet recognized as having a link with iron metabolism will no doubt appear on the scene in the near future, influencing the phenotype of iron-overload diseases.

9.5.4 Heterogeneity of Phenotypes in Hereditary Haemochromatosis

Clinical expression of iron-overload disease in subjects with a homozygous C282Y mutation of the HFE gene is highly variable, also with regard to increase of severity with age (Olynyk *et al.*, 1999). On the other hand, subjects lacking the homozygous C282Y mutation of the HFE gene may develop a clinical picture that is identical to, and sometimes more severe than, those with the classical mutation (Pietrangelo *et al.*, 1999). Therefore, other genetic and environmental factors must affect the severity of iron overload. In this context, the role of lymphocyte subpopulations has been suggested from previous observations of lymphocyte abnormalities in HH patients (Porto *et al.*, 1997; Arosa *et al.*, 1997). To test directly the role of lymphocytes in cellular iron handling, a double knockout mouse was developed by crossing $RAG1^{-/-}$ and $\beta 2m^{-/-}$ mice (Santos *et al.*, 2000c). RAG1-single deficient mice, which lack mature lymphocytes, have a normal capacity to regulate their iron absorption, but iron depositions are found in the liver when they are iron

Table 9.2 Causes of iron overload.

Primary haemochromatosis, caused by inappropriately high absorption of iron
    Hereditary haemochromatosis, associated with a homozygous Cys282Tyr mutation of the
        HFE gene
    Idiopathic haemochromatosis, not associated with a homozygous Cys282Tyr mutation of the
        HFE gene
    Porphyria cutanea tarda (very often associated with HFE mutations)
    Neonatal haemochromatosis
    Juvenile haemochromatosis
    Haemochromatosis associated with insulin resistance

Secondary iron overload, with increased iron absorption
    Haemolytic and dyserythropoietic anaemias, not receiving erythrocyte infusions (e.g.
        thalassaemias, sideroblastic anaemias, congenital dyserythropoietic anaemias, hexokinase
        and pyruvate kinase deficiency)

Secondary iron overload, with normal or decreased iron absorption
    Multiple erythrocyte transfusions in patients with haemolytic and dyserythropoietic anaemias
    Multiple erythrocyte transfusions in patients with hypoplastic anaemias
    Iatrogenic causes: long-term non-indicated (parenteral) iron therapy
    Frequent iron injections in rH-erythropoietin treated patients with end-stage renal disease
    Genetic defects of some proteins with a function in iron transport (e.g. atransferrinaemia)

Local iron overload
    Morbus Hallervorden–Spatz (brain)
    Idiopathic pulmonary haemosiderosis (lung)
    Goodpasture syndrome (lung, kidney)
    Intravascular haemolysis, such as paroxysmal noctural haematuria (kidney)
    Severe local bleeding, e.g. haemophilia (joint, muscle)

---

loaded through their diet, in a pattern similar to that seen in $\beta 2m^{-/-}$ mice. The $\beta 2m$ RAG1-double knockout mice develop a more severe phenotype involving increased iron absorption, with iron accumulation in the liver, heart and pancreas. Iron deposition in the heart deserves special interest, because heart failure is the most frequent cause of death in untreated HH and post-transfusional secondary haemosiderosis patients. Iron excess in myocytes could cause oxidative stress and alteration of myocyte functions due to iron-catalysed Fenton chemistry (Halliwell, 1994). We observed that $\beta 2mRAG1$-double knockout mice develop heart fibrosis, which could be prevented by reconstitution with normal haematopoietic cells. The possible influence of lymphocytes in cellular iron storage and iron-mediated cellular damage may include cytokine regulation (Weiss *et al.*, 1997) and/or a role in macrophage differentiation and function. The generation of HFE $\beta 2m$-double mutant mice, that deposit more tissue iron than mice lacking HFE only (Levy *et al.*, 2000), suggests that other $\beta 2m$-interacting proteins may be involved in iron regulation and may be the causative gene in non-HFE haemochromatosis (Pietrangelo *et al.*, 1999) or in juvenile haemochromatosis (Roetto *et al.*, 1999).

9.5.5 Findings in C282Y Heterozygotes

Heterozygosity for the C282Y mutation of the HFE gene has always been considered to be of no clinical consequence. There are now some studies showing that, as a

group, patients with this show slight but significant changes in some parameters of iron metabolism (Bulaj *et al.*, 1996; de Valk *et al.*, 2000b). Differences with genetically normal subjects are even more evident in compound heterozygotes, carrying one C282Y and one H63D mutation. More important is the finding that C282Y heterozygosity appears to be an independent risk factor for cardiovascular mortality and myocardial infarction (Roest *et al.*, 1999; Tuomainen *et al.*, 1999). This can hardly be explained by some discrete biochemical differences between heterozygotes and normal subjects. It has been suggested that the role of iron may be to increase LDL oxidation, which is an important feature in the development of atherosclerosis, or an interaction with endothelial NO catabolism. Transferrin-bound iron is considered to be safe and not a source for catalytically active iron. This is different for non-transferrin bound iron (NTBI). This iron species has been known for many years to be present in the plasma of patients with severe forms of secondary iron overload like β-thalassaemia major (Graham *et al.*, 1979). Recently, using more sensitive techniques, this noxious iron species could be identified in adequately treated hereditary haemochromatosis homozygotes, and even in heterozygotes (Loreal *et al.*, 2000; de Valk *et al.*, 2000a,b; Gosriwatana *et al.*, 1999). These findings will have important consequences for screening of populations for haemochromatosis, for phlebotomy treatment protocols, and in determining the clinical approach to heterozygotes.

9.5.6 Haemochromatosis and Porphyria Cutanea Tarda

Porphyria cutanea tarda (PCT) is a clinical condition associated with photosensitization of the skin by porphyrins and is caused by deficient hepatic uroporphyrinogen decarboxylase activity (see Chapter 7 for a detailed description of porphyrin biosynthesis). A familial and sporadic variant of PCT exists. It has been known for many years that all skin symptoms of PCT disappear after phlebotomy treatment. The amount of iron which must be removed to cure patients is very variable, but often iron overload exists. Initially PCT was envisaged as a form of secondary haemosiderosis, although some relationship with hereditary haemochromatosis was suspected. Detection of HFE and genotyping of patients with mutations of HFE enabled us to demonstrate that the majority of patients with PCT were either homozygous or heterozygous for either the C282Y or H63D mutation (Santos *et al.*, 1997b). This was the first indication that the H63D mutation might also have some clinical relevance, although neither H63D heterozygotes or homozygotes have any sign of iron overload. Clinical expression of skin symptoms and hepatic damage is particularly accelerated in C282Y homozygotes (Brady *et al.*, 2000; Bulaj *et al.*, 2000), acquired contributing factors being alcohol, hepatitis C virus and oestrogens.

9.5.7 Treatment of Iron Overload

The aim of treatment of iron overload is to remove all potentially toxic iron from the body. In hereditary haemochromatosis this can be achieved by weekly phlebotomies of 500 ml until the desired serum ferritin concentration (mostly <50 µg/l) or a normal transferrin iron saturation is reached (Brissot *et al.*, 2000).

During maintenance therapy, such values can be maintained by 2–12 phlebotomies per year, which is a remarkably wide range and one of the many signs of the heterogeneity in genotype of HH. The aim of treatment should not be to relieve the patient of complaints related to iron overload in order to induce symptoms resulting from chronic iron-deficiency anaemia. Although much effort has been given to reach a consensus about the optimal treatment of HH patients, there is no sound basis, and certainly no evidence-based medicine, for maintaining these patients at the limit of iron-deficiency anaemia. It may be more important to prevent generation of NTBI in iron-overload patients than to maintain a very low plasma ferritin concentration. This would necessitate the development of sensitive clinical tests to detect NTBI (Breuer *et al.*, 2000), and of novel absorbable iron chelators that would be able to remove NTBI from plasma but do not enter cells (Liu *et al.*, 2000).

It is of pathophysiological interest that it should be easy to remove iron rapidly from the body without inducing anaemia. This implies massive release of iron from both ferritin and haemosiderin (Ward *et al.*, 2000), a process that may be associated with destruction of these proteins. This touches one of remaining secrets of iron metabolism. We are well informed now of the way in which iron enters cells, but we know hardly anything about the mechanism of iron release from these two storage proteins (Chapter 6) and from macrophages and hepatocytes. One point is clear, however: if there is an increased demand for erythropoiesis, this signal effectively reaches iron-storing cells and molecules. An interesting observation comes from experiments on the utilization of intracellular ferritin iron for haemoglobin synthesis in developing human erythroid precursors (Meyron-Holtz *et al.*, 1999; Vaisman *et al.*, 1997). Strong evidence has been obtained that proteolytic degradation of ferritin in a lysosomal-like acid compartment was necessary for iron release. It may be that the iron storage compartment does not have the static nature that seems to be apparent when we study Perl's Blue-stained cells under the microscope. It may well be that there is a continuous synthesis and breakdown of iron storage proteins, releasing iron to the labile iron pool where it can be utilized for the synthesis of other iron-containing proteins, be exported from the cell for utilization in other cells, be chelated by iron chelators in case of the treatment of secondary iron overload, or be incorporated into newly synthesized ferritin.

9.6 Conclusion

Clinicians usually study diseases in order to improve the diagnosis and treatment of their patients. Careful evaluation of clinical symptoms and functional and biochemical defects is, however, of pivotal importance in appreciating and evaluating results from biochemical and cellular experiments. There should be no discrepancy between a hypothesis based on *in vitro* experiments and pathophysiological findings in patients or relevant animal models. If such a discrepancy exists, either the interpretation of such experiments is wrong, or they cannot be projected to an *in vivo* cell system or whole organism, or else something very interesting has been found. Conflicting *in vitro* results in, for example, the function of HFE and the HFE-TfR complex need be solved using existing observations in patients and animals with iron transport disorders.

9.7 References

Abboud, S. and Haile, D.J. (2000). *J. Biol. Chem.*, **275**, 19906–12.

Aguilar-Martinez, P., Biron, C., Masmejean, C., Jeanjean, P. and Schved, J.F. (1996). *Blood*, **88**, 1895.

Aisen, P. (1982). *Clin. Haematol.*, **11**, 241–57.

Aisen, P., Wessling-Resnick, M. and Leibold, E.A. (1999). *Curr. Opin. Chem. Biol.*, **3**, 200–6.

Anderson, G.J., Murphy, T.L., Cowley, L., Evans, B.A., Halliday, J.W. and McLaren, G.D. (1998). *Genomics*, **48**, 34–9.

Andrews, N.C., Fleming, M.D. and Levy, J.E. (1999). *Curr. Opin. Hematol.*, **6**, 61–4.

Arosa, F.A., Oliveira, L., Porto, G., da Silva, B.M. *et al.* (1997). *Clin. Exp. Immunol.*, **107**, 548–54.

Barosi, G., Cazzola, M., Morandi, S., Stefanelli, M. and Perugini, S. (1978). *Br. J. Haematol.*, **39**, 409–23.

Baynes, R.D. (1994). In *Iron Metabolism in Health and Disease* (eds Brock, J.H., Halliday, J.W., Pippard, M.J. and Powell, L.W.), W.B. Saunders, London, pp. 190–225.

Bennett, M.J., Lebron, J.A. and Bjorkman, P.J. (2000). *Nature*, **403**, 46–53.

Bernstein, S.E. (1987). *J. Lab. Clin. Med.*, **110**, 690–705.

Bothwell, T.H. (1968). *Br. J. Haematol.*, **14**, 453–6.

Brady, J.J., Jackson, H.A., Roberts, A.G., Morgan, R.R. *et al.* (2000). *J. Invest Dermatol.*, **115**, 868–74.

Breuer, W., Epsztejn, S. and Cabantchik, Z.I. (1995). *J. Biol. Chem.*, **270**, 24209–15.

Breuer, W., Hershko, C. and Cabantchik, Z.I. (2000). *Transfusion Sci.*, **23**, 185–92.

Brissot, P., Guyader, D., Loreal, O., Laine, F. *et al.* (2000). *Transfusion Sci.*, **23**, 193–200.

Brock, J.H. (1994). In *Iron Metabolism in Health and Disease* (eds Brock, J.H., Halliday, J.W., Pippard, M.J. and Powell, L.W.) W.B. Saunders, London, pp. 353–89.

Bulaj, Z.J., Griffen, L.M., Jorde, L.B., Edwards, C.Q. and Kushner, J.P. (1996). *New England J. Med.*, **335**, 1799–805.

Bulaj, Z.J., Phillips, J.D., Ajioka, R.S., Franklin, M.R. *et al.* (2000). *Blood*, **95**, 1565–71.

Cairo, G., Recalcati, S., Montosi, G., Castrusini, E., Conte, D. and Pietrangelo, A. (1997). *Blood*, **89**, 2546–553.

Cairo, G. and Pietrangelo, A. (2000). *Biochem. J.*, **352**, 241–50.

Camaschella, C., Roetto, A., Cali, A., De Gobbi, M. *et al.* (2000). *Nat. Genet.*, **25**, 14–15.

Campuzano, V., Montermini, L., Molto, M.D., Pianese, L. *et al.* (1996). *Science*, **271**, 1423–7.

Canonne-Hergaux, F., Gruenheid, S., Ponka, P. and Gros, P. (1999). *Blood*, **93**, 4406–17.

Celsing, F., Ekblom, B., Sylven, C., Everett, J. and Astrand, P.O. (1988). *Acta Med. Scand.*, **223**, 451–7.

Cossee, M., Puccio, H., Gansmuller, A., Koutnikova, H. *et al.* (2000). *Human Mol. Genet.*, **9**, 1219–26.

Craven, C.M., Alexander, J., Eldridge, M., Kushner, J.P., Bernstein, S. and Kaplan, J. (1987). *Proc. Natl Acad. Sci. USA*, **84**, 3457–61.

Custer, G., Balcerzak, S. and Rinehart, J. (1982). *Am. J. Hematol.*, **13**, 23–36.

Dearborn, D.G. (1997). *Curr. Opin. Pediatr.*, **9**, 219–24.

DeMaeyer, E. and Adiels-Tegman, M. (1985). *World Health Stat. Q.*, **38**, 302–16.

Dennery, P.A., Spitz, D.R., Yang, G., Tatarov, A. *et al.* (1998). *J. Clin. Invest.*, **101**, 1001–11.

De Sousa, M., Reimao, R., Lacerda, R., Hugo, P., Kaufmann, S.H. and Porto, G. (1994). *Immunol. Lett.*, **39**, 105–11.

De Valk, B., Addicks, M.A., Gosriwatana, I., Lu, S., Hider, R.C. and Marx, J.J. (2000a). *Eur. J. Clin. Invest.*, **30**, 248–51.

De Valk, B., Witlox, R.S., van der Schouw, Y.T. and Marx, J.J. (2000b). *Eur. J. Intern. Med.*, **11**, 317–21.

Dhur, A., Galan, P. and Hercberg, S. (1989). *J. Nutr.*, **119**, 40–7.

Donovan, A., Brownlie, A., Zhou, Y. *et al.* (2000). *Nature*, **403**, 776–81.

Dreyfuss, M.L., Stoltzfus, R.J., Shrestha, J.B., Pradhan, E.K. *et al.* (2000). *J. Nutr.*, **130**, 2527–36.

D'Souza, S.W., Lakhani, P., Waters, H.M., Boardman, K.M. and Cinkotai, K.I. (1987). *Early Human Dev.*, **15**, 103–11.

Fairbanks, V.F., Fahey, J.L. and Beutler, E. (1971). In *Clinical Disorders of Iron Metabolism* (eds Fairbanks, V.F., Fahey, J.L. and Beutler, E.), Grune and Stratton, New York, London, pp. 1–41.

Feder, J.N., Gnirke, A., Thomas, W., Tsuchihashi, Z. *et al.* (1996). *Nat. Genet.*, **13**, 399–408.

Feder, J.N., Penny, D.M., Irrinki, A., Lee, V.K. *et al.* (1998). *Proc. Natl Acad. Sci. USA*, **95**, 1472–7.

Ferreira, C., Bucchini, D., Martin, M.E., Levi, S. *et al.* (2000). *J. Biol. Chem.*, **275**, 3021–4.

Fleming, M.D., Trenor, C.C., III, Su, M.A., Foernzler, D. *et al.* (1997). *Nat. Genet.*, **16**, 383–6.

Fleming, M.D., Romano, M.A., Su, M.A., Garrick, L.M., Garrick, M.D. and Andrews, N.C. (1998). *Proc. Natl Acad. Sci. USA*, **95**, 1148–53.

Fleming, R.E., Migas, M.C., Zhou, X., Jiang, J. *et al.* (1999). *Proc. Natl Acad. Sci. USA*, **96**, 3143–8.

Fleming, R.E., Migas, M.C., Holden, C.C., Waheed, A. *et al.* (2000). *Proc. Natl Acad. Sci. USA*, **97**, 2214–9.

Fodor, I. and Marx, J.J. (1988). *Biochim. Biophys. Acta*, **961**, 96–102.

Francanzani, A.L., Fargion, S., Romano, R., Piperno, A. *et al.* (1989). *Gastroenterology*, **96**, 1071–8.

Geisser, P. (1998). *Iron Therapy with Special Emphasis on Oxidative Stress*, Vifor International Inc, St Gallen, Switzerland.

Girelli, D., Corrocher, R., Bisceglia, L., Olivieri, O. *et al.* (1995). *Blood*, **86**, 4050–3.

Gosriwatana, I., Loreal, O., Lu, S., Brissot, P., Porter, J. and Hider, R.C. (1999). *Anal. Biochem.*, **273**, 212–20.

Goya, N., Miyazaki, S., Kodate, S. and Ushio, B. (1972). *Blood*, **40**, 239–45.

Graham, G., Bates, G.W., Rachmilewitz, E.A. and Hershko, C. (1979). *Am. J. Hematol.*, **6**, 207–17.

Griffiths, W.J., Kelly, A.L. and Cox, T.M. (1999). *Mol. Med. Today*, **5**, 431–8.

Gross, C.N., Irrinki, A., Feder, J.N. and Enns, C.A. (1998). *J. Biol. Chem.*, **273**, 22068–74.

Gunshin, H., Mackenzie, B., Berger, U.V., Gunshin, Y. *et al.* (1997). *Nature*, **388**, 482–8.

Gutierrez, J.A., Yu, J. and Wessling-Resnick, M. (1998). *Biochem. Biophys. Res. Commun.*, **253**, 739–42.

Gutteridge, J.M. (1994). *Chem. Biol. Interact.*, **91**, 133–40.

Halliwell, B. (1994). *Lancet*, **344**, 721–4.

Harding, A.E. (1981). *J. Med. Genet.*, **18**, 436–41.

Harris, Z.L., Durley, A.P., Man, T.K. and Gitlin, J.D. (1999). *Proc. Natl Acad. Sci. USA*, **96**, 10812–7.

Hashimoto, K., Hirai, M. and Kurosawa, Y. (1997). *Biochem. Biophys. Res. Commun.*, **230**, 35–9.

Heinrich, H.C., Gabbe, E.E., Meineke, B. and Whang, D.H. (1966). *Klin. Wochenschr.*, **44**, 827–33.

Hershko, C., Cook, J.D. and Finch, C.A. (1972). *J. Lab Clin. Med.*, **80**, 624–34.

Hershko, C. (1975). *Br. J. Haematol.*, **29**, 199–204.

Hershko, C., Konijn, A.M., Link, G., Moreb, J., Grauer, F. and Weissenberg, E. (1985). *Clin. Lab Haematol.*, **7**, 259–69.

Huebers, H., Huebers, E., Forth, W. and Rummel, W. (1973). *Hoppe Seylers Z. Physiol. Chem.*, **354**, 1156–8.

Huggenvik, J.I., Craven, C.M., Idzerda, R.L., Bernstein, S., Kaplan, J. and McKnight, G.S. (1989). *Blood*, **74**, 482–6.

Kino, K., Tsunoo, H., Higa, Y., Takami, M., Hamaguchi, H. and Nakajima, H. (1980). *J. Biol. Chem.*, **255**, 9616–20.

Kondo, H., Saito, K., Grasso, J.P. and Aisen, P. (1988). *Hepatology*, **8**, 32–8.

Lamarche, J.B., Lemieux, B. and Lieu, H.B. (1984). *Can. J. Neurol. Sci.*, **11**, 592–600.

Levy, J.E., Jin, O., Fujiwara, Y., Kuo, F. and Andrews, N.C. (1999). *Nat. Genet.*, **21**, 396–9.

Levy, J.E., Montross, L.K. and Andrews, N.C. (2000). *J. Clin. Invest.*, **105**, 1209–16.

Liu, Z.D., Piyamongkol, S. and Hider, R.C. (2000). *Transfus. Sci.*, **23**, 269–70.

Logan, J.I., Harveyson, K.B., Wisdom, G.B., Hughes, A.E. and Archbold, G.P. (1994). *Quarterly J. Med.*, **87**, 663–70.

Loreal, O., Gosriwatana, I., Guyader, D., Porter, J., Brissot, P. and Hider, R.C. (2000). *J. Hepatol.*, **32**, 727–33.

Manis, J. (1971). *Am. J. Physiol.*, **220**, 135–9.

Martin, M.E., Fargion, S., Brissot, P., Pellat, B. and Beaumont, C. (1998). *Blood*, **91**, 319–23.

Marx, J.J. (1979a). *Haematologica*, **64**, 479–93.

Marx, J.J. (1979b). *Scand. J. Haematol.*, **23**, 293–302.

Marx, J.J.M. (1982). In *The Biochemistry and Physiology of Iron* (eds Saltman, P. and Hegenauer, J.), Elsevier North Holland Inc, New York, pp. 245–7.

Marx, J.J.M. (1997). *Eur. J. Clin. Nutr.*, **51**, 491–4.

Marx, J.J. and Aisen, P. (1981). *Biochim. Biophys. Acta*, **649**, 297–304.

Marx, J.J. and van den Bent, B. (1981). *Nuklearmedizin*, **20**, 191–4.

Marx, J.J. and van Asbeck, B.S. (1996). *Acta Haematol.*, **95**, 49–62.

Marx, J.J., van den Bent, B., van Dongen, R. and Strackee, L.H. (1980). *Nuklearmedizin*, **19**, 140–5.

Mast, A.E., Blinder, M.A., Gronowski, A.M., Chumley, C. and Scott, M.G. (1998). *Clin. Chem.*, **44**, 45–51.

McKie, A.T., Marciani, P., Rolfs, A., Brennan, K. *et al.* (2000). *Mol. Cell*, **5**, 299–309.

Mete, A., Dorrestein, G.M. and Marx, J.J.M. (2001). *Eur. J. Clin. Invest* (in press).

Meyron-Holtz, E.G., Vaisman, B., Cabantchik, Z.I., Fibach, E. *et al.* (1999). *Blood*, **94**, 3205–11.

Miltenburg, G.A., Wensing, T., Breukink, H.J. and Marx, J.J. (1993). *Vet. Res. Commun.*, **17**, 209–17.

Montosi, G., Paglia, P., Garuti, C., Guzman, C.A. *et al.* (2000). *Blood*, **96**, 1125–9.

Moura, E., Verheul, A.F. and Marx, J.J. (1997). *Scand. J. Immunol.*, **46**, 399–405.

Moura, E., Noordermeer, M.A., Verhoeven, N., Verheul, A.F. and Marx, J.J. (1998a). *Blood*, **92**, 2511–9.

Moura, E., Verheul, A.F. and Marx, J.J. (1998b). *Eur. J. Clin. Invest.*, **28**, 164–73.

Mumford, A.D., Vulliamy, T., Lindsay, J. and Watson, A. (1998). *Blood*, **91**, 367–8.

Oates, P.S., Thomas, C., Freitas, E., Callow, M.J. and Morgan, E.H. (2000). *Am. J. Physiol Gastrointest. Liver Physiol.*, **278**, G930–G936.

Olsen, A., Magnussen, P., Ouma, J.H., Andreassen, J. and Friis, H. (1998). *Trans. R. Soc. Trop. Med. Hyg.*, **92**, 643–9.

Olynyk, J.K., Cullen, D.J., Aquilia, S., Rossi, E., Summerville, L. and Powell, L.W. (1999). *New England J. Med.*, **341**, 718–24.

Oski, F.A. (1993). *New England J. Med.*, **329**, 190–3.

Parkkila, S., Parkkila, A.K., Waheed, A., Britton, R.S. *et al.* (2000). *Haematologica*, **85**, 340–5.

Pietrangelo, A., Montosi, G., Totaro, A., Garuti, C. *et al.* (1999). *New England J. Med.*, **341**, 725–32.

Porto, G., Vicente, C., Teixeira, M.A., Martins, O. *et al.* (1997). *Hepatology*, **25**, 397–402.

Poss, K.D. and Tonegawa, S. (1997). *Proc. Natl Acad. Sci. USA*, **94**, 10919–24.

Raja, K.B., Simpson, R.J., Pippard, M.J. and Peters, T.J. (1988). *Br. J. Haematol.*, **68**, 373–8.

Ramm, G.A. (2000). In *Hemochromatosis. Genetics, Pathophysiology, Diagnosis and Treatment* (eds Barton, J.C. and Edwards, C.Q.), Cambridge University Press, Cambridge, pp. 494–507.

Recalcati, S., Pometta, R., Levi, S., Conte, D. and Cairo, G. (1998). *Blood*, **91**, 2565–72.

Ricketts, C. and Cavill, I. (1978). *Clin. Nucl. Med.*, **3**, 159–64.

Ricketts, C., Jacobs, A. and Cavill, I. (1975). *Br. J. Haematol.*, **31**, 65–75.

Riedel, H.D., Remus, A.J., Fitscher, B.A. and Stremmel, W. (1995). *Biochem. J.*, **309**, 745–8.

Roest, M., van der Schouw, Y.T., de Valk, B., Marx, J.J. *et al.* (1999). *Circulation*, **100**, 1268–73.

Roetto, A., Totaro, A., Cazzola, M., Cicilano, M. *et al.* (1999). *Am. J. Human Genet.*, **64**, 1388–93.

Rothenberg, B.E. and Voland, J.R. (1996). *Proc. Natl Acad. Sci. USA*, **93**, 1529–34.

Rotig, A., de Lonlay, P., Chretien, D., Foury, F. *et al.* (1997). *Nat. Genet.*, **17**, 215–7.

Roy, C.N., Penny, D.M., Feder, J.N. and Enns, C.A. (1999). *J. Biol. Chem.*, **274**, 9022–28.

Santos, M., Schilham, M.W., Rademakers, L.H., Marx, J.J., de Sousa, M. and Clevers, H. (1996). *J. Exp. Med.*, **184**, 1975–85.

Santos, M., Wienk, K.J., Schilham, M.W., Clevers, H., de Sousa, M. and Marx, J.J. (1997a). *Lab. Anim.*, **31**, 264–70.

Santos, M., Clevers, H.C. and Marx, J.J. (1997b) *New England J. Med.*, **336**, 1327–8.

Santos, M., Clevers, H., de Sousa, M. and Marx, J.J. (1998). *Blood*, **91**, 3059–65.

Santos, M., Sousa, M. and Marx, J.J. (2000a). *Transfusion Sci.*, **23**, 225–35.

Santos, M., Marx, J.J.M., Clevers, H. and de Sousa, M. (2000b). In *Haemochromatosis. Genetics, Pathophysiology, Diagnosis and Treatment* (eds Barton, J.C. and Edwards, C.Q.), Cambridge University Press, Cambridge, pp. 487–93.

Santos, M.M., de Sousa, M., Rademakers, L.H., Clevers, H., Marx, J.J. and Schilham, M.W. (2000c). *Am. J. Pathol.*, **157**, 1883–92.

Scheiber-Mojdehkar, B., Zimmermann, I., Dresow, B. and Goldenberg, H. (1999). *J. Hepatol.*, **31**, 61–70.

Sibille, J.C., Kondo, H. and Aisen, P. (1988). *Hepatology*, **8**, 296–301.

Skikne, B.S., Flowers, C.H. and Cook, J.D. (1990). *Blood*, **75**, 1870–6

Smith, J.E. (2000). In *Haemochromatosis. Genetics, Pathophysiology, Diagnosis and Treatment* (eds Barton, J.C. and Edwards, C.Q.), Cambridge University Press, Cambridge, pp. 508–16.

Stefanelli, M., Barosi, G., Cazzola, M. and Orlandi, E. (1980). *Br. J. Haematol.*, **45**, 297–308.

Stoltzfus, R.J., Dreyfuss, M.L., Chwaya, H.M. and Albonico, M. (1997). *Nutr. Rev.*, **55**, 223–32.

Takahashi, Y., Miyajima, H., Shirabe, S., Nagataki, S., Suenaga, A. and Gitlin, J.D. (1996). *Human Mol. Genet.*, **5**, 81–4.

Tsuchihashi, Z., Hansen, S.L., Quintana, L., Kronmal, G.S. *et al*. (1998). *Blood Cells Mol. Dis.*, **24**, 317–21.

Tuomainen, T.P., Kontula, K., Nyyssonen, K., Lakka, T.A., Helio, T. and Salonen, J.T. (1999). *Circulation*, **100**, 1274–9.

Vaisman, B., Fibach, E. and Konijn, A.M. (1997). *Blood*, **90**, 831–8.

Verloop, M.C. (1970). *Blood*, **36**, 657–71.

Vulpe, C.D., Kuo, Y.M., Murphy, T.L., Cowley, L. *et al*. (1999). *Nat. Genet.*, **21**, 195–9.

Waheed, A., Parkkila, S., Zhou, X.Y., Tomatsu, S. *et al*. (1997). *Proc. Natl Acad. Sci. USA*, **94**, 12384–9.

Waheed, A., Parkkila, S., Saarnio, J., Fleming, R.E. *et al*. (1999). *Proc. Natl Acad. Sci. USA*, **96**, 1579–84.

Ward, R.J., Legssyer, R., Henry, C. and Crichton, R.R. (2000). *J. Inorg. Biochem.*, **79**, 311–7.

Weber, J., Werre, J.M., Julius, H.W. and Marx, J.J. (1988). *Ann. Rheum. Dis.*, **47**, 404–9.

Weiss, G., Bogdan, C. and Hentze, M.W. (1997). *J. Immunol.*, **158**, 420–5.

Werner, E. and Kaltwasser, J.P. (1987). *Arzneimittelforschung*, **37**, 116–21.

Wienk, K.J., Marx, J.J., Santos, M., Lemmens, A.G. *et al*. (1997). *Br. J. Nutr.*, **77**, 123–31.

Wienk, K.J., Marx, J.J. and Beynen, A.C. (1999). *Eur. J. Nutr.*, **38**, 51–75.

Wollenberg, P., Mahlberg, R. and Rummel, W. (1990). *Biol. Met.*, **3**, 1–7.

Zahringer, J., Baliga, B.S. and Munro, H.N. (1976). *Proc. Natl Acad. Sci. USA*, **73**, 857–61.

Zhou, X.Y., Tomatsu, S., Fleming, R.E., Parkkila, S. *et al*. (1998). *Proc. Natl Acad. Sci. USA*, **95**, 2492–7.

Zoller, H., Pietrangelo, A., Vogel, W. and Weiss, G. (1999). *Lancet*, **353**, 2120–3.

10 Iron and Oxidative Stress

10.1 Introduction

Iron and oxidative stress are intertwined; increasing amounts of low molecular weight, redox-active iron, are synonymous with activation of reactive oxygen species (ROS); a scientific fact that is not new – as far back as the 1900s, the consequences of increased iron loading to the detriment of the cell had been realized. However, as in *Through the Looking Glass* by Lewis Carroll, 'all is not as it seems' and progress in this subject has been advancing dramatically since the last edition of this book.

Life in an oxygen-rich environment is not without its hazards, and oxygen-derived free radicals (molecules which have one or more unpaired electrons are called free radicals; they are generally very reactive and will act as chain carriers in chemical reactions) are formed in the course of normal aerobic life. In mammals, metabolism is normally dependent upon oxygen that, as we have seen (Chapter 1) can give rise to reactive oxygen species, the most potentially dangerous of which is the hydroxyl ion, a highly reactive, short-lived, free radical, that can do enormous damage to biological molecules. As well as oxygen-derived free radicals that are formed in the course of normal aerobic life, reactive nitrogen species (RNS) are also generated. During normal cellular metabolism, such radicals will rapidly detoxify; however, if somewhat higher levels are generated these could initiate cellular toxicity as well as acting as signalling molecules to mobilize certain cellular defence mechanisms.

Free radicals are involved in a multitude of normal biochemical reactions; both reactive oxygen and nitrogen species are implicated in cell regulation where oxidants and redox status are important factors in signal transduction. Free-radical oxygen species are involved in enzyme-catalysed reactions, in mitochondria as by-products of the consumption of molecular oxygen in the electron transport chain, in signal transduction and gene expression, and in activation of nuclear transcription factors. Reactive nitrogen species also play an important role as messengers in cells.

10.2 Iron and Fenton Chemistry

Ferrous iron, by its reaction with hydrogen peroxide in the Fenton reaction, can yield the toxic hydroxyl radical, OH$^\bullet$, which will further potentiate oxygen toxicity.

$$Fe^{2+} + H_2O_2 \longrightarrow OH^\bullet + OH^- + Fe^{3+} \qquad \text{Fenton chemistry}$$
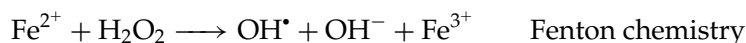
Hydroxyl radicals are the most reactive free-radical species known and have the ability to react with a wide number of cellular constituents including amino-acid residues, and purine and pyrimidine bases of DNA, as well as attacking membrane lipids to initiate a free-radical chain reaction known as lipid peroxidation.

It is, therefore, vital that iron is carefully sequestered into non-toxic forms, since an increase in the low-molecular-weight iron pool (Chapter 7), could exacerbate free-radical generation. The low-molecular-weight pool is considered to be an equilibrium between Fe^{2+} and Fe^{3+} at concentrations of 10^{-8} M and 10^{-16} M respectively. (Crichton and Ward, 1992). More recent estimates using the fluorescent metallosensor calcein give somewhat higher values, calculated to be of the order of 10^{-6} M (Epsztejn *et al.*, 1997). In normal circumstances excess iron will be incorporated into one of the iron storage proteins, ferritin or haemosiderin, the synthesis of the former in iron repletion is induced in the cytosol of the cell by lack of binding by the iron sensor proteins IRP1 and IRP2 to the 5′-IREs of the cognate mRNAs (see Chapter 7).

10.2.1   Reactive Nitrogen Species

Reactive nitrogen species also play an important role as messengers in cells. NO is produced by the enzyme nitric oxide synthase, NOS, from arginine generating NO and citrulline. Various isoforms of this enzyme exist which modulate diverse physiological responses: for example vasodilation is induced by NO produced by endothelial NOS, eNOS, in the brain; NO functions as a signal messenger (neuronal NOS, nNOS) and NO also acts as an antimicrobial agent to combat infection (inducible NOS, iNOS). In this latter function it has been suggested that there is direct interaction between catalytic iron-centres of enzymes, for example, aconitase, succinate dehydrogenase and ribonucleotide reductase within the microbe (Lepoivne *et al.*, 1991; Drapier and Hibbs, 1988) and NO, such that the enzymes are inactivated. NO also plays an important role in the regulation of iron homeostasis, interacting with the iron-sulfur centres of IRP (see later).

Peroxynitrite, a non-radical product, is formed by the reaction of $NO^{\bullet}$ and $O_2^{\bullet-}$ and is highly toxic to cells.

$$NO^{\bullet} + O_2^{\bullet-} \longrightarrow ONOO^-$$
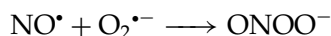
At physiological pH, $ONOO^-$ protonates to peroxynitrous acid (ONOOH) which disappears within a few seconds, the end product being largely nitrate. The chemistry of peroxynitrite/peroxynitrous acid is extremely complex, although addition of ONOO to cells and tissues leads to oxidation and nitration of proteins, DNA and lipids with a reactivity that is comparable to that of hydroxyl radicals.

10.3   Importance of Cytoprotection

Such a plethora of radicals produced as a result of normal cellular metabolism needs to be rapidly scavenged by cytoprotective enzymes and antioxidants present in the cell and cellular membranes, both hydrophobic and hydrophilic compartments. The
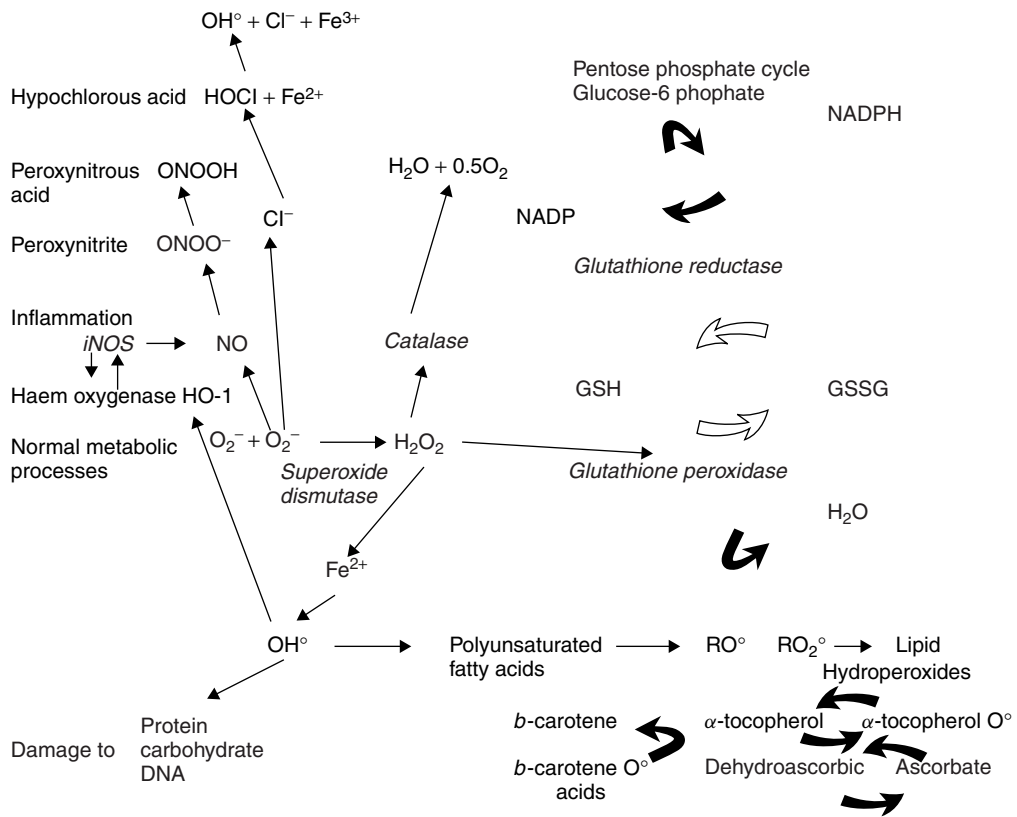
Figure 10.1 'Ward' cascade showing the cooperation between cytoprotective enzymes and antioxidants for scavenging of reactive oxygen and reactive nitrogen species.

vast array of protective mechanisms do not act independently of one another, but rather function cooperatively in the form of a cascade, (Figure 10.1).

The glutathione redox system is an essential player in controlling the redox state within the cell, the glutathione/glutathione reductase pathway attempts to keep a stable cellular redox balance

Glutathione (GSH)

Glutathione (GSH), the tripeptide γ-glutamylcysteinyl glycine, can exist both in a reduced and an oxidized form (the latter composed of two GSH molecules linked by a disulfide bridge). It is one of the most important cellular antioxidants since it supplies the electrons for the reduction of peroxides by the action of glutathione peroxidase. The oxidized glutathione GSSH formed is subsequently regenerated by the NADPH dependent glutathione reductase. Inside the cell, glutathione is present in millimolar concentrations mainly in the reduced form, GSH; small changes in the ratio of reduced GSH to oxidized GSSG may have significant biological effects. GSH/GSSG ratios vary enormously between intracellular compartments, being the highest in the nucleus 100 : 1 and lowest in the endoplasmic reticulum (Hwang

et al., 1992). The ability of cells to up-regulate their levels of intracellular glutathione (GSH) synthesis in times of oxidative stress will be an important factor in the ability of the cell to protect itself from toxicity.

Glutathione has specific transporters for its entry into mitochondria (as has iron, see later) such that any defects in its transport into the mitochondria will be important contributing factors in precipitating mitochondrial toxicity. Evidence that dicarboxylate and 2-oxoglutamate may be carriers for glutathione into the mitochondria has recently been published (Chen *et al.*, 2000).

10.3.1 Glutathione Reductase

Glutathione reductase is a NADPH flavoprotein which reduces GSSG to GSH at the expense of oxidizing NADPH. The NADPH required is provided in animal tissues by the pentose phosphate pathway. Glutathione reductase contains two protein subunits, each with a flavin FAD at its active site. The NADPH reduces the FAD which then passes its electron onto a disulfide bridge, S—S, between the two cysteine residues in the protein. The two—SH formed then interact with GSSG and reduce it to 2GSH. Glutathione reductase activity has been assayed in both the cytosol and mitochondria (where GSH and GSSG would be present). *In vitro*, glutathione reductase activity is stimulated by melatonin (Reiter *et al.*, 1997s 1999) by Fe^{2+}, but not Fe^{3+}, after 24-h incubation with cultures of Vero monkey kidney cells (Garcia-Alfonso *et al.*, 1996) and by peroxynitrite (Francescutti *et al.*, 1996), and *in vivo* by *N*-nitroso compounds in the livers of mice (Sheweita and Mostafe, 1996), and by ferric chloride intracortically injected into the cerebral cortex of rats (Singh and Pathak, 1990). *In vitro* experiments have shown that glutathione reductase is inhibited by plant polyphenols (Zhang *et al.*, 1997), ascorbate/iron in synaptosome culture (Cardoso *et al.*, 1998), and by dinitrosyliron diglutamate and dinitrosyliron di-L-cysteine (Keese *et al.*, 1997).

Since glutathione reductase is a cornerstone of the malaria parasite antioxidant defence and repair mechanism, it is a potential target for antimalarial and cytostatic agents.

10.3.2 Glutathione Peroxidase

This is a tetrameric enzyme with identical subunits, each monomer containing one atom of selenium in the form of a selenocysteine residue. Non-selenium containing glutathione peroxidase enzymes have also been described (Ketterer and Meyer, 1989). Glutathione peroxidase is found both in the cytosol and the mitochondria, and catalyses the removal of hydrogen peroxide from the cell, converting reduced glutathione to oxidized glutathione in the process – thus being one of the key enzymes of the antioxidant system. Glutathione peroxidase can also terminate the chain reaction of lipid peroxidation by removing lipid hydroperoxides from the cell membrane.

Within nervous tissue glutathione peroxidase is localized predominantly in microglia with relatively lower amounts in neurons (Lindenau *et al.*, 1998). When

oxidative stress is induced, glutathione peroxidase activity is elevated in microglia and may provide one of the important mechanisms for nervous tissue to withstand oxidative stress.

10.3.3 Superoxide Dismutase

Two forms of SOD exist in eukaryote cells, a Cu/Zn SOD present in the cytosol while a MnSOD is present within the mitochondria. In bacteria an iron-containing SOD has been identified (Lim *et al.*, 1997). Superoxide dismutase plays an important protective role by catalysing the dismutation of superoxide radicals to hydrogen peroxide and dioxygen. In nervous tissue, superoxide dismutase is considered to be a major factor in the protection against oxidative stress; specific antibodies to the Cu/Zn SOD and Mn-SOD showed that the cytoplasm of astrocytes, cellular processes and the nucleolus were predominantly Cu/Zn-SOD. Mn-SOD was localized predominantly to the mitochondria of astroglia (Lindenau *et al.*, 2000) After insult with ROS and RNS, Mn-SOD increased twofold, thereafter decreasing slowly, while Cu/Zn-SOD increased in astroglial cells. Both SOD isoforms are assumed to be induced to prevent oxidative and nitric oxide/peroxynitrite mediated damage.

10.3.4 Catalase

Catalases, in common with many peroxidases, are haem enzymes in which the high spin iron–porphyrin system can generate a ferryl type of iron (Chapter 2) to participate in the oxidation of molecules at the expense of hydrogen peroxide. While both catalases and peroxidases can oxidize a variety of organic substrates, catalases differ by their ability to use hydrogen peroxide both as electron donor and acceptor, thus catalysing the disproportionation reaction in which two molecules of hydrogen peroxide give two molecules of water and one molecule of dioxygen. Catalase is located essentially within the peroxisomes of mammalian cells. The exact role it might play in cells where there is increased oxidative stress remains unclear – it would be presumed that any excess hydrogen peroxide generated in the cell would be effectively removed by glutathione peroxidase present in the cytosol and would never reach the peroxisomes. The catalase present in the peroxisomes might therefore function to protect the peroxisome from the hydrogen peroxide produced by some of the many oxidases present in this intracellular compartment.

10.3.5 Pentose Phosphate Pathway, PPP

The importance of having adequate supplies of NADPH for the regeneration of these various enzymes cannot be over emphasized. In normal situations this cofactor can be adequately provided by the reductive pentose phosphate pathway. Monitoring the activity of the pentose phosphate pathway has been proposed as a unique way to study the metabolic response to oxidative stress, since the glutathione peroxidase activity is coupled via glutathione reductase to the enzyme glucose-6-phosphate dehydrogenase (Ben Yoseph *et al.*, 1994).

Exposure of 9L gliosarcoma cells to hydrogen peroxide stimulated PPP, which could be attenuated when the neurons were preincubated with the iron chelator desferrioxamine.

10.3.6   Haem Oxygenase

Haem oxygenase, HO-1 (also referred to as heat shock protein (hsp) 32) is a highly inducible stress protein that oxidatively cleaves haem molecules (derived from haemoglobin, cytochromes, etc.) to the bile pigments, biliverdin and bilirubin, together with the gaseous cellular messenger carbon monoxide and Fe^{2+}. Ferris *et al*. (1999) suggested that HO-1 augmented iron efflux thereby modulating intracellular iron levels. The induction of HO-1 is reputed to be a protective event: transition metal ions and oxidative stress can induce its transcription. Several authors have suggested that HO-1 confers cellular protection against a wide range of oxidant stresses both *in vivo* and *in vitro*, but the mechanism of protection is unclear. Neither bilirubin or biliverdin have strong antioxidant properties, particularly *in vivo*, while the production of free iron could be considered to be a prooxidant event. Some authors suggest that this free redox-active iron could induce ferritin synthesis, hence an antioxidant effect could be inferred. In recent *in vitro* studies by Lamb *et al*. (1999) who isolated microsomes and incubated them with haemoglobin (to induce HO-1), a time-dependent increase in lipid peroxidation was observed, thereby suggesting that there was an HO-driven iron dependent mechanism. The significance of such a prooxidant pathway in cellular protection has yet to be established although the authors suggest that it might have important beneficial functions to the cell through an unidentified iron-signalling mechanism. Earlier a tenuous relationship between HO-1 and iNOS had been identified, indicating that if HO-1 activity was increased (by addition of haemin 24 h prior to LPS stimulation), NO release was impaired, reputedly because of a decrease in haem bioavailability for iNOS synthesis (Turcanu *et al*., 1998). It has also been demonstrated that both NO, NO donors (Foresti and Motterlini, 1999), and peroxynitrite (Foresti *et al*., 1999), are capable of inducing HO-1 protein expression, while LPS is known to activate the HO-1 gene in liver cultures and macrophage cells through oxidative activation of NFKappaB (Oshiro *et al*., 1999).

10.4   Importance of Cell Type in Response to Oxidative Stress

Over the past years it has become apparent that the cell type is an important determinant of the extent of oxidative stress that may occur. Both the latent activities of cytoprotective enzymes in specific cell types, as well as the ability of the cell to respond rapidly to an oxidative insult by the upregulation of such enzymes, will be important predeterminants of the fate of the cell. Table 10.1 shows the concentrations of both antioxidants and cytoprotective enzymes in a variety of tissues. While the liver is well provided with antioxidant protection, the brain has very low levels, so the ability to respond rapidly to an oxidative insult by upregulation of gene transcription and translation will be an important determinant of survival or death. Cells such as hepatocytes have high levels of expression and

Table 10.1 Antioxidant and cytoprotective enzyme content in a variety of rat tissues.

	Antioxidants			Cytoprotective enzymes		
	a-tocopherol	*glutathione*	*Superoxide dismuatase*	*Catalase*	*Glutathione peroxidase*	*Glutathione reductase*
	nmol/g. tissue	*μmol/g. tissue*		*Unites/g. tissue*		
Liver	380 ± 8.5	5.6 ± 2.1	$12,000 \pm 3120$	47.5 ± 9.5	41.1 ± 12.3	6.59 ± 2.6
Spleen	62.4 ± 27.5	3.01 ± 0.22	2022 ± 424	2.0 ± 0.7	11.2 ± 1.7	1.7 ± 0.54
Brain	22.4 ± 1.4	0.90 ± 0.09	1679 ± 246	0.04 ± 0.002	0.69 ± 0.08	2.67 ± 0.03
Heart (Aerobic muscle)	46.6 ± 20.9	2.63 ± 2.09	2060 ± 703	0.97 ± 0.15	11.2 ± 2.1	1.28 ± 0.52
Plantaris (Anaerobic muscle)	13.8 ± 3.3	1.33 ± 0.23	398 ± 144	0.08 ± 0.02	0.54 ± 0.39	0.42 ± 0.14

Results are mean ± standard deviation of at least six determinations in different animals of body weight 201–300g (from Ward *et al.*, 1994).

translation of cytoprotective enzymes as well as biosynthesis of glutathione, so ROS could be very effectively scavenged. In contrast, astrocytes noted for their low protection appear to be extremely vulnerable to oxygen species, cells in culture taking up to 36 hours for the upregulation of certain cytoprotective enzymes such as catalase, superoxide dismutase and glutathione peroxidase. Iron is actively excluded from the brain, the transfer of excess iron from the peripheral system to the brain being extremely low, even when the circulating low-molecular-weight iron is high, for example, in untreated genetic haemochromatosis and thalassaemia patients there is little evidence to suggest an increased burden of iron in the brain. However, as we shall see, iron deposits in the brain due to localized degradation of tissue will have a devastating effect and induce massive ROS generation because of the relatively low cytoprotection in an oxidizing environment.

10.4.1 Cancer Cells

Interestingly, the activity of some cytoprotective enzymes, particularly catalase and glutathione peroxidase, is low in animal and human cancers, suggesting that most cancer cell types cannot detoxify hydrogen peroxide, this reactive oxygen intermediate being an important secondary messenger for the stimulation of various pathways. Whether this reflects utilization or poor upregulation is unknown. Furthermore it is reported that all cancer cells have some imbalance in antioxidant enzyme levels by comparison with their cells of origin (Oberley and Oberley, 1997).

In vitro studies in which cells are treated with H_2O_2, show that the cells become resistant towards subsequent increased amounts of ROS that would be lethal without such pretreatment. Such observations indicate that cells can activate an adaptive genetic programme against oxidative stress.

Resting cells do not express iNOS but the capacity to express this enzyme after specific stimuli is present in several tissues. Cells such as macrophages, endothelial cells, kidney cells, chondrocytes, cardiac myocytes, pancreatic islets and fibroblasts

have the ability to express iNOS. Factors that will induce iNOS differ between cell types. However microbes are the most important factor for the induction of iNOS.

10.4.2 Neutrophils and Macrophages

Specific cell types can also utilize the cytotoxicity of the reactive oxygen species, ROS, that are generated *in vivo* to attack and kill invading microorganisms. Monocytes, neutrophils, eosinophils and macrophages play an important role in combating infection through the production of a wide armoury of ROS and RNS. During phagocytosis, these professional killer cells increase their consumption of molecular oxygen, generating a large quantity of ROS and RNS, referred to as the respiratory burst. The oxidase responsible for the respiratory burst consists of one membrane-bound and four cytosolic components. Upon activation, the cytosolic proteins translocate to the membrane-bound component, a *b*-type cytochrome, and a multi-component electron transfer system is formed that catalyses the reduction of molecular oxygen at the expense of NADPH (reviewed in Dahlguen and Karlsson, 1999), Figure 10.2. Superoxide and hydrogen peroxide are generated by the NADPH oxidase which can give rise to other ROS and RNS, e.g. H_2O_2, NO and peroxynitrite. NO formation in macrophages is one of the major mechanisms of the macrophage defence against invading microorganisms.

In macrophages there is an autoregulatory feedback loop that links iron home-ostasis with optimal formation of NO for host defence. In both *in vivo* and *in vitro* iron-loaded cells (Legssyer *et al.*, 2000; Weiss *et al.*, 1994), the ability of the macrophage to release NO after challenge with LPS and interferon-γ is reduced. However, the underlying mechanism by which iron exerts transcriptional regula-tion of iNOS has remained elusive although recent data suggests that activation of hypoxia inducible factor 1 (HIF-1) might be involved (see Chapter 12).

In neutrophils the presence of myeloperoxidase, MPO, within the granules will catalyse the formation of hypochlorous acid from the reaction between hydrogen peroxide and chloride ions while eosinophils MPO preferentially use Br^- ions.

$$H_2O_2 + Cl^- \longrightarrow HOCl + OH^-$$
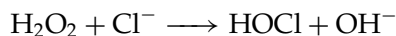
Iron can react with hypochlorous acid, (in neutrophils) to generate the hydroxyl radical:

$$Fe^{2+} + HOCl \rightarrow OH^\bullet + Cl^- + Fe^{3+}$$
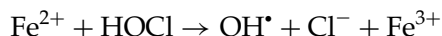
Low levels of hypochlorous acid can function as a mediator in cell activation, induce NFKB heterodimer p50/p65 in a T-lymphocytic cell line through proteolysis of IKB and p105 inhibitors. Hypochlorous acid will also contribute to the release of TNFα in cellular supernatants of T-lymphocytes which are capable of commencing activation in non-induced cells (Schoonbroodt *et al.*, 1997). Hypochlorous acid can react with amines to produce chloramines and *N*-chlorinated derivatives that have a long lifetime in plasma. Taurine, a sulfonated amino acid, will finally combine with these two products to reduce their toxicity.
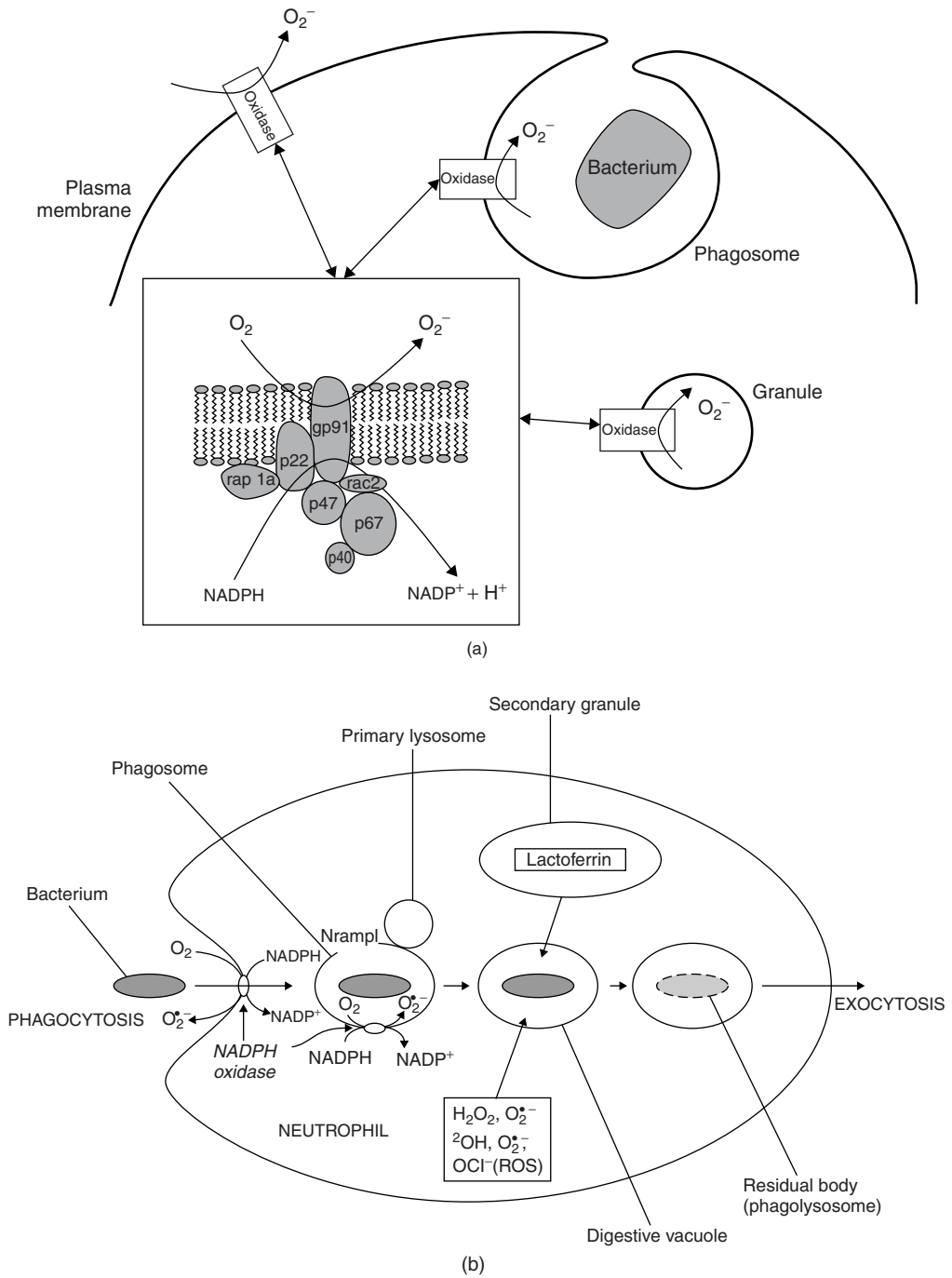
Figure 10.2 Possible sites for NADPH-oxidase assembly and activity in human neutrophils. Reprinted from Dahlgren and Karlsson, 1999. Copyright (1999), with permission from Elsevier Science.

10.5 Natural Resistance-associated Macrophage Protein (Nramp1)

Over the past 10 years interest has been directed at Nramp1 which is reputed to play an important role in controlling intracellular homeostasis of iron in macrophages, such that the proliferation of intracellular pathogens can be limited (Barton *et al.*, 1999). Nramp1 is a divalent cation transporter, is localized to the membrane of the phagolysosome and functions either to transport iron into the phagosome where it serves as a catalyst for the Fe^{2+}-mediated stimulation of the Fenton reaction, producing hydroxyl radicals (Kuhn *et al.*, 1999) or, alternatively, to transport iron out of the parasite-harbouring phagosome (Gomes and Appelberg, 1998), thus decreasing the amount of iron available for bacterial growth. Nramp1 is upregulated in macrophages after LPS and IFNγ treatment, iron or sodium nitroprusside treatment (Baker *et al.*, 2000). However, growth rates are decreased because of decreased iron availability, shown by an increase in IRP-2. These authors suggested that Nramp1 might control its own expression through a negative autoregulatory loop that is important for iron homeostasis and maintenance of low redox active iron in the macrophage.

10.6 Ageing of Cells

The ageing of cells is associated with the loss of ability of the cell to maintain a variety of factors that include iron homeostasis and metabolic rate, so that the cell is more vulnerable to ROS, the net result being increased oxidative stress. In general there are significant decreases in the glutathione redox index with increasing age in both the heart and the liver (Stio *et al.*, 1994). Other factors are also involved, including increase in iron content, decrease in antioxidant protection and over-expression of certain cytoprotective enzymes, for instance MnSOD is ageing brain – although the mechanisms mediating such upregulation are unknown. Generation of ROS by electrons escaping from the electron transport chain in mitochondria is by far the predominant process during the lifetime of a normal healthy cell. Mitochondrial malfunction has been suggested as the intracellular basis of ageing. There is also clear evidence that free-radical dependent reactions lead to lipofuscin formation, and its accumulation has been demonstrated to be dependent upon the iron-catalysed Fenton reaction (von Zglinicki and Brunk, 1993).

10.7 Cell Signalling and Iron

When marginally higher levels of ROS are generated in eukaryotic cells, certain response mechanisms are activated in order to combat the harmful effects, which involve changes in gene expression patterns in the cell, i.e. transcriptional changes. Since the underlying mechanisms are highly conserved, the responses are quite similar in organisms ranging from bacteria to man. Many of the signals derive from the extracellular environment and accordingly these signals require transduction from the cell surface to the nucleus. Stimulation of these pathways leads to the

increased activity of specific transcription factors and consequently the increased expression of certain stress-related genes.

10.7.1 Oxidative Stress in Bacteria

The genetic response to oxidative stress has been studied extensively in *E. Coli*. The synthesis of over 80 proteins is induced upon exposure to H_2O_2 and $O_2^{\bullet-}$, and two transcription factors have been identified. Firstly the system OxyR which is activated by H_2O_2, resulting in the formation of an intracellular disulfide bond, that then switches on several genes encoding for antioxidant functions such as catalase. During aerobic growth, OxyR acts homeostatically to regulate cellular H_2O_2 levels. Secondly the transcription factors SoxR/S are induced by superoxide anions or nitric oxide and activate expression of genes, the products of which are involved either in protection from oxidative stress or repair of ROS-mediated damage. The SoxR protein is activated by oxidation of its 2Fe–2S component and stimulates the SoxS gene. The SoxS protein then induces transcription of at least 15 genes encoding antioxidant functions, e.g. SOD, metabolic functions and antibiotic resistance by activation of efflux pumps. The SoxRS system may function in resistance to NO-generating immune cells and may contribute to clinical antibiotic resistance.

10.7.2 Oxidative Signalling in Yeast

In *Saccharomyces cerevisiae* the binding of a haem group, the synthesis of which needs oxygen, activates the transcription factor HAP-1 which controls transcription of the catalase and SOD genes (Zitomer and Lowry, 1992). The oxidant defence system of budding yeast *Saccharomyces cerevisiae* has a number of inducible adaptive stress responses to oxidants such as H_2O_2, superoxide anion and lipid peroxidation products. The oxidative responses appear to be regulated, at least in part, at the level of transcription, and there is considerable overlap between them and many diverse stress responses, allowing the yeast cell to integrate its response towards environmental stress (Jamieson, 1998). Mutations in Ras and other signal transduction proteins increase survival and resistance to oxidative stress in stationary phase yeast.

10.7.3 Oxidative Stress in Plants

Atmospheric pollutants represent an important source of oxidative and nitrosative stress to terrestrial plants. In plants, salicylic acid is known to be the mediator for systemic acquired resistance. The salicylic-binding protein shows catalase activity, which decreases significantly upon ligand binding, thereby resulting in the accumulation of hydrogen peroxide (Chen *et al*., 1993). The plant immune system involves the generation of ROS messengers by ligand-induced inhibition of an ROS-eliminating enzyme. However the molecular and biological mechanisms of

adaptation are still poorly understood and the signalling pathways remain elusive (Dat *et al.*, 2000). Calcium signalling has been implicated in plant responses to oxidative stress, constituting a signal that is transduced via calmodulin, calcium dependent protein kinase and other calcium controlled proteins to effect a wide array of downstream responses (Knight, 2000).

10.7.4 Oxidative Stress in Mammalian Cells

Transcription factors that are exclusively activated by ROS, or those that selectively control expression of ROS-protective and repair enzymes, are slowly being identified. Much of this work has used different cell lines, indicating that ROS show cell type specificity with respect to transcription factors and their activation (Bonizzi *et al.*, 1999). NFKappaB (NF-KB) was the first eukaryotic transcription factor shown to respond directly to oxidative stress, the oxidative stress being induced by hydrogen peroxide from which hydroxyl radicals were generated via Fenton chemistry (Schreck *et al.*, 1991). However incubation with other ROS, e.g. superoxide, hydroxyl radical and NO donors, failed to activate NFKB. In other words NFKB is selectively mediated by peroxides in a fashion comparable to the bacterial activation of OxyR, and over-expression of either catalase or Cu/Zn-SOD in cell lines induced either suppression or superinduction of NFKB respectively (Schmidt *et al.*, 1995), while depletion of GSH induced NF-KB. A variety of antioxidants including GSH precursors, L-cysteine, thiols, vitamin E and its derivatives are able to block its activation.

In most cell types NFKB is present in the cytosol as an inactive heterodimer (p50 and p65; or p50/c-Rel) bound to a third inhibitory subunit IKB. Removal of this inhibitory subunit is the signal for the translocation of the transcription factor to the nucleus to bind to consensus DNA sequences, where NF-KB plays a key role in the regulation of numerous genes involved in pathogen responses and cellular defence mechanisms, Figure 10.3. These include many immunologically relevant genes, cytokines and cytokine receptors, growth factors, and cell adhesion molecules, each of which contain functional NF-KB binding sites in their promoter and enhancer regions. In T lymphocytes, IL-2 and IL-2 receptor α-chain are controlled by NF-KB while in retroviruses, e.g. HIV-1, the NF-KB binding sites are found in their regulatory LTR region. NF-KB activation does not require new protein synthesis: a great variety of pathogens and inflammatory stimuli, e.g. LPS, viral infection, cytokines IL-1, IFNγ and TNFα, activate the transcription factor within minutes (Baeuerle and Henkel, 1994).

Activation of cells results in the release of IKB, followed by the rapid proteolysis of IKB. Although phosphorylation of serine 32 and 36 in the amino-terminal part of IKBα occurs when the proinflammatory cytokines or mitogens are administered to a T lymphocytic cell line, a different site of action has been found after H_2O_2 incubation (Schoonbroodt *et al.*, 2000). The tyrosine residue 42 and the *C*-terminal PEST (Pro–Glu–Ser–Thr) domain plays a major role in the phosphorlylation of IKB after treatment with H_2O_2. Furthermore the H_2O_2-inducible phosphorylation was not dependent upon IKB kinase activation but involved casein kinase II. The importance of iron for the activation of NFKB was underlined by the fact that
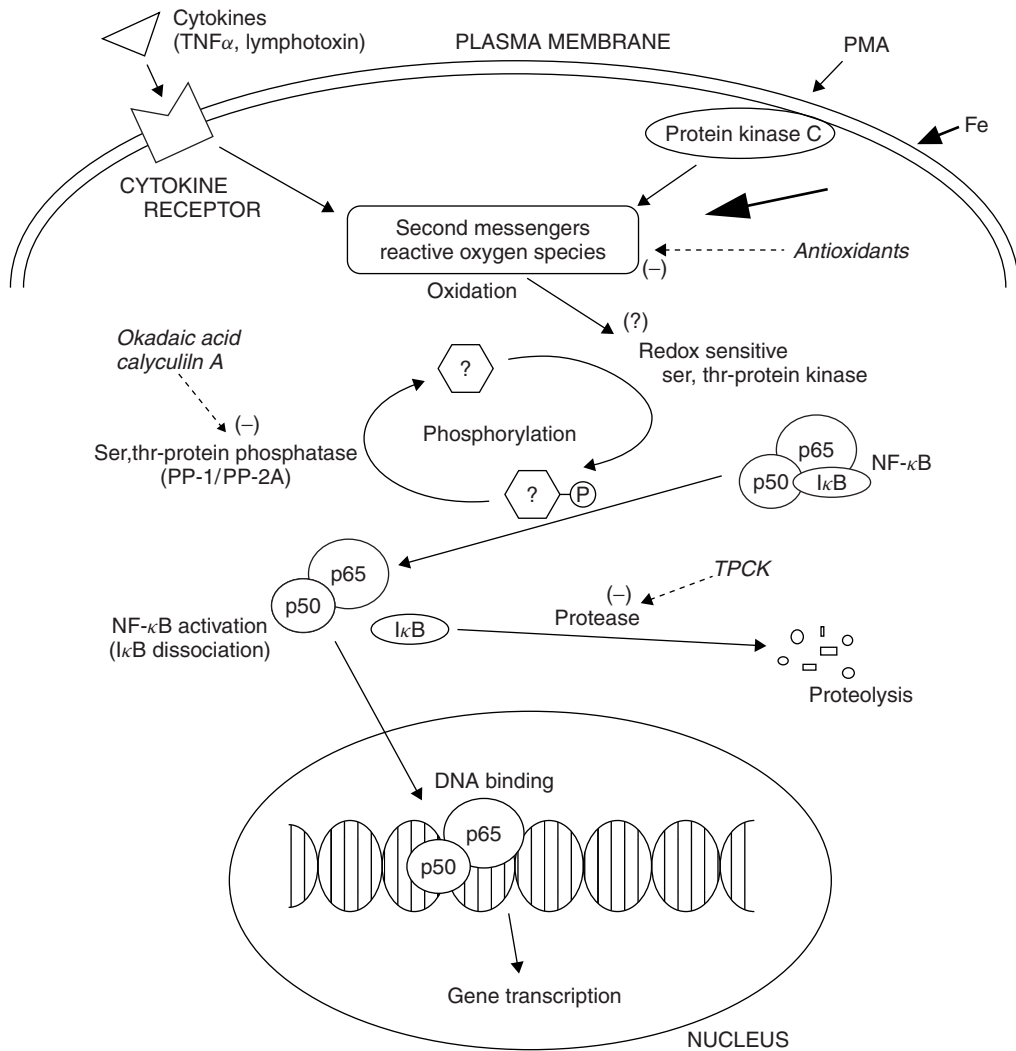
Signal transduction pathways for NF-κB activation

(a)

Figure 10.3 (a) Proposed mechanism for induction of NF*K*B proteins (from Suzuki *et al.*, 1994); (b) interaction with iron metabolism. Reproduced with permission from Cairo and Pietrangelo, 2000, © the Biochemical Society.

administration of either DFO or hydroxypyridone diminished the activation of the transcription factor induced by hydrogen peroxide.

A common observation has been that different times are needed for the activation of NF*K*B by different stimuli; in the case of proinflammatory cytokines the kinetics of the activation is fast, while in the case of H_2O_2 the kinetics of the activation are slow and sustained. This led to the realization that perhaps different target regions on the IKB were affected by the stimulant, or that other transcription factors were involved. NF*K*B is frequently associated with other transcription factors so that they
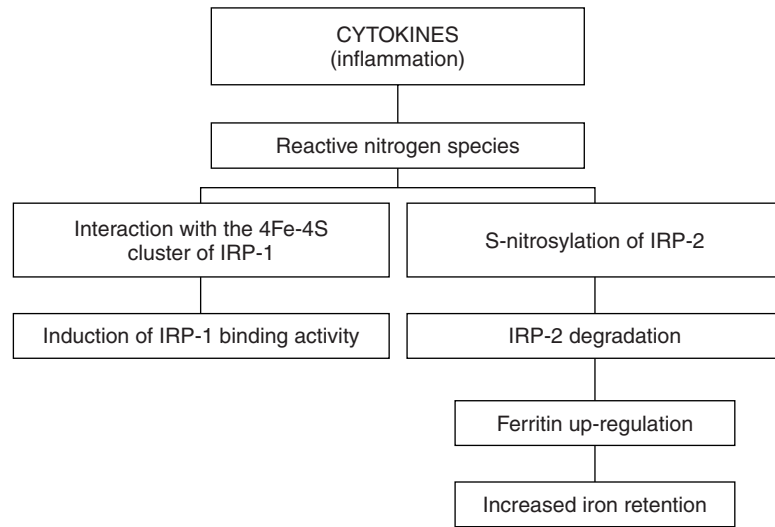
(b)

Figure 10.3   (*continued*)

cooperate for full induction of various genes. Using iNOS induction as an example, Dlaska and Weiss (1997) identified a regulatory region on the iNOS gene between −153 to −142 bp upstream of the transcriptional start site of the iNOS promoter that was sensitive to regulation by iron perturbation. The protein responsible was identified as NF-IL6, a member of the CCAAT/enhancer binding protein family of transcription factors. The binding of NF-IL6 to the consensus motif with iNOS was induced by both IFNγ and LPS, reduced by iron and enhanced by DFO. Iron by itself regulated expression of iNOS transcriptionally. The NF-IL6 binding site on iNOS is of central importance for the high transcriptional rate of the iNOS gene after IFNγ and LPS stimulation. It was suggested that after cytokine/LPS stimulation of cells, activation of the NF-IL6 occurred later than that of NF*K*B such that NF-IL6 would maintain the active transcription rate while NF*K*B would initiate transcription. Another transcription factor has also been implicated, HIF-1 (hypoxia inducible factor-1), which may cooperate with NF-IL6 in iron-mediated regulation of iNOS in ANA-1 macrophages. Binding of HIF-1 to target sequences is induced by DFO.

   A recent review has cast doubt upon the exact role played by ROS in activating NF*K*B, suggesting that the activation of NF*K*B by hydrogen peroxide is cell specific and distinct from physiological activators such as Il-1 and TNF. In addition, inhibition by antioxidants was also found to be cell- and stimulus specific and can involve a variety of factors not related to redox modulation (Bowie and O'Neill, 2000). Only recently have studies of NF*K*B activation in various human diseases commenced, e.g. into Parkinson's disease, while only a few studies of human cell lines, e.g. hepatocytes and phagocytic leucocytes and macrophages, have been reported so far. Our recent studies (Legssyer *et al.*, 2001) show that macrophages loaded *in vivo* with iron, were unable to increase NF*K*B activation after challenge with LPS *ex vivo*, thereby suggesting that such cells are compromised and do not respond adequately to infection.

Recent results have demonstrated that oxidant stress generated directly by exogenous H_2O_2 differentially induces IL-8 and ICAM-1 transcription in epithelial and endothelial cells. H_2O_2 induces IL-8 but not ICAM-1 in the A549 type-II-like epithelial cell line, whereas in a microvessel endothelial cell line (HMEC-1) as well as in primary endothelial cells, H_2O_2 induces ICAM-1 but not IL-8, which is spontaneously expressed. In contrast, the proinflammatory cytokine TNFα, whose activity is dependent on the generation of intracellular ROS, induces IL-8 and ICAM-1 in both cell types. The differential induction of IL-8 and ICAM-1 by H_2O_2 and TNFalpha suggests that the two inflammatory stimuli target distinct redox responsive signalling pathways to activate cell type-specific gene expression.

Heterdimers of the Jun and Fos transcription factor family constitute the transcription factor AP-1. Oxidative stress results in the increased transcription of the c-fos and c-jun genes although only a moderate induction of AP-1 occurs.

10.8 Apoptosis

Signals from neighbouring cells or tissues will instruct a particular cell to proliferate, differentiate into another cell type or to commit suicide by programmed cell death. Figure 10.4 shows that NFKB can play a major role in countering programmed cell death and hence survival of the cell after stimulation of the TNFα pathway. Such a pathway depends upon the activation of NFKB which will activate a variety of anti-apoptopic genes.

The role of ROS in DNA damage has been widely debated (Wiseman and Halliwell, 1996). Whether increasing iron content in various tissues will exacerbate DNA damage is debatable. Our studies of livers from rats iron loaded for four weeks with ferrocene or iron dextran failed to show any modification of DNA bases (Ward *et al.*, 1995). Since iron is carefully sequestered into ferritin and haemosiderin in iron loading-syndromes it is unclear how it might be released to react with DNA. An increased incidence of hepatic carcinoma has been reported in genetic haemochromatosis patients with iron loading thereby indicating that over a period of years modification of DNA may occur. Ultimately DNA damage can lead to a death-inducing signalling complex, Figure 10.5 (Plate 15). Caspases are thought to be the central executioners of the apoptopic pathway (Hengarten, 2000). The Bcl-2 family is also important in the regulation of the cytochrome *c* pathway across the mitochondrial outer membrane, the Bcl-2 proteins might act by inserting into the outer mitochondrial membrane to form channels or holes by interacting with other proteins or by control homeostasis of mitochondria (reviewed by Hengarten, 2000). The release of cytochome *c* from the mitochondria is an almost universal feature of apoptopic cell death although apoptosis induced by death receptors often bypasses the mitochondrial pathway.

10.9 Relationship Between NFKB and NO

One of the major sites of action of NFKB is the activation of iNOS. In 1993, it was shown that the murine gene coding iNOS contained two putative NFKB
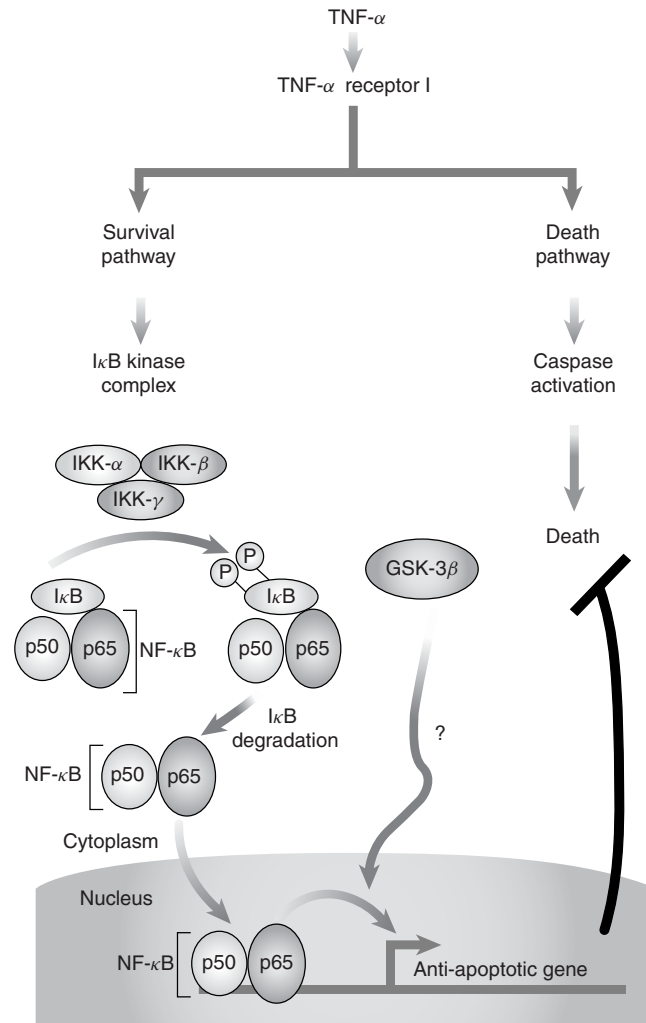
Figure 10.4 Life and death decisions in cells. Cellular stimulation with tumour necrosis factor-α (TNFα) simultaneously activates survival and death signalling pathways. Reprinted with permission from Nature (from Pomerantz and Baltimore, 2000). Copyright (2000) Macmillan Magazines Limited. p50 and p65 are subunits of NFKB

binding sites, one of which, NF-KBd, is necessary to confer inducibility by bacterial lipopolysaccharide (Xie *et al*., 1993). Stimulation of RAW 264.7 macrophages with LPS showed NFKB/Rel activation (p50-p50 and p50-p60) and binding to both NFKB sites in the mouse iNOS promoter (Goldring *et al*., 1995). Therefore activation of NFKB should lead to the transcription of iNOS. The regulatory cross-talk between iron metabolism and NO in macrophages is further highlighted by the transcriptional regulation of the iNOS gene by iron. Hence in macrophages the regulation of iron metabolism and NO is tightly connected. Recent studies in our laboratories have shown that alveolar macrophages, isolated from iron loaded rats decrease NO release after an LPS/IFNγ challenge (Legssyer *et al*., 2001), possibly

reflecting two pathways: (i) the presence of iron acting as a catalyst in NFKB activation via production of hydroxyl radicals from Fenton chemistry, and (ii) a decrease in iNOS transcription and translation due to its regulatory loop between iron metabolism and the NO/NOS pathway of iron metabolism (Weiss *et al.*, 1994).

10.10 How Does NO and H₂O₂ Affect the Iron Regulatory Proteins IRP-1 and IRP-2

Stimulation of murine peritoneal macrophages with IFNγ and LPS induced NO synthesis and activated IRE binding by IRP-1 and IRP-2. This activation is NO dependent and accompanied by a loss of the aconitase activity of IRP-1. This was also shown to occur in other cell types, such as the erythroid cell line K562, rat brain slices and mouse fibroblast lines and did not require cytokine stimulation. The activating effects of NO may depend on a direct interaction with the 4Fe−4S cluster or a slow effect on the low-molecular-weight iron pool. Activation of IRP-2 by LPS and IFN-γ has not been universally confirmed (reviewed by Cairo and Pietrangelo, 2000).

Early studies by Pantopoulos and Hentze (1995) showed that exposure of murine B6 fibroblasts to H_2O_2 leads to a reduction of ferritin synthesis and stimulation of transferrin receptor mRNA expression, both as a result of induction of IRP binding to IREs in ferritin and transferrin receptors. However it has been emphasized that such a response would indicate an increased low-molecular-weight iron pool which would be conducive to enhancing oxidative stress rather than reducing it. Cairo and Pietrangelo (2000) suggested that this effect occurred more as a response to the phosphorylation-dependent signalling pathway, rather than oxidative stress. Moreover, further studies showed that neither *in vivo* or *in vitro* H_2O_2 generation caused any stimulatory effect on IRP in mammalian cells, and in fact IRP was inactivated after simultaneous generation of H_2O_2 and $O_2^{\bullet-}$. In contrast IRP-2 is more susceptible to redox changes and is not activated by extracellular H_2O_2. Further studies are needed to identify the exact role played by H_2O_2 upon IRP-1 and IRP-2 activity *in vivo* in tissues and different cell types.

However, the activation of IRP-1 by H_2O_2 and NO differs considerably. NO requires up to 15 h for complete activation of IRP-1 while H_2O_2 achieves maximum IRP-1 activation within 60 minutes. Such results suggest that H_2O_2 activation does not simply result from a direct oxidative attack on IRP-1 but involves additional cellular activities (phosphorylation) for IRP-1 activation. Bouton *et al.* (1997) suggested that the formation of peroxynitrite might be important for IRP-1 activation. However, as yet, other investigators have not confirmed this.

Changes in redox state or oxidative stress in the cell can modulate binding of the IRPs to the IREs. Multiple factors, such as NO, peroxynitrite, and ROS as well as phosphorylation by protein kinase, modulate the RNA binding of IRP-1 and IRP-2. Peroxynitrite caused IRP-1 to lose its aconitase activity but it did not gain increased capacity to bind IRE, indicating that Fe−S is the target of peroxynitrite. In addition, peroxynitrite caused IRP-2 to lose its spontaneous binding activity, thus showing that peroxynitrite can regulate IRP-2 by a post translational event (Bouton *et al.*, 1997).

10.11 Diseases in which Increases in Iron may be Associated with Increased Oxidative Stress in the Cell

10.11.1 Iron and Inflammation

It has been well documented that the anaemia of chronic disease, ACD, results in a lowering of various haematological parameters. Several mediators are involved, among them histamine, serotonin, bradykinin, prostaglandins and, as found more recently, cytokines and nitric oxide. ACD is a parameter of systemic autoimmune disorders. The severe inflammatory stimuli lead to several systemic changes, mediated by inflammation-associated cytokines, e.g. IL-6, IL-1 TNFa, TGF beta that regulate hepatic synthesis of the acute phase proteins.

In rheumatoid arthritis iron accumulates in the joints, specifically the synovium, and this was reputed to exacerbate joint injury by the production of ROS. Later studies indicated that ischaemia/reperfusion injury, associated with increased iron loading, might be more relevant to the joint damage. Circulating levels of TNFα and IL-1β serum levels are significantly increased in RA with ACD. RA patients treated with TNFα antibodies show disease improvement including an increase in haemoglobin levels. The most controversial and stimulating aspect of the pathogenesis of ACD in system autoimmune disease is the role of iron metabolism and nitric oxide; the latter, as we have already mentioned, contributes to the regulation of iron metabolism. Both iron deficiency and iron overload influence the proliferation of B and T lymphocytes and differentially affect T−helper and TH-2 lymphocytes. Furthermore TH-1 cytokines and TH-2 type cytokines inhibit NO production. For these reasons cell-mediated immunity may influence NO synthesis and mechanisms leading to iron accumulation in the RE systems (Bertero and Caligaris Cappio, 1997).

10.12 Diseases in which Iron Plays an Important Role

10.12.1 Genetic Haemochromatosis

One of the most notable features of this inherited defect of iron homeostasis (Chapter 9) is the ability of individuals to accumulate large amounts of iron over many years and yet show no apparent adverse effects. This may in part be due to the ability of tissues, notably the liver, to increase their iron stores gradually over a long period of time, successfully sequestrating excess iron into ferritin and, predominantly, haemosiderin. However with time the excessive deposition of iron will cause a variety of toxic effects including diabetes and arthritis which are caused by deposition of iron in these tissues. Removal of this iron by venesection can often reduce these iron-induced symptoms.

10.12.12 Secondary Iron Overload

Thalassaemia

There is massive accumulation of iron in the tissues of thalassaemia patients primarily as a result of the influx of excessive haem breakdown both from the use of regular blood transfusions to correct the anaemia, and the increased breakdown of the erythrocytes as a result of the compromised status of the erythrocytes due to the imbalance in globin synthesis. In addition, iron absorption is increased as a result of the underlying anaemia. Splenectomy is often required because of the increased susceptibility of the patient to infection, resulting in even higher iron loading. The antioxidant status of such individuals is compromised, e.g. vitamin E and beta carotene levels are lower than controls while LDL conjugated dienes are three times higher than controls. This could lead to oxidative modification of low-density lipoprotein and an increased atherogenetic risk in beta thalassaemia patients.

Removal of the iron by chelation with the intramuscularly injected desferrioxamine or the newer oral chelators, such as the hydroxypyridone L1, will enhance the longevity of the patients.

HIV

The progression of human immunodeficiency virus (HIV) towards its more advanced stages is accompanied by increasing body stores of iron. Iron accumulates in macrophages as well as microglia, endothelial cells and myocytes. The iron burden is especially intense in the bone marrow, brain white matter, muscle and liver. Such excesses of iron will enhance oxidative stress, impair several already compromised immune defence mechanisms and directly promote the growth of microbes (Boelaert *et al.*, 1996).

10.13 Neurodegenerative Diseases

An inevitable consequence of ageing is an increase of iron in specific brain regions that may be contributory to a generalized increased oxidative stress. Cell type also appears to be important; neurons alone are highly sensitive to oxidative stress, although if cultured in the presence of astrocytes or microglia they remain viable after exposure to ROS or RNS (Tanaka *et al.*, 1999). It has also been shown that soluble and insoluble factors secreted by the astrocytes protect the neurons against ROS and RNS.

Iron has been implicated in many neurodegenerative diseases, particularly microglia activation and mitochondrial dysfunction.

Parkinson's Disease

In this progressive neurodegenerative disease there is increased deposition of iron within neuromelanin, specifically in the substantia nigra region. Gross cellular

dysfunction occurs, with iron-induced oxidative stress accompanied by the destruction of the neuromelanin-containing neurons in the substantia nigra, locus coeruleus as well as C1 and C3 medullary group.

Significant decreases in glutathione content occur in specific brain regions of Parkinson's patients, not necessarily accompanied by increased levels of oxidized GSSH. Furthermore, since mitochondrial glutathione is one of the major defence mechanisms for removing hydrogen peroxide its depletion will potentiate oxidant-induced loss of mitochondrial function as well as promoting extramitochondrial activation of NFKB. The increase in haem oxygenase 1 in both Lewy bodies and PD nigra neurons (Schipper *et al.*, 1998) will cause excessive cellular levels of haem-derived free iron and carbon monoxide and may contribute to the pathogenesis of PD.

Interestingly it has been noted that Indian vegetarians have a low incidence of Parkinson's disease in comparison with the Indian meat eaters, the Parsees. The reason for this difference has been suggested as the inhibition of iron absorption by the polyphenols that are present in high amounts in Indian spices. Further long-term studies of people with low iron status throughout their life time may give an indication as to whether decreasing iron intake may be beneficial in preventing the deposition of iron in the brain during the life time of an individual.

Alzheimer's Disease

In Alzheimer's disease, perturbation of iron homeostasis occurs (Ward and Crichton, 2001) although the mechanisms responsible await elucidation. Changes in iron homeostasis would appear to be a contributory factor in Alzheimer's disease although whether this is a primary or secondary effect remains unanswered. The abnormal distribution of iron in Alzheimer brains may result from a disequilibrium of IRP-1 and IRP-2. IRP-2 shows a striking difference from control age-matched brain and is associated with intraneuronal lesions (Smith *et al.*, 1998). *In vitro* studies of murine erythnoleukaemia cell lines indicated that the presence of aluminium in such cells antagonized the iron-induced decrease in the IRE binding activity of IRP-2, the aluminium stabilizing the IRP-2 and preventing its degradation such that the IRE binding of IRP-2 was enhanced (Yamanaka *et al.*, 1999). This would result in upregulation of transferrin receptors with an increased flux of metals associated with transferrin, namely iron and aluminium.

Despite initial studies implicating aluminium as a major factor in the development of senile plaques and neurofibrillary tangles, present results would indicate that the brain regions of Alzheimer patients do not always show significant increases in aluminium content. Microglia are a primary cellular component of plaque in Alzheimer's disease, and may contribute to the oxidative stress associated with the disease. However, studies of cytoprotective enzymes in the frontal cortex of Alzheimer patients have reported no changes in either SOD or glutathione peroxidase activities (Hayn *et al.*, 1996), which might indicate that the iron present is not redox active.

Friedrich's Ataxia

The import of metals into the mitochondria is poorly understood. Clearly with the generation of ROS it is essential that the presence of low-molecular-weight iron be kept to a minimum to prevent Fenton chemistry occurring. Iron is required by mitochondria for the biosynthesis of haem (Lange *et al.*, 1999) and iron-sulfur proteins (Lill *et al.*, 1999) (see Chapter 7). Experiments in yeast (Chapter 4) have shown that iron is not only imported into the mitochondrial matrix but is also transported out of the mitochondria across the inner membrane, constituting a veritable dynamic mitochondrial iron cycle (Radisky *et al.*, 1999). The yeast gene YFH1 is homologous to the mammalian gene frataxin, which is mutated in Friedrich's ataxia. YFH1 is involved in mitochondrial iron efflux (Babcock *et al.*, 1997); its deletion results in mitochondrial iron accumulation and ultimately respiratory incompetence. In man, frataxin, is localized to mitochondria, where it may play a role either in mitochondrial iron transport or in iron−sulfur cluster assembly or transport (Puccio and Koenig, 2000). Friedrich's ataxia (Chapter 7) is a mitochondrial disease associated with excessive mitochondrial accumulation of iron, particularly in brain and heart, leading to oxidative damage and mitochondrial dysfunction.

10.14 References

Babcock, M., de Silva, D., Oaks, R., Davis-Kaplan, S. *et al.* (1997). *Science,* **276**, 1709−12.

Baeuerle, P.A. and Henkel, T. (1994). *Ann. Rev. Immunol.,* **12**, 141−79.

Baker, S.T., Barton, C.H. and Biggs, T.E. (2000). *J. Leukoc. Biol.,* **67**, 501−7.

Barton, C., Biggs, T., Baker, S., Bowen, H. and Atkinson, P. (1999). *J. Leukoc. Biol.,* **66**, 757−62.

Ben-Yoseph, O., Boxer, P.A. and Ross, B.D. (1994). *Dev. Neurosci.,* **16**, 328−36.

Bertero, M.T. and Caligaris Cappio, F. (1997). *Haematologica,* **82**, 375−81.

Boelaert, J.R., Weinberg, G.A. and Weinberg, E.D. (1996). *Infect. Agents Dis.,* **5**, 36−46.

Bonizzi, G., Schoonbroolt, S., Havard, L., Piette, J., Merville, M.-P. and Bours, V. (1999). *Mol. Cell Biol.,* **19**, 1950−60.

Bouton, C., Hirling, H. and Drapier, J.C. (1997). *J. Biol. Chem.,* **272**, 19969−75.

Bowie, A. and O'Neill, L.A. (2000). *Biochem. Pharmacol.,* **59**, 13−23.

Cairo, G. and Pietrangelo, A. (2000). *Biochem. J.,* **352**, 241−50.

Cardoso, S.M., Pereira, C. and Oliveira, C.R. (1998). *Arch. Environ. Contam. Toxicol.,* **246**, 703−10.

Chen, Z., Putt, D.A. and Lash, L.H. (2000). *Arch. Biochem. Biophys.,* **373**, 193−202.

Chen, Z., Silva, H. and Klessing, D.F. (1993). *Science,* **262**, 1883−86.

Crichton, R.R. and Ward R.J. (1992). *Biochem.,* **31**, 11255−64.

Dahlgren, C. and Karlsson, A. (1999). *J. Immunol. Meth.,* **232**, 3−14.

Dat, J., Vandenabeele, S., Vranova, E., Van Montagu, M., Inze, D. and Van Breusegem' F. (2000). *Cell Mol. Life Sci.,* **57**, 779−95.

Dlaska, M. and Weiss, G. (1997). *J. Immunol.,* **162**, 6171−77.

Drapier, J.C. and Hibbs, J.B. (1988). *J. Immunol.*, **140**, 2829–38.

Epsztejn, S., Kakhlon, O., Glickstein, H., Breuer, W. and Cabantchik, I. (1997). *Anal Biochem.*, **248**, 31–40.

Ferris, C., Jaffrey, S., Takahashi, M., Brady, S. *et al.* (1999). *Nat. Cell. Biol.*, **1**, 152–7.

Foresti, R. and Motterlini, R. (1999). *Free Radic. Res.*, **31**, 459–75.

Francescutti, D., Baldwin, J., Lee, L. and Mutus, B. (1996). *Protein Eng.*, **9**, 189–94.

Garcia-Alfonsa, C., Lapez-Barea, J., Sanz, P., Repetto, G. and Repetto, M. (1996). *Arch. Enviro. Contam. Toxicol.*, **30**, 431–6.

Ghosh, S., May, M.J. and Kopp, E.B. (1998). *Ann. Rev. Immunol.*, **16**, 225–60.

Goldring, C.E., Narayanan, R., Lagadec, P. and Jeannin, J.F. (1995). *Biochem. Biophys. Res.*, **209**, 73–9.

Gomes, M.S. and Appelberg, R. (1998). *Immunology*, **95**, 165–8.

Hayn, M., Kremser, K., Singewald, N., Cairns, N. *et al.* (1996). *Life Science*, **58**, 537–44.

Hengartner M.O. (2000). *Nature*, **407**, 770–6.

Hentze, M.W. and Kuhn, L.C. (1996). *Proc. Natl Acad. Sci. USA.*, **93**, 8175–82.

Hwang, C., Sinskey, J. and Lodish, H.F. (1992). *Science*, **257**, 1496–1502.

Jamieson, D.J. (1998). *Yeast*, **14**, 1511–27.

Keese, M.A., Bose, M., Mulsch, A., Schirmer, R.H. and Becker, K. (1997). *Biochem. Pharmacol.*, **54**, 1307–13.

Ketterer, B. and Meyer, D.J. (1989). *Mutat. Res.*, **214**, 33–40.

Knight, H. (2000). *Int. Rev. Cytol.*, **195**, 269–324.

Kuhn, D.E., Baker, B.D., Lafuse, W.P. and Zwilling, B.S. (1999). *J. Leukoc. Biol.*, **66**, 113–9.

Lamb, N.J., Quinlan, G.J., Mumby, S., Evans, T.W. and Gutteridge, J.M. (1999). *Biochem. J.*, **344**, 153–8.

Lange, H., Kispal, G. and Lill, R. (1999). *J. Biol. Chem.*, **274**, 18989–96.

Lavrovsky, Y., Song, C.S., Chatterjee, B. and Roy, A.K. (2000). *Mech. Ageing Dev.*, **114**, 49–60.

Legssyer, R., Josse, C., Piette, J., Ward, R.J. and Crichton, R.R. (2001). *Biochem. Pharmacol.*, submitted for publication.

Lepoivre, M., Fieschi, F., Cowes, L., Thelander, L. and Fontecave, M. (1991). *Biochem. Biophys. Acta.*, **179**, 442–8.

Lill, R., Diekert, K., Kaut, A., Lange, H. *et al.* (1999). *Biol. Chem.*, **380**, 1157–66.

Lim J.H., Yu, Y.G., Choi, I.G., Ryu, J.R. *et al.* (1997). *FEBS Lett.*, **406**, 142–46.

Lindenau, J., Noack, H., Asazyama, K. and Wolf, G. (1998). *Glia*, **24,** 252–6.

Lindenau, J., Noack, H., Possel, H., Asayama, K. and Wolf, G. (2000). *Glia*, **29**, 25–34.

Oberley, T.D. and Oberley, L.W. (1997). *Histol. Histopathol.*, **12**, 525–35.

Oshiro, S., Takeuchi, H., Matsumoto, M. and Kurata, S. (1999). *Cell Biol. Int.*, **23**, 465–74.

Pantopoulos, K. and Hentze, M. (1995). *EMBO J.*, **14**, 2917–24.

Pomerantz, J.L. and Baltimore, D. (2000). *Nature* **406** 26–9.

Puccio, H. and Koenig, M. (2000). *Human Mol. Genet.*, **9**, 887–92.

Radisky, D.C., Babcock, M.C. and Kaplan, J. (1999). *J. Biol. Chem.*, **274**, 4497–99.

Reiter, R., Tang, L., Garcia, J.J. and Munoz-Hoyos, A. (1997). *Life Sci.* **60**, 2255–71.

Reiter, R., Cabrera, J., Sainz, R.M., Mayo, J.C., Manchester, L.C. and Tan, D.X.(1999). *Ann. NY Acad. Sci.*, **890**, 471–85.

Schipper, H., Liberman, A. and Stopa E. (1998). *Exp. Neurology*, **150**, 60–8.

Schmidt, K.N., Amstad, P., Cerutti, P. and Bazzuerle, P.A. (1995). *Chem. Biol.*, **2**, 13–22.

Schreck, R., Rieber, P. and Baeuerle, P.A. (1991). *EMBO J.*, **10**, 2247–58.

Schoonbroodt, S., Legrand Poels, S., Best Belpomme, M. and Piette, J. (1997). *Biochem. J.*, **321**, 777–85.

Schoonbroodt, S., Ferreira, V., Best Belpomme, M., Boelaert, J. *et al.* (2000). *J. Immunol.*, **164**, 4292–300.

Sheweita, S.A. and Mostafa, M.H.(1996). *Cancer Lett.*, **99**, 29–34.

Singh, R. and Pathak, D.N. (1990). *Epilepsia*, **31**, 15–26.

Smith, M., Wehe, K., Harris, P., Siedlak, S., Connor, J. and Perry, G. (1998). *Brain Res.*, **788,** 232–6.

Stio, M., Iantomasi, T., Favilli, F., Marraccini, P. *et al.* (1994) *Biochem. Cell Biol.*, **72**, 58–61.

Suzuki, Y.J., Mizuna, M. and Packer, L. (1994). *J. Immunal.*, **153**, 5008–15.

Tanaka, J., Toku, K., Zhang, B., Ishihara, K., Sakanaka, M. and Maeda, N. (1999). *Glia*, **28**, 85–96.

Turcanu, V. Dhouib, M. and Poindron, P. (1998). *Res. Immunol.*, **149**, 741–4.

von Zglinicki, T. and Brunk, U.T. (1993). *Z. Gerontol.*, **26**, 215–20.

Ward, R.J. and Crichton, R.R. (2001). In *Aluminium in Alzheimers Disease* (ed. Exley, C.), Elsevier, The Netherlands.

Ward R.J., Abiaka, C. and Peters, T.J. (1994). *J. Nephrol.*, **7** 89–96.

Ward, R.J., Zhang, Y., Crichton, R.R., Portman, B. *et al.* (1995). *Arch. Int. Biochem. Physiol.*, **B30**.

Weiss, G., Werner Felmayer, G., Werner, E., Grunewald, K., Wachter, H. and Hentze, M. (1994). *J.Exp. Med.*, **180**, 969–76.

Wiseman, H. and Halliwell, B. (1996). *Biochem. J.*, **313**, 17–29.

Xie, Q.W., Whisnant, R. and Nathan, C. (1993). *J. Exp. Med.*, **177**, 1779–84.

Yamanaka, K., Minato, N. and Iwai, K. (1999). *FEBS Lett.*, **462,** 216–20.

Zhang, K., Yang, E.B., Tang, W.Y., Wong, K. and Mack, P. (1997). *Biochem. Pharmacol.*, **54**, 1047–53.

Zitomer, R.S. and Lowry, C.V. (1992). *Microbiol. Rev.*, **56**, 1–11.

11 Iron and Infection

11.1 Introduction

In biological systems, iron, although practically ubiquitous, is only present in a free soluble form in vanishingly small amounts. As we saw in Chapter 3, it is essential for the growth of almost all microorganisms, including the vast majority of those that cause microbial infections in man and animals. Even the growth of the primitive single-celled organisms that constitute the bulk of oceanic phytoplankton, is limited by iron availability, which can be enhanced by massive iron enrichment, causing a huge, temporary bloom of phytoplankton (Mullineaux, 1999). The importance of iron for the proliferation and extended growth of living organisms makes *iron withholding* by host cells a logical defensive strategy, very widely applied in nature to limit the growth of invading parasitic organisms. Perhaps the best example is the chemically erudite hen (Weinberg, 1984) – the egg still represents the simplest iron-withholding defensive strategy, namely stationing iron-binding proteins at potential sites of invasion. Although the embryo is supplied with generous quantities of iron (1 mg in chicken yolk), potential microbial invaders that manage to penetrate through the porous shell are starved of iron, which is absent from the egg white, and further confronted with the powerful iron-binding protein, ovotransferrin, which constitutes 12 % of the egg-white solids. The bacteriostatic activity of ovotransferrin not only suppresses the growth of bacteria, both Gram-positive and Gram-negative, but also of fungi.

11.2 Microbial Strategies to Overcome the Iron-withholding Imposed by the Host, and its Potential Clinical Consequences

11.2.1 Siderophore Production

Many microorganisms, when in iron-depleted conditions, are able to mobilize environmental iron by secreting low-molecular weight, high-affinity iron-chelating compounds called siderophores, as well as cell-surface receptors for the ferric−siderophore complex and other proteins necessary for their uptake. Over the last three decades we have learned a lot about the chemical nature of these

siderophores, their receptors, their genetics and the precise mechanism of iron assimilation by these systems (for detailed information on these topics, see Chapter 3). In view of the crucial necessity for microbes to acquire iron, it is not astonishing that some of them do not rely on the synthesis of one single type of siderophore but rather synthesize several different siderophores. Others, on the contrary, do not synthesize siderophores but only the receptors for ferric-siderophores, therefore relying upon siderophore production by other species. The fact that some microbes are able to utilize iron from ferric-siderophores that they are not themselves capable of producing may have major clinical consequences that are worth mentioning here in more detail.

The experimental and clinical data that follow are related to the use of a microbial siderophore in medicine. It concerns desferrioxamine (DFO), the natural hydroxamate siderophore produced by *Streptomyces pilosus*. Incidentally, the *Streptomyces* genus has been the source of other major drugs in the history of medicine, such as the tuberculostatic drug streptomycin. Historically, DFO has been used for the last four decades in clinical practice as an iron chelator, mainly to remove excess iron from thalassaemic patients. Since the 1970s, there has been an increasing awareness of the potential risk of certain types of bacterial infections linked to DFO therapy. More particularly, it was found that patients on DFO treatment were at increased risk of developing serious infections caused by strains of *Yersinia* spp., mainly *Y. enterocolitica* (Robins-Browne and Prpic, 1983). It is not always clear to what extent the relative contribution of iron overload versus DFO therapy played the major role in the pathogenesis of this infection, as both iron overload and DFO alone have been shown both *in vitro* and *in vivo*, and in experimental animals as well as in patients, to enhance the growth of this microorganism (Robins-Browne and Prpic, 1985; Boelaert *et al.*, 1987). Strains of *Y. enterocolitica* of certain serotypes (e.g. O3 and O9) do not produce a siderophore during iron starvation and can acquire iron from the exogenous siderophore ferrioxamine (Heesemann *et al.*, 1993). Very recently, DFO conjugated to hydroxyethyl starch in order to increase its serum half-life, was also found to exacerbate *Y. enterocolitica* infection in mice, though to a lesser extent than DFO (Schubert and Autenrieth, 2000). Physicians caring for thalassaemic patients should be well aware of the possibility of this infection, which presents either as bacteraemia or as abdominal syndrome. In case of such a clinical event, they should draw specimens for culture, stop DFO therapy and institute antimicrobial therapy against *Yersinia* species. Such utilization of iron from ferrioxamine (FO) is not limited to *Yersinia* spp. and may occur in other bacterial species, such as *Salmonella* and *Aeromonas* (Jones *et al.*, 1977; Boelaert *et al.*, 1993b). Infection due to the latter species has been reported during DFO therapy (Shi-Hua *et al.*, 1996).

In the beginning of the eighties, the clinical application of DFO expanded to a new type of patient, namely those on maintenance dialysis. As we will see in Chapter 12, some patients suffered from aluminium overload, mostly due to the use of aluminium salts as phosphate binders, while others had obvious transfusional iron overload in the pre-erythropoietin era. DFO was therefore used either to remove aluminium, excess iron or both. Nephrologists established that DFO therapy did not increase the overall incidence of bacterial infections but that it slightly increased the risk of bacteraemia caused by *Y. enterocolitica* or *Y. pseudotuberculosis*, as had been previously observed in thalassaemic patients (Boelaert *et al.*, 1987; Tielemans *et al.*,

1989). However, an even more threatening infectious complication became known when reports of mucormycosis in dialysis patients treated with DFO appeared in the literature. Mucormycosis, better called 'zygomycosis', is an infection caused by fungi belonging to the class of *Zygomycetes*, order Mucorales. Together with colleagues from the USA, a worldwide registry of zygomycosis in dialysis patients was established, and a total of 49 patients was reported in whom this infection had developed while on DFO therapy (Boelaert *et al.*, 1991). The infection was severe, as it was disseminated in several organs in about half of the cases. This dissemination explains the gloomy outcome in this cohort, with a fatality rate of 90 %. We, and others, developed experimental models of zygomycosis both in the guinea pig (Van Cutsem and Boelaert, 1989) and in the mouse (Abe *et al.*, 1990; Anand *et al.*, 1992) and showed that in each of these different models, the administration of DFO at the time of infection resulted in shortened survival time of the experimental animals. More importantly, when *Rhizopus* was cultured in iron-poor medium with serum containing FO radiolabelled with iron, a FO concentration as low as 0.01 µM induced uptake of radiolabelled iron by the fungus and concomitant enhancement of fungal growth (Boelaert *et al.*, 1993a). These experiments proved that zygomycosis during DFO therapy is mediated by fungal iron uptake from FO. It was important to assess whether this severe infectious complication was restricted to the use of DFO or might also occur when using an iron chelator from another chemical class, such as deferiprone, belonging to the hydroxypyridinones. When the *in vitro* growth of *Rhizopus* was studied in the presence of either FO or the iron complex of deferiprone, only FO was found to be a fungal growth promoter (Boelaert *et al.*, 1994). Next to the chelator specificity, we examined the fungal specificity of this severe infection which had developed in at least 49 DFO-treated dialysis patients. In other words, are there other fungi or yeasts that can utilize FO as iron source and that may lead potentially to infection in DFO-treated patients? *In vitro*, both *Cryptococcus neoformans* and *Aspergillus fumigatus* can take up iron from FO (Boelaert *et al.*, 1993a,b; Jacobson and Petro, 1987; Jacobson *et al.*, 1998), which explains the increased pathogenicity of both fungi in experimental infections with concomitant DFO administration (Boelaert *et al.*, 1993a). Nevertheless, to the best of our knowledge, no case of human cryptococcosis or aspergillosis has been reported during DFO therapy. Why has this problem of DFO-associated zygomycosis not been observed earlier, as DFO has been extensively used for treating thalassaemics since the end of the 1950s? Indeed, this infection has only rarely been reported as occurring in DFO-treated patients suffering from a non-malignant haematological disease (e.g. thalassaemia). One of the differences between dialysis and thalassaemia patients concerns the altered pharmacokinetic handling of drugs in uraemia. The pharmacokinetics of FO after injection of DFO differ greatly between uraemics and normal non-uraemic individuals, with a very slow FO elimination in uraemic patients, leading to increased serum levels of this complex for prolonged periods of time (Verpooten *et al.*, 1992). In summary, both the specific ability of *Zygomycete* fungi to acquire iron from the ferrated DFO and the prolonged serum retention of the complex in uraemic patients forms the physiopathological basis of DFO-related zygomycosis in dialysis patients. This major drug-related complication led to the abandonment of the use of DFO in dialysis units and to a decline in the use of aluminium-containing phosphate binders, to be replaced by calcium salts. Moreover, since the advent of

erythropoietin for clinical use, the problem of transfusional iron overload in this group of patients has drastically declined. DFO-associated zygomycosis is therefore no longer a threat to the patients on maintenance dialysis nowadays. However, one has to remain careful. New formulations of DFO are currently designed to overcome the short plasma half-life of the drug; they are either slow-release formulations or DFO bound to a macromolecule such as hydroxyethylstarch. These new-generation DFO formulations are currently undergoing clinical testing. Hopefully they will not result in the infectious problems, just described. The main message that should be retained from this history is that 'playing' with substances produced by nature in order to obtain the vitally essential metal may be a double-edged sword. The second message is that specific infections, occurring in a very specific subset of patients, may be helpful for uncovering disease mechanisms. The following two examples of iron-related infections that developed in a very narrow spectrum of patients, illustrate this point, where detailed studies revealed hitherto unknown microbial iron-acquisition systems. The first example concerns DFO-related zygomycosis, that 'exploded' in the dialysis setting. When studying iron acquisition by *Rhizopus*, we found that this fungus, like other members of the class of zygomycetes, can not only utilize iron from FO, as discussed above, but with the help of G. Winkelmann, it was found that all zygomycetes produce a polycarboxylate siderophore, rhizoferrin, unlike most other siderophore-producing fungi, which produce hydroxamate siderophores (Drechsel *et al.*, 1991). Another fascinating example of an iron-related infection that is restricted to a very narrow spectrum of patients concerns pythiosis, which is caused by the fungus *Pythium insidiosum*. This oomycete fungus causes severe human disease in untreated thalassaemic patients, as has been reported from Thailand and this will be discussed later in this chapter. Suspecting some peculiarities in the iron transport mechanism of this fungus, the same group from Tübingen discovered that this phylogenetically primitive fungus produces citric acid as siderophore, the simplest siderophore ever identified in fungi (Boelaert *et al.*, 1999).

Even if, as discussed above, DFO can enhance the growth of selected microorganisms that have the capacity to extract the iron from FO, the drug may, by withdrawing iron, limit the growth of many other microorganisms (Boelaert *et al.*, 1993b). Whether this may have clinical application in the prevention or cure of some infectious diseases will be discussed later in this chapter.

The importance of microbial iron acquisition by siderophores, of course, also clears the way for the host to try to interfere with the microbe's iron-acquisition strategy. This can occur in some circumstances by making antibodies to siderophores or, in the case of human phagocytes by extracting the iron from the *Pseudomonas aeruginosa* siderophores at the phagocyte surface (Britigan *et al.*, 2000). Finally, further research on siderophore structures may result in therapeutic applications. For instance, natural mycobactins yielded promising results when tested against virulent *Mycobacterium* tuberculosis *in vitro* (Vergne *et al.*, 2000).

11.2.2   Binding of Diferric-transferrin or -lactoferrin

A number of Gram-negative microorganisms, including the important human pathogens *Neisseria gonorrhoeae*, *Neisseria meningitidis* and *Haemophilus influenzae*,
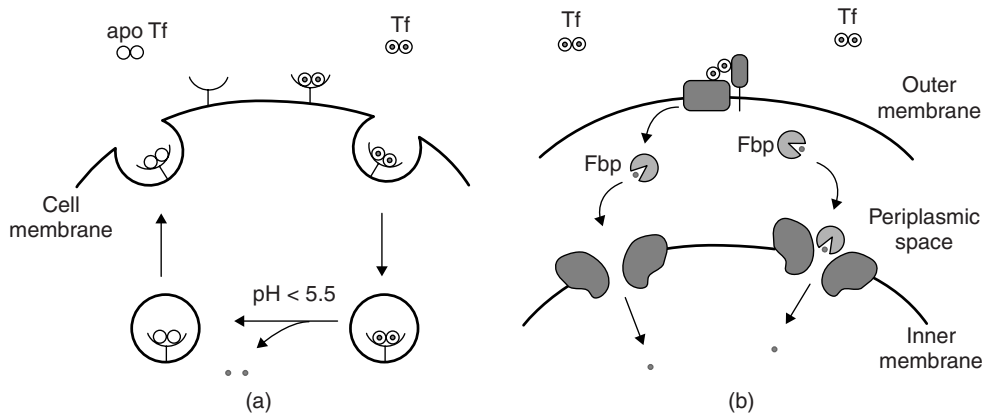
Figure 11.1 Schematic representation of iron uptake mechanisms. (a) The transferrin-mediated pathway in animals involves receptor-mediated endocytosis of diferric transferrin (Tf), release of iron at the lower pH of the endocytic vesicle and recycling of apoTf. (b) The mechanism in *H. influenzae* involves extraction of iron from Tf at outer membrane receptors and transport to the inner membrane permease system by a periplasmic ferric binding protein (Fbp). From Baker, 1997. Reproduced by permission of Nature Publishing Group.

are able to bind diferric-transferrin or -lactoferrin from specific mammalian hosts (Cornelissen and Sparling, 1994). The microbes that bind diferric-transferrin therefore mimic an essential host cell function, iron acquisition via binding of Fe−Tf to a cell surface transferrin receptor (TfR). However, fundamental differences exist between host cell and invader mechanisms of transferrin-borne iron acquisition (Figure 11.1). First, the molecular structure of the receptor differs. Whereas the host TfR is a 90-kDa homodimer, the microbial receptor system consists of two different outer membrane transferrin binding proteins, TbpA and TbpB, respectively (Lbp1 and Lbp2 are the corresponding receptors for lactoferrin). TbpB is a lipoprotein that is surface exposed and anchored by its fatty acyl tail. It is assumed to interact with the other subunit, TbpA, to increase the specificity of the functional receptor system to Tf. Secondly, there is a different mechanism of iron entry. The host cell internalizes the receptor−Fe−Tf complex, with subsequent removal of iron from the complex within the acidic endosome and recycling of the apoTf back to the plasma membrane (Chapter 5). In contrast, the microbial cell does not internalize the Fe−Tf. Once bound to the TbpA/TbpB complex, iron is released from the Fe−Tf molecule. TbpA behaves as a TonB-dependent outer membrane protein that allows iron, derived from Fe−Tf, to cross the microbial outer membrane through a gated pore. Within the periplasmic space iron is bound by a ferric binding protein, Fbp, which as we saw in Chapter 5 in the case of *Haemophilus influenzae*, is a member of the transferrin superfamily. Fbp then transports the iron across the periplasm to an inner membrane permease, which releases the iron into the cytoplasm. Although fundamental differences exist between host cell and pathogen in acquisition of transferrin-iron, there may be a competition in availability from this source. A recent report indicating that neisserial infection of human epithelial cells reduces the cellular levels of TfR mRNA and hence the uptake of transferrin from the extracellular milieu, may be

interpreted as a microbial strategy to increase the extracellular concentration of transferrin-bound iron available to the essentially extracellular bacteria (Bonnah *et al.*, 2000).

The unravelling of the detailed mechanisms by which selected microorganisms acquire iron by binding to Fe–Tf and or Fe–Lf allows greater understanding of several biological consequences that are of great clinical relevance. Four of them are discussed here. First, the direct binding of one or both of the host Fe-binding proteins Fe–Tf and Fe–Lf is host specific, or only concerns a narrow range of hosts. In other words, microbial strains can only invade hosts that have the iron-binding protein corresponding to their receptor system. For example, the success of *Neisseria meningitidis* in causing fulminant human meningitis, and of *Helicobacter pylori* in causing human gastric ulcer disease, are partially related to their binding of human Fe–Tf and Fe–Lf for the former and human Fe–Lf for the latter species. They are known to colonize and infect only humans. Similarly, *Actinobacillus pleuropneumoniae* leads to pulmonary infection is swine but not in humans, because of its receptor specificity towards swine but not human Fe–Tf. Second, the choice between Tf-derived or Lf-derived iron within a given host may dictate the localization of the infection. Tf is found mainly in serum and also in cerebrospinal fluid, especially during inflammation, whereas Lf is found on mucosal surfaces, such as those of the respiratory, digestive and urogenital tracts. Thus we can infer that *Neisseria meningitidis*, when colonizing the respiratory tract, will utilize Fe–Lf, whereas if it invades the blood stream and the meninges it will utilize Fe–Tf. For *Helicobacter pylori*, the Fe–Lf present in the human gastric mucosa will be used as iron source for chronic subsistence of the pathogen in this peculiar niche. Third, as will be discussed at the end of this chapter, these concepts raise the possibility of developing immunization strategies by vaccinating against some of these bacterial receptors. Finally, these iron acquisition systems are logical drug design targets. For example, it might be possible to design drugs that would prevent iron release from the relatively exposed iron binding site of Fbp (Baker, 1997).

11.2.3 Binding of Haem-containing Compounds

Haem is the most abundant carrier of iron in vertebrates because of the high haemoglobin content of erythrocytes. It is also released by tissue damage and by desquamation of epithelial cells making it an important source of iron for bacteria colonizing the gut. A large number of mainly pathogenic bacteria can use haem (Braun *et al.*, 1998) as an iron source (Table 11.1), employing multiple strategies for obtaining haem iron. The most obvious is for the microorganism to take up residence within the erythrocyte and to digest host-cell haemoglobin. This is the well-known case of *Plasmodium* sp., the protozoa that causes malaria, but may also occur with the bacterial *Bartonella* spp., which includes *B. henselae*, that causes cat scratch disease. A variant on this strategy is used by *Candida albicans*, which binds to erythrocytes, causes their lysis, and utilizes their haemoglobin (Manns *et al.*, 1994). Yet another strategy is to extract iron either directly from free haemoglobin or haem, or from their complexes with haptoglobin and haemopexin respectively.

Table 11.1 Bacterial haem transport systems.

TonB-dependent receptor I (kDa)	Additional proteins (kDa)	Substrates	Organism
HemR	HemP HemS HemTUV	Haem	*Y. enterocolitica*
HmuR	HmuP HmuS HmuTUV	Haem	*Y. pestis*
ShuA, ChuA		Haem	*S. dysenteriae,* *E. coli*
HutA	HutB	Haem	*V. cholerae*
HmbR		Haemoglobin	*N. meningitidis*
HgbA [= HupA]		Haemoglobin, Haemoglobin-Haptoglobin	*H. ducreyi*
HhuA		Haemoglobin-Haptoglobin	*H. influenzae*
HpuB	HpuA	Haemoglobin-Haptoglobin	*N. meningitidis* *N. gonorrhoeae*
HxuC	HxuA HxuB	Haem, Haemopexin	*H. influenzae*
HasR	HasA HasD HasE HasF	Haem, Haemoglobin	*S. marcescens*
	HupA	Haem	*B. fragilis*

The first of the haem uptake systems to be characterized at molecular level was that of *Yersinia enterolitica*, which closely resembles a typical siderophore uptake system (Stojiljkovic and Hantke, 1992, 1994), including a TonB-dependent outer membrane receptor for haem, a periplasmic binding protein, and a cytoplasmic membrane transport system. There also seems to be a protein that degrades haem and liberates haem iron within the cell. TonB-dependent outer membrane receptor proteins for haem have been cloned and sequenced from *Shigella dysenteriae* and *E. coli* (Mills and Payne, 1995; Torres and Payne, 1997), while in *Vibrio cholera* two genes are required for haem utilization, one an outer membrane receptor a second which may have a TonB-like function (Henderson and Payne, 1994).

Vibrio cholera can also take up iron from haemoglobin as can several other bacteria. The haemoglobin receptor HmbR has been cloned from *N. meningitidis* (Stojiljkovic *et al.*, 1995) and has sequence homology with the transferrin (TbpA) and lactoferrin (LbpA) receptors and the haem receptors of *V. cholera* (HutA) and *Y. enterocolitica*. HmbR illustrates rather well the remark made previously concerning host specificity, since it binds human haemoglobin with much higher affinity than it does other animal haemoglobins (Stojiljkovic *et al.*, 1996).

The haemoglobin released upon lysis of erythrocytes is bound by haptoglobin in the serum, which prevents haemoglobin utilization by many bacteria such as *E. coli*. However, the specialized pathogens *Haemophilus* and *Neisseria* have systems for obtaining iron from the haemoglobin–haptoglobin complex (Stevens *et al.*, 1996; Lewis *et al.*, 1997). When serum haptoglobin is depleted, free haemoglobin is

oxidized and haem is liberated, which is bound by serum albumin and, more tightly, by haemopexin ($K_D < 1$ pM). *Haemophilus* strains can use the haem–haemopexin complex as a source of iron, and three proteins HxuABC are required for efficient uptake. HxuA binds haem–haemopexin, and is secreted into the medium by the outer membrane protein HxuB (Cope *et al.*, 1994). HxuC, which has similarities with TonB-dependent receptors, is thought to interact with HxuA to transport haem across the outer membrane of the bacteria (Cope *et al.*, 1995).

In *S. marescens* a small (19 kD) haem-binding protein, HasA, is secreted into the medium by an ABC-transporter (Letoffe *et al.*, 1994; Binet and Wandersman, 1996), where it binds haem from haemoglobin and delivers it to the membrane receptor HasR (Ghigo *et al.*, 1997). By analogy with siderophores, HasA can be considered as a haemophore (Braun *et al.*, 1998).

11.2.4 Reduction of Fe(III) and Uptake of Fe(II)

Selected microorganisms can reduce extracellular Fe(III) to Fe(II), and actively take up the Fe(II). This mechanism is used by both the bacteria *Listeria monocytogenes* and *Legionella pneumophila*, and the yeasts *Saccharomyces cerevisiae* and *Cryptococcus neoformans*. In the latter yeast, two reduction mechanisms have been distinguished: the expression of a cell membrane ferric reductase, and the secretion of an extracellular reductant (Nyhus and Jacobson, 1996). The components of both iron reduction and iron uptake that have been characterized at the genetic and molecular levels in the model organism *Saccharomyces cerevisiae* are discussed in Chapter 4. Detailed insight into these iron acquisition systems has been extremely instructive for the understanding of iron acquisition in mammalian cells.

11.2.5 Multiple Intracellular Microbial Strategies

When macrophages ingest particulate material, such as a microorganism, an intracellular vacuole, called a phagosome, is constituted, that undergoes a step-wise maturation. This process consists of a progressive acidification and several fusion events, finally resulting in fusion with a lysosome to form a phagolysosome. This organelle contains enzymes and the acidic environment necessary to degrade the phagocytosed material. This pathway is an important component of the macrophage's defence against invading pathogens. For an obligate or facultative intracellular pathogen to be successful, i.e. to survive and to multiply within the macrophage, it has to evolve one or more strategies to escape or to combat this phagosomal maturation process (Garcia-del-Portillo and Finlay, 1995). Schematically (and in a simplified manner), these strategies are: (i) to escape from the phagosome into the cytoplasm and spread directly from cell to cell; (ii) to inhibit phagosomal acidification and phagosome–lysosome fusion. Other evasion strategies that help microorganisms to survive within macrophages, and that will not be further discussed here, are: (iii) adaptation to the hostile phagolysosome conditions; (iv) modulation of macrophage apoptosis (e.g. several viral genomes encode for proteins that exert an antiapoptotic effect, which may ensure a sustained

infection); (v) modulation of macrophage cytokine production, i.e. suppression or lack of induction of activating cytokines, or induction of deactivating cytokines; (vi) inhibition of antigen presentation and T-cell stimulation. These multiple and complex microbial strategies to counteract the cellular defences have been categorized in to three (anthropomorphic) attitudes: stealth, sabotage and exploitation (Brodsky, 1999). Detailed discussion of these microbial strategies is beyond the scope of this chapter. However, it is worth concentrating on some of the evasion manoeuvres that impact directly upon microbial iron availability. When the first strategy, that of escape to the cytosol, is operative, the microorganism probably finds its iron source within the so-called 'labile iron pool' (LIP), where the metal is thought to be in its reduced Fe(II) form and bound to low-molecular-weight molecules (see Chapter 7). It is possible that *Listeria monocytogenes*, which escapes from the phagosome to the cytoplasm, uses its reductase and Fe(II) uptake system to capture iron from the low-molecular-weight iron ligands of the LIP. In the case of the second strategy, where the microbe blocks the maturation of the phagosome, we could well ask at which stage in phagosome maturation it would be most effective for the block to occur. As we saw in Chapter 5, the uptake of transferrin-bound iron occurs in the early endosome, and so it might be useful for such microorganisms to arrest phagosome maturation precisely at this stage, before fusion with lysosomes, which should facilitate access to the metal. This may be the case for *Mycobacterium tuberculosis*, whose dual 'mycobactin T' siderophore system (De Voss *et al.*, 1999) is well equipped to acquire iron from transferrin. *Mycobacterium tuberculosis* arrests the maturation of its phagosome at a stage at which the phagosome interacts with early and late endosomes, but not yet with lysosomes (Clemens and Horwitz, 1996). It is therefore possible that 'freezing' of the *M. tuberculosis*-containing vacuole at the early endosome stage evolved in part to facilitate iron acquisition. How this 'freezing' occurs is not fully established, although the persistence of the Rab5 protein on the *M. tuberculosis*-containing phagosome may help in maintaining its early endosomal properties (Clemens *et al.*, 2000).

During the invasion of macrophages by a microorganism, both the host and the pathogen may elicit mechanisms that alter iron metabolism within the macrophage. The interested reader is referred to a recent elegant review on this topic by Eugene Weinberg, who for decades has pioneered research on iron and infection (Weinberg, 2000). One of the major weapons utilized by the macrophage against intracellular parasitism is associated with its stimulation by γ-interferon. This T-cell derived cytokine promotes several activities that are relevant to iron metabolism. First, it induces a decreased expression of the number of transferrin receptors at the surface of the macrophage, resulting in a limited cellular iron uptake and impaired iron acquisition by microorganisms such as *Legionella pneumophila* that escapes into the cytosol and are likely to be dependent on the LIP for growth (Byrd and Horwitz, 1989). The same authors recently reported an 'experiment of nature', namely a patient, whose non-activated monocytes were uniquely non-permissive for *L. pneumophila* growth. This was associated with abnormally low levels of transferrin receptor expression, possibly as a result of systemic inflammation due to chronic periodontal disease, as the abnormality resolved after definitive cure of the gingivitis (Byrd and Horwitz, 2000). As this transferrin pathway of iron acquisition may be essential to certain pathogens, they – not astonishingly – have evolved opposing

strategies, consisting in upregulating host cell expression of the transferrin receptor mRNA, resulting in a selective accumulation of diferric-transferrin. This is reported for *Coxiella burnettii* (Howe and Mallavia, 1999) and *Ehrlichia chaffeensis*. In the latter case, this upregulation of TfR mRNA may be secondary to a direct activation of IRP-1 (Barnewall *et al.*, 1999).

A second way by which the T-helper 1 lymphocyte-derived γ-interferon can alter iron metabolism in the macrophage is by inducing synthesis of NO by the cytokine-inducible isoform of nitric oxide synthase (iNOS, NOS2). There is now ample evidence that iNOS is expressed in human and not just in rodent mononuclear macrophages (Weinberg, 1999). The interactions of NO and iron metabolism are discussed in more detail in Chapters 7 and 10. Of importance for the present topic are: (i) NO and its complexes with other cellular compounds ('reactive nitrogen intermediates' such as peroxynitrite) exert a potent antimicrobial effect on an impressive number of pathogens by virtue of their reaction with non-haem iron prosthetic groups of enzymes involved in DNA synthesis and electron transport, eventually resulting in damage to or even death of the pathogens; (ii) NO production results in efflux of iron from the cell, while iron loading of the cell results in a suppression of nitric oxide production (Weiss *et al.*, 1994). In view of the importance of NO as key effector molecule, it could be anticipated that some pathogens might try to subvert this machinery. We give two examples. The first concerns *Leishmania major*, an obligate intracellular parasite of macrophages in mammalian hosts that has proved so useful for studying the immune components of the parasite/host interactions. Lipophosphoglycan, a surface molecule of *Leishmania* promastigotes, was shown to reduce the expression of nitric oxide synthase mRNA in murine macrophages, at least when present prior to activation of the host cell by γ-interferon (Proudfoot *et al.*, 1996). The second concerns the ability of *Cryptococcus neoformans* to produce an unknown compound that can capture NO, allowing the fungus to evade the host defence mechanism (Trajkovic *et al.*, 2000).

It is likely that γ-interferon also uses other pathways to modulate iron metabolism during microbial cell invasion. This cytokine is reported to enhance the synthesis by the host macrophage of a protein (Nramp1) to be discussed later in this chapter, that may act by modulating iron transport at the phagosomal membrane. Finally, γ-interferon was found to inhibit *Toxoplasma gondii* replication in a non-macrophage type of cell (the primary rat enterocyte) by limiting the availability of intracellular iron by an unidentified mechanism, unrelated to those just discussed, namely suppression of host-cell transferrin receptors or enhanced NO formation (Dimier and Bout, 1998). This is of interest, as enterocytes may be viewed as one of the first lines of defence against pathogen invasion.

Recently, another interaction was reported between an intracellular pathogen and the key regulator system of intracellular iron concentration, i.e. the degree of binding of the IRPs to IRE (see Chapter 7). In extracts from *Leishmania tarentolae*, a protein has been detected that binds specifically to the mammalian IRE. However, the exact nature and function of this protein is unclear up to now. In contrast to mammalian IRPs, the *L. tarentolae* IRE-binding activity was not induced by growth in iron-depleted medium (Meehan *et al.*, 2000).

11.2.6 Comment

The reader should realize that the schematic subdivisions of methods of iron acquisition by microorganisms, even if useful for didactic reasons, are oversimplifications. For instance, many microbes utilize – in an apparently redundant manner – several of the outlined strategies according to their site of growth within or outside of the body. To give just two examples of very common pathogens: *Candida albicans* can produce a hydroxamate siderophore, can lyse erythrocytes and bind haemoglobin, and can produce a ferric reductase; *Staphylococcus aureus* can bind transferrin, can produce siderophores staphyloferrin A and B and can digest haemoglobin and haem.

11.3 The Impact of Chronic Inflammation/Infection on Iron Metabolism

Inflammation results in important changes in iron metabolism that have been referred to as the 'hypoferraemic response', characterized by lowering of serum iron and transferrin iron saturation, increase in serum ferritin and an accompanying 'anaemia of chronic disease'. It was known for decades that inflammation results in: (i) the suppression of intestinal assimilation of iron; and (ii) a decreased release of iron from the macrophage together with an increased macrophage ferritin synthesis. In other words, iron traffic is modified, so that the metal is diverted from both the circulation and sites of erythropoiesis to the storage compartment in the reticuloendothelial system. Although it has been clear for more than two decades that the macrophage plays a major role in the hypoferraemic response, views on the mechanisms involved have shifted over the years, with a growing interest now in the roles played by inflammatory mediators such as cytokines. The literature on this subject is somewhat confusing and the interested reader will find more details in the reviews by Brock (1993) and by Weiss (1999). We limit ourselves here to the essential points. As discussed above, the Th-1-derived γ-interferon depresses TfR expression in activated macrophages. The latter cells produce proinflammatory cytokines such as TNF-α and IL-1 (and perhaps IL-6) that transcriptionally induce ferritin synthesis, which favours iron storage within the macrophage. Reactive nitrogen intermediates that follow the production of nitric oxide, NO (see Chapter 10) are other products of the Th-1 proinflammatory reaction. Their effect on macrophage iron handling is complex, as indicated by contradictory reports. Apparently, their main effect is to decrease RNA binding to IRP-2 (see Chapter 10) and to degrade IRP-2 independently of cellular iron levels. This degradation results posttranscriptionally in decreased TfR and increased ferritin levels in the activated macrophage (Recalcati *et al.*, 1998; Kim and Ponka, 2000). On the other hand, Th-2-derived cytokines such as IL-4 and IL-13 seem to reverse the inhibitory effect of γ-interferon on TfR expression, and hence enhance TfR-mediated iron uptake in activated macrophages. These Th-1- and Th-2-derived cytokines may therefore collaborate, the primary effect of the Th-2-derived cytokines being an increased iron uptake by the activated macrophage, and the primary effect of the Th-1-derived cytokines being increased iron storage

in ferritin. It can be anticipated that in the coming years a clearer picture of the mechanisms by which inflammation tunes the handling of iron by macrophages will emerge.

As indicated above, chronic inflammation is frequently accompanied by the so-called 'anaemia of chronic disease', renamed with more precision 'anaemia of inflammation'. Even if the mechanism is not entirely clear and may be multifactorial, it is generally accepted to be mainly due to the decreased production of red cells secondary to: (i) the decreased availability of iron, and (ii) the blunted action of erythropoietin (EPO). Decreased iron availability occurs as a result of decreased intestinal iron absorption and, more importantly, the above mentioned expansion of the iron-storage compartment in the activated reticuloendothelial cells that withhold the metal and prevent its release. The proinflammatory cytokines not only impair this macrophage iron release, but they also impair EPO metabolism in two ways. First, for a given degree of anaemia, the EPO production is decreased during inflammation; second, the EPO response of the erythroid progenitor cells is decreased (relative EPO unresponsiveness or resistance). It is not absolutely clear what the role of this 'anaemia of chronic disease' may be. The most widely held theory is that its characteristic iron withholding is a host defence mechanism to deprive invading microorganisms of iron. Other explanations have been proposed, such as a reduction of the iron flux, or a strengthening of the protective Th-1 immune effector mechanisms (Weiss, 1999; Brock, 1999; Jurado, 1997).

As a corollary, an important clinical question is whether or not the administration of iron compounds (red blood cell transfusion or iron supplementation) to combat the anaemia in a patient suffering from inflammation or infection is useful or may even be risky. This question is not so simple to answer and was recently reviewed (Brock, 1999). We start with some general considerations. First, the anaemia of chronic disease (e.g. in rheumatoid arthritis) is usually moderate and well tolerated; if asymptomatic, it should not be treated. Second, iron supplementation during an inflammatory situation is likely to be relatively inefficient for two reasons: oral iron absorption is suppressed and parenteral iron will mostly be directed to the reticuloendothelial stores rather than being incorporated into red blood cells. Third, parenterally administered iron carries the risk of being ingested by neutrophils – thus decreasing their antimicrobial defence – resulting in the transient appearance in the circulation of non-transferrin-bound iron, NTBI (see Chapter 5), which may result in a decrease of lymphocyte function. On top of these theoretical considerations come important clinical questions. One of them concerns both the efficacy and the risk of iron supplementation in areas where malaria is endemically prevalent. Although this subject remains controversial (for discussion, see Brock, 1999), a recent study on oral supplementation of iron in infants found no increased risk of developing clinical malaria and a reduced incidence of severe anaemia (Menendez *et al.*, 1997). Therapy with recombinant erythropoietin may be considered in certain cases of 'anaemia of chronic disease'. However, as discussed, the decreased responsiveness to EPO during inflammation results in the requirement of high doses of recombinant human EPO, with obvious financial consequences.

11.4 The Impact of Iron Excess on Infection

11.4.1 Iron Excess Increases the Risk and Aggravates the Outcome of Many Infections

There is ample evidence to indicate that iron loading directly enhances the *in vitro* growth of a multitude of pathogens, both protozoal, bacterial and fungal. Likewise, there is considerable evidence from *in vivo* experimental data that iron in excess enhances the risk and aggravates the outcome of numerous infections. The interested reader may find lists of these pathogens in a recent review by Weinberg (1999). Rather than commenting on these experimental data, we prefer to restrict the discussion to human infections. Table 11.2 does not pretend to provide a complete list but rather shows some typical examples of human infections that are more

Table 11.2 Some examples of clinical infections tending to occur particularly in patients with generalized or local iron excess or dysregulated iron metabolism.

Main pathophysiological mechanisms of iron loading that may result in an increased infectious risk

I.1	Increased gastrointestinal absorption of iron
I.2a	Parenteral administration of iron
I.2b	Increased release of iron in the blood stream (haemolysis)
I.3	Increased inhalation of iron
II	Chronic inflammation
III	Diabetic ketoacidosis

Type of microorganism	Underlying condition	Mechanism of iron loading
Bacteria		
Legionella pneumophila	Tobacco smoking	I.3
Listeria monocytogenes	Transfusional iron overload (e.g. dialysis)	I.2a
Mycobacterium avium	HIV-1 infection with iron loading	II
Mycobacterium tuberculosis	African iron overload	I.1
Salmonella spp.	Sickle cell anaemia	I.2b
Vibrio vulnificus	Primary haemochromatosis Alcoholic liver cirrhosis	I.1
Yersinia enterocolitica and *pseudotuberculosis*	Primary haemochromatosis	I.1
	Transfusional iron overload (e.g. thalassaemia dialysis)	I.2a
	African iron overload	I.1
Fungi/Yeasts		
Candida albicans	Haematologic malignancies with iron overload	I.2a; II
Cryptococcus neoformans	HIV-1 infection: tobacco smoking as risk	I.3; II
Pythium insidiosum	Thalassaemia	I.1
Rhizopus spp.	Diabetic ketoacidosis	III

prevalent or are aggravated in states of iron excess. The mechanisms leading to a state of generalized or local increase in iron burden are also indicated schematically.

A first category of patients is those who accumulate an excessive amount of iron either by an enhanced gastrointestinal absorption, by parenteral administration or excessive release, or by inhalation. The classical causes of major iron overload are genetically determined and characterized by a huge increase in gastrointestinal absorption of the metal (see Chapter 9). Primary haemochromatosis, thalassaemia and African iron overload (the latter due to both genetic and alimentary factors) are all accompanied by an increased risk of infection by *Yersinia enterocolitica*, presenting most often as either liver abscess or as right-lower-quadrant abdominal pain with bacteraemia. In thalassaemic patients, even if therapy with DFO presents an additional risk for this infection (see above), as is the case with splenectomy, iron overload is an independent risk factor (Adamkiewicz *et al.*, 1998). Primary haemochromatosis patients, particularly when cirrhotic, also are at risk of severe infection caused by *Vibrio vulnificus*. Pythiosis is a peculiar and severe infection that is restricted to thalassaemic patients and is caused by the oomycete fungus *Pythium insidiosum*. In its most classical presentation, it is characterized by an obstructive arthritis of the lower extremities due to fungal growth within the arterial tree and it frequently necessitates amputation. African iron overload patients also are at increased risk of fatal tuberculosis (Gordeuk *et al.*, 1996). Regular parenteral administration of iron or transfusion of packed red cells can also result in iron loading. This was the case in the dialysis population prior to the advent of recombinant erythropoietin and may partially remain a problem in the present erythropoietin era, due to the accompanying need for parenteral iron therapy. As in the previous patient groups, dialysis patients with iron excess are at risk of bacteraemias caused by *Yersinia* spp., as discussed earlier in this chapter. They may also be at enhanced risk of infection caused by *Listeria monocytogenes*. Other cohorts of patients requiring frequent transfusion of packed red cells, such as those with myelodysplasia and other haematological malignancies, share a similar risk, and an increased risk of candidal infection (Iglesias-Osma *et al.*, 1995). However, the infectious risk in patients on regular parenteral iron and/or transfusion is not restricted to these specific pathogens. Indeed, we found in a prospective study that haemodialysis patients with a serum ferritin value >1000 µg/l had three times as many bacteraemic episodes than those with a serum ferritin value <500 µg/l, and the causative pathogens were the ones usually encountered in this cohort (Boelaert *et al.*, 1990a). An enhanced breakdown of red cells, as during the vasoocclusive haemolytic crises in sickle cell anaemia, may also result in an excessive release of iron and is probably one of the factors that may explain the enhanced prevalence of osteomyelitis due to *Salmonella* spp. in this patient category. Tobacco smoking is another way to increase the iron burden, at least locally, mainly in the bronchoalveolar macrophages (Mateos *et al.*, 1998). Iron in excess in these cells is particularly evident when tobacco smoking is associated with chronic bronchitis. As the bronchoalveolar macrophages represent a major line of defence against inhaled pathogens, it is likely that the well-known association between 'legionnaires' disease' caused by *Legionella pneumophila* and smoking is iron related. Similarly, we hypothesized that the doubled risk of cryptococcal meningitis in HIV-1

positive current smokers versus non-smokers may have the same pathophysiology (Boelaert and Blasi, 1999).

As discussed in the previous section, long-standing inflammation may result in accumulation of iron in the reticuloendothelial system. In HIV-1 infection, a good example of a prolonged inflammatory process, such an excessive deposition of iron has been documented, and it may be responsible for an enhanced risk of certain infections (Boelaert *et al.*, 1996). For instance, two studies reported an increased risk of *Mycobacterium avium* infection when such an excess of iron was present, as histologically documented (Al Khafaie *et al.*, 1997; De Monyé *et al.*, 1999).

In the above examples, the increased risk of infection is related to an excessive deposition of iron, either at many body sites or within one particular organ. In the following example, the increased risk is due to a temporary disruption of the so-called 'iron withholding'. Diabetic ketoacidosis is a major cause of zygomycosis, a severe fungal infection that has already been discussed in this chapter. During the time of profound acidosis that often accompanies diabetic ketoacidosis, iron is released from its binding sites on transferrin; this pH-related effect results in an iron supply that suffices to trigger an overwhelming fungal infection in the rhinocerebral territory.

11.4.2 What may be the Mechanisms?

Very schematically, iron in excess can result in an increased risk and worse outcome of infections for the three following reasons. First, it is clear that the growth of most microorganisms is inhibited by iron restriction and enhanced by the presence of iron in the growth medium (Weinberg, 1978). Second, some important iron-withholding strategies of the host may become ineffective in the presence of an excessive amount of iron. To cite just one example, the iron restriction afforded by physiologic iron saturation of transferrin (only 30 %) is abrogated when transferrin is nearly fully iron saturated and even more in the presence of NTBI (see Chapter 5) in the serum. Third, iron in excess grossly impairs the immune system and phagocyte functions in particular. Let us consider macrophages and neutrophils. Iron-loaded macrophages/monocytes exhibit a decreased responsiveness to γ-interferon and a decreased production of both TNF-α and NO (Weiss *et al.*, 1994, 1995). They also have a limited phagocytic capacity toward microorganisms (Van Asbeck *et al.*, 1982). Polymorphonuclear leucocytes, when iron loaded, also have impaired functions of phagocytosis and killing, as has been demonstrated in patients with transfusional iron overload, such as dialysis and thalassaemic patients (Cantinieaux *et al.*, 1993). We observed that recombinant EPO treatment of iron-loaded dialysis patients reversed the neutrophil dysfunction when iron overload had been resolved (Boelaert *et al.*, 1990b).

11.5 The Role of Iron-related Genes on the Risk and Outcome of Infection

Among the genetic diseases that cause iron overload, rank several entities that were discussed in the previous section, such as haemochromatosis, thalassaemias and

African iron overload. In this section, we discuss the effects of two other genes that seem to modulate the distribution and fate of intracellular iron and hence to alter the risk of (susceptibility to) and/or the course (outcome) of some infectious diseases.

11.5.1 The *Nramp1* Gene

The first gene to be discussed is *Nramp1*. This acronym describes 'natural resistance-associated macrophage protein 1'. This gene was formerly known as the *Bcg* gene, because it confers resistance to *Mycobacterium bovis* (Bcg strain) in inbred mice during the initial phase of infection (Gros *et al.*, 1981). Subsequently, when it was found that the same gene controls innate resistance/susceptibility not only to several *Mycobacteria* species but also to other intracellular pathogens, such as *Salmonella typhimurium* and *Leishmania donovani*, the gene was renamed *Bcg/Ity/Lsh*. More recently, the same gene in the mouse was found to control, at least to some extent, resistance to infection caused by some other microorganisms as well, as shown in Table 11.3. It should be noted that *Mycobacterium tuberculosis* does not belong to this list (North and Medina, 1998). When a candidate for this gene was found on the mouse chromosome 1, it was designated *Nramp1*. It encodes a 548 amino-acid protein with 10 to 12 transmembrane domains. Sequence analysis of *Nramp1* revealed that susceptibility to the above mentioned microorganisms is associated with a single glycine-to-aspartic acid substitution at position 169 (Gly169Asp) within the predicted fourth transmembrane domain of the Nramp1 protein (Vidal *et al.*, 1993). Transfer of the Gly-169 allele of *Nramp1* into transgenic mice of susceptible (Asp-169) background restored the resistance to the above mentioned microorganisms. The exact mechanisms of the *Nramp1*-mediated innate resistance to organisms indicated in Table 11.3 and of the functional defect in the *Nramp1* mutants are still not well understood. However, some insight has been gained. In mice, expression of the gene is restricted to spleen and liver, more specifically to the macrophage populations of these organs, which may explain its prominent role in defence against intracellular parasites that inhabit these type of cells. This contrasts with the ubiquitous expression of the related *Nramp2* gene (discussed in Chapters 5, 8 and 8). *Nramp1* gene expression is enhanced by macrophage activators, including interferon-γ. During microbial phagocytosis, the Nramp1 protein is recruited to the membrane of the phagosome where it remains during the course of phagolysosomal biogenesis. This intimate localization of Nramp1 close to the intracellular pathogens suggests that it may control the replication of intracellular microorganisms by altering the internal milieu of the microbe-containing phagosome (Gruenheid *et al.*, 1997). Several research groups are trying to unravel the exact mechanism by which Nramp1 controls microbial proliferation in the phagosome and very divergent hypotheses have been put forward. They will not be discussed in detail, except for the putative role of iron in the Nramp1-mediated microbiostasis. Let us first recall that the murine *Nramp2* gene (discussed in Chapter 8) carries a defect in models of microcytic anaemia in the *mk* mouse, and in the Belgrade rat, associated with impaired intestinal iron absorption. It encodes a metal-ion transporter protein that transports Fe^{2+} together with other

divalent cations. Other members of this highly conserved gene family function as metal-ion transporters. In view of the importance of iron for the replication of many microorganisms and the high degree (78 %) of homology between the Nramp1 and Nramp2 proteins, is was therefore logical to suspect that Nramp1 might interfere with the transport of iron across the phagosomal membrane. What is the evidence for this so far? Two groups reached totally opposite conclusions based on *in vitro* studies. In one model, Nramp1 is assumed to transport iron out of the phagosome into the cytoplasm, depriving the pathogen of the metal (Barton *et al.*, 1999). In the other model, Nramp1 is supposed to transport a limited amount of iron from the cytoplasm into the phagosome, where it may serve as a catalyst to generate microbicidal hydroxyl radicals (Zwilling *et al.*, 1999). At the time of writing, this controversy has not been settled. However, an *in vivo* study tends to support the first of these two models. In that study, *Mycobacterium avium*-infected mice of both the resistant type (wild type *Nramp1*) and the susceptible type (mutated *Nramp1*) were subjected to iron loading. Whereas this iron load little affected the outcome of the infection in the susceptible mice, it strongly diminished the capacity of the resistant mice to control the infection (Gomes and Appelberg, 1998). To further complicate the picture, several microorganisms themselves may express Nramp homologues. For instance, *Mycobacterium tuberculosis* and *M. bovis* Bcg express mRNA encoding a Nramp homologue called 'Mramp' that seems to function as a divalent cation transporter (Agranoff *et al.*, 1999).

In humans, NRAMP1, a homologue of the murine *Nramp1*, has also been characterized. It is located on chromosome 2q and shows a 88 % sequence homology with its mouse counterpart. Apparently, humans bear a functional NRAMP1 protein and the susceptible allelic variant of murine *Nramp1* (Gly169Asp) has not so far been found. Nevertheless, several polymorphisms have been identified in the human *NRAMP1* gene but they were found outside the coding regions. Although, as indicated in Table 11.3, the *Nramp1* gene does not govern mouse resistance to virulent *Mycobacterium tuberculosis* but rather to related strains (such as *M. bovis* Bcg), and the so-called atypical mycobacteria, one should question whether differential resistance or susceptibility to tuberculosis may be related to sequence variations in the human *NRAMP1* gene. A genetic difference in the ability of the host macrophage to kill tuberculous bacillus is established. A few studies have been undertaken to examine whether some of these polymorphisms were more prevalent in patients with mycobacterial infections. A recent study performed in Gambia compared the prevalence of different NRAMP1 polymorphisms in several hundreds of patients

Table 11.3 Selected microorganisms toward which innate resistance in the mouse is governed by the *Nramp1* gene.

Bacteria	Fungi/Yeasts	Protozoa
Mycobacterium avium	*Candida albicans*	*Leishmania donovani*
Mycobacterium bovis (BCG)	*Cryptococcus neoformans*	*Toxoplasma gondii*
Mycobacterium intracellulare		
Mycobacterium lepraemurium		
Mycobacterium smegmatis		
Salmonella typhimurium		

with tuberculosis and uninfected controls that were ethnically matched. In the tuberculosis group, there was a significant over-representation of heterozygotes for two of the polymorphisms studied (Bellamy *et al.*, 1998). However, the importance of this finding is uncertain, as the studied polymorphisms again were outside the coding regions.

To sum up, it is possible that the murine *Nramp1* gene (and possibly its human counterpart) affect resistance toward major intracellular parasites via modulation of the iron distribution in the macrophage phagosome. This hypothesis is actively tested and it is likely that more definitive answers will be provided in the coming years. Moreover, should *NRAMP1* be confirmed as contributing to human susceptibility to tuberculosis, the NRAMP1 protein might then represent an interesting target for pharmacological intervention.

11.5.2   The Haptoglobin Gene

Haptoglobin is an alpha-2 globulin present in plasma. Its primary function is the binding of free haemoglobin during haemolysis. It consists of an α- and a β-chain. In humans (but not in other species), haptoglobin presents a genetic polymorphism in its α-chain, due to the existence of two alleles Hp^1 and Hp^2. The three major phenotypes, Hp 1-1, Hp 2-1 and Hp 2-2, can be distinguished by starch gel electrophoresis. In the northwestern European population, their phenotypic distribution is 16 %, 48 % and 36 %, respectively. Several disease associations have been observed, most notably a higher risk of atheromatosis in Hp 2-2 individuals (Langlois and Delanghe, 1996). Interestingly, normal Hp 2-2 individuals were found to have higher serum transferrin saturation and higher serum ferritin values as well as lower serum vitamin C levels than their Hp 1-1 and Hp 2-1 counterparts (Delanghe *et al.*, 1998). More recently, the same group of investigators observed that peripheral blood monocytes from Hp 2-2 individuals have a higher L-ferritin content than those from persons with the other phenotypes, possibly due to a facilitated macrophage cell entry of haemoglobin, when bound to Hp 2-2 as opposed to the other haptoglobin types (Langlois *et al.*, 2000). This suggests that the genetic polymorphism of the α-chain of haptoglobin is a determinant of iron distribution within the macrophage. On account of the different iron status in the serum and in the monocytes/macrophages, Hp 2-2 individuals might have an altered course of some infectious diseases. Up to now, this has only been investigated for two infections: HIV-1 infection and tuberculosis. The first study concerns a cohort of 653 HIV-1 infected patients. Hp 2-2 carriers presented some degree of iron accumulation; when studied prior to any antiretroviral therapy, they had significantly higher plasma levels of HIV-1 RNA. More importantly, their median survival was 3.7 years less than that of patients with the other phenotypes (Delanghe *et al.*, 1998). The other study by the same group prospectively examined the course of pulmonary tuberculosis in a rural Zimbabwean population after standard therapy. The odds of death were 6.1-times greater in Hp 2-2 carriers than in patients with Hp 1-1 (Kasvosve *et al.*, 2000).

To sum up, there is evidence to suggest that the Hp_α gene influences macrophage iron distribution. Obviously, more studies are required on the effect of the

haptoglobin polymorphism on iron status and its pathophysiological link to certain infectious diseases.

11.6 Can Iron Depletion be Applied to Combat Infection?

11.6.1 Phlebotomy

Experimental dietary iron loading of hepatitis C-virus-infected chimpanzees results in exacerbation of liver injury (Bassett *et al.*, 1999). Patients with chronic hepatitis C virus infection often have elevated serum iron, transferrin saturation and ferritin levels, with a mild to moderate increase in hepatic iron concentration. As some studies suggested that this increased iron status is associated with a decreased response to interferon-α, phlebotomy has been tried to improve the response rate to this drug (Bonkovsky *et al.*, 1997). Recently, the results of a randomized and controlled trial on iron reduction in chronic hepatitis C were reported (Fontana *et al.*, 2000). It concerned treatment-naïve patients who were randomized in two treatment groups; patients in both groups were treated with interferon-α for 6 months but in one group phlebotomy was added, starting prior to and continuing during the drug treatment period, aimed at reaching a mild iron-deficiency state. In confirmation of previous studies, a lower serum-transferrin saturation at baseline was predictive of a higher percentage of patients with undetectable viral load 6 months after therapy. More importantly, inflammation found upon liver biopsy was significantly lower after treatment in the interferon-plus-iron reduction group than in the group without iron reduction. Standard therapy of chronic hepatitis C virus infection has recently moved from interferon-α monotherapy to combination therapy with ribavirin. As the latter drug may cause haemolysis and resulting anaemia, it seems unlikely that phlebotomy will be used in association with this new therapeutic drug combination. In a double-blind controlled trial, comparing ribavirin with placebo therapy for 36 weeks in hepatitis C virus-infected patients, a significant increase in hepatocyte iron was observed in the ribavirin group as compared with the placebo group. It is presently unclear as to whether or not this excessive iron accumulation in the liver will limit the usefulness of ribavirin (Fiel *et al.*, 2000).

Phlebotomy has not been used as strategy against other infectious diseases, although prudent phlebotomy may be beneficial at the outset of HIV-1 infection. No clinical study has addressed this issue up to now. Furthermore, even if this apparently outreaches the scope of this chapter, we should mention here the results obtained by Solonen's group, who studied the association of voluntary blood donation and the risk of myocardial infarction. Blood donors had a relative risk of myocardial infarction of 0.14 as compared to non-donors (Tuomainen *et al.*, 1997). If the hypothetical association between atherosclerosis and infection by *Chlamydia pneumoniae* gains more weight in the future, one of the ways to explain the beneficial effect of blood donation is that the iron restriction it induces may limit the growth of this pathogen (Freidank and Billing, 1997).

11.6.2   Iron Chelators

Can iron restriction be used as a therapeutic measure to prevent or eliminate infections without compromising the host organism? At present, the only iron chelator widely available for clinical use is desferrioxamine (DFO), which is very efficient in preventing clinical consequences in thalassaemic patients (Brittenham,1992). Has this drug any antiinfectious potential? This question on its potential usefulness against infection should be answered at three levels: (i) its *in vitro* effect on the growth of microorganisms; (ii) its *in vivo* effect on the course of experimental infections; and most importantly, (iii) its effect on clinical infections in humans. DFO is indeed able to suppress the *in vitro* growth and to protect against experimental infections caused by several microbes (Boelaert *et al.*, 1993b). On the other hand, one should not forget that a limited number of microorganisms can utilize the iron from ferrioxamine to enhance their growth, as discussed in Section 1 of this chapter. Malaria is the only infectious disease against which iron chelation has been clinically tried because iron chelators act as growth suppressors, mainly by depriving *Plasmodium* spp. of essential iron at critical stages of their intraerythrocytic development, such as DNA replication. Gordeuk and collaborators showed that, when added to the standard quinine regimen, DFO was significantly more likely than placebo to result in a fast recovery from coma and improved plasmodial blood clearance in children with cerebral malaria due to *Plasmodium falciparum* (Gordeuk *et al.*, 1992). However, subsequent results were less convincing. In further studies by the same group, addition of DFO to quinine (including a loading dose of the latter) did not result in a beneficial effect on mortality of children with cerebral malaria (Thuma *et al.*, 1998). Second, the orally administered hydroxypyridinone iron chelator deferiprone, although more membrane permeant than DFO, proved ineffective in malaria because of its limited capacity to attain antiinfective levels in the blood for prolonged periods. Third, malaria is caused by the plasmodial infection of the red blood cell, a cell type that is only very rarely infected by other microorganisms, so that care should be taken in extrapolating results obtained on malaria to other infectious diseases. Apart from malaria, iron chelation has been advocated as a possible strategy to reduce the iron burden existing in long-standing HIV-1 infection (Boelaert *et al.*, 1996). Although DFO and other chelators are effective *in vitro* in reducing HIV-1 activation due to oxidative stress (Sappey *et al.*, 1995; Georgiou *et al.*, 2000), no clinical study has been reported on the use of iron chelation in the context of HIV-1 infection, except for its use in HIV-1-infected thalassaemic patients, where it was found effective in a retrospective study (Costagliola *et al.*, 1994). Generally speaking, in order to restrict selectively the availability of iron to intracellular pathogens, it is essential that the drugs under consideration not only target as specifically as possible the types of cells inhabited by these pathogens – usually macrophages – but also target the cellular compartment(s) where they reside. In other words, the fact that either DFO or deferiprone are effective in reducing liver iron in patients with thalassaemia does not allow extrapolation to antiinfective efficacy.

In summary, there is still little justification for the use of the currently available iron chelators in the prevention or therapy of human infectious diseases. However,

there is a strong need for designing and studying new types of iron chelators, which should be targeted to the site of microbial proliferation within the macrophage.

11.6.3 Chloroquine

The 4-aminoquinoline compound chloroquine is widely known as a classical antimalarial and it is also used in clinical medicine to treat some autoimmune diseases such as rheumatoid arthritis and systemic lupus eryth-ematosus. The drug has been shown experimentally to be endowed with antiinfectious properties against selected intracellular microorganisms. It is likely that the mechanism whereby chloroquine inhibits the growth of pathogens in the macrophage is not uniform. Three mechanisms may be evoked: first, impairment of iron availability to the pathogen; second, the consequences of the increased pH within acidic organelles that are unrelated to iron metabolism; third, direct toxicity to the pathogen, due to the very high rate of pH-driven accumulation of the diprotic weak base within the acidic phagosome and phagolysosome and/or within the acid vesicles of the microorganism itself. The first of these mechanisms, i.e. chloroquine's ability to impair the availability of iron to the pathogen, has been elegantly demonstrated for the following pathogens residing within the macrophage: *Legionella pneumophila* (Byrd and Horwitz, 1991), *Histoplasma capsulatum* (Newman *et al.*, 1994) and *Francisella tularensis* (Fortier *et al.*, 1995). In these three cases, the effect of chloroquine could be mimicked by another weak base, such as ammonium chloride, and it was abrogated by the addition of a transferrin-independent iron source such as iron nitrilotriacetate (which enters the macrophage by a pH-independent pathway) but not by the addition of holotransferrin. As chloroquine impairs the mobilization of the metal from either holotransferrin in the endosome or from ferritin that is degraded in the lysosome, this indicates that an acidic environment is critical for these microorganisms to access cellular iron for growth. Other microorganisms whose intracellular growth is inhibited by chloroquine *in vitro* are: *Mycobacterium tuberculosis*, *M. avium, Cryptococcus neoformans, Penicillium marneffei* and *Leishmania* spp. (Boelaert *et al.*, 2001). In the case of *C. neoformans*, the effect of chloroquine is clearly iron unrelated (Mazzolla *et al.*, 1997; Levitz *et al.*, 1997). The mechanism underlying the inhibitory effect of chloroquine toward the other mentioned pathogens requires further study.

Chloroquine's effects on the functions of intracellular organelles may also explain the drug's anti-HIV-1 activity. It has been shown to inhibit HIV-1 *in vitro* (Tsai *et al.*, 1990; Sperber *et al.*, 1993) and also *in vivo* in patients. The most likely mechanism involved is the inhibition of intravesicular glycosylation of the HIV-1 envelope protein gp120, whereby the produced virion loses its infectivity. Although this anti-HIV-1 effect of chloroquine is likely to be iron unrelated, it is noteworthy that the drug decreases cellular iron availability, as demonstrated in a lymphocytic cell line (Morra *et al.*, 2000) and *in vivo* (Legssyer *et al.*, 1999). In the latter study, chronic administration of chloroquine to rats for 5 weeks resulted in a significantly decreased iron content in liver and spleen; the drug also abrogated iron loading of the macrophages during experimental administration of iron dextran to the animals. This iron-restricting property of chloroquine would be welcome in states of chronic

infection, characterized by a progressive iron loading of the reticuloendothelial cells, as discussed earlier in this chapter. HIV-1 infection is a typical example of a long-standing inflammatory process where such iron loading has been documented (Boelaert *et al.*, 1996).

11.6.4 Vaccination

Among the multiple mechanisms that microorganisms have invented to acquire iron, some may lend themselves to preventive medicine by vaccination. Two such microbial strategies, manipulated to the benefit of the host, are briefly discussed here.

First, the critical role played by Tbp and Lbp subunits in bacterial iron acquisition from host-specific Tf and Lf suggests that these receptor proteins may serve as good candidates for vaccination. Understandably, most of the work in this direction has been performed on *Neisseria meningitidis*, but the same approach is being taken with *Haemophilus influenzae*, *Moraxella catarrhalis* and other pathogens. The TbpB and LbpB subunits are presently viewed as better immunogens than their TbpA and LbpA counterparts. Convalescent-phase sera from patients infected with the above mentioned organisms contain antibodies directed against TbpB. The fact that recombinant TbpBs generate protective antibodies indicates that industrial production of TbpBs for vaccination purposes is an achievable goal. The above examples concern Gram-negative bacteria. The same concepts may apply to some Gram-positive bacteria. For example, the pneumococcal surface protein A, PspA, that binds human Lf, is a promising vaccine candidate that may act by impeding iron acquisition at the mucosal surface (Hammerschmidt *et al.*, 1999).

Next to immunity induced against some Tbp or Lbp subunits, it is conceivable that immunity against other microbial iron acquisition systems may be elicited. One example concerns the haemolysin produced by *Haemophilus ducreyi* (the aetiologic agent of chancroid, an important cause of genital ulcers in the populations of developing countries), that is homologous to the *Serratia marcescens* haemolysin. Immunization of rabbits with this haemolysin resulted in an attenuation of the experimental infection (Dutro *et al.*, 1999).

11.7 References

Abe, F., Inaba, H., Katoh, T. and Hotchi, M. (1990). *Mycopathologia*, **110**, 87–91.

Adamkiewicz, T.V., Berkovitch, M., Krishnan, C., Polsinelli, C., Kermack, D. and Olivieri, N. (1998). *Clin. Infect. Dis.*, **27**, 1362–6.

Agranoff, D., Monahan, I.M., Mangan, J.A., Butcher, P.D. and Krishna, S. (1999). *J. Exp. Med.*, **190**, 717–24.

Al Khafaie, B.B., Kralovic, S. and Smith, R.D. (1997). *Modern Pathol.*, **10**, 474–80.

Anand, V.K., Alemar, G. and Griswold, J.A. (1992). *Laryngoscope*, **102**, 656–62.

Artis, W.M., Fountain, J.A., Delcher, H.K. and Jones, H.E. (1982). *Diabetes*, **31**, 1109–14.

Baker, E.N. (1997). *Nature Struct. Biol.*, **4**, 869–71.

Barnewall, R.E., Ohashi, N. and Rikihisa, Y. (1999). *Infect. Immun.*, **67**, 2258–65.

Barton, C.H., Biggs, T.E., Baker, S.T., Bowen, H. and Atkinson, P.G.P. (1999). *J. Leukoc. Biol.*, **66**, 757–62.

Bassett, S.E., Di Bisceglie, A.M., Bacon, B.R., Sharp, R.M. *et al.* (1999). *Hepatology*, **29**, 1884–92.

Bellamy, R., Ruwende, C., Corrah, T., McAdam, K.P.W.J., Whittle, H.C. and Hill, A.V.S. (1998). *New Engl. J. Med.*, **338**, 640–4.

Binet, R. and Wandersman, C. (1996). *Mol. Microbiol.*, **22**, 265–73.

Boelaert, J.R. and Blasi, E. (1999). *J. Infect. Dis.*, **180**, 1412–3.

Boelaert, J.R., Van Landuyt, H.W., Valcke, Y.L., Cantinieaux, B. *et al.* (1987). *J. Infect. Dis.*, **156**, 384–7.

Boelaert, J.R., Daneels, R.F., Schurgers, M.L., Matthys, E.G., Gordts, B.Z. and Van Landuyt, H.W. (1990a). *Nephrol. Dial. Transplant.*, **5**, 130–4.

Boelaert, J.R., Cantinieaux, B.F., Hariga, C.F. and Fondu, P.G. (1990b). *Nephrol. Dial. Transplant*, **5**, 504–7.

Boelaert, J.R., Fenves, A.Z. and Coburn, J.W. (1991). *Am. J. Kidney Dis.*, **18**, 660–7.

Boelaert, J.R., de Locht, M., Van Cutsem, J., Kerrels, V. *et al.* (1993a). *J. Clin. Invest.*, **91**, 1979–86.

Boelaert, J.R., de Locht, M. and Van Cutsem, J. (1993b). *Rev. Med. Microbiol.*, **4**, 171–5.

Boelaert, J.R., Van Cutsem, J., de Locht, M., Schneider, Y.-J. and Crichton, R.R. (1994). *Kidney Intern.*, **45**, 667–71.

Boelaert, J.R., Weinberg, G.A. and Weinberg, E.D. (1996). *Infect. Agents Dis.*, **5**, 36–46.

Boelaert, J.R., Pootrakul, P., Chaiprasert, A., Van Landuyt, H.W., Lambert, A. and Winkelmann, G. (1999s). Pathophysiology of pythiosis in thalassemic patients. *Abstracts of the World Congress of Iron Metabolism 'Bioiron 99'*, Sorrento, May 23–28, abstr. p. 372.

Boelaert, J.R., Appelberg, R., Gomes, M.S., Blasi, E. *et al.* (2001). *J. AIDS*, in press.

Bonkovsky, H., Banner, B.F. and Rothman, A.L. (1997). *Hepatology*, **25**, 759–68.

Bonnah, R.A., Lee, S.W., Vasquez, B.L., Enns, C.A. and So, M. (2000). *Cell Microbiol.*, **2**, 207–18.

Braun, V., Hantke, K. and Köster, W. (1998). in *Metal Ions in Biological Systems* (eds Sigel, A. and Sigel, H.), **35**, 68–145.

Britigan, B.E., Rasmussen, G.T., Olakanmi, O. and Cox, C.D. (2000). *Infect. Immun.*, **68**, 1271–5.

Brittenham, G.M. (1992). *Blood*, **80**, 569–74.

Brock, J.H. (1993). *J. Nutr. Immunol.*, **2**, 47–106.

Brock, J.H. (1999). *Curr. Opin. Clin. Nutr. Metab. Care*, **2**, 507–10.

Brodsky, F.M. (1999). *Immunol. Rev.*, **168**, 5–11.

Byrd, T.F. and Horwitz, M.A. (1989). *J. Clin. Invest.*, **83**, 1457–65.

Byrd, T.F. and Horwitz, M.A. (1991). *J. Clin. Invest.*, **88**, 351–7.

Byrd, T.F. and Horwitz, M.A. (2000). *J. Infect. Dis.*, **181**, 1394–400.

Cantinieaux, B. and Boelaert, J.R. (1993). *Eur. J. Haematol.*, **51**, 161–5.

Clemens, D.L. and Horwitz, M.A. (1996). *J. Exp. Med.*, **184**, 1349–55.

Clemens, D.L., Lee, B.-Y. and Horwitz, M.A. (2000). *Infect. Immun.*, **68**, 2671–84.

Cope, L.D., Thomas, S.E., Latimer, J.L., Slaughter, C.A., Muller Eberhard, U. and Hansen, E.J. (1994). *Mol. Microbiol.*, **13**, 863–73.

Cope, L.D., Yogev, R., Muller Eberhard, U. and Hansen, E.J. (1995). *J. Bacteriol.*, **177**, 2644–53.

Cornelissen, C.N. and Sparling, P.F. (1994). *Mol. Microbiol.*, **14**, 843–50.

Costagliola, D., de Montalembert, M., Lefrère, J.-J., Briand, C. *et al.* (1994). *Brit. J. Haematol.*, **87**, 849–52.

Delanghe, J., Langlois, M., Boelaert, J.R., Van Acker, J. *et al.* (1998). *AIDS*, **12**, 1027–32.

De Monyé, C., Karcher, D.S., Boelaert, J.R. and Gordeuk, V.R. (1999). *AIDS*, **13**, 375–80

De Voss, J.J., Rutter, K., Schroeder, B.G. and Barry. C.E. (1999). *J. Bacteriol.*, **181**, 4443–51.

Dimier, I.H. and Bout, D.T. (1998). *Immunol.*, **94**, 488–95.

Drechsel, H., Metzger, J., Freund, S., Jung, G., Boelaert, J.R. and Winkelmann, G. (1991). *Biol. Met.*, **4**, 238–343.

Dutro, S., Wood, G.E. and Totten, P.A. (1999). *Infect. Immun.*, **67**, 3317–28.

Fiel, M.I., Schiano, T.D., Guido, M., Thung, S.N. *et al.* (2000). *Am. J. Clin. Path.*, **113**, 29–34.

Fontana, R.J., Israel, J., Le Clair, P., Banner, B.F. *et al.* (2000). *Hepatology*, **31**, 730–6.

Fortier, A.H., Leiby, D.A., Narayanan, R.B., Asafoadjei, E. *et al.* (1995). *Infect. Immun.*, **63**, 1478–83.

Freidank, H.M. and Billing, H. (1997). *Clin. Microbiol. Infect.*, **3**, suppl. 2, 193.

Garcia-del-Portillo, F. and Finlay, B.B. (1995). *Trends Microbiol.*, **3**, 373–80.

Georgiou, N.A., van der Bruggen, T., Oudshoorn, M., Nottet, H.S.L.M., Marx, J.J.M. and van Asbeck, B.S. (2000). *J. Infect. Dis.*, **181**, 484–90.

Ghigo, J.M., Letoffe, S. and Wandersman, C. (1997). *J. Bacteriol.*, **179**, 3572–9.

Gomes, M.S. and Appelberg, R. (1998). *Immunol.*, **95**, 165–8.

Gordeuk, V.R., Thuma, P., Brittenham, G., McLaren, C. *et al.* (1992). *New. Engl. J. Med.*, **327**, 1473–7.

Gordeuk, V.R., McLaren, C.E., MacPhail, A.P., Deichsel, G. and Bothwell, T.H. (1996). *Blood*, **87**, 3470–6

Gros, P., Skamene, E. and Forget, A. (1981). *J. Immunol.*, **127**, 2417–21.

Gruenheid, S., Pinner, E., Desjardins, M. and Gros, P. (1997). *J. Exp. Med.*, **185**, 717–30.

Hammerschmidt, S., Bethe, G., Remane, P.H. and Chhatwal, G.S. (1999). *Infect. Immun.*, **67**, 1683–7.

Heesemann, J., Hantke, K., Vocke, T., Saken, E. *et al.* (1993). *Mol. Microbiol.*, **8**, 397–408.

Henderson, D.P. and Payne, S.M. (1994). *J. Bacteriol.*, **176**, 3269–77.

Howe, D. and Mallavia, L.P. (1999). *Infect. Immun.*, **67**, 3236–41.

Iglesias-Osma, C., Gonzalez-Villaron, L., San Miguel, J.F., Vazquez, L. and de Castro, S. (1995). *Cell. Microbiol.*, **48**, 223–5.

Jacobson, E.S. and Petro, M.J. (1987). *J. Med. Vet. Mycol.*, **25**, 415–8.

Jacobson, E.S., Goodner, A.P. and Nyhuis, K.J. (1998). *Infect. Immun.*, **66**, 4169–75.

Jones, R.L., Peterson, C.M., Grady, R.W., Kumbaraci, T., Cerami, A. and Graziano, C.H. (1977). *Nature*, **267**, 63–4.

Jurado, R.L. (1997). *Clin. Infect. Dis.*, **25**, 888−95.

Kasvosve, I., Gomo, Z.A.R., Mvundura, E., Moyo, V.M. *et al*. (2000). *Int. J. Tuberculosis Lung Dis.*, in press.

Kim, S. and Ponka, P. (2000). *J. Biol. Chem.*, **275**, 6220−6.

Langlois, M.R. and Delanghe, J.R. (1996). *Clin. Chem.*, **42**, 1589−600.

Langlois, M.R., Martin, M.-E., Boelaert, J.R., Beaumont, C. *et al*. (2000). *Clin. Chem.*, **46**, 1619−25.

Legssyer, R., Ward, R., Crichton, R.R. and Boelaert, J.R. (1999). *Biochem. Pharmacol.*, **57**, 907−11.

Letoffe, S., Ghigo, J.M. and Wandersmann, C. (1994). *J. Bacteriol.*, **176**, 5372−7.

Levitz, S.M., Harrison, T.S., Tabuni, A. and Liu, X. (1997). *J. Clin. Invest.*, **100**, 1640−6.

Lewis, L.A., Gray, E., Wang, Y.P., Roe, B.A. and Dyer, D.W. (1997). *Mol. Microbiol.*, **23**, 737−49.

Manns, J.M., Mosser, D.M. and Buckley, H.R. (1994). *Infect. Immun.*, **62**, 154−6.

Mateos, F., Brock, J.H. and Pérez-Arellano, J.L. (1998). *Thorax*, **53**, 594−600.

Mazzolla, R., Barluzzi, R., Brozzetti, R., Boelaert, J.R. *et al*. (1997). *Antimicrob. Ag. Chemother*, **41**, 802−7.

Meehan, H.A., Lundberg, R.A. and Connell, G.J. (2000). *Parasitol. Res.*, **86**, 109−14.

Menendez, C., Kahigwa, E., Hirt, R. and Vounatsou, P. *et al*. (1997). *Lancet*, **350**, 844−50.

Mills, M. and Payne, S. (1995). *J. Bacteriol.*, **177**, 3004−9.

Morra, E., Savarino, A., Gennero, L. and Pescarmona, G.P. (2000). *J. Clin. Virol.*, **16**, 91−2 (abstr.).

Mullineaux, C.W. (1999). *Science*, **283**, 801−2.

Murray, M.J., Murray, A.B., Murray, M.B. and Murray, C.J. (1978). *Br. Med. J.*, **2**, 1113−5.

Newman, S.L., Gootee, L., Brunner, G. and Deepe, G.S. Jr. (1994). *J. Clin. Invest.*, **93**, 1422−9.

North, R.J. and Medina, E. (1998). *Trends in Microbiol.*, **6**, 441−3.

Nyhus, K.J. and Jacobson, E.S. (1996). *Infect. Immun.*, **65**, 434−8.

Proudfoot, L., Nikolaev, A.V., Feng, G.-J., Wei, X.-G. *et al*. (1996). *Proc. Natl Acad. Sci. USA*, **93**, 10984−9.

Recalcati, S., Taramelli, D., Conte, D. and Cairo, G. (1998). *Blood*, **91**, 1059−66.

Robins-Browne, R.M. and Prpic, J.K. (1983). *Lancet*, **2**, 1372.

Robins-Browne, R.M. and Prpic, J.K. (1985). *Infect. Immun.*, **47**, 774−9.

Sappey, C., Boelaert, J.R., Legrand-Poels, S., Forceille, C., Favier, A. and Piette, J. (1995). *AIDS Res. Hum. Retroviruses*, **11**, 1049−61.

Schubert, S. and Autenrieth, I.B. (2000). *Clin. Diagn. Lab. Immunol.*, **7**, 457−62.

Shi-Hua, Lin, Shang-Der, Shieh, Kuo-Chang, Lu, Yuh-Feng, Lin *et al*. (1996). *Am. J. Kidney Dis.*, **27**, 733−5.

Sperber, K., Kalb, T.H., Stecher, V.J., Banerjee, R. and Mayer, L. (1993). *Aids Res. Human. Retroviruses*, **9**, 91−8.

Stevens, M.K., Porcella, S., Klesney Tait, J., Lumbley, S. *et al*. (1996). *Infect. Immunol.*, **64**, 1724−35.

Stojiljkovic, I. and Hantke, K. (1992). *EMBO J.*, **11**, 4359–67.

Stojiljkovic, I. and Hantke, K. (1994). *Mol. Microbiol.*, **13**, 719–32.

Stojiljkovic, I., Hwa, V., de Saint Martin, L. O'Gaoro, P. *et al.* (1995). *Mol. Microbiol.*, **15**, 531–41.

Stojiljkovic, I., Larsen, J., Hwa, V., Anic, S. and So, M. (1996). *J. Bacteriol.*, **178**, 4670–8.

Thuma, P.E., Mabeza, G.F., Biemba G., Bhat, G.J. *et al.* (1998). *Trans. Roy. Soc. Trop. Med. Hyg.*, **92**, 214–8.

Tielemans, C., Boelaert, J., Vergauwe, P., Van Roost, G. *et al.* (1989). *Nephron.*, **53**, 276–7.

Torres, A.G. and Payne, S.M. (1997). *Mol. Microbiol.*, **23**, 825–33.

Trajkovic, V., Stepanovic, S., Samardzic, T., Jankovic, V. *et al.* (2000). *Scand. J. Immunol.*, **51**, 384–91.

Tsai, W.P., Nara, P.L., Kung, H.F. and Oroszlan, S. (1990). *AIDS Res. and Human. Retrov.*, **6**, 481–9.

Tuomainen, T.-P., Salonen, R., Nyyssönen, K. and Salonen, J.T. (1997). *Br. Med. J.*, **314**, 793–4.

Van Asbeck, B.S., Verbrugh, H.A., Van Oost, B.A. and Marx, J.J.M. (1982). *Br. Med. J.*, **284**, 542–4.

Van Cutsem, J. and Boelaert, J.R. (1989). *Kidney Int.*, **36**, 1061–8.

Vergne, A.F., Walz, A.J. and Miller, M.J. (2000). *Nat. Prod. Rep.*, **17**, 99–116.

Verpooten, G.A., d'Haese, P.C., Boelaert, J.R., Becaus, I., Lamberts, L.V. and De Broe, M.E. (1992). *Nephrol. Dial. Transplant.*, **7**, 931–8.

Vidal, S.M., Malo, D., Vogan, K., Skamene, E. and Gros, P. (1993). *Cell*, **73**, 469–85.

Weinberg, B. (1998). *Molecular Medicine*, **4**, 557–91.

Weinberg, E.D. (1978). *Microbiol. Rev.*, **42**, 45–66.

Weinberg, E.D. (1984). *Physiol. Rev.*, **64**, 65–102.

Weinberg, E.D. (1999). *Emerging Infectious Diseases*, **5**, 346–52.

Weinberg, E.D. (2000). *Microbes and Infection*, **2**, 85–9.

Weiss, G. (1999). *Kidney Intern.*, **55**, suppl. 69: S12–S17.

Weiss, G., Werner-Felmayer, G., Werner, E.R., Grunewald, K., Wachter, H. and Hentze, M.W. (1994). *J. Exp. Med.*, **180**, 969–76.

Weiss, G., Wachter, H. and Fuchs, D. (1995). *Immunol. Today*, **16**, 495–500.

Zwilling, B.S., Kuhn, D.E., Wikoff, L., Brown, D. and Lafuse, W. (1999). *Infect. Immun.*, **67**, 1386–92.

12 Interactions between Iron and other Metals

12.1 Introduction

In the course of evolution, the importance of particular metal ions in biological systems has ebbed and flowed, as a function of environmental conditions. Before the arrival of photosynthesis, when there was no oxygen, elements like Fe and Ni were extremely important, whereas, for example, Cu was virtually inaccessible for reasons of solubility. With the arrival of an oxidizing environment, Ni virtually disappeared from the equation, Cu became bioavailable, and Fe, although it was now insoluble and poorly available, had proved of such fundamental importance in biological catalysis that specific systems were developed for its uptake from the environment, such that it continues to play a key role in life as we know it today.

   We have chosen, somewhat arbitrarily, to classify metals in terms of their interaction with iron into two groups, and to consider particularly iron–metal interactions in mammals. First we consider essential metals which are required for living organisms, and the way in which they interact with iron (and reciprocally). In this category we include Cu, which has played Venus to the Mars of iron since the cyanobacterial evolution of molecular dioxygen, and which is intimately involved in iron metabolism as we have seen in the earlier parts of this book. Zn is another transition metal which has important interactions with iron, as does Co through its role in cobalamine cofactors. Mn is also an essential metal ion, that poses problems when in excess due to its accumulation in brain, resulting in Parkinson-like symptoms and aggressive behaviour. Iron also interacts in a biological context with Ni, and with Mo and V in bacterial systems, but few effects of these metals on mammalian iron metabolism have been reported. Then we have toxic metal ions like Pb, some of which interfere with essential metabolic pathways that depend on iron, and others which, like Al, on account of their chemical similarity to iron, take advantage of iron-transport pathways.

12.2 Interactions Between Iron and Essential Metals

It would be surprising to find that there were no interactions between iron and a number of other divalent transition-metal ions in mammalian systems, not least

because, at the level of the gastrointestinal tract (Chapter 8), they can compete with the same DMT1 transporter localized at the apical (brush border) membrane of the villus epithelium for uptake into the mucosal cell. In the initial publication of Gunshin *et al.* (1997) the proton-coupled divalent transporter was reported to transport Fe^{2+}, Zn^{2+}, Mn^{2+}, Co^{2+}, Cd^{2+}, Cu^{2+}, Ni^{2+} and Pb^{2+}. In the present context we will deal with Cu^{2+}, Zn^{2+}, Mn^{2+}, and Co^{2+}.

12.2.1 Mars and Venus – Iron and Copper

Introduction

Iron and copper have long exerted a fascination for man. Chemists gave the name Mars, the Roman god of war, to iron, while Venus, the Roman goddess of love and beauty, was the alchemist's name for copper. Copper and its alloy, bronze, were used for several thousand years prior to iron for metallurgy.[†] Fe(0) is easy to oxidize, giving rust, while Cu(0) is difficult to oxidize because of its high electrode potential, such that copper is often found in nature in the metallic state. Iron has long been considered not only as a precious metal, but as the strong metal and, at the dawn of the Twentieth century, Rudyard Kipling wrote:

> *'Gold is for the mistress – silver for the maid –*
> *Copper for the craftsman cunning at his trade.'*
> *'Good !' said the Baron, sitting in his hall,*
> *'But Iron – Cold Iron – is master of them all.'*

Copper is associated with two important life-threatening diseases in man, the pathologies of both being due to defective intracellular copper transport. Menke's disease is characterized by progressive cerebral degeneration, essentially due to insufficient copper absorption, and Wilson's disease is due to excessive copper accumulation in liver, accompanied by liver disease and haemolytic crises.

Trace amounts of copper are essential for life. However, as with iron, excess copper is also toxic, on account of its capacity to catalyse the Fenton reaction. There are analogies and differences between these two elements successively selected by Nature as it was obliged to adapt life to the first general irreversible pollution of the earth, namely the advent of dioxygen.

> *'There was a primitive separation between organisms heavily dependent on iron, nickel (especially) and cobalt, the archebacteria, and other prokaryotes where the dominance of iron is more obvious. It is also clear that copper is of little significance in most of these organisms relative to its multitude of roles in multicellular eukaryotes, while in these eukaryotes the role of nickel and cobalt is further diminished. We may conjecture that biological systems did not use copper extensively before the advent of an oxidizing atmosphere based on dioxygen' (Frausto da Silva and Williams, 1991).*

[†] The Iron Age was a phase of human civilization (in Europe from about 1000 BC to 100 AD), characterized by the introduction and development of iron tools and weapons; it followed the Bronze Age.

Copper Chemistry, Its Interactions with Iron, and Evolution

Two oxidation states are usual for copper, Cu(I) and Cu(II). Although some earlier reports suggested the occurrence of Cu(III) in galactose oxidase, it is now known that this is due to the generation of a tyrosyl radical on a tyrosine liganded to copper during the reaction cycle, and it is unlikely that this oxidation state has any biological relevance. The Cu(II)/Cu(III) redox potential is generally high and hence, one electron oxidation of the protein ligand occurs. The $3d^9$ outer electronic configuration of Cu(II) lacks cubic symmetry and hence yields distorted forms of the basic stereochemistry. The coordination numbers 4 (square planar), 5 (trigonal bipyramid or square pyramid) or 6 predominate. With coordination 6, the Jahn–Teller effect excludes the regular octahedron. The stable Cu(II)–N bonds are often inert while the bonds with oxygen donor ligands are more labile. Cu(I) prefers coordination numbers 2, 3 or 4 (tetrahedral geometry) and is stabilized by soft ligands. Coordination 5 is known (square pyramid). Cu(I) is a closed shell d^{10} transition metal ion and thus is diamagnetic. The disproportionation of Cu(I) is usual:

$$\mathbf{2Cu^+ \longleftrightarrow Cu + Cu^{2+}}$$
$$E_0 = 0.182 \text{ V}$$
$$E_0(Cu^{2+}/Cu^+) = 0.34 \text{ V}$$
$$E_0(Cu^+/Cu) = 0.52 \text{ V}$$
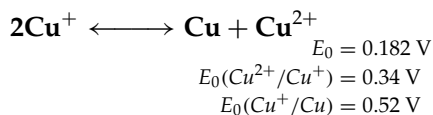
The equivalent reaction is not observed with iron. Cu(I) catalyses the Fenton reaction with hydrogen peroxide, just as Fe(II) does. The Cu(I) state exhibits the ability to bind and activate dioxygen via $Cu_2(\mu\text{-}\eta^2{:}\eta^2\text{-}O_2)$ and $Cu_2(\mu\text{-}O)_2$ species.

Copper proteins are widely distributed in living organisms, and have two main functions, electron transfer and dioxygen transport and activation (Kaim and Rall, 1996; Klinman, 1996; Salomon *et al.*, 1996; Koch *et al.*, 1997). A great many copper proteins are extracellular; exceptions are cytochrome *c* oxidase, which is bound to the external face of the inner mitochondrial membrane, and the copper–zinc superoxide dismutase found in the cytosol of eukaryotic cells. At least three spectroscopically distinct classes of copper occur in biology, designated Types 1, 2 or 3, which can be found either alone or in combination. Type 1 centres, exemplified by the electron transfer proteins plastocyanin and azurin, have deeply blue coloured Cu(II) centres, high reduction potentials and unusual ground-state EPR spectra, indicative of significant delocalization of the metal unpaired-electron density. They have highly unusual coordination geometry, in that their mononuclear Cu centre is designed for binding Cu(I) rather than Cu(II). This constrained coordination site in plastocyanin is already preformed in the apoprotein (Garrett *et al.*, 1984), constituting the so-called 'entatic state'. The reduction potentials of Type 1 centres are modulated to fit the overall $\Delta G°$ of the reaction catalysed, with very low reorganization energies, such that there is practically no difference in ligand positions between oxidized, reduced and apoproteins (Gray *et al.*, 2000).[‡] Whereas Type 1 centres are only used for electron transfer, Type 2 mononuclear copper centres have vacant coordination

---

[‡] This article is dedicated by Harry Gray and Bob Williams to the memory of the third author, Bo Malmström, who passed away on 9 February, 1999. Bo made many contributions to the field of biological inorganic chemistry and blue copper proteins in particular.

sites and can be involved in catalytic redox reactions with substrate molecules; they have weak bands in electronic absorption spectra, and hyperfine coupling constants in EPR spectra typical of tetragonal coordination. Type 2 centres may act in isolation, e.g. galactose oxidase, amine oxidase, dopamine-β-hydroxylase, or in concert with other copper centres. Galactose oxidase and amine oxidase are interesting because they catalyse the two-electron oxidation of substrates coupled to the two-electron reduction of dioxygen to hydrogen peroxide. This is accomplished by using an additional organic cofactor covalently bound to the site. Type 3 centres are binuclear, EPR silent in the oxidized Cu(II)–Cu(II) state (due to antiferromagnetic coupling between the two Cu centres). They participate in dioxygen transport (haemocyanin), dioxygen activation and oxygenation reactions (tyrosinase). The Cu(I)–Cu(I) state binds dioxygen to give $[(Cu(II))_2O_2]$ complexes. Proteins such as ascorbate oxidase, laccase and ceruloplasmin, involved in dioxygen activation and oxidase functions, contain all three types of copper centre (illustrated in Figure 12.1 for ascorbate oxidase).

During prebiotic times, water-soluble ferrous iron was present and was used in the first stage of life, while copper was in the water-insoluble Cu(I) state, as highly insoluble sulphides. About 10^9 years ago the metabolism of a primitive prokaryote (cyanobacteria) led to the evolution of dioxygen into the Earth's atmosphere. A
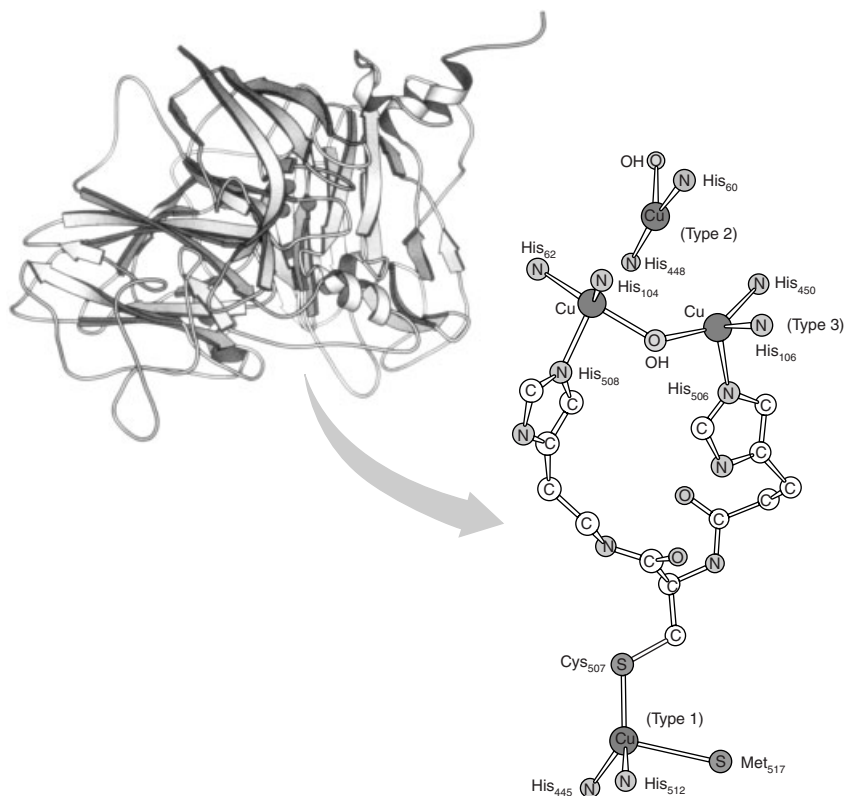
Figure 12.1 Structure of the four copper sites in ascorbate oxidase showing their spatial relationship. From Lippard and Berg, 1994. Reproduced by permission of University Science Books.

lag of 200–300 million years is estimated to have been required between the first production of O_2 and the appearance of a significant O_2 concentration in the atmosphere, because the O_2 produced was initially consumed by the oxidation of ferrous ions in the oceans. However, as iron was oxidized and transformed into insoluble iron hydroxides, the bioavailability of iron was lost. At the same time, the oxidation of insoluble copper(I) led to soluble copper(II). While the proteins and enzymes involved in anaerobic metabolism were designed to act in the lower portion of the redox potential spectrum, the presence of dioxygen created the need of a new redox active metal with E_o M^{n+1}/M^n from 0 to 0.8 V. Copper, now bioavailable, was ideally suited with a redox potential between +0.25 and +0.75 V. Copper began to be used in enzymes, firstly in the extracellular space (lysine oxidase, laccase, phenol oxidase, amine oxidase). While the new role of copper evolved, the role of iron changed. Inside cells, iron could still be used for catalytic functions. For aerobic metabolism, proteins and enzymes with higher redox potentials came to be utilized, taking advantage of the oxidizing power of dioxygen in energy-capture systems like cytochrome oxidase which involves two haem iron centres and two copper centres (Cu_A and Cu_B).

Copper was found to be necessary for haemoglobin formation in rats fed on a milk-based diet (Hart *et al.*, 1928). In rapidly growing piglets, copper deficiency lowered body iron content and interfered with iron distribution to tissues (Gubler *et al.*, 1956), and it was subsequently shown that reticulocytes from copper-deficient pigs took up iron poorly and were deficient in haem synthesis (Lee *et al.*, 1968). While it is now clearly established that copper deficiency is associated with anaemia in animals, acquired copper deficiency in humans is mainly a pathology of infants: most cases of clinical manifestation have been described in malnourished children (Olivares and Uauy, 1996). The most constant clinical manifestations are anaemia, neutropenia and bone abnormalities. Haemolysis is associated with copper overload in domestic animals (dogs, sheep, cattle), in acute copper sulphate poisoning in humans, and it appears that the haemolytic episodes in Wilson's disease are similar to those in animals with heavy copper overload, and that the periodic release of copper from the liver is responsible for these acute episodes (Thompson, 1977). There seems to be no documented evidence of interference with copper metabolism in conditions of either iron deficiency or overload.

Copper Chaperones

On account of its capacity to catalyse the production of highly toxic hydroxyl radicals, the management of cellular copper is of great importance. It has become apparent recently that this involves a ubiquitous family of copper chaperones – proteins that transport copper in the cytoplasm to its site of utilization by copper-dependent proteins (Pufahl *et al.*, 1997). These proteins have been identified in species from bacteria to man. The simplest system (Figure 12.2, Plate 16) is the *cop* operon involved in copper homeostasis in the Gram-positive bacteria *Enterococcus hirae*. It consists of four genes, two of which, *copA* and *copB*, encode copper pumps belonging to the P-type ATPase family of universal ATP-driven ion pumps (Odermatt *et al.*, 1993). Members of this subgroup transport

transition metal ions, and have been called Cpx- or P_1-type ATPases (Lutsenko and Kaplan, 1995; Solioz and Vulpe, 1996). CopAp appears to be responsible for Cu^+ uptake when copper is limiting, whereas copBp secretes Cu^+ when it is in excess (Solioz and Odermatt, 1995). Expression of the *cop* operon is regulated by the DNA-binding repressor protein CopYp and the copper chaperone CopZp. When cytoplasmic copper levels rise two Cu^+–CopZp molecules deliver their copper to CopYp, displacing a structurally required Zn^{2+} and releasing CopYp from the DNA thereby inducing transcription of the *cop* operon (Cobine *et al*., 1999).

Members of a homologous family of metallochaperones, which bind and transport metals (to date Cu and Hg) specifically have been found in humans, in the nematode worm *C. elegans*, plants (*Arabidopsis*), and in yeast and bacteria (reviewed in Harrison *et al*., 2000). They have very similar protein folds, an open-faced β-sandwich consisting of four β-strands forming an antiparallel β-sheet, situated below two α-helices, illustrated for CopZp in Figure 12.3 (Plate 13). Interestingly the *N*-termini of cadmium, silver and copper-pumping Cpx-type ATPases contain domains that are similar to the copper chaperones CopZp and Atx1p. These domains occur in one or two copies in microbial enzymes, through to six copies in human Menkes and Wilson disease ATPases (Solioz and Vulpe, 1996). In the metallochaperones and chaperon-like modules the metal-binding sequence motif – CxxxC–, occurs on the mobile loop between the first β-strand and the first α-helix (Figure 12.3).

In the yeast *Saccharomyces cerevisiae*, both extracellular ferric iron and cupric copper are reduced by plasma-membrane ferric reductases, encoded by the gene products Fre1p and Fre2p. Reduction of environmental Cu(II) to Cu(I) by Fre1p is followed by high affinity copper uptake across the yeast plasma membrane (Figure 12.2) mediated by the copper transporter proteins Ctr1p and Ctr3p (Dancis *et al*., 1994; Knight *et al*., 1996). A low-affinity system also exists involving Ctr2p (Kampfenkel *et al*., 1995). Once copper has entered the cell it is transported to specific destinations by cytosolic copper chaperones (Harrison *et al*., 1999, 2000). Whether they interact directly with the CTR copper import pumps directly at their cytosolic face, or whether an as yet unidentified protein facilitates copper transport between them is not known. The 74-residue cytoplasmic protein Atx1p (Lin *et al*., 1997) delivers copper to Ccc2p, the post-Golgi vesicular copper transporter that is responsible for copper loading and hence the activation of Fet3p (Askwith and Kaplan, 1998; Harrison *et al*., 1999). Ccc2p has all the characteristics of a Cpx-type ATPase and has copper-chaperone-like subdomains in its *N*-terminus. The proposed path for intracellular transfer by Atx1p is represented in Figure 12.4. Also included is a proposed mechanism for the exchange of Cu(I) between Atx1p and Ccc2p involving two- and three-coordinate Cu-bridged intermediates (Pufahl *et al*., 1997). Lys7p, a 249 residue cytosolic copper chaperone, appears to deliver copper *in vivo* to the cytoplasmic copper/zinc superoxide dismutase (Horecka *et al*., 1995; Gamonet and Loaquin, 1998), whereas Cox 17p (Figure 12.2), another cytoplasmic protein of 69 residues, delivers copper to the Cu_A site of mitochondrial cytochrome *c* oxidase (Glerum *et al*., 1996). Cox 17p, 60 % of which is found in the intermembrane space in mitochondria, does not have a classical mitochondrial import sequence, and probably transfers its copper directly to the Cu_A binuclear site, which protrudes into the mitochondrial intermembrane space (Harrison *et al*., 1999). Of the copper
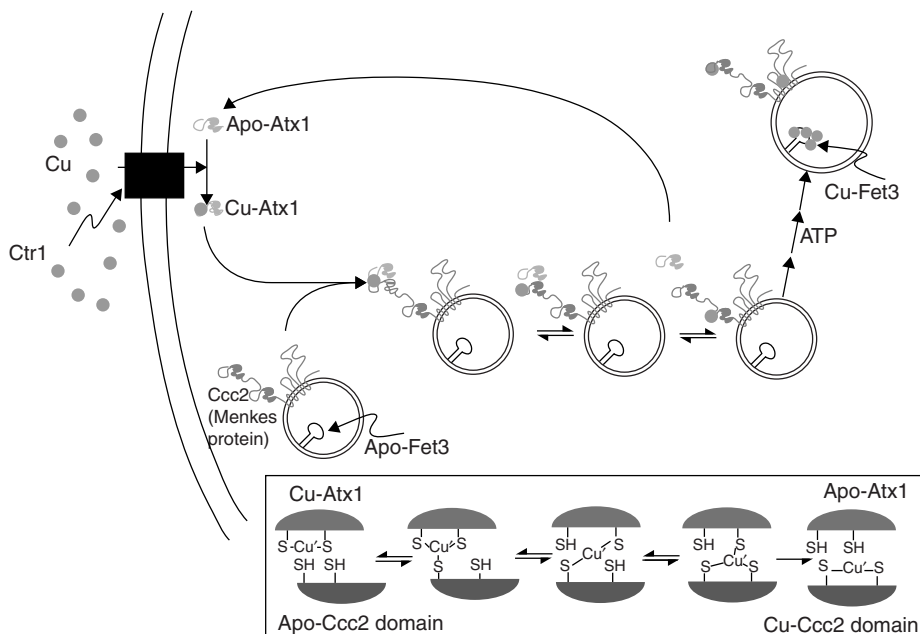
Figure 12.4 Proposed path for the intracellular transfer of Cu(I) by Atx1. Copper destined for incorporation into the vascular multicopper oxidase Fet3 requires both Ctr1 and Ccc2. Cytoplasmic Cu(I)-Atx1, but not apo-Atx1, associates with the amino-terminal domain of Ccc2 and Cu(I) is transferred to the latter. (*Inset*) A proposed mechanism for the exchange of Cu(I) involving two- and three-coordinate Cu-bridged intermediates. The human homologues of Atx1 (Hah1), Ccc2 (Menkes and Wilson's proteins) and Fet3 (ceruloplasmin) are likely to employ similar mechanisms. Reprinted with permission from Pufahl *et al*., 1997. Copyright (1997) American Association for the Advancement of Science.

chaperones described above for yeast, functional homologues have been found for Atx1p, Lys7p and Cox17p in human cells which complement the function of the yeast chaperones.

Metallothioneins are ubiquitous, low molecular weight, thiol-rich proteins which have a selective capacity to bind metal ions such as zinc, cadmium, mercury and copper. In the yeast *Saccharomyces cerevisiae* a family of metallothioneins, encoded by the amplified CUP1 gene locus and the single copy CRS5 gene, both under the regulation of their copper-dependent transcriptional activator ACE1, play a key role in mediating copper resistance (Strain and Culotta, 1996; Jensen *et al*., 1996).

In response to copper, the expression of the high affinity Cu(I) uptake genes CTR1, CTR3 and FRE1 are all regulated by the nutritional copper sensor Mac1p, while the transcriptional activation of the detoxification genes CUP1 and CRS5 (the metallothioneins) and SOD1 (the cytosolic Cu/Zn superoxide dismutase) are regulated by the toxic copper sensor Ace1p (Pena *et al*., 1998). To date however, the prediction that other redox-active metal ions such as iron and cobalt will also be transported by corresponding chaperone proteins to their sites of utilization (Harrison *et al*., 1999) remains to be established.

We have already described the link between the uptake of iron and copper in yeast (Chapter 4). Iron uptake by yeast requires two proteins (Dancis *et al*., 1994; Askwith

et al., 1994), one, Ctr1p, required for high affinity copper transport across the plasma membrane and the other, Fet3p, a member of the family of blue multicopper oxidoreductases, involved in cellular iron uptake through its ferroxidase activity. Iron can enter the cell via a high affinity iron-transport system consisting of Ftr1p, a transmembrane iron permease, and Fet3p, an integral membrane protein with an extracellular multicopper oxidase domain (Stearman *et al.*, 1996). Disruption of any one of the genes involved in the cellular copper transport system composed of Ctr1p, Atx1p, Ccc2p results in a deficiency of both Fet3p activity and high-affinity iron transport (Askwith and Kaplan, 1998).

Iron and Copper Interactions in Mammals and Man

All of the genes required for copper loading of Fet3p in yeast have homologues in man with considerable sequence conservation. Although the transport of copper into mammalian cells is not well established, a functional human homologue, *HCTR1*, of the yeast copper transporter gene, *CTR1*, has been identified by complementation (Zhou and Gitschier, 1997). HCTR can transfer copper to the human copper chaperone CCS (Casareno *et al.*, 1998), which delivers iron to cytoplasmic Cu/Zn superoxide dismutase (SOD1) (Figure 12.2). The function of CCS has been inferred from its sequence homology to the yeast Lys7p, and its ability to complement *Lys7⁻* yeast cells. The human homologue to Atx1p, the chaperone that delivers copper to the CPx-type ATPases in the post-Golgi apparatus is HAH1, a 68-residue protein, which can restore Fet3p function in yeast mutants lacking functional Atx1p (Klomp *et al.*, 1997), and it is inferred that in man HAH1 delivers copper to a trans-Golgi compartment where it is required for copper loading of ceruloplasmin (Sato and Gitlin, 1991). The proteins involved in Menkes and Wilson's diseases, respectively ATP7Ap and ATP7Bp, are both CPx-type ATPases, homologous to yeast Ccc2p (Yuan *et al.*, 1995), which is responsible for Fet3p copper loading. The Menkes protein, ATPAp, which is expressed in most tissues except the liver (Vulpe *et al.*, 1993; Chelly *et al.*, 1993; Mercer *et al.*, 1993), causes defective intestinal copper absorption and decreased tissue copper mobilization leading to copper deficiency. In Wilson's disease, the tissues that normally express ATPBp are unable to export copper and so accumulate it (Bull *et al.*, 1993; Chelly and Monaco, 1993; Tanzi *et al.*, 1993), causing tissue damage, particularly in liver and brain. The loss of ATPBp leads to defective copper transport into the intracellular vesicles in which ceruloplasmin is normally loaded with copper. Since the liver is the principal site of ceruloplasmin synthesis, plasma ceruloplasmin levels are low (Scheinberg and Gitlin, 1952), in some cases resulting in anaemia similar to that observed in copper-deficient pigs. Since the Menkes and Wilson's proteins can complement yeast *CCC2* knockout mutants, it is likely that these ATPases play a similar role to Ccc2p, a view which is supported by their localization in the trans-Golgi network (Petris *et al.*, 1996; Nagano *et al.*, 1998). It has been shown recently (Hamza *et al.*, 1999) that HAH1 can be detected in lysates of human cell lines and tissues and that HAH1 interacts with both the Wilson and Menkes proteins *in vivo*. When similar studies were repeated using three disease-associated mutations in the amino terminus of the Wilson protein, a marked diminution in HAH1 interactions was observed,

suggesting that impaired copper delivery by HAH1 constitutes the molecular basis of Wilson's disease in patients harbouring these mutations. This provides a mechanism for HAH1's function as a copper chaperone with an essential role in copper homeostasis, and further suggests that the defect, at least in Wilson's disease, is probably at the level of transfer of copper to the CPx-type ATPase, rather than from the ATPase to ceruloplasmin.

In mammals, as in yeast, several different metallothionein isoforms are known, each with a particular tissue distribution (Vasak and Hasler, 2000). Their synthesis is regulated at the level of transcription not only by copper (as well as the other divalent metal ions cadmium, mercury and zinc) but also by hormones, notably steroid hormones, that affect cellular differentiation. Intracellular copper accumulates in metallothionein in copper overload diseases, such as Wilson's disease, forming two distinct molecular forms; one with 12 Cu(I) equivalents bound, in which all 20 thiolate ligands of the protein participate in metal binding; the other with eight Cu(I)/metallothionein a molecules, with between 12–14 cysteines involved in Cu(I) coordination (Pountney *et al.*, 1994). Although the role of specific metallothionein isoforms in zinc homeostasis and apoptosis is established, its primary function in copper metabolism remains enigmatic (Vasak and Hasler, 2000).

The biochemical links between dietary copper and iron metabolism in animals that were outlined in physiological terms earlier, have tended to focus on the principal copper-containing protein of plasma, ceruloplasmin. Ceruloplasmin is a blue copper protein synthesized mainly in the liver. In the pioneering studies of the Utah group, dietary copper restriction was reflected in decreased plasma levels of ceruloplasmin, defective mobilization of iron into the plasma with hypoferraemia, and accumulation of iron in parenchymal tissues (Lee *et al.*, 1968). Injection of ceruloplasmin repairs the hypoferraemia (Ragan *et al.*, 1969). It was proposed that it was the ferroxidase activity of ceruloplasmin (Osaki *et al.*, 1966) which was necessary for the oxidation of Fe^{2+} to Fe^{3+} to enable its uptake into apotransferrin (Williams *et al.*, 1974). The importance of ceruloplasmin in normal human iron homeostasis has been confirmed by the recent description of the human congenital disease, aceruloplasminaemia, in which mutations in the ceruloplasmin gene lead to its absence from plasma (Yoshida *et al.*, 1995; Harris *et al.*, 1995). No detectable changes in copper transport are observed, but iron loading is found in parenchymal tissues, principally liver and pancreas, similar to that in copper-deficient pigs. While the anaemia observed in aceruloplasmic humans is not as severe as in the copper-deficient pigs, severe iron loading is also found in brain (accompanied by neurological symptoms such as extrapyrimidal disorders and cerebral ataxia), indicative of a role for ceruloplasmin in iron export from human brain (Harris *et al.*, 1995; Klomp and Gitlin, 1997). A murine model of aceruloplasminaemia showed no abnormalities in cellular iron uptake but a striking impairment in the movement of iron out of reticuloendothelial cells and hepatocytes (Harris *et al.*, 1999). In order to explain the findings in both copper deficient animals and in man, it is proposed that plasma ceruloplasmin mediates iron mobilization from cells (after reduction and transport of Fe^{2+} out of the cell), facilitating iron binding to apotransferrin and hence its delivery to other iron-requiring cells (Askwith and Kaplan, 1998), as described in Chapter 4.

It has been reported that ceruloplasmin increases iron uptake into cultured human cells (Mukhopadhyay *et al*., 1998), although this apparently contradictory *in vitro* observation must be set against the *in vivo* evidence presented above from both animal and human studies. Plasma ceruloplasmin levels increase markedly in anaemia, consistent with a physiological role in tissue iron mobilization, and this effect is due to transcriptional activation of ceruloplasmin mRNA synthesis (Mukhopadhyay *et al*., 2000).

Recently a genetic approach has been used to identify the gene mutant in *sla* (sex-linked anaemia) mice, which have a block in intestinal iron transport. Mice carrying the sla mutation develop moderate to severe anaemia, and although they take up iron from the intestinal lumen into mature epithelial cells normally, subsequent exit of iron into the circulation is diminished, and iron accumulates in the enterocytes and is lost during turnover of the intestinal epithelium. The mutant gene in sla mice, Heph (hephaestin) has been identified as a transmembrane-bound ceruloplasmin homologue, which is highly expressed in the intestine (Vulpe *et al*., 1999). It is proposed that the hephaestin protein is a multicopper ferroxidase necessary for the egress of iron from intestinal enterocytes into the circulation, establishing yet another important link between copper and iron metabolism in mammals. In recent studies, a reciprocal relationship between liver copper and iron status has been observed in iron-loaded rats (Ward *et al*., 1998). Whether this is related to a possible role of DMT1 in intestinal copper uptake, and its regulation by the IRP system remains to be established.

12.2.2 Iron and Zinc

Introduction

The first recognition of a role for zinc in biochemistry was the discovery in1939 that it was an essential component of carbonic anhydrase, a key enzyme in erythrocytes that catalyses the formation of bicarbonate:

$$CO_2 + H_2O \longleftrightarrow H^+ + HCO_3^-$$

Carboxypeptidase A was the next zinc-requiring enzyme to be discovered, in 1955, and since then over two-hundred enzymes catalysing all sorts of reactions have been found. Some of these zinc enzymes are involved in pathways of major importance in iron metabolism, such as δ-aminolaevulinate dehydratase (also known as porphobilinogen synthase), which catalyses the condensation of two molecules of δ-aminolaevulinate to yield porphobilinogen in the haem biosynthetic pathway. Zinc is also found in many nucleic-acid-binding proteins, which contain characteristic structural motifs known as zinc fingers (Schwabe and Klug, 1994). Severe zinc deficiency in man is manifested by poor growth and development and impaired immune response, although the precise defects in zinc metabolism are not clear. Zinc is now thought to play a role in fetal development, brain function, taste perception and wound healing. A number of symptoms associated with anaemias of various sorts may be linked to dietary deficiency of zinc, and inversely, particularly

in developing countries, zinc deficiency is common among populations that are iron deficient.

Zinc Chemistry and Biochemistry

Zinc is the second most ubiquitous transition element in biological systems after iron. It is much more available than nickel, cadmium, iron, copper, etc., and has a striking number of intrinsic chemical properties that help to explain its natural selection (Frausto da Silva and Williams, 1991; Holm *et al.*, 1996). These are: (i) the Zn^{2+} readily undergoes ligand substitution, the aquo exchange rate of $[Zn(OH_2)_6]^{2+}$ is about 10^7 sec^{-1}, which is at least one order of magnitude higher than for hexaquo ions of other divalent first-order transition series elements, with the exception of $[Cu(OH_2)_6]^{2+}$ (k around 10^9 sec^{-1}), whose axial sites are labilized by a Jahn–Teller distortion. (ii) Zn(II) is not subject to the effects of ligand field stabilization energy, which means that its coordination number (almost always 4 or 5 in proteins) and stereochemistry are entirely set by ligand charge and size, ensuring flexible coordination geometry (>nickel, magnesium). (iii) Zn(II) is a borderline hard–soft acid, and hence has affinity not only for soft ligands like Met$^{\bullet}$S and Cys$^{\bullet}$S, but also for harder ligands like X$^{\bullet}$CO$_2$, His$^{\bullet}$N and H_2O/OH^-. Its affinity for hard ligands extends to the binding of carbonyl oxygen atoms not only in protein side chains and backbone, but also in substrates and inhibitors; carbonyl oxygen ligands are rarely encountered in binding sites of other transition metals. (iv) Zn(II), unlike Cu, Fe and Mn, cannot participate in redox reactions at biological potentials. (v) Its high charge/ionic radius ratio (3.3 and 2.9 in 4- and 5-coordination, respectively) allow it to function as an extremely effective Lewis acid (only Cu(II) is better amongst divalent ions) in polarizing carbonyl groups subject to nucleophilic attack. In addition, the positive charge on the metal ion lowers the pK_a of coordinated water, thus providing a locally high concentration of OH^- at or near physiological pH and generating an internal nucleophile for attack on a substrate. The combination of highly localized charge and high electron affinity makes Zn^{2+} a very effective attacking group, capable of binding and activating substrate and releasing product efficiently. This explains the use of zinc for attack on small substrates (H_2O and CO_2 in carbonic anhydrase, for example) and the 'hydroxide-carbonyl' mechanism whereby bound hydroxide nucleophilically attacks a carbonyl group activated by coordination to the same (or a bridged) Zn(II) centre.

In the yeast *S. cerevisiae*, analysis of the genome sequence indicates that around 2 % of all genes encode transcriptional regulators containing either the Cys_2His_2 zinc finger domain or the Cys_6 zinc cluster motif (Eide, 1998). Zinc uptake in yeast involves at least two uptake systems, a high-affinity system using the transporter protein encoded by the *ZRT1* gene, and the other a low-affinity system, encoded by the *ZRT2* gene. Both ZRT1 and ZRT2 are similar in sequence and predicted topology to the IRT1 iron transporter in *Arabadopsis* (Eide *et al.*, 1996). These three metal-ion transporters are members of the ZIP family (ZRT, IRT-like proteins), and at least two members of the ZIP family of proteins have been identified in humans (Eide, 1998). Zinc uptake in yeast is controlled at the level of transcription of both ZRT1 and ART2 by the product of the *ZAP1* gene (Zhao and Eide, 1997), itself apparently

a Zn-finger transcriptional activator. Two intracellular zinc transporters have been identified in *S. cerevisiae*, ZRC1 and COT1, which belong to yet another family of metal transport proteins, referred to as the CDF (cation diffusion facilitator) family. Three mammalian CDF proteins are zinc transporters. ZnT-1 is a zinc efflux transporter in the plasma membrane (Palmiter and Findley, 1995). ZnT-2 is found in the membrane of an acidic endosomal/lysosomal compartment and may play a role in zinc sequestration (Palmiter *et al.*, 1996a). ZnT-3 is expressed only in the brain and testis. It is most abundant in the neurons of the hippocampus and the cerebral cortex, and is localized to the synaptic vesicle membranes, suggesting that ZrT-3 transports zinc into this compartment (Palmiter *et al.*, 1996b).

Iron and Zinc Interactions in Man

Zinc deficiency is associated with poor growth, loss of appetite, skin lesions, impaired taste acuity, delayed wound healing, hypogonadism, delayed sexual maturation and impaired immune response. Zinc status seems to be regulated by strong homeostatic control of both absorption and excretion (reviewed in Whittaker, 1998). Zinc is more efficiently absorbed in small amounts than in large amounts, and individuals with poor zinc status absorb zinc more efficiently than those with normal status. The lack of a suitable index for measuring body zinc status has led to uncertainties in establishing recommended dietary allowances. Decreased zinc absorption because of dietary fibre and phytates leads to zinc deficiency in children in rural areas of Iran and Egypt, and zinc supplementation leads to improved growth (Prasad, 1990). Several Third World countries are taking measures to increase dietary intake of iron and zinc with fortification of foods or dietary supplements. While several studies have shown that high iron concentrations can negatively affect zinc absorption when given in solution, no such interference is observed when iron and zinc are given in a meal. It was postulated that a total dose of >25 mg iron could produce a measurable effect on zinc absorption (Solomons, 1986), which could happen if iron supplements are taken with a meal, and it is recommended that iron supplements be taken between meals. However, recent studies using the stable isotope ^{65}Zn show that fortifying foods with iron at current fortification levels has no adverse effect on zinc absorption (Valberg *et al.*, 1984; Sandstrom *et al.*, 1985; Davidsson *et al.*, 1995). This may reflect the increased amount of zinc compounds in food – in the USA, during the period from 1970 to 1987 the total amount of zinc compounds in the US food supply increased by a factor of 32 (Whittaker, 1998).

Zinc protoporphyrin IX is a normal metabolite that is formed in trace amounts during haem biosynthesis. However, in iron deficiency or in impaired iron utilization, zinc becomes an alternative substrate for ferrochelatase and elevated levels of zinc protoporphyrin IX, which has a known low affinity for oxygen, are formed. This zinc-for-iron substitution is one of the first biochemical responses to iron depletion, and erythrocyte zinc protoporphyrin is therefore a very sensitive index of bone-marrow iron status (Labbe *et al.*, 1999). In addition, zinc protoporphyrin may regulate haem catabolism by acting as a competitive inhibitor of haem oxygenase, the key enzyme of the haem degradation pathway. However, it has been reported

that zinc fails to induce the synthesis of erythropoietin[¶] at normal oxygen tensions, and suppresses the synthesis of erythropoietin in hypoxic cells. It has recently been found that zinc inactivates the nuclear transcription factor HIF-1 (hypoxia-inducible factor-1) and suppresses erythropoietin mRNA transcription in hypoxic cells (Chun *et al.*, 2000a).

While it seems that there is little interference between iron and zinc metabolism under normal dietary situations, the possibility of interference must be taken into account when considering iron or zinc supplementation in developing countries.

12.2.3 Iron and Manganese

Introduction

While the importance of manganese in biological systems remains undisputed, its precise function remains poorly explored. In green plants, photosystem II uses a Mn-based enzyme system to cleave water, producing molecular oxygen, protons and electrons. Within the confines of the mitochondria, yet another oxygen-evolving enzyme, superoxide dismutase is found (it is also present in many prokaryotic cells), transforming superoxide anion produced by the respiratory chain into molecular oxygen and hydrogen peroxide.

Manganese Chemistry and Biochemistry

Manganese is not a rare element, being about as common as Fe or Zn. In aqueous solution the most striking features of manganese chemistry are the stability of Mn^{2+} in acid solution and the greater stability of MnO_2 in alkaline solutions and in the presence of oxygen. In contrast to iron, the Mn(III) state readily disproportionates to Mn(II) and Mn(IV). We might conclude that Mn biochemistry ought to be dominated by (i) the chemistry of Mn(II), which should be intermediate between that of Mg(II) and that of Ca(II) and Zn(II), and (ii) the powerful oxidizing action of the stable higher oxidation state, Mn(IV). In reality considerable Mn(III) chemistry is observed in biology, for example mitochondrial superoxide dismutase and lysosomal acid phosphatase. In yeast, Mn^{2+} appears to be taken up by two separate uptake systems (Gadd and Laurence, 1996), a high affinity system with an apparent K_m of 0.3 μM and a low affinity system with a K_m of 60 μM. The *SMF1* gene encodes a plasma membrane protein that is probably the high-affinity transporter (Supek *et al.*, 1996). Two other genes, *SMF2* (West *et al.*, 1992) and *SMF3* (Supek *et al.*, 1997), encode proteins that are closely related to SMF1. Smf1p and smf2p also

---

[¶] Erythropoietin is the protein growth factor secreted by the kidney which stimulates the production of red blood cells, and is used in the treatment of anaemia arising from kidney disease. Erythropoietin, now available as a recombinant human protein for routine clinical use, is the latest in a series of 'illegal substances' whose utilization by professional athletes has caused scandal and shame in events as different as the Tour de France and the Olympic games. The rationale for its use is that by increasing the red cell mass, it makes more oxygen available to muscle during prolonged physical effort – a kind of short cut to achieving the kinds of performances that may underly the dominance of long distance running events by Ethiopean and Kenyan athletes.

have broad metal specificity and are not regulated transcriptionally by manganese, which may suggest that they are not the high affinity Mn transporters. However, Smf1p-mediated transport is regulated post-transcriptionally by the product of the *BSD2* gene (Culotta *et al.*, 1998), an endoplasmic reticulum membrane protein. Cells deleted for Bsd2p have increased activities of Smf1p and Smf2p and accumulate high levels of Mn, Cu, Cd and Co.

All three SMF proteins are members of the Nramp family of metal transporters. The mammalian Nramp2 /DCT1 (divalent cation transport) is the H^+-coupled transport protein responsible for the absorption of dietary Fe^{2+} – and perhaps also of other metals including Mn^{2+} – at the intestinal apical surface, as well as its transport across the endosomal membrane within the cell in the transferrin–receptor iron-uptake pathway (see Chapters 5 and 8). That DCT1 may be involved in manganese transport in mammals is supported by the observation that analysis of the Belgrade rat (which is defective in DCT1) shows deficiencies in manganese (Chua and Morgan, 1997).

Iron–Manganese Interactions in Man

Manganese is an essential trace element at low concentrations, but at higher concentrations it is neurotoxic, accumulating particularly in the globus pallidus. While the clinical symptoms are typical of Parkinson's disease, with rhythmic tremor and muscular rigidity, there is an important psychiatric aspect associated with Mn intoxication, manifested by behavioural aggression. An increasingly popular hypothesis is that the continued degeneration of dopaminergic neurones in Parkinson's disease may be the consequence of aberrant oxidation of dopamine and resultant generation of DNA-reactive species in those patients receiving L-dopa therapy. Chronic occupational metal exposure, particularly to Mn and Cu, has been shown to be a risk factor for Parkinsonism (Gorell *et al.*, 1999), and Mn has been shown to be a true catalyst for dopamine oxidation, lending support to this hypothesis. Studies in the rat have shown that Mn and Fe interact during transfer from the plasma to the brain and other organs, and that this transfer is synergistic rather than competitive in nature (Chua and Morgan, 1996), suggesting that excessive intake of Fe plus Mn may accentuate the risk of tissue damage by one metal alone, particularly in the brain. Chronic Mn exposure in rats alters iron homeostasis apparently by causing a unidirectional influx of iron from the systemic circulation across the blood–brain barrier (Zheng *et al.*, 1999). Manganese intoxication in rhesus monkeys results in a Parkinsonian syndrome (in two of three animals), which did not respond to L-dopa (Olanow *et al.*, 1996). Focal mineral deposits, primarily consisting of iron and aluminium, were found in both the globus pallidus and the substantia nigra pars reticularis. Both the cytotoxicity and clastogenicity of laevodopa and dopamine in cultured cell lines is enhanced by concomitant exposure to either Mn or Cu salts (Snyder and Friedman, 1998). Manganese was found to increase LPS-stimulated NO production from microglial cells (Chang and Liu, 1999), unlike other transition metals tested including iron, cobalt, copper and zinc. Mn appeared to exert its effect at the level of transcription of the inducible NO synthase (Chapter 10), and unlike other transition metals Mn did not appear to be cytotoxic to microglial

cells. It is suggested that Mn could induce sustained production of neurotoxic NO by activated microglial cells, which might be detrimental to surrounding neurones.

The mitochondrial dysfunctionality seen in manganese neurotoxicity might be related to the accumulation of reactive oxygen species (Verity, 1999). Mitochondrial Mn superoxide dismutase (MnSOD) is found to be low or absent in tumour cells and may act as a tumour suppressor. It is induced by inflammatory cytokines like TNF, presumably to protect host cells. In a rat model, iron-rich diets were found to decrease MnSOD activity, although a recent study reported that in rat epithelial cell cultures iron supplementation increased MnSOD protein levels and activity, but did not compromise the ability of inflammatory mediators like TNF to further increase the enzyme activity (Kuratko, 1999).

While our present dietary heterogeneity (at least in the developed world) makes it unlikely that we will encounter many cases of Mn deficiency, the association of low Mn-dependent SOD activity with cancer susceptibility is a cause for concern (Finley and Davis, 1999). The dangers of Mn toxicity may be greater than we imagine. Vegetarian lifestyles are being adopted by an increasing number of young people, which may simultaneously increase Mn intake, and increase the risk of iron deficiency with concomitant increased dietary Mn absorption.[§]

12.2.4   Iron and Cobalt

Cobalt Chemistry and Biochemistry

Cobalt, like iron and nickel, has access to a variety of oxidation and spin states and has more than five 3d electrons in its lower oxidation state (i.e. it is electron rich). Cobalt (and nickel) are special, in that they are not only generally electron rich, especially in lower oxidation states and in low-spin states, but that some of their 3d electrons are forced into exposed σ- (or π-) orbitals in these low-spin states by the preferred symmetry of their complexes. This means that the tetragonal low-spin d^7 Co(II) ion is a reactive free radical, and this property is exploited in vitamin B_{12}, a coenzyme required for many enzymatic transformations requiring a source of free radicals, such as the Class II ribonucleotide reductases of *Lactobacillus* sp. (Chapter 2). Some eight years after its isolation in 1948, the structure of the 'anti pernicious anaemia factor', vitamin B_{12}, was determined. Vitamin B_{12} is an alkyl–cobalt(III) complex of a substituted corrin (Figure 12.5), certainly the best studied organometallic system in biology. The original structure determination was carried out on cyanocobalamine, in which cyanide is the second axial ligand together

---

[§] Yet another hazard may also be waiting just around the corner. After successfully eliminating lead from petrol (see later in this chapter), there are proposals to extend the use of a Mn compound, MMT, (methylcyclopentadienyl manganese tricarbonyl), as an antiknock additive in unleaded petrol. MMT has been used in Canada since 1976, but its importation and interprovincial trade was banned by the Canadian Federal Government in 1997. It has been approved for use in Argentina, Australia, Bulgaria, New Zealand and Russia (Frumkin and Solomon, 1997). The proposal was initially turned down by the US Environmental Protection Agency, but has since been approved on appeal (Davis, 1999). With the recent recognition of the serious condition known as 'road rage', we can do very well without a fuel petrol supplement that might raise brain Mn levels leading to even more aggressive behaviour.

R = CN (Vitamin B$_{12}$)
R = Adenosyl (Coenzyme B$_{12}$)
R = Me
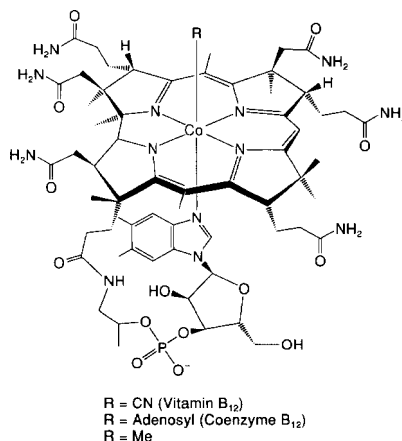
Figure 12.5 Cobalamine structures. From Lippard and Berg, 1994. Reproduced by permission of University Science Books.

with the pendant dimethylbenzimidazole nucleotide, which is covalently linked to the corrin D ring. In the active B$_{12}$ coenzyme the sixth ligand is a 5′-deoxyadenosyl group (Figure 12.5). While some of the reactions involving B$_{12}$ coenzyme involve radical-based redox chemistry, like the ribonucleotide reductases, many are simple rearrangements involving 1–2 carbon shifts (e.g. methylmalonyl mutase). Many of the reactions that use the B$_{12}$ coenzyme take place by free-radical pathways initiated or catalysed by homolytic cleavage of the Co–C bond,[‖] to form a Co(II) species and a deoxyadenosyl radical. The radical then abstracts a hydrogen atom from substrate to produce a substrate radical, which then rearranges. From recent X-ray studies on methionine synthase and methylmalonyl-coenzyme A mutase, it appears that upon binding to the enzyme the dimethylbenzimidazole ligand to the cobalt is displaced by a histidine residue from the protein. In the mutase a significant feature, which may facilitate homolytic cleavage of the carbon–cobalt bond, may be the long cobalt–nitrogen bond linking histidine to the cofactor (Ludwig and Matthews, 1997).

While little is known about cobalt transport and uptake in mammals, SMF2 has been linked to Co^{2+} uptake in yeast (Liu *et al.*, 1997). Most of the cobalt-containing enzymes described in the literature contain cobalamine cofactors, although a few examples, mostly in bacteria, have been described of enzymes that require the metal ion cobalt. The crystal structure of one of these, methionine aminopeptidase from *E. coli* is available, and has five amino acids liganding the two cobalt ions, which are conserved in all methionine aminopeptidases sequenced to date. The *C*-terminal domain of methionine aminopeptidase 1 from *S. cerevisiae* has 41 % identity to the *E. coli* enzyme and has all five cobalt-coordinating amino acids conserved (Klinkenberg *et al.*, 1997). Using partial amino-acid sequence data from porcine methionyl aminopeptidase, a full length clone of the homologous human enzyme has been

---

[‖] For a more detailed analysis of Co chemistry and B$_{12}$ in particular, see Frausto da Silva and Williams (1991) and Lippard and Berg (1994), and for a recent review of B$_{12}$-dependent enzymes, see Ludwig and Mathews (1997).

obtained; it can be readily accomodated in the *E. coli* methionyl aminopeptidase structure, and the Co^{2+} ligands are fully preserved (Arfin *et al.*, 1995).

Iron – Cobalt Interactions in Man

In 1926 it was found that pernicious anaemia, an often fatal disease of the elderly characterized by decreased red blood cell numbers, low haemoglobin levels and progressive neurological deterioration, could be treated by feeding patients large amounts of liver, a cure considered by some patients as worse than the disease. Vitamin B_{12} is not synthesized by plants or animals, and is only sythesized by a few species of bacteria, and in man the major source of the vitamin is the diet. However, its transport across the intestinal mucosa requires its binding to a glycoprotein intrinsic factor secreted by the stomach. The B_{12}-intrinsic factor complex is taken up by a specific receptor in the intestinal mucosa, and transported across the mucosal cell to the basolateral membrane where it is released into the bloodstream. It is then transported to the tissues by a member of the family of plasma globulins, transcobalamine II. Pernicious anaemia is not due to dietary insufficiency of vitamin B_{12}, but rather to insufficient secretion of intrinsic factor – daily requirements for cobalamine are around 3 μg, and the liver typically stores a 3 to 5 year supply of B_{12}. This explains not only the insidious onset of pernicious anaemia, but also the fact that true dietary B_{12} deficiency is rarely seen even in vegetarians. Congenital absence or defective synthesis of intrinsic factor or transcobalamine II result in megaloblastic anaemia.[††] In all mammals, cobalamine regulates DNA synthesis indirectly by its effect on the step in folate metabolism in which N^5-methyltetrahydrofolate and homocysteine are converted to methionine and tetrahydrofolate. This reaction is catalysed by the cytosolic enzyme methionine synthase, which requires methyl cobalamine as cofactor. Defects in the generation of methylcobalamine result in homocystinuria; affected infants present with megaloblastic anaemia, retardation, neurological and ocular defects. The cofactor of methylmalonyl-CoA mutase, the mitochondrial enzyme that converts methylmalonyl CoA to succinyl CoA as the final step in the oxidation of branched-chain fatty acids, is 5′-deoxyadenosylcobalamine, and defects in its synthesis in infants results is methylmalonic aciduria, mental retardation and hypotonia. These infants do not, however, develop megaloblastic anaemia because they have adequate amounts of methylcobalamine (Kapadia, 1995). We cannot at present pinpoint the exact molecular nature of the interaction between cobalamine and iron that leads to megaloblastic anaemia, although the clinical findings described above would seem to point to a more important role being played by methylcobalamine than by 5′-deoxyadenosylcobalamine.

The physiological regulation of the red blood cell mass depends upon the enhanced transcription of the gene for erythropoietin, a protein growth factor secreted by the kidneys, in response to hypoxia. This regulation by feedback mechanisms that sense levels of tissue oxygenation is thought to involve a putative oxygen sensor, whose mechanism remains to be elucidated. Interestingly, cobalt

---

[††] Pernicious anaemia, due to B_{12} deficiency, is one example of the class of anaemias known as megaloblastic anaemias, resulting from an abnormality in erythroblast maturation.

(and nickel) also stimulate erythropoeitin production, as does iron chelation with desferrioxamine. It has been proposed that the oxygen-sensing signal pathway may involve one or more haem proteins, possibly *b*-type cytochromes (Ehleben *et al.*, 1998) as oxygen sensor, together with a multi-subunit assembly containing an NAD(P)H oxidase capable of producing peroxide and hydroxyl radicals (Bunn *et al.*, 1998). The hydroxyl radicals generated by the Fenton reaction are important for triggering erythropoietin production (Ehleben *et al.*, 1998; Porwol *et al.*, 1998; Daghman *et al.*, 1999). The up-regulation of erythropoietin gene transcription is mediated by the heterodimeric DNA transcription factor HIF-1 (hypoxia inducible factor 1) and the orphan nuclear receptor HNF-4 (hepatic nuclear factor 4), which bind to cognate response elements in a critical 3′-enhancer that is approximately 50 base-pairs in length. HIF-1 binding is induced by cobalt, as well as by hypoxia (Bunn *et al.*, 1998). While both of the haem-binding ligands, NO and CO, inhibited HIF-1 DNA binding by suppressing activation of erythropoietin mRNA transcription, they had no effect on the induction of HIF-1 binding activity and erythropoietin expression by cobalt or desferrioxamine (Huang *et al.*, 1999). The authors conclude that while NO and CO act proximally as haem ligands binding to the oxygen sensor, cobalt and the iron chelator desferrioxamine act at a site downstream from the oxygen sensor. This is in line with recent studies showing that exposure of cells to either iron chelation or cobalt causes dissociation of HIF-1 from its complex with a tumour suppressor protein (Maxwell *et al.*, 1999).

12.3 Iron and Toxic Metals

12.3.1 Iron and Aluminium

Introduction

Aluminium forms 8 % of the earth's crust; it is the most abundant metal, and the third most abundant element after oxygen and silicon. It only occurs naturally in a combined form – as an oxide in bauxite, and in complex aluminosilicates (like sands) such as micas and feldspar. Aluminium is a toxic metal, but does not usually cause adverse effects on health among the general population. Biology has managed to avoid using aluminium, despite its natural abundance, although we are not quite sure how it has done so. Despite its abundance in the earth's crust, aluminium concentration in the oceans is less than 40 nM, possibly reflecting the accumulation of aluminium and silicon by diatoms.[‡] Until recently, most natural waters contained insignificant amounts of aluminium, and any free Al^{3+} usually disappeared into sediment as the insoluble hydroxide. However, one of the principal consequences of burning fossil fuels has been to release acid gases which result in the massive acidification of fresh water sources. This causes release of metal ions like aluminium, mercury and lead from mineral deposits in the soil, leading to aluminium concentrations in fresh water lakes at pH<6 to μM levels. This has disastrous consequences for plants and animals (particularly fish, for whom

[‡] Diatoms constitute a family of unicellular microscopic algae whose cell walls consist of two boxlike parts which contain silica. They are an important source of food for all kinds of marine organisms.

concentrations as low as $5\,\mu M$ are toxic) that come into direct contact with the element. There are exceptions such as the tea plant which has an extraordinary propensity for accumulating aluminium from acid soils (as much as 3 % is found in older leaves). An average tea infusion contains about fifty-times as much aluminium as does an infusion from coffee. The greater concentrations of aluminium in fresh water from the effects of acid rain on soils has made this enigmatic element accessible for the first time to living organisms. Despite this, the uptake of aluminium from drinking water does not appear to pose a significant threat to human health (Doll, 1993; Priest *et al.*, 1998). A much more serious cause of aluminium intoxication is the use of aluminium as a phosphate binder in the dialysis fluids used in patients with renal insufficiency. Because of the large volumes of fluid used, the frequency of haemodialysis and the long-term nature of the treatment, even small levels of aluminium may become deleterious with time.

Aluminium Chemistry and Biochemistry

The chemistry of aluminium combines features in common with two other groups of elements, namely (i) divalent magnesium and calcium, and (ii) trivalent chromium and iron (Williams, 1999). It is likely that the toxic effects of aluminium are related to its interference with calcium directed processes, whereas its access to tissues is probably a function of its similarity to ferric iron (Ward and Crichton, 2001). The effective ionic radius of Al^{3+} in sixfold coordination (54 pm) is most like that of Fe^{3+} (65 pm), as is its hydrolysis behaviour in aqueous solution:

$$Al^{3+} + 4OH^- \longleftrightarrow [Al(OH)_4]^-$$
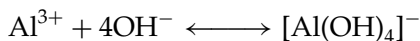
Aluminium is amphoteric[¶¶] in its stable trivalent state, acting either as a cation or an anion, occurring as Al^{3+} in complex ions with many inorganic or organic donors, yet giving salts – aluminates – with many simple cations. However, Al^{3+} is a much stronger acid than Mg^{2+} and Ca^{2+}, which makes it a powerful competitor for oxygen-donor ligands for these two important biological cations, and leads to profound interference with their metabolism. In contrast, Al^{3+} is a weaker acid than Fe^{3+} and therefore causes less interference with iron metabolism (particularly since much of this requires redox cycling between Fe^{2+} and Fe^{3+} forms). The most likely ligands for Al^{3+} are oxygen atoms, particularly if they are negatively charged, with carboxylate, catecholate and phosphate groups being the strongest binders. Sulphydryl groups, even when part of a potential chelate ring, do not bind Al^{3+}, and amines do not bind strongly except as part of multidentate ligand systems like NTA and EDTA. The rate of ligand exchange into and out of the metal coordination sphere, is extremely slow for Al^{3+}; thus, essential metabolic processes involving rapid Ca^{2+} exchange which is 10^8-times slower with Al^{3+}, would be seriously affected by substitution, as would Mg^{2+}-dependent enzymes (10^5-times slower with Al^{3+}). For Al^{3+} in aqueous solutions only two species predominate over the entire pH range, the octahedral hexahydrate $(Al(H_2O)_6^{3+}$, usually abbreviated as

¶¶ Amphoteric – having both acid and a basic qualities.

Al^{3+} at pH < 5, and the tetrahedral $Al(OH)_4^-$ at pH > 6.2. Of course the amount of free aqueous Al^{3+} in solution will be significantly influenced by the presence of ligands, their stability constants with Al^{3+} and the ratio of Al(III) to ligand. In the extracellular fluids of mammals, the iron-binding protein transferrin usually has nearly 70 % of its metal-binding capacity free. If Al^{3+} could get into the circulation, it could certainly occupy those binding sites. The stability constants for the two binding sites on transferrin are similar: $\log K_a$ of 12.9 and 12.3 (Martin, 1994), substantially lower than for iron. In the following section we will consider how Al^{3+} could enter the human body, and how it could get into cells.

Iron–Aluminium Interactions and Aluminium Toxicity

The daily intake of aluminium in man is reputed to be 3 mg/day, although only 0.06–0.1 % of an ingested dose of ^{26}Al was found to be absorbed (Moore *et al.*, 2000). It is clear that neither of the major mechanisms for iron uptake which were discussed in Chapter 8, the ferrireductase/DCT1 pathway and the haem pathway, are appropriate for aluminium transfer across the gastrointestinal tract. This leaves two possible routes, the integrin–mobilferrin pathway (Conrad *et al.*, 1999), reported to transport ferric iron directly across the mucosal cell, and the passage of Al^{3+} through the gap junctions between the enterocytes, thereby bypassing both the apical and basolateral membranes. In view of the apparent requirement for IREG1 and hephaestin at the basolateral membrane, again involving transport of Fe^{2+} followed by redox chemistry, the most likely way for Al^{3+} to get across the gut in man could well be through the gap junctions.

Once in the serum, aluminium can be transported bound to transferrin, and also to albumin and low molecular-weight ligands like citrate. Fractionation of serum from a haemodialysis patient (with a high plasma aluminium concentration of 5 μM) gave a distribution of 60% bound to transferrin, 34% to albumin and 6% to citrate (Fatemi *et al.*, 1991). This may simply reflect the lower stability of the transferrin–aluminium complex. However, the transferrin–aluminium complex will be able to enter the cell via the transferrin–transferrin-receptor pathway (Chapter 8). Within the acidic environment of the endosome we assume that aluminium will be released from transferrin, but how it exits from this compartment remains unknown – as at the basolateral membrane of the mucosa, DCT1 is thought to transport Fe^{2+} into the cytosol. Studies of the subcellular distribution of aluminium in various cell lines and animal models have shown that most accumulates in the mitochondrial fraction (reviewed in Ward and Crichton, 2001), where it may interfere with the mitochondrial respiratory chain (Swegert *et al.*, 1999), as does increased iron loading (Chapter 7). Mitochondria obtained from fibroblasts of Alzheimer patients have decreased calcium uptake, whereas exposure of such cells to iron increases their calcium uptake and their sensitivity to reactive oxygen species (Kumar *et al.*, 1994). This underlines the probability that the mitochondrial toxicity of both aluminium and iron is due to their interference with calcium homeostasis.

Once aluminium has reached the circulation, there seems little doubt that it can cross the blood–brain barrier – the best proof being that in renal dialysis patients

with high plasma aluminium levels, increased deposition of aluminium is found in brain (Edwardson *et al.*, 1992). The form in which it crosses the barrier is not known.

Aluminium toxicity is the likely cause of three human disorders arising from long-term haemodialysis: vitamin D-resistant osteomalacia, iron adequate microcytic anaemia, and dialysis dementia (Martin, 1994). The first of these conditions is consistent with interference with calcium deposition into bone, and the accumulation of aluminium in the bone matrix.

Aluminium is also a possible cause of the high frequency of sclerosis and Parkinsonian dementia among the natives of certain regions of South East Asia, where the soils are high in Al(III) and low in Mg^{2+} and Ca^{2+}.

Elevated levels of Al(III) have been reported in the brains of Alzheimer's patients[§§] and of renal dialysis patients as well as in animal models of aluminium intoxication (reviewed in Ward and Crichton, 2001), and since it has been suggested that iron homeostasis (Chapter 7) is disrupted in Alzheimer's disease (Good *et al.*, 1992) the hypothesis that aluminium might exert its toxic effects by interfering with iron homeostasis has been advanced. It has been shown that IRP-1 levels in brains of Alzheimer patients were similar to controls, although aluminium levels were not determined (Smith *et al.*, 1998). In contrast, IRP-2 showed important differences, and was found to be associated with intraneuronal lesions. *In vitro* studies in an erythroleukaemic cell line indicated that aluminium antagonized the iron-induced decrease in IRP-2 binding to IREs, stabilized IRP-2 against degradation and enhanced its binding to IREs (Yamanaka *et al.*, 1999). This would of course result in up-regulation of transferrin receptors, resulting in increased influx of both iron and aluminium into the cells. In previous studies (Abreo *et al.*, 1994), increased iron uptake by transferrin receptor-mediated endocytosis and decreased ferritin synthesis were observed in aluminium-loaded Friend erythroleukaemic cells. More recently (Abreo *et al.*, 1999), murine neuroblastoma cells incubated in culture with either aluminium–transferrin or aluminium citrate were shown to accumulate aluminium, which not only enhanced iron uptake from transferrin, but also the expression of neurofibrillary tangle protein. However, Oshiro *et al.* (1998) reported that aluminium-loading of fetal rat cerebral cortical cells increased transferrin-independent iron uptake, but decreased transferrin receptor mRNA levels, increasing the aconitase activity (i.e. decreased IRE binding activity) of IRP-1 protein. Subsequent studies on primary cultures of neuronal and glial cells showed that aluminium loading with Al-NTA decreased transferrin receptor expression and decreased the amount of IRP/IRE complex (Oshiro *et al.*, 2000).

It was reported that brain ferritin from aluminium-loaded rats and from Alzheimer's patients contained significant amounts of aluminium (Fleming and

---

[§§] Alzheimer's disease, first described more than a century ago, is the most common cause of senile dementia, accounting for about two-thirds of cases. There are over 4 million sufferers of Alzheimer's disease in the United States, where the disease afflicts 3 % of adults aged between 65 and 74, one in six of those between 75 and 84, and one in three of those above 85. As Bruce Martin eloquently points out 'Alzheimer's disease is a progressive senile dementia characterized not by minor failures, such as the sufferer forgetting where she put her glasses, but rather by a complete loss of input from a memory bank so that she forgets that she wears glasses at all' (Martin, 1994). Autopsies of Alzheimer's brains reveal the deposition of fibrillar amyloid proteins as neurofibrillary tangles with paired helical filaments (the defining characteristic of the disease) and of senile plaques, both of which have been reported to contain aluminium. The role of aluminium in the formation of the neurological lesions associated with Alzheimer's disease remains a matter of debate.

Joshi, 1878), as did ferritin which had been incubated with aluminium citrate (Cochran and Chawtur, 1988). In later studies of isolated ferritin from the brains of either renal dialysis patients (with high circulating plasma aluminium levels) or Alzheimer's patients (Dedman *et al.*, 1992a), or horse spleen ferritin that had been incubated with aluminium citrate (Dedman *et al.*, 1992b) less than ten aluminium atoms per ferritin molecule were found. This is consistent with the mechanism of iron incorporation into ferritin, presented in Chapter 6, that requires oxidation of ferrous iron to ferric in the initial stages of iron uptake. Dedman *et al.* (1992b) did show that aluminium citrate could be incorporated into ferritin (up to 120 atoms of aluminium/molecule), suggesting that once the nucleation centre within ferritin is formed, aluminium can indeed enter into ferritin *in vitro*. Whether or not aluminium can interfere with iron uptake into ferritin, or indeed be incorporated into ferritin *in vivo* remains to be established.

Changes in iron homeostasis would appear to be a major contributory factor in Alzheimer's disease, although the possible role of aluminium in this remains uncertain. Despite initial studies which implicated aluminium in the development of senile plaques and neurofibrillary tangles, current results fail to confirm consistently the presence of the metal at the sites of the lesions and hence cast serious doubts on it playing a causal role in Alzheimer's disease. Chronic exposure to aluminium results in selective cognitive impairment in rats, with altered calcium homeostasis (Jope and Jackson, 1992). Taken together with the demonstration that aluminium causes dementia in haemodialysis patients, there can be no doubt that aluminium is neurotoxic. The potential therapeutic benefit of long-term chelation therapy to prevent accumulation of both aluminium and iron in brain as a function of ageing could complement a greater understanding of the role of both metal ions in the aetiology and pathogenesis of many neurological diseases.

12.3.2   Iron and Lead

Chronic lead poisoning (saturnism) is a major cause of environmental concern in all countries worldwide. While lead toxicity affects several organ systems, including the nervous, haematopoietic, renal, endocrine and skeletal, the effect of major concern is the impairment of cognitive and behavioural development in infants and young children (Goyer, 1997). Low-level exposure to lead from various environmental sources, including lead-based paint, and household dust from surfaces covered with such paints, as well as lead in air, food and water, can be involved. The removal of lead additives from petrol has greatly reduced the levels of the metal in air, food, water and dust. Lead in water is more efficiently absorbed than lead in food, hence the danger of lead in tap water from solder or pipes in residential plumbing[‖] is of particular concern. Because iron deficiency and lead poisoning share common environmental risk factors, it is common practice to supplement the diets of children at risk from lead toxicity with iron (Wright, 1999), as well as calcium (as we might expect, lead also seriously interferes with

---

[‖] Plumbers (lead workers) nowadays rarely use lead, since most modern houses have water pipes in other metals or in plastic.

cellular calcium metabolism). Lead toxicity correlates with blood Pb levels and progresses from biochemical and subclinical abnormalities at levels of around 10 µg/dl to coma and death at levels in excess of 100 µg/dl (Markowitz, 1999). The anaemia of lead poisoning is associated with elevated serum iron levels, which may reflect lower transferrin levels; lead has been shown to suppress human transferrin protein and mRNA levels *in vitro* (Barnum-Huckins *et al.*, 1997). Elevated levels of erythrocyte zinc protoporphyrin are found in lead toxicity, together with evidence of increased oxidative stress, as reflected by decreased glutathione peroxidase levels and increased production of thiobarbituric-acid-reactive substances. Lead has been found to promote lipid oxidation and alterations in physical properties of membranes (Adonaylo and Oteiza, 1999), while chronic lead intoxication affects the structure of myelin in the central nervous system of rats (Dabrowska-Bouta *et al.*, 1999). Lead has been found to elicit a positive response in tests for fidelity of DNA synthesis, mutation, chromosome aberrations, cancer and birth defects, thus indicating that it can also have long term genetic effects on the evolution of exposed plant and animal populations (Johnson, 1998).

The Zn-requiring enzyme δ-aminolaevulinate dehydratase (otherwise known as porphobilinogen synthase) catalyses the condensation of two molecules of δ-aminolaevulinate to form the pyrrole porphobilinogen. In the haem biosynthetic pathway, four porphobilinogen molecules are subsequently condensed to form a linear tetrapyrrole, which is cyclized and oxidized to form porphobilinogen IX. The inhibition of δ-aminolaevulinate dehydratase is an important feature of acute lead poisoning, in view of the exceptional affinity of the enzyme for the metal ($K_i = 7$ fM) (Simons, 1995) and close parallels in the neurological symptoms of lead intoxication and inherited deficiency of the enzyme (Doss *et al.*, 1979). It has been suggested that the accumulation of δ-aminolaevulinate in the blood, which mimics the neurotransmitter γ-aminobutyrate (GABA), and is a potent agonist for GABA receptors, may be responsible for the neurological symptoms and psychosis that often accompanies lead poisoning (Brennan and Cantrill, 1979). It is this inhibition of δ-aminolaevulinate dehydratase that is presumed to account for the anaemia of lead poisoning, and direct replacement of Zn in the unique triple cysteine site of porphobilinogen synthase by Pb has been shown in a dramatic fashion in the crystal structure of Pb-porphobilinogen synthase (Erskine *et al.*, 1997). Lead is also thought to inhibit ferrochelatase, which may explain the elevated values of zinc protoporphyrin found in lead intoxication.

12.3.3 Cadmium

Cadmium is nutritionally non-essential, toxic and a ubiquitous environmental pollutant. It is found in leafy vegetables, grains and cereals, and since it is present in substantial amounts in tobacco leaves, cigarette smokers on a packet a day can easily double their cadmium intake. It has a long biological half-life (17–30 years in man), accumulates in liver and kidneys and its toxicity involves principally kidney and bone (Goyer, 1997).While Cd interferes primarily with calcium, it also interacts with zinc and can induce the synthesis of metallothionein. Cadmium bound to metallothionein in liver or kidney is thought to be non-toxic, but cadmium in plasma

bound to metallothionein is toxic to the renal tubule while being excreted in the urine (Chan and Cherian, 1993). Cadmium administration to rats induces iron deficiency (Crowe and Morgan, 1997), and iron-deficiency anaemia is also seen in the severe bone disease discovered in Japan, known as itai-itai disease, which is though to result from excess cadmium exposure from rice compounded by nutritional deficiencies of calcium, vitamin D, zinc and iron. Iron deficiency increases cadmium absorption from the gastrointestinal tract in both experimental animals and humans (Flanagan *et al.*, 1978). Cadmium seriously impairs erythropoiesis, and has been shown to aggravate anaemia by suppressing erythropoietin gene expression in anaemic patients (reference cited in Chun *et al.*, 2000). In Hep3B cells cadmium was found to block the HIF-1 response to hypoxia, cobalt or desferrioxamine by stimulating the proteasome-dependent degradation of the HIF-1 alpha subunit (Chun *et al.*, 2000b).

12.4 References

Abreo, K., Glass, J., Jain, S. and Sella, M. (1994). *Kidney Internat.*, **45**, 636–41.

Abreo, K., Abreo, F., Sella, M. and Jain, S. (1999). *J. Neurochem.*, **72**, 2059–64.

Adonaylo, V.N. and Oteiza, P.I. (1999). *Toxicology*, **132**, 19–32.

Arfin, S.M., Kendall, R.L., Hall, L., Weaver, L.H. *et al.* (1995). *Proc. Natl Acad. Sci., USA*, **92**, 7714–8.

Askwith, C. and Kaplan, J. (1998). *Trends Biochem. Sci.*, **23**, 135–8.

Askwith, C., Eide, D., Van Ho, A., Bernard, P.S. *et al.* (1994). *Cell*, **76**, 403–10.

Barnum-Huckins, K.M., Martinez, A.O., Rivera, E.V., Adrian, E.K. *et al.* (1997). *Toxicology*, **118**, 11–22.

Brennan, M.J.W. and Cantrill, R.C. (1979). *Nature*, **280**, 514–5.

Bull, P.C., Thomas, G.R., Rommens, J.M., Forbes, J.R. and Cox, D.A. (1993). *Nat. Genet.*, **5**, 327–37.

Bunn, H.F., Gu, J., Huang, L.E., Park, J.W. and Zhu, H. (1998). *J. Exp. Biol.*, **201**, 1197–201.

Casareno, R.L., Waggoner, D. and Gitlin, J.D. (1998). *J. Biol. Chem.*, **273**, 23625–8.

Chan, H. and Cherian, M.G. (1993). *Toxicol. Appl. Pharmacol.*, **120**, 308–14.

Chang, J.Y. and Liu, L.Z. (1999). *Brain Res. Mol. Brain Res.*, **68**, 22–8.

Chelly, J. and Monaco, A.P. (1993). *Nat. Genet.*, **5**, 317–8.

Chelly, J., Tumer, Z., Tonneson, T., Patterson, A. *et al.* (1993). *Nat. Genet.*, **3**, 14–19.

Chua, A.C. and Morgan, E.H. (1996). *Biol. Trace Elem. Res.*, **55**, 39–54.

Chua, A.C. and Morgan, E.H. (1997). *J. Comp. Physiol. B*, **167**, 361–9.

Chun, Y.S., Choi, E., Kim, G.T., Lee, M.J. *et al.* (2000a). *Biochem. Biopys. Res. Commun.*, **268**, 652–656.

Chun, Y.S., Choi, E., Kim, G.T., Choi, H. *et al.* (2000b). *Eur. J. Biochem.*, **267**, 4198–204.

Cobine, P., Wickramasinghe, W.A., Harrison, M.D., Weber, T., Solioz, M. and Dameron, C.T. (1999). *FEBS Lett.*, **445**, 27–30.

Cochran, M. and Chawtur, V.(1988). *Biochem. J.*, **287**, 515–20.

Conrad, M.E., Umbreit, J.N. and Moore, E.G. (1999). *Am. J. Med. Sci.*, **318**, 213–9.

Cousins, R.J. (1985). *Physiol. Rev.*, **95**, 238–309.

Crowe, A. and Morgan, E.H. (1997). *Toxicol. Appl. Pharmacol.*, **145**, 136–46.

Culotta, V.C., Liu, X.F. and Schmidt, P. (1998). In *Metals and Genetics* (ed. Sarkar, B.) Plenum Press, New York.

Dabrowska-Bouta, B., Sulkowski, G., Bartosz, G., Walski, M. and Rafalowska, U. (1999). *J. Mol. Neurosci.*, **13**, 127–39.

Daghman, N.A., Elder, G.E., Savage, G.A., Winter, P.C., Maxwell, A.P. and Lappin, T.R. (1999). *Ann. Hematol.*, **78**, 275–8.

Dancis, A., Yuan, D.S., Halle, D., Askwith, C. *et al*. (1994). *Cell*, **76**, 393–402.

Davidsson, L., Almgren, A., Sandstrom, B. and Hurrell, R.F. (1995). *Br. J. Nutr.*, **74**, 417–25.

Davis, J.M. (1999). *Neurotoxicology*, **20**, 511–8.

Dedman, D.J., Treffry, A., Candy, J.M., Taylor, G.A. *et al*. (1992a). *Biochem. J.*, **287**, 509–14.

Dedman, D.J., Treffry, A. and Harrison, P.M. (1992b). *Biochem. J.*, **287**, 515–20.

Doll, S.R. (1993). *Age Ageing*, **22**, 138–53.

Doss, M., von Tiepermann, R., Schneider, J. and Schmid, H. (1979). *Klin. Wochenschr.*, **57**, 1123–7.

Edwardson, J.A., Candy, J.M., Ince, P.G., McArthur, F.K. *et al*. (1992). *CIBA Fdn Symp.*, **169**, 165–79.

Ehleben, W., Bolling, B., Merten, E., Porwol, T., Strogmaier, A.R. and Acker, H. (1998). *Respir. Physiol.*, **114**, 25–36.

Eide, D.J. (1998). *Ann. Rev. Nutr.*, **18**, 441–69.

Eide, D., Broderius, M., Fett, J. and Guerinot, M.L. (1996). *Proc. Natl Acad. Sci. USA*, **93**, 5624–8.

Erskine, P.T., Senior, N., Awan, S., Lambert, R. *et al*. (1997). *Nature Struct. Biol.*, **4**, 1025–31.

Fatemi, S.J., and Moore, G.R. (1991). *Biochem. J.*, **280**, 527–32.

Finley, J.W. and Davis, C.D. (1999). *Biofactors*, **10**, 15–24.

Flanagan, P.R., McLellan, J.S., Haist, J., Cherian, M.D. *et al*. (1978). *Gastroenterology*, **74**, 841–6.

Fleming, J. and Joshi, J.G. (1987). *Proc. Natl Acad. Sci. USA*, **84**, 7866–70.

Frausto da Silva, J.J.R. and Williams, R.J.P. (1991). In *The Biological Chemistry of the Elements*, Oxford University Press, Oxford.

Frumkin, H. and Solomon, G. (1997). *Am. J. Ind. Med.*, **31**, 107–15.

Gadd, G.M. and Laurence, O.S. (1996). *Microbiology*, **142**, 1159–67.

Gamonet, F. and Loaquin, G.J.M. (1998). *Eur. J. Biochem.*, **251**, 716–23.

Garrett, T.P., Clingeleffer, D.J., Guss, J.M., Rogers, S.J. and Freeman, H.C. (1984). *J. Biol. Chem.*, **259**, 2822–5.

Glerum, D.M., Koerner, T.J. and Tzagaloff, A. (1996). *J. Biol. Chem.*, **271**, 14504–9.

Good, P., Perl, D., Bierer, L. and Schmeidler, J. (1992). *Ann. Neurol.*, **31**, 286–92.

Gorell, J.M., Johnson, C.C., Rybicki, B.A., Peterson, E.L. *et al*. (1999). *Neurotoxicology*, **20**, 239–47.

Goyer, R.A. (1997). *Ann. Rev. Nutr.*, **17**, 37–50.

Gray, H.B., Malmström, B.G. and Williams, R.J.P. (2000). *J. Biol. Inorg. Chem.*, **5**, 551–9.

Gubler, C.J., Cartwright, G.E. and Wintrobe M.M. (1956). *J. Biol. Chem.*, **224**, 533–46.

Gunshin, H., McKenzie, B., Berger, U.V., Gunshin, Y. *et al.* (1997). *Nature*, **388**, 482–8.

Hamza, I., Schaeffer, M., Klomp, L.J. and Gitlin, J.D. (1999). *Proc. Natl Acad. Sci. USA*, **96**, 13363–8.

Harris, Z.L., Takahashi, T., Miyajima, H., Serizawa, M., MacGillevray, R.T. and Gitlin, J.D. (1995). *Proc. Natl Acad. Sci. USA*, **92**, 2539–43.

Harris, Z.L., Durley, A.P., Man, T.K. and Gitlin, J.D. (1999). *Proc. Natl Acad. Sci. USA*, **96**, 10812–7.

Harrison, M.D., Jones, C.E. and Dameron C.T. (1999). *J. Biol. Inorg. Chem.*, **4**, 145–53.

Harrison, M.D., Jones, C.E., Solioz, M. and Dameron, C.T. (2000). *Trends Biochem. Sci.*, **25**, 29–32.

Hart E.B., Steenbock, H., Waddell J. and Elvehjem C.A. (1928). *J. Biol. Chem.*, **77**, 797–812.

Holm, R.H., Kennepohl, P. and Solomon, E.I. (1996). *Chem. Rev.*, **96**, 2239–314.

Horecka, J., Kinsey, P.T. and Sprague, J.F. (1995). *Gene*, **162**, 87–92.

Huang, L.E., Willmore, W.G., Gu, J., Goldberg, M.A. and Bunn, H.F. (1999). *J. Biol. Chem.*, **274**, 9038–44.

Jensen, L.T., Howard, W.R., Strain, J.J., Winge, D.R. and Culotta, V.C. (1996). *J. Biol. Chem.*, **271**, 18514–19.

Johnson, F.M. (1998). *Mutat. Res.*, **410**, 123–40.

Jope, R.S. and Jackson, G.V.W. (1992). *CIBA Fdn Symp.*, **169**, 254–7.

Kaim, W. and Rall, J. (1996) *Angew. Chem. Int. Ed. Engl.*, **35**, 43–60.

Kampfenkel, K., Kushnir, S., Baviychuk, E., Inze, D. and Van Montagu, M. (1995). *J. Biol. Chem.*, **270**, 28479–86.

Kapadia, C.R. (1995). *Gastroenterologist*, **3**, 329–44.

Klinkenberg, M., Ling, C. and Chang, Y.H. (1997). *Arch. Biochem. Biophys.*, **347**, 193–200.

Klinman, J.P. (1996) *Chem. Rev.*, **96**, 2541–61.

Klomp, L.W.J, Lin, S.J., Yuan, D.S., Klausner, R.D., Culotta, V.C. and Gitlin, J.D. (1997). *J. Biol. Chem.*, **272**, 9221–6.

Klomp, L.W. and Gitlin, J.D. (1996) Human *Mail. Genet.*, **5**, 1989–96.

Knight, S.A., Labbe, S., Kwon, L.F., Kossman, D.J. and Theile, D.J. (1996). *Genes Dev.*, **10**, 1917–29.

Koch, K.A., Pena, M.M. and Thiele, D.J. (1997) *Chem. Biol.*, **4**, 549–60.

Kumar, U., Dunlop, D.M. and Richardson, J.S. (1994). *Life Science*, **54**, 1855–60.

Kuratko, C.N. (1999). *Toxicol. Lett.*, **104**, 151–8.

Labbe, R.F., Vreman, H.J. and Stevenson, D.K. (1999). *Clin. Chem.*, **45**, 2060–72.

Lee, G.R., Nacht, S., Lukens, J.N. and Cartwright, G.E. (1968). *J. Clin. Invest.*, **47**, 2058–69.

Lin, S.J., Pufahl, R.A., O'Halloran, T.V. and Culotta, V.C. (1997). *J. Biol. Chem.*, **272**, 9215–20.

Lippard, S.J. and Berg, J.M. (1994). *Principles of Bioinorganic Chemistry*, University Science Books, Mill Valley, California, USA, pp. 336–43.

Liu, X.F., Supek, F., Nelson, N. and Culotta, V.C. (1997). *J. Biol. Chem.*, **272**, 11763–9.

Ludwig, M.L. and Matthews, R.G. (1997). *Ann. Rev. Biochem.*, **66**, 269–313.

Lutsenko, S. and Kaplan, J. (1995). *Biochem.*, **34**, 15608–13.

Markowitz, M. (1999). *Curr. Prob. Pediatr.*, **30**, 62–70.

Martin, R.B. (1994). *Acc. Chem. Res.*, **27**, 204–10.

Maxwell, P.H., Wiesener, M.S., Chang, G.W., Clifford, S.C. *et al.* (1999). *Nature*, **399**, 271–5.

Mercer, J.F., Livingston, J., Hall, B., Paynter, J.A. *et al.* (1993). *Nat. Genet.*, **3**, 20–5.

Moore, P.B., Day, J.P., Taylor, G.A., Ferrier, I.N., Fifield, L.K. and Edwardson, J.A. (2000). *Dementia Geriatric Cogn. Disord.*, **11**, 66–9.

Mukhopadhyay, C.K., Attieh, Z.K. and Fox, P.L. (1998). *Science*, **279**, 714–7.

Mukhopadhyay, C.K., Mazumder, B. and Fox, P.L. (2000). *J. Biol. Chem.*, **275**, 21048–54.

Nagano, K., Nakamura, K., Urakami, K.I., Uchiyama, H. *et al.* (1998). *Hepatology*, **27**, 799–807.

Odermatt, A., Suter, H., Krapf, R. and Solioz, M. (1993). *J. Biol. Chem.*, **268**, 12775–9.

Olanow, C.W., Good, P.F., Shinotoh, H., Hewitt, K.A. *et al.* (1996). *Neurology*, **46**, 492–8.

Olivares, M. and Uauy, R. (1996). *Am. J. Clin. Nutr.*, **63**, 791S–796S.

Osaki, S., Johnson, D.A. and Frieden, E. (1966). *J. Biol. Chem.*, **241**, 2476–81.

Oshiro, S., Kawahara, M., Mika, S., Muramoto, K. *et al.* (1998). *J. Biochem. (Tokyo)*, **123**, 42–6.

Oshiro, S., Kawahara, M., Kurudo, Y., Zhang, C. *et al.* (2000). *Biochem. Biophys. Acta*, **1502**, 405–14.

Palmiter, R.D. and Findley, S.D. (1995). *EMBO J.*, **14**, 639–49.

Palmiter, R.D., Cole, T.B. and Findley, S.D. (1996a). *EMBO J.*, **15**, 1784–91.

Palmiter, R.D., Cole, T.B., Quaife, C.J. and Findley, S.D. (1996b). *Proc. Natl Acad. Sci., USA*, **93**, 14934–9.

Pena, M.M., Koch, K.A. and Thiele, D.J. (1998). *Mol. Cell. Biol.*, **18**, 2514–23.

Petris, M.J., Mercer, J.F., Culvenor, J.G., Lockhart, P., Gleeson, P.A. and Camakaris, J. (1996). *EMBO J.*, **15**, 6084–95.

Porwol, T., Ehleben, W., Zierold, K., Fandrey, J. and Acker, H. (1998). *Eur. J. Biochem.*, **256**, 16–23.

Pountney, D.L., Schauwecker, I., Zarn J. and Vasak, M. (1994). *Biochem.*, **33**, 9699–715.

Prasad, A.S. (1990). In *Modern Nutrition in Health and Disease* (ed. Tomita, H.) Springer Verlag, Tokyo, pp. 3–14.

Priest, N.D., Talbot, R.J., Newton, D., Day, J.P., King, S.J. and Fifield, L.K. (1998). *Human Exp. Toxicol.*, **17**, 296–301.

Pufahl, R.A., Singer, C.P., Peariso, K.L., Lin, S.-J. *et al.* (1997). *Science*, **278**, 853–6.

Ragan, H.A., Nacht, S., Lee, G.R., Bishop, C.R. and Cartwright, G. (1969). *Am. J. Physiol.*, **217**, 1320–3.

Salamon, E.I., Sundaram, U.M. and Machankin, T.E. (1996). *Chem. Rev.*, **96**, 2563–605.

Sandstrom, B., Davidsson, L., Cederblad, A. and Lonnerdal, B. (1985). *J. Nutr.*, **115**, 411–4.

Sato, M. and Gitlin, J. (1991). *J. Biol. Chem.*, **266**, 5128–34.

Scheinberg, I.H. and Gitlin, J.D. (1952). *Science*, **116**, 484–5.

Schwabe, J.W.R. and Klug, A. (1994). *Nature Struct. Biol.*, **1**, 345–9.

Simons, T.J.B. (1995). *Eur. J. Biochem.*, **234**, 178–83.

Smith, M.A., Wehr, K., Harris, P.O.R, Siedlak, S.L., Connor, J.R. and Perry, G. (1998). *Brain Res.*, **788**, 232–6.

Snyder, R.D. and Friedman, M.B. (1998). *Mutat. Res.*, **405**, 1–8.

Solioz, M. and Odermatt, A. (1995). *J. Biol. Chem.*, **270**, 9217–21.

Solioz, M. and Vulpe, C. (1996). *Trends Biochem. Sci.*, **21**, 237–41.

Solomons, N.W. (1986). *J. Nutr.*, **116**, 927–35.

Stearman, R., Yuan, D.S., Yamaguchi-Iwai, Y., Klausner, R.D. and Dancis, A. (1996). *Science*, **271**, 1552–7.

Strain, J. and Culotta, V.C. (1996). *Mol. Gen. Genet.*, **251**, 139–45.

Supek, F., Suekova, L., Nelson, H. and Nelson, N. (1996). *Proc. Natl Acad. Sci. USA*, **93**, 5105–10.

Supek, F., Suekova, L., Nelson, H. and Nelson, N. (1997). *J. Exp. Biol.*, **200**, 321–30.

Swegert, C.V., Dave, K.R. and Katyare, S.S. (1999). *Mech. Ageing Develop.*, **112**, 27–42.

Tanzi, R.E., Petrukhin, K., Chernov, I., Pellequer, J.L. *et al.* (1993). *Nat. Genet.*, **5**, 344–50.

Thompson, R.B. (1977). In *Disorders of the Blood*, Churchill Livingstone Edinburgh, pp. 338–339.

Valberg, L.S., Flanagan, P.R. and Chamberlain, M.J. (1984). *Am. J. Clin. Nutr.*, **40**, 536–41.

Verity, M.A. (1999). *Neurotoxicology*, **20**, 489–97.

Vasak, M. and Hasler, D.W. (2000). *Curr. Opin. Chem. Biol.*, **4**, 177–83.

Vulpe, C., Levison, B., Whitney, S., Packman, S. and Gitschier, J. (1993). *Nat. Genet.*, **3**, 7–13.

Vulpe, C.D., Kuo, Y.M., Murphy, T.L., Cowley, L. *et al.* (1999). *Nature Genet.*, **21**, 195–9.

Ward, R.J. and Crichton, R.R. (2001). In *Aluminium and Alzheimer's Disease* (ed. Exley, C.). Elsevier, pp. 293–310.

Ward, R.J., Scarino, L., Leone, A., Crichton, R.R. and McArdle, H.J. (1998). *Biochem. Soc. Trans.*, **26**, S191.

West, A.H., Clark, D.J., Martin, J., Neupert, W., Hartl, F.U. and Horwich, A.L. (1992). *J. Biol. Chem.* **267**, 24625–33.

Whittaker, P. (1998). *Am. J. Clin. Nutr.*, **68**, 442S–446S.

Williams, D.M., Lee, G.R. and Cartwright, G.E. (1974). *Am. J. Physiol.*, **227**, 1094–7.

Williams D.M., Loukopoulus D., Lee G.R. and Cartwright G.E. (1976). *Blood*, **48**, 77–85.

Williams, R.J.W. (1999). *J. Inorg. Biochem.*, **76**, 81–8.

Wright, R.O. (1999). *Curr. Opin. Pediatr.*, **11**, 255–8.

Yamanaka, K., Minato, N. and Iwai, K. (1999). *FEBS Lett.*, **462**, 216–20.

Yoshida, K., Furihata, K., Takeda, S., Nakamura, A. *et al.* (1995). *Nature Genet.*, **9**, 267–72.

Yuan, D.S., Stearman, R., Dancis, A., Dunn, T., Beeler, T. and Klausner, R.D. (1995). *Proc. Natl Acad. Sci., USA*, **92**, 2632–6.

Zhao, H. and Eide, D.J. (1997). *Mol. Cell. Biol.*, **17**, 5044–52.

Zheng, W., Zhao, Q., Slavkovich, V., Ascher, M. and Graziano, J.H. (1999). *Brain Res.*, **833**, 125–32.

Zhou, B. and Gitschier, J. (1997). *Proc. Natl Acad. Sci., USA*, **94**, 7481–6.

13 Concluding Remarks

There comes a time in any literary endeavour when one has to recognize that time has run its course, that a line has to be drawn in the sand, that one simply cannot continue to surf the Internet, that there is an ultimate limit to the recent publications that one can include in the final text. As the Thirteenth century Chinese scholar Tai T'ung (*The Six Scripts: Principles of Chinese Writing*) wrote 'Were I to await perfection, my book would never be finished.' So, at the beginning of the veritable Twenty-first century, the real Third millenium, it is time to conclude, with all of the regrets which that implies. That perfection could ever be attained in a field which is undergoing such an explosive expansion and development at the present time is quite simply impossible.

So, in the context of the sequencing of the entire human genome, and the almost weekly publication of the complete genome of yet another organism (over one-hundred complete genomes, almost all of bacteria, are predicted to be published by the end of 2000), how will access to the basic linear DNA sequence structure of hundreds of thousands of genes, in this post-genomic era, change our understanding of how these genes, or more particularly their products, function in a biological context? Is it enough to cite the magical key word *functional genomics*, which has been described as 'the development and application of global – meaning genome-wide or system-wide – experimental approaches to assess gene function by making use of the information and reagents that are provided by the sequencing and mapping of genomes' in order magically to transform biology into a Brave New World, where we know not only what the proteins encoded by genes look like, but also what they do and how they fit into the global economy of the organism concerned. Despite protestations that genome sequencing is simply brute force molecular biology[†] with little or no intellectual input, there are others who claim that with the appropriate Rosetta Stone[‡] to predict which proteins interact with each other (Eisenberg *et al.*,

---

[†] A sheep farmer comes across a young man in one of his fields; the young man proposes guessing how many sheep are in the field, in return for a sheep if his prediction is correct: the farmer, bemused, agrees and the intruder correctly estimates exactly how many sheep are present. By way of compensation the farmer asks the young man, who has claimed his prize, and tucked it under his arm, whether he will return his trophy if the farmer can correctly guess his profession. He agrees, and the farmer declares that he is a molecular biologist. Stupefied the young man asks 'How did you know that?' The farmer simply replies 'I'll tell you when you give me back my dog!'

[‡] The Rosetta Stone, a tablet of black basalt found in 1799 in Rosetta, a town in Egypt, had parallel inscriptions in Greek and in ancient Egyptian demotic and hieroglyphic characters, and was of crucial importance in deciphering ancient Egyptian writing.

2000), and better algorithms to predict protein structure from primary sequence, the secrets of the large number of unknown ORFs (open reading frames) in the human genome, which have little or no sequence homology to other proteins of known function, will be uncovered. The answer is, of course, *not so easily!* What leads us to believe that via genomics, proteomics, transcriptomics and even metabolomics, by transforming ourselves into informaticians we can solve all of the problems of biology?

John Walker, Nobel laureate for Chemistry in 1997, quoted Sidney Brenner in his plenary lecture to the *Eighteenth International Congress of Biochemistry and Molecular Biology: Beyond the Genome*, in Birmingham in July 2000: 'Will the world be a different place on Tuesday? [27th June, 2000, the day after the announcement of the completion of the human genome] No. We have a huge task ahead: the interpretation of this mass of data. We need to find out what all these proteins do, and how they link together. This is a task for *'traditional' biochemistry* and *physiology*.'

When the first edition of this book was written 10 years ago, the structures of very few metalloproteins were known. In the interval, metalloprotein crystallography has come of age with more and more structures appearing, at higher and higher resolution, in seemingly unending succession. With these structures have come surprises as well. While it is true that the *Haemophilus influenzae* periplasmic ferric-binding protein hFBP is indeed a member of the transferrin superfamily (Chapter 5), the recently determined crystal structure of FhuD, the periplasmic ferrichrome transporter with bound gallichrome (ferrichrome in which Fe^{3+} is replaced by Ga^{3+}) (Clarke *et al.*, 2000) shows a totally different class of structure (Chapter 3). We must however emit a word of caution: although we have many crystal structures, they do not in themselves allow us to understand the mechanisms by which any given protein functions – much good old fashioned solution biochemistry remains to be done. And while our understanding of iron uptake by *Escherichia coli* continues to advance rapidly, as can be seen from the progress reported in Chapter 3, the same is still far from being the case in other bacteria, with a particularly alarming absence of knowledge about iron uptake *and* metabolism in archaebacteria. Even in *E. coli* we still understand little about intracellular iron metabolism and its regulation.

Our understanding of iron metabolism in plants has made enormous progress, particularly since molecular biological techniques have been applied, more easily controlled culture systems used, and genome sequencing, notably for *Arabadopsis thaliana*, undertaken. Yet, much remains to be done, particularly with regard to our understanding of regulatory pathways. From a more practical point of view, appropriate treatment for chlorosis still remains a major problem in plant husbandry. Of course, the gigantic strides in research into bakers' yeast, *Saccharomyces cerevisiae*, have highlighted the important interactions between iron and copper, and identified a number of genes that have homologues in the human genome. This still leaves open the question as to just how close to that in man yeast-iron metabolism really is. This is particularly underlined by the apparently contradictory roles of Fet3 in yeast as compared with ceruloplasmin and hephaestin in mammalian cells: the former brings iron into the cell while the other two take iron out of cells. There is, however, no doubt that the identification of genes involved in mitochondrial iron metabolism in yeast is likely to advance our understanding of a number of

disorders in man characterized by accumulation of iron in this key organelle, such as Friedrich's ataxia.

I must confess that I never cease to wonder at the surprises that the transferrin molecule continues to reserve for us. Pushing the power of X-ray crystallography to its limits, Ted Baker's group has managed to capture within the same crystalline lattice two different occupancies of the iron-binding site, lending enormous weight to the argument that protonation of the carbonate anion is indeed the first step in the release of iron from transferrin at acidic pH values. There are, however, still a few links missing in our understanding of how iron is delivered from transferrin within the cell. While the important role of DCT1 in shifting iron out of the endosomal compartment seems well established, we still lack convincing evidence for a ferrireductase within the endosome or the endosomal membrane. The role of such recently discovered proteins as SFT, which stimulates Fe transport of both transferrin- and non-transferrin-bound iron (NTBI) remains enigmatic, particularly in view of its cytolocalization to recycling endosomes, its linkage to a cell-surface ferrireductase activity, and its stimulation of both ferrous and ferric iron at pH 7.4 (Wessling-Resnick, 2000). Yet another anomaly is posed by the ceruloplasmin-stimulated iron uptake for trivalent metal ions described by Attieh *et al.* (1999), which seems to fly in the face of accepted physiological wisdom that supports a crucial role for ceruloplasmin in iron mobilization from cells (Harris *et al.*, 1999). Perhaps the use of cell lines instead of primary cell cultures or studies on whole organisms[¶], is to some extent the cause of the problem.

By comparison with iron transport proteins, that constitute a veritable hierarchy with little apparent similarity of structure except for the transferrin superfamily (which includes the Venus Fly Trap proteins of the bacterial periplasm), ferritin turns out to be an almost ubiquitous feature of the living organism, with the possible exceptions of a few archaebacteria and the common bakers' yeast, *Saccharomyces cerevisiae*. However, while its role in iron storage is uncontested in plants and animals, as well as in other eukaryotes, it is still not entirely clear what its function really is in bacteria. The best known bacterial system, *E. coli*, regulates its iron requirements at the level of the uptake systems, and does not seem either to store much iron in its ferritins, or to suffer much from their knock-out. This contrasts significantly with the situation in mammals, where knock-out of the H ferritin gene has no effect on heterozygotes, but is rapidly lethal in homozygotes (Ferreira *et al.*, 2000). I suppose that this at least tells us that H-chain ferritin is important, but for what? Perhaps this also reflects the iron storage function of mammalian ferritins, and the importance of having two types of subunits, one involved in initial iron uptake and oxidation, and the other in consolidation of the biomineralization of the ferritin iron micelle. Perhaps the fairly general absence of heteropolymers in prokaryotic ferritins is telling us something about their eventual physiological function. And what about haem-binding in certain bacterioferritins, or even more peculiar, haem demetallation in mammalian ferritins? Does this have a possible role in haem

---

[¶] While I fully understand concern about animal welfare, it is difficult to see how our understanding of iron metabolism, not to mention the development of new drugs, can evolve without carrying out animal studies. It is difficult to see how one can extrapolate from results obtained using cultured cell lines which typically have very large numbers of transferrin receptors when compared with the normal cells from which they are derived.

catabolism? Despite our increasing confidence about the pathway of iron uptake into ferritins, we still know practically nothing about storage iron mobilization, whether from ferritin (or as seems increasingly likely, from haemosiderin and its precursors in the lysosomal compartment) or for that matter about the origin of the different iron core structures that we find in different circumstances (Ward *et al.*, 2000).

When we consider iron homeostasis, the discovery that there are at least two IRPs with potentially different target binding IRE sequences complicates the situation, to put it mildly. To make matters worse (if possible) so does the finding of IREs in the 5′- and 3′-UTRs of the mRNAs of iron transporters located respectively at the basolateral (IREG1) and apical DCT1) membranes of the enterocyte, whose expressions are both up-regulated under conditions of iron deficiency. Perhaps the simple model of translational regulation of mRNAs is not the whole story, and there really are other regulatory mechanisms waiting to be discovered in mammalian cells, perhaps this time at the level of transcription. One of the long-standing enigmas of the biological inorganic chemistry of iron, namely how iron is inserted into iron-containing proteins, is slowly beginning to be understood. The recent progress on ferrochelatase, as well as in elucidating the steps involved in Fe–S cluster assembly and their incorporation into Fe–S proteins, together with better information about mitochondrial iron metabolism, hold great promise. We should, however, not forget how little we still know about the pathways of iron insertion into non-haem, non-Fe–S, iron-containing proteins, which are clearly associated with the question of whether there might be iron chaperone proteins. My personal intuition is that there are not, in the same sense as for copper, chaperones for iron. However, there are the ferrochelatases which insert iron into protoporphyrin IX, and the recently discovered proteins involved in Fe–S protein biosynthesis. We already know, from studies in *E. coli*, that the constitution of the tyrosyl radical at the catalytic site of the key diiron enzyme ribonucleotide reductase, requires several proteins *in vivo*. So we might just ask, what do we mean by the word chaperone[§]?

More detailed knowledge of the mechanisms of iron absorption from the gastrointestinal tract of mammals has advanced by leaps and bounds in the last few years, with the cloning of key participants at both the apical and basolateral faces of the mucosal endothelial cells. The extraordinarily far-sighted contribution of William Crosby and Marcel Conrad, nearly 40 years ago (Conrad and Crosby, 1963; Crosby, 1963), reminded us of the key role of body iron status in determining the level at which iron absorption will be set within the cells of the crypts of Lieberkühn when they differentiate and move up to the villus tips to play their key role in

[§] It may finally come down to 'what's in a name'. If we go by the book, a chaperon/chaperone is an older or married person who accompanies young unmarried people in public, or who is present at their parties, dances, etc, for the sake of propriety or to supervise their behaviour. In our more licentious Twentieth century this was interpreted, notably by protein chemists to describe accompanying protein molecules that protected other protein molecules from degradation or denaturation during their transit across membranes, particularly by preventing improper folding and aggregation of the target protein. Perhaps the best definition is that given by John Ellis, who points out that molecular chaperones function in an analogous way to their human counterparts: *They inhibit inappropriate interactions between potentially complementary surfaces and disrupt unsuitable liasons so as to facilitate more favourable associations*. In that sense, any protein which fulfills these criteria would qualify; in necessity the corresponding synonyms are: companion, duenna, protectress, or escort – you may take your choice!

iron absorption from the gastrointestinal tract. We mentioned earlier the questions concerning how IRPs in their high affinity binding form can not only up-regulate the synthesis of proteins with IREs in their 3′-UTR, such as DCT1, but also those like IREG1 (ferroportin, MTP1) which have an IRE in their 5′-UTR. This is not the only outstanding question that we still face concerning iron absorption. Not the least of the enigmas which remain involves the nature of the interaction between the haemochromatosis gene product HFE and the transferrin receptor, and above all how it deregulates the setting of the preenterocyte within the crypt of Lieberkühn such that, arriving at the absorptive villus, it allows too much iron across despite all the plasma appearances of iron surfeit. The role of enterocyte ferritin in the maintenance of global iron homeostasis now seems clear, supporting the 'mucosal block' hypothesis of Granick (1946), reinforced by Crosby's observation that there were decreased amounts of ferritin in the absorbing cells of the upper gut in haemochromatosis patients (Crosby, 1963). This already indicated that there was some abnormality either in mucosal ferritin or, as we now know, in lower levels of ferritin protein expression within the villus enterocyte, thus setting the 'iron thermostat' at a level which results in the transfer of a larger proportion than normal of the iron entering mucosal cells into the body.

Now that we have diagnostic tools that allow the early diagnosis of genetic haemochromatosis, and an increased awareness of the frequency of iron deficiency, together with the prospects of application of extensive therapeutic programmes in developing countries, one might have thought that the entire field of iron metabolism was about to enter into its 'golden age'. Alas, iron metabolism is considered by funding bodies to be 'well understood', while those of us in the field recognize how much still remains to be done before we can proceed to a rational therapeutic approach to disorders of iron metabolism[‖]. Of course, the problem with the treatment of disorders of iron metabolism such as genetic haemochromatosis, and secondary iron-loading diseases like thalasaemia, is that they are not 'sexy', when compared for example with AIDS. The important role of iron in many infectious diseases has also been underlined as another target area in which therapeutic measures to remove excess iron from specific cellular and tissue locations could prove extremely useful. However, phlebotomy and iron chelators are not exactly high technology.

This situation may be about to change as we look at the role of iron and its implications in the formation of reactive oxygen species, with their potential to attack, modify, and ultimately destroy cells. The signalling function of ROS, not to mention RNS, has been underlined earlier. Yet, we tread a delicate, and poorly understood balance between low levels of ROS, required both for cell signalling and to maintain the antioxidative defences of the cell in a state of alert[††], and levels which become toxic. This remains an extremely important area of therapeutic concern, since oxidative stress, whether proven to be due to iron or not, is

---

[‖] I am reminded of the remark of the celebrated pianist Artur Schnabel, quoted by Alfred Brendel, concerning the piano sonatas of Mozart – 'too easy for children, too difficult for adults'.

[††] A fire station that was manned by personnel who were allowed to sleep between fixed hours of the day and night, would not be effective in responding to emergencies precisely during these periods. Likewise, cellular defences against oxidative stress cannot afford to sleep 'by day or by night'. They need to be in a state of permanent alert maintained by not only the threat of ROS, but by their very presence.

involved in disorders as diverse as carcinogenesis, ischaemia/reperfusion damage (with all its implications for organ transplantation), inflammatory/immune injury, alcohol abuse, atherosclerosis, microbial infection and neurological disorders. The latter category of disease, including Parkinson's disease, Alzheimer's disease, Huntingdon's chorea, multiple sclerosis and Friedrich's ataxia (the latter also involving cardiac tissue), are all characterized by excessive accumulation of iron in the brain. With the increased life expectancy of the population in developed countries, any measures that could prevent the onset of debilitating neurological disease, and in addition bring a better quality of life as the inexorable process of ageing comes upon us like a shipwreck (*sic* Sacha Distel), would be an enormous boon and blessing.

We know from reliable statistical data that low haemoglobin levels (at the upper limits of iron deficiency anaemia) correlate with longevity. We have seen the potential role of excessive iron accumulation in the potentiation of clinical disorders, particularly as a function of age. It would seem that a carefully evaluated clinical study, in which an orally active iron chelator was applied over an relatively long period of time, together with assessment of the possible positive effects on retarding the onset of a whole series of disorders, would be of considerable interest. And we should not undervalue the potential of a new generation of iron chelators, not only in this area, but also as therapeutic agents in secondary iron overload, in infectious diseases, particularly of the respiratory tract, and for many applications in agriculture and biotechnology, some of which we may not even have thought about to date.

When one looks at this rich panorama of unsolved questions, also having potential for solutions still waiting to be found, I can only end by evoking, as at the outset of this long Odyssey, Robert Frost:

> *Whose woods these are I think I know.*
> *His house is in the village, though;*
> *He will not see me stopping here*
> *To watch his woods fill up with snow.*
>
> *The woods are lovely, dark and deep,*
> *But I have promises to keep,*
> *And miles to go before I sleep,*
> *And miles to go before I sleep.*

Robert Frost 'Stopping by woods on a snowy evening' from *New Hampshire* (1923)

13.1 References

Attieh, Z.K., Mukhopadhyay, C.K., Seshadri, V., Tripoulos, N.A. and Fox, P.L. (1999). *J. Biol. Chem.*, **274**, 1116–23.

Clarke, T.E., Ku, S.-Y., Dougan, D.R., Vogel, H.J. and Tari, L.W. (2000). *Nature Struct. Biol.*, **7**, 287–91.

Conrad, M.E. and Crosby, W.H. (1963). *Blood*, **22**, 406–15.

Crosby, W.H. (1963). *Blood*, **22**, 441–9.

Eisenberg, D., Marcotte, E.M., Xenarios, I. and Yeates, T.O. (2000). *Nature*, **405**, 823–6.

Ferreira, C., Bucchini, D., Martin, M.E., Levi, S. *et al*. (2000). *J. Biol. Chem.*, **275**, 3021–4.

Granick, S. (1946). *J. Biol. Chem.*, **164**, 737–46.

Harris, Z.L., Durley, A.P., Man, T.K. and Gitlin, J.D. (1999). *Proc. Natl Acad. Sci., USA*, **96**, 10812–7.

Ward, R.J., Legssyer, R., Henry, C. and Crichton, R.R. (2000). *J. Inorg. Biochem.*, **79**, 311–7.

Wessling-Resnick, M. (2000). *Ann. Rev. Nutr.*, **20**, 129–51.

Index

Page numbers in italic, e.g. *56*, signify references to figures. Page numbers in bold, e.g. **10**, denote references to tables.